

**Traditional polymers with nontraditional side-chain functionality:
Carboalkoxylated polyvalerolactones and polyisoprenes from malic acid
and glucose**

A DISSERTATION SUBMITTED TO THE FACULTY OF
UNIVERSITY OF MINNESOTA

BY

Grant William Fahnhorst

IN PARTIAL FULFILLMENT OF THE REQUIREMENTS
FOR THE DEGREE OF
DOCTOR OF PHILOSOPHY

Thomas R. Hoye, advisor

June 2019

© Grant William Fahnhorst

June 2019

Acknowledgements

Not making the fifth grade “A” hockey team was one of the best things that has ever happened to me. At the time, my dad was the first person to notice how devastated I was, and he immediately encouraged me to “use that net we bought you more” and told me that I would need to work hard if I really wanted to become a good hockey player. After countless hours of shooting pucks and perfecting my skills in hockey, I was not cut from another team for the next 10 years. I tell this story because first and foremost, I would like to thank my parents, Jim and Kim. Their constant love and support provided me a strong work ethic and the belief that I could achieve anything I set my mind to. I also must thank my siblings, Jamie and Logan. Growing up, they were always lovingly competitive, which provided a great environment for each of us to push each other to become better in the classroom and in sports.

Next, I would like to thank my academic mentors. My undergraduate advisor, Professor Rita Majerle, noticed how much I enjoyed her organic chemistry course and was the person to really push me into chemistry and research. I also cannot thank my graduate advisor, Professor Thomas Hoye, enough for shaping me into the chemist I am today. His attention to detail and passion for chemistry are contagious. He has provided a culture where it feels like I have not worked a day in my graduate career.

I would also like to thank Dr. Sean Ross, Shu Xu, Severin Thompson, Xiao Xiao, Sahil Arora, Dr. Andrew Michel, Guilhem De Hoe, Amy Ott, Pat Crossland, Curtis Payne, Robin Harkins, Xin Yi, and Ethan Gormung that have made the Hoye group and the University of Minnesota an enjoyable place to learn. Also, thank you to Dr. Bryce Sundahl, Dr. Nicolas Ball-Jones, Dr. David Guptill, and Dr. Rajasekhar “Reddy” Naredla,

who were mentors that were always willing to help me with a problem early in my graduate career.

Finally, I thank my wife Monica. She provides me with love and support every day. We first met a few weeks before I started graduate school and have grown together throughout the past five years to become husband and wife. I cannot wait to see what the future has in store for us.

*I dedicate this thesis to my parents, Jim and Kim,
and my wife, Monica.*

Abstract

The compounding environmental effects of non-degradable plastics have attracted increased attention to sustainable polymers. This dissertation is focused on producing polymers from plant-based, renewable feedstocks while also emphasizing novel methods to chemically recycle polymers into valuable fragments. Plant-based feedstocks provide reagents with increased oxidation relative to petroleum and offer the opportunity to access traditional monomers with novel functionality. In this document, approaches to producing biobased monomers in addition to ring-opening transesterification polymerization (ROTEP) are introduced (Chapter 1). After, my research (in Part 1) on the two-step synthesis and ROTEP of 4-carboalkoxyvalerolactones is discussed. The ROTEP of these monomers, which are derived from malic acid, can either provide (i) tough and flexible, semicrystalline polyesters that can be chemically recycled by two independent pathways (Chapter 2 and 4) or (ii) an amorphous, hyperbranched polyester also capable of being chemically recycled (Chapter 3). The architecture of the product polymer is determined by the catalyst used for ROTEP or the position of the carboalkoxy on the lactone ring (Chapter 5). These characteristics are unique to this relatively unstudied family of monomers. In Part 2, anhydromevalonolactone, which can be fermented from glucose, is converted into isoprenecarboxylic acid, isoprenecarboxylate esters, and isoprenecarboxamides. These isoprene derivatives are radically polymerized to provide linear polymers (Chapter 6) or crosslinked superabsorbent hydrogels (Chapter 7). This series of polymers may provide a biobased alternative to polyacrylates.

Table of Contents

| | |
|---|----------|
| Acknowledgements..... | i |
| Dedication..... | iii |
| Abstract..... | iv |
| Table of Contents..... | v |
| List of Figures..... | ix |
| List of Schemes..... | xiii |
| List of Tables..... | xiv |
| ◆PART 1◆ Carboalkoxylated polyvalerolactones from malic acid..... | 1 |
| Chapter 1. Approaches to bioderived monomers and an introduction to ring-opening transesterification polymerization..... | 2 |
| 1.1 Plastics today..... | 2 |
| 1.2 Approaches to sustainable monomers from biomass..... | 3 |
| 1.2.1 Drop-in monomers..... | 3 |
| 1.2.2 Novel monomers: Biobased replacements..... | 4 |
| 1.2.3 Novel monomers: Novel biobased monomers..... | 5 |
| 1.3 Ring-opening transesterification polymerization..... | 7 |
| 1.3.1 Thermodynamics of ROTEP..... | 8 |
| 1.3.2 Thermal properties and kinetic considerations for substituted lactones..... | 11 |
| 1.3.3 Chemical recycling of polylactones..... | 12 |
| 1.3.4 Remaining needs for chemically recyclable polyesters..... | 14 |
| 1.4 Thesis Overview..... | 15 |
| 1.5 Previously reported carboalkoxylated lactones..... | 17 |
| 1.6 References..... | 19 |

| | |
|---|-----------|
| Chapter 2. A carbomethoxylated polyvalerolactone from malic acid: Synthesis and divergent chemical recycling..... | 24 |
| 2.1 Introduction | 25 |
| 2.2 Monomer synthesis | 26 |
| 2.3 Polymer synthesis and CMVL degradation | 27 |
| 2.4 Divergent chemical recycling of poly(CMVL)..... | 32 |
| 2.5 Conclusion..... | 35 |
| 2.6 References | 36 |
| | |
| Chapter 3. Isomerization of Linear to Hyperbranched Polymers: Two Isomeric Lactones Converge, via Metastable Isostructural Polyesters, to a Highly Branched Analogue | 40 |
| 3.1 Introduction | 42 |
| 3.2 Analysis of EQ-PCMVL from CMVL and PCMVL using catalyst 302 | 43 |
| 3.3 MALDI spectrometry reveals cyclic structure | 48 |
| 3.4 Isomerization of isoCMVL to EQ-PCMVL..... | 51 |
| 3.5 Chemical recycling through methanolysis of EQ-PCMVL | 52 |
| 3.6 Conclusion..... | 54 |
| 3.7 References | 55 |
| | |
| Chapter 4. Tough and flexible carboalkoxylated polyvalerolactones from malic acid: Influence of the carboalkoxy sidechain on polymer thermal and mechanical properties | 57 |
| 4.1 Introduction | 58 |
| 4.2 Results and discussion..... | 59 |
| 4.2.1 Monomer syntheses | 59 |
| 4.2.2 Synthesis and characterization of low molecular weight PCRVLs (ca. 50 repeat units per chain)..... | 62 |

| | |
|--|-----------|
| 4.2.3 High molecular weight PCRVLs: Polymerization and molar mass distribution | 64 |
| 4.2.3 High molecular weight PCRVLs: Thermal and mechanical properties | 66 |
| 4.3 Conclusion..... | 70 |
| 4.4 References | 72 |
| Chapter 5. Effects of carboalkoxy sidechain position on lactone monomers: | |
| Polymerization or isomerization? | 75 |
| 5.1 Introduction | 76 |
| 5.2 Monomer syntheses | 78 |
| 5.2.1 Carboalkoxylated valerolactones..... | 78 |
| 5.2.2 Carboalkoxylated caprolactones..... | 79 |
| 5.3 Polymerization studies: Past and present | 80 |
| 5.3.1 Previous observations and our hypothesis..... | 80 |
| 5.3.2 Polymerization or isomerization? Carboalkoxylated valerolactones | 81 |
| 5.3.3 Polymerization or isomerization? Carboalkoxylated caprolactones | 82 |
| 5.4 Future directions..... | 86 |
| 5.5 Conclusion..... | 88 |
| 5.5 References | 89 |
| ◆PART 2◆ Carboalkoxylated polyisoprene from glucose..... | 91 |
| Chapter 6. Poly(isoprenecarboxylates) and poly(isoprenecarboxamides) from glucose via anhydromevalonolactone..... | |
| 92 | 92 |
| 6.1 Introduction | 93 |
| 6.2 Isoprenecarboxylates: Synthesis, polymerization, and polymer properties | 95 |
| 6.3 Isoprenecarboxamides: Synthesis, polymerization, and polymer properties | 98 |
| 6.4 Conclusion..... | 100 |

| | |
|---|------------|
| 6.5 References | 101 |
| Chapter 7. Superabsorbent poly(isoprenecarboxylate) hydrogels..... | 104 |
| 7.1 Introduction | 105 |
| 7.2 Results and Discussion..... | 106 |
| 7.3 Conclusion..... | 113 |
| 7.4 References | 115 |
| Bibliography | 119 |
| Appendix A. Supporting Information for Chapter 2 (S2)..... | 133 |
| Appendix B. Supplementary information for Chapter 3 (S3) | 168 |
| Appendix C. Supplementary information for Chapter 4 (S4) | 199 |
| Appendix D. Supplementary information for Chapter 5 (S5) | 254 |
| Appendix E. Supporting information for Chapter 6 (S6) | 272 |
| Appendix F. Supporting information for Chapter 7 (S7) | 307 |
| Appendix G. Copies of NMR spectra for Chapter 4 and 5 | 332 |

List of Figures

| | |
|-------------------|-----|
| Figure 1.1 | 9 |
| Figure 1.2 | 11 |
| Figure 1.3 | 13 |
| Figure 2.1 | 28 |
| Figure 2.2 | 28 |
| Figure 3.1 | 43 |
| Figure 3.2 | 44 |
| Figure 3.3 | 46 |
| Figure 3.4 | 47 |
| Figure 3.5 | 49 |
| Figure 3.6 | 50 |
| Figure 3.7 | 51 |
| Figure 3.8 | 52 |
| Figure 3.9 | 53 |
| Figure 4.1 | 59 |
| Figure 4.2 | 60 |
| Figure 4.3 | 61 |
| Figure 4.4 | 61 |
| Figure 4.5 | 63 |
| Figure 4.6 | 65 |
| Figure 4.7 | 66 |
| Figure 4.8 | 67 |
| Figure 4.9 | 69 |
| Figure 4.10 | 70 |
| Figure 5.1 | 76 |
| Figure 5.2 | 77 |
| Figure 5.3 | 78 |
| Figure 5.4 | 79 |
| Figure 5.5 | 80 |
| Figure 5.6 | 82 |
| Figure 5.7 | 83 |
| Figure 5.8 | 84 |
| Figure 5.9 | 87 |
| Figure 6.1 | 94 |
| Figure 6.2 | 97 |
| Figure 6.3 | 100 |
| Figure 7.1 | 106 |
| Figure 7.2 | 107 |
| Figure 7.3 | 109 |

| | |
|--------------------|-----|
| Figure 7.4 | 111 |
| Figure 7.5 | 113 |
| Figure S2.1 | 139 |
| Figure S2.2 | 142 |
| Figure S2.3 | 151 |
| Figure S2.4 | 153 |
| Figure S2.5 | 154 |
| Figure S2.6 | 154 |
| Figure S2.7 | 156 |
| Figure S2.8 | 159 |
| Figure S2.9 | 159 |
| Figure S2.10 | 160 |
| Figure S2.11 | 160 |
| Figure S2.12 | 161 |
| Figure S2.13 | 161 |
| Figure S2.14 | 162 |
| Figure S2.15 | 162 |
| Figure S2.16 | 163 |
| Figure S2.17 | 163 |
| Figure S2.18 | 164 |
| Figure S2.19 | 165 |
| Figure S2.21 | 165 |
| Figure S2.22 | 166 |
| Figure S3.1 | 171 |
| Figure S3.2 | 179 |
| Figure S3.3 | 181 |
| Figure S3.4 | 186 |
| Figure S3.5 | 187 |
| Figure S3.6 | 189 |
| Figure S3.7 | 191 |
| Figure S3.8 | 192 |
| Figure S3.9 | 193 |
| Figure S3.10 | 194 |
| Figure S3.11 | 194 |
| Figure S3.12 | 195 |
| Figure S3.13 | 196 |
| Figure S3.14 | 197 |
| Figure S3.15 | 197 |
| Figure S4.1 | 233 |
| Figure S4.2 | 235 |
| Figure S4.3 | 235 |
| Figure S4.4 | 237 |

| | |
|-------------------|-----|
| Figure S4.5..... | 237 |
| Figure S4.6..... | 238 |
| Figure S4.7..... | 239 |
| Figure S4.8..... | 240 |
| Figure S4.9..... | 241 |
| Figure S4.10..... | 241 |
| Figure S4.11..... | 242 |
| Figure S4.12..... | 243 |
| Figure S4.13..... | 245 |
| Figure S4.14..... | 245 |
| Figure S4.15..... | 246 |
| Figure S4.16..... | 248 |
| Figure S4.17..... | 249 |
| Figure S4.18..... | 250 |
| Figure S4.19..... | 251 |
| Figure S4.20..... | 251 |
| Figure S4.21..... | 252 |
| Figure S4.22..... | 252 |
| Figure S5.1..... | 268 |
| Figure S5.2..... | 268 |
| Figure S5.3..... | 269 |
| Figure S5.4..... | 269 |
| Figure S5.5..... | 270 |
| Figure S6.1..... | 281 |
| Figure S6.2..... | 282 |
| Figure S6.3..... | 283 |
| Figure S6.4..... | 284 |
| Figure S6.5..... | 285 |
| Figure S6.6..... | 287 |
| Figure S6.7..... | 295 |
| Figure S6.8..... | 296 |
| Figure S6.9..... | 297 |
| Figure S6.10..... | 298 |
| Figure S6.11..... | 298 |
| Figure S6.12..... | 299 |
| Figure S6.13..... | 299 |
| Figure S6.14..... | 300 |
| Figure S6.15..... | 301 |
| Figure S6.16..... | 302 |
| Figure S6.17..... | 303 |
| Figure S6.18..... | 303 |
| Figure S6.19..... | 304 |

| | |
|-------------------|-----|
| Figure S6.20..... | 304 |
| Figure S6.21..... | 305 |
| Figure S6.22..... | 305 |
| Figure S7.1..... | 317 |
| Figure S7.2..... | 318 |
| Figure S7.3..... | 319 |
| Figure S7.4..... | 320 |
| Figure S7.5..... | 321 |
| Figure S7.6..... | 322 |
| Figure S7.7..... | 323 |
| Figure S7.8..... | 324 |
| Figure S7.9..... | 325 |
| Figure S7.10..... | 327 |
| Figure S7.11..... | 328 |
| Figure S7.12..... | 329 |
| Figure S7.13..... | 330 |

List of Schemes

| | |
|------------------|----|
| Scheme 1.1 | 4 |
| Scheme 1.2 | 5 |
| Scheme 1.3 | 6 |
| Scheme 1.4 | 14 |
| Scheme 2.1 | 27 |
| Scheme 2.2 | 31 |
| Scheme 2.3 | 32 |
| Scheme 2.4 | 34 |
| Scheme 2.5 | 35 |
| Scheme 6.1 | 93 |
| Scheme 6.2 | 95 |
| Scheme 6.3 | 96 |
| Scheme 6.4 | 98 |

List of Tables

| | |
|------------------|-----|
| Table 1.1 | 17 |
| Table 5.1 | 86 |
| Table 6.1 | 98 |
| Table 7.1 | 110 |
| Table S2.1 | 151 |
| Table S2.2 | 152 |
| Table S7.1 | 314 |
| Table S7.2 | 318 |
| Table S7.3 | 323 |
| Table S7.4 | 325 |
| Table S7.5 | 326 |
| Table S7.6..... | 328 |
| Table S7.7 | 330 |

◆PART 1◆

Carboalkoxylated polyvalerolactones from malic acid

Chapter 1. Approaches to bioderived monomers and an introduction to ring-opening transesterification polymerization

1.1 Plastics today

Plastics play a vital role in our everyday lives. Due to their low cost, numerous varieties, and endless applications, approximately 300 to 350 million tons of plastic are produced annually worldwide.¹ To put this into perspective, the height of the worldwide annual production of plastic piled in a city block (200 m x 100 m) would be ca. 15 km tall—equivalent to thirty-three John Hancock Towers. Forty to fifty percent of this vast amount of plastic is single-use packaging, which is thrown away, recycled, incinerated, or leached into the environment.²

The compounding effects of non-degradable plastics on our environment are well-documented, and our dependence on crude oil to produce commodity polymers is a growing concern. A broad range of expertise from scientists and engineers are currently being used to produce polymers from sustainable, plant-based feedstocks and also to develop novel ways to recycle or degrade polymers using environmentally friendly conditions.³ However, replacing traditional plastics is a difficult task due to their (i) highly optimized syntheses (over 50 years of research), (ii) inexpensive feedstock (petroleum oil), (iii) excellent materials properties (over 50 years of structure-property characterization), and (iv) preexisting capital infrastructure. With all these challenges, “there is still a great future in sustainable polymers”⁴ and there remains a need to explore novel, biobased monomers and polymers using robust and scalable processes that may one day form our next generation of polymers.

1.2 Approaches to sustainable monomers from biomass

A broad array of chemical targets can be synthesized from biomass. A number of biobased chemicals are already being produced in large quantities for biofuels, and many potential commodity chemicals from biomass have been identified by the United States Department of Energy.⁵ In order to one day be competitive with petroleum-derived monomers, most strategies to convert these potential commodity chemicals into monomers focus on: using as few steps as possible; using high-yielding, scalable, sustainable, and inexpensive reagents (such as acid, base, and/or hydrogen gas); and performing high-yielding transformations. Each of these biobased product monomers are either considered drop-in monomers or novel monomers. The latter group can be split into two additional subcategories: (i) biobased replacements and (ii) novel biobased monomers.

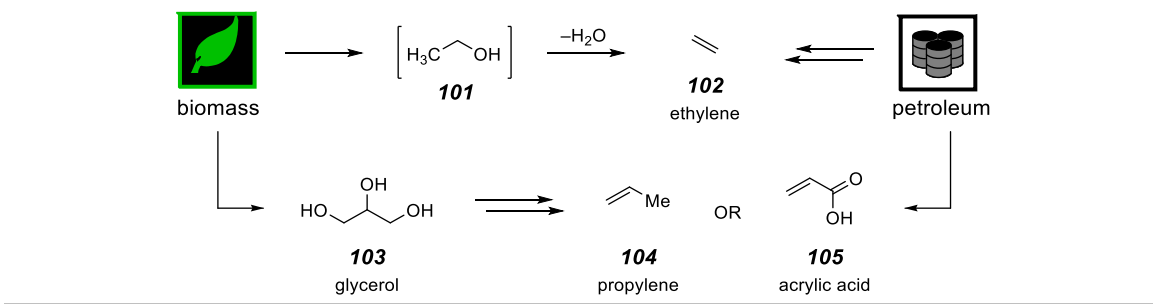
1.2.1 Drop-in monomers

A monomer obtained through a biosynthetic route, when traditionally made from petroleum, is considered a drop-in monomer.⁶ In such cases, the monomers and corresponding polymers are identical to those from petroleum but vary merely in the starting feedstock and synthetic route by which they are obtained. This approach to biobased monomers is very attractive because there is already a market for the product polymer. Additionally, the polymerization of the monomer and the processing of the polymer should be identical to existing technologies (thus they are called “drop-in” replacements).

Ethylene (**102**), the world’s most used monomer, can be obtained through the dehydration of ethanol (**101**) and has already seen considerable investment since bioethanol is produced in large quantities for biofuels (Scheme 1.1).^{7,8} Additionally, biobased propylene (**104**) and acrylic acid (**105**) and have garnered substantial attention since these

3-carbon monomers can be obtained, for example, from glycerol (**103**), a waste product in the production of biodiesel. In these routes, glycerol can be dehydrated and either reduced to propylene⁹ or oxidized to acrylic acid.¹⁰ Other examples include the production of isoprene from itaconic acid using a fermentation/multifunctional cascade synthesis¹¹ and ethylene glycol through oxidation of biobased ethylene.¹²

Scheme 1.1 Examples of drop-in monomers

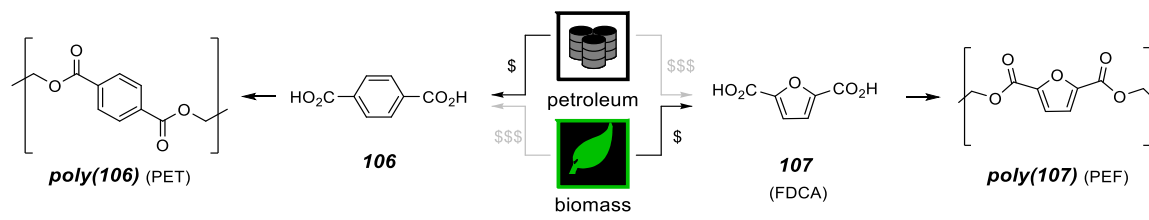


1.2.2 Novel monomers: Biobased replacements

Biobased replacement monomers produce polymers with similar properties to their corresponding counterparts derived from petroleum. However, biobased replacements take advantage of the more oxidized precursors available from biomass compared to petroleum to produce monomers with very similar, yet distinct, chemical functionality. In this case, the monomers are developed and optimized specifically to replace certain preexisting petroleum-based monomers that are difficult or expensive to obtain from biomass. This is an advantageous strategy since the polymerizations and processes of these new monomers and polymers are very similar to those already developed for petroleum-based ones. Additionally, the markets for these polymers are relatively easy to identify. Biobased replacements, however, will still require new optimizations and formulations for each product in which the new polymer is used for.¹³

An example of a biobased replacement is shown in Scheme 1.2. 2,5-Furandicarboxylic acid (FDCA, **107**) is an aromatic diacid that is obtained in one step from hydroxymethylfurfural,¹⁴ a chemical readily available from biomass.^{5,15} This renewable diacid is analogous to terephthalic acid (**106**) but is more easily accessible from biorenewable precursors. These two chemicals are both aromatic diacids that proceed through analogous condensation polymerization to form poly(ethylene furanoate) [PEF, **poly(107)**] and poly(ethylene terephthalate) [PET, **poly(106)**], respectively. PEF and PET behave very similarly in terms of their performance and applications—specifically for single-use bottle packaging.

Scheme 1.2 2,5-Furandicarboxylic acid (**107**) and PEF [**poly(107)**] as biobased replacements for terephthalic acid (**106**) and PET [**poly(106)**]

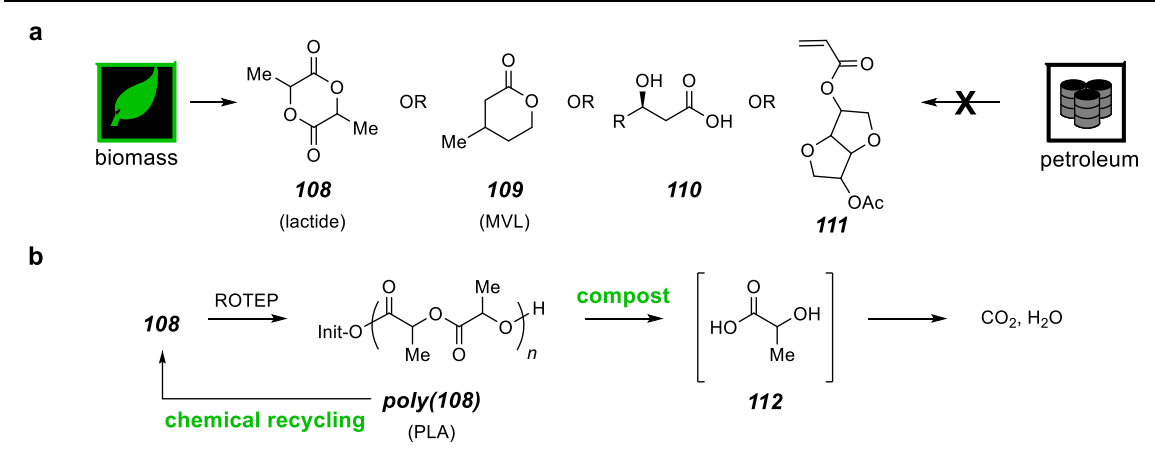


1.2.3 Novel monomers: Novel biobased monomers

Novel biobased monomers are more easily derived from biomass than from petroleum resources. Moreover, these monomers do not have an easily identifiable petroleum-based counterpart. The market and suitable applications for the corresponding polymers therefore must be generated and often can be difficult to identify. In today's market, these novel biobased monomers must produce polymers that have advantageous properties in order to drive companies to invest in developing new formulations for their products. In some cases, the advantageous property may be price (including the ability to use less of this new polymer compared to the traditional polymer), mechanical and thermal polymer performance, or non-traditional avenues for post-consumer processing such as

composting, biodegradability, or chemical recycling (chemical recycling will be further discussed in Section 1.3.5).

Scheme 1.3 (a) Examples of novel biobased monomers and (b) the polymerization and degradation of PLA [**poly(108)**]



It is worth noting that many of these “novel” biobased monomers and polymers have commonly been screened using chemical means from other resources prior to developing biorenewable platforms. For example, a synthesis of lactic acid was reported in 1845,¹⁶ and a US patent was filed in 1955 that converted propylene into lactic acid using nitric acid and nitrogen tetroxide at elevated temperatures.¹⁷ Today lactic acid can be fermented from biomass where it is then converted into lactide (**108**) and subjected to ring-opening transesterification polymerization (ROTEP) to poly(lactic acid) [PLA, **poly(108)**, Scheme 1.3b]. PLA is one of the most successful sustainable polymers and can be chemically recycled (depolymerized) back to **108** or composted into lactic acid (**112**) and mineralized into CO₂ and water.

3-Methylvalerolactone (**109**) and 3-hydroxyalkanoic acids (**110**) are two additional examples of novel biobased monomers (Scheme 1.3a). Methyl-substituted valerolactone **109** can be chemically recycled back to its monomer like PLA but has complementary thermal and mechanical properties.¹⁸ Additionally, polyesters from hydroxyalkanoates **110**

can be synthesized *in vivo* through polycondensation within enzymes and produce non-toxic degradation products.¹⁹ A final, common strategy for novel biobased polymers is to add a polymerizable (methyl)acrylate moiety to a bio-sourced alcohol. For example, isosorbide acrylate **111** produces a polymer with a high glass transition temperature (T_g , 95 °C) and has been incorporated into thermoplastic pressure-sensitive adhesives.²⁰

1.3 Ring-opening transesterification polymerization

To make a plastic, the building block of a polymer (or monomer), is chemically linked together (or polymerized) to make long-chain molecules called polymers. The mechanism by which a monomer can be polymerized is dictated by the monomer's specific chemical functionalities: each chemical functional group requires a specific method(s) to link one monomer to the next. For example, α -olefins such as ethylene and propylene are polymerized using either Ziegler-Natta organometallic catalysts or radical polymerization. Alternatively, lactic acid can be polymerized using condensation polymerization, or it can be cyclized to lactide and be polymerized through ROTEP. The growing demand to replace petroleum-based polymers with bioderived variants has generated increased interest in polyesters due to their hydrolyzable backbone ester linkages. Throughout the majority of this dissertation I utilize ROTEP to produce novel polyesters (Chapters 2–5). Therefore, further discussion will emphasize ROTEP over other polymerization strategies.

The polymerization conditions for ROTEP can have dramatic effects on the product polymer. These effects are controlled by initial reactions conditions. For example, readily available mono- or multifunctional initiators, such as alcohols or amines, are used to make linear or branched polymer architectures, and the molecular weight of each polymer can be controlled by the initial molar ratio of the lactone monomer vs. the initiator. Moreover, both the initial monomer concentration and the temperature for polymerization can have a

significant impact on the overall monomer conversion depending on the free energy of polymerization (ΔG_p°) for the monomer used. In general, higher monomer concentrations and lower temperatures used for polymerization lead to higher equilibrium monomer conversion.²¹

1.3.1 Thermodynamics of ROTEP

ROTEP of lactones is an equilibrium-driven polymerization. The enthalpy of polymerization (ΔH_p°) is closely tied to the ring-strain of each lactone monomer, which is influenced by variations in bond angles and bond lengths in the cyclic structure, eclipsing hydrogen interactions, and steric strain imparted by added substituents (if any). The entropy of polymerization (ΔS_p°) is a balance between: (i) lower entropy due to loss of translational degrees of freedom from a monomer converting into a polymer (this value is similar from monomer to monomer) and (ii) higher entropy from an increase in the number of rotational degrees of freedom gained by the carbon and oxygen atoms as they are no longer restricted in the cyclic lactone conformation. These rotational degrees of freedom gained in polymerization and the ring strain in the monomer are directly related to the ring-size and the substitution on each lactone.²¹⁻²³ Experimentally, ΔH_p° and ΔS_p° are determined by Van't Hoff analysis, which is derived from analyzing the influence of temperature on the equilibrium monomer conversion.

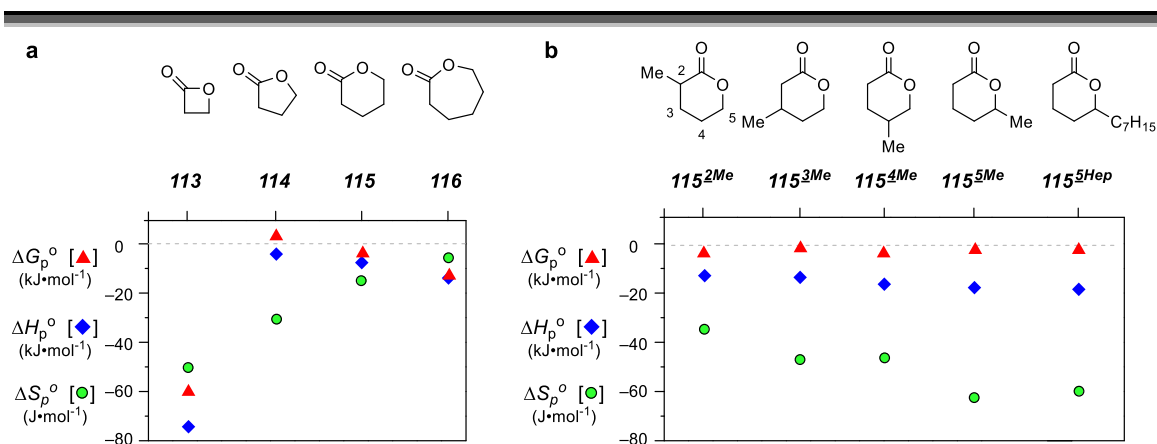


Figure 1.1 Enthalpy and entropy of polymerization for (a) unsubstituted lactones and (b) selected alkyl-substituted valerolactones. * ΔH_p° and ΔS_p° values were taken from Table 1 in Schneiderman and Hillmyer, and ΔG_p° were calculated using these values at 25 °C.²⁴ Lactones **113**, **115**^{2Me} to **115**^{5Hep} were polymerized neat and lactones **114–116** were polymerized in solution (1M). Although these phase differences can account for changes in the ΔS_p° ,²³ the overall trends in ΔG_p° , ΔH_p° and ΔS_p° are well-reflected nonetheless.

In the family of unsubstituted lactones, propiolactone (or β -lactone, **113**) featuring a four-atom ring size, and caprolactone (or ϵ -caprolactone, **116**) containing a seven-atom ring size, each polymerize to nearly untraceable levels of remaining monomer. However, these two polymerizations differ in thermodynamic driving forces (see Figure 1.1a). Propiolactone **113** has a large free energy of polymerization (ΔG_p°) due to its high enthalpic ring strain even though the polymerization is the most entropically disfavored (since there are only a few conformational degrees of freedom gained in polymerization).²⁵ Conversely, caprolactone **116** is not nearly as ring-strained as propiolactone **113** but is driven entropically by larger contributions from the many conformational/rotational degrees of freedom gained upon polymerization.²⁶ The six-atom ring valerolactone (δ -valerolactone, **115**), which has a small but negative ΔG_p° , can be polymerized to high conversions under many conditions (>99% conversion, solvent free, ambient temperature) because it has both intermediate ring strain and intermediate gain in rotational degrees of freedom. Finally, the

five-atom ring butyrolactone (γ -butyrolactone, **114**) has only recently been polymerized²⁷ and does not polymerize under standard ROTEP conditions because of its positive ΔG_p° . Butyrolactone **114** is considered strain-free²⁸ and is not significantly entropically favored for polymerization.

Added alkyl or functional group substitution on a lactone ring can also play a significant role in a monomer's ability to polymerize. For example, substituents can inhibit the equilibrium monomer conversion of a caprolactone monomer, which normally polymerizes efficiently.^{29,30} Conversely, additional substitution can make the ΔG_p° of butyrolactones convert from being unfavorable to favorable.^{28,31} Subtle substituent effects are more intricate for valerolactones compared to other ring sizes because its ΔG_p° is only slightly favored ($\Delta G_p^\circ = \text{ca. } -4 \text{ kJ}\cdot\text{mol}^{-1}$) toward polymerization. As shown in Figure 1.1b, the addition of a methyl (**115^{2Me}** through **115^{5Me}**) [where **115^{#Me}** represents a valerolactone ring (**115**) with a methyl (**Me**) substituted at the **#** position] or heptyl group (**115^{5Hep}**) to a valerolactone can change the ΔH_p° from $-8 \text{ kJ}\cdot\text{mol}^{-1}$ for unsubstituted valerolactone **115** to $-19 \text{ kJ}\cdot\text{mol}^{-1}$ for **115^{5Me}** by increasing the associated ring strain. Alternatively, these substituents penalize the overall ΔG_p° by decreasing the ΔS_p° . The effects of having substitution at the 3- and 4- positions (as in **115^{3Me}** and **115^{4Me}**) are very subtle (Figure 1.1b), and yet **115^{3Me}** will polymerize to 91% equilibrium monomer conversion while **115^{4Me}** will polymerize to 98% equilibrium monomer conversion (neat, room temperature). Furthermore, the length of the alkyl group (as shown in **115^{5Me}** and **115^{5Hep}**) has little effect on the ΔG_p° and equilibrium monomer conversion.²⁴ From an economic standpoint, minor changes in ΔG_p° lead to slight differences in monomer conversion, but these differences will increase processing costs for polymers. These studies suggest that **115^{4Me}** is the most attractive monomer in this valerolactone series in terms of ΔG_p° .

1.3.2 Thermal properties and kinetic considerations for substituted lactones

Poly(valerolactone) and poly(caprolactone) are both semicrystalline polymers with low T_g s around $-60\text{ }^\circ\text{C}$ and melting temperatures (T_m s) around $60\text{ }^\circ\text{C}$.³² One methyl (or alkyl) group added at any position in the valerolactone ring (e.g., **115**^{2Me}–**115**^{5Me}, Figure 1.2a) completely inhibits the formation of crystal domains and instead produces completely amorphous polyesters with T_g s similar to valerolactone ($-50\text{ }^\circ\text{C}$).²⁴ This loss of crystallinity has also been reported for polycaprolactones with a methyl (polymerized from **116**^{4Me} and **116**^{6Me}, Figure 1.2b)^{33,34} or isopropyl³⁵ group (substituted at the 4-position, not shown).

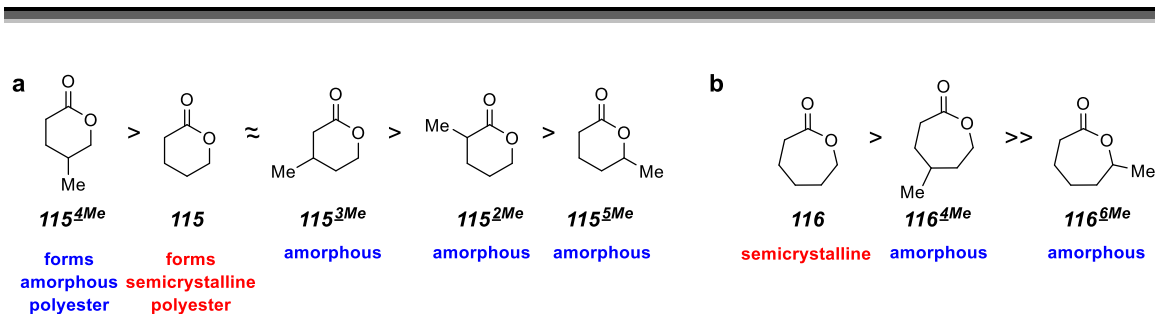


Figure 1.2 Relative rates of polymerization and general polymer thermal properties for (a) methyl-substituted valerolactones using diphenyl phosphate as a catalyst without solvent (neat)²⁴ and (b) alkyl-substituted caprolactones using an aluminum salen catalyst in toluene.³⁶

The relative rates of polymerization for valerolactone (**115**) and each methyl-substituted valerolactone (**115**^{#Me}) are shown in Figure 1.2a. Lactone **115**^{4Me} is the fastest to polymerize followed by **115**, **115**^{3Me}, **115**^{2Me}, and finally **115**^{5Me}. Likewise, the rates of polymerization for caprolactones **116**, **116**^{4Me}, and **116**^{6Me} showed that unsubstituted caprolactone **116** polymerizes fastest followed by 4-methylcaprolactone (**116**^{4Me}), with 6-methylcaprolactone (**116**^{6Me}) polymerizing significantly slower than the other two monomers (Figure 1.2b).

These reports demonstrate that lactones with a methyl (or alkyl) group on the carbon bearing the cyclic ester oxygen polymerize the slowest due to the secondary (rather than primary) propagating alcohol that is formed during propagation. Additionally, the rate of polymerization for a lactone containing a methyl (or alkyl) group at the 2-position is reduced as a consequence of the added steric crowding around the carbonyl. Finally, methyl substitution not directly adjacent to the lactone can either polymerize faster [for 4-methylvalerolactone (**115**^{4Me})] or slower [3-methylvalerolactone (**115**^{3Me}) or 4-methylcaprolactone (**116**^{4Me})] than its unsubstituted parent lactone.

1.3.3 Chemical recycling of polylactones

Currently the “lifecycle” of a polymer is rarely cyclic (Figure 1.3). A starting material is derived either from petroleum or bio-based sources, converted into a monomer, then a polymer, and finally a commercial product. The nature of the product allows for it to potentially be collected and mechanically recycled. Yet, only about 2% of single-use plastic packaging is recycled in a closed-loop fashion (i.e., recycled into products with equal value to the recycled material)² due to variations regarding purity and molecular weight of the recycled material. Ultimately the remaining polymer products are either placed into landfill, leached into the environment, or incinerated for energy.³⁷

Converting a polymer back into its respective monomer after use would be one way to close this lifecycle. This general strategy of chemical recycling—chemical degradation of a macromolecule into valuable fragments—is appealing since the recovered monomer could be repolymerized to produce a polymer with the desired molecular weight, composition, and architecture.³⁸ This process would bring added value to a polymer after consumer use and could decrease dependence on monomer feedstocks. This concept has already been adopted by the BASF chemical company.³⁹

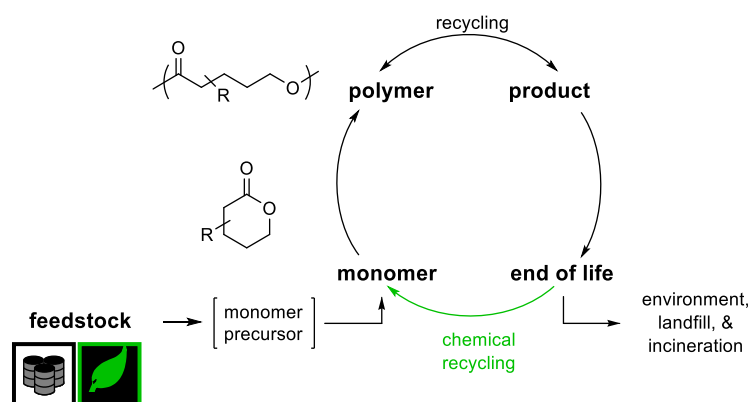
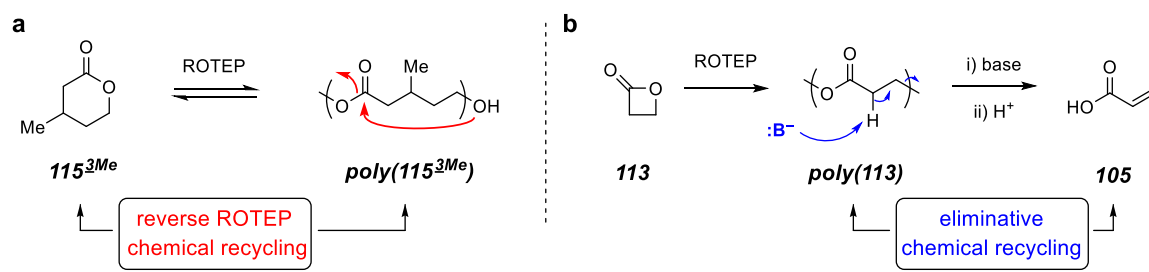


Figure 1.3 Lifecycle of a polymer

Polyesters derived from lactones are attractive from a chemical recycling perspective. The polymerization of lactones (sometimes) proceed to lower-than-ideal equilibrium monomer conversions. This is especially problematic on a processing-scale when costs of the monomer itself and the process for removing the unreacted monomer is necessary. Yet since this equilibrium for lactones is accessible even at room temperature, polyesters derived from lactones can be chemically recycled back to their precursor monomer using relatively mild conditions. As shown in Scheme 1.4a, **115^{3Me}** can be polymerized to **poly(115^{3Me})** using ROTEP. **Poly(115^{3Me})** can also be degraded back to lactone **115^{3Me}** by way of reverse-ROTEP. Commonly, these reverse-ROTEP conditions utilize a catalyst (e.g. tin octanoate), elevated temperatures (ca. 150 °C), and vacuum to reestablish the monomer-polymer equilibrium while distillatively removing the monomer as it is generated. The recycled **115^{3Me}** can be polymerized again to **poly(115^{3Me})** with a desired polymer architecture and molecular weight. To the extent that this process is efficient enough, chemically recyclable monomers can, in theory, be infinitely recycled.⁴⁰

Scheme 1.4 Polymerization and chemical recycling of (a) **poly(115^{3Me})** via reverse ROTEP and (b) **poly(113)** to acrylic acid (**105**) via elimination



Polyesters (and polyvalerolactones in general) can also be strategically degraded to other chemicals in a complementary manner (as shown in Scheme 1.4b). Propiolactone **113** can be polymerized to **poly(113)**. It is unfavorable for **poly(113)** to undergo reverse ROTEP due to **113**'s high ring strain (see Section 1.3.1), but **poly(113)** can be thermally or chemically degraded to acrylic acid.⁴¹ This eliminative-type degradation has also recently been performed on PLA to produce acrylic acid (not shown).⁴²

1.3.4 Remaining needs for chemically recyclable polyesters

Today, a number of limitations still remain for advancing renewable polymers, which does not even include the largest limitations of polymer price and cost to research new formulations. For instance, the most-used biorenewable polymer, PLA, is already being used to make compostable, single-use cups and silverware; however, this polymer has a relatively low glass transition temperature (ca. 50–60 °C) and low melt strength.⁴³ The low glass transition temperature limits the potential of PLA to be used in applications where higher temperatures are necessary (e.g., single-use coffee cups), and the limited melt strength of PLA hinders its applicability for plastic bag packaging (although considerable work has been devoted on solutions to this problem, such as long-chain branched PLA).⁴⁴ A similar limitation of currently sustainable lactones is that there are relatively few chemically recyclable polymers that have thermal transitions well-outside of a user's

reachable temperatures. In other words, these polymers are not thermally stable over a temperature range that is required for hot beverages as well as cold Minnesota winters. As such, there remains a need to explore novel chemically recyclable monomers, polymers, and materials with complementary properties to those currently available.

The installation of new functionality onto the sidechain of reactive monomers has been shown to drastically affect a polymer's thermal transitions and mechanical properties. For example, changing the sidechain substituent from a methyl (e.g., polypropylene) to a carboxyl group [e.g. poly(acrylic acid)] directly alters the polymer properties and, therefore, the application of each polymer. Additionally, the increased oxidation state of reagents provided by biomass compared to petroleum oil creates an opportunity to utilize this over-oxidation to produce *traditional monomers with non-traditional sidechain functionality*. To this end, I have developed syntheses to carboalkoxylated lactone monomers from biorenewable feedstocks (Part 1). To date, there have been relatively few examples of polylactones that (i) have substituents more complex than alkyl groups, (ii) can be readily accessible from biomass, and (iii) have controllable polymer molecular weights (see Table 1.1). In Part 2, I will discuss a fortuitous route to produce isoprenecarboxylic acid, and the impacts that this carboxyl group imparts on the polymerizability of this monomer and the material properties of its corresponding polymer.

1.4 Thesis Overview

With the goal of installing novel functionality onto monomers derived from biomass, I will discuss the synthesis and properties of two novel monomer systems each containing a carboxy substituent. Part 1 will focus on carboalkoxylated polylactones and the repercussions of installing a pendant side chain ester onto a cyclic ester monomer. More specifically, in Chapter 2 I will discuss the synthesis, polymerization, and divergent

chemical recycling of the novel monomer 4-carbomethoxyvalerolactone (CMVL) into linear poly(4-carbomethoxyvalerolactone) (polyCMVL) using an acid catalyst. Next, I will demonstrate that the linear polyCMVL is merely a metastable state and can isomerize to a hyperbranched polymer using a more highly active zinc catalyst (Chapter 3, in collaboration with Dr. Daniel Stasiw and Professor William Tolman). Having understood the chemical reactivity of CMVL, I will detail the influence of other alkoxy substituents on this 4-carboalkoxyvalerolactone scaffold to explore the corresponding polymers' thermal and mechanical properties (Chapter 4). In Chapter 5, I will discuss some preliminary findings on the effects of carboalkoxy positioning on lactones as well as a basic model to predict whether a carboalkoxylated lactone will polymerize to a linear polymer, a branched polymer, or isomerize into a non-polymerizable lactone.

Part 2 of this thesis will discuss my work on isoprenecarboxylic acid. Namely, Chapter 6 will discuss the fundamental radical polymerizability of isoprenecarboxylic acid, its ester derivatives, and its amide derivatives. Finally, Chapter 7 will demonstrate how isoprenecarboxylic acid can be used felicitously toward superabsorbent hydrogels.

1.5 Previously reported carboalkoxylated lactones

Table 1.1 Reported carboalkoxylated polyesters ^{a-i} See Ref.45^{a-i}

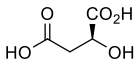
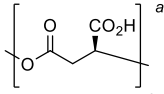
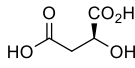
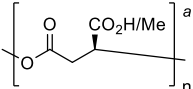
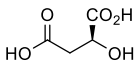
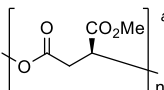
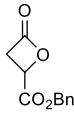
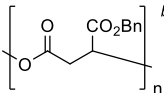
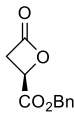
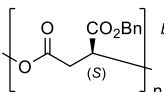
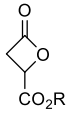
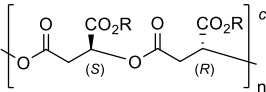
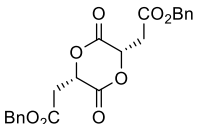
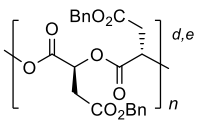
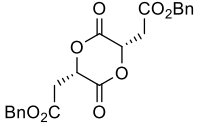
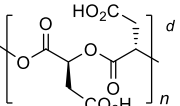
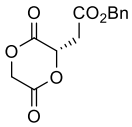
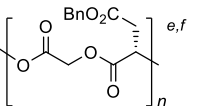
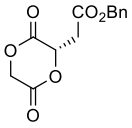
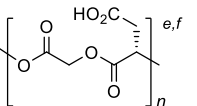
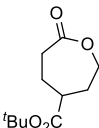
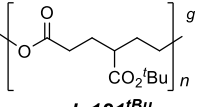
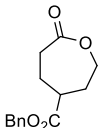
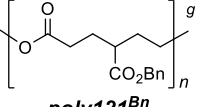
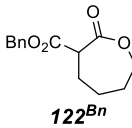
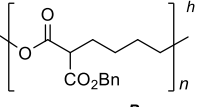
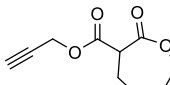
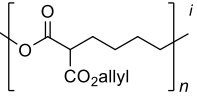
| Monomer | Polymer | T_g (°C) | T_m (°C) | ΔH_m (J·g ⁻¹) | Notes | |
|--|--|------------------------|--------------------|--------------------------------------|--|--|
|  <p>117</p> |  <p>poly117^H poly(β,L-malic acid)</p> | 110 | 216 | 42 | polymerized via microbes <i>P. polycephalum</i> | |
|  <p>117</p> |  <p>poly(117^{H/Me}) poly(β,L-malic acid) statistically methylated</p> | 20 47 75 | N.A. N.A. 45 | % Me 174 172 171 | 42 58 41 | polymerized via microbes followed by methylation with diazomethane |
|  <p>117</p> |  <p>poly(117^{Me}) poly(methyl β,L-malate)</p> | 41 | 148 | 42 | polymerized via microbes followed by methylation with diazomethane | |
|  <p>118^{Bn}</p> |  <p>a-poly(118^{Bn}) atactic poly(benzyl β-malate)</p> | "amorphous polyesters" | | | – | |
|  <p>118^{Bn}</p> |  <p>iso-poly(118^{Bn}) isotactic poly(benzyl β-malate)</p> | N.A. | 165–185 | N.A. | – | |
|  <p>118^R</p> |  <p>s-poly(118^R) syndiotactic poly(alkyl β-malate)</p> | R Me allyl Bn | 40 12 30–35 | 137–151 112 111–117 | 101 N.A. N.A. | polymerized from racemic lactones |
|  <p>119^{Bn}</p> |  <p>poly(119^{Bn}) poly(benzyl α,L-malide)</p> | N.A. | | | little polymerization or no polymerization reported. Can be copolymerized with lactide | |

Table 1.1 (continued) Reported carboalkoxylated polyesters ^{a-i} See Ref. 45^{a-i}

| Monomer | Polymer | T_g (°C) | T_m (°C) | ΔH_m (J•g ⁻¹) | Notes |
|--|--|---------------|---------------|--------------------------------------|--|
|  <p>119^{Bn}</p> |  <p>poly(119^H) poly(α,L-malic acid)</p> | N.A. | | | Little polymerization or no polymerization reported. Synthesized by hydrogenolysis of a benzyl ester on every repeat unit after polymerization |
|  <p>120^{Bn}</p> |  <p>poly120^{Bn} poly(glycolide-co-α,L-malic acid)</p> | N.A. | | | polymerizes with controllable molecular weights |
|  <p>120^{Bn}</p> |  <p>poly120^H poly(glycolide-co-benzyl α,L-malate)</p> | N.A. | | | benzyl groups removed post-polymerization using hydrogenation |
|  <p>121^{tBu}</p> |  <p>poly121^{tBu} poly(4-carbo^tbutoxycaprolactone)</p> | N.A. | | | lower molar mass than targeted. M_n reported ca. 1400 g•mol ⁻¹ . Could be copolymerized with caprolactone |
|  <p>121^{Bn}</p> |  <p>poly121^{Bn} poly(4-carbobenzyloxycaprolactone)</p> | N.A. | | | lower molar mass than targeted. M_n reported ca. 2000 g•mol ⁻¹ . Could be copolymerized with caprolactone |
|  <p>122^{Bn}</p> |  <p>poly122^{Bn} poly(2-carbobenzyloxycaprolactone)</p> | N.A. | | | block copolymers were synthesized using PEG-OH as an initiator. ¹ H NMR spectra show broad resonances. |
|  <p>123</p> |  <p>poly123 poly(2-carboallyloxycaprolactone)</p> | N.A. | | | block copolymers were synthesized using PEG-OH as an initiator |

1.6 References

- ¹ Jambeck, J. R.; Geyer, R.; Wilcox, C.; Siegler, T. R.; Perryman, M.; Andrady, A.; Narayan, R.; Law, K. L. Plastic Waste Inputs from Land into the Ocean. *Science* **2015**, *347*, 768–771.
- ² World Economic Forum; Ellen MacArthur Foundation; McKinsey and Company. The New Plastics Economy Rethinking the Future of Plastics. <http://www.ellenmacarthurfoundation.org/publications>, 2016.
- ³ Zhang, X.; Fevre, M.; Jones, G. O.; Waymouth, R. M. Catalysis as an enabling science for sustainable polymers. *Chem. Rev.* **2017**, *118*, 839–885.
- ⁴ Schneiderman, D. K.; Hillmyer, M. A. *50th anniversary perspective*: There is a great future in sustainable polymers. *Macromolecules* **2017**, *50*, 3733–3749.
- ⁵ Werpy, T.; Petersen, G. Top Value Added Chemicals From Biomass Volume I: Results of Screening for Potential Candidates; U.S. Department of Energy: Oak Ridge, TN, **2004**.
- ⁶ Sara, M., Brar, S. K.; Blais, J. F. Production of drop-in and novel bio-based platform chemicals in *Platform Chemical Biorefinery*. Elsevier, **2016**, ch. 14. pp 249–283.
- ⁷ (a) Nordqvist Melander, A.; Qvint, K. Assessing the sustainability of first generation ethanol for bioethylene production. Chalmers University of Technology Report no. 2016:6. (b) Broeren, M. *Production of Bio-ethylene*, Technology brief, International Renewable Energy Agency (IRENA), Abu Dhabi, **2013**. (c) Mahsenzadeh, A.; Zamani, A.; Taherzadeh, M. J. Bioethylene production from ethanol: A review and techno-economical evaluation. *ChemBioEng Rev.* **2017**, *4*, 75–91.
- ⁸ In 2007, Dow announced the construction of an ethylene plant in Brazil, which converted sugar cane into ethanol and further dehydrated ethanol to ethylene (Tullo, A. H. Dow to make polyethylene from sugar in Brazil. *C&EN.* **2007**, *30*, 17.). At the time of this announcement, petroleum prices were increasing and, following the decline of the price of petroleum and a slowing economy, Dow delayed the project. (Tullo, A. H. Dow will delay biopolymers plant. *C&EN.* **2012**, *90*, 22.). Today, the company Braskem sells biobased polyethylene.
- ⁹ Yu, L.; Yuan, J.; Zhang, Q.; Li, Y.-M.; He, H.-Y.; Fan, K.-N.; Cao, Y. Propylene from renewable resources: Catalytic conversion of glycerol into propylene. *ChemSusChem* **2014**, *7*, 743–747.
- ¹⁰ A recent review: Sun, D.; Yamada, Y.; Sato, S.; Ueda, W. Glycerol as a potential renewable raw material for acrylic acid production. *Green. Chem.* **2017**, *19*, 3186–3213.
- ¹¹ Abdelraham, O. A.; Park, D. S.; Vinter, K. P.; Spangers, C. S.; Ren, L.; Cho, H. J.; Zhang, K.; Fan, W.; Tsapatsis, M.; Dauenhauer. Renewable isoprene of sequential

-
- hydrogenation of itaconic acid and dehydra-decyclization of 3-methyl-tetrahydrofuran. *ACS Catal.* **2017**, *7*, 1428–1431.
- ¹² Tulio, A. H. Coke plays spin the bottle. *C&EN.* **2012**, *90*, 19–20
- ¹³ Bomgardner, M. M. Building a better plastic bottle. *C&EN.* **2017**, *95*, 17–19.
- ¹⁴ A few recent examples: (a) Kim, M.; Su, Y.; Fukuoka, A.; Hensen, E. J. M.; Nakajima, K. Aerobic oxidation of 5-(hydroxymethyl)furfural cyclic acetal enables selective furan-2,5-dicarboxylic acid formation with CeO₂-supported gold catalyst. *Angew. Chem. Int. Ed.* **2018**, *57*, 8235–8239. (b) Barwe, S.; Weinder, J.; Cychy, S.; Morales, D. M.; Dieckhöfer, S.; Hiltrop, D.; Masa, J.; Muhler, M.; Schuhmann. Electrocatalytic oxidation of 5-(hydroxymethyl)furfural using high-surface-area nickel boride. *Angew. Chem. Int. Ed.* **2018**, *57*, 11460–11464. (c) Xia, H.; Xu, S.; Hu, H.; An, J.; Li, C.; Efficient conversion of 5-hydroxymethylfurfural to high-value chemicals by chemo- and bio-catalysis. *RSC Advances* **2018**, *54*, 30875–30886.
- ¹⁵ Yu, I. K. M.; Tsang, D. C. W. Conversion of biomass to hydroxymethylfurfural: A review of catalytic systems and underlying mechanisms. *Bioresour. Technol.* **2017**, *238*, 716–732.
- ¹⁶ At the time of publication of this thesis, the first reported lactic acid synthesis using the search engines Reaxys and SciFinder was: Pelouze, J. Ueber die Milchsäure. *Liebigs Ann.* **1845**, *53*, 112–124
- ¹⁷ Robertson, N. C.; Schoenbrunn, E. F. US Patent 2847464A, December 5, 1955.
- ¹⁸ Xiong, M.; Schneiderman, D. K.; Bates, F. S.; Hillmyer, M. A.; Zhang, K. *Proc. Natl. Acad. Sci. U. S. A.* **2014**, *111*, 8357–8362.
- ¹⁹ Koller, M. Biodegradable and biocompatible polyhydroxy-alkanoates (PHA): Auspicious microbial macromolecules from pharmaceutical and therapeutic applications. *Molecules* **2018**, *23*, 362.
- ²⁰ Gallagher, J. M.; Hillmyer, M. A.; Reineke, T. M. Acrylic triblock copolymers incorporating isosorbide for pressure sensitive adhesives. *ACS Sustainable Chem. Eng.* **2016**, *4*, 3379–3387.
- ²¹ Duda, A.; Kowalski, A. Thermodynamics and kinetics of ring-opening polymerization. In *Handbook of ring-opening polymerization*; Dubois, P., Coulembier, O., Raquez, J.-M., Eds.; Wiley-VCH Verlag GmbH & Co. KGaA: Weinheim, 2009; pp 1–51.
- ²² Sawada, H. Thermodynamics of polymerization. II. Thermodynamics of ring-opening polymerization. *J. Macromol. Sci.-Revs. Macromol. Chem.* **1970**, *C5*, 151–174.
- ²³ Olsén, P.; Odelius, K.; Albertsson, A.-C. Thermodynamic presynthetic considerations for ring-opening polymerization. *Biomacromolecules* **2016**, *17*, 699–709.
- ²⁴ Schneiderman, D. K.; Hillmyer, M. A. Aliphatic polyester block polymer design. *Macromolecules* **2016**, *49*, 2419–2428.

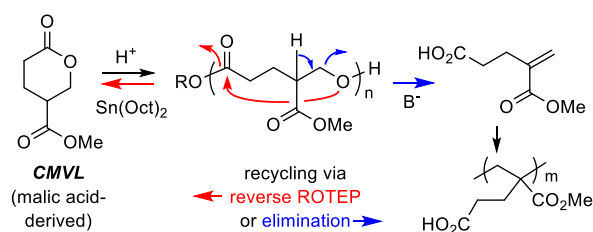
-
- ²⁵ Yevstropov, A. A.; Lebedev, B. V.; Kulagina, T. G.; Lyudvig, Ye. B.; Belenkaya, B. G. The thermodynamic properties of β -propiolactone, its polymer, and its polymerization in the 0–400 K range. *Polym. Sci. U.S.S.R.* **1979**, *21*, 2249–2256.
- ²⁶ Save, M.; Schappacher, M.; Soum, A. Controlled ring-opening polymerization of lactones and lactides initiated by lanthanum isopropoxide, 1. General aspects and kinetics. *Macromol. Chem. Phys.* **2002**, *203*, 889–899.
- ²⁷ Hon, M.; Chen, E. Y.-X. Completely recyclable biopolymers with linear and cyclic topologies via ring-opening polymerization of γ -butyrolactone. *Nat. Chem.* **2016**, *8*, 42–49.
- ²⁸ Zhu, J.-B.; Watson, E. M.; Tang, J.; Chen, E. Y.-X. A synthetic polymer system with repeatable chemical recyclability. *Science* **2018**, *360*, 398–403.
- ²⁹ MacDonald, J. P.; Shaver, M. P. An aromatic/aliphatic polyester prepared via ring-opening polymerization and its remarkably selective and cyclable depolymerization to monomer. *Polym. Chem.* **2016**, *7*, 553–559.
- ³⁰ Zhang, D.; Hillmyer, M. A.; Tolman, W. B. Catalytic polymerization of a cyclic ester derived from a “cool” natural precursor. *Biomacromolecules* **2005**, *6*, 2091–2095.
- ³¹ Haba, O.; Itabashi, H. Ring-opening polymerization of a five-membered lactone *trans*-fused to a cyclohexane ring. *Polym. J.* **2014**, *46*, 89–93.
- ³² Aubin, M.; Prud'homme, R. E. Preparation and properties of poly(valerolactone). *Polymer* **1981**, *22*, 1223–1226.
- ³³ Watts, A.; Kurokawa, N.; Hillmyer, M. A. Strong, resilient, and sustainable aliphatic polyester thermoplastic elastomers. *Biomacromolecules* **2017**, *18*, 1845–1854.
- ³⁴ Seefried Jr., C. G.; Koleske, J. V. Lactone polymers. VI. Glass-transition temperatures of methyl-substituted ϵ -caprolactones and polymer blends. *J. Polym. Sci., Part B: Polym. Phys.* **1975**, *13*, 851–856.
- ³⁵ Quilter, H. C.; Hutchby, M.; Davidson, M. G.; Jones, M. D.; Polymerisation of a terpene-derived lactone: A bio-based alternative to ϵ -caprolactone. *Polym. Chem.* **2016**, *8*, 833–837.
- ³⁶ Ten Breteler, M. R.; Zhong, Z.; Dijkstra, P. J.; Palmans, A. R. A.; Peeters, J.; Feijen, J. Ring-opening polymerization of substituted ϵ -caprolactones with a chiral (salen) AlO_iPr Complex. *J. Polym. Sci. A* **2007**, *45*, 429–436.
- ³⁷ Hopewell, J.; Dvorak, R.; Kosior, E. Plastics recycling: Challenges and opportunities. *Philos. Trans. R. Soc., B* **2009**, *364*, 2115–2126.
- ³⁸ For a recent review see: Hong, M.; Chen, E. Y.-X. Chemically Recyclable Polymers: A Circular Economy Approach to Sustainability. *Green Chem.* **2017**, *19*, 3692–3706.

-
- ³⁹ For example, BASF's "ChemCycling." Chemical recycling of plastic waste. <https://www.basf.com/global/en/who-we-are/sustainability/management-and-instruments/circular-economy/chemcycling.html>. Accessed January 2019.
- ⁴⁰ Tan, X.; Chen, E. Y.-X. Toward infinitely recyclable plastics from renewable cyclic esters. *Chem* **2018**, DOI: 10.1016/j.chempr.2018.10.011.
- ⁴¹ Mahoney, J. E. Acrylic acid production methods. International Patent WO 2013/126375 A1, 2013.
- ⁴² Terrade, F. G.; van Krieken, J.; Verkuijl, B. J. V.; Bouwman, E. Catalytic cracking of lactide and poly(lactic acid) to acrylic acid at low temperatures. *ChemSusChem* **2017**, *10*, 1904–1908.
- ⁴³ Nagarajan, V.; Mohanty, A. K.; Misra, M. Perspective on polylactic acid (PLA) based sustainable materials for durable applications: Focus on toughness and heat resistance. *ACS Sustainable Chem. Eng.* **2016**, *4*, 2899–2916.
- ⁴⁴ Gu, L.; Xu, Y.; Fahnhorst, G. W.; Macosko, C. W. Star vs long chain branching of poly(lactic acid) with multifunctional aziridine. *J. Rheol.* **2017**, *61*, 785–796.
- ⁴⁵ (a) Portilla-Arias, J. A.; García-Alvarez, M.; Martínez de Ilarduya, A.; Holler, E.; Galbis, J. A.; Muñoz-Guerra, S. Synthesis, degradability, and drug releasing properties of methyl esters of fungal poly(β ,L-malic acid). *Macromol. Biosci.* **2008**, *8*, 540–550. (b) Lenz, R. W.; Guerin, P. Functional polyesters and polyamides for medical applications of biodegradable polymers. In *Polymers in medicine. Biomedical and pharmacological applications*; Chiellini, E.; Giusti, P., Ed.; Springer: Boston, 1983; Vol. 23, pp 219–231. (c) Jaffredo, C. G.; Chapurina, Y.; Kirillov, E.; Carpentier, J.-F.; Guillaume, S. M.; Highly stereocontrolled ring-opening polymerization of racemic alkyl β -malolactonates mediated by yttrium [amino-alkoxybis(phenolate)] complexes. *Chem. Eur. J.* **2016**, *22*, 7629–7641. (d) Ouchi, T.; Fujino, A. Synthesis of poly(α -malic acid) and its hydrolysis behavior *in vivo*. *Makromol. Chem.* **1989**, *190*, I523–I530 (e) Pounder, R. J.; Dove, A. P. Synthesis and organocatalytic ring-opening polymerization of cyclic esters derived from L-malic acid. *Biomacromolecules* **2010**, *11*, 1930–1939. (f) Taguchi, K.; Yano, S.; Hiratani, K.; Minoura, N.; Okahata, Y.; Ring-opening polymerization of 3(S)-[(benzyloxycarbonyl)methyl]-1,4-dioxane-2,5-dione: A new route to a poly(α -hydroxy acid) with pendant carboxyl groups. *Macromolecules* **1988**, *21*, 3338–3340. (g) Trollsas, M.; Lee, Y. V.; Mecerreyes, D.; Löwenhielm, P.; Möller, M.; Miller, R. D.; Hedrick, J. L. Hydrophilic aliphatic polyesters: Design, synthesis, and ring-opening polymerization of functional cyclic esters. *Macromolecules* **2000**, *33*, 4619–4627. (h) Mahmud, A.; Xiong, X.-B.; Lavasanifar, A. Novel self-associating poly(ethylene oxide)-block-poly(ϵ -caprolactone) block copolymers with functional side groups on the polyester block for drug delivery. *Macromolecules* **2006**, *39*, 9419–9428. (i) Garg, S. M.; Xiong, X.-B.; Lu, C.; Lavasanifar, A. Application of click chemistry in the preparation of

poly(ethylene oxide)-block-poly(ϵ -caprolactone) with hydrolyzable cross-links in the micellar core. *Macromolecules* **2011**, *44*, 2058–2066.

Chapter 2. A carbomethoxylated polyvalerolactone from malic acid:

Synthesis and divergent chemical recycling*



Summary: In this chapter, we report the synthesis of a novel substituted polyvalerolactone from the renewable monomer, 4-carbomethoxyvalerolactone (**CMVL**, two steps from malic acid). We show that the polymerization of **CMVL** proceeds to high equilibrium monomer conversion to give the semicrystalline carbomethoxylated polyester with low dispersity. The material displays a glass transition temperature of $-18\text{ }^\circ\text{C}$ and two melting temperatures at 68 and $86\text{ }^\circ\text{C}$. This polymer can be chemically recycled by either of two independent pathways. The first (red, to the left) cleanly returns **CMVL** by a backbiting depolymerization from the hydroxy terminus; the second (blue, to the right) uses base to cleave the polyester in a retro-oxa-Michael fashion. This affords a methacrylate-like monomer that we have polymerized radically to a new polymethacrylate analogue. This is a rare example of a polymer that has been shown to have two independent chemical recycling pathways leading to two different classes of monomers.

* Reproduced in part with permission from Fahnhorst G. W.; Hoye, T. R. *ACS Macro Lett.* **2018**, 7, 143–147. Copyright 2018 American Chemical Society

2.1 Introduction

The multi-billion-dollar plastics industry produces around 300 million tons of plastic annually.¹ However, only a small portion is recycled,² and the performance and properties of new materials derived from previously used polymers is virtually always an important issue.³ Biodegradable and compostable polymers like poly(lactic acid) (PLA) are incorporated into products to help address issues of sustainability and degradation. Yet, biodegradable and compostable polymers sometimes require burdensome degradation conditions.⁴ Moreover, one can question the value of biodegrading polymers to invisible chemicals (i.e., small molecules or oligomers) vs. coping with the environmental consequences of more macroscopic, solid plastic debris itself.⁵

More recently, some research has been focused on utilizing chemically recyclable polymers (CRPs),⁶ defined as macromolecules that can be chemically degraded to valuable molecular fragments, most typically back to the monomer from which the polymer was derived. These can then be re-polymerized in the same manner as the initial, virgin-quality monomers. CRPs most commonly include polyesters and polyamides, derived from ring-opening polymerization (ROP) of lactones^{6,7} and lactams,⁸ and polycarbonates from epoxide/CO₂ copolymerizations.⁹

The synthesis of CRPs from renewable feedstocks and useful properties is attractive. Malic acid (**201**), known as a “top value-added chemical,”¹⁰ is a promising renewable and scalable feedstock. Synthesized microbially from biomass as an intermediate in the Krebs cycle, it is abundantly available.¹¹

Here we report the synthesis of 4-carbomethoxyvalerolactone (**204** ≡ **CMVL**) from malic acid (Scheme 2.1) and its ring-opening transesterification polymerization (ROTEP) to produce the new polyester, poly(4-carbomethoxyvalerolactone) [**poly(204)**],

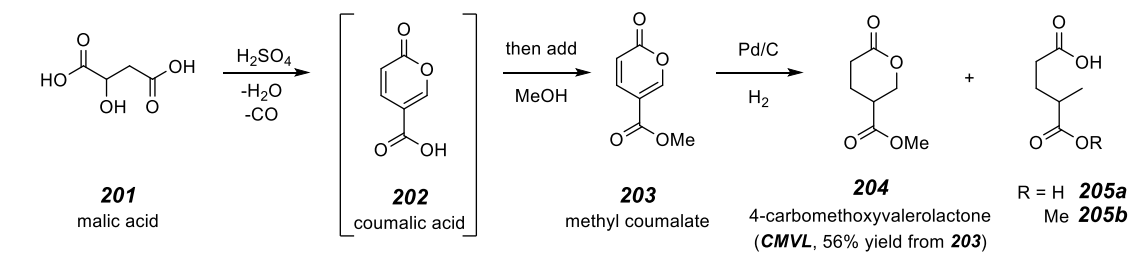
poly(CMVL)]. We also show the chemical (or back-to-monomer) recyclability of **poly(204)** by virtue of two complementary degradation pathways: i) a reverse ROTEP back to **CMVL** or ii) an eliminative process leading to a methacrylate derivative, which can further be polymerized to a new poly(methacrylate)-like material. To the best of our knowledge, this is the first report of a polymerization of a carboalkoxyvalerolactone.¹² Additionally, this is a rare example¹³ of depolymerization via two independent, chemical recycling pathways to yield two different types of monomers.

2.2 Monomer synthesis

The transformation of malic acid (**201**) to coumalic acid (**202**) using sulfuric acid (or fuming sulfuric acid) is well-studied, the initial report dating back to the late 1800s (Scheme 2.1).^{14,15} Fisher esterification with methanol allows access to methyl coumalate (**203**) in a one-pot process.¹⁶ The mechanism of this malic acid dimerization is proposed to proceed through an initial loss of carbon monoxide and H₂O, followed by an aldol condensation to produce coumalic acid (**202**).¹⁷ Because we could find no studies that confirmed whether CO or CO₂ is the gas evolved in this process and because a variation of the mechanism in which sulfuric is reduced to sulfurous acid is plausible, we captured the gaseous byproduct and confirmed (IR spectroscopy) that it was, indeed, carbon monoxide (see SI).

We initially isolated acid **202** using a modified Wiley and Smith protocol.¹⁵ Subjecting **202** to only a catalytic amount of sulfuric acid in methanol led to esterification of the pyrone ester moiety even at low conversions. This indicates that **203** forms more selectively in the 1-pot synthesis with the high concentrations of sulfuric acid.

Scheme 2.1 Two-step synthesis of **CMVL** (**204**) from malic acid (**201**)



Diels-Alder reactions of **202** or **203** with various dienophiles have been used to prepare biorenewable terephthalic acid and methyl terephthalate derivatives.¹⁸ Hydrogenation reactions of **202**¹⁹ or of **203**²⁰ are reported, but in no case has the saturated lactone product been fully characterized. A significant, competing hydrogenolysis of the C5–O bond during these reactions leads to the competitive production of products **205a** or **205b**. In our hands, the hydrogenation of **203** over 5% Pd/C afforded a mixture of **CMVL** and **205b** in a ratio of ca. 1.2:1 at 1 atm of H₂. We found that we could increase this ratio to 2.5:1 in favor of **CMVL** using a H₂ pressure of 80 psi. Unfortunately, increasing the pressure to 1400 psi gave no significant further improvement. Other hydrogenation catalysts provided lower portions of **CMVL** and/or other byproducts (Figure S2.2). However, lactone-ester **CMVL** and acid-ester **205b** can easily be separated via partitioning of the latter into aqueous NaHCO₃ solution. Overall, **CMVL** can be obtained in two operations from malic acid, typically in yields >30%.

2.3 Polymer synthesis and **CMVL** degradation

Aware that 4-methylvalerolactone (**207**, cf. Figure 2.1a) can be polymerized to high conversion,²¹ we surmised that **CMVL** would do so as well. Indeed, this proved to be the case. Exposure of a bulk sample of **CMVL** to 1,4-benzenedimethanol (**206**) and diphenyl phosphate [DPP, (PhO)₂PO₂H] at ambient temperature smoothly produced **poly(204)**

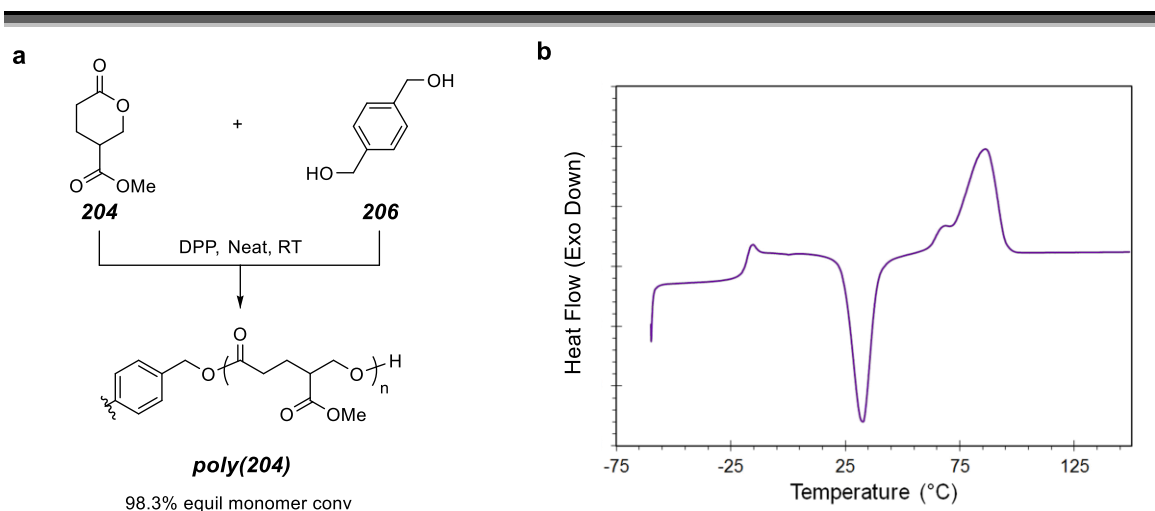


Figure 2.1 a) Polymerization of **CMVL (204)** using **DPP** as a catalyst. b) DSC thermogram (with downward exotherm) of **poly(204)** at a heating rate of $5\text{ }^{\circ}\text{C}\cdot\text{min}^{-1}$ taken on the third heating cycle. The thermogram shows that **poly(204)** has a $T_g = -18\text{ }^{\circ}\text{C}$, a $T_c = 32\text{ }^{\circ}\text{C}$, and two T_m 's = 68 and $86\text{ }^{\circ}\text{C}$.

(Figure 2.1a) as a semicrystalline material. Diol **206** was chosen as the initiator because it provides two sets of readily distinguished singlets in the ^1H NMR spectrum of the polymer that can be used for MW analysis. We could effectively target the molar mass of the polymer by adjusting the monomer to initiator ratio. Starting with a 200:1 or 500:1 ratio of **CMVL** to **206**, we achieved a polymer with a molar mass of 31 or $71\text{ kg}\cdot\text{mol}^{-1}$ (^1H NMR), respectively. The former proceeded to an equilibrium monomer conversion of 98.3% (analogous to conversion Schneiderman reported for **207**), and the dispersity (D) of the higher molecular weight sample was 1.2 (SEC, DMF). Additionally, there was no evidence for any chain-transfer involving transesterification between a carbomethoxy group and the growing chain end. This is consistent with the considerably higher basicity of an aliphatic lactone vs. ester functional group, resulting in a much higher concentration of the protonated lactone carbonyl intermediate species.²²

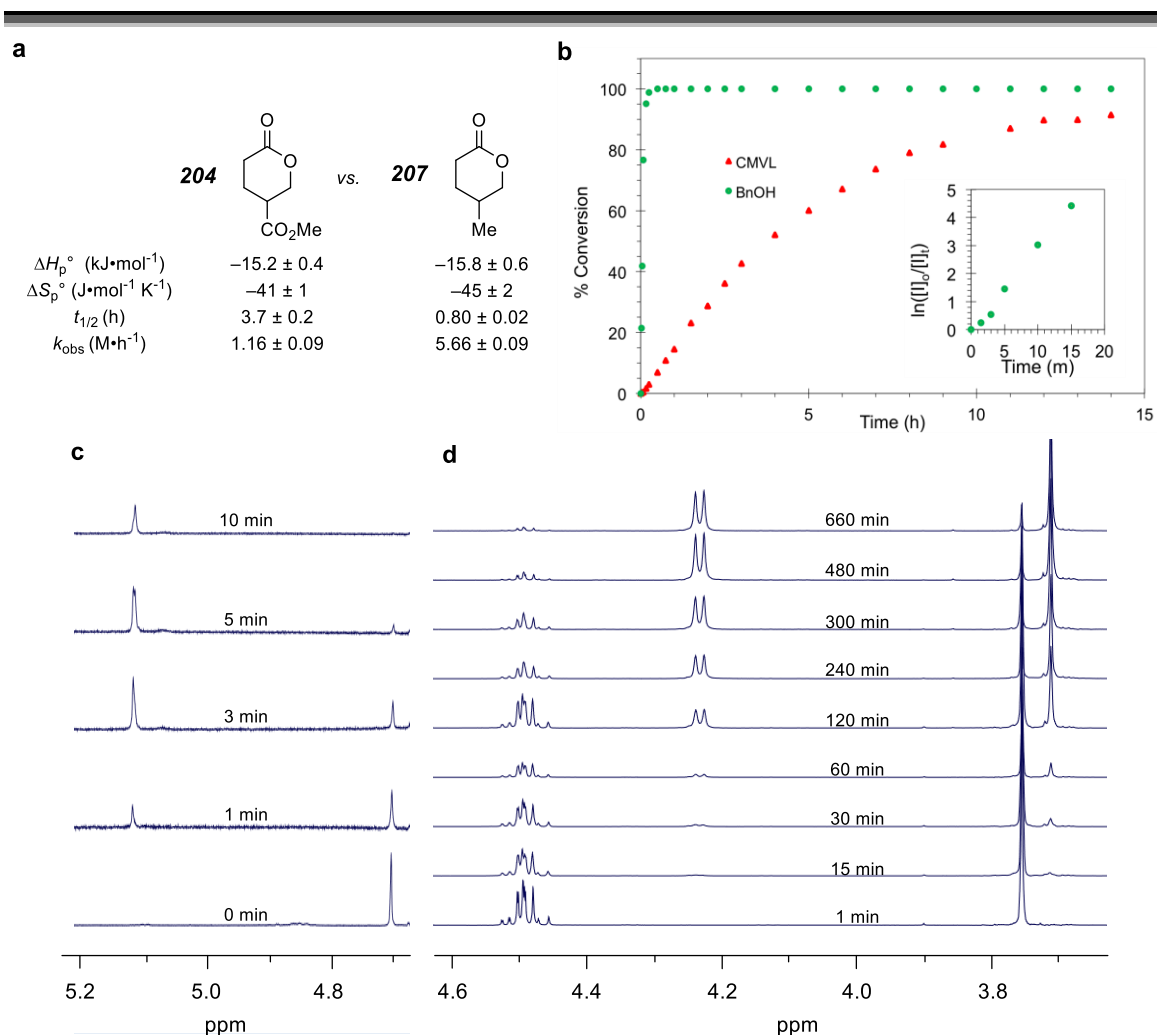


Figure 2.2 a) Kinetic and thermodynamic data comparing the polymerization of **CMVL** (**204**) and **207**. The data for **207** are taken from Schneiderman and Hillmyer.²¹ Kinetic data for both **CMVL** and **207** were collected using a **CMVL**:**BnOH**:**DPP** ratio of 200:1:1. b) Conversion of the **BnOH** initiator (**I**) and the **CMVL** monomer during bulk polymerization. The insert plot suggests that initiation is first order in the **BnOH**. Overlaid NMR spectra of c) **BnOH** alcohol (4.7 ppm) initiation to a benzyl ester (5.1 ppm) and d) ring-opening of **CMVL** to **poly(204)**. In the latter, there is an upfield shift of both the methylene at 4.49 ppm to 4.23 ppm and the methyl ester resonance (3.76 to 3.71 ppm).

Most substituted poly(valerolactones) are amorphous.²¹ The known exception is isotactic poly(4-methylvalerolactone), prepared from enantioenriched 4-methylvalerolactone (**207**).²³ The DSC thermogram of the 71 kg•mol⁻¹ sample of **poly(204)** (Figure 2.1b) reveals it to be a semicrystalline polymer, with a low T_g (-18 °C) and two T_m 's (68 and 86 °C).²⁴ This is somewhat surprising, because monomer **204** is racemic and **poly(204)** is likely to be highly atactic. We have not determined the degree of crystallinity (briefly discussed in Chapter 4) nor the impact of using an enantioenriched monomer.

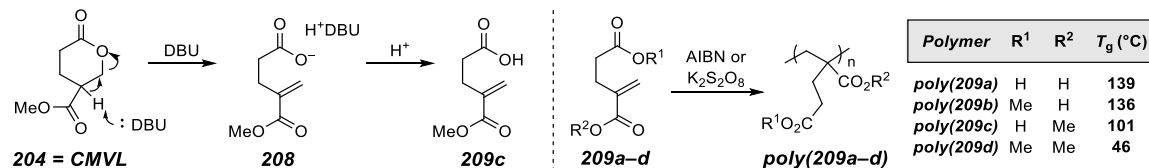
We determined the thermodynamics of the solution-phase polymerization (Figure 2.2a) using Van't Hoff analysis (Figure S2.3). We used starting monomer concentrations of 1.0 M²⁵ (in chloroform). The enthalpy (ΔH_p^0) and entropy (ΔS_p^0) of polymerization were -15.2 ± 0.4 kJ•mol⁻¹ and -41 ± 1 J•mol⁻¹, respectively. These values were essentially identical to those measured for the polymerization of **207** (-15.8 ± 0.6 kJ•mol⁻¹ and -42 ± 2 J•mol⁻¹).²¹ Not surprisingly, the equilibrium monomer conversions of **CMVL** and **207** (both in bulk) are also nearly identical.

We also studied the rate of polymerization of **CMVL** in order to compare its reactivity vs. that of other substituted valerolactones. The half-lives ($t_{1/2}$) and rate constants (k_{obs}) for polymerization of the four, isomeric, monomethyl-substituted valerolactones have previously been determined for the bulk polymerization using a ratio of lactone monomer to benzyl alcohol initiator (BnOH) to DPP catalyst of ~200:1:1.²¹ Using the same conditions, we measured the $t_{1/2}$ for consumption of **CMVL** to be 3.7 ± 0.2 hours with a $k_{obs} = 1.16 \pm 0.09$ M h⁻¹ (Figure 2.2b). We measured these values using ¹H NMR spectroscopy of quenched polymerization aliquots (Figure 2.2c and Figure 2.2d). The progress of the reaction slows in the second half because the reaction mixture shows the onset of turbidity, the intensity of which progresses over time, just prior to the time for 50% conversion. Overall, the rate of **CMVL** ROTEP (k_{obs}) is slower than that of

unsubstituted valerolactone (ca. 2.5x), 3-methylvalerolactone (ca. 2.1x), and 4-methylvalerolactone (**207**, ca. 4.9x) and faster than that of 2-methylvalerolactone (ca. 1.3x) and 5-methylvalerolactone (ca. 3.7x).²¹

We briefly explored 1,8-diazabicyclo[5.4.0]undec-7-ene (DBU) for its potential to polymerize **CMVL** (in dichloromethane, DCM). At low mol% levels, DBU was an ineffective ROTEP catalyst. The reason was revealed when 1 full equivalent of DBU was used. This cleanly led to the formation of methacrylate **208**, a process that, in effect, incapacitates the DBU (Scheme 2.2). This retro-oxa-Michael addition (i.e., elimination) may occur through either an E2 or E1_{cb} mechanism.²⁶ Acidification leads to the 2-methyleneglutaric monomethyl ester **209c** in 95% yield without purification beyond liquid-liquid partitioning. This material appeared to be quite pure (see NMR data in SI) and was used directly for polymerizations.

Scheme 2.2 Eliminative ring opening of **CMVL** to the methacrylate analogue **208** (and **209c**) using DBU and polymerization of analogues **209a-d**



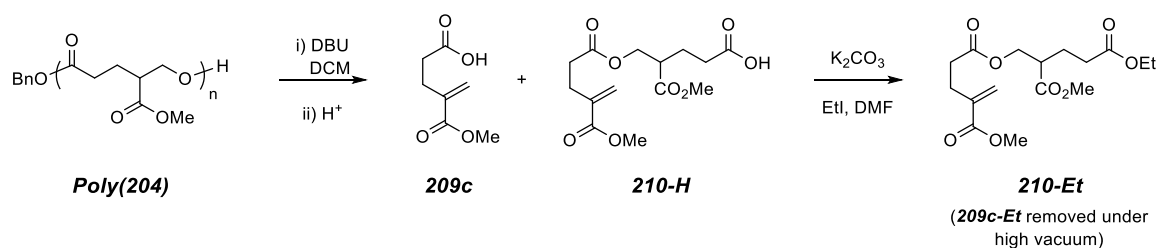
We also briefly explored the polymerization of analogues of **209c** with the goal of exploring the effect of carboxyl substitution on the T_g of the resulting poly(methacrylate)-type polymers. We synthesized the following monomers using known procedures:²⁷ 2-methyleneglutaric acid (**209a**), 5-methoxy-2-methylene-5-oxopentanoic acid (**209b**), and dimethyl 2-methyleneglutarate (**209d**). The polymerization of diacid **209a** and the dimethyl ester **209d** have each been reported using radical initiators.²⁸ We polymerized each of **209a-d** using azobisisobutyronitrile (AIBN) or potassium persulfate (K₂S₂O₈)

initiators at 65 °C to access the set of four polymers, **poly(209a–d)** (see SI for details). The T_g s of these analogues varied with the nature of the carboxyl functional groups on each repeat unit in the polymer backbone. **Poly(209a)** and **poly(209b)**, with a carboxylic acid nearer the polymer chain, both have high T_g s (139 and 136 °C, respectively); **poly(209c)** and **poly(209d)**, with a methyl ester closer to the main chain, show lower T_g s (101 and 46 °C, respectively).

2.4 Divergent chemical recycling of poly(CMVL)

We wanted to expand this eliminative degradation of **CMVL** and apply it to **poly(204)** to bring added value to the polymer after its end-of-life. **Poly(204)** was dissolved in DCM containing DBU (ca. 1.1 equivalents DBU per repeat unit of polymer, Scheme 2.3), which are nearly identical conditions to those used to degrade **CMVL**. After 20 h, the degradation was incomplete and did not appear to further progress even when longer reaction times or higher temperatures (which also led to polymerization of **209c**) were used.

Scheme 2.3 Degradation of **poly(204)** with DBU in DCM leads to a mixture of **209c** and dimer **210-H**

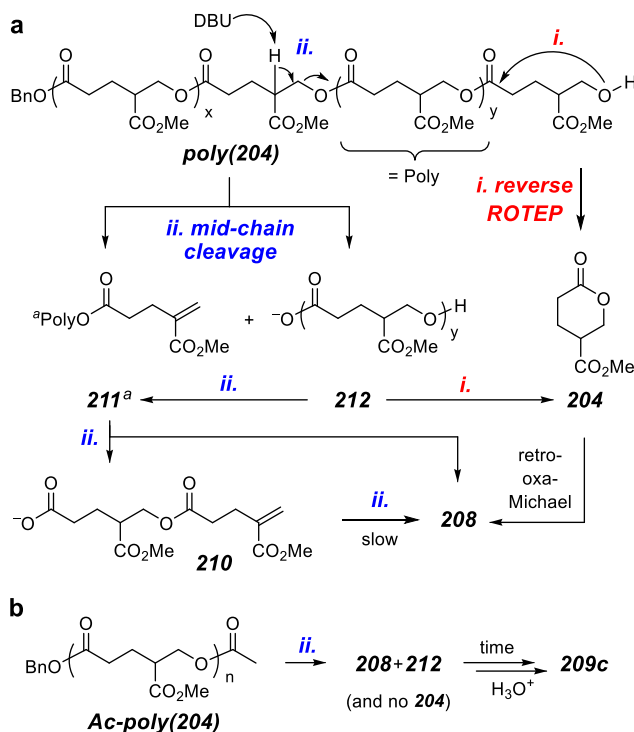


The acidified degradation mixture appeared to contain equimolar amounts of **209c** and **210-H**. To support this analysis, we first confirmed the presence of **209c** through doping a small amount of purified **209c** (prepared in the degradation of **CMVL**) into an ^1H NMR aliquot containing the crude, basic reaction mixture. After, each newly formed

carboxylic acid (of **209c** and **210-H**) was functionalized using potassium carbonate and ethyl iodide (Scheme 2.3). The compounds were placed under high vacuum to remove the more volatile ethylated **209c** (not shown) and cleanly afford ethylated dimer **210-Et**.

We next monitored this base degradation process via ^1H NMR spectroscopy in CDCl_3 (Figure S2.7) and found that depolymerization occurs via two competitive pathways as depicted in Scheme 2.4. In mode *i.*, DBU can catalyze the reverse ROTEP of **poly(204)** to give, initially, **CMVL**. **CMVL** can then proceed through the retro-oxa-Michael addition to give **208**, as previously discussed (Scheme 2.2). Alternatively in mode *ii.*, DBU can cleave (through elimination) along the main chain to give two shorter **poly(204)** fragments. One, **212**, is still terminated by a hydroxyl group and the other, **211**, by the new alkene. The latter can now only continue to degrade via additional mid-chain cleavages; the former can continue to degrade via the competitive reverse ROTEP (*i.*) vs. eliminative (*ii.*) pathways. Both pathways ultimately result in a metastable mixture of **208** and dimer **210** (1-2 days at rt in CDCl_3). Dimer **210** was observed to then further transform into **208** at a significantly slower rate, presumably because the final elimination needs to occur in the vicinity of a proximal carboxylate anion. To support this interpretation of the base-promoted degradation, we synthesized the acetylated **poly(204)** [**Ac-poly(204)**]. In this case, the reverse ROTEP pathway *i.* was thwarted and no intermediate **CMVL** was observed upon treatment with DBU in CDCl_3 (Scheme 2.4b).

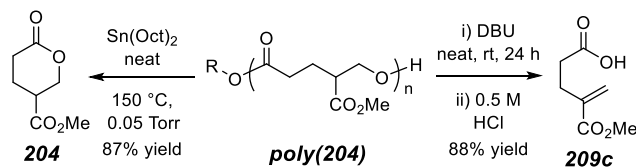
Scheme 2.4 Mechanistic analysis of eliminative degradation of **poly(204)**



^aPartially degraded polymers **210** can bear either a terminal benzyl ester^b or a carboxylate salt. ^bA few percent of the benzyl ester analogue of **209c** was observed in the crude degradation product mixture.

We envisioned that we could further drive the eliminative degradation of **poly(204)** to completion by forcing the DBU base into proximity of anionic dimer **210** simply by performing this degradation without solvent (Scheme 2.5). When a *neat* sample of **poly(204)** ($M_n = 22 \text{ kg}\cdot\text{mol}^{-1}$) was treated with DBU (>1 equiv per repeat unit), it cleanly degraded in an eliminative sense to give, following acidification, the monomer **209c** in 88% yield. In a complementary fashion and under orthogonal reaction conditions, neat **poly(204)** ($M_n = 70 \text{ kg}\cdot\text{mol}^{-1}$) was heated (150 °C, ca. 0.05 torr) in the presence of tin octanoate (SnOct₂), depolymerization provided an 87% yield of recovered monomer **CMVL (204)**.

Scheme 2.5 Divergent chemical recycling of **poly(204)** to **CMVL** [Sn(Oct)₂] or enoate **209c** (DBU)



2.5 Conclusion

In summary, we have synthesized the novel carbomethoxylated polyvalerolactone **poly(204)**. The precursor monomer, **CMVL**, can be obtained in two steps from malic acid. The polymer has a $T_g = -18$ °C, $T_c = 32$ °C, and two T_m 's at 68 and 86 °C. The polymerization shows an equilibrium monomer conversion of >98% in bulk at room temperature. An additional novel feature of this work is that the **poly(204)** can be degraded efficiently, yet divergently, to two different monomers under complementary sets of conditions. First, transesterification degradation (reverse ROTEP) promoted by Sn(Oct)₂ returns **CMVL**. On the other hand, base-promoted degradation gives the methacrylate analogue **209c**. This monomer was radically polymerized to give the new polymethacrylate derivative **poly(209c)**.

2.6 References

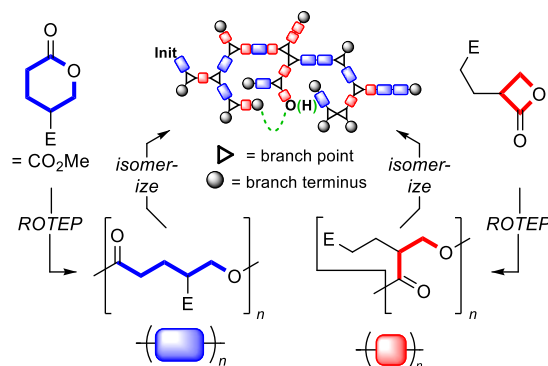
- ¹ Jambeck, J. R.; Geyer, R.; Wilcox, C.; Siegler, T. R.; Perryman, M.; Andrady, A.; Narayan, R.; Lavender Law, K. Plastic waste inputs from land into the ocean. *Science* **2015**, *347*, 768–771.
- ² World Economic Forum, Ellen MacArthur Foundation and McKinsey and Company, the new plastics economy rethinking the future of plastics; 2016; [report] <http://www.ellenmacarthurfoundation.org/publications>.
- ³ Hopewell, J.; Dvorak, R.; Kosior, E. Plastics recycling: Challenges and opportunities. *Phil. Trans. R. Soc. B* **2009**, *364*, 2115–2126.
- ⁴ Kyrikou, I.; Briassoulis, D. Biodegradation of agricultural plastic films: A critical review. *J. Polym. Environ.* **2007**, *15*, 125–150.
- ⁵ Laycock, B.; Nickolic, M.; Colwell, J. M.; Gauthier, E.; Halley, P.; Bottle, S.; George, G. Lifetime prediction of biodegradable polymers. *Prog. Polym. Sci.* **2017**, *71*, 144–189.
- ⁶ For a recent review see: Hong, M.; Chen, E. Y.-X. Chemically recyclable polymers: A circular economy approach to sustainability. *Green Chem.* **2017**, *19*, 3692–3706.
- ⁷ (a) Hong, M.; Chen, E. Y.-X. Completely recyclable biopolymers with linear and cyclic topologies via ring-opening polymerization of γ -butyrolactone. *Nat. Chem.* **2016**, *8*, 42–49. (b) X. Y. Tang, M. Hong, L. Falivene, L. Caporaso, L. Cavallo and E. Y.-X. Chen. The quest for converting biorenewable bifunctional α -methylene- γ -butyrolactone into degradable and recyclable polyester: Controlling vinyl-addition/ring-opening/cross-linking pathways. *J. Am. Chem. Soc.* **2016**, *138*, 14326–14337. (c) MacDonald, J. P.; Shaver, M. P. An aromatic/aliphatic polyester prepared via ring-opening polymerisation and its remarkably selective and cyclable depolymerisation to monomer. *Polym. Chem.* **2016**, *7*, 553–559. (d) Schneiderman, D. K.; Vanderlaan, M. E.; Mannion, A. M.; Panthani, T. R.; Batiste, D. C.; Wang, J. Z.; Bates, F. S.; Macosko, C. W.; Hillmyer, M. A. Chemically recyclable biobased polyurethanes. *ACS Macro Lett.* **2016**, *5*, 515–518. (e) Brutman, J. P.; De Hoe, G. P.; Schneiderman, D. K.; Le, T. N.; Hillmyer, M. A. Renewable, degradable, and chemically recyclable cross-linked elastomers. *Ind. Eng. Chem. Res.* **2016**, *55*, 11097–11106.
- ⁸ Kamimura, A.; Shigehiro, Y. An efficient method to depolymerize polyamide plastics: A new use of ionic liquids. *Org. Lett.* **2007**, *9*, 2533–2535.
- ⁹ (a) Li, C.; Sablong, R. J.; van Benthem, R. A. T. M.; Koning, C. E. Unique base-initiated depolymerization of limonene-derived polycarbonates. *ACS Macro Lett.* **2017**, *6*, 684–658. (b) Liu, B.; Chen, L.; Zhang, M.; Yu, A. Degradation and stabilization of poly(propylene carbonate). *Macromol. Rapid Commun.* **2002**, *23*, 881–884. (c) Darensbourg, D. J.; Wei, S.-H. Depolymerization of polycarbonates derived

-
- from carbon dioxide and epoxides to provide cyclic carbonates. A kinetic study. *Macromolecules* **2012**, *45*, 5916–5922.
- ¹⁰ Werpy, T.; Petersen, G. Top value added chemicals from biomass volume I — Results of screening for potential candidates from sugars and synthesis gas. Top value added chemicals from biomass volume I: Results of screening for potential candidates; 2004.
- ¹¹ Chi, Z.; Wang, Z.-P.; Wang, G.-Y.; Khan, I.; Chi, Z.-M. Microbial biosynthesis and secretion of L-malic acid and its applications. *Crit. Rev. Biotechnol.* **2016**, *36*, 99–107.
- ¹² Polymers incorporating poly(4-carbotertbutoxycaprolactone),^a poly(2-carbobenzoxycaprolactone),^b and poly(2-carbopropargyloxycaprolactone)^c moieties each been reported. Relatively few details about their properties have been described. (a) Trollsås, M.; Lee, Y. V.; Mecerreyes, D.; Löwenhielm, P.; Möller, M.; Miller, R. D.; Hedrick, J. L. Hydrophilic aliphatic polyesters: Design, synthesis, and ring-opening polymerization of functional cyclic esters. *Macromolecules* **2000**, *33*, 4619–4627. (b) Mahmud, A.; Xiong, X.-B.; Lavasanifar, A. Novel self-associating poly(ethylene oxide)-block-poly(ϵ -caprolactone) block copolymers with functional side groups on the polyester block for drug delivery. *Macromolecules* **2006**, *39*, 9419–9428. (c) Garg, S. M.; Xiong, X.-B.; Lu, C.; Lavasanifar, A. Application of click chemistry in the preparation of poly(ethylene oxide)-block-poly(ϵ -caprolactone) with hydrolyzable cross-links in the micellar core. *Macromolecules* **2011**, *44*, 2058–2066.
- ¹³ PLA can be degraded to either acrylic acid or lactide. Terrade, F. G.; van Krieken, J.; Verkuijl, B. J. V.; Bouwman, E. Catalytic cracking of lactide and poly(lactic acid) to acrylic acid at low temperatures. *ChemSusChem* **2017**, *10*, 1904–1908.
- ¹⁴ von Pechmann, H. On the Cleavage of α -Oxyacids. *Liebigs Ann. Chem.* **1891**, *264*, 261–309.
- ¹⁵ Wiley, R. H.; Smith, N. R. Coumalic Acid. *Org. Synth.* **1951**, *31*, 23–24.
- ¹⁶ Zhu, W.; Shen, J.; Li, Q.; Pei, Q.; Chen, J.; Chen, Z.; Liu, Z.; Hu, G. Synthesis, pharmacophores, and mechanism study of pyridin-3(1*H*)-one derivatives as regulators of translation initiation factor 3A. *Arch. Pharm. Chem. Life Sci.* **2013**, *346*, 654–666.
- ¹⁷ Ashworth, L. W.; Bowden, M. C.; Dembofsky, B.; Levin, D.; Moss, W.; Robinson, E.; Szczur, N.; Virica, J. A new route for manufacture of 3-cyano-1-nathalenecarboxylic acid. *Org. Process Res. Dev.* **2003**, *7*, 74–81.
- ¹⁸ (a) Lee, J. J.; Kraus, G. A. One-pot formal synthesis of biorenewable terephthalic acid from methyl coumalate and methyl pyruvate. *Green Chem.* **2014**, *16*, 2111–2116. (b) Lee, J. J.; Kraus, G. A. Divergent Diels-Alder methodology from methyl coumalate toward functionalized aromatics. *Tet. Lett.* **2013**, *54*, 2366–2368. (c) Lee, J. J.; Pollock III, G. R.; Mitchell, D.; Kasuga, L.; Kraus, G. R. Upgrading malic acid to bio-based benzoates via a Diels–Alder-initiated sequence with the methyl coumalate platform. *RSC Adv.* **2014**, *4*, 45657–45664. (d) Pfennig, T.; Johnson, R. L.; Shanks, B. H. The

-
- formation of *p*-toluic acid from coumalic acid: A reaction network analysis. *Green Chem.* **2017**, *19*, 3263–3271.
- ¹⁹ (a) Wiley, R. H.; Hart, A. J. 2-Pyrones. XIV. The hydrogenation of 2-pyrones. *J. Am. Chem. Soc.* **1955**, *77*, 2340–2341. (b) Cao, J.; Wang, S.; Jia L.; Hua, R. Liquid crystal compound containing tetrahydropyran difluoro methoxy-linking group and preparation method and application thereof. Chinese Patent CN 201410088636, March 12, 2014.
- ²⁰ Fried, J.; Elderfield, R. C. Studies on the lactone related to the cardiac aglycones. VI. The action of diazomethane on certain derivatives of α -pyrone. *J. Org. Chem.* **1941**, *6*, 577–583.
- ²¹ Schneiderman, D. K.; Hillmyer, M. A. Aliphatic polyester block polymer design. *Macromolecules* **2016**, *49*, 2419–2428.
- ²² (a) Bouchoux, G.; Drancourt, D.; Leblanc, D. Gas-phase basicities of lactones. *New J. Chem.* **1995**, *19*, 1243–1257. (b) Bouchoux, G. Gas-phase basicities of polyfunctional molecules. Part 4: Carbonyl groups as basic sites. *Mass Spectrum. Rev.* **2015**, *34*, 493–534. (c) Basko, M.; Kubisa, P. Cationic copolymerization of ϵ -caprolactone and L,L-lactide by an activated monomer mechanism. *J. Polym. Sci. A Polym Chem.* **2006**, *44*, 7071–7081.
- ²³ (a) Ishmuratov, G. Y.; Yakovleva, M. P.; Zaripova, G. V.; Botsman, L. P.; Muslukhov, R. R.; Tolstikov, G. A. Novel synthesis of (4R)-4-methylpentanolide from (L)-(-)-menthol. *Chem. Nat. Compd.* **2004**, *40*, 548–551. (b) Zhang, C.; Schneiderman, D. K.; Cai, T.; Tai, Y.-S.; Fox, K.; Zhang, K. Optically active β -methyl- δ -valerolactone: Biosynthesis and polymerization. *ACS Sustainable Chem. Eng.* **2016**, *4*, 4396–4402.
- ²⁴ Tanaka, N. Two equilibrium melting temperatures and physical meaning of DSC melting peaks in poly(ethylene terephthalate). *Polymer* **2008**, *49*, 5353–5356.
- ²⁵ Olsen, P.; Odelius, K.; Albertsson, A.-C. Thermodynamic presynthetic considerations for ring-opening polymerization. *Biomacromolecules* **2016**, *17*, 699–709.
- ²⁶ An analogous eliminative transformation, in which **CMVL** was presumed to be formed in situ, has been induced by fluoride ion. Bartley, D. M.; Coward, J. K. Regioselective synthesis of α -methyl 2-methyleneglutarate via a novel lactonization-elimination rearrangement *J. Org. Chem.* **2006**, *71*, 372–374.
- ²⁷ (a) Feng, Y.; Coward, J. K. Prodrug forms of N-[(4-deoxy-4-amino-10-methyl)pteroyl]glutamate- γ -[ψ P(O)(OH)]-glutarate, A potent inhibitor of folylpoly- γ -glutamate synthetase: Synthesis and hydrolytic stability. *J. Med. Chem.*, **2006**, *49*, 770–788. (b) Tello-Aburto, R.; Lucero, A. N.; Rogelj, S. A catalytic approach to the MH-031 lactone: Application to the synthesis of geraldin analogs. *Tetrahedron Lett.* **2014**, *55* 6266–6268.
- ²⁸ (a) Kobatake, S.; Yamada, B.; Radical polymerization and copolymerization of methyl α -(2-carbomethoxyethyl)acrylate, a dimer of methyl acrylate, as a polymerizable α -substituted acrylate. *J. Polym. Sci. A Polym. Chem.* **1996**, *34*, 95–108. (b) Trumbo, D.

L.; Zander, R. A. The copolymerization behavior of acrylate dimers: Copolymers of methyl, ethyl, and *n*-butyl acrylate dimers. *J. Polym. Sci. A Polym. Chem.* **1991**, *29*, 1053–1059. (c) Harada, T.; Zetterlund, P. B.; Yamada, B. Preparation of macromonomers by copolymerization of methyl acrylate dimer involving β fragmentation. *J. Polym. Sci. A.* **2004**, *43*, 597–607.

Chapter 3. Isomerization of linear to hyperbranched polymers: Two isomeric lactones converge, via metastable isostructural polyesters, to a highly branched analogue*



Summary: We report in Chapter 3, the Zn(II)-catalyzed convergence of two metastable and isostructural polyesters to an isomeric polymer having a hyperbranched architecture. Ring-opening transesterification polymerization (ROTEP) of 4-carbomethoxyvalerolactone (**CMVL**) under Brønsted catalysis gave the linear polyester **PCMVL** as discussed in Chapter 2. We show here that both **CMVL** and **PCMVL** can be (polymerized and) isomerized to the equilibrated (and highly branched) polyester **EQ-PCMVL**. Analysis of the fragments obtained from eliminative degradation of **EQ-PCMVL** were critical in the formulation of its structure. The isomerization of **PCMVL** to **EQ-PCMVL** is a direct consequence of the presence of the second ester functional group in the **CMVL** ester-lactone, a rarely studied class of monomer (see Chapter 1, Table 1). Zn(II)-catalysis for the ROTEP of the isomeric β -lactone, 2-(2-

* This work was performed in collaboration with Dr. Daniel Stasiw and Bill Tolman. This chapter has been reproduced in part with permission from Fahnhorst, G. W.; Stasiw, D. E.; Tolman, W. B.; Hoye, T. R. *ACS Macro Lett.* **2018**, 7, 1144–1148. Copyright 2018 American Chemical Society

carbomethoxyethyl)propiolactone (*iso*CMVL), as well as isomerization of the isostructural linear homopolymer derived from that isomeric monomer, led to the same **EQ-PCMVL**. These results suggest a new strategy for the introduction of branching into various polyesters.

3.1 Introduction

The extent and nature of branching architecture in both synthetic and natural polymers have significant ramifications on material properties.¹ Methods and strategies for incorporating these features are valuable. An illustrative example is the synthesis of either linear or branched polyolefins from a common monomer, a feature that can be controlled by the choice of catalyst that either permits, or not, chain walking during the polymerization reaction.² A second example is the synthesis of hyperbranched polyesters by ring-opening transesterification polymerization (ROTEP) of lactone monomers bearing a hydroxy group, which polymerize to give highly branched polyesters.³ This example involves a class of monomers known as inimers³ (or dual initiator/monomer compounds) that, per force, produce polymers with a highly branched architecture.⁴

In the examples described above the linear or (hyper)branched nature of the polymer is dictated from the outset of the polymerization. By contrast, we are unaware of any instances of the isomerization of a preformed, linear polymer to an isomeric (hyper)branched polymer. We report such a process here.⁵

We recently described⁶ the polymerization of 4-carbomethoxyvalerolactone (**CMVL**, Figure 1a), readily available from malic acid (via coumalic acid⁷) in Chapter 2. Under the action of Brønsted acid catalysis [diphenyl phosphate (DPP)], **CMVL** gave poly(**CMVL**) (**PCMVL**) as a semicrystalline, linear homopolymer via ROTEP (Figure 3.1a). Exchange at the methyl ester carboxyls—a process that would have introduced branching (or a ring)—was not detected. The assignment of a linear structure to **PCMVL** was supported by its highly efficient, reagent-dependent degradations. Namely, when **PCMVL** was heated in the presence of a Sn(II) catalyst, reverse-ROTEP⁸ smoothly converted it back to **CMVL**. On the other hand, when treated with the organobase 1,8-

diazabicyclo[5.4.0]undec-7-ene (DBU), **PCMVL** gave the methacrylate derivative **301a** by elimination at every backbone ester junction.

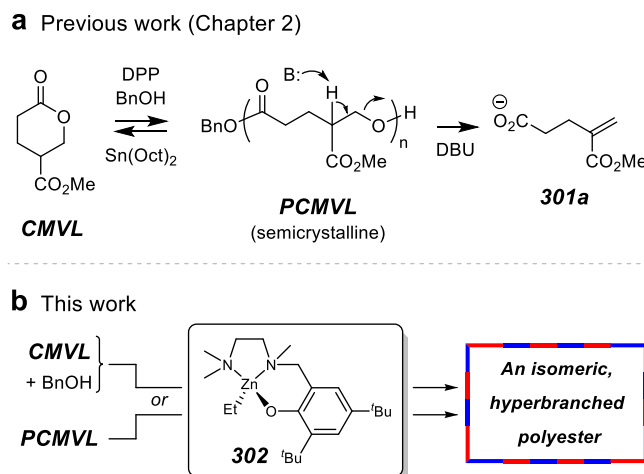


Figure 3.1 (a) Brønsted acid catalyzed ROTEP of **CMVL** to (linear) **PCMVL**. (b) Use of the Zn(II) catalyst **302** leads to a new, isomeric polyester.

We now report (Figure 3.1b) that the zinc complex **302**⁹ catalyzes the conversion of **CMVL** to a highly branched, isostructural (and equilibrated) polyester, **EQ-PCMVL**. We further show i) that the linear **PCMVL** is a metastable intermediate enroute to **EQ-PCMVL** and ii) that catalyst **302** is capable of isomerizing preformed linear **PCMVL** to **EQ-PCMVL**. The key enabler of the intricate and fascinating interconversions associated with the overall equilibration is the presence of a carboalkoxy substituent on every repeat unit in the polyester—to our knowledge, a unique structural feature. Significantly, these findings pave the way for use of related strategies for introducing branching in a considerable array of polyesters.

3.2 Analysis of EQ-PCMVL from CMVL and PCMVL using catalyst **302**

The polymerization of neat **CMVL** by catalyst **302** (Figure 3.2a), initiated by benzyl alcohol (BnOH), was rapid and proceeded to essentially the same equilibrium

monomer conversion (>98%) as the DPP-promoted polymerization. However, the resulting **EQ-PCMVL** had a different macroscopic morphology—the melting characteristic of **PCMVL** was no longer observed in the DSC of this now amorphous polyester and only a T_g was observed at $-20\text{ }^\circ\text{C}$. The proton NMR spectra revealed distinguishing features between **EQ-PCMVL** and **PCMVL** (Figure 3.2b)—most notably, a second methyl ester and broadening of the backbone resonances.

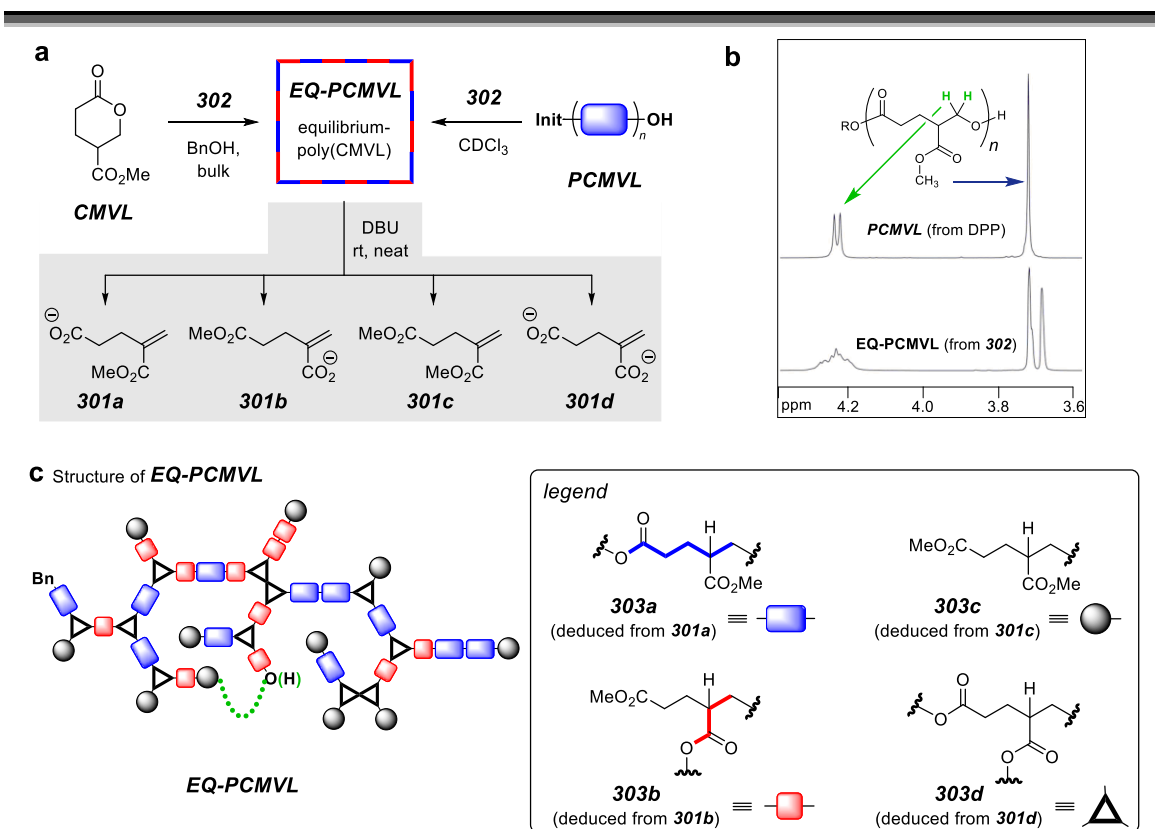


Figure 3.2 (a) Polymerization/reorganization of **CMVL** and **PCMVL** with catalyst **302**. (b) Overlaid NMR spectra of **PCMVL** and **EQ-PCMVL** (c) Structure of **EQ-PCMVL** deduced from the eliminative fragments **301a**–**301d**. Green dotted line depicts a closure to a cyclic substructure (see MALDI discussion below).

We again used degradation experiments to give valuable information about the structure of the new **EQ-PCMVL**. Exposure to $\text{Sn}(\text{Oct})_2$ under the retro-ROTEP conditions used for complete **PCMVL** degradation ($150\text{ }^\circ\text{C}$, 24 h, 0.1 torr) gave, now, only

a trace amount of **CMVL**, leaving the remainder of the macromolecular sample intact. On the other hand, incubation in DBU (3 equiv, ambient T, neat, 20 h) resulted in ca. 75% overall degradation, producing substantial amounts of each of the four methyleneglutarates **301a–301d** as the only monomeric decomposition products (gray box in Figure 3.2a). This contrasts with the formation of **301a** alone from analogous eliminative fragmentation of the homopolymer **PCMVL**.⁶

Through retrodegradative reasoning, we deduced that the structure of **EQ-PCMVL** contains the four unique subunits **303a–303d** (Figure 3.2c). Each of these gives rise to one of the four corresponding elimination products **301a–301d**. The 4-atom backbone repeat unit **303b** (red square) is isomeric with the 6-atom unit **303a** (blue rectangle)—the only backbone subunit present in **PCMVL**. The remaining two subunits suggest that **EQ-PCMVL** is highly branched (cf. **303d**, triangle) and that each branch has at its terminus a dimethyl ester (cf. **303c**, ball). A corollary is that the structure of **EQ-PCMVL** (Figure 3.2c) contains essentially an equivalent number of triangles (**303d**) and balls (**303c**). Moreover, the total number of backbone ester moieties and methyl esters in the ensemble of macromolecules is conserved during the multiple transesterification events through which they arise (see SI for a more detailed discussion). The absence of crystallinity in **EQ-PCMVL** is also consistent with this highly branched structure.

We then investigated the polymerization of **CMVL** with catalyst **302** more carefully by in situ ¹H NMR monitoring in CDCl₃ (Figure 3.3) rather than in the bulk. A typical plot of reaction progress showed the consumption of monomeric **CMVL** and growth of **PCMVL** at the same rate in the early phase of reaction, as measured by the resonances for their methyl esters at δ 3.75 (green circle) and 3.71 (blue diamond), respectively. The half-life for monomer loss was less than one hour. However, even at early time points a third methyl ester resonance (at δ 3.67, red square) had appeared and this

continued to grow with time. Gradually, as the amount of **EQ-PCMVL** increased, the concentration of **PCMVL** diminished until, ultimately, the isomerization progressed to the point of having an ca. 1:1 ratio of the two methyl ester resonances at 3.71 and 3.67.¹⁰ This result is consistent with the presence of a similar number of each of the subunits **3a–3d10** in **EQ-PCMVL**. The ratio of these resonances remained essentially invariant even after extended time, a hallmark of a process having reached equilibrium.

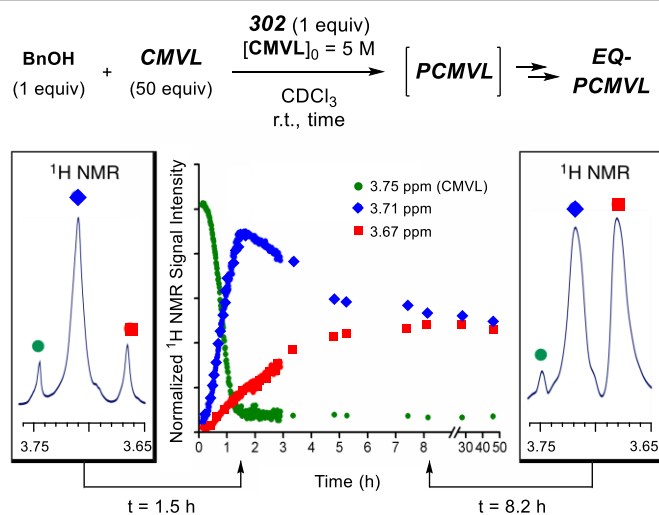


Figure 3.3 Time courses for polymerization of **CMVL** by zinc complex **302** to produce the equilibrated **EQ-PCMVL**.

In an independent experiment that further solidifies the interpretation that **PCMVL** is isomerizing to **EQ-PCMVL**, preformed **PCMVL** homopolymer (from the DPP ROTEP) was exposed to the zinc catalyst **302** in bulk at $80 \text{ }^\circ\text{C}$ with no added initiator alcohol (Figure 3.2a). The ^1H NMR spectrum recorded at the final resting-state was essentially indistinguishable from that of the sample of **EQ-PCMVL** produced starting from the **CMVL** monomer. Thus, the zinc complex **302** and the lone hydroxy group in **PCMVL** are capable of promoting the chain-scrambling, transesterification events.

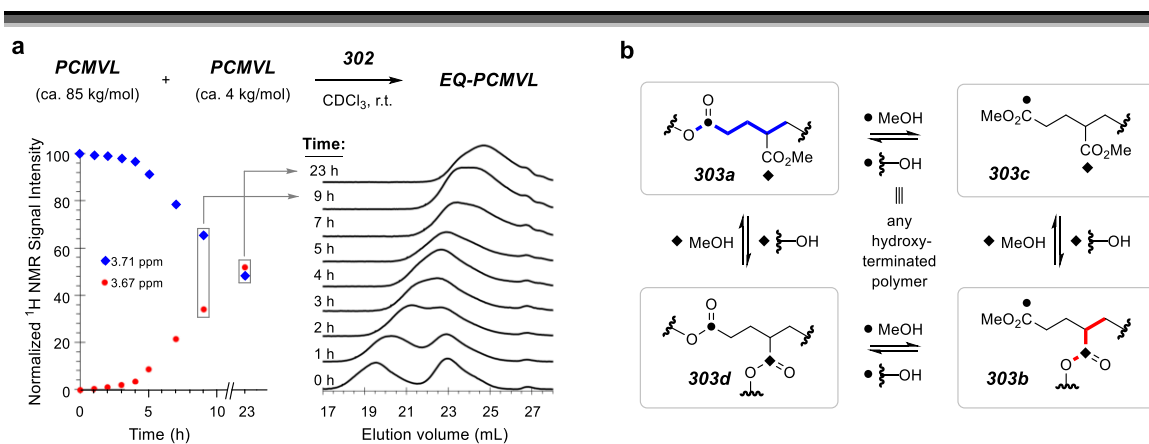


Figure 3.4 (a) Time course for the isomerization of preformed homomeric **PCMVL** by zinc complex **302** to produce the equilibrated **EQ-PCMVL**. (b) A scheme that demonstrates the multiple transesterification events that occur to obtain **EQ-PCMVL**.

A related experiment, also using preformed **PCMVL**, provided additional perspective (Figure 3.4a). Equivalent masses of two samples of **PCMVL** of different molecular weight ($M_n = 4$ vs. $85 \text{ kg}\cdot\text{mol}^{-1}$) were treated with **302** (in CDCl_3 at ambient temperature). Aliquots were analyzed in parallel by both ^1H NMR spectroscopy and SEC. The latter showed initial broadening of both polymers with eventual merging of their retention volumes. These changes, however, occurred considerably faster than the growth of the new methyl ester resonance. Ultimately, both the SEC and NMR data converged to those of the resting state. These complementary experiments indicate that transesterification at the backbone esters (chain transfer) is faster than that at the methyl ester side chains in **PCMVL**, consistent with the fact that the latter are more sterically hindered (α -branched¹¹) than the former. The greatly increased SEC retention volume of the final sample of **EQ-PCMVL**, significantly greater than even that of the 4K starting sample of **PCMVL**, is a clear reflection of a reduced radius of gyration¹² in the equilibrated polymer, reflecting the high degree of branching and the presence, perhaps, of cyclic structures.

These experiments suggest that the four subunits **303a–303d** can each arise through intermolecular transesterification from *either* of the two adjacent (Figure 3.4b, up/down or right/left) subunits with either MeOH or a polymeric terminal hydroxy. For example, **303a** can arise from the transesterification of **303d** with MeOH or the transesterification of **303c** with a terminal polymer hydroxy. However, two transesterification events are required to interconvert any of the diagonal pairs—for example, **303b** from **303a**.

3.3 MALDI spectrometry reveals cyclic structure

We turned to MALDI analysis to provide further insight about the nature of the end-groups present in **EQ-PCMVL**. To this end, we synthesized **PCMVL** with a $M_n = 2.54 \text{ kg}\cdot\text{mol}^{-1}$ and isomerized it to **EQ-PCMVL** by reacting it with the zinc catalyst **302** neat for 20 h. The mass spectrum (Figure 3.5) of pre-isomerized, linear **PCMVL** shows the major mass distribution associated with sodiated **PCMVL** ($\text{BnOH} + x\cdot\text{CMVL} + \text{Na}^+$) in addition to a less intense distribution of the potassiated ions ($\text{BnOH} + x\cdot\text{CMVL} + \text{K}^+$). We were surprised to see another less intense distribution, which we initially surmised was associated with water initiation ($\text{H}_2\text{O} + x\cdot\text{CMVL} + \text{Na}^+$). However, when the terminal hydroxy of **PCMVL** was acetylated with acetic anhydride and triethylamine, we observed in the resulting polymer sample an ca. 1.0:1.0 molar ratio of resonances for PhCH_2OCO -polymer to the terminal acetate CH_3CO_2 -polymer by ^1H NMR spectroscopy—indicating that there had been a negligible amount of water initiation in the **PCMVL** polymerization. This subset of ions with 90 amu less than that of the major set of (sodiated) ions likely arise from an ester pyrolysis reaction¹³ at any of the upstream backbone ester moieties, which, necessarily, fragments away the OBn-containing, initiating terminus, leaving a free CO_2H at the new terminus. Ionization by adduction of these species produces ions of 90 fewer amu's.

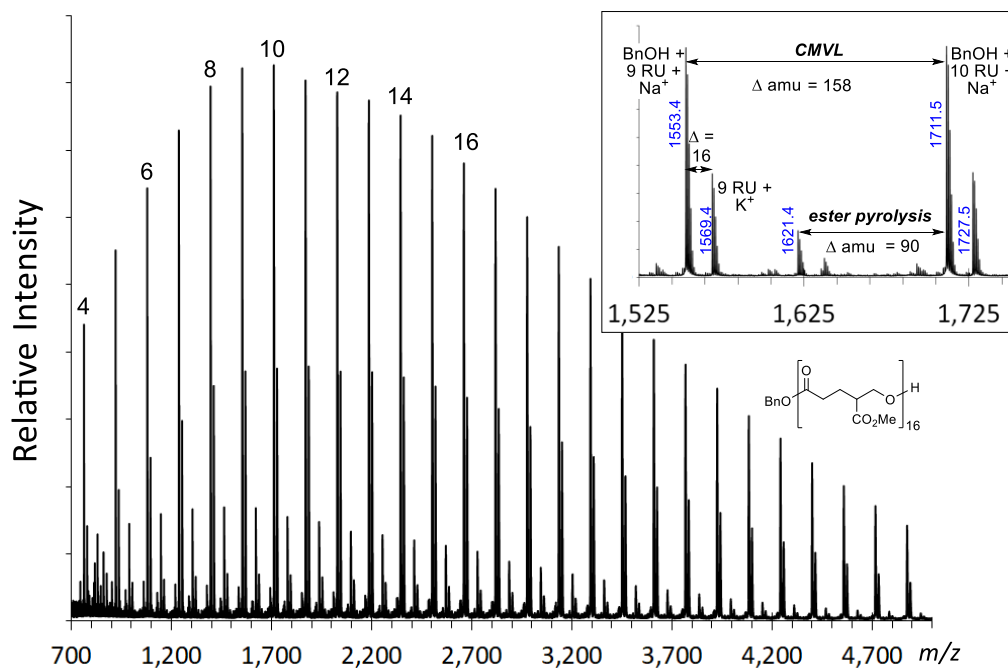


Figure 3.5 MALDI/TOF-MS spectrum (taken in reflectron mode) of pre-isomerized, linear **PCMVL** [initiated with benzyl alcohol ($M_n = 2.54 \text{ kg}\cdot\text{mol}^{-1}$ from ^1H NMR spectroscopy)] using dihydroxybenzene as a matrix. **CMVL** molar mass = $158 \text{ g}\cdot\text{mol}^{-1}$.

The mass spectrum of isomerized, branched **EQ-PCMVL** (Figure 3.6) shows significant differences from the mass spectrum of the precursor, linear **PCMVL**. Specifically, the most intense peaks are shifted to lower m/z , and overall a larger variety of types of ions within the range of one repeat unit (158 amu). The two main distributions arise from intramolecular transesterification of the terminal hydroxy on either a polymer backbone ester [red circle, ($\text{Na}^+ + \text{X}\cdot\text{CMVL}$)] or a side-chain methyl ester [blue diamond, ($\text{BnOH} + \text{X}\cdot\text{CMVL} + \text{Na}^+ - \text{MeOH}$)] to form, in either case, a cyclic (and hyperbranched) polymer.

An expansion of the **EQ-PCMVL** mass spectrum is shown in Figure S3.4 that more clearly shows the mass distributions associated with the two modes of cyclization (red circle and blue diamond) as discussed for Figure 3.6. Additionally, we observed (i) molar

mass distributions associated with ions containing two Bn groups [Figure S3.4, (2•BnOH + X•CMVL + Na⁺ – 2•MeOH)] and (ii) ester pyrolysis (analogous to **PCMVL**, loss of Bn) of the cyclized polymers.

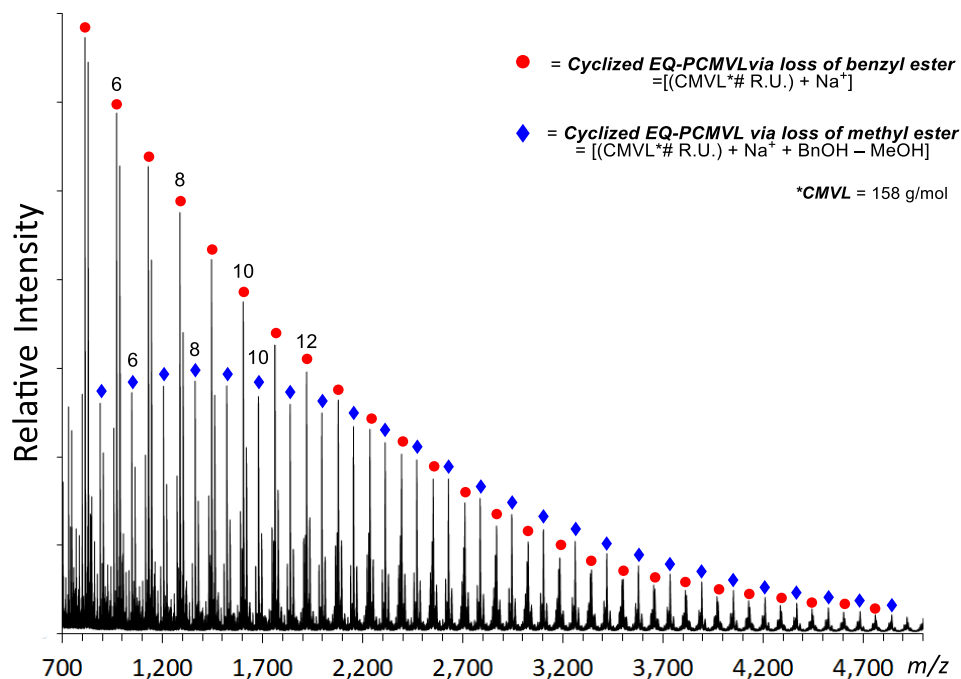


Figure 3.6 MALDI/TOF-MS spectrum taken in reflectron mode of **EQ-PCMVL** (isomerized from **PCMVL** with $M_n = 2.54 \text{ kg}\cdot\text{mol}^{-1}$ from ^1H NMR spectroscopy) using dihydroxybenzene as a matrix. **CMVL** molar mass = $158 \text{ g}\cdot\text{mol}^{-1}$. See expansion in Figure S3.4 for a set of specific amu values across a representative pair of ions differing by one (or two) repeat units.

This MALDI data indicated that isomerized **EQ-PCMVL** formed from (a low MW) **PCMVL** contained a large portion of hyperbranched polymers containing a ring (see green dotted line in Figure 2b). This feature quite likely arises from intramolecular transesterification of either a side-chain or mid-chain ester by the terminal hydroxy group, processes that are again supported by interpretation of the MALDI data.¹⁴ The result is a

lower than targeted molar mass, a feature also observed by light scattering SEC of higher MW samples of **EQ-PCMVL** (see SI).

3.4 Isomerization of *iso*CMVL to EQ-PCMVL

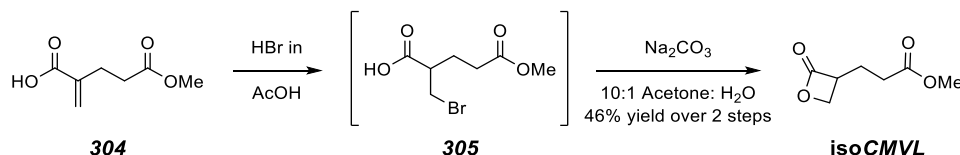


Figure 3.7 Two-step synthesis of *iso*CMVL from 2-methyleneglutarate **304**

*iso*CMVL is the β -lactone constitutional isomer of CMVL (Figure 3.7) and shares the same carbon skeleton. We wondered whether the isomeric homopolymer composed only of four-atom backbone repeat units **303b** [i.e., **P(*iso*CMVL)**, Figure 3.8a] could be prepared from *iso*CMVL. Moreover, could the overall isomerization to **EQ-PCMVL** be accessed from *iso*CMVL by way of **P(*iso*CMVL)**? We synthesized *iso*CMVL in two steps from methacrylic acid analogue **304** (Figure 3.7), which was prepared using the same conditions we used in Chapter 2. Exposure of **304** to anhydrous HBr in acetic acid cleanly gave the hydrobrominated acid ester **305**. Subsequent base treatment of **305** afforded *iso*CMVL in 46% yield over two steps (Figure 3.7).

Treating *iso*CMVL with zinc catalyst **302** (and BnOH as initiator) gave rise, initially, to the methyl ester resonance at 3.67 ppm, consistent with formation of **P(*iso*CMVL)**. Again, growth of resonances associated with **303a** and **303c** at 3.71 ppm, indicative of the onset of formation of **EQ-PCMVL**, was observed prior to full consumption of the β -lactone (see Figure S3.2 for a kinetic scan analogous to that shown in Figure 3.3). Under these polymerization conditions, **P(*iso*CMVL)** is, like **PCMVL**, a metastable state. Indeed, treating preformed, linear **P(*iso*CMVL)**¹⁵ with catalyst **302** gave **EQ-PCMVL** (see associated experimental section).

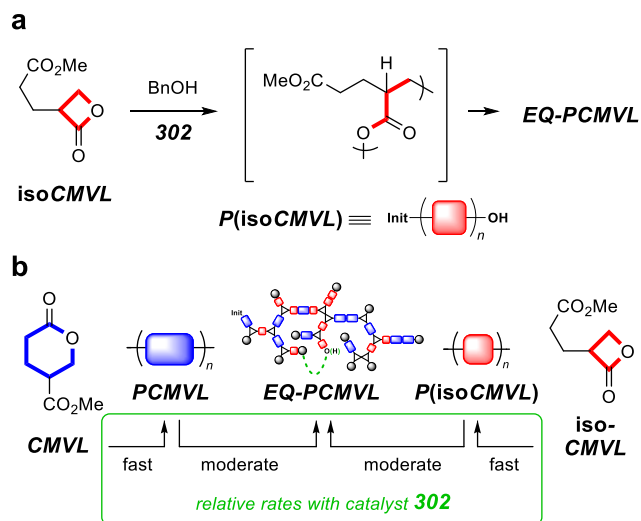


Figure 3.8 (a) ROTEP of the β -lactone *isoCMVL* to (linear) *P(isoCMVL)* and *EQ-PCMVL*. (b) Relative rates of ROTEP of *CMVL* and *isoCMVL* and their convergence to *EQ-PCMVL* with **302**.

The following overall picture emerges (Figure 3.8b). i) The rates of ROTEP of *CMVL* and *isoCMVL* catalyzed by **302** are quite similar to one another. ii) The isomerizations of each of the respective homopolymers are again (and surprisingly), similar to one another. iii) Each isomerization is somewhat slower than the ROTEP but sets in prior to equilibrium consumption of each lactone monomer. iv) Finally, both reactions eventually converge to essentially the same final resting state—*EQ-PCMVL*.

3.5 Chemical recycling through methanolysis of *EQ-PCMVL*

To gain one final piece of evidence for the structure of *EQ-PCMVL*, as well as to demonstrate recovery of *CMVL* from *EQ-PCMVL*, we performed a two-stage chemical recycling. Namely, *EQ-PCMVL* was fully degraded in methanol containing H_2SO_4 (Figure 3.9). The intermediate dimethyl ester **306**, the common sink from methanolysis of all four subunits **303a–d**, was then converted to *CMVL* using $\text{Sn}(\text{Oct})_2$. These conditions allowed continuous removal of recovered monomer from a dynamic mixture of species

interconverting by ROTEP/retro-ROTEP events. The highest mass recovery in this two-stage degradation was 84%, with an approximate 4:1 ratio of **CMVL** to **306**.

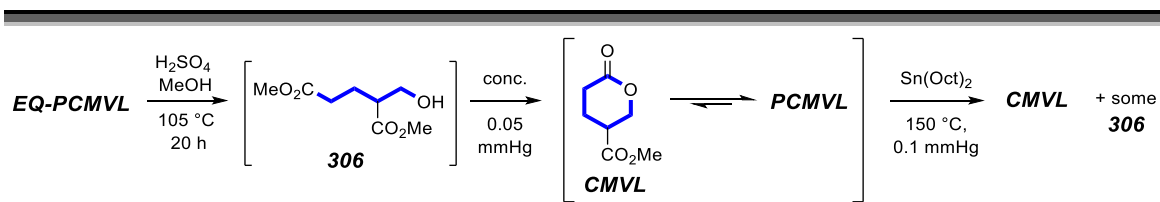


Figure 3.9 Chemical recycling of **EQ-PCMVL**

We were surprised to see that other Brønsted acid catalysts were unable to affect this two-stage recycling. We initially used HCl in order to easily remove the acid after methanolysis *in vacuo*. However, a large release of pressure was noticeable when opening the sealed methanolic **EQ-PCMVL** solution (even when cooled to -15 °C prior to opening), and the degradation never reached full conversion even at long reaction times and high HCl loadings. These observations suggest that HCl and MeOH were reacting to form methyl chloride, a volatile gas at room temperature, which incapacitate the acid catalyst to further catalyze the polymer methanolysis.

We also attempted to use poly(phosphoric acid) or diphenyl phosphate (DPP) to use as the catalyst for *both* the methanolysis and reverse-ROTEP steps. Yet, each of these catalysts were unable to degrade **EQ-PCMVL** or invoke the second stage of the degradation. We initially felt that esterification of DPP to form the diphenyl monoalkyl phosphate was occurring, but ³¹P NMR spectroscopy revealed only one phosphorous signal that we confirmed to be DPP using NMR spectroscopy. The heterogeneous catalyst Amberlyst 15 did also effect this two-stage transformation but required large catalyst loadings to promote the degradation in reasonable reaction times and temperatures.

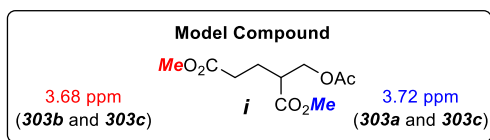
3.6 Conclusion

In conclusion, we have demonstrated an unprecedented isomerization pathway by which a preformed linear polymer is converted to a highly branched architecture. The process here involved multiple transesterification events and is a direct ramification of the use of monomeric lactones containing a carboalkoxy substituent. The nature of the catalyst can influence whether the linear homopolymer from initial ROTEP predominates or whether the isomerization to a highly branched polymer ensues. Degradation studies of these isomeric polymers were essential for deducing the structures of each. The work here also demonstrates that two isomeric monomers can converge, through the intermediacy of isostructural, linear homopolymers, to the same, equilibrated, final resting state—an intricate example of a classic chemical principle. Finally, we note that other lactones bearing a pendant ester group should function in a very similar fashion and that the fundamental concepts exposed through this investigation should allow for the introduction of branching into other families of polyesters, a potential strategy for management of polyester properties.¹⁶

3.7 References

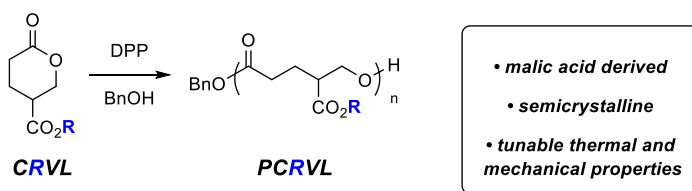
- ¹ (a) Viot, B. I.; Lederer, A. Hyperbranched and highly branched polymer architectures—Synthetic strategies and major characterization aspects. *Chem. Rev.* **2009**, *109*, 5924–5973. (b) Zheng, Y.; Li, S.; Weng, Z.; Gao, G. Hyperbranched polymers: Advances from synthesis to applications. *Chem. Soc. Rev.* **2015**, *44*, 4091–4130.
- ² Dong, Z.; Ye, Z. Hyperbranched polyethylenes by chain walking polymerization: Synthesis, properties, functionalization, and applications. *Polym Chem.* **2012**, *3*, 286–301.
- ³ Trollsås, M.; Löwenhielm, P.; Lee, V. Y.; Möller, M.; Miller, R. D.; Hedrick, J. L. New approach to hyperbranched polyesters: Self-condensing cyclic ester polymerization of bis(hydroxymethyl)-substituted ϵ -caprolactone. *Macromolecules* **1999**, *32*, 9062–9066.
- ⁴ Fréchet, J. M. J.; Henmi, M.; Gitsov, I.; Aoshima, S.; Leduc, M. R.; Grubbs, R. B. Self-condensing vinyl polymerization: An approach to dendritic materials. *Science* **1994**, *263*, 1080–1083.
- ⁵ A related concept, using reversible Diels-Alder reactions and resulting in architectural reorganization of a preformed polymer was recently reported. Sun, H. Kabb, C. P.; Dai, Y.; Hill, M. R.; Ghiviriga, I.; Bapat, A. P.; Sumerlin, B. S. Macromolecular metamorphosis via stimulus-induced transformations of polymer architecture. *Nat. Chem.* **2017**, *9*, 817–823.
- ⁶ Fahnhorst, G. W.; Hoyer, T. R. A carbomethoxylated polyvalerolactone from malic acid: Synthesis and divergent chemical recycling. *ACS Macro Lett.* **2018**, *7*, 143–147.
- ⁷ (a) von Pechmann, H. On the cleavage of α -oxyacids. *Liebigs Ann. Chem.* **1891**, *264*, 261–309. (b) Wiley, R. H.; Smith, N. R. Coumalic acid. *Org. Synth.* **2003**, *31*, 23–24.
- ⁸ (a) Zhu, J.-B.; Watson, E. M.; Tang, J.; Chen, E. Y.-X. A synthetic polymer system with repeatable chemical recyclability. *Science* **2018**, *360*, 398–403. (b) Hong, M.; Chen, E. Y.-X. Chemically recyclable polymers: A circular economy approach to sustainability. *Green Chem.* **2017**, *19*, 3692–3706. (c) Hong, M.; Chen, E. Y.-X. Completely recyclable biopolymers with linear and cyclic topologies via ring-opening polymerization of γ -butyrolactone. *Nat. Chem.* **2016**, *8*, 42–49. (d) Schneiderman, D. K.; Vanderlaan, M. E.; Mannion, A. M.; Panthani, T. R.; Batiste, D. C.; Wang, J. Z.; Bates, F. S.; Macosko, C. W.; Hillmyer, M. A. Chemically recyclable biobased polyurethanes. *ACS Macro Lett.* **2016**, *5*, 515–518.
- ⁹ Williams, C. K.; Breyfogle, L. E.; Kyung Choi, S.; Nam, W.; Young Jr., V. G.; Hillmyer, M. A.; Tolman, W. B. A highly active zinc catalyst for the controlled polymerization of lactide. *J. Am. Chem. Soc.* **2003**, *125*, 11350–11359.

- ¹⁰ The resonance at 3.71 ppm reflects the total content of both **3a** and **3c** whereas that at 3.67 ppm reflects the total amount of the **3b** and **3c** subunits. The ¹H NMR methyl ester resonances of the bis-methyl ester **i** (prepared by methanolysis of **CMVL** followed by acetylation, see SI) are nearly identical to those in **PCMVL** and **EQ-PCMVL**.



- ¹¹ Rule of six: "In reactions involving addition to an unsaturated function containing a double bond, the greater the number of atoms in the six position the greater will be the steric effect." (a) Newman, M. S. Some observations concerning steric factors. *J. Am. Chem. Soc.* **1950**, 72, 4783–4786. (b) Newman, M. S. In *Steric effects in organic chemistry*; Newman, M. S., Ed.; Wiley: New York, 1956; p 206.
- ¹² (a) Gaborieau, M.; Castignolles, P. Size-exclusion chromatography (SEC) of branched polymers and polysaccharides. *Anal. Bioanal. Chem.* **2011**, 399, 1413–1423. (b) McKee, M. G.; Unal, S.; Wilkes, G. L.; Long, T. E. Branched polyesters: Recent advances in synthesis and performance. *Prog. Polym. Sci.* **2005**, 30, 507–539.
- ¹³ Ladavière, C.; Lacroix-Desmazes, P.; Delolme, F. First systematic MALDI/ESI mass spectrometry comparison to characterize polystyrene synthesized by different controlled radical polymerizations. *Macromolecules* **2009**, 42, 70–84.
- ¹⁴ Dušek, K.; Šomvásky, J.; Smrdková, M.; Simonsick, Jr., W. J.; Wilczek, L. Role of cyclization in the degree-of-polymerization distribution of hyperbranched polymers. Modeling and experiment. *Polym. Bull.* **1999**, 42, 489–496.
- ¹⁵ We attempted to polymerize *iso***CMVL** to the linear **P(isoCMVL)** using catalysts such as Al(O^{*i*}Pr)₃, DPP, and Sn(Oct)₂. However, we were unable to obtain the linear polymer and instead formed **EQ-PCMVL** with varying levels of branching. Fortunately, in two separate occasions a sample of neat *iso***CMVL** slowly polymerized over the course of ca. 3–4 months to the homopolymeric, linear **P(isoCMVL)** while stored in a nitrogen-filled glovebox. This linear **P(isoCMVL)** was enough to be used for characterization (SEC, TGA, DSC, NMR, degradation).
- ¹⁶ Corneillie, S.; Smet, M. PLA architectures: The role of branching. *Polym. Chem.* **2015**, 6, 850–867.

**Chapter 4. Tough and flexible carboalkoxylated polyvalerolactones
from malic acid: Influence of the carboalkoxy sidechain on polymer
thermal and mechanical properties**



Summary: In this chapter, eight 4-carboalkoxyvalerolactones (**CRVLs**), which vary in their alkyl sidechains, were synthesized from malic acid (or methyl acrylate) and subjected to ring-opening transesterification polymerization (ROTEP) using diphenyl phosphate [DPP, (PhO)₂PO₂H] as a catalyst. Each **CRVL** produced a semicrystalline poly(4-carboalkoxyvalerolactone) (**PCRVL**), and the alkyl group on each carboalkoxy directly influenced the thermal transitions of these polyesters. Polymerizations at 70 °C to synthesize high molecular weight samples led to polyesters containing very small amounts of branching, which was supported using ¹H NMR spectroscopy, MALDI spectrometry, size-exclusion chromatography, and eliminative degradation. Mechanical testing of these lightly branched, high molecular weight samples revealed that these polyesters are tough (up to 88 ± 33 MJ•m⁻³) and flexible [Young's modulus (*E*) up to 186 ± 13 MPa]. Importantly, these tough and flexible thermoplastics derived from malic acid are, in theory, chemically recyclable by two independent pathways.

4.1 Introduction

With the growing demand to replace petroleum-derived plastics with biobased alternatives, polyesters such as poly(lactic acid) (PLA) and poly(3-hydroxyalkanoates) [P(3-HAs)]¹ have emerged as leading replacements. However, broad applicability of these polymers has been limited due to their relatively narrow range of properties.² Research has focused on modifying the mechanical properties of these polymers through, for example, the incorporation of branching³⁻⁵ or the use of comonomers to prepare statistical⁶ or block copolymers.⁷⁻⁹ Alternatively, there remains a need to explore new biobased monomers and polymers with tunable and complementary properties to those currently available.

Sidechain substituents play an important role in dictating the thermal and mechanical properties of polymers.¹⁰⁻¹² The differences can be either dramatic [e.g., the methyl group in poly(propylene) vs. the carboxyl group in poly(acrylic acid)] or subtle in nature. That is, even slight modifications in backbone substituents can promote useful changes in polymer properties.^{13,14} These subtle changes are exemplified by poly[alkyl (meth)acrylates], where glass transition temperatures (T_g s) and entanglement molecular weights (M_e s) are readily manipulated by modifying the alkyl chain on the monomer used for polymerization.¹⁵

In Chapter 2,¹⁶ we demonstrated that poly(4-carbomethoxyvalerolactone) [PCMeVL, Figure 4.1a] from CMeVL has thermal properties distinct from alkyl-substituted valerolactones.¹⁷ Importantly, CMeVL is the first racemic substituted valerolactone to afford a semicrystalline polyester. PCMeVL can also be chemically recycled by two independent routes: (i) reverse-ring-opening transesterification polymerization (reverse-ROTEP) back to CMeVL and (ii) base-induced eliminative degradation to a methacrylate analogue. The latter chemical recycling pathway is enabled

by the presence of the methyl ester on every repeat. Additionally, this side chain methyl ester allowed for a post-polymerization isomerization from linear **PCMeVL** to an isomeric, hyperbranched polyester using a highly active zinc catalyst (Chapter 3).¹⁸

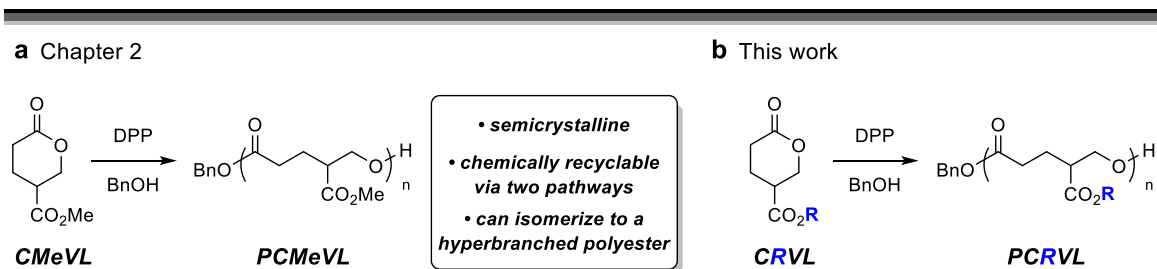


Figure 4.1 (a) Previous work with **CMeVL** to its polyester, **PCMeVL** (b) This work exploring the influence of the alkoxy group on the properties of **PCRVLs**

Herein we report the synthesis and thermal and mechanical properties of poly(4-carboalkoxyvalerolactones) (**PCRVLs**, Figure 4.1b) using [DPP, (PhO)₂PO₂H] as the catalyst for ROTEP of **CRVL** monomers. The **PCRVLs** differ in the identity of the alkyl chain within their sidechain carboalkoxy group. This subtle modification leads to novel polyesters with complimentary and tunable properties to **PCMeVL** (as well as other sustainable polymers). These polymers should also be chemically recyclable in two ways and may be capable of a post-polymerization isomerization to a hyperbranched polyester.

4.2 Results and discussion

4.2.1 Monomer syntheses

Monomer **CRVLs** containing an ethyl (**CEtVL**), isopropyl (**CIPrVL**), and *n*-butyl (**CnBuVL**) carboalkoxys were synthesized following our previous procedure for **CMeVL** (Figure 4.2).¹⁶ Malic acid (**401**) was heated in sulfuric acid (65 °C for 16 to 24 h) to form coumalic acid (**402-H**) as an intermediate.^{19,20} Ethanol, isopropanol, or *n*-butanol was

added directly to this reaction mixture (65 °C for 4 to 18 h) to form alkyl coumalates **402-R** in 37–59% yield following distillation and a recrystallization. Hydrogenation of **402-R** using Pd/C and hydrogen gas (ca. 80 psi) gave **CEtVL**, **CiPrVL**, and **CnBuVL** in good yields (56–61%). Yet, 2-methylglutaric acid monoalkyl esters were always observed (compounds S401, S402, and S403). These byproducts were easily removed from the **CRVLs** by extraction into aqueous base.

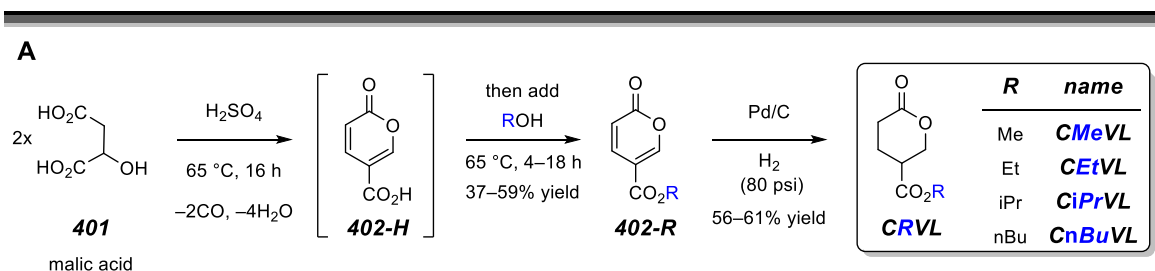


Figure 4.2 Two-step synthesis of **CRVL** (*R* = Me, Et, iPr, nBu) from malic acid (**401**).

tert-Butyl coumalate (**402-tBu**) was much more difficult to synthesize from **402-H**. Common methods to convert carboxylic acids to *tert*-butyl esters such as isobutylene with sulfuric acid or conversion of coumalic acid to coumalic acid chloride, followed by the addition of *t*-BuOH and base, led to no conversion and low yields (ca. 15%), respectively.²¹ Exposure of **2-H** to di-*tert*-butyl dicarbonate [(Boc)₂O] with DMAP and *t*-BuOH also afforded low yields (10–35%, Figure 4.3)^{22,23} but provided enough **2-tBu** to explore preliminary polymer properties, following hydrogenation of **2-tBu** to **CtBuVL** (67% yield).

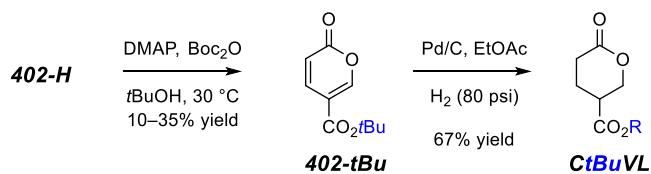


Figure 4.3 Synthesis of **CtBuVL** from coumalic acid (**402-H**)

To expand the set of these **CRVLs**, we made 4-carbobenzoxy, 4-carbo(2-ethylhexoxy), and 4-carboundecoxyvalerolactones [**CBnVL**, **C²EtHexVL**, and **CC₁₁VL** (Figure 4.4)]. The two-step synthesis starting from malic acid and sulfuric acid previously discussed (Figure 4.2) was not suitable for this series because these less polar alcohols were not miscible with the H_2SO_4 reaction mixture. Also, addition of these alcohols to coumalic acid chloride (not shown) often led to esterification of the pyrone ester moiety. Deprotonation of **402-H** with Na_2CO_3 in DMF and displacement of an alkyl bromide was effective for making **402-R** that contained longer alkyl chains. Hydrogenation of these **402-Rs** gave similar conversion of **CRVLs** and 2-methylglutaric acid monoalkyl esters. However, these two products were more difficult to separate by simple partitioning into a basic aqueous solution.

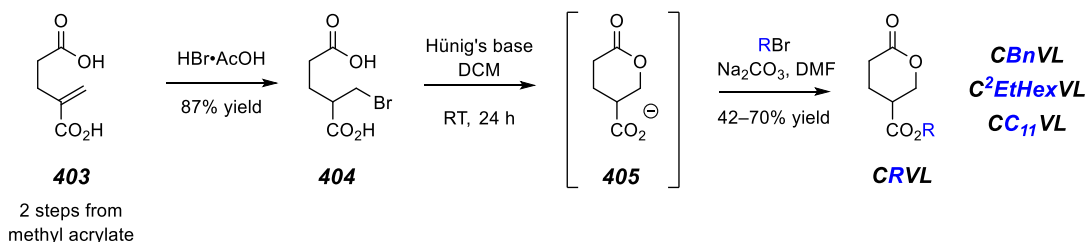


Figure 4.4 Two-step synthesis of **CBnVL**, **C²EtHexVL**, and **CC₁₁VL** from **403**.

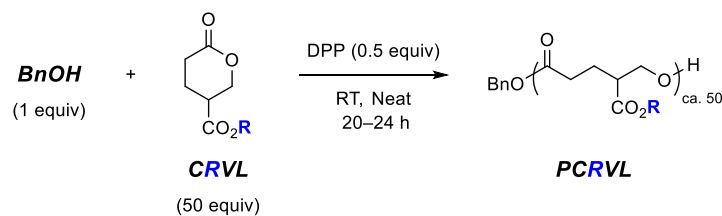
These challenges led us to develop an alternative synthesis to obtain **CRVLs** with longer alkyl chains (Figure 4.4). 2-Methyleneglutaric acid (**403**, prepared in two steps from methyl acrylate)²⁴ was treated with $\text{HBr}\cdot\text{AcOH}$ to give bromodiacid **404**. Exposure of **404**

to Hünig's base in DCM caused cyclization to lactone **405**, which was then alkylated to **CRVLs** using Na_2CO_3 and alkyl bromides. This two-step sequence afforded **CBnVL**, **C²EtHexVL**, and **CC₁₁VL** in 42–70% yield, in these instances following chromatographic purification on silica gel.

4.2.2 Synthesis and characterization of low molecular weight PCRVLs (ca. 50 repeat units per chain)

Each of these seven **CRVLs** was polymerized to relatively low molecular weight **PCRVLs** using a 50:1:0.5 ratio of **CRVL**:BnOH:DPP (neat, ambient temperature, 20–24 h, Figure 4.5). Each **PCRVL** was purified by precipitation and characterized by NMR spectroscopy, size-exclusion chromatography (SEC), thermogravimetric analysis (TGA), and differential scanning calorimetry (DSC) (tabulated in Figure 4.5). The measured molar masses (¹H NMR and SEC) for these samples matched well with those targeted, and the SEC traces exhibited unimodal distributions with low dispersities (D), suggesting that the polymerization proceeded without intermolecular transesterification of the growing polymer ester or sidechain esters. TGA analysis also showed reasonable degradation temperatures for polyesters.²⁵ The lowest degradation occurred for **PCtBuVL** and the highest for **PCBnVL** (1% mass loss).

Notably, each **PCRVL** was semicrystalline, and the thermal characteristics [T_g , crystallization temperature (T_c), melting temperatures (T_m), and enthalpy of melting (ΔH_m)] of each was influenced by the nature of the alkyl group in the sidechain esters (Table in Figure 4.5). In the linear alkyl series, polymers with longer alkyls in the sidechain esters had lower T_g s (–18 °C for **PCMeVL** to <–75 °C for **PC₁₁VL**). Overall, the lowest T_m was observed for **PC²EtHexVL** (–7 °C) while the highest T_m corresponded to **PCtBuVL** (95 °C). The undecyl-containing **PC₁₁VL** showed an intermediate T_m to those of **PCMeVL**



| Polymer | —SEC + NMR— | | | —TGA— | —DSC— | | | |
|------------------------------|------------------|----------------|--------------------|------------------------|---------------|------------------|-----------------|--------------------------------------|
| | M_n (theor) | M_n (NMR) | \bar{D} (SEC) | T_d [[1%, 5%] °C] | T_g (°C) | T_c (°C) | T_m (°C) | ΔH_m (J·g ⁻¹) |
| <i>PCMeVL</i> ^a | 8.0 | - | - | 213, 263 | -18 | 32 | 68, 86 | 35.7 |
| <i>PCEtVL</i> | 8.7 | 8.2 | 1.1 | 218, 249 | -29 | n.o. | 52 ^d | 6.4 ^e |
| <i>PCiPrVL</i> | 9.4 | 8.9 | 1.0(3) | 228, 269 | -24 | 36 | 62 | 19.8 |
| <i>PCnBuVL</i> | 10.1 | 9.7 | 1.5 | 252, 292 | -44 | 11 | 50 | 30.4 |
| <i>PCtBuVL</i> | 10.1 | 11.7 | 1.2 | 197, 214 | -7 | 44 ^c | 95 | 30.7 |
| <i>PCBnVL</i> ^b | 11.2 | 12.6 | 1.1 | 289, 307 | -6 | n.o. | 47 ^d | 4.4 ^e |
| <i>PC²EtHexVL</i> | 13.6 | 13.3 | 1.2 | 226, 269 | -55 | -29 ^c | -7 | 13.4 |
| <i>PCC₁₁VL</i> | 15.0 | 14.1 | 1.2 | 236, 268 | <-75 | 16 | 55 | 30.8 |

Figure 4.5 Polymerization of **CRVLs** to **PCRVLs** using DPP and benzyl alcohol (BnOH) neat at room temperature. Each **PCRVL** had ca. 50 repeat units per polymer chain. TGA data was taken using a heating rate of 10 °C·min⁻¹. DSC results were taken on the third heating cycle, and each DSC sample was cooled from 150 °C to -60 °C (5 °C·min⁻¹) and subsequently heated to 150 °C (5 °C·min⁻¹) for analysis. No T_c was observed for **PCEtVL** or **PCBnVL** (n.o. = not observed). ^a Data taken from our previous report.¹⁶ ^b Contains an acetylated end group (H=Ac). ^c T_c observed during cooling prior to heating cycle. ^d No T_m was observed on the third heating cycle and reported values were taken from the first, initial heating cycle.

and **PCnBuVL**, a phenomenon that suggests crystallization within both the backbone and sidechain alkyl moieties of **PC₁₁VL**. Finally, the ΔH_m s and the crystallization rates in **PCRVLs** varied greatly from sample to sample. In particular, **PCEtVL** and **PCBnVL** were the slowest to crystallize and no melting endotherms were observed for either of these samples after the initial heating cycle.

Last, we repeated the polymerization for **PCtBuVL**, **PC²EtHexVL**, and **PC₁₁VL** and monitored their monomer conversion to equilibrium. Each monomer reached 97% to 99% equilibrium conversion, indicating that the alkyl substituents play a minor role in the free energy of polymerization.

4.2.3 High molecular weight PCRVLs: Polymerization and molar mass distribution

PCMeVL, **PCEtVL**, **PCiPrVL**, and **PCnBuVL** were synthesized to molecular weights of ca. 100 kg•mol⁻¹ for use in uniaxial tensile testing (Figure 4.6a). Initial attempts to polymerize **CMeVL** to **PCMeVL** with a molar mass of ca. 100 kg•mol⁻¹ took 5 days to reach 90% conversion at room temperature (RT) with 0.4 mol% DPP. Viscosity and crystallization were apparently slowing the propagation rate. Therefore 70 °C was used as the polymerization temperature for each **CRVL**, which led to ca. 90% monomer conversion within 9 to 24 h.

The SEC chromatograms of **PCMeVL**, **PCEtVL**, **PCiPrVL**, and **PCnBuVL** revealed bimodal distributions wherein the larger peak had a slightly lower than targeted molar mass (Figure 4.6b). The shorter retention volume signal had ca. twice the M_w of that of the major component. This was surprising considering the lower molecular weight samples polymerized at room temperature were unimodal. Monitoring the SEC behavior of **PCiPrVL** (**CiPrVL**:BnOH = ca. 300:1) throughout the polymerization revealed that this bimodal distribution was present even at low monomer conversion. The polymer distribution thereafter broadened, and the bimodality persisted until ca. 9 h, when the two modes converged together (Figure 4.6c). These observations are consistent with slow intra- and intermolecular chain transfer reactions that occur during the polymerization.²⁶⁻²⁸

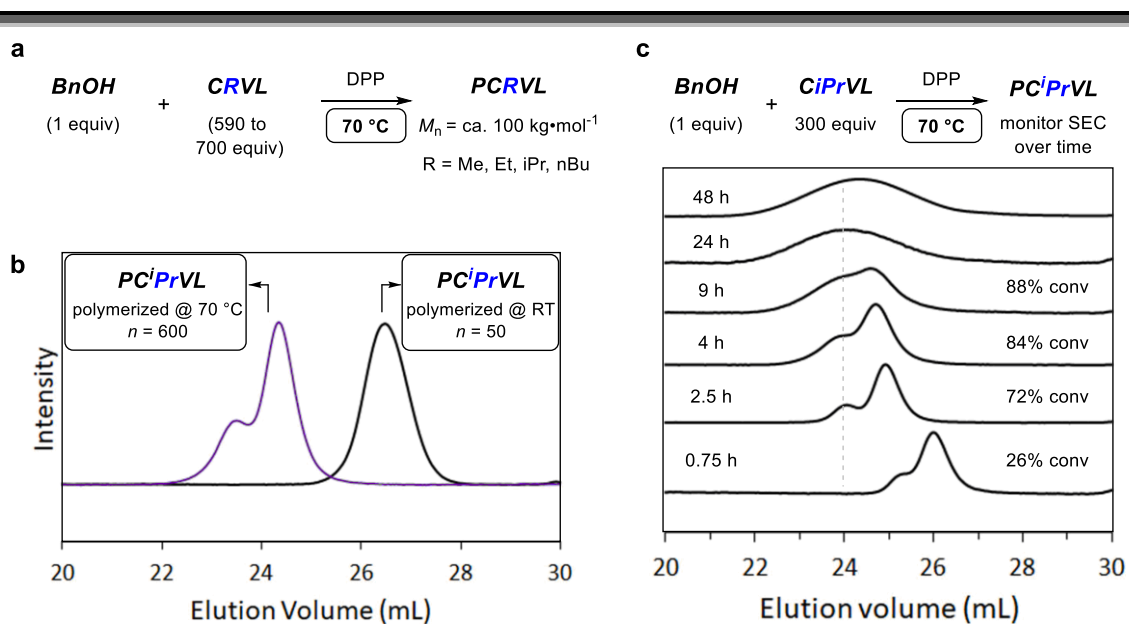


Figure 4.6 (a) Polymerization of **CRVLs** (R = Me, Et, iPr, nBu) to **PCRVLs** at 70 °C with targeted molar masses of ca. 100 kg•mol⁻¹. (b) The SEC behavior of **PCiPrVL** with ca. 600 (polymerized at 70 °C) and ca. 50 (polymerized at RT) repeat units per chain. (c) Overlaid normalized SEC distributions taken over the course of the polymerization for **CiPrVL** to **PCiPrVL** at 70 °C.

¹H NMR and MALDI analysis further supported these chain transfer reactions. For example, the ¹H NMR spectrum of **PCnBuVL** contained integrations corresponding to fewer terminal hydroxy end groups (POLY-CH₂OH) compared to initiator (PhCH₂O-) end group resonances. Additionally, MALDI analysis of **PCnBuVL** [number-average molecular weight (M_n) = ca. 2.5 kg•mol⁻¹ polymerized at 70 °C for 24 h] contained signals related to five unique series of molar mass distributions. The two most intense distributions corresponds to sodiated or potassiated linear **PCnBuVL** (BnOH + #•CnBuVL + Na⁺ or BnOH + #•CnBuVL + K⁺), and the next most intense series arises from backbone ester cleavage (pyrolytic to oligomeric alkenes and carboxylic acids), which occurs during the MALDI excitation.¹⁸ The remaining two, smallest series are indicative of intramolecular

cyclization (Figure 4.7) to form small amounts of cyclic chains. The first of these corresponds to cyclization of **PCnBuVL**'s terminal hydroxy group with a side chain ester (labeled as *loss of nBuOH*); the second supports cyclization of **PCnBuVL**'s terminal hydroxy into a backbone ester (labeled as *loss of BnOH*). These analyses suggest that the higher temperature for polymerization enables small amounts of transesterification reactions with the sidechain and backbone esters. The end result is that **PCRVL** contains small amounts of branched and cyclic polymer chains, which likely accounts for the bimodality observed in the SEC traces.

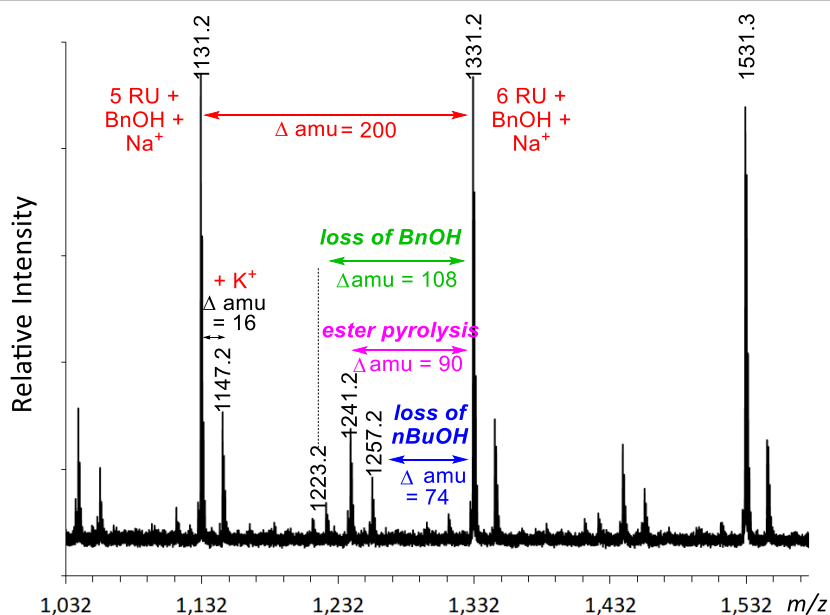


Figure 4.7 An expanded MALDI spectrum of **PCnBuVL** ($M_n = 2.5 \text{ kg}\cdot\text{mol}^{-1}$) polymerized with BnOH and DPP at 70 °C (see Figure S4.1 for a full MALDI spectrum). The two series containing the *loss of BnOH* and *loss of nBuOH* support that presence of small amounts of cyclic products in **PCnBuVL**

Other studies using **PCMeVL** support that branching and cyclization only occur a small fraction of the time. When **PCMeVL** was subjected to DBU to effect eliminative

degradation of the polymer backbone, very minor ^1H NMR resonances associated with degradative subunits characteristic of branched **PCMeVL** were present.¹⁸ Additionally, a polymerization of **CMeVL** with DPP at 85 °C for 4 days (polymerization at this temperature reaches equilibrium within hours) showed the growth of a new methyl ester singlet (3.67 ppm), which is again associated with light branching within **PCMeVL**.¹⁸

4.2.3 High molecular weight PCRVLs: Thermal and mechanical properties

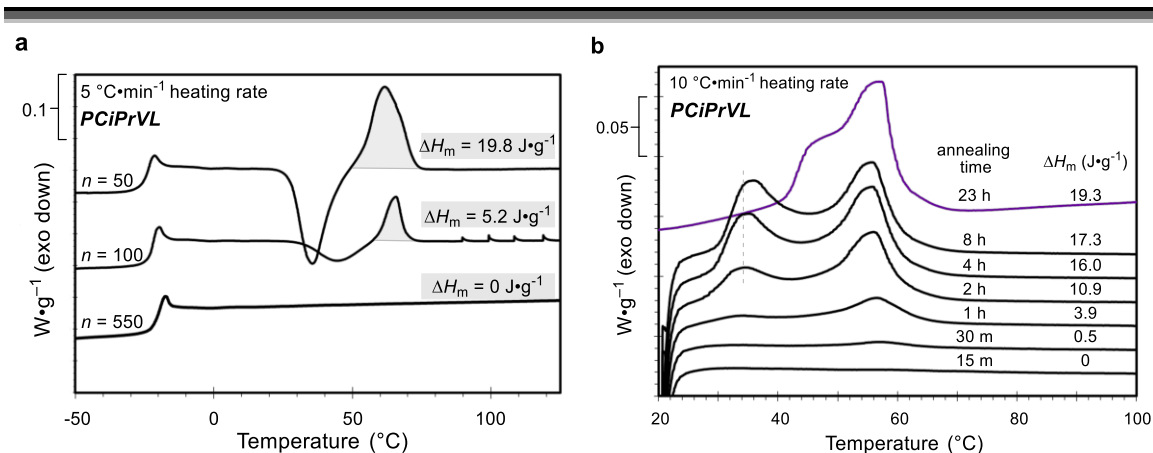


Figure 4.8 (a) DSC thermograms of **PCiPrVL** with varying M_n taken on the third heating cycle (5 °C·min⁻¹) that show a reduction in ΔH_m as the M_n of each sample increases. This suggests that the crystallization rate of each sample is reduced with higher M_n . (b) DSC annealing study of **PCiPrVL**. This sample was heated to 150 °C (10 °C·min⁻¹), cooled to and held at 22 °C for the annealing time, heated to 150 °C (10 °C·min⁻¹), and repeated. The top trace (23 h) is of the fully annealed bulk sample of **PCiPrVL** prior to mechanical testing.

The thermal behavior as assessed by DSC of each high molecular weight ($M_w = \text{ca. } 67\text{--}129 \text{ kg}\cdot\text{mol}^{-1}$) **PCRVL** was noticeably different than their analogous lower molecular weight (8–15 kg·mol⁻¹) samples. The DSC traces of three **PCiPrVL** samples (ca. 50, 100, and 550 repeat units per chain) showed similar ΔH_m s on their first heating cycle. However,

a reduction in the ΔH_m s was observed on the following heating cycles as the molecular weight of the sample increased until **PCiPrVL** with ca. 550 repeat units per chain showed no melting endotherm on the latter cycles (Figure 4.8a). This supports that the crystallization rate of each polymer sample is reduced as the molecular weight increases.²⁹

We studied the crystallization of each **PCRVL** using DSC heat-and-hold experiments for a range of temperatures (Figures S4.4, S4.6, S4.8, and S4.9) and lengths of time (Figure 4.8b and Figures S4.5, S4.7, and S4.10). An example of the effect of hold time is shown in Figure 4.8b. **PCiPrVL** was heated to 150 °C, cooled to (10 °C•min⁻¹) and held at 22 °C³⁰ for the indicated time, and reheated to 150 °C (10 °C•min⁻¹). The sample was again cooled to 22 °C, and this cycle was repeated for each of the subsequent hold times. These DSC traces (Figure 4.8b) show that little crystallization occurs within the first hour ($\Delta H_m = 3.9 \text{ J}\cdot\text{g}^{-1}$ at 1 h) of annealing, and that **PCiPrVL** crystallizes the most from 1 to 4 hours ($\Delta H_m = 16.0 \text{ J}\cdot\text{g}^{-1}$ at 4 h). After 4 h there is little change in the overall ΔH_m (final $\Delta H_m = 19.3 \text{ J}\cdot\text{g}^{-1}$). However, with longer annealing times the lower melting maximum slowly shifts to higher temperatures until, ultimately, reaching its resting state at 47 °C.

The DSC traces of the final, annealed, bulk samples of **PCMeVL**, **PCEtVL**, **PCiPrVL**, and **PCnBuVL** are shown in Figure 4.9. These samples show slightly higher T_g s and slightly lower T_m s than their analogous lower molecular weight samples (see Figure 4.5). Overall, **PCMeVL** has the highest T_m (49 and 78 °C) and the largest ΔH_m (35.4 J•g⁻¹). **PCnBuVL** has the lowest T_m (45 °C), and **PCEtVL** has the smallest ΔH_m (13.0 J•g⁻¹) in this series. The ΔH_m s, listed from largest to smallest are observed for **PCMeVL**, **PCnBuVL**, **PCiPrVL**, and **PCEtVL**.

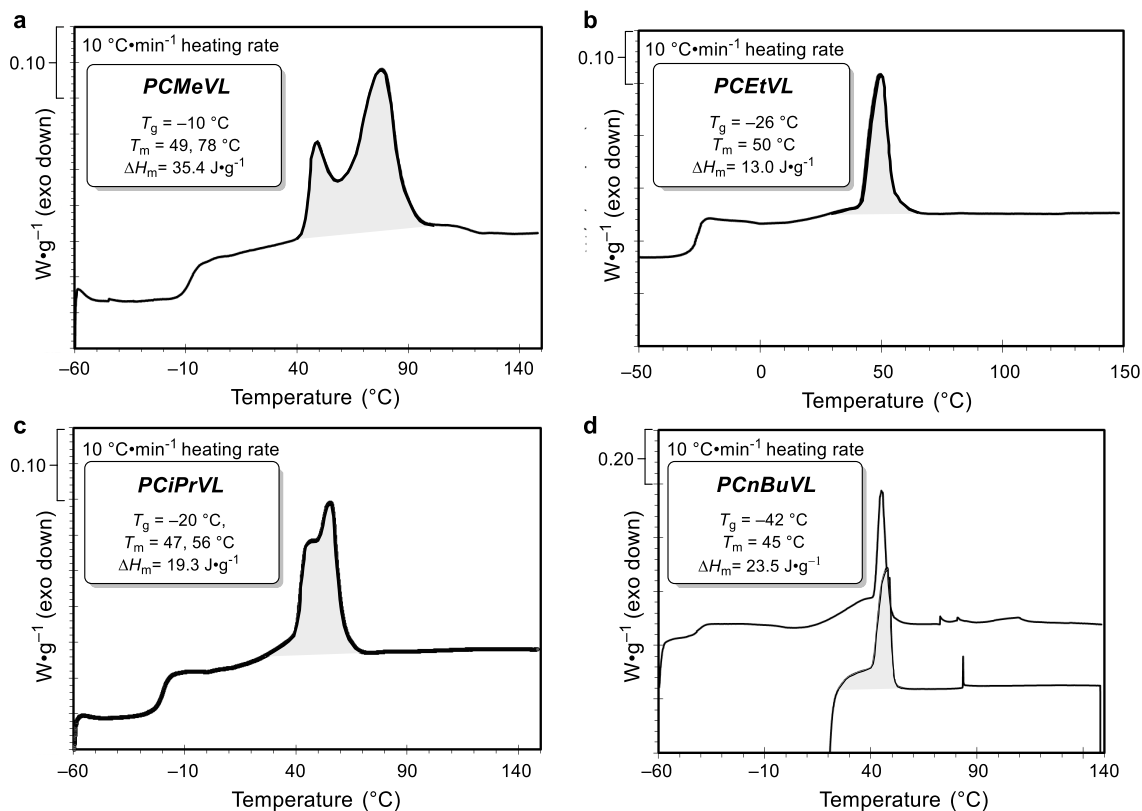


Figure 4.9 DSC thermograms of PCRVLs prior to mechanical testing. Each sample was annealed, cooled to $-60\text{ }^{\circ}\text{C}$, and heated to $150\text{ }^{\circ}\text{C}$ at a heating rate of $10\text{ }^{\circ}\text{C}\cdot\text{min}^{-1}$. Due to the broadening of the melting exotherm of **PCnBuVL** while cooling to $-60\text{ }^{\circ}\text{C}$, another DSC run was performed and cooled only to $20\text{ }^{\circ}\text{C}$ prior to heating to $150\text{ }^{\circ}\text{C}$. **PCMeVL** was annealed at $35\text{ }^{\circ}\text{C}$ for 24 h followed by room temperature for 4 days. **PCEtVL**, **PCiPrVL**, and **PCnBuVL** were annealed at room temperature for 5 days.

We next analyzed the high molecular weight PCRVLs using uniaxial tensile testing (Figure 4.10). Each sample was uniaxially extended at an extension rate of $50\text{ mm}\cdot\text{min}^{-1}$ until failure. The alkyl group on each carboalkoxy dramatically impacted these properties. In this series, **PCMeVL** has the most rigid, strongest, and toughest tensile features in terms of elastic modulus ($E = 186 \pm 13\text{ MPa}$), tensile strength ($\sigma_B = 34.5 \pm 9.1\text{ MPa}$), stress at yield ($\sigma_y = 11.4 \pm 0.3\text{ MPa}$), and toughness ($88 \pm 33\text{ MJ}\cdot\text{m}^{-3}$). **PCMeVL** also has a high

strain at break ($\epsilon_B = 480 \pm 100\%$). These tensile properties are comparable to many plastics used today (low-density polyethylene $E = \text{ca. } 250 \text{ MPa}$ and $\epsilon_B = \text{ca. } 400\text{--}500\%$, high-density polyethylene $\sigma_B = \text{ca. } 32 \text{ MPa}$).³¹ Additionally, **PCMeVL** behaves very similarly to poly(3-hydroxypropionate)³² and is much tougher than PLA (ca. $2 \text{ MJ}\cdot\text{m}^{-3}$ —two of the leading biobased polymers today).

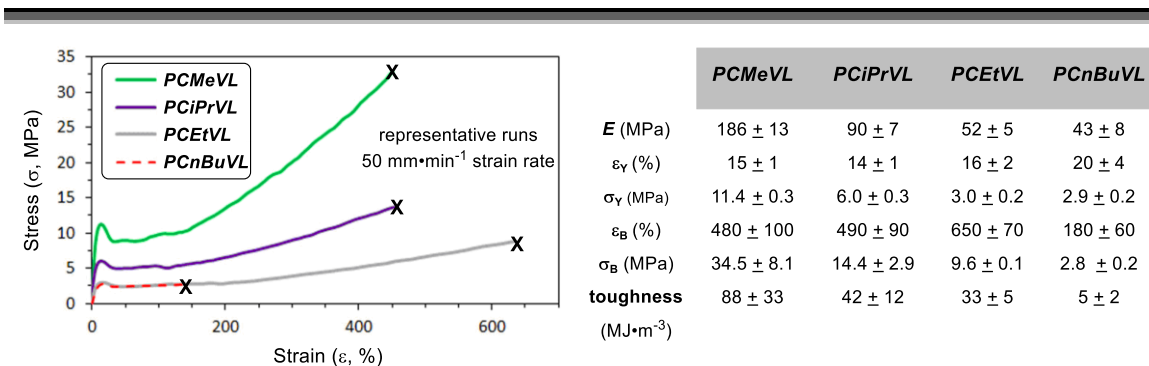


Figure 4.10 Stress-strain curves and tabulated results for four **PCRVLs**. Each sample was uniaxially extended at $50 \text{ mm}\cdot\text{min}^{-1}$ until sample failure. Plotted curves are representative samples of a minimum of five replicates.

The E , σ_B , σ_Y , and toughness of these samples decreases from **PCMeVL**, to **PCiPrVL**, to **PCEtVL**, and to **PCnBuVL**. In a contrasting fashion the strain at break (ϵ_B) decreases from **PCEtVL**, to **PCiPrVL**, to **PCMeVL**, and to **PCnBuVL**, respectively. **PCnBuVL**, which had the lowest tensile strength, strain at break, and toughness, was liquid-like after mechanical failure. This early failure may be due to strain-induced melting.

4.3 Conclusion

CRVLs that vary in their alkyl sidechains were synthesized from malic acid or methyl acrylate. The ROTEP of each **CRVL** using DPP as a catalyst resulted in thermoplastic, semicrystalline **PCRVLs**, which produced monomodal distributions when

polymerized at room temperature (for lower molecular weight samples) and bimodal distributions when polymerized at 70 °C (for higher molecular weight samples). ¹H NMR spectroscopy, MALDI spectrometry, size-exclusion chromatography, and eliminative degradation support that this bimodality is likely caused by chain transfer reactions during the polymerization that lead to very low levels of branching or cyclic polymers. The alkyl group on each carboalkoxy greatly influenced the T_g , T_m , ΔH_m , and mechanical properties of these tough, flexible, and chemically recyclable polyesters.

4.4 References

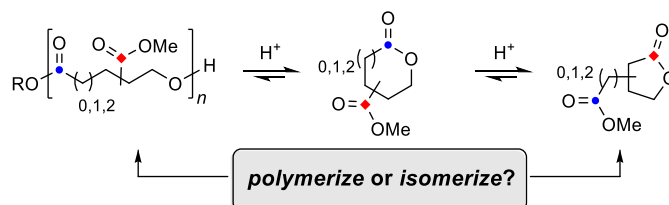
- ¹ Andreeßen, B.; Taylor, N.; Steinbüchel. Poly(3-hydroxypropionate): A promising alternative to fossil fuel-based materials. *Appl. Environ. Microbiol.* **2014**, *80* 6574–6582.
- ² Nagarajan, V.; Mohanty, A. K.; Misra, M. Perspective on polylactic acid (PLA) based sustainable materials for durable applications: Focus on toughness and heat resistance. *ACS Sustainable Chem. Eng.* **2016**, *4*, 2899–2916.
- ³ Corneillie, S.; Smet, M. PLA architectures: The role of branching. *Polym. Chem.* **2015**, *6*, 850–867.
- ⁴ Gu, L.; Xu, Y.; Fahnhorst, G. W.; Macosko, C. W. Star vs long chain branching of poly(lactic acid) with multifunctional aziridine. *J. Rheol.* **2017**, *61*, 785–796.
- ⁵ Haugan, I. N.; Maher, M. J.; Chang, A. B.; Lin, T.-P.; Grubbs, R. H.; Hillmyer, M. A.; Bates, F. S. – Consequences of grafting density on the linear viscoelastic behavior of graft polymers. *ACS Macro Lett.* **2018**, *7*, 525–530.
- ⁶ Qian, H.; Wohl, A. R.; Crow, J. T.; Macosko, C. W.; Hoyer, T. R. A strategy for control of “random” copolymerization of lactide and glycolide: Application to synthesis of PEG-*b*-PLGA block polymers having narrow dispersity. *Macromolecules*, **2011**, *44*, 7132–7140.
- ⁷ Aluthge, D. C.; Xu, C.; Othman, N.; Noroozi, N.; Hatzikiriakos, S. G.; Mehrkhodavandi, P. PLA-PHB-PLA triblock copolymers: Synthesis by sequential addition and investigation of mechanical and rheological properties. *Macromolecules* **2013**, *46*, 3965–3974.
- ⁸ Schneiderman, D. K.; Hillmyer, M. A. Scalable production of mechanically tunable block polymers from sugar. *Proc. Natl. Acad. Sci. U. S. A.* **2014**, *111*, 8357–8362.
- ⁹ Watts, A.; Kurokawa, N.; Hillmyer, M. A. Strong, resilient, and sustainable aliphatic polyester thermoplastic elastomers. *Biomacromolecules* **2017**, *18*, 1845–1854.
- ¹⁰ Bicerano, J. In *Prediction of Polymer Properties*, 3rd ed.; Marcel Dekker: New York, 2002.
- ¹¹ Boyle, B. M.; Heinz, O.; Miyake, G. M.; Ding, Y. Impact of the pendant group on the chain conformation and bulk properties of norbornene imide-based polymers. *Macromolecules* **2019**, *52*, 3426–3434.
- ¹² Ball-Jones, N. R.; Fahnhorst, G. W.; Hoyer, T. R.; Poly(isoprenecarboxylates) from glucose via anhydromevalonolactone. *ACS Macro Lett.* **2016**, *5*, 1128–1131.

-
- ¹³ Mark, H. F. Internal polyolefins and a few highly substituted polyvinyls. In *Advances in Polyolefins: The World's Most Widely Used Polymers*; Seymour, R. B., Cheng, T. C., Eds.; Springer: New York, 1987; pp 15–22, DOI: 10.1007/978-1-4757-9095-5.
- ¹⁴ Aime, J. P.; Ramakrishnan, S.; Chance, R. R.; Kim, M. W. The effect of substituent groups on polymer conformation in good solvent: Polyoctene and polydecene. *J. Phys. France* **1990**, *51*, 963–975.
- ¹⁵ Penzel, E. Polyacrylates. In *Ullmann's Encyclopedia of Industrial Chemistry*; Wiley-VCH Verlag GmbH & Co. KGaA: Weinheim, Germany, 2000; Vol. 28, pp 515–536.
- ¹⁶ Fahnhorst, G. W.; Hoye, T. R. A Carbomethoxylated polyvalerolactone from malic acid: Synthesis and divergent chemical recycling. *ACS Macro Lett.* **2018**, 143–147.
- ¹⁷ Schneiderman, D. K.; Hillmyer, M. A. Aliphatic polyester block polymer design. *Macromolecules* **2016**, *49*, 2419–2428.
- ¹⁸ Fahnhorst, G. W.; Stasiw, D. E.; Tolman, W. B.; Hoye, T. R. Isomerization of linear to hyperbranched polymers: Two isomeric lactones converge via metastable isostructural polyesters to a highly branched analogue. *ACS Macro Lett.* **2018**, *7*, 1144–1148.
- ¹⁹ von Pechmann, H. On the cleavage of α -oxyacids. *Liebigs Ann. Chem.* **1891**, 264, 261–309.
- ²⁰ Wiley, R. H.; Smith, N. R. Coumalic acid. *Org. Synth.* **1951**, *31*, 23–24.
- ²¹ Yamashita, T.; Nishikawa, H.; Kawamota, T. Scale-up synthesis of a deuterium-labeled cis-cyclobutane-1,3-dicarboxylic acid derivative using continuous photo flow chemistry. *Tetrahedron* **2019**, *75*, 617–623.
- ²² Takeda, K.; Akiyama, A.; Nakamura, H.; Takizawa, S.-I.; Mizuno, Y.; Takayanagi, H.; Harigaya, Y. Dicarbonates: Convenient 4-dimethylaminopyridine catalyzed esterification reagents. *Synthesis* **1994**, *10*, 1063–1066.
- ²³ Phillips, A. J.; Nasveschuk, C. G.; Henderson, J. A.; Liang, Y.; Chen, C.-L.; C.; Duplessis, M.; He, M.; Larzarski, K. Amine-linked C3-glutarimide degronimers for target protein degradation. World patent WO2017197051(A1). November 16, 2017.
- ²⁴ Tello-Aburto, R.; Lucero, A. N.; Rogelj, S. A. Catalytic approach to the MH-031 lactone: Application to the synthesis of geralcin analogs. *Tetrahedron Lett.* **2014**, *55*, 6266–6268.
- ²⁵ See, for example: Kopinke, F.-D.; Remmler, M.; Mackenzie, K.; Möder, M.; Wachsen, O. Thermal decomposition of biodegradable polyester—II. Poly(lactic acid). *Polym. Degrad. Stabil.* **1996**, *53*, 329–342.
- ²⁶ Baran, J.; Duda, A.; Kowalski, A.; Szymanski, R.; Penczek, S. Intermolecular chain transfer to polymer with chain scission: General treatment and determination of k_p/k_{tr} in L,L-lactide polymerization. *Macromol. Rapid Commun.* **1997**, *18*, 325–333.

-
- ²⁷ Penczek, S.; Duda, A.; Szymanski, R. Intra- and intermolecular chain transfer to macromolecules with chain scission. The case of cyclic esters. *Macromol. Symp.* **1998**, *132*, 441–449.
- ²⁸ Catalytic polymerization of a cyclic ester derived from a “cool” natural precursor. *Biomacromolecules* **2005**, *6*, 2091–2095.
- ²⁹ Hiemenz, P. C.; Lodge, T. P. Crystalline polymers: Kinetics of nucleation and growth. In *Polymer Chemistry*: CRC Press. **2007**; pp 536–545.
- ³⁰ The appropriate annealing temperature for these **PCRVLs** was determined by DSC heat and hold experiments at four to five temperatures near each samples T_c (see SI). The temperature that provided the largest ΔH_m after 1 hour was used to anneal each sample.
- ³¹ Compton, T. R. Mechanical properties of polymers. In *Physical Testing of Plastics*: Smithers Rapra; Shropshire, 2012; pp 1–148.
- ³² Meng, D.-C.; Shi, Z.-Y.; Wu, L-P.; Zhou, Q.; Wu, Q.; Chen, J.-C. Chen, G.-Q. Production and characterization of poly(3-hydroxypropionate-co-4-hydroxybutyrate) with fully controllable structures by recombinant *Escherichia coli* containing an engineered pathway. *Metab. Eng.* **2012**, *14*, 317–324.

Chapter 5. Effects of carboalkoxy sidechain position on lactone

monomers: Polymerization or isomerization?*



Summary: In this chapter we find that the position of a carboalkoxy group on a lactone ring is crucial to whether a carboalkoxylated lactone will polymerize or isomerize when treated with an acid catalyst [e.g., diphenyl phosphate, $(\text{PhO})_2\text{PO}_2\text{H}$]. These divergent pathways are dictated by the proximity between the propagating hydroxy and sidechain carboalkoxy. When a propagating hydroxy and the sidechain carbonyl carbon are positioned to form a more stable lactone isomer (e.g., butyro- or valerolactone), an intramolecular transesterification can occur (see discussion in Chapter 1 on thermodynamics of ring-opening transesterification polymerization). When isomerization occurs the newly formed lactone will either be non-polymerizable (if butyrolactone is formed) or further polymerize (if a valerolactone is formed) to a lightly branched polyester. Polymerization to a linear polyester is favorable when the propagating hydroxy and sidechain carbonyl are unable to undergo intramolecular transesterification.

* Monomers **501**^{2Me} and **501**^{2nBu} were synthesized and polymerized by Severin Thompson

5.1 Introduction

In Chapters 2 and 4, we described the ring-opening transesterification polymerization (ROTEP) of 4-carboalkoxyvalerolactones [**501^{4R}**, where **501^{#R}** represents a valerolactone ring **501** substituted at the # position with a carboalkoxy group and (**R**) as its alkyl group, Figure 5.1a] to the linear, semicrystalline poly(4-carboalkoxyvalerolactones) [**poly(501^{4R})**] using diphenyl phosphate [DPP, (PhO)₂PO₂H] as the catalyst.¹ These polymers could also be chemically recycled in two-independent pathways. The semicrystalline nature and the divergent chemical recycling are enabled through the presence of the sidechain ester on each repeat unit. Moreover, the alkoxy substituent on the sidechain ester plays a crucial role on the thermal and mechanical properties of these polymers (Chapter 4).

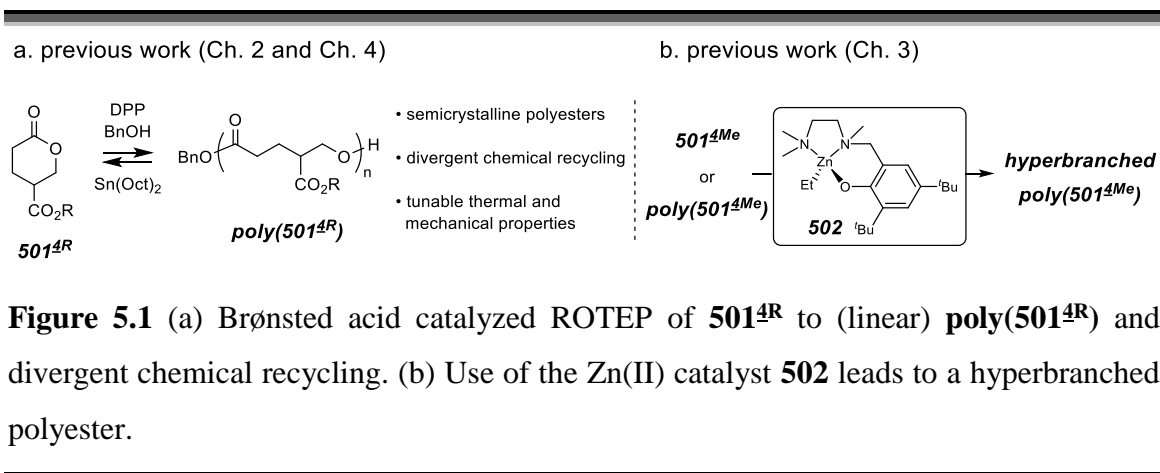


Figure 5.1 (a) Brønsted acid catalyzed ROTEP of **501^{4R}** to (linear) **poly(501^{4R})** and divergent chemical recycling. (b) Use of the Zn(II) catalyst **502** leads to a hyperbranched polyester.

In Chapter 3, we showed that the catalyst used for polymerization of **501^{4Me}** is vital to the architecture of the product polyester. The highly active zinc catalyst **502** polymerized **501^{4Me}** to a hyperbranched polyester **hyperbranched poly(501^{4Me})** (Figure 5.1b) and also enabled the post-polymerization isomerization of **poly(501^{4Me})** to **hyperbranched poly(501^{4Me})**.² This phenomenon occurs through multiple intermolecular and

intramolecular transesterifications of the polymer terminal hydroxy with the sidechain ester. In this case, the ester sidechain is now reactive under these polymerization conditions—contrary to what we observed with DPP at room temperature—when the organometallic catalyst **502** is used for polymerization.

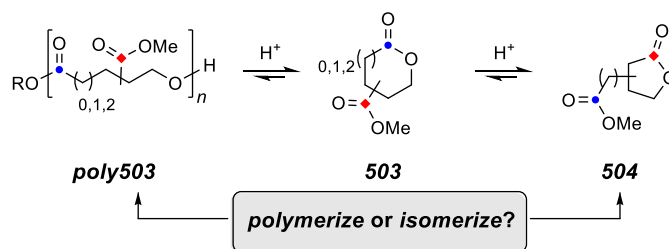


Figure 5.2 This work aims to develop a better understanding of how carboalkoxy positioning on a lactone ring influences whether a carboalkoxylated lactone will polymerize or isomerize.

In this chapter, we explore the influence of the *carboalkoxy position* on valero- and caprolactones to understand the reactivity of these potential monomers with an acid catalyst. The position of alkyl substituents on lactone monomers has been reported to alter the rates of polymerization and entanglement molecular weights (see Chapter 1).³ However, previous reports suggest that carboalkoxylated lactones can have another level of reactivity that can severely alter or inhibit polymerization (see Table 1.1 and discussion below).⁴ We find that the position of the sidechain ester can either (i) be unreactive in the polymerization and lead to a linear polyester such as **poly(503)** (polymerized from **503**); (ii) be moderately reactive and afford a lightly branched polyester (not shown); or (iii) be highly reactive and terminate the polymerization by isomerization to a non-polymerizable butyrolactone **504** (Figure 5.2). The project described herein is the furthest from completion, and the motivation for this chapter is to offer insight from preliminary observations and findings to provide guidance for future work on this project.

5.2 Monomer syntheses

5.2.1 Carboalkoxylated valerolactones

We first synthesized 2-carboethoxyvalerolactone (**501^{2Et}**) by α -functionalizing valerolactone (**505**) using sodium ethoxide and diethyl carbonate (**506**) in yields ranging from 40–55% (Figure 5.3a).⁵ To our surprise, similar conditions with sodium methoxide and dimethyl carbonate or sodium butoxide with dibutyl carbonate were unsuccessful; this likely arises from the low solubility of the alkoxide in the dialkyl carbonate solution. However, the use of lithium diisopropylamide (LDA) with methyl or butyl chloroformate in THF proved to be a viable alternative to obtain **501^{2Me}** and **501^{2nBu}** (monomer structures shown in Figure 5.6).

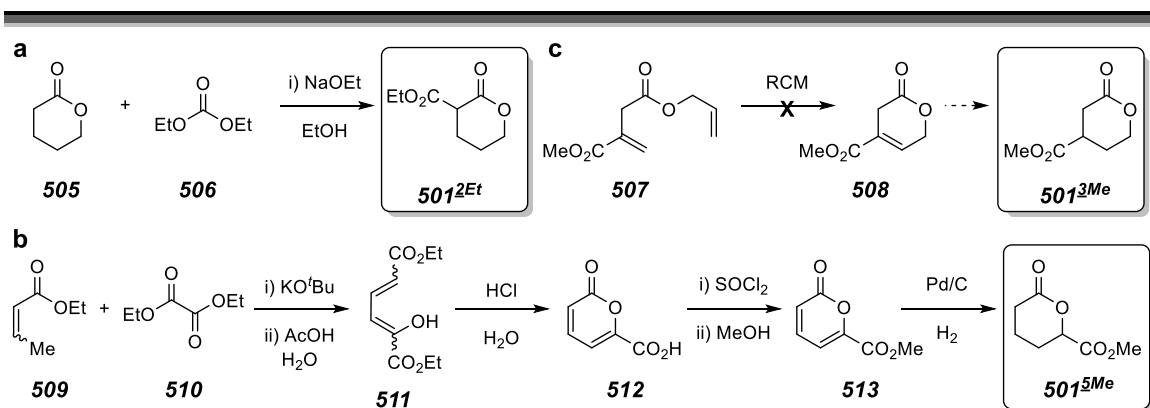


Figure 5.3 Synthesis of carboalkoxylated valerolactones (a) **501^{2Et}** and (b) **501^{5Me}** and (c) attempted synthesis of **501^{3Me}**.

5-Carbomethoxyvalerolactone **501^{5Me}** was synthesized from pyrone precursor **513** (Figure 5.3b) following a modified literature procedure.^{6,7} A Claisen condensation between diethyl oxalate (**510**) and ethyl crotonate (**509**) gave diene **511**, following acidification. This intermediate was very sensitive to both light and air and would degrade to a product

that was insoluble in common organic solvents. Thus, **511** was immediately refluxed in concentrated HCl following its preparation to give pyrone **512** in yields of ca. 20% over three steps. Subsequently treating **512** with thionyl chloride and a drop of DMF gave the acid chloride that was, following concentration, immediately added to MeOH at 0 °C to give **513**. Enough of pyrone **513** was produced to allow for its hydrogenation to **501^{5Me}** in sufficient quantities to preliminarily explore its polymer properties.

Unfortunately, attempts to synthesize the 3-carbomethoxyvalerolactone (**501^{3Me}**, Figure 5.3c) were unsuccessful. One strategy we attempted was the ring-closing metathesis of diene **507**. However, we did not observe unsaturated lactone **508** and instead found that these conditions led to dimerization of **507**.

5.2.2 Carboalkoxylated caprolactones

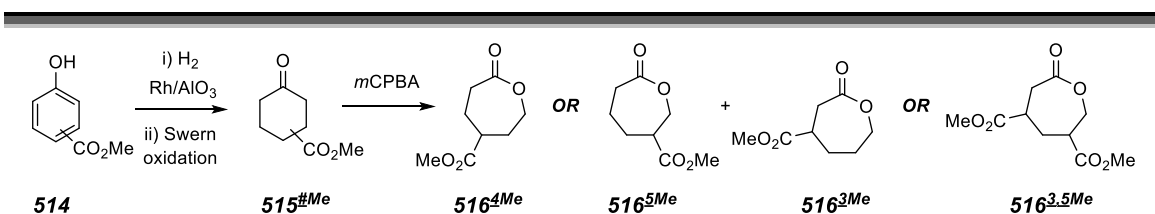


Figure 5.4 Three-step synthesis of carboalkoxylated caprolactones **516^{4Me}**, **516^{3Me}**, **516^{5Me}**, and **516^{3,5Me}** from hydroxybenzoates **514**.

Carbomethoxylated caprolactones **516^{#Me}** were successfully prepared in three steps (Figure 5.4). Commercially available hydroxybenzoates **514** were hydrogenated using rhodium on alumina under ca. 80 psi hydrogen gas followed by a Swern oxidation to give carbomethoxycyclohexanones **515^{#Me}**.⁸ Baeyer-Villiger oxidation to 4-carbomethoxycaprolactone [**516^{4Me}**, from 4-carbomethoxycyclohexanone (**515^{4Me}**)], 5-carbomethoxycaprolactone and 3-carbomethoxycaprolactone [**516^{5Me}** and **516^{3Me}** as a 1:9 mixture, from 3-carbomethoxycyclohexanone (**515^{3Me}**)], and 3,5-

dicarbomethoxycaprolactone [**516**^{3,5Me}, from 3,5-dicarbomethoxycyclohexanone (**515**^{3,5Me})] afforded the desired monomers in good yields.

5.3 Polymerization studies: Past and present

5.3.1 Previous observations and our hypothesis

Previous studies on the polymerization of carboalkoxylated lactones have produced diverse outcomes (see Table 1.1 in Chapter 1). 4-Carbo-*tert*-butoxycaprolactone (**516**^{4tBu}) was only capable of producing low molecular weight polymers (ca. 1500 g•mol⁻¹) using either tin octanoate or aluminum isopropoxide as a catalyst (Figure 5.5a).⁴ Yet, 4-carbomethoxyvalerolactone (**501**^{4Me}) proceeded selectively to the linear polyester **poly(501**^{4Me}) using the acid catalyst DPP (Figure 5.5b). Finally, the polymerization of propiolactone **518** using DPP afforded the branched polyester **poly(518)** (Figure 5.5c).

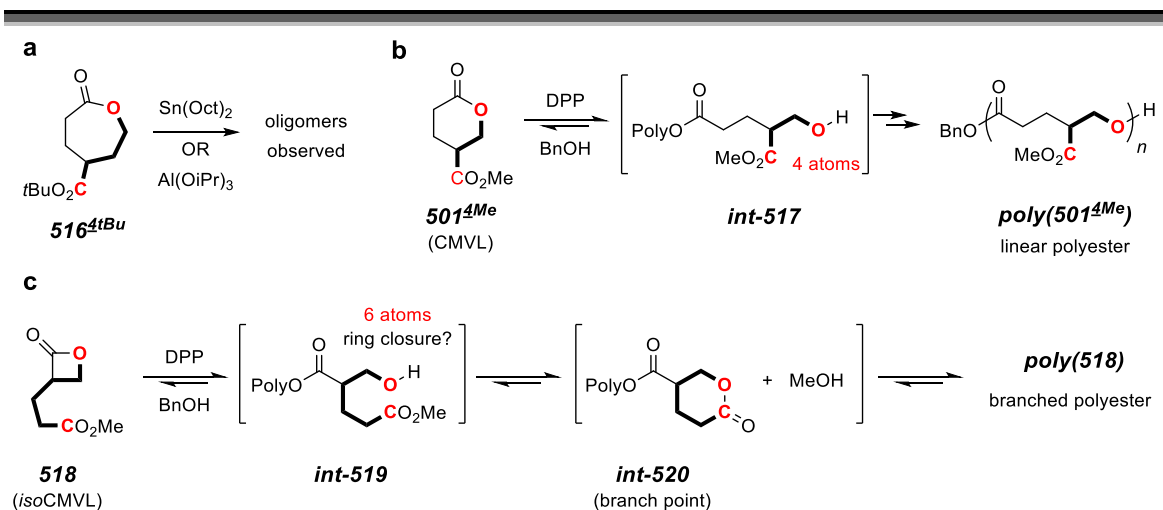


Figure 5.5 Hypothesis on the reactivity of previously studied carboalkoxylated lactones (a) **516**^{4tBu}, (b) **501**^{4Me}, and (c) **518**.

We hypothesized that these diverse outcomes are related to the proximity of the propagating hydroxy to the sidechain carbonyl carbon. Monomer **501^{4Me}** produces **int-517**, where the propagating hydroxy is four-atoms away from the sidechain carbonyl carbon (Figure 5.5b). A four-atom ring is kinetically unfavorable to form and would also form a thermodynamically unfavorable propiolactone (see Chapter 1 discussion). Thus, intramolecular ring closure does not occur and the linear polyester **poly(501^{4Me})** is cleanly formed. However, the isomeric monomer **518** produces, once ring opened, **int-519** where the hydroxy and sidechain carbonyl are now six atoms apart from each other (Figure 5.5c). This intermediate can form a kinetically and thermodynamically favorable valerolactone (compared to a propiolactone) at its polymer terminus **int-520** (Figure 5.5c). This valerolactone terminus provides the opportunity for branching if intermolecularly ring-opened by a propagating polymer chain. These events lead to the highly branched polyester **poly(518)**.

5.3.2 Polymerization or isomerization? Carboalkoxylated valerolactones

We first polymerized valerolactone **501^{5Me}** using DPP and BnOH to cleanly afford the amorphous **poly(501^{5Me})** with a glass transition temperature (T_g) at -5 °C (Figure 5.6a). Like **501^{4Me}**, intramolecular transesterification of this propagating hydroxy and the sidechain carbonyl is unfavorable since this would lead to the three-membered lactone. We also briefly explored the polymerization of carboxylated valerolactone **501^{5H}** and note that **poly(501^{5H})** (not shown) is water soluble.

Under identical conditions, the 2-carboalkoxyvalerolactones **501^{2R}** gave amorphous polyesters **poly(501^{2R})** with T_g s of -21 for **poly(501^{2Me})**, -31 for **poly(501^{2Et})**, and -46 °C for **poly(501^{2nBu})** (Figure 5.6b). The polymerizations of each appeared to afford linear polymers. However, analysis of crude aliquots from the polymerization mixture showed the formation of free alcohol (MeOH, EtOH, or *n*-BuOH) using ¹H NMR

spectroscopy. These observations suggest that there is likely some level of branching in these polyesters, which can arise from intramolecular cyclization of propagating **int-523** to **int-524**. It is interesting to note that in these ROTEP equilibrium-based polymerizations, **int-523** will rapidly be consuming and reforming the starting monomer **501^{2R}**, but it is equally likely that **int-523** can cyclize on its sidechain alkyl ester to **int-524**.

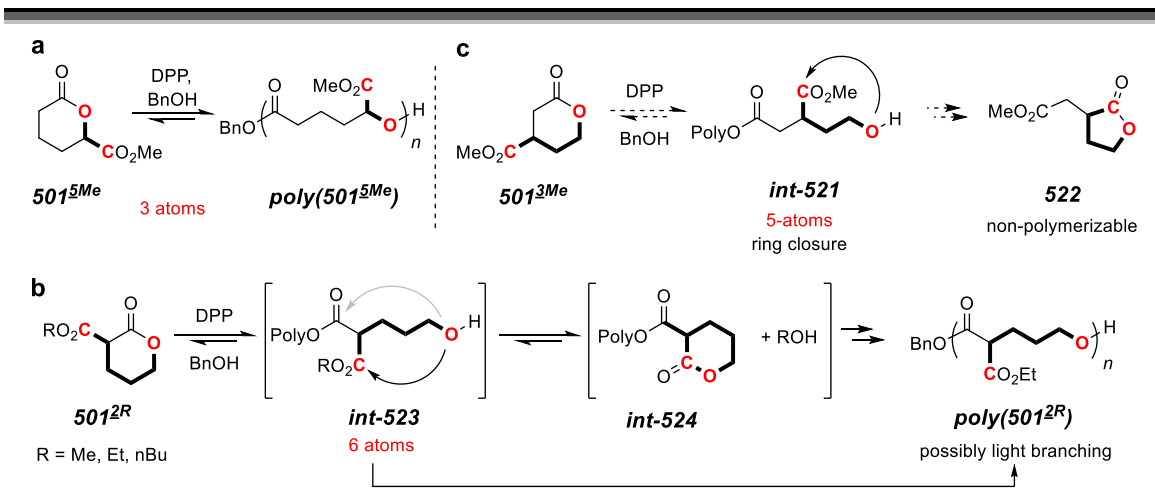


Figure 5.6 Acid-catalyzed polymerization of carboalkoxylated valerolactones (a) **501^{5Me}** and (b) **501^{2Et}**. (c) Predicted isomerization pathway of **501^{3Me}**

Lastly in the valerolactone series, we hypothesize that **501^{3Me}** would rapidly form butyrolactone **522**. Ring-opened **int-521** can quickly cyclize to the five-membered ring, which prevents further polymerization (Figure 5.6c).

5.3.3 Polymerization or isomerization? Carboalkoxylated caprolactones

We next studied the acid-catalyzed polymerization of caprolactone **516^{4Me}** (Figure 5.7) to understand why Trollsas and coworkers were only able to obtain oligomers rather than polymers.⁴ The attempted polymerization of **516^{4Me}** with benzene dimethanol (**525**) and a catalytic amount of DPP led to full consumption of the starting caprolactone with 67% conversion to butyrolactone **527** (Figure 5.7). This lactone presumably formed from

int-526 where the propagating hydroxy and sidechain carbonyl carbon are five atoms apart. The remaining material was consistent with oligomerization of either **516^{4Me}** or **527**, but we were unable to further analyze this material since it was not isolable via precipitation or silica gel chromatography. In the future, subjecting the product butyrolactone **527** to the polymerization conditions to see if any oligomerization can occur could help determine which polymer repeat unit was forming. Overall, this observation is consistent with the report that carbo-*tert*-butoxycaprolactone (**516^{4tBu}**) only produced oligomers⁴ and also supports our hypothesis that 3-carbomethoxyvalerolactone (**501^{3Me}**, Figure 5.6) would isomerize to a non-polymerizable butyrolactone since the ring-opened product of **516^{4Me}** and **501^{3Me}** each contain a propagating hydroxy and sidechain carbonyl carbon five atoms apart.

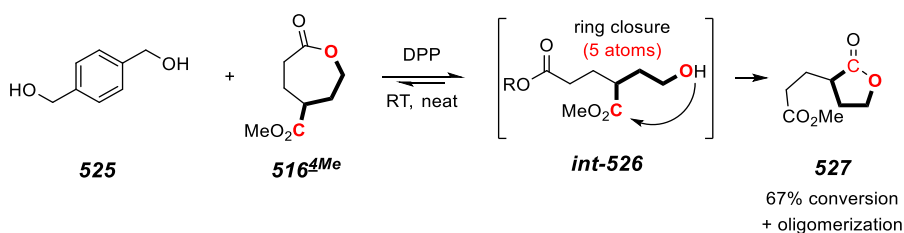


Figure 5.7 Acid catalyzed isomerization of **516^{4Me}** to butyrolactone **527**.

We exposed a 9:1 mixture of **516^{3Me}** and **516^{5Me}** to acidic conditions (Figure 5.8), which resulted in full consumption of the starting caprolactones. Yet the ¹H NMR spectrum of the crude polymerization mixture suggested that a new lactone had formed in a very small concentration. Additionally, these resonances disappeared when the polymer was purified by precipitation, which is consistent with the formation of a new lactone.

Monomer **516^{5Me}** should polymerize to **poly(516^{5Me})** cleanly since the propagating hydroxy and sidechain carbonyl are four atoms apart (similar to valerolactone **501^{4Me}** in Figure 5.5b). Our hypothesis proposes that **516^{3Me}** can isomerize to valerolactone **528**,

which is still a reactive monomer. Monomer **516^{3Me}** could then lead to either subunit **poly(516^{3Me})** through ROTEP or isomerize to **528** prior to polymerizing to subunit **poly(528)**. A mixture of **516^{3Me}** and **516^{5Me}** would then lead to the statistical copolymer **poly(516^{3Me}-co-516^{5Me})** or **poly(516^{3Me}-co-528)** (Figure 5.8). Differentiation of these two copolymer structures was inconclusive using ¹H NMR spectroscopy.

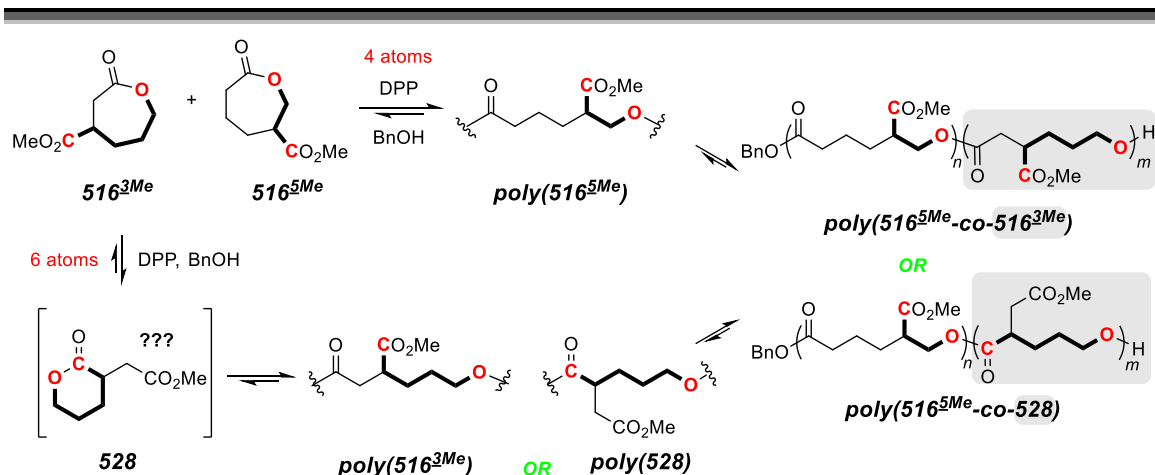


Figure 5.8 Acid-catalyzed polymerization of **516^{3Me}** and **516^{5Me}** to the statistical copolymers of **poly(516^{3Me}-co-516^{5Me})** or **poly(516^{3Me}-co-528)**. The polymerization of **516^{3Me}** may isomerize to **528** prior to polymerizing.

We wanted to see if we could “trap” the isomerized lactone **528** (or a derivative thereof) prior to its polymerization. We envisioned that adding an unreactive substituent to the caprolactone ring of **516^{3Me}** would be helpful. This added substituent could enable the ring opening and ROTEP of the disubstituted variant of *caprolactone* **516^{3Me}** but could also strongly inhibit the polymerization of the disubstituted variant of *valerolactone* **528**.⁹

To this end, 3,5-dicarbomethoxycaprolactone (**516^{3,5Me}**) was synthesized in three steps from dimethyl 5-hydroxyisophthalate (Figure 5.4) and was subjected to ROTEP conditions using DPP and a catalytic amount of methanol as the initiator (Figure 5.9). To

our delight, this reaction led to an 89% yield of **529** after MPLC purification, suggesting that **516**^{3Me} is likely capable of isomerization to **528** prior to polymerization. However, this evidence is not conclusive. I have recently been able to chromatographically separate **516**^{3Me} from **516**^{5Me} on a small scale using MPLC, which could help to further evaluate this isomerization event.

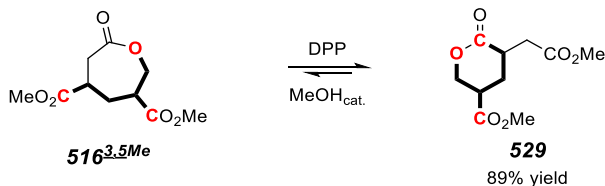
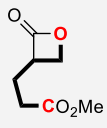
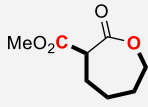
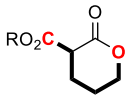
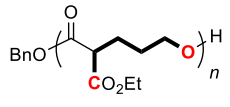
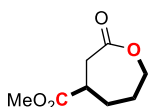
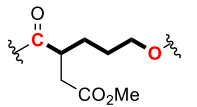
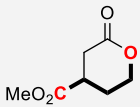
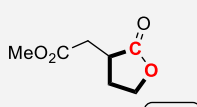
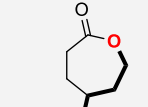
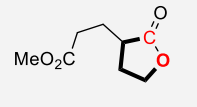
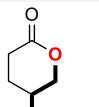
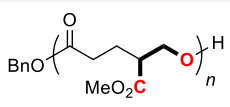
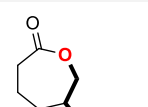
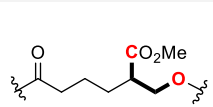
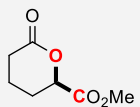
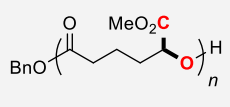
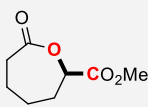
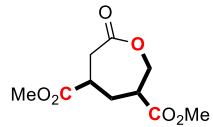
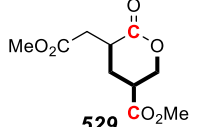


Figure 5.9 Isomerization of **516**^{3,5Me} to valerolactone **529**. This experiment suggests that the mono-substituted **516**^{3Me} likely isomerizes to six-membered ring **528** prior to polymerizing.

Through these studies we can begin to build a model to determine the product derived from carboalkoxylated lactones when treated with an acid catalyst and alcohol initiator. A propagating hydroxy tends to undergo intramolecular transesterification with a sidechain carboalkoxy group when the hydroxy and sidechain carbonyl carbon are five or six atoms away. When this isomerization occurs for the five-atom case, an isomerized substituted butyrolactone is formed, which is incapable of polymerization. When six-atoms apart, an isomerized substituted valerolactone can form at the growing polymer's terminus, which can lead to a branched polyester with undetermined levels of branch density. Isomerization does not occur for the three- and four-atom case since isomerization would unfavorably lead to highly strained lactones. For this reason, the polymerization of such carboalkoxylated lactones proceeds to give linear polyesters. Lastly, it is important to note that each of these polyesters may undergo *intermolecular* transesterification to generate some branching as observed in Chapter 3 and 4; however, this should be reduced using DPP at room temperature (Chapter 2).

5.4 Future directions

Table 5.1 Summary of carboalkoxylated lactone polymerizations using DPP as a catalyst.

| Monomer | Product | Monomer | Product |
|---|---|--|--|
|  <p>518 (isoCMVL)</p> | <p>poly(518) highly branched</p> |  <p>516^{2Me}</p> | <p>??</p> |
|  <p>501^{2R}</p> |  <p>poly(501^{2R}) possibly light branching</p> |  <p>516^{3Me}</p> |  <p>poly(528) copolymer with poly(516^{5Me})</p> |
|  <p>501^{3Me}</p> |  <p>522 ??</p> |  <p>516^{4Me}</p> |  <p>527 67% conversion</p> |
|  <p>501^{4Me}</p> |  <p>poly(501^{4Me}) linear polyester</p> |  <p>516^{5Me}</p> |  <p>poly(516^{5Me}) copolymer with poly(528) ??</p> |
|  <p>501^{5Me}</p> |  <p>poly(501^{5Me}) linear polyester</p> |  <p>516^{6Me}</p> | <p>??</p> |
| | |  <p>516^{3,5Me}</p> |  <p>529 89% yield</p> |

A summary of these results as well as other potential carboalkoxylated valero- and caprolactones to be studied are shown in Table 5.1. In addition to pursuing these new

monomers, each of the already studied monomers should be reexamined across a consistent series of polymerization conditions and molecular weights.

Of the monomers we have not studied, it would be ideal to synthesize and subject valerolactone **516^{3Me}** (5-atoms) to the acid polymerization conditions to determine if, indeed, this monomer isomerizes to a valerolactone ring prior to polymerization. Caprolactone **516^{2Me}** would also be interesting since the propagating hydroxy and sidechain ester are now 7-atoms apart, which is something we have not considered but has been reported by others in copolymers with caprolactone.^{10,11} Based on our model, we would predict that monomer **516^{2Me}** would produce a linear polyester.

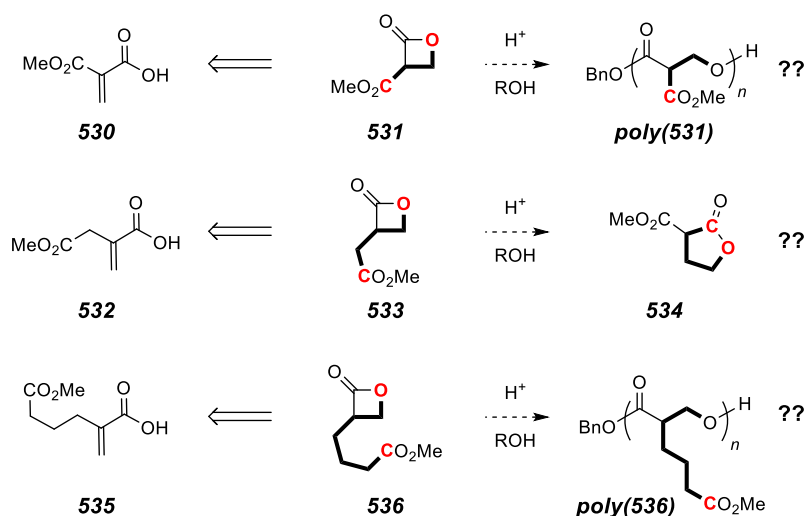


Figure 5.10 Potential 2-(carbomethoxyalkyl)propiolactones to synthesize and subject to polymerization conditions to further expand the scope of this study

Additional carboalkoxylated propiolactones such as 2-(carbomethoxyalkyl)propiolactones **531**, **533**, and **536** (Figure 5.10) would also add significant understanding to this study. Now highly strained 4-membered ring lactones can isomerize to less-strained, larger-ring lactones. We hypothesize that **531** (four atoms) will

polymerize cleanly to **poly(531)**, **533** (five atoms) will isomerize to a butyrolactone, and **536** (seven atoms) will polymerize to linear **poly(536)**. These propiolactones can theoretically be synthesized from the unsaturated acid esters **530**, **532**, and **535**. Treatment of each with HBr•AcOH to hydrobrominate the alkene followed by treatment with base to cyclize to the lactone, should afford these propiolactones in an analogous fashion to our previous report for **518**.² It is envisioned that the unsaturated acid ester **530** could be synthesized from malonic acid (or other routes¹²) and itaconate **532** is commercially available. The synthesis of **535** may be more complicated, but has been reported^{13,14} and can be made, for example, in one-step from methyl hex-5-ynoate. Alternatively, regioisomers of these propiolactones substituted at the 3-position could be made by carbonylation of epoxy esters in the Coates lab.¹⁵

5.5 Conclusion

In this chapter we studied the influence of the carboalkoxy position on valero- and caprolactones. The position of the carboalkoxy group is crucial to whether a carboalkoxylactone will isomerize to a non-polymerizable isomer or polymerize to a linear or branched polyester. Importantly, when the propagating hydroxy and the sidechain carbonyl are 5-atoms apart, an intramolecular transesterification leads to a substituted butyrolactone isomer, which can no longer polymerize. Additionally, when a more thermodynamically stable lactone (e.g., propiolactone to a valerolactone) can form, these monomers can polymerize to polyesters with varied levels of branching (see **518** and **501^{2R}**, Table 5.1). Finally, when the propagating hydroxy and sidechain carbonyl are incapable of forming a more stable lactone than the starting material, the monomer will polymerize to a linear polyester (such as **501^{4Me}**). We believe this study has led to a rational model to use when targeting new polymers made from biomass-derived carboalkoxylated lactones.

5.5 References

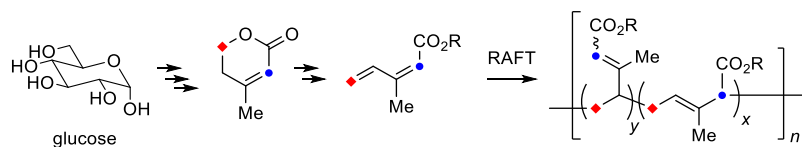
- ¹ Fahnhorst, G. W.; Hoye, T. R. A carbomethoxylated polyvalerolactone from malic acid: Synthesis and divergent chemical recycling. *ACS Macro Lett.* **2018**, 143–147.
- ² Fahnhorst, G. W.; Stasiw, D. E.; Tolman, W. B.; Hoye, T. R. Isomerization of linear to hyperbranched polymers: Two isomeric lactones converge via metastable isostructural polyesters to a highly branched analogue. *ACS Macro Lett.* **2018**, 7, 1144–1148.
- ³ Schneiderman, D. K.; Hillmyer, M. A. Aliphatic polyester block polymer design. *Macromolecules* **2016**, 49, 2419–2428.
- ⁴ Trollsas, M.; Lee, Y. V.; Mecerreyes, D.; Löwenhielm, P.; Möller, M.; Miller, R. D.; Hedrick, J. L. Hydrophilic aliphatic polyesters: Design, synthesis, and ring-opening polymerization of functional cyclic esters. *Macromolecules* **2000**, 33, 4619–4627.
- ⁵ Wright, J. L.; Caprathe, B. W.; Downing, D. M.; Glase, S. A.; Heffner, T. G.; Jaen, J. C.; Johnson, S. J.; Kesten, S. R.; MacKensie, R. G.; Meltzer, L. T.; Pugsley, T. A.; Smith, S. J.; Wise, L. D.; Wustrow, D. J. The discovery and structure-activity relationships of 1,2,3,6-tetrahydro-4-phenyl-1-[(arylcyclohexenyl)alkyl]pyridines. Dopamine autoreceptor agonists and potential antipsychotic agents. *J. Med. Chem.* **1994**, 37, 3523–3533.
- ⁶ Lapworth, A. CXXXIV.—The form of change in organic compounds, and the function of the α -meta-orientating groups. *J. Chem. Soc., Trans.* **1901**, 79, 1265–1284.
- ⁷ Wiley, R. H.; Hart, A. J. 2-Pyrones. IX. 2-Pyrone-6-carboxylic acid and its derivatives. *J. Am. Chem. Soc.* **1954**, 76, 1943–1944.
- ⁸ Cregge, R. J.; Lentz, N. L.; Sabol, J. S. Conformationally restricted leukotriene antagonists. Synthesis of chiral 4-hydroxy-4-alkylcyclohexanecarboxylic acids as leukotriene D4 analogues. *J. Org. Chem.* **1991**, 56, 1758–1763.
- ⁹ Disubstituted caprolactones have been efficiently polymerized (Zhang, D.; Hillmyer, M. A.; Tolman, W. B. Catalytic polymerization of a cyclic ester derived from a “cool” natural precursor. *Biomacromolecules* **2005**, 6, 2091–2095.). Contrarily, we can find no reports of polymers made from disubstituted valerolactones and, in our hands, have been unable to polymerize some disubstituted valerolactones.
- ¹⁰ Mahmud, A.; Xiong, X.-B.; Lavasanifar, A. Novel self-associating poly(ethylene oxide)-block-poly(ϵ -caprolactone) block copolymers with functional side groups on the polyester block for drug delivery. *Macromolecules* **2006**, 39, 9419–9428.
- ¹¹ Garg, S. M.; Xiong, X.-B.; Lu, C.; Lavasanifar, A. Application of click chemistry in the preparation of poly(ethylene oxide)-block-poly(ϵ -caprolactone) with hydrolyzable cross-links in the micellar core. *Macromolecules* **2011**, 44, 2058–2066.

-
- ¹² Wang, Y.; Liu, X.; Laurini, E.; Posocco, P.; Ziarelli, F.; Fermeglia, M.; Qu, F.; Pricl, S.; Zhang, C.-C.; Peng, L. Mimicking the 2-oxoglutaric acid signaling function using molecular probes: Insights from structural and functional investigations. *Org. Biomol. Chem.* **2014**, *12*, 4723–4729.
- ¹³ Hierold, J.; Hsia, T.; Lupton, D. W. The Grob/Eschenmoser fragmentation of cycloalkanones bearing β -electron withdrawing groups: A general strategy to acyclic synthetic intermediates. *Org. Biomol. Chem.* **2011**, *9*, 783–792.
- ¹⁴ Jones, E. R. H.; Whitham, G. H.; Whiting, M. C. Researches on acetylenic compounds. Part XLIV. The reaction between nickel carbonyl and some esters of ω -acetylenic acids. *J. Chem. Soc.* **1954**, *0*, 1865–1868.
- ¹⁵ Schmidt, J. A. R.; Lobkovsky, E. B.; Coates, G. W. Chromium(III) octaethylporphyrinato tetracarbonylcobaltate: A highly active, selective, and versatile catalyst for epoxide carbonylation. *J. Am Chem. Soc.* **2005**, *127*, 11425–11435.

◆PART 2◆

Carboalkoxylated polyisoprene from glucose

Chapter 6. Poly(isoprenecarboxylates)* and poly(isoprenecarboxamides) from glucose via anhydromevalonolactone



Summary: A short and efficient synthesis of a series of isoprenecarboxylic acid esters (ICAEs) and isoprenecarboxamides (ICAs) and their corresponding polymers is presented. The base-catalyzed eliminative ring opening of anhydromevalonolactone provides isoprenecarboxylic acid, which was further transformed to ICAEs and ICAs. Reversible addition-fragmentation chain-transfer (RAFT) polymerization was used to synthesize high molecular weight ($>100 \text{ kg mol}^{-1}$) poly(isoprenecarboxylates) with dispersities (D) of ca. 1.5. The glass transition temperatures (T_g) and entanglement molecular weights (M_e) of the poly(isoprenecarboxylates) were determined and showed similar trends to the T_g and M_e values for analogous poly(acrylate esters). These new glucose-derived materials could provide a sustainable alternative to poly(acrylates). ICAs were polymerized using uncontrolled radical polymerization and provided polymers with T_g s much higher than those of the poly(isoprenecarboxylates).

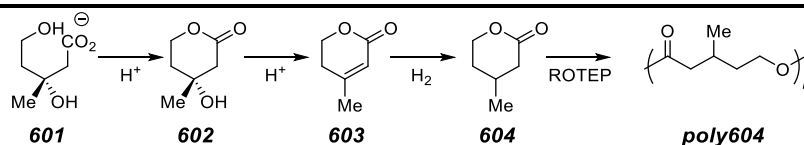
* Reproduced in part with permission from Ball-Jones, N. R.; Fahnhorst, G. W.; Hoye, T. R. *ACS Macro Lett.* **2016**, 5, 1128–1131. Copyright 2016 American Chemical Society

The work on poly(isoprenecarboxylate esters) was led by Dr. Nicolas R. Ball-Jones.

6.1 Introduction

The synthesis of polymers from renewable feedstocks is of growing importance to a sustainable society. We sought to capitalize on the ready availability of mevalonate (**601**), for which an efficient bioengineered preparation via fermentation of glucose was developed in the Zhang laboratory.¹ The carboxylate **601** can be readily converted (Scheme 6.1) through acidification to mevalonolactone (**602**) and, in turn, anhydromevalonolactone (**603**). Simple hydrogenation then gives β -methyl- δ -valerolactone (or 3-methylvalerolactone, **604**). This saturated lactone has been demonstrated by investigators in the Hillmyer, Bates, and Macosko laboratories to be an effective monomer for ring-opening transesterification polymerization (ROTEP) enroute to valuable polyesters containing **poly604**.^{1,2}

Scheme 6.1 The facile chemical conversion of mevalonate (**601**) to β -methyl- δ -valerolactone (**604**) via mevalonolactone (**602**) and anhydromevalonolactone (**603**)



We were exploring various alternative strategies that capitalize on the ready availability of **602–604** in ways that might lead to additional novel monomers and/or polymers. (*Z*)-3-Methylpenta-2,4-dienoic acid (or isoprenecarboxylic acid, **606-H**, Figure 6.1) has been prepared from anhydromevalonolactone (**603**).^{3,4} However, we can find no reports of the polymerization of **606-H** or any of its esters (**606-R**). In contrast, 4-methylpenta-2,4-dienoate (**607**),⁵ sorbic acid esters (**608**),⁶ pentadienoates (**609**),⁷ and 3-methylene-4-pentenoates (**610**)⁸ have all been polymerized under one or more of radical, anionic, or cationic conditions. Light-induced topochemical polymerizations of the related

dienoate salts **611a-d** have also been described.⁹ All of these unsymmetrical dienic monomers can, in principle, give rise to a variety of regioisomeric relationships in the derived polymeric backbones. For example, methyl penta-2,4-dienoate (**609** or β -vinylacrylate) has been radically polymerized to give a homopolymer comprising an 85:15 mixture of backbone repeat units arising from competitive 1,4- vs. 1,2-addition.⁷ Finally, we also note the recent work of Boday and coworkers, who polymerized "methylidenelactide"¹⁰ and pointed out that this compound was one of only a few examples of acrylate-like monomers in which all atoms are bio-derived (the others arising from itaconic or levulinic acid or via bioengineered routes to acrylic acid from sugars).¹¹ We report here the preparation of a series of esters and amides derived from **606-H** and their radical polymerization to poly(isoprenecarboxylates) and poly(isoprenecarboxamides).

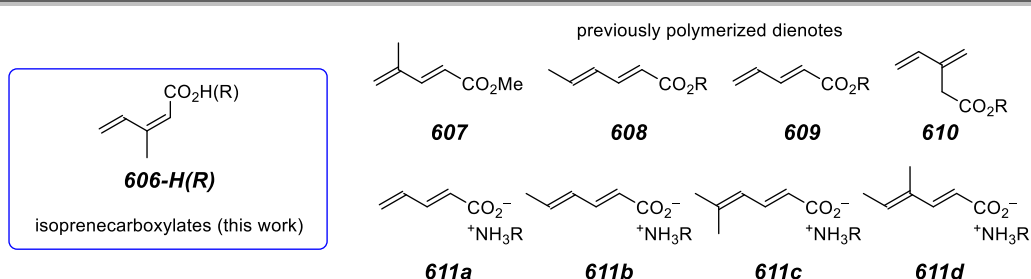


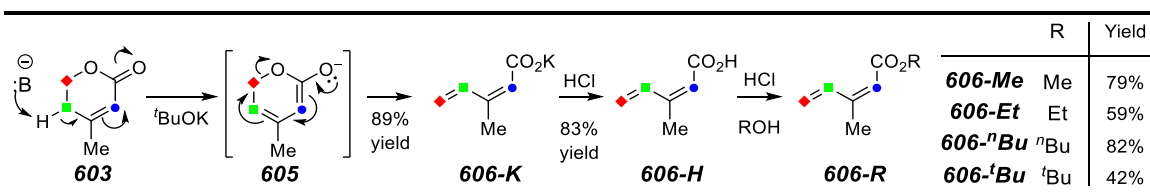
Figure 6.1 Isoprenecarboxylic acid (**606-H**) and its esters (**606-R**) described here and related dienoates (**607–611**) whose polymerizations have been previously described.

In this chapter, we will discuss radical polymerization (rather than ring-opening transesterification polymerization in previous chapters) and will reference reversible deactivation polymerization strategies, namely, reversible addition-fragmentation chain-transfer (RAFT) polymerization. Reversible deactivation strategies decrease the concentration of “active” propagating radical species by reversibly trapping them in a dormant state. In doing so, termination reactions are reduced and lead to a better control of

a polymer's molecular weight and dispersity. For RAFT polymerization, trithiocarbonates are often used as the chain-transfer agent.¹²

6.2 Isoprenecarboxylates: Synthesis, polymerization, and polymer properties

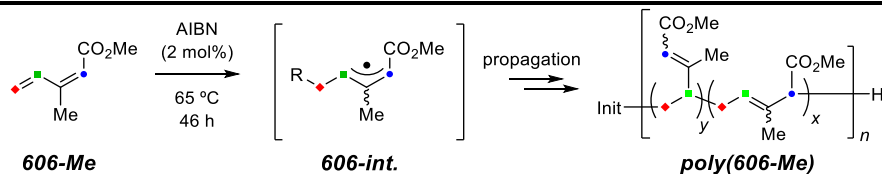
Scheme 6.2 Elimination reaction to form the dienoate potassium salt **606-K** and subsequent Fischer esterification of the conjugate acid **606-H** to provide isoprenecarboxylate esters **606-R**



Cornforth first demonstrated³ the eliminative opening of lactone **603**, most likely via **605** and an E1cB mechanism, under the action of potassium tert-butoxide (Scheme 6.2). Acidification gives the acid **606-H**. We have routinely prepared and isolated the potassium salt **606-K** on multi-ten-gram scales. Non-nucleophilic bases 1,8-diazabicyclo[5.4.0]undec-7-ene (DBU) also effect this transformation, but weaker bases such as diisopropylethylamine were unable to. Other known methods for accessing this penta-2,4-dienoic acid are less attractive from a preparative point of view: e.g. cross-coupling of alkenylstannanes,¹³ multi-step sequences,¹⁴ or generation as a mixture of 3- and 4-methylpentadienoic acids from isoprene.¹⁵ Fischer esterification of **606-H** with any of the alcohols MeOH, EtOH, or *n*-BuOH gave, following distillation, each of the esters **606-Me**, **606-Et**, and **606-*n*Bu**, respectively, in the yield indicated in Scheme 6.2. Alternatively, the *tert*-butyl ester **606-*t*Bu** was prepared by suspension of **606-H** in isobutylene and treatment with H₂SO₄ as a Brønsted acid catalyst.

We first used azobisisobutyronitrile (AIBN) to initiate a polymerization of methyl isoprenecarboxylate (**606-Me**) (Scheme 6.3) to provide poly(methyl isoprenecarboxylate) [**poly(606-Me)**]. This demonstrated that **606-Me** behaves in a similar fashion to other conjugated dienoates (Figure 6.1). ^1H and ^{13}C NMR analysis of the **poly(606-Me)** suggested that polymerization occurs by radical addition to the terminal methylene (C5), which produces the delocalized radical (**606-int.**) that propagates in competing 1,4- and 1,2-addition modes in a ratio of ca. 1.5:1. Additionally, the broad nature of nearly all resonances were indicative of the likely formation of multiple diastereomeric relationships among the new stereogenic alkene (*E/Z*) and sp^3 carbon atoms (*R/S*) that arise from the addition of each monomer.

Scheme 6.3 Free radical polymerization of **606-Me**, initiated by AIBN



To gain additional control over M_n and lower the dispersities of the polymer products, especially when made via bulk polymerization,¹⁶ we explored several reversible deactivation radical polymerization strategies.¹⁷ Nitroxide mediated radical polymerization of **606-Me** in the bulk initiated by TIPNO-St¹⁸ behaved in a manner characteristic of a living polymerization; the M_n increased linearly with conversion (see Figure S6.6 in the Supporting Information). This product showed a substantially lower dispersity ($D = 1.45$) than that of the polymer prepared from the AIBN bulk polymerization (cf. Scheme 6.3).

Because of the somewhat exotic nature of the TIPNO-St initiator, we also explored reversible addition-fragmentation chain-transfer (RAFT) polymerization of the esters **606-R** (Figure 6.2). When **606-Me** (1 equiv) was polymerized in the presence of AIBN

(8×10^{-5} equiv) and the trithiocarbonate **612** (DDMAT,¹⁹ 1×10^{-3} equiv) as the RAFT agent, the resulting **poly(606-Me)** showed a M_n of $150 \text{ kg} \cdot \text{mol}^{-1}$ and a dispersity of 1.5 (SEC vs. PS). The T_g of the sample was $34 \text{ }^\circ\text{C}$ and its entanglement molecular weight ($M_e = 4\rho RT/5G_n^\circ$) was $17 \text{ kg} \cdot \text{mol}^{-1}$. The RAFT polymerization of **606-Me** again appeared to be living (Figure 6.2) as the M_n increased linearly with conversion. It is also worth noting that neither of these controlled polymerization methods altered the ratio of 1,4- vs. 1,2-addition modes of polymerization (i.e., the ratio remained ca. 1.5:1).

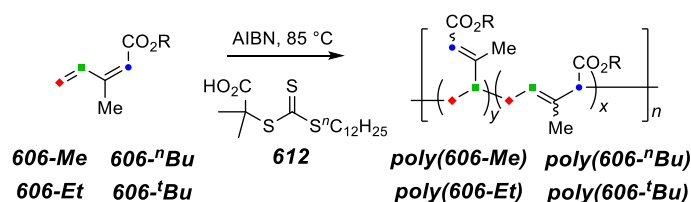


Figure 6.2 RAFT polymerization of isoprenecarboxylates **606-R**. Conditions used for the polymerization of bulk samples of each of **606-Me**, **606-Et**, **606-ⁿBu**, and **6-^tBu**.

With the goal of establishing the effect of the ester alkyl moiety on T_g and M_e , we also prepared high molecular weight polymer samples from the series of esters **606-Et**, **606-ⁿBu**, and **606-^tBu**. Samples of each of **poly(606-Me)**, **poly(606-Et)**, **poly(606-ⁿBu)**, and **poly(606-^tBu)** having $M_n > 100 \text{ kg} \cdot \text{mol}^{-1}$ were prepared using AIBN and **612**. The T_{gs} and M_{es} of these poly(isoprenecarboxylates) are given in Table 6.1a. The T_{gs} decrease as the ester alkyl moiety grows in size until the *t*-butyl analogue is reached, in which case there is a substantial increase in the T_g . This is quite analogous to the trend seen for simple poly(acrylate) esters (cf. Table 6.1b). Similarly, the M_{es} for the poly(isoprenecarboxylates) parallel those for the analogous poly(acrylates). The former tend to be higher than the latter for most of the same ester alkyl groups, perhaps reflecting the contribution from the larger sidechain moieties arising from the 1,2-mode of polymerization of the isoprenecarboxylate monomers **606-R**.

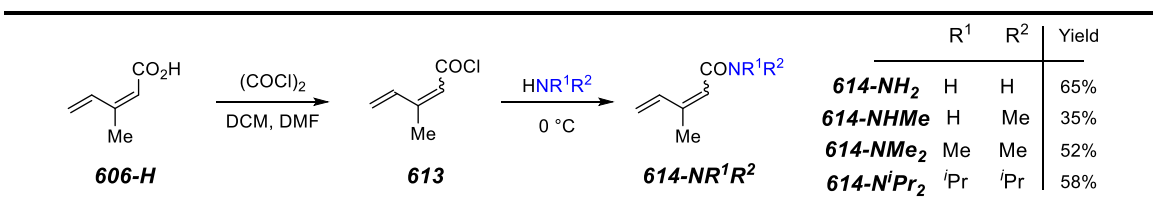
Table 6.1 (a) Comparison of glass transition temperatures (T_g) and entanglement molecular weights (M_e) for the four **poly(606-R)** esters; all five samples had $M_n > 100 \text{ kg}\cdot\text{mol}^{-1}$. (b) T_g and M_e for poly(methyl acrylate) (**PMA**), poly(ethyl acrylate) (**PEA**), poly(*n*-butyl acrylate) (**PⁿBA**), and poly(*t*-butyl acrylate) (**P^tBA**).^{a-d} Ref. 20a-d

| a Poly(isoprenecarboxylates) | | | | | b Poly(acrylates) | | | | |
|------------------------------|---------------------|---------------------|---------------------------------|---------------------------------|-------------------|-----------------|-----------------|------------------------|------------------------|
| | <i>poly(606-Me)</i> | <i>poly(606-Et)</i> | <i>poly(606-ⁿBu)</i> | <i>poly(606-^tBu)</i> | | PMA | PEA | PⁿBA | P^tBA |
| T_g (°C) | 34 | 10 | -19 | 55 | T_g (°C) | 22 ^a | -8 ^a | -43 ^a | 55 ^a |
| M_e (kg/mol) | 17 | 22 | 41 | 39 | M_e (kg/mol) | 9 ^b | 12 ^c | 29 ^d | NA |

6.3 Isoprenecarboxamides: Synthesis, polymerization, and polymer properties

Poly(isoprenecarboxylates) [**poly(606-R)**] behaved very similarly to polyacrylates in relation to their ester alkyl influence on the polymers' T_g s and M_e s. Because of this, we felt that it would be advantageous to expand the scope of this novel family of polymers and produce isoprenecarboxamides **614-NR¹R²** and their corresponding polymers. Polyacrylamides are known to have higher T_g s than ester acrylates and can be water soluble. We hypothesized that poly(isoprenecarboxamides) [**poly(614-NR¹R²)**] would behave similarly.

Scheme 6.4 One-pot, two-step synthesis of isoprenecarboxamides (**614-NR¹R²**) from isoprenecarboxylic acid (**606-H**)



We synthesized isoprenecarboxamides (**614-NR¹R²**) by subjecting acid **606-H** to oxalyl chloride and a drop of DMF to afford acid chloride **613** (Scheme 6.4). After ca. 2 h, an amine was added directly to this reaction mixture in a one-pot, two-step transformation. Initial attempts to isolate and purify **613** prior the addition of an amine were unsuccessful and led to decomposition of **613** to a dark brown oil upon concentration. Regardless, the four isoprenecarboxamides were obtained as mixtures of *E:Z* isomers by recrystallization (**614-NH₂** in toluene) or distillation.

We polymerized **614-NH₂** using AIBN (65 °C, 24 h) and observed ca. 70% monomer conversion to **poly(614-NH₂)** (Figure 6.3a). This polymer was highly hygroscopic as observed by the ca. 10% mass loss below 150 °C prior to the onset of polymer degradation (ca. 165 °C) as analyzed by thermogravimetric analysis (TGA, Figure 6.3b). No *T_g* was observed in the DSC thermogram prior to its degradation. Additionally, an insoluble polymer formed when **poly(614-NH₂)** was heated to 165 °C, which swelled in the presence of DMF.

Attempts to use higher polymerization temperatures with AIBN or other thermal radical initiators after this initial attempt gave irreproducible results. Common problems were low conversion or formation of cross-linked gels. Using radical photoinitiator 2,2-dimethoxy-2-phenylacetophenone (DMPA) did help to prevent the formation of cross-linked materials, but often led to low conversions (<40% with 0.2 equiv DMPA per monomer). Fortunately, we were able to obtain enough **poly(614-NHMe)** and **poly(614-NMe₂)** to study their DSC properties. **Poly(614-NHMe)** has a high *T_g* at 147 °C and **poly(614-NMe₂)** has a *T_g* at 87 °C. In one instance **poly(614-NⁱPr₂)** was polymerized and did so efficiently. However, this polymer was never purified or characterized.

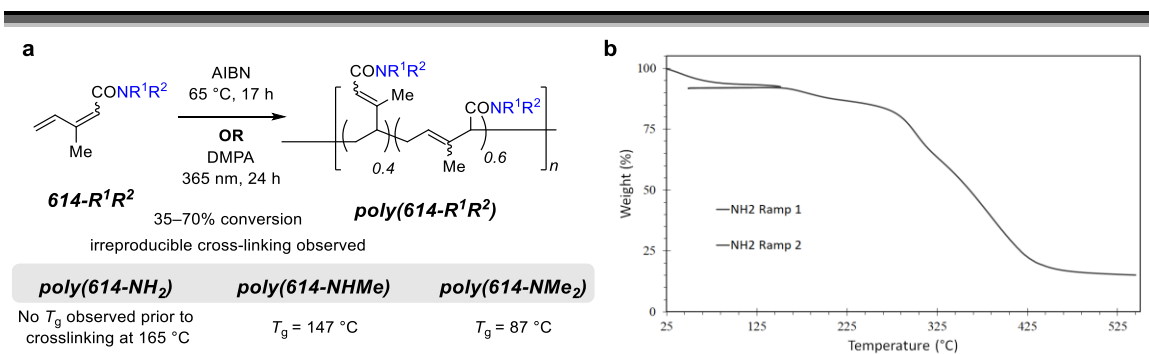


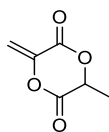
Figure 6.3 (a) Free radical polymerization of **614-NR¹R²** to **poly(614-NR¹R²)** using either AIBN at 65 °C or DMPA at 365 nm (b) TGA thermogram of the hygroscopic **poly(614-NR¹R²)**. The TGA sample was first heated to 150 °C (10 °C•min⁻¹), cooled to 50 °C (10 °C•min⁻¹), and heated to 550 °C (10 °C•min⁻¹).

6.4 Conclusion

In summary, we have prepared a series of four esters **604-R** and four amides **613-NR¹R²** of isoprenecarboxylic acid (**606-H**) that differ in the size of the ester or *N*-amide alkyl moiety. This parent acid was made by an eliminative opening of anhydromevalonolactone (**603**), a commodity efficiently available in large quantities from glucose.¹ Each ester was polymerized under RAFT conditions to provide a series of high molecular weight polymers. The glass transition temperature and entanglement molecular weight of each was determined. The ester alkyl group in these polymers affected the T_g and M_e in a very similar fashion as is known for simple poly(acrylates). This work establishes the feasibility of using glucose as a source of polymers with acrylate-like properties. Additionally, we briefly explored the polymerization and thermal polymer properties of amides **613-NR¹R²**. Poly(isoprenecarboxamides) [**poly(613-NR¹R²)**] have high T_g s (>165 °C, 147 °C, and 87 °C). However, these monomers are difficult to polymerize to high monomer conversion without cross-linking.

6.5 References

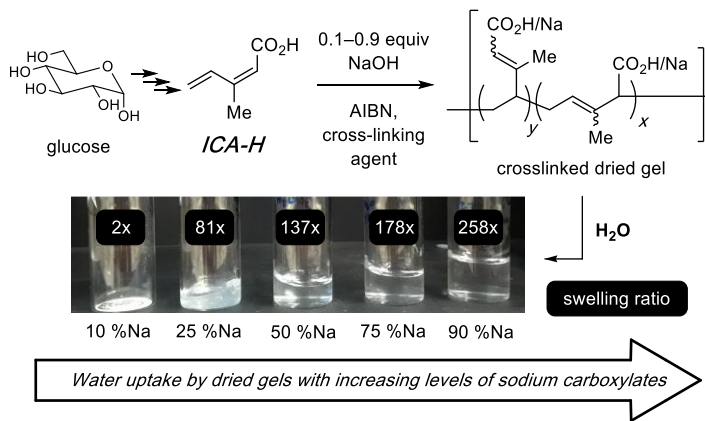
- ¹ Xiong, M.; Schneiderman, D. K.; Bates, F. S.; Hillmyer, M. A.; Zhang, K. Scalable production of mechanically tunable block polymers from sugar. *Proc. Natl. Acad. Sci.* **2014**, *111*, 8357–8362.
- ² (a) Zhang, J.; Li, T.; Mannion, A. M.; Schneiderman, D. K.; Hillmyer, M. A.; Bates, F. S. Tough and sustainable graft block copolymer thermoplastics. *ACS Macro Lett.* **2016**, *5*, 407–412. (b) Schneiderman, D. K.; Vanderlaan, M. E.; Mannion, A. M.; Panthani, T. R.; Batiste, D. C.; Wang, J. Z.; Bates, F. S.; Macosko, C. W.; Hillmyer, M. A. Chemically recyclable biobased polyurethanes. *ACS Macro Lett.* **2016**, *5*, 515–518.
- ³ Cornforth, J. W.; Cornforth, R. H.; Popjak, G.; Gore, I. Y. Studies on the biosynthesis of cholesterol. 5. Biosynthesis of squalene from D,L-2-hydroxy-3-methyl-[2-¹⁴C]pentano-5-lactone. *Biochem. J.* **1958**, *69*, 146–155.
- ⁴ Moriconi, E. J.; Meyer, W. C. Reaction of dienes with chlorosulfonyl isocyanate. *J. Org. Chem.* **1971**, *36*, 2841–2849.
- ⁵ Arbutova, I. A.; Efremova, V. N.; Eliseeva, A. G.; Mikhailova, N. V.; Nikitin, V. N.; Sidorovich, A. V.; Klushin, N. A.; Kuvshinskii, E. V. *Vysokomolekulyarnye Soedineniya, Seriya A.* **1970**, *12*, 697–704.
- ⁶ For example, Takasu, A.; Ishii, M.; Inai, Y.; Hirabayashi, T. Highly threo diastereoselective anionic polymerization of (*E,E*)-methyl sorbate catalyzed by a bulky organoaluminum lewis acid. *Macromolecules* **2001**, *34*, 6548–6550.
- ⁷ Ueda, M.; Shimada, S.; Ogata, T.; Oikawa, K.; Ito, H.; Yamada, B. Radical polymerization of methyl *trans*- β -vinylacrylate. *J. Polym. Sci. A Polym. Chem.* **1995**, *33*, 1059–1067.
- ⁸ Sheares, V. V. Functionalized diene monomers and polymers containing functionalized dienes and methods for their preparation. US Patent 6,344,538 B1, February 5, 2002.
- ⁹ Matsumoto, A.; Sada, K.; Tashiro, K.; Miyata, M.; Tsubouchi, T.; Tanaka, T.; Odani, T.; Nagahama, S.; Tanaka, T.; Inoue, K.; Saragai, S.; Nakamoto, S. Reaction principles and crystal structure design for the topochemical polymerization of 1,3-dienes. *Angew. Chem. Int. Ed.* **2002**, *41*, 2502–2505.



- ¹⁰ Methylidenelactide:
- ¹¹ Mauldin, T. C.; Wertz, J. T.; Boday, D. J. *ACS Macro Lett.* **2016**, *5*, 544–546.
- ¹² Perrier, S. *50th Anniversary perspective: RAFT polymerization—A user guide.* *Macromolecules* **2017**, *50*, 7433–7447.
- ¹³ Abarbri, M.; Parrain, J.-L.; Duchêne, A. Stereospecific synthesis of (*Z*) or (*E*)-3-methylalk-2-enoic acids. *Tetrahedron Lett.* **1995**, *36*, 2469–2472.
- ¹⁴ Nakai, T.; Mikami, K.; Taya, S.; Kimura, Y.; Mimura, T. The [2,3]Wittig rearrangement of 2-alkenyloxyacetic acids and its applications to the stereocontrolled synthesis of β , γ -unsaturated aldehydes and conjugated dienoic acids. *Tetrahedron Lett.* **1981**, *22*, 69–72.
- ¹⁵ Huguet, N.; Jevtovikj, I.; Gordillo, A.; Lejkowski, M. L.; Lindner, R.; Bru, M.; Khalimon, A. Y.; Rominger, F.; Schunk, S. A.; Hofmann, P.; Limbach, M. Nickel-catalyzed direct carboxylation of olefins with CO₂: One-pot synthesis of α,β -unsaturated carboxylic acid salts. *Chem. Eur. J.* **2014**, *20*, 16858–16862.
- ¹⁶ Dvornić, P. R.; Jaćović, M. S. The viscosity effect on autoacceleration of the rate of free radical polymerization. *Polym. Eng. Sci.* **1981**, *21*, 792–796.
- ¹⁷ Jenkins, A. D.; Jones, R. G.; Moad, G. Terminology for reversible-deactivation radical polymerization previously called “controlled” radical or “living” radical polymerization (IUPAC Recommendations 2010). *Pure Appl. Chem.* **2009**, *82*, 483–491.
- ¹⁸ TIPNO-St: *N*-(*tert*-butyl)-*N*-(2-methyl-1-phenylpropyl)-*O*-(1-phenylethyl)hydroxylamine: Benoit, D.; Chaplinski, V.; Braslau, R.; Hawker, C. J. Development of a universal alkoxyamine for “living” free radical polymerizations. *J. Am. Chem. Soc.* **1999**, *121*, 3904–3920.
- ¹⁹ DDMAT: 2-[[[(dodecylthio)carbonothioyl]thio]-2-methylpropanoic acid.
- ²⁰ (a) Penzel, E. Polyacrylates. In *Ullmann’s Encyclopedia of Industrial Chemistry*; Wiley-VCH Verlag GmbH & Co. KGaA: Weinheim, Germany, 2000; Vol. 28, pp 515–536. (b) Fetters, L.J.; Lohse, D.J.; Richter, D.; Witten, T.A.; Zirkelt, A. Connection between polymer molecular weight, density, chain dimensions, and melt viscoelastic properties. *Macromolecules* **1994**, *27*, 4639–4647. (c) Andreatti, L.; Castelvetro, V.; Faetti, M.; Giordano, M.; Zulli, F. Rheological and thermal properties

of narrow distribution poly(ethyl acrylate)s. *Macromolecules* **2006**, *39*, 1880–1889. (d) Yamazaki, H.; Takeda, M.; Kohno, Y.; Ando, H.; Urayama, K; Takigawa, T. Dynamic viscoelasticity of poly(butyl acrylate) elastomers containing dangling chains with controlled lengths. *Macromolecules* **2011**, *44*, 8829–8834.

Chapter 7. Superabsorbent poly(isoprenecarboxylate) hydrogels*



Summary: In this chapter, isoprenecarboxylic acid (**ICA-H**) is used to synthesize cross-linked networks by radical polymerization. Monomer feeds comprising various ratios of **ICA-H** and its sodium salt (**ICA-Na**) were used to give hydrogels that show attractive performance in comparison with (non-bioderived) poly(acrylate) hydrogels. In particular, these new materials show increasing levels of water uptake (i.e., swelling ratio) across the entire range of ionization (10–90 %Na). This behavior is attributed to the larger distance between carboxylate moieties in the hydrogels, a feature that reduces the average amount of charge repulsion between proximal sodium carboxylate ion pairs (counterion condensation).

* Reproduced in part with permission from Fahnhorst, G. W.; Hoyer, T. R. *ACS Sustainable Chem. Eng.* **2019**, 7, 7491–7495. Copyright 2019 American Chemical Society

7.1 Introduction

Hydrogels—cross-linked polymer networks that swell in the presence of water—are widely used in everyday applications. Their unique ability to retain water have made them suitable for applications ranging from personal-care, commodity and specialty products such as diapers, shampoos, lotions, and cosmetics to more sophisticated applications such as drug-delivery agents and contact lenses. Most commonly, hydrogels are derived from water-soluble monomers of the acrylic acid family [e.g., (meth)acrylic acid, (meth)acrylamide, *N*-isopropylacrylamide, dimethylacrylamide, etc.]. Superabsorbent polymers (SAPs) are capable of retaining very large amounts of water [e.g., >100x the mass of the dried polymer network (aka, dried gel)]. These typically comprise copolymers of ionizable carboxylic acids, portions of which are present as their corresponding alkali metal carboxylate salts (e.g., sodium acrylate with acrylic acid). The ionic nature of such copolymers provides the enthalpic driving force that renders them hydrophilic.¹

With the growing demand toward replacing petroleum-based polymers with sustainable alternatives, researchers have explored producing acrylic acid from renewable feedstocks like lactic acid,^{2–5} 3-hydroxypropionic acid,^{6,7} and glycerol.^{8,9} Although technically feasible, at present these are not deemed to be economically viable. Additionally, considerable research has been focused on incorporating other renewable monomers such as α -methylene- γ -butyrolactone,¹⁰ starch,¹¹ alginates,¹² cellulose,^{13–17} itaconic acid,^{18–20} and chitosan^{21,22} into hydrogels, but this nearly always involves incorporation of acrylate moieties for the polymerization chemistry. There remains a need for viable alternatives in which the content of the hydrogel polymer is largely bio-derived.

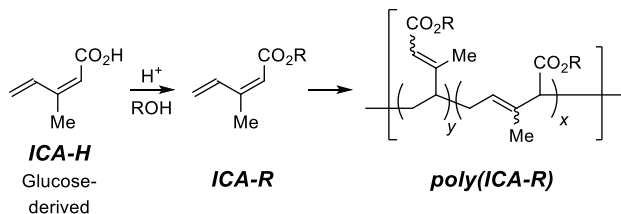


Figure 7.1 Previous work: conversion of isoprenecarboxylic acid (**ICA-H**) to its corresponding esters **ICA-R** and their polymerization to poly(isoprenecarboxylic acid esters) [**poly(ICA-R)**].²³

Recently, we prepared isoprenecarboxylic acid (**ICA-H**, Figure 7.1) from anhydromevalonolactone, which can be efficiently obtained from glucose via mevalonate.²³ We proceeded to synthesize and radically polymerize the corresponding isoprenecarboxylate esters (**ICA-R**) to poly(isoprenecarboxylic acid esters) [**poly(ICA-R)**]. We observed that these behave similarly to poly(acrylates) in terms of entanglement molecular weights and glass transition temperatures. To expand on this technology, we envisioned that **ICA-H** could be used as a new platform for the development of novel hydrogels and SAPs. This route is attractive because **ICA-H** has the potential to be produced at a price point where it perhaps could serve as a major component of a specialty hydrogel.²⁴ This study was, therefore, undertaken to explore a potential practical application of this new polymer.

7.2 Results and Discussion

We synthesized a series of sodiated poly(isoprenecarboxylates) [**poly(ICA-H/Na)**] as shown in Figure 7.2a. The relative number of carboxylates to carboxylic acids was controlled by varying the relative amounts of **ICA-H** and its sodium salt **ICA-Na** in the monomer feed by pre-titrating the former with controlled amounts of NaOH. Use of 50:50 MeOH/H₂O as solvent allowed for maintenance of homogeneity at the reaction temperature

(65 °C) throughout the entire polymerization. The ratio of the two monomers had little effect on the 1,2- vs. 1,4-mode of addition in the radical polymerization. The ratio of these competing additions was assessed by ¹H NMR analysis (D₂O) of the resulting linear **poly(ICA-H/Na)**; the value of 1.0:1.5 was the same as that observed in **poly(ICA-R)**.²³ However, the rate of the polymerization slowed as the percentage of sodium carboxylates in the feed was increased. This phenomenon is also reported for (meth)acrylic acid and sodium (meth)acrylate co-polymerizations.^{25–27}

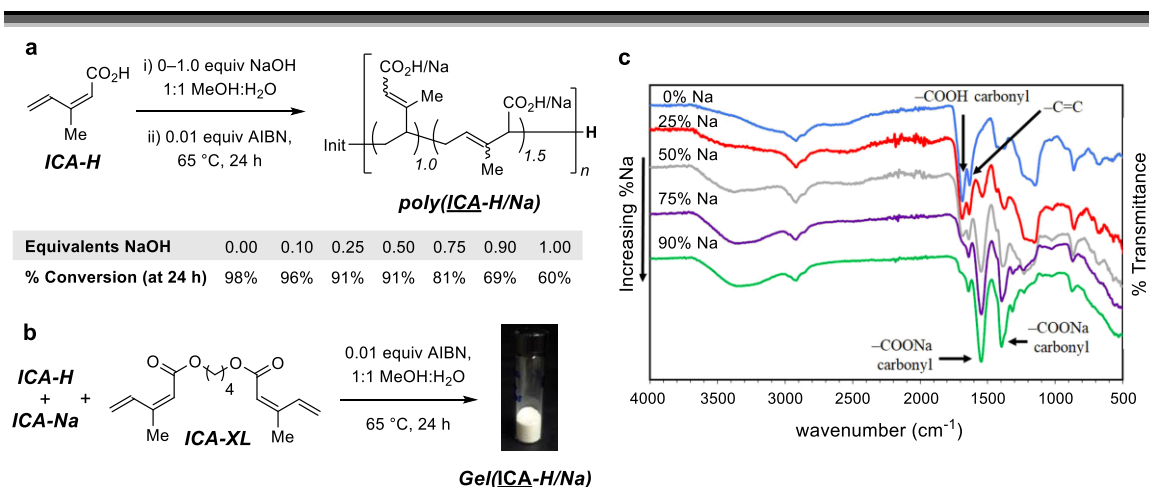


Figure 7.2 (a) Synthesis of linear poly(isoprenecarboxylic acid/carboxylate) [**poly(ICA-H/Na)**]. (b) Synthesis of cross-linked hydrogels **Gel(ICA-H/Na)** from monomers **ICA-H** and **ICA-Na** and the cross-linking agent **ICA-XL**. (c) IR spectra of hydrogels containing varying amounts of sodium carboxylates.

We proceeded to use solution polymerization to synthesize cross-linked networks of sodiated poly(isoprenecarboxylic acid) [**Gel(ICA-H/Na)**] (Figure 7.2b). We used analogous conditions described for the linear **poly(ICA-H/Na)** preparation, now in the presence of 1 mol% of the cross-linking agent **ICA-XL**. Each sample was polymerized to gel state, from which any soluble components were leached with water and acetone. The resulting gels were dried (100 °C, vacuum) and ground to fine powders (see SI for details)

having particle sizes ranging from tens to low hundreds of μm (see representative SEM images in Figure S7.4). Overall mass recovery of the final dried powder was typically in the range of 70–90% based on monomer conversion.

The IR spectra of the dried sodiated isoprenecarboxylic acid gels are shown in Figure 7.2c. With increasing ionization, the spectra show (i) a decrease in the intensity of the C=O stretch corresponding to the acid repeat units (1688 cm^{-1}) and (ii) an increase in that of two C=O stretches at 1547 (asymmetric stretch) and 1395 (symmetric stretch) cm^{-1} , indicative of the sodium carboxylate repeat units.²⁸ Additionally, more water is incorporated within those dried gels that contain higher percentages of **ICA-Na** in the starting polymerization mixture as observed by the intensity of the broad OH stretch between $\sim 3100\text{--}3600\text{ cm}^{-1}$ [distinct from the underlying OH stretch from CO_2H groups (ca. $2500\text{--}3500\text{ cm}^{-1}$)]. This interpretation of water retention at higher %Na is supported by the observed early mass loss (<10% below $200\text{ }^\circ\text{C}$) prior to the onset of polymer degradation (thermogravimetric analysis, Figure S7.3).

We then evaluated the swelling properties of the **Gel(ICA-H/Na)** samples of varying %Na content. Deionized water was added to each dried gel (Figure 7.3a) and mass gain was determined following centrifugation and excess water removal. The results are indicated by the black bars in Figure 7.3a. A barely discernable amount of swelling was observed for the gel having only 10 %Na, but a nearly linear increase in the extent of swelling was seen for the samples containing 25 up to 90 %Na. For the last, the 25 mg sample of dried gel swelled to 6.11 g of hydrogel [swelling ratio (SR) = 245x]. The presence of additional alkali ions is known to decrease swelling efficiency, so we repeated measurement using a 0.17 M (1% w/w) aqueous solution of NaCl instead of DI water (black bars, Figure 7.3b). A nearly identical trend in SR vs. %Na was observed, and the extent of

swelling was reduced by ca. five times (note y-axis values in Figure 7.3a vs. 3b). The data represented by the gray bars in Figure 7.3 is for analogous poly(acrylic acid) (**PAA**) carboxylate gels [**Gel(AA-H/Na)**] and is discussed in further detail later.

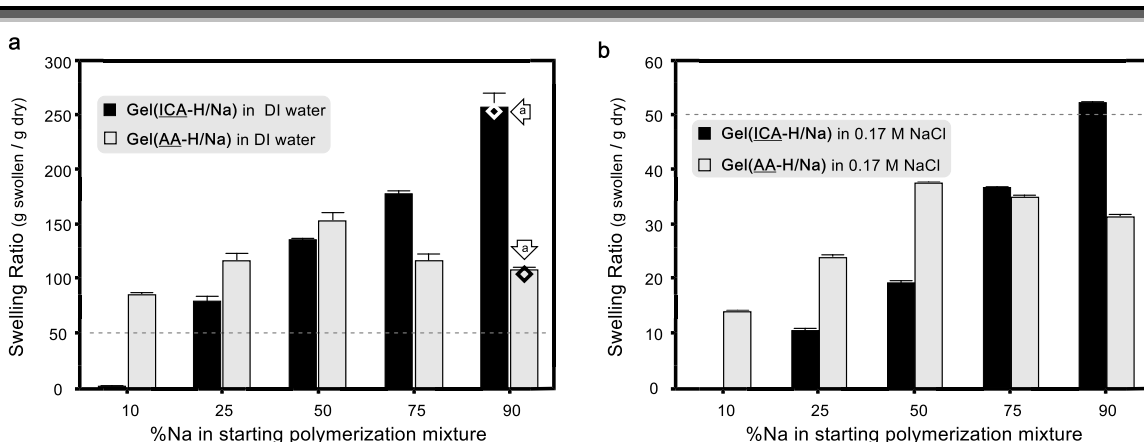


Figure 7.3 Swelling ratio (SR = g of swollen gel/g of dried gel) vs. percent sodiation in the starting monomer feed for both **Gel(ICA-H/Na)** (black) and **Gel(AA-H/Na)** hydrogels (gray) prepared under identical conditions in (a) DI H₂O and (b) 0.17 M (1% w/w) NaCl aqueous solution. ^a Diamond represents the SR in DI water for a sample of 90 %Na **Gel(ICA-H/Na)** or **Gel(AA-H/Na)** prepared by titrating a 50 %Na gel with additional NaOH.

The effect of the nature of the alkali counterion was examined. We synthesized two analogous series of ICA gels with ionizations ranging between 10–90% having Li⁺ [**Gel(ICA-H/Li)**] and K⁺ [**Gel(ICA-H/K)**] counterions (from the addition of metered amounts of LiOH or KOH to the **ICA-H** monomer prior to polymerization). As with sodium, as the %Li or %K increases, the swelling ratios also increase in a linear fashion (see Figures S11 and S13). The swelling ratios also decrease by ca. five times when upon changing from DI H₂O vs. either 0.17 M NaCl or KCl solution. The swelling ratios comparing the counterion effect for the 90% ionized samples are shown in Table 7.1a. Overall, the trend is that **Gel(ICA-H/Li)** swells the most and **Gel(ICA-H/K)** the least,

although the magnitude of those changes are relatively small when one further factors in that the number of metal ions per mass of each dried gel decreases in the series of Li > Na > K. In the presence of excess (5-8 fold) 0.17 M NaCl or KCl solution, the differences among the SRs as well as their overall magnitude are considerably compressed.

Table 7.1 (a) Effect of alkali metal counterion (Met) on the SR for 90 % ionization of Li, Na, and K **Gel(ICA-H/Met)s**. (b) Effect of cross-link density on the SR for 90 % Na of **Gel(ICA-H/Na)s**

| a) Alkali metal counterion vs. swelling ratio for Gel(ICA-H/Met) | | | | b) Cross-link density vs. swelling ratio for Gel(ICA-H/Na) (90%Na) | | | |
|---|---------------------|-------------|------------|---|--------------------------|-------------|------------|
| <i>M</i> | DI H ₂ O | 0.17 M NaCl | 0.17 M KCl | <i>mol% ICA-XL</i> | DI H ₂ O | 0.17 M NaCl | 0.17 M KCl |
| 90%Li | 322 ± 12 | 56 ± 1 | 54 ± 2 | 0.1 | No gel fraction detected | | |
| 90%Na | 258 ± 15 | 52 ± 1 | 48 ± 1 | 1.0 | 258 ± 15 | 52 ± 1 | 48 ± 1 |
| 90%K | 224 ± 21 | 46 ± 0.3 | 44 ± 2 | 2.5 | 185 ± 6 | 48 ± 1 | 49 ± 1 |
| | | | | 5.0 | 116 ± 3 | 35 ± 2 | 25 ± 2 |

We also briefly studied the effect of cross-link density vs. swelling. The data are shown in Table 7.1b (and Table 7.S3, Figure S7.7). A reduction in SR is observed **Gel(ICA-H/Na)** as the number of cross-links increases within a given volume, a common phenomenon for many hydrogels.²⁹

Finally, we were also interested in benchmarking the swelling performance of these new bioresourced **Gel(ICA-H/Na)** samples against that of samples of sodiated, cross-linked poly(acrylic acid) gels [**Gel(AA-H/Na)**]. Because many factors are known to influence the precise nature of the poly(acrylic acid)-based gels made by polymerization of acrylic acid/sodium acrylate feeds,^{30,31} we opted to synthesize our own **Gel(AA-H/Na)s** for this comparative study by an analogous protocol to that used to prepare **Gel(ICA-H/Na)** (see SI). The results for the swelling of **Gel(AA-H/Na)** are shown by the gray bars in Figures 3a and 3b. The most significant difference in the observed trends is that **Gel(AA-H/Na)** swelling reaches a maximum at 50% sodiation of its acid groups and then wanes at higher levels of ionization,³²⁻³⁴ whereas the **Gel(ICA-H/Na)** samples continue to increase

their extent of swelling at increasingly higher amounts of sodiation. This behavior is parallel for the swelling data in either DI water (Figure 7.3a) or 0.17 M (1% w/v) NaCl solution (Figure 7.3b). This difference can be explained by a phenomenon known as counterion condensation.^{35–37} Because the average distance

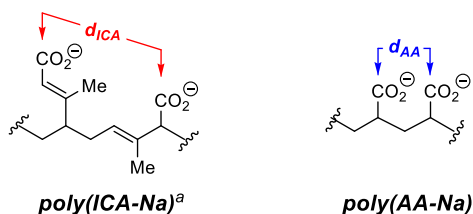


Figure 7.4 The average distance between carboxylates is larger for **poly(ICA-Na)** than for **poly(AA-Na)** (i.e., $d_{ICA} > d_{AA}$). “The representative substructure shown for the former (here for a pair of adjacent 1,2- and 1,4-ICA subunits) is one of several present in **poly(ICA-Na)**).

between any two carboxylate groups is smaller for **Gel(AA-H/Na)** than for **Gel(ICA-H/Na)** (see red vs. blue in Figure 7.4), the average “tightness” of the ion pairing of each Na⁺ with its carboxylate is greater in the former than in the latter in order to minimize repulsion between neighboring anionic carboxylates. This leads to a reduced driving force for water solvation of the sodium counterions present in **Gel(AA-H/Na)**. From the alternative perspective, the carboxylate ions are less repulsive in **Gel(ICA-H/Na)**, allowing its sodium counterions to take on higher levels of solvation. Thus, the greater average spacing between the carboxylates in **Gel(ICA-H/Na)** imparts a significant performance advantage to these novel hydrogels.

Because each series of polymeric gels was made by using different ratios of RCO₂H:RCO₂Na monomer feeds, it is possible that differences in the morphologies of the resulting networks contribute to the differences in swelling behavior. This was explored by

taking a sample of the 50% sodiated material for each of the acrylate [**Gel(AA-H/Na)**] and isoprenecarboxylate [**Gel(ICA-H/Na)**] and titrating it to 90% sodiation by addition of aqueous NaOH. The SRs of the resulting hydrated gels, in each case, were, within error, identical to those observed for the material made directly by starting with a 10:90 RCO₂H:RCO₂Na ratio of monomers [see diamonds (◆) in Figure 7.3a].

We also briefly explored the effect of pH on the swelling ratio³⁸ of a single gel sample for each of **Gel(ICA-H/Na)** and **Gel(AA-H/Na)** (25 %Na in various buffered solutions at constant ionic strength; Table S7.5, Figure 7.5). The observed trends mirror reasonably well those observed for the swelling studies portrayed in Figure 7.3. These final two experiments suggest that any morphological differences associated with the method of gel synthesis is not contributing significantly to the differences in the trends for these two classes of hydrogels, further supporting the counterion condensation interpretation.

The phenomenon of lack of counterion condensation across a full range of %ionization has been observed for poly(styrenesulfonic acid)³⁹ and poly(2-acrylamido-2-methylpropanesulfonic acid),⁴⁰ polymers in which the ionizable groups are also spatially separated to a greater extent than in poly(acrylic acid). However, we are not aware of this being observed previously for carboxylic acid-containing polymers or those that are bioresourcable. In addition, we have not seen examples of reports of continuous increase in SRs across the full spectrum of ionization.

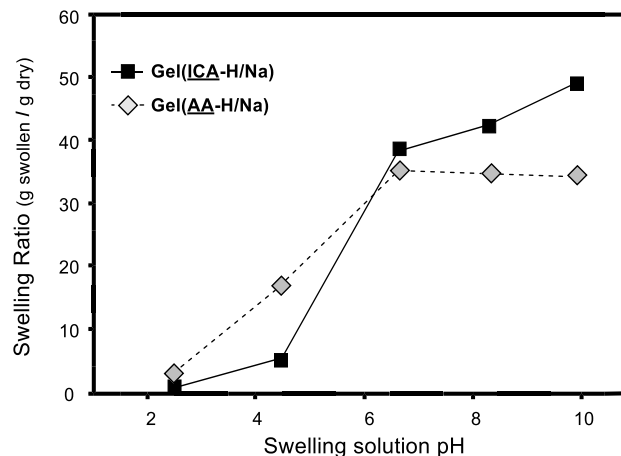


Figure 7.5 Graph of swelling ratio data (Table S7.5) for sodiated (25 %Na) hydrogels, each made using 1% cross-linking agent [**Gel(ICA-H/Na)** as black squares and **Gel(AA-H/Na)** as gray diamonds] in swelling solutions with pH ranging from 2.4–9.9. These observations are similar to the data in Figure 3a, where the % ionizations vs. swelling ratios are compared.

7.3 Conclusion

Using the bio-derived isoprenecarboxylic acid monomer **ICA-H**, we have synthesized and studied the swelling properties of **Gel(ICA-H/Na)**. A series of these cross-linked, polymeric hydrogels varying in the extent of ionization (i.e., %Na loading) of the carboxyl groups present in each backbone repeat unit was prepared. The swelling behavior of each gel was benchmarked against similar hydrogels that we made by the same polymerization protocol from acrylic acid/sodium acrylate monomer feeds. The novel **Gel(ICA-H/Na)** materials retain ever-increasing amounts of water across the entire range of %Na loading, a phenomenon that distinguishes them from and is advantageous to the behavior we observed for the analogous acrylate-based gels. The poly(acrylate)s [**Gel(AA-**

H/Na)] showed a maximum amount of swelling at 50 %Na (140x in DI water) whereas the new **Gel(ICA-H/Na)** gels showed continuously increased uptake even at the highest (90 %Na) degree of ionization (260x in DI water). We attribute this difference to a reduced amount of counterion condensation in the **Gel(ICA-H/Na)** samples because of the greater spatial separation of the carboxyl groups in the ICA-based gels, a potentially more broadly exploitable phenomenon. It is notable that (i) all of the carbon atoms in mevalonate, the organic raw material whose production from glucose by an engineered metabolic pathway²⁴ has been performed on large scale, are present in the hydrogel; (ii) >99% of the entire carbon content of the gel is derived from mevalonate; and (iii) only straightforward chemistry (water is the sole byproduct) is needed for the three reactions that transform mevalonate into the network gel: an acid-catalyzed dehydration, a base-mediated eliminative ring-opening, and a radical initiated polymerization.

7.4 References

- ¹ Thakur, S.; Thakur, V. K.; Arotiba, O. A. History, classification, properties and application of hydrogels: An overview. In *Hydrogels: Recent advances*. Thakur, V. K.; Thakur, M. K., Eds.; Springer: Singapore, 2018; Ed. 1. pp 29–50, DOI 10.1007/978-981-10-6077-9_2.
- ² Aida, T. M.; Ikarashi, A.; Saito, Y.; Watanabe, M.; Smith Jr., R. L.; Arai, K. Dehydration of lactic acid to acrylic acid in high temperature water at high pressures. *J. Supercrit. Fluids* **2009**, *50*, 257–264, DOI 10.1016/j.supflu.2009.06.006.
- ³ Yee, G. M.; Hillmyer, M. A.; Tonks, I. A. Bioderived acrylates from alkyl lactates via Pd-catalyzed hydroesterification. *ACS Sustainable Chem. Eng.* **2018**, *6*, 9579–9584, DOI 10.1021/acssuschemeng.8b02359.
- ⁴ Holmen, R. E. Acrylates by catalytic dehydration of lactic acid and lactates. U.S. Patent 2,859,240, November 4, 1958.
- ⁵ Sawicki, R. A. Catalyst for dehydration of lactic acid to acrylic acid. U.S. Patent 4,729,978, March 8, 1988.
- ⁶ Velasquez, J. E.; Collias, D. I.; Godlewski, J. E.; Wireko, F. C. Catalytic dehydration of hydroxypropionic acid and its derivatives. U.S. Patent 20170057900A1, March 2, 2017.
- ⁷ Li, C.; Zhu, Q.; Cui, Z.; Wang, B.; Fang, Y.; Tan, T. Highly efficient and selective production of acrylic acid from 3-hydroxypropionic acid over acidic heterogeneous catalysts. *Chem. Eng. Sci.* **2018**, *183*, DOI 288–294, 10.1016/j.ces.2018.03.030.
- ⁸ Kim, M.; Lee, H. Highly selective production of acrylic acid from glycerol via two steps using Au/CeO₂ catalysts. *ACS Sustainable Chem. Eng.* **2017**, *5*, 11371–11376, DOI 10.1021/acssuschemeng.7b02457.
- ⁹ Wisuthammakul, A.; Sooknoi, T. Direct conversion of glycerol to acrylic acid via integrated dehydration-oxidation bed system. *Appl. Catal. A* **2012**, *413*, 109–116, DOI 10.1016/j.apcata.2011.10.045.
- ¹⁰ Kollár, J.; Mrlík, M.; Moravčíková, D.; Kroneková, Z.; Liptaj, T.; Lacík, T.; Mosnáček, J. Tulips: A renewable source of monomer for superabsorbent hydrogels. *Macromolecules* **2016**, *49*, 4047–4056, DOI 10.1021/acs.macromol.6b00467.

-
- ¹¹ Castel, D.; Ricard, A.; Audebert, R. Swelling of anionic and cationic starch-based superabsorbents in water and saline solution *J. App. Polym. Sci.* **1990**, *39*, 11–29, DOI 10.1002/app.1990.070390102.
- ¹² Chan, A. W.; Whitney, R. A.; Neufeld, R. J. Semisynthesis of a controlled stimuli-responsive alginate hydrogel. *Biomacromolecules* **2009**, *10*, 609–616, DOI 10.1021/bm801316z.
- ¹³ Marci, G.; Mele, G.; Palmisano, L.; Pulitob, P.; Sannino, A. Environmentally sustainable production of cellulose-based superabsorbent hydrogels. *Green Chem.* **2006**, *8*, 439–444, DOI 10.1039/B515247J.
- ¹⁴ Sannino, A.; Demitri, C.; Madaghiale, M. Biodegradable cellulose-based hydrogels: Design and applications. *Materials* **2009**, *2*, 353–373, DOI 10.3390/ma2020353.
- ¹⁵ Chang, C.; He, M.; Zhou, J.; Zhang L. Swelling behaviors of pH- and salt-responsive cellulose-based hydrogels. *Macromolecules* **2011**, *44*, 1642–1648, DOI 10.1021/ma102801f.
- ¹⁶ Dai, H.; Huang, H. Enhanced swelling and responsive properties of pineapple peel carboxymethyl cellulose-*g*-poly(acrylic acid-co-acrylamide) superabsorbent hydrogel by the introduction of carclazyte. *J. Agric. Food Chem.* **2017**, *65*, 565–574, DOI 10.1021/acs.jafc.6b04899.
- ¹⁷ For a review on cellulose-based hydrogels see. Ma, J.; Li, X.; Bao, Y. Advances in cellulose-based superabsorbent hydrogels. *RSC Adv.* **2015**, *5*, 59745–59757, DOI 10.1039/C5RA08522E.
- ¹⁸ Krušić, M. K.; J. Filipović, J. Copolymer hydrogels based on *N*-isopropylacrylamide and itaconic acid. *Polymer* **2006**, *47*, 148–155, DOI 10.1016/j.polymer.2005.11.002.
- ¹⁹ Karadağ, E.; Saraydin, D.; Güven, O. Radiation induced superabsorbent hydrogels. acrylamide/itaconic acid copolymers. *Macromol. Mater. Eng.* **2001**, *286*, 34–42, DOI 10.1002/1439-2054(20010101)286:1<34::AID-MAME34>3.0.CO;2-J.
- ²⁰ Saggu, S.; Bajpai, S. K. Water uptake behavior of poly(methacrylamide-co-*N*-vinyl-2-pyrrolidone-co-itaconic acid) as pH-sensitive hydrogels: Part I. *J. Macromol. Sci., Pure Appl. Chem.* **2006**, *43*, 1135–1150, DOI 10.1080/10601320600735116.
- ²¹ Zhang, R.-Y.; Zaslavski, E.; Vasilyev, G.; Boas, M.; Zussman, E. Tunable pH-responsive chitosan-poly(acrylic acid) electrospun fibers. *Biomacromolecules* **2018**, *19*, 588–595, DOI 10.1021/acs.biomac.7b01672.

-
- ²² For a recent review see: Cheng, B.; Pei, B.; Wang, Z.; Hu, Q. Advances in chitosan-based superabsorbent hydrogels. *RSC Adv.* **2017**, *7*, 42036–42046, DOI 10.1039/C7RA07104C.
- ²³ Ball-Jones, N. R.; Fahnhorst, G. W.; Hoyer, T. R. Poly(isoprenecarboxylates) from glucose via anhydromevalonolactone. *ACS Macro Lett.* **2016**, *5*, 1128–1131, DOI 10.1021/acsmacrolett.6b00560.
- ²⁴ Xiong, M.; Schneiderman, D. K.; Bates, F. S.; Hillmyer, M. A.; Zhang, K. Scalable production of mechanically tunable block polymers from sugar. *Proc. Natl. Acad. Sci. U. S. A.* **2014**, *111*, 8357–8362. DOI 10.1073/pnas.1404596111.
- ²⁵ Noble, B. B.; Coote, M. L. Effects of ionization on tacticity and propagation kinetics in methacrylic acid polymerization; Matyjaszewski, K.; Sumerlin, B. S.; Tsarevsky, N. V.; Chiefari, J., Eds.; ACS Symposium Series 1187; American Chemical Society: Washington DC, 2015; pp 51–72, DOI 10.1021/bk-2015-1187.ch003.
- ²⁶ Pinner, S. H. Polymerization rate of methacrylic acid. *J. Polym. Sci.* **1952**, *9*, 282–285, DOI 10.1002/pol.1952.120090310.
- ²⁷ Blauer, G. Rate of polymerization of methacrylic acid in alkaline solution. *J. Polym. Sci.* **1953**, *11*, 189–192, DOI 10.1002/pol.1953.120110211.
- ²⁸ Max, J. J.; Chapados, C. Infrared spectroscopy of aqueous carboxylic acids: A Comparison between different acids and their salts. *J. Phys. Chem. A* **2004**, *108*, 3324–3337, DOI 10.1021/jp036401t.
- ²⁹ Flory, P. J.; Rehner, J. Statistical mechanics of cross-linked polymer networks II. Swelling. *J. Chem. Phys.* **1943**, *11*, 521–526, DOI 10.1063/1.1723792.
- ³⁰ Elliot, J. E.; Macdonald, M.; Nie, J.; Bowman, C. N. Structure and swelling of poly(acrylic acid) hydrogels: Effect of pH, ionic strength, and dilution on the crosslinked polymer structure. *Polymer* **2004**, *45*, 1503–1510, DOI 10.1016/j.polymer.2003.12.040.
- ³¹ Riahinezhad, M.; Kazemi, K.; McManus, N.; Penlidis, A. Effect of ionic strength on the reactivity ratios of acrylamide/acrylic acid (sodium acrylate) copolymerization. *J. Appl. Polym. Sci.* **2014**, *131*, 40959, DOI 10.1002/app.40949.
- ³² Kuhn, W.; Hargitay, B.; Katchalsky, A.; Eisenberg, H.; Reversible dilation and contraction by changing the state of ionization of high-polymer acid networks. *Nature* **1950**, *165*, 514–516, DOI 10.1038/165514a0.
- ³³ Kuhn et. al. (ref. 32) showed for a series of poly(acrylic acid)-based gels a plateauing (or leveling off) rather than a fall-off effect for the swelling ratios at high levels of

-
- ionization (from ca. 50% to 90% ionization). These differences may be attributed to the additional mass gained by the hydrogel in the formation of sodium carboxylate salts upon addition of a titrated amount NaOH to the acrylic acid gels. The change in mass associated with exchange of sodium for hydrogen does not appear to have been accounted for in determining the swelling ratios of those samples, which would lead to a greater fall-off, more similar to our observations (Figure 7.3).
- ³⁴ Ikegami, A. Hydration and ion binding of polyelectrolytes. *J. Polym. Sci. A.* **1964**, *2*, 907–921, DOI 10.1002/pol.1964.100020226.
- ³⁵ Manning, G.S. The molecular theory of polyelectrolyte solutions with applications to the electrostatic properties of polynucleotides. *Q. Rev. Biophys.* **1978**, *11*, 179–246, DOI 10.1017/S0033583500002031.
- ³⁶ Stevens, M.J.; Kremer, K. The nature of flexible linear polyelectrolytes in salt free solution: A molecular dynamics study. *J. Chem. Phys.* **1995**, *103*, 1669–1690, DOI 10.1063/1.470698.
- ³⁷ Rička, J.; Tanaka, T. Swelling of ionic gels: quantitative performance of the Donnan theory. *Macromolecules* **1984**, *17*, 2916–2921, DOI 10.1021/ma00142a081.
- ³⁸ Bao, Y.; Ma, J.; Li, N. Synthesis and swelling behaviors of sodium carboxymethyl cellulose-g-poly(AA-co-AM-co-AMPS)/MMT superabsorbent hydrogels. *Carbohydr. Polym.* **2011**, *84*, 76–82, DOI 10.1016/j.carbpol.2010.10.061.
- ³⁹ Kwak, J. C. T.; Hayes, R. C. Electrical conductivity of aqueous solutions of salts of polystyrenesulfonic acid with univalent and divalent counterions. *J. Phys. Chem.* **1975**, *79*, 265–269, DOI 10.1021/j100570a014.
- ⁴⁰ Gong, J. P.; Komsatsu, N.; Nitta, T.; Osada, Y. Electrical conductance of polyelectrolyte gels. *J. Phys. Chem. B.* **1997**, *101*, 740–745, DOI 10.1021/jp963059u.

Bibliography

Chapter 1

- ¹ Jambeck, J. R.; Geyer, R.; Wilcox, C.; Siegler, T. R.; Perryman, M.; Andrady, A.; Narayan, R.; Law, K. L. Plastic Waste Inputs from Land into the Ocean. *Science* **2015**, *347*, 768–771.
- ² World Economic Forum; Ellen MacArthur Foundation; McKinsey and Company. The New Plastics Economy Rethinking the Future of Plastics. <http://www.ellenmacarthurfoundation.org/publications>, 2016.
- ³ Zhang, X.; Fevre, M.; Jones, G. O.; Waymouth, R. M. Catalysis as an enabling science for sustainable polymers. *Chem. Rev.* **2017**, *118*, 839–885.
- ⁴ Schneiderman, D. K.; Hillmyer, M. A. *50th anniversary perspective*: There is a great future in sustainable polymers. *Macromolecules* **2017**, *50*, 3733–3749.
- ⁵ Werpy, T.; Petersen, G. Top Value Added Chemicals From Biomass Volume I: Results of Screening for Potential Candidates; U.S. Department of Energy: Oak Ridge, TN, **2004**.
- ⁶ Sara, M., Brar, S. K.; Blais, J. F. Production of drop-in and novel bio-based platform chemicals in *Platform Chemical Biorefinery*. Elsevier, **2016**, ch. 14. pp 249–283.
- ⁷ (a) Nordqvist Melander, A.; Qvint, K. Assessing the sustainability of first generation ethanol for bioethylene production. Chalmers University of Technology Report no. 2016:6. (b) Broeren, M. *Production of Bio-ethylene*, Technology brief, International Renewable Energy Agency (IRENA), Abu Dhabi, **2013**. (c) Mahsenzadeh, A.; Zamani, A.; Taherzadeh, M. J. Bioethylene production from ethanol: A review and techno-economical evaluation. *ChemBioEng Rev.* **2017**, *4*, 75–91.
- ⁸ (a) Tullo, A. H. Dow to make polyethylene from sugar in Brazil. *C&EN.* **2007**, *30*, 17. (b) Tullo, A. H. Dow will delay biopolymers plant. *C&EN.* **2012**, *90*, 22.
- ⁹ Yu, L.; Yuan, J.; Zhang, Q.; Li, Y.-M.; He, H.-Y.; Fan, K.-N.; Cao, Y. Propylene from renewable resources: Catalytic conversion of glycerol into propylene. *ChemSusChem* **2014**, *7*, 743–747.
- ¹⁰ A recent review: Sun, D.; Yamada, Y.; Sato, S.; Ueda, W. Glycerol as a potential renewable raw material for acrylic acid production. *Green. Chem.* **2017**, *19*, 3186–3213.
- ¹¹ Abdelraham, O. A.; Park, D. S.; Vinter, K. P.; Spangers, C. S.; Ren, L.; Cho, H. J.; Zhang, K.; Fan, W.; Tsapatsis, M.; Dauenhauer. Renewable isoprene of sequential hydrogenation of itaconic acid and dehydra-decyclization of 3-methyl-tetrahydrofuran. *ACS Catal.* **2017**, *7*, 1428–1431.
- ¹² Tulio, A. H. Coke plays spin the bottle. *C&EN.* **2012**, *90*, 19–20
- ¹³ Bomgardner, M. M. Building a better plastic bottle. *C&EN.* **2017**, *95*, 17–19.
- ¹⁴ (a) Kim, M.; Su, Y.; Fukuoka, A.; Hensen, E. J. M.; Nakajima, K. Aerobic oxidation of 5-(hydroxymethyl)furfural cyclic acetal enables selective furan-2,5-dicarboxylic acid formation with CeO₂-supported gold catalyst. *Angew. Chem. Int. Ed.* **2018**, *57*, 8235–8239. (b) Barwe, S.; Weinder, J.; Cychy, S.; Morales, D. M.; Dieckhöfer, S.; Hiltrop, D.; Masa, J.; Muhler, M.; Schuhmann. Electrocatalytic oxidation of 5-(hydroxymethyl)furfural using high-surface-area nickel boride. *Angew. Chem. Int. Ed.* **2018**, *57*, 11460–11464. (c) Xia, H.; Xu, S.; Hu, H.; An, J.; Li, C.; Efficient conversion of 5-hydroxymethylfurfural to high-value chemicals by chemo- and bio-catalysis. *RSC Advances* **2018**, *54*, 30875–30886.

- ¹⁵ Yu, I. K. M.; Tsang, D. C. W. Conversion of biomass to hydroxymethylfurfural: A review of catalytic systems and underlying mechanisms. *Bioresour. Technol.* **2017**, *238*, 716–732.
- ¹⁶ At the time of publication of this thesis, the first reported lactic acid synthesis using the search engines Reaxys and SciFinder was: Pelouze, J. Ueber die Milchsäure. *Liebigs Ann.* **1845**, *53*, 112–124
- ¹⁷ Robertson, N. C.; Schoenbrunn, E. F. US Patent 2847464A, December 5, 1955.
- ¹⁸ Xiong, M.; Schneiderman, D. K.; Bates, F. S.; Hillmyer, M. A.; Zhang, K. *Proc. Natl. Acad. Sci. U. S. A.* **2014**, *111*, 8357–8362.
- ¹⁹ Koller, M. Biodegradable and biocompatible polyhydroxy-alkanoates (PHA): Auspicious microbial macromolecules from pharmaceutical and therapeutic applications. *Molecules* **2018**, *23*, 362.
- ²⁰ Gallagher, J. M.; Hillmyer, M. A.; Reineke, T. M. Acrylic triblock copolymers incorporating isosorbide for pressure sensitive adhesives. *ACS Sustainable Chem. Eng.* **2016**, *4*, 3379–3387.
- ²¹ Duda, A.; Kowalski, A. Thermodynamics and kinetics of ring-opening polymerization. In *Handbook of ring-opening polymerization*; Dubois, P., Coulembier, O., Raquez, J.-M., Eds.; Wiley-VCH Verlag GmbH & Co. KGaA: Weinheim, 2009; pp 1–51.
- ²² Sawada, H. Thermodynamics of polymerization. II. Thermodynamics of ring-opening polymerization. *J. Macromol. Sci.-Revs. Macromol. Chem.* **1970**, *C5*, 151–174.
- ²³ Olsén, P.; Odelius, K.; Albertsson, A.-C. Thermodynamic presynthetic considerations for ring-opening polymerization. *Biomacromolecules* **2016**, *17*, 699–709.
- ²⁴ Schneiderman, D. K.; Hillmyer, M. A. Aliphatic polyester block polymer design. *Macromolecules* **2016**, *49*, 2419–2428.
- ²⁵ Yevstropov, A. A.; Lebedev, B. V.; Kulagina, T. G.; Lyudvig, Ye. B.; Belenkaya, B. G. The thermodynamic properties of β -propiolactone, its polymer, and its polymerization in the 0–400 K range. *Polym. Sci. U.S.S.R.* **1979**, *21*, 2249–2256.
- ²⁶ Save, M.; Schappacher, M.; Soum, A. Controlled ring-opening polymerization of lactones and lactides initiated by lanthanum isopropoxide, 1. General aspects and kinetics. *Macromol. Chem. Phys.* **2002**, *203*, 889–899.
- ²⁷ Hon, M.; Chen, E. Y.-X. Completely recyclable biopolymers with linear and cyclic topologies via ring-opening polymerization of γ -butyrolactone. *Nat. Chem.* **2016**, *8*, 42–49.
- ²⁸ Zhu, J.-B.; Watson, E. M.; Tang, J.; Chen, E. Y.-X. A synthetic polymer system with repeatable chemical recyclability. *Science* **2018**, *360*, 398–403.
- ²⁹ MacDonald, J. P.; Shaver, M. P. An aromatic/aliphatic polyester prepared via ring-opening polymerization and its remarkably selective and cyclable depolymerization to monomer. *Polym. Chem.* **2016**, *7*, 553–559.
- ³⁰ Zhang, D.; Hillmyer, M. A.; Tolman, W. B. Catalytic polymerization of a cyclic ester derived from a “cool” natural precursor. *Biomacromolecules* **2005**, *6*, 2091–2095.
- ³¹ Haba, O.; Itabashi, H. Ring-opening polymerization of a five-membered lactone *trans*-fused to a cyclohexane ring. *Polym. J.* **2014**, *46*, 89–93.
- ³² Aubin, M.; Prud’homme, R. E. Preparation and properties of poly(valerolactone). *Polymer* **1981**, *22*, 1223–1226.
- ³³ Watts, A.; Kurokawa, N.; Hillmyer, M. A. Strong, resilient, and sustainable aliphatic polyester thermoplastic elastomers. *Biomacromolecules* **2017**, *18*, 1845–1854.

- ³⁴ Seefried Jr., C. G.; Koleske, J. V. Lactone polymers. VI. Glass-transition temperatures of methyl-substituted ϵ -caprolactones and polymer blends. *J. Polym. Sci., Part B: Polym. Phys.* **1975**, *13*, 851–856.
- ³⁵ Quilter, H. C.; Hutchby, M.; Davidson, M. G.; Jones, M. D.; Polymerisation of a terpene-derived lactone: A bio-based alternative to ϵ -caprolactone. *Polym. Chem.* **2016**, *8*, 833–837.
- ³⁶ Ten Breteler, M. R.; Zhong, Z.; Dijkstra, P. J.; Palmans, A. R. A.; Peeters, J.; Feijen, J. Ring-opening polymerization of substituted ϵ -caprolactones with a chiral (salen) AlO_iPr Complex. *J. Poly. Sci. A* **2007**, *45*, 429–436.
- ³⁷ Hopewell, J.; Dvorak, R.; Kosior, E. Plastics recycling: Challenges and opportunities. *Philos. Trans. R. Soc., B* **2009**, *364*, 2115–2126.
- ³⁸ Hong, M.; Chen, E. Y.-X. Chemically Recyclable Polymers: A Circular Economy Approach to Sustainability. *Green Chem.* **2017**, *19*, 3692–3706.
- ³⁹ Chemical recycling of plastic waste. <https://www.basf.com/global/en/who-we-are/sustainability/management-and-instruments/circular-economy/chemcycling.html>. Accessed January 2019.
- ⁴⁰ Tan, X.; Chen, E. Y.-X. Toward infinitely recyclable plastics from renewable cyclic esters. *Chem* **2018**, DOI: 10.1016/j.chempr.2018.10.011.
- ⁴¹ Mahoney, J. E. Acrylic acid production methods. International Patent WO 2013/126375 A1, 2013.
- ⁴² Terrade, F. G.; van Krieken, J.; Verkuijl, B. J. V.; Bouwman, E. Catalytic cracking of lactide and poly(lactic acid) to acrylic acid at low temperatures. *ChemSusChem* **2017**, *10*, 1904–1908.
- ⁴³ Nagarajan, V.; Mohanty, A. K.; Misra, M. Perspective on polylactic acid (PLA) based sustainable materials for durable applications: Focus on toughness and heat resistance. *ACS Sustainable Chem. Eng.* **2016**, *4*, 2899–2916.
- ⁴⁴ Gu, L.; Xu, Y.; Fahnhorst, G. W.; Macosko, C. W. Star vs long chain branching of poly(lactic acid) with multifunctional aziridine. *J. Rheol.* **2017**, *61*, 785–796.
- ⁴⁵ (a) Portilla-Arias, J. A.; García-Alvarez, M.; Martínez de Ilarduya, A.; Holler, E.; Galbis, J. A.; Muñoz-Guerra, S. Synthesis, degradability, and drug releasing properties of methyl esters of fungal poly(β ,L-malic acid). *Macromol. Biosci.* **2008**, *8*, 540–550. (b) Lenz, R. W.; Guerin, P. Functional polyesters and polyamides for medical applications of biodegradable polymers. In *Polymers in medicine. Biomedical and pharmacological applications*; Chiellini, E.; Giusti, P., Ed.; Springer: Boston, 1983; Vol. 23, pp 219–231. (c) Jaffredo, C. G.; Chapurina, Y.; Kirillov, E.; Carpentier, J.-F.; Guillaume, S. M.; Highly stereocontrolled ring-opening polymerization of racemic alkyl β -malolactonates mediated by yttrium [amino-alkoxybis(phenolate)] complexes. *Chem. Eur. J.* **2016**, *22*, 7629–7641. (d) Ouchi, T.; Fujino, A. Synthesis of poly(α -malic acid) and its hydrolysis behavior *in vivo*. *Makromol. Chem.* **1989**, *190*, I523–I530 (e) Pounder, R. J.; Dove, A. P. Synthesis and organocatalytic ring-opening polymerization of cyclic esters derived from L-malic acid. *Biomacromolecules* **2010**, *11*, 1930–1939. (f) Taguchi, K.; Yano, S.; Hiratani, K.; Minoura, N.; Okahata, Y.; Ring-opening polymerization of 3(S)-[(benzyloxycarbonyl)methyl]-1,4-dioxane-2,5-dione: A new route to a poly(α -hydroxy acid) with pendant carboxyl groups. *Macromolecules* **1988**, *21*, 3338–3340. (g) Trollsas, M.; Lee, Y. V.; Mecerreyes, D.; Löwenhielm, P.; Möller, M.; Miller, R. D.; Hedrick, J. L. Hydrophilic aliphatic polyesters: Design, synthesis, and ring-opening polymerization of functional cyclic esters. *Macromolecules* **2000**, *33*, 4619–4627. (h) Mahmud, A.; Xiong, X.-B.; Lavasanifar, A. Novel self-associating poly(ethylene oxide)-block-poly(ϵ -caprolactone) block copolymers with

functional side groups on the polyester block for drug delivery. *Macromolecules* **2006**, *39*, 9419–9428. (i) Garg, S. M.; Xiong, X.-B.; Lu, C.; Lavasanifar, A. Application of click chemistry in the preparation of poly(ethylene oxide)-block-poly(ϵ -caprolactone) with hydrolyzable cross-links in the micellar core. *Macromolecules* **2011**, *44*, 2058–2066.

Chapter 2

- ¹ Jambeck, J. R.; Geyer, R.; Wilcox, C.; Siegler, T. R.; Perryman, M.; Andrady, A.; Narayan, R.; Lavender Law, K. Plastic waste inputs from land into the ocean. *Science* **2015**, *347*, 768–771.
- ² World Economic Forum, Ellen MacArthur Foundation and McKinsey and Company, the new plastics economy rethinking the future of plastics; 2016; [report] <http://www.ellenmacarthurfoundation.org/publications>.
- ³ Hopewell, J.; Dvorak, R.; Kosior, E. Plastics recycling: Challenges and opportunities. *Phil. Trans. R. Soc. B* **2009**, *364*, 2115–2126.
- ⁴ Kyrikou, I.; Briassoulis, D. Biodegradation of agricultural plastic films: A critical review. *J. Polym. Environ.* **2007**, *15*, 125–150.
- ⁵ Laycock, B.; Nickolic, M.; Colwell, J. M.; Gauthier, E.; Halley, P.; Bottle, S.; George, G. Lifetime prediction of biodegradable polymers. *Prog. Polym. Sci.* **2017**, *71*, 144–189.
- ⁶ For a recent review see: Hong, M.; Chen, E. Y.-X. Chemically recyclable polymers: A circular economy approach to sustainability. *Green Chem.* **2017**, *19*, 3692–3706.
- ⁷ (a) Hong, M.; Chen, E. Y.-X. Completely recyclable biopolymers with linear and cyclic topologies via ring-opening polymerization of γ -butyrolactone. *Nat. Chem.* **2016**, *8*, 42–49. (b) X. Y. Tang, M. Hong, L. Falivene, L. Caporaso, L. Cavallo and E. Y.-X. Chen. The quest for converting biorenewable bifunctional α -methylene- γ -butyrolactone into degradable and recyclable polyester: Controlling vinyl-addition/ring-opening/cross-linking pathways. *J. Am. Chem. Soc.* **2016**, *138*, 14326–14337. (c) MacDonald, J. P.; Shaver, M. P. An aromatic/aliphatic polyester prepared via ring-opening polymerisation and its remarkably selective and cyclable depolymerisation to monomer. *Polym. Chem.* **2016**, *7*, 553–559. (d) Schneiderman, D. K.; Vanderlaan, M. E.; Mannion, A. M.; Panthani, T. R.; Batiste, D. C.; Wang, J. Z.; Bates, F. S.; Macosko, C. W.; Hillmyer, M. A. Chemically recyclable biobased polyurethanes. *ACS Macro Lett.* **2016**, *5*, 515–518. (e) Brutman, J. P.; De Hoe, G. P.; Schneiderman, D. K.; Le, T. N.; Hillmyer, M. A. Renewable, degradable, and chemically recyclable cross-linked elastomers. *Ind. Eng. Chem. Res.* **2016**, *55*, 11097–11106.
- ⁸ Kamimura, A.; Shigehiro, Y. An efficient method to depolymerize polyamide plastics: A new use of ionic liquids. *Org. Lett.* **2007**, *9*, 2533–2535.
- ⁹ (a) Li, C.; Sablong, R. J.; van Benthem, R. A. T. M.; Koning, C. E. Unique base-initiated depolymerization of limonene-derived polycarbonates. *ACS Macro Lett.* **2017**, *6*, 684–658. (b) Liu, B.; Chen, L.; Zhang, M.; Yu, A. Degradation and stabilization of poly(propylene carbonate). *Macromol. Rapid Commun.* **2002**, *23*, 881–884. (c) Darensbourg, D. J.; Wei, S.-H. Depolymerization of polycarbonates derived from carbon dioxide and epoxides to provide cyclic carbonates. A kinetic study. *Macromolecules* **2012**, *45*, 5916–5922.
- ¹⁰ Werpy, T.; Petersen, G. Top value added chemicals from biomass volume I — Results of screening for potential candidates from sugars and synthesis gas. Top value added chemicals from biomass volume I: Results of screening for potential candidates; 2004.
- ¹¹ Chi, Z.; Wang, Z.-P.; Wang, G.-Y.; Khan, I.; Chi, Z.-M. Microbial biosynthesis and secretion of L-malic acid and its applications. *Crit. Rev. Biotechnol.* **2016**, *36*, 99–107.

- ¹² (a) Trollsås, M.; Lee, Y. V.; Mecerreyes, D.; Löwenhielm, P.; Möller, M.; Miller, R. D.; Hedrick, J. L. Hydrophilic aliphatic polyesters: Design, synthesis, and ring-opening polymerization of functional cyclic esters. *Macromolecules* **2000**, *33*, 4619–4627. (b) Mahmud, A.; Xiong, X.-B.; Lavasanifar, A. Novel self-associating poly(ethylene oxide)-block-poly(ϵ -caprolactone) block copolymers with functional side groups on the polyester block for drug delivery. *Macromolecules* **2006**, *39*, 9419–9428. (c) Garg, S. M.; Xiong, X.-B.; Lu, C.; Lavasanifar, A. Application of click chemistry in the preparation of poly(ethylene oxide)-block-poly(ϵ -caprolactone) with hydrolyzable cross-links in the micellar core. *Macromolecules* **2011**, *44*, 2058–2066.
- ¹³ PLA can be degraded to either acrylic acid or lactide. Terrade, F. G.; van Krieken, J.; Verkuijl, B. J. V.; Bouwman, E. Catalytic cracking of lactide and poly(lactic acid) to acrylic acid at low temperatures. *ChemSusChem* **2017**, *10*, 1904–1908.
- ¹⁴ von Pechmann, H. On the Cleavage of α -Oxyacids. *Liebigs Ann. Chem.* **1891**, *264*, 261–309.
- ¹⁵ Wiley, R. H.; Smith, N. R. Coumalic Acid. *Org. Synth.* **1951**, *31*, 23–24.
- ¹⁶ Zhu, W.; Shen, J.; Li, Q.; Pei, Q.; Chen, J.; Chen, Z.; Liu, Z.; Hu, G. Synthesis, pharmacophores, and mechanism study of pyridin-3(1*H*)-one derivatives as regulators of translation initiation factor 3A. *Arch. Pharm. Chem. Life Sci.* **2013**, *346*, 654–666.
- ¹⁷ Ashworth, L. W.; Bowden, M. C.; Dembofsky, B.; Levin, D.; Moss, W.; Robinson, E.; Szczur, N.; Virica, J. A new route for manufacture of 3-cyano-1-nathalenecarboxylic acid. *Org. Process Res. Dev.* **2003**, *7*, 74–81.
- ¹⁸ (a) Lee, J. J.; Kraus, G. A. One-pot formal synthesis of biorenewable terephthalic acid from methyl coumalate and methyl pyruvate. *Green Chem.* **2014**, *16*, 2111–2116. (b) Lee, J. J.; Kraus, G. A. Divergent Diels-Alder methodology from methyl coumalate toward functionalized aromatics. *Tet. Lett.* **2013**, *54*, 2366–2368. (c) Lee, J. J.; Pollock III, G. R.; Mitchell, D.; Kasuga, L.; Kraus, G. R. Upgrading malic acid to bio-based benzoates via a Diels-Alder-initiated sequence with the methyl coumalate platform. *RSC Adv.* **2014**, *4*, 45657–45664. (d) Pfennig, T.; Johnson, R. L.; Shanks, B. H. The formation of *p*-toluic acid from coumalic acid: A reaction network analysis. *Green Chem.* **2017**, *19*, 3263–3271.
- ¹⁹ (a) Wiley, R. H.; Hart, A. J. 2-Pyrones. XIV. The hydrogenation of 2-pyrones. *J. Am. Chem. Soc.* **1955**, *77*, 2340–2341. (b) Cao, J.; Wang, S.; Jia L.; Hua, R. Liquid crystal compound containing tetrahydropyrans difluoro methoxy-linking group and preparation method and application thereof. Chinese Patent CN 201410088636, March 12, 2014.
- ²⁰ Fried, J.; Elderfield, R. C. Studies on the lactone related to the cardiac aglycones. VI. The action of diazomethane on certain derivatives of α -pyrone. *J. Org. Chem.* **1941**, *6*, 577–583.
- ²¹ Schneiderman, D. K.; Hillmyer, M. A. Aliphatic polyester block polymer design. *Macromolecules* **2016**, *49*, 2419–2428.
- ²² (a) Bouchoux, G.; Drancourt, D.; Leblanc, D. Gas-phase basicities of lactones. *New J. Chem.* **1995**, *19*, 1243–1257. (b) Bouchoux, G. Gas-phase basicities of polyfunctional molecules. Part 4: Carbonyl groups as basic sites. *Mass Spectrum. Rev.* **2015**, *34*, 493–534. (c) Basko, M.; Kubisa, P. Cationic copolymerization of ϵ -caprolactone and L,L-lactide by an activated monomer mechanism. *J. Polym. Sci. A Polym Chem.* **2006**, *44*, 7071–7081.
- ²³ (a) Ishmuratov, G. Y.; Yakovleva, M. P.; Zaripova, G. V.; Botsman, L. P.; Muslukhov, R. R.; Tolstikov, G. A. Novel synthesis of (4*R*)-4-methylpentanolide from (L)-(-)-menthol. *Chem. Nat. Compd.* **2004**, *40*, 548–551. (b) Zhang, C.; Schneiderman, D. K.; Cai, T.; Tai, Y.-S.; Fox,

- K.; Zhang, K. Optically active β -methyl- δ -valerolactone: Biosynthesis and polymerization. *ACS Sustainable Chem. Eng.* **2016**, *4*, 4396–4402.
- ²⁴ Tanaka, N. Two equilibrium melting temperatures and physical meaning of DSC melting peaks in poly(ethylene terephthalate). *Polymer* **2008**, *49*, 5353–5356.
- ²⁵ Olsen, P.; Odelius, K.; Albertsson, A.-C. Thermodynamic presynthetic considerations for ring-opening polymerization. *Biomacromolecules* **2016**, *17*, 699–709.
- ²⁶ Bartley, D. M.; Coward, J. K. Regioselective synthesis of α -methyl 2-methyleneglutarate via a novel lactonization-elimination rearrangement *J. Org. Chem.* **2006**, *71*, 372–374.
- ²⁷ (a) Feng, Y.; Coward, J. K. Prodrug forms of N-[(4-deoxy-4-amino-10-methyl)pteroyl]glutamate- γ -[ψ P(O)(OH)]-glutarate, A potent inhibitor of folylpoly- γ -glutamate synthetase: Synthesis and hydrolytic stability. *J. Med. Chem.*, **2006**, *49*, 770–788. (b) Tello-Aburto, R.; Lucero, A. N.; Rogelj, S. A catalytic approach to the MH-031 lactone: Application to the synthesis of geraldin analogs. *Tetrahedron Lett.* **2014**, *55* 6266–6268.
- ²⁸ (a) Kobatake, S.; Yamada, B.; Radical polymerization and copolymerization of methyl α -(2-carbomethoxyethyl)acrylate, a dimer of methyl acrylate, as a polymerizable α -substituted acrylate. *J. Polym. Sci. A Polym. Chem.* **1996**, *34*, 95–108. (b) Trumbo, D. L.; Zander, R. A. The copolymerization behavior of acrylate dimers: Copolymers of methyl, ethyl, and *n*-butyl acrylate dimers. *J. Polym. Sci. A Polym. Chem.* **1991**, *29*, 1053–1059. (c) Harada, T.; Zetterlund, P. B.; Yamada, B. Preparation of macromonomers by copolymerization of methyl acrylate dimer involving β fragmentation. *J. Polym. Sci. A.* **2004**, *43*, 597–607.

Chapter 3

- ¹ (a) Viot, B. I.; Lederer, A. Hyperbranched and highly branched polymer architectures—Synthetic strategies and major characterization aspects. *Chem. Rev.* **2009**, *109*, 5924–5973. (b) Zheng, Y.; Li, S.; Weng, Z.; Gao, G. Hyperbranched polymers: Advances from synthesis to applications. *Chem. Soc. Rev.* **2015**, *44*, 4091–4130.
- ² Dong, Z.; Ye, Z. Hyperbranched polyethylenes by chain walking polymerization: synthesis, properties, functionalization, and applications. *Polym Chem.* **2012**, *3*, 286–301.
- ³ Trollsås, M.; Löwenhielm, P.; Lee, V. Y.; Möller, M.; Miller, R. D.; Hedrick, J. L. New approach to hyperbranched polyesters: Self-condensing cyclic ester polymerization of bis(hydroxymethyl)-substituted ϵ -caprolactone. *Macromolecules* **1999**, *32*, 9062–9066.
- ⁴ Fréchet, J. M. J.; Henmi, M.; Gitsov, I.; Aoshima, S.; Leduc, M. R.; Grubbs, R. B. Self-condensing vinyl polymerization: An approach to dendritic materials. *Science* **1994**, *263*, 1080–1083.
- ⁵ A related concept, using reversible Diels-Alder reactions and resulting in architectural reorganization of a preformed polymer was recently reported. Sun, H. Kabb, C. P.; Dai, Y.; Hill, M. R.; Ghiviriga, I.; Bapat, A. P.; Sumerlin, B. S. Macromolecular metamorphosis via stimulus-induced transformations of polymer architecture. *Nat. Chem.* **2017**, *9*, 817–823.
- ⁶ Fahnhorst, G. W.; Hoye, T. R. A carbomethoxylated polyvalerolactone from malic acid: Synthesis and divergent chemical recycling. *ACS Macro Lett.* **2018**, *7*, 143–147.
- ⁷ (a) von Pechmann, H. On the cleavage of α -oxyacids. *Liebigs Ann. Chem.* **1891**, *264*, 261–309. (b) Wiley, R. H.; Smith, N. R. Coumalic acid. *Org. Synth.* **2003**, *31*, 23–24.
- ⁸ (a) Zhu, J.-B.; Watson, E. M.; Tang, J.; Chen, E. Y.-X. A synthetic polymer system with repeatable chemical recyclability. *Science* **2018**, *360*, 398–403. (b) Hong, M.; Chen, E. Y.-X. Chemically recyclable polymers: A circular economy approach to sustainability. *Green Chem.*

- 2017**, *19*, 3692–3706. (c) Hong, M.; Chen, E. Y.-X. Completely recyclable biopolymers with linear and cyclic topologies via ring-opening polymerization of γ -butyrolactone. *Nat. Chem.* **2016**, *8*, 42–49. (d) Schneiderman, D. K.; Vanderlaan, M. E.; Mannion, A. M.; Panthani, T. R.; Batiste, D. C.; Wang, J. Z.; Bates, F. S.; Macosko, C. W.; Hillmyer, M. A. Chemically recyclable biobased polyurethanes. *ACS Macro Lett.* **2016**, *5*, 515–518.
- ⁹ Williams, C. K.; Breyfogle, L. E.; Kyung Choi, S.; Nam, W.; Young Jr., V. G.; Hillmyer, M. A.; Tolman, W. B. A highly active zinc catalyst for the controlled polymerization of lactide. *J. Am. Chem. Soc.* **2003**, *125*, 11350–11359.
- ¹¹ (a) Newman, M. S. Some observations concerning steric factors. *J. Am. Chem. Soc.* **1950**, *72*, 4783–4786. (b) Newman, M. S. In *Steric effects in organic chemistry*; Newman, M. S., Ed.; Wiley: New York, 1956; p 206.
- ¹² (a) Gaborieau, M.; Castignolles, P. Size-exclusion chromatography (SEC) of branched polymers and polysaccharides. *Anal. Bioanal. Chem.* **2011**, *399*, 1413–1423. (b) McKee, M. G.; Unal, S.; Wilkes, G. L.; Long, T. E. Branched polyesters: Recent advances in synthesis and performance. *Prog. Polym. Sci.* **2005**, *30*, 507–539.
- ¹³ Ladavière, C.; Lacroix-Desmazes, P.; Delolme, F. First systematic MALDI/ESI mass spectrometry comparison to characterize polystyrene synthesized by different controlled radical polymerizations. *Macromolecules* **2009**, *42*, 70–84.
- ¹⁴ Dušek, K.; Šomvásky, J.; Smrdková, M.; Simonsick, Jr., W. J.; Wilczek, L. Role of cyclization in the degree-of-polymerization distribution of hyperbranched polymers. Modeling and experiment. *Polym. Bull.* **1999**, *42*, 489–496.
- ¹⁶ Corneillie, S.; Smet, M. PLA architectures: The role of branching. *Polym. Chem.* **2015**, *6*, 850–867.
- * References 10 and 15 in Chapter 3 were footnotes. These footnotes have been removed here.

Chapter 4

- ¹ Andreeßen, B.; Taylor, N.; Steinbüchel. Poly(3-hydroxypropionate): A promising alternative to fossil fuel-based materials. *Appl. Environ. Microbiol.* **2014**, *80*, 6574–6582.
- ² Nagarajan, V.; Mohanty, A. K.; Misra, M. Perspective on polylactic acid (PLA) based sustainable materials for durable applications: Focus on toughness and heat resistance. *ACS Sustainable Chem. Eng.* **2016**, *4*, 2899–2916.
- ³ Corneillie, S.; Smet, M. PLA architectures: The role of branching. *Polym. Chem.* **2015**, *6*, 850–867.
- ⁴ Gu, L.; Xu, Y.; Fahnhorst, G. W.; Macosko, C. W. Star vs long chain branching of poly(lactic acid) with multifunctional aziridine. *J. Rheol.* **2017**, *61*, 785–796.
- ⁵ Haugan, I. N.; Maher, M. J.; Chang, A. B.; Lin, T.-P.; Grubbs, R. H.; Hillmyer, M. A.; Bates, F. S. – Consequences of grafting density on the linear viscoelastic behavior of graft polymers. *ACS Macro Lett.* **2018**, *7*, 525–530.
- ⁶ Qian, H.; Wohl, A. R.; Crow, J. T.; Macosko, C. W.; Hoyer, T. R. A strategy for control of “random” copolymerization of lactide and glycolide: Application to synthesis of PEG-*b*-PLGA block polymers having narrow dispersity. *Macromolecules*, **2011**, *44*, 7132–7140.

- ⁷ Aluthge, D. C.; Xu, C.; Othman, N.; Noroozi, N.; Hatzikiriakos, S. G.; Mehrkhodavandi, P. PLA-PHB-PLA triblock copolymers: Synthesis by sequential addition and investigation of mechanical and rheological properties. *Macromolecules* **2013**, *46*, 3965–3974.
- ⁸ Schneiderman, D. K.; Hillmyer, M. A. Scalable production of mechanically tunable block polymers from sugar. *Proc. Natl. Acad. Sci. U. S. A.* **2014**, *111*, 8357–8362.
- ⁹ Watts, A.; Kurokawa, N.; Hillmyer, M. A. Strong, resilient, and sustainable aliphatic polyester thermoplastic elastomers. *Biomacromolecules* **2017**, *18*, 1845–1854.
- ¹⁰ Bicerano, J. In *Prediction of Polymer Properties*, 3rd ed.; Marcel Dekker: New York, 2002.
- ¹¹ Boyle, B. M.; Heinz, O.; Miyake, G. M.; Ding, Y. Impact of the pendant group on the chain conformation and bulk properties of norbornene imide-based polymers. *Macromolecules* **2019**, *52*, 3426–3434.
- ¹² Ball-Jones, N. R.; Fahnhorst, G. W.; Hoyer, T. R.; Poly(isoprenecarboxylates) from glucose via anhydromevalonolactone. *ACS Macro Lett.* **2016**, *5*, 1128–1131.
- ¹³ Mark, H. F. Internal polyolefins and a few highly substituted polyvinyls. In *Advances in Polyolefins: The World's Most Widely Used Polymers*; Seymour, R. B., Cheng, T. C., Eds.; Springer: New York, 1987; pp 15–22, DOI: 10.1007/978-1-4757-9095-5.
- ¹⁴ Aime, J. P.; Ramakrishnan, S.; Chance, R. R.; Kim, M. W. The effect of substituent groups on polymer conformation in good solvent: Polyoctene and polydecene. *J. Phys. France* **1990**, *51*, 963–975.
- ¹⁵ Penzel, E. Polyacrylates. In *Ullmann's Encyclopedia of Industrial Chemistry*; Wiley-VCH Verlag GmbH & Co. KGaA: Weinheim, Germany, 2000; Vol. 28, pp 515–536.
- ¹⁶ Fahnhorst, G. W.; Hoyer, T. R. A Carbomethoxylated polyvalerolactone from malic acid: Synthesis and divergent chemical recycling. *ACS Macro Lett.* **2018**, 143–147.
- ¹⁷ Schneiderman, D. K.; Hillmyer, M. A. Aliphatic polyester block polymer design. *Macromolecules* **2016**, *49*, 2419–2428.
- ¹⁸ Fahnhorst, G. W.; Stasiw, D. E.; Tolman, W. B.; Hoyer, T. R. Isomerization of linear to hyperbranched polymers: Two isomeric lactones converge via metastable isostructural polyesters to a highly branched analogue. *ACS Macro Lett.* **2018**, *7*, 1144–1148.
- ¹⁹ von Pechmann, H. On the cleavage of α -oxyacids. *Liebigs Ann. Chem.* **1891**, 264, 261–309.
- ²⁰ Wiley, R. H.; Smith, N. R. Coumalic acid. *Org. Synth.* **1951**, *31*, 23–24.
- ²¹ Yamashita, T.; Nishikawa, H.; Kawamota, T. Scale-up synthesis of a deuterium-labeled cis-cyclobutane-1,3-dicarboxylic acid derivative using continuous photo flow chemistry. *Tetrahedron* **2019**, *75*, 617–623.
- ²² Takeda, K.; Akiyama, A.; Nakamura, H.; Takizawa, S.-I.; Mizuno, Y.; Takayanagi, H.; Harigaya, Y. Dicarbonates: Convenient 4-dimethylaminopyridine catalyzed esterification reagents. *Synthesis* **1994**, *10*, 1063–1066.
- ²³ Phillips, A. J.; Nasveschuk, C. G.; Henderson, J. A.; Liang, Y.; Chen, C.-L.; C.; Duplessis, M.; He, M.; Larzarski, K. Amine-linked C3-glutarimide degronimers for target protein degradation. World patent WO2017197051(A1). November 16, 2017.

- ²⁴ Tello-Aburto, R.; Lucero, A. N.; Rogelj, S. A. Catalytic approach to the MH-031 lactone: Application to the synthesis of geraldin analogs. *Tetrahedron Lett.* **2014**, *55*, 6266–6268.
- ²⁵ See, for example: Kopinke, F.-D.; Remmler, M.; Mackenzie, K.; Möder, M.; Wachsen, O. Thermal decomposition of biodegradable polyester—II. Poly(lactic acid). *Polym. Degrad. Stabil.* **1996**, *53*, 329–342.
- ²⁶ Baran, J.; Duda, A.; Kowalski, A.; Szymanski, R.; Penczek, S. Intermolecular chain transfer to polymer with chain scission: General treatment and determination of k_p/k_{tr} in L,L-lactide polymerization. *Macromol. Rapid Commun.* **1997**, *18*, 325–333.
- ²⁷ Penczek, S.; Duda, A.; Szymanski, R. Intra- and intermolecular chain transfer to macromolecules with chain scission. The case of cyclic esters. *Macromol. Symp.* **1998**, *132*, 441–449.
- ²⁸ Catalytic polymerization of a cyclic ester derived from a “cool” natural precursor. *Biomacromolecules* **2005**, *6*, 2091–2095.
- ²⁹ Hiemenz, P. C.; Lodge, T. P. Crystalline polymers: Kinetics of nucleation and growth. In *Polymer Chemistry*: CRC Press. **2007**; pp 536–545.
- ³¹ Compton, T. R. Mechanical properties of polymers. In *Physical Testing of Plastics*: Smithers Rapra; Shropshire, 2012; pp 1–148.
- ³² Meng, D.-C.; Shi, Z.-Y.; Wu, L.-P.; Zhou, Q.; Wu, Q.; Chen, J.-C. Chen, G.-Q. Production and characterization of poly(3-hydroxypropionate-co-4-hydroxybutyrate) with fully controllable structures by recombinant *Escherichia coli* containing an engineered pathway. *Metab. Eng.* **2012**, *14*, 317–324.
- * Reference 30 in Chapter 4 was a footnote. This footnote has been removed here.

Chapter 5

- ¹ Fahnhorst, G. W.; Hoyer, T. R. A carbomethoxylated polyvalerolactone from malic acid: Synthesis and divergent chemical recycling. *ACS Macro Lett.* **2018**, 143–147.
- ² Fahnhorst, G. W.; Stasiw, D. E.; Tolman, W. B.; Hoyer, T. R. Isomerization of linear to hyperbranched polymers: Two isomeric lactones converge via metastable isostructural polyesters to a highly branched analogue. *ACS Macro Lett.* **2018**, *7*, 1144–1148.
- ³ Schneiderman, D. K.; Hillmyer, M. A. Aliphatic polyester block polymer design. *Macromolecules* **2016**, *49*, 2419–2428.
- ⁴ Trollsas, M.; Lee, Y. V.; Mecerreyes, D.; Löwenhielm, P.; Möller, M.; Miller, R. D.; Hedrick, J. L. Hydrophilic aliphatic polyesters: Design, synthesis, and ring-opening polymerization of functional cyclic esters. *Macromolecules* **2000**, *33*, 4619–4627.
- ⁵ Wright, J. L.; Caprathe, B. W.; Downing, D. M.; Glase, S. A.; Heffner, T. G.; Jaen, J. C.; Johnson, S. J.; Kesten, S. R.; MacKensie, R. G.; Meltzer, L. T.; Pugsley, T. A.; Smith, S. J.; Wise, L. D.; Wustrow, D. J. The discovery and structure-activity relationships of 1,2,3,6-tetrahydro-4-phenyl-1-[(arylcyclohexenyl)alkyl]pyridines. Dopamine autoreceptor agonists and potential antipsychotic agents. *J. Med. Chem.* **1994**, *37*, 3523–3533.
- ⁶ Lapworth, A. CXXXIV.—The form of change in organic compounds, and the function of the α -meta-orientating groups. *J. Chem. Soc., Trans.* **1901**, *79*, 1265–1284.
- ⁷ Wiley, R. H.; Hart, A. J. 2-Pyrones. IX. 2-Pyrone-6-carboxylic acid and its derivatives. *J. Am. Chem. Soc.* **1954**, *76*, 1943–1944.

- ⁸ Cregge, R. J.; Lentz, N. L.; Sabol, J. S. Conformationally restricted leukotriene antagonists. Synthesis of chiral 4-hydroxy-4-alkylcyclohexanecarboxylic acids as leukotriene D4 analogues. *J. Org. Chem.* **1991**, *56*, 1758–1763.
- ⁹ Zhang, D.; Hillmyer, M. A.; Tolman, W. B. Catalytic polymerization of a cyclic ester derived from a “cool” natural precursor. *Biomacromolecules* **2005**, *6*, 2091–2095.
- ¹⁰ Mahmud, A.; Xiong, X.-B.; Lavasanifar, A. Novel self-associating poly(ethylene oxide)-block-poly(ϵ -caprolactone) block copolymers with functional side groups on the polyester block for drug delivery. *Macromolecules* **2006**, *39*, 9419–9428.
- ¹¹ Garg, S. M.; Xiong, X.-B.; Lu, C.; Lavasanifar, A. Application of click chemistry in the preparation of poly(ethylene oxide)-block-poly(ϵ -caprolactone) with hydrolyzable cross-links in the micellar core. *Macromolecules* **2011**, *44*, 2058–2066.
- ¹² Wang, Y.; Liu, X.; Laurini, E.; Posocco, P.; Ziarelli, F.; Fermeglia, M.; Qu, F.; Pricl, S.; Zhang, C.-C.; Peng, L. Mimicking the 2-oxoglutaric acid signaling function using molecular probes: Insights from structural and functional investigations. *Org. Biomol. Chem.* **2014**, *12*, 4723–4729.
- ¹³ Hierold, J.; Hsia, T.; Lupton, D. W. The Grob/Eschenmoser fragmentation of cycloalkanones bearing β -electron withdrawing groups: A general strategy to acyclic synthetic intermediates. *Org. Biomol. Chem.* **2011**, *9*, 783–792.
- ¹⁴ Jones, E. R. H.; Whitham, G. H.; Whiting, M. C. Researches on acetylenic compounds. Part XLIV. The reaction between nickel carbonyl and some esters of ω -acetylenic acids. *J. Chem. Soc.* **1954**, *0*, 1865–1868.
- ¹⁵ Schmidt, J. A. R.; Lobkovsky, E. B.; Coates, G. W. Chromium(III) octaethylporphyrinato tetracarbonylcobaltate: A highly active, selective, and versatile catalyst for epoxide carbonylation. *J. Am Chem. Soc.* **2005**, *127*, 11425–11435.

Chapter 6

- ¹ Xiong, M.; Schneiderman, D. K.; Bates, F. S.; Hillmyer, M. A.; Zhang, K. Scalable production of mechanically tunable block polymers from sugar. *Proc. Natl. Acad. Sci.* **2014**, *111*, 8357–8362.
- ² (a) Zhang, J.; Li, T.; Mannion, A. M.; Schneiderman, D. K.; Hillmyer, M. A.; Bates, F. S. Tough and sustainable graft block copolymer thermoplastics. *ACS Macro Lett.* **2016**, *5*, 407–412. (b) Schneiderman, D. K.; Vanderlaan, M. E.; Mannion, A. M.; Panthani, T. R.; Batiste, D. C.; Wang, J. Z.; Bates, F. S.; Macosko, C. W.; Hillmyer, M. A. Chemically recyclable biobased polyurethanes. *ACS Macro Lett.* **2016**, *5*, 515–518.
- ³ Cornforth, J. W.; Cornforth, R. H.; Popjak, G.; Gore, I. Y. Studies on the biosynthesis of cholesterol. 5. Biosynthesis of squalene from D,L-2-hydroxy-3-methyl-[2-¹⁴C]pentano-5-lactone. *Biochem. J.* **1958**, *69*, 146–155.
- ⁴ Moriconi, E. J.; Meyer, W. C. Reaction of dienes with chlorosulfonyl isocyanate. *J. Org. Chem.* **1971**, *36*, 2841–2849.
- ⁵ Arbuzova, I. A.; Efremova, V. N.; Eliseeva, A. G.; Mikhailova, N. V.; Nikitin, V. N.; Sidorovich, A. V.; Klushin, N. A.; Kuvshinskii, E. V. *Vysokomolekulyarnye Soedineniya, Seriya A.* **1970**, *12*, 697–704.

- ⁶ Takasu, A.; Ishii, M.; Inai, Y.; Hirabayashi, T. Highly threo diastereoselective anionic polymerization of (*E,E*)-methyl sorbate catalyzed by a bulky organoaluminum Lewis acid. *Macromolecules* **2001**, *34*, 6548–6550.
- ⁷ Ueda, M.; Shimada, S.; Ogata, T.; Oikawa, K.; Ito, H.; Yamada, B. Radical polymerization of methyl *trans*- β -vinylacrylate. *J. Polym. Sci. A Polym. Chem.* **1995**, *33*, 1059–1067.
- ⁸ Sheares, V. V. Functionalized diene monomers and polymers containing functionalized dienes and methods for their preparation. US Patent 6,344,538 B1, February 5, 2002.
- ⁹ Matsumoto, A.; Sada, K.; Tashiro, K.; Miyata, M.; Tsubouchi, T.; Tanaka, T.; Odani, T.; Nagahama, S.; Tanaka, T.; Inoue, K.; Saragai, S.; Nakamoto, S. Reaction principles and crystal structure design for the topochemical polymerization of 1,3-dienes. *Angew. Chem. Int. Ed.* **2002**, *41*, 2502–2505.
- ¹¹ Mauldin, T. C.; Wertz, J. T.; Boday, D. J. *ACS Macro Lett.* **2016**, *5*, 544–546.
- ¹² Perrier, S. 50th Anniversary perspective: RAFT polymerization—A user guide. *Macromolecules* **2017**, *50*, 7433–7447.
- ¹³ Abarbri, M.; Parrain, J.-L.; Duchêne, A. Stereospecific synthesis of (*Z*) or (*E*)-3-methylalk-2-enoic acids. *Tetrahedron Lett.* **1995**, *36*, 2469–2472.
- ¹⁴ Nakai, T.; Mikami, K.; Taya, S.; Kimura, Y.; Mimura, T. The [2,3]Wittig rearrangement of 2-alkenyloxyacetic acids and its applications to the stereocontrolled synthesis of β , γ -unsaturated aldehydes and conjugated dienoic acids. *Tetrahedron Lett.* **1981**, *22*, 69–72.
- ¹⁵ Huguet, N.; Jevtovikj, I.; Gordillo, A.; Lejkowski, M. L.; Lindner, R.; Bru, M.; Khalimon, A. Y.; Rominger, F.; Schunk, S. A.; Hofmann, P.; Limbach, M. Nickel-catalyzed direct carboxylation of olefins with CO₂: One-pot synthesis of α,β -unsaturated carboxylic acid salts. *Chem. Eur. J.* **2014**, *20*, 16858–16862.
- ¹⁶ Dvornić, P. R.; Jačović, M. S. The viscosity effect on autoacceleration of the rate of free radical polymerization. *Polym. Eng. Sci.* **1981**, *21*, 792–796.
- ¹⁷ Jenkins, A. D.; Jones, R. G.; Moad, G. Terminology for reversible-deactivation radical polymerization previously called “controlled” radical or “living” radical polymerization (IUPAC Recommendations 2010). *Pure Appl. Chem.* **2009**, *82*, 483–491.
- ¹⁸ TIPNO-St: *N*-(*tert*-butyl)-*N*-(2-methyl-1-phenylpropyl)-*O*-(1-phenylethyl)hydroxylamine: Benoit, D.; Chaplinski, V.; Braslau, R.; Hawker, C. J. Development of a universal alkoxyamine for “living” free radical polymerizations. *J. Am. Chem. Soc.* **1999**, *121*, 3904–3920.
- ²⁰ (a) Penzel, E. Polyacrylates. In *Ullmann's Encyclopedia of Industrial Chemistry*; Wiley-VCH Verlag GmbH & Co. KGaA: Weinheim, Germany, 2000; Vol. 28, pp 515–536. (b) Fetters, L.J.; Lohse, D.J.; Richter, D.; Witten, T.A.; Zirkelt, A. Connection between polymer molecular weight, density, chain dimensions, and melt viscoelastic properties. *Macromolecules* **1994**, *27*, 4639–4647. (c) Andreatti, L.; Castelvetro, V.; Faetti, M.; Giordano, M.; Zulli, F. Rheological and thermal properties of narrow distribution poly(ethyl acrylate)s. *Macromolecules* **2006**, *39*, 1880–1889. (d) Yamazaki, H.; Takeda, M.; Kohno, Y.; Ando, H.; Urayama, K.; Takigawa, T. Dynamic viscoelasticity of poly(butyl acrylate) elastomers containing dangling chains with controlled lengths. *Macromolecules* **2011**, *44*, 8829–8834.

* References 10 and 19 in Chapter 6 were footnotes. These footnotes have been removed here.

Chapter 7

- ¹ Thakur, S.; Thakur, V. K.; Arotiba, O. A. History, classification, properties and application of hydrogels: An overview. In *Hydrogels: Recent advances*. Thakur, V. K.; Thakur, M. K., Eds.; Springer: Singapore, 2018; Ed. 1. pp 29–50.
- ² Aida, T. M.; Ikarashi, A.; Saito, Y.; Watanabe, M.; Smith Jr., R. L.; Arai, K. Dehydration of lactic acid to acrylic acid in high temperature water at high pressures. *J. Supercrit. Fluids* **2009**, *50*, 257–264.
- ³ Yee, G. M.; Hillmyer, M. A.; Tonks, I. A. Bioderived acrylates from alkyl lactates via Pd-catalyzed hydroesterification. *ACS Sustainable Chem. Eng.* **2018**, *6*, 9579–9584.
- ⁴ Holmen, R. E. Acrylates by catalytic dehydration of lactic acid and lactates. U.S. Patent 2,859,240, November 4, 1958.
- ⁵ Sawicki, R. A. Catalyst for dehydration of lactic acid to acrylic acid. U.S. Patent 4,729,978, March 8, 1988.
- ⁶ Velasquez, J. E.; Collias, D. I.; Godlewski, J. E.; Wireko, F. C. Catalytic dehydration of hydroxypropionic acid and its derivatives. U.S. Patent 20170057900A1, March 2, 2017.
- ⁷ Li, C.; Zhu, Q.; Cui, Z.; Wang, B.; Fang, Y.; Tan, T. Highly efficient and selective production of acrylic acid from 3-hydroxypropionic acid over acidic heterogeneous catalysts. *Chem. Eng. Sci.* **2018**, *183*.
- ⁸ Kim, M.; Lee, H. Highly selective production of acrylic acid from glycerol via two steps using Au/CeO₂ catalysts. *ACS Sustainable Chem. Eng.* **2017**, *5*, 11371–11376.
- ⁹ Wisuthammakul, A.; Sooknoi, T. Direct conversion of glycerol to acrylic acid via integrated dehydration-oxidation bed system. *Appl. Catal. A* **2012**, *413*, 109–116.
- ¹⁰ Kollár, J.; Mrlík, M.; Moravčíková, D.; Kroneková, Z.; Liptaj, T.; Lacík, T.; Mosnáček, J. Tulips: A renewable source of monomer for superabsorbent hydrogels. *Macromolecules* **2016**, *49*, 4047–4056.
- ¹¹ Castel, D.; Ricard, A.; Audebert, R. Swelling of anionic and cationic starch-based superabsorbents in water and saline solution *J. App. Polym. Sci.* **1990**, *39*, 11–29.
- ¹² Chan, A. W.; Whitney, R. A.; Neufeld, R. J. Semisynthesis of a controlled stimuli-responsive alginate hydrogel. *Biomacromolecules* **2009**, *10*, 609–616.
- ¹³ Marci, G.; Mele, G.; Palmisano, L.; Pulitob, P.; Sannino, A. Environmentally sustainable production of cellulose-based superabsorbent hydrogels. *Green Chem.* **2006**, *8*, 439–444.
- ¹⁴ Sannino, A.; Demitri, C.; Madaghiale, M. Biodegradable cellulose-based hydrogels: Design and applications. *Materials* **2009**, *2*, 353–373, DOI 10.3390/ma2020353.
- ¹⁵ Chang, C.; He, M.; Zhou, J.; Zhang L. Swelling behaviors of pH- and salt-responsive cellulose-based hydrogels. *Macromolecules* **2011**, *44*, 1642–1648.

- ¹⁶ Dai, H.; Huang, H. Enhanced swelling and responsive properties of pineapple peel carboxymethyl cellulose-g-poly(acrylic acid-co-acrylamide) superabsorbent hydrogel by the introduction of carclazyte. *J. Agric. Food Chem.* **2017**, *65*, 565–574.
- ¹⁷ Ma, J.; Li, X.; Bao, Y. Advances in cellulose-based superabsorbent hydrogels. *RSC Adv.* **2015**, *5*, 59745–59757.
- ¹⁸ Krušić, M. K.; J. Filipović, J. Copolymer hydrogels based on *N*-isopropylacrylamide and itaconic acid. *Polymer* **2006**, *47*, 148–155.
- ¹⁹ Karadağ, E.; Saraydin, D.; Güven, O. Radiation induced superabsorbent hydrogels. acrylamide/itaconic acid copolymers. *Macromol. Mater. Eng.* **2001**, *286*, 34–42.
- ²⁰ Saggiu, S.; Bajpai, S. K. Water uptake behavior of poly(methacrylamide-co-*N*-vinyl-2-pyrrolidone-co-itaconic acid) as pH-sensitive hydrogels: Part I. *J. Macromol. Sci., Pure Appl. Chem.* **2006**, *43*, 1135–1150.
- ²¹ Zhang, R.-Y.; Zaslavski, E.; Vasilyev, G.; Boas, M.; Zussman, E. Tunable pH-responsive chitosan-poly(acrylic acid) electrospun fibers. *Biomacromolecules* **2018**, *19*, 588–595.
- ²² For a recent review see: Cheng, B.; Pei, B.; Wang, Z.; Hu, Q. Advances in chitosan-based superabsorbent hydrogels. *RSC Adv.* **2017**, *7*, 42036–42046.
- ²³ Ball-Jones, N. R.; Fahnhorst, G. W.; Hoyer, T. R. Poly(isoprenecarboxylates) from glucose via anhydromevalonolactone. *ACS Macro Lett.* **2016**, *5*, 1128–1131.
- ²⁴ Xiong, M.; Schneiderman, D. K.; Bates, F. S.; Hillmyer, M. A.; Zhang, K. Scalable production of mechanically tunable block polymers from sugar. *Proc. Natl. Acad. Sci. U. S. A.* **2014**, *111*, 8357–8362.
- ²⁵ Noble, B. B.; Coote, M. L. Effects of ionization on tacticity and propagation kinetics in methacrylic acid polymerization; Matyjaszewski, K.; Sumerlin, B. S.; Tsarevsky, N. V.; Chiefari, J., Eds.; ACS Symposium Series 1187; American Chemical Society: Washington DC, 2015; pp 51–72.
- ²⁶ Pinner, S. H. Polymerization rate of methacrylic acid. *J. Polym. Sci.* **1952**, *9*, 282–285.
- ²⁷ Blauer, G. Rate of polymerization of methacrylic acid in alkaline solution. *J. Polym. Sci.* **1953**, *11*, 189–192.
- ²⁸ Max, J. J.; Chapados, C. Infrared spectroscopy of aqueous carboxylic acids: A Comparison between different acids and their salts. *J. Phys. Chem. A* **2004**, *108*, 3324–3337.
- ²⁹ Flory, P. J.; Rehner, J. Statistical mechanics of cross-linked polymer networks II. Swelling. *J. Chem. Phys.* **1943**, *11*, 521–526.
- ³⁰ Elliot, J. E.; Macdonald, M.; Nie, J.; Bowman, C. N. Structure and swelling of poly(acrylic acid) hydrogels: Effect of pH, ionic strength, and dilution on the crosslinked polymer structure. *Polymer* **2004**, *45*, 1503–1510.

- ³¹ Riahihinezhad, M.; Kazemi, K., McManus, N., Penlidis, A. Effect of ionic strength on the reactivity ratios of acrylamide/acrylic acid (sodium acrylate) copolymerization. *J. Appl. Polym. Sci.* **2014**, *131*, 40959.
- ³² Kuhn, W.; Hargitay, B.; Katchalsky, A.; Eisenberg, H.; Reversible dilation and contraction by changing the state of ionization of high-polymer acid networks. *Nature* **1950**, *165*, 514–516.
- ³⁴ Ikegami, A. Hydration and ion binding of polyelectrolytes. *J. Polym. Sci. A.* **1964**, *2*, 907–921.
- ³⁵ Manning, G.S. The molecular theory of polyelectrolyte solutions with applications to the electrostatic properties of polynucleotides. *Q. Rev. Biophys.* **1978**, *11*, 179–246.
- ³⁶ Stevens, M.J.; Kremer, K. The nature of flexible linear polyelectrolytes in salt free solution: A molecular dynamics study. *J. Chem. Phys.* **1995**, *103*, 1669–1690.
- ³⁷ Rička, J.; Tanaka, T. Swelling of ionic gels: quantitative performance of the Donnan theory. *Macromolecules* **1984**, *17*, 2916–2921.
- ³⁸ Bao, Y.; Ma, J.; Li, N. Synthesis and swelling behaviors of sodium carboxymethyl cellulose-g-poly(AA-co-AM-co-AMPS)/MMT superabsorbent hydrogels. *Carbohydr. Polym.* **2011**, *84*, 76–82.
- ³⁹ Kwak, J. C. T.; Hayes, R. C. Electrical conductivity of aqueous solutions of salts of polystyrenesulfonic acid with univalent and divalent counterions. *J. Phys. Chem.* **1975**, *79*, 265–269.
- ⁴⁰ Gong, J. P.; Komsatsu, N.; Nitta, T.; Osada, Y. Electrical conductance of polyelectrolyte gels. *J. Phys. Chem. B.* **1997**, *101*, 740–745.
- * Reference 33 in Chapter 6 was a footnote and has been removed here.

Appendix A. Supporting Information for Chapter 2 (S2)

| | |
|---|------------|
| S2.1 General Experimental Protocols | 134 |
| S2.2 Preparation and Characterization of non-Polymeric Compounds | 137 |
| S2.2.1 Methyl coumalate (methyl 2-oxo-2H-pyran-5-carboxylate, 203) | 137 |
| S2.2.2 4- Carbomethoxyvalerolactone (methyl 6-oxotetrahydro-2H-pyran-3-carboxylate, CMVL , 204) and 5-Methoxy-4-methyl-5-oxopentanoic acid (205b) ... | 139 |
| S2.2.3 5-Methoxy-4-methylene-5-oxopentanoic acid (209c)..... | 142 |
| S2.2.4 Dimethyl 2-Methyleneglutarate (209d)..... | 143 |
| S2.2.5 2-Methylene glutaric acid (209a) | 144 |
| S2.2.6 5-Methoxy-2-methylene-5-oxopentanoic acid (209b) | 144 |
| S2.3 Preparation and Characterization of Polymers..... | 145 |
| S2.3.1 Poly(CMVL) [poly(204)] | 145 |
| S2.3.2 Poly(5-methoxy-4-methylene-5-oxopentanoic acid) [poly(209c)] | 146 |
| S2.3.3 Poly(dimethyl 2-methyleneglutarate) [poly(209d)] | 147 |
| S2.3.4 Poly(2-methyleneglutaric acid) [poly(209a)]..... | 148 |
| S2.3.5 Poly(5-methoxy-2-methylene-5-oxoglutaric acid) [poly(9b)] | 149 |
| S2.4 Poly(204): Thermodynamics of Polymerization | 150 |
| S2.5 Poly(204): Kinetics of Polymerization | 152 |
| S2.6.1 CMVL recovery from poly(204) using Sn(Oct) ₂ | 153 |
| S2.6.2 Production of 209c from poly(204) using DBU..... | 155 |
| S2.7 SEC, TGA, and DSC data of polymers..... | 159 |
| S2.8 References..... | 167 |

S2.1 General Experimental Protocols

Materials:

D,L-Malic acid ($\geq 99\%$) was purchased from Sigma Aldrich and used as received. Solvents were purchased and used as received unless otherwise noted. Anhydrous dichloromethane and THF were passed through an activated alumina column prior to use. Chloroform used for the thermodynamics experiments was first washed with H₂O, dried (MgSO₄), filtered, distilled over CaH₂, and stored under N₂ in a glovebox prior to use. CDCl₃ used for polymer degradation experiments was distilled over CaH₂ and stored over 3 Å molecular sieves prior to use. DBU and NEt₃ were distilled over CaH₂ and stored over 3 Å sieves and KOH, respectively. BnOH was distilled over CaH₂ and stored under a N₂ atmosphere in a glovebox. Crystalline 1,4-benzenedimethanol (BDM) was placed under high vacuum for a minimum of 48 h prior to use. Pd/C [5% (w/w)] was purchased from Engelhard and was washed with THF prior to use. Powdered diphenyl phosphate (DPP; phosphoric acid, diphenyl ester) was purchased from Sigma Aldrich and placed in a vial under high vacuum for a minimum of 72 h prior to use. Upon storage, the (hygroscopic) commercial sample would begin to clump, in which case the material was pulverized back to a powder and then stirred magnetically under high vacuum for 72 h.

Instrumental methods:

NMR: Spectra for ¹H and ¹³C NMR were taken using Bruker Avance 500 and 400 spectrometers (500 MHz and 400 MHz). ¹H NMR chemicals shift using CD₃OD, DMSO-*d*₆ and CDCl₃ are referenced to CHD₂OD at δ 3.34 ppm, CHD₂SOCD₃ at δ 2.50 ppm, and TMS at 0.00 ppm, respectively. ¹³C NMR spectra are referenced to the CDCl₃ carbon resonance at 77.16 ppm. Coupling constants were analyzed by previously described methods.¹ The acronym ‘nfom’ is used non-first-order multiplets in a ¹H NMR spectrum. Reported resonances use the format chemical shift (in ppm) followed by [multiplicity, coupling constant(s), relative number of protons (to the nearest whole proton), and substructural environment]. Substructural environments are assigned and italicized by, e.g., CH_aH_b.

ATR-FTIR: A Bruker Alpha Platinum ATR-FTIR instrument fitted with a diamond single-bounce crystal was used to measure Fourier transform infrared spectra. Measurements were recorded commonly using thirty-two scans with a four second acquisition time.

Mass spectrometry of non-polymeric samples: An Agilent 5975 mass selective detector (MSD) GC-MS operating at 70 eV (electron ionization) was used to obtain low resolution mass spectra. The column was an Agilent HP-5 with a 0.25 μm film thickness, 15 m length, \times 0.32 mm inner diameter. High resolution mass spectra (HRMS) of CMVL were obtained in electrospray ionization mode (ESI) using a Bruker BioTOF (ES-TOF) instrument. CMVL was dissolved in MeOH and PEG was used as an internal calibrant/standard.

Size Exclusion Chromatography (SEC): Two SEC instruments were used according to the solubility of the polymer being analyzed. The polymer samples were dissolved in the elution solvent at $\sim 1 \text{ mg}\cdot\text{mL}^{-1}$, and the samples were eluted at a flow rate of $1 \text{ mL}\cdot\text{min}^{-1}$. An RI detector [HP1047A (CHCl_3) and Agilent 1200 Series G1362A Infinity (DMF)] and polystyrene standards as calibrants were used to determine the M_n , M_w , and \bar{D} .

Chloroform: (Agilent 1100 series) Three consecutive Varian PL gel Mixed C Columns (7.5 mm inner diameter; 25 cm length) were used. The injection volume was 50 μL .

DMF: Two successive Styragel HT4 columns (7.8 mm id, 30 cm length) were used. The injection volume was 20 μL . The reported M_w and M_n values were determined vs. polystyrene calibration; accordingly, it may be that the actual absolute values of the molar masses of the samples analyzed in that fashion could be significantly different.

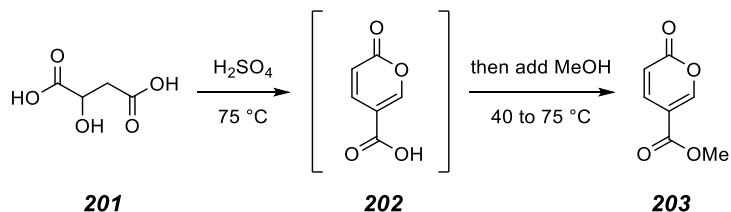
Thermogravimetric Analysis (TGA): Typical sample sizes used for TGA (TA Instruments Q500) ranged from 5–10 mg. TGA samples were heated under N_2 at a heating rate of $10 \text{ }^\circ\text{C}\cdot\text{min}^{-1}$. Due to the hygroscopic nature of some polymers, some samples were heated at $10 \text{ }^\circ\text{C}\cdot\text{min}^{-1}$ to $100 \text{ }^\circ\text{C}$, cooled to $35 \text{ }^\circ\text{C}$ at $10 \text{ }^\circ\text{C}\cdot\text{min}^{-1}$, and reheated to $550 \text{ }^\circ\text{C}$ at $10 \text{ }^\circ\text{C}\cdot\text{min}^{-1}$. The 1% and 5% mass loss are recorded for these samples, excluding the initial

mass loss on the first heating cycle (e.g., if 2% mass loss was observed for the initial ramp to removed water, the “1% mass loss” that is recorded occurs at 97% mass of the initial loading).

Differential Scanning Calorimetry (DSC): Samples for differential scanning calorimetry (TA Instruments Q-1000 DSC) were sealed hermetically in aluminum pans unless otherwise noted. The glass transition temperature of each sample is reported as the inflection point observed on the second heating cycle. The samples were typically heated to 150 °C, cooled to -60 °C (10 °C•min⁻¹), and heated again to 150 °C (10 °C•min⁻¹). For poly(204), the heating procedure was followed as noted above; an additional cycle of cooling to -60 °C (5 °C•min⁻¹) and heating to 150 °C (5 °C•min⁻¹) was then performed.

S2.2 Preparation and Characterization of non-Polymeric Compounds

S2.2.1 Methyl coumalate (methyl 2-oxo-2H-pyran-5-carboxylate, **203**)



D,L-Malic acid (**201**, 100.0 g, 745.7 mmol) was added portion wise (ca. 20 g/addition) to a stirring solution of sulfuric acid (250 mL) in a 1 L round bottom flask at 75 °C over the course of ca. 45 minutes. Gas evolution was vigorous immediately following the addition of each portion. The mixture was allowed to stir for 16 h, at which time the color had progressed to dark red. The mixture was allowed to cool to ambient temperature, and the flask was placed into an ice bath. MeOH (300 mL) was added dropwise over 1.5 h. The internal temperature of the solution was monitored during the addition so that it did not exceed 45 °C. Upon complete addition, the solution was heated to 75 °C and stirred for 16 h. The solution was cooled and poured over ice (500 mL), extracted with CHCl₃, washed (NaHCO₃ and brine), dried (MgSO₄), and concentrated to give a yellow oil (43.3 g crude) that crystallized upon standing. A portion (654 mg) was purified via column chromatography (silica, 3:1 Hex:EtOAc) to give methyl coumalate (**203**, 478 mg, 56% yield).

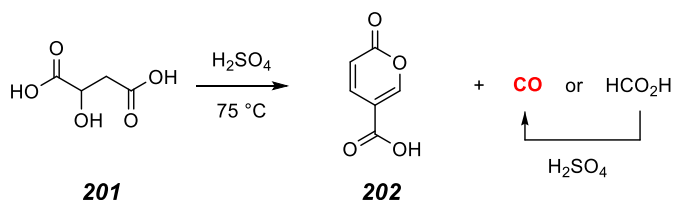
Alternatively, and for easier separation on larger scale, **203** was distilled via bulb-to-bulb distillation (0.15 mm Hg, external bath temperature at 110 °C) and then recrystallized (EtOAc) to give methyl coumalate as a white solid (22.9 g, 40% yield). The recovered mother liquor from multiple reactions has been recycled, distilled, and recrystallized to give additional amounts of **203**.

¹H NMR (500 MHz, CDCl₃) δ 8.31 (dd, *J* = 2.6, 1.1 Hz, 1H, (CO)O-CH=C), 7.79 (dd, *J* = 9.8, 2.6 Hz, 1H, -CHCH(C=O)-), 6.35 (dd, *J* = 9.8, 1.1 Hz, 1H, -CHCH(C=O)-), and 3.89 (s, 3H, -CH₃).

^{13}C NMR (125 MHz, CDCl_3) δ 163.5, 159.9, 158.3, 141.7, 115.4, 112.1, and 52.6.

mp: 70–73 °C, with sublimation (lit. 67–71 °C).²

Identification of the gaseous byproduct (carbon monoxide) accompanying the production of coumalic acid



In a separate, but analogous experiment, sulfuric acid (30 mL) and a stir bar were placed into a two-neck, 50-mL round-bottom flask. One neck was fitted with a rubber septum, the other was connected to an IR gas cell, the outlet of which was connected to an oil bubbler. Nitrogen was used to purge the headspace of the flask and IR cell for ca. 30 minutes. The septum was removed, and malic acid (3.00 g) was added. The septum was replaced, nitrogen was flowed through the headspace for 5 more minutes, and the flask was placed into an oil bath at $50\text{ }^\circ\text{C}$. The contents were stirred as gas evolved. After 45 minutes, the IR cell was closed, and an IR spectrum was taken. The spectrum (immediately below) clearly indicated that carbon monoxide was the main gas produced in the transformation of the malic acid to coumalic acid, consistent with what has been reported in the literature³ (although we could not locate experimental evidence to document that fact).

The carbon monoxide could be produced either in the elementary step of the mechanism involving C–C bond cleavage³ or by a secondary decomposition of formic acid, a process known to be catalyzed by sulfuric acid.

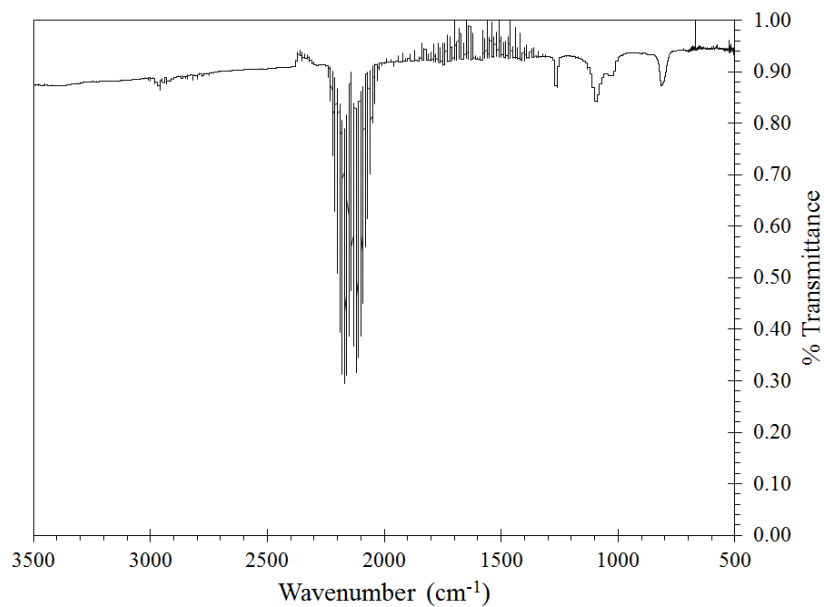
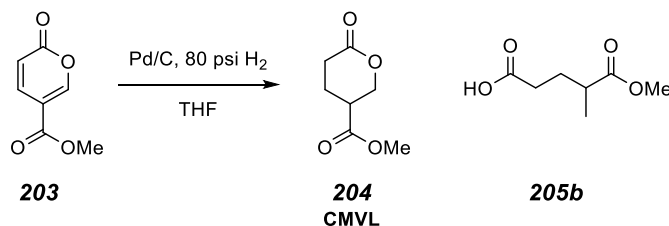


Figure S2.1 Infrared (IR) spectrum of the off gas collected in the synthesis of coumalic acid **202**. This spectrum is consistent with the IR spectrum of carbon monoxide.

S2.2.2 4- Carbomethoxyvalerolactone (methyl 6-oxotetrahydro-2H-pyran-3-carboxylate, CMVL, **204**) and 5-Methoxy-4-methyl-5-oxopentanoic acid (**205b**)



Methyl coumalate (**203**, 15.68 g, 101.8 mmol), Pd/C [5% (w/w), 1.00 g], and THF (150 mL) were placed and sealed in a 500 mL Fisher-Porter vessel. The headspace was, twice, pressurized with hydrogen gas (80 psi) and the pressure was vented. Hydrogen was then admitted and frequently replenished to maintain the pressure between ca. 60–80 psi. When the reaction no longer consumed hydrogen (ca. 8 h), the pressure was released, the mixture was filtered (Celite), and the filtrate was concentrated to afford a 1.00:0.37 mixture of 4-carbomethoxy- δ -valerolactone (CMVL, **204**) and 5-methoxy-2-methyl-5-oxopentanoic acid (**205b**). The mixture was diluted in EtOAc (400 mL) and washed with

NaHCO₃ (3x). The aqueous bicarbonate layers were combined, saturated with NaCl, and extracted with (EtOAc, 3x). The combined organic layers were washed with brine, dried (MgSO₄), and concentrated to afford 4-carboxymethyl- δ -valerolactone (**204**, 8.74 g, 56% yield). The lactone was stirred for ca. 12 h over CaH₂ under nitrogen and distilled *in vacuo* (48% distilled yield). Typically, the lactone was distilled two to three times prior to polymerization. A portion of the above aqueous NaHCO₃ layer was acidified with 3 M HCl and extracted with EtOAc (3x). The combine organic layers were washed with brine, dried (MgSO₄), and concentrated to give a colorless oil containing, predominantly, the known acid **204**.^{4,5} A portion was purified via column chromatography (silica, 7:3 Hex: EtOAc) to afford 5-methoxy-4-methyl-5-oxopentanoic acid (**205b**) as a colorless oil.

Data for CMVL

¹H NMR (500 MHz, CDCl₃) δ 4.51 (ddd, $J = 11.5, 5.3, 1.0$ Hz, 1H, (CO)O-CH_{eq}H_{ax}CH), 4.47 (dd, $J = 11.6, 7.6$ Hz, 1H, (CO)O-CH_{eq}H_{ax}CH), 3.75 (s, 3H, -CO₂Me), 2.94 (dddd, $J = 7.7, 7.7, 6.6, 5.3$ Hz, 1H, CH-CO₂Me), 2.70 (ddd, $J = 17.5, 6.9, 6.9$ Hz, 1H, -CH_aH_b(CO)OCH₂), 2.56 (ddd, $J = 17.5, 7.5, 7.5$ Hz, 1H, -CH_aH_b(CO)OCH₂), 2.22 (dddd, 1H, $J = 13.9, 7.6, 7.6, 7.6$ Hz, -O₂CCH₂H_{ea}CH_{ax}CH-), and 2.19 (dddd, $J = 14.0, 7.6, 7.6, 6.7, 1.0$ Hz, 1H, -O₂CCH₂H_{ea}CH_{ax}CH-).

¹³C NMR (125 MHz, CDCl₃) δ 171.8, 170.5, 68.8, 51.5, 38.1, 28.2, and 21.7.

IR (neat, selected peaks): 2957, 1724, 1456, 1436, and 1164 cm⁻¹.

bp: 119–123 °C @ 0.16 mm Hg or 101–105 °C @ 0.05 mm Hg.

GC-MS (30 m x 0.25 mm ID, HP-5, 50 °C/2.0 min/20 °C min⁻¹ /250 °C) $t_R = 5.83$ min; MS [70 eV, m/z (rel int)]: 158 (11, M⁺), 130 (39, M⁺-CO), 127 (25, M⁺-OMe), and 55 (100, C₄H₇).

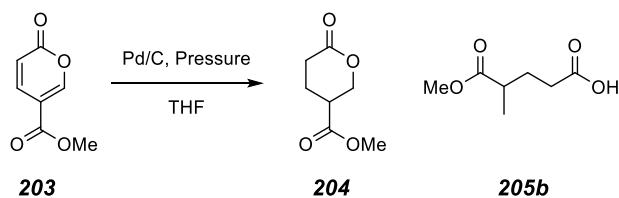
HRMS (ESI-TOF): Calculated for (C₇H₁₀O₄Na)⁺ 181.0471; found: 181.0477.

Data for 5-methoxy-4-methyl-5-oxopentanoic acid (205b)

¹H NMR (500 MHz, CDCl₃) δ 11.30 (br s, 1H, -CO₂H), 3.69 (s, 3H, CO₂Me), 2.53 (dq, *J* = 8.4, 7.0, 5.7 Hz, 1H, CHCO₂Me), 2.42 (ddd, *J* = 16.6, 8.5, 6.6 Hz, 1H, HO₂CCH_aH_b), 2.39 (ddd, *J* = 16.6, 8.2, 6.9 Hz, 1H, HO₂CCH_aH_b), 1.98 (dddd, *J* = 13.9, 8.2, 8.2, 6.7 Hz, 1H, CH_cH_dCHCO₂Me), 1.79 (dddd, *J* = 13.9, 8.6, 7.0, 5.9 Hz, CH_cH_dCHCO₂Me), and 1.19 (d, *J* = 7.0 Hz, 3H, CH₃CHCO₂Me).

Hydrogenation Screening

Methyl coumalate (**203**, ~20 mg), Pd/C (~2 mg), and THF (0.12 mL) were placed into a ½-dram vial fitted with a stir bar. The vial was either placed into (i) a wide-mouth glass jar (for hydrogenations at 1 atm) and capped with a large neoprene stopper, through which a needle was inserted to admit gas from a hydrogen balloon (1 atm), (ii) a Fisher-Porter vessel (for hydrogenations at 25–80 psi), or (iii) a Parr reactor for the hydrogenation at 1400 psi. The sample at 1 atm were stirred for ca. 24 h, 25–80 psi samples for 120–150 minutes, and 30 minutes for the 1400 psi sample. All samples were filtered through Celite and concentrated, and conversion was analyzed via ¹H NMR spectroscopy. All reactions went to full conversion unless otherwise noted.

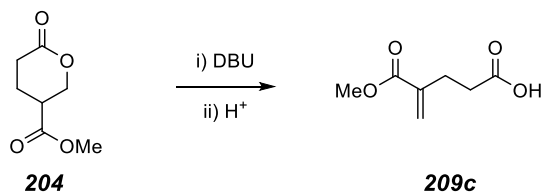


| Pressure | Solvent | Ratio of 204:205b |
|----------|---------|-------------------|
| 1 atm | THF | 1.2:1 |
| 25 psi | THF | 1: 0.6 |
| 80 psi | THF | 1:0.4 |
| 1400 psi | THF | 1:0.4 |

| Catalyst | Pressure | Solvent | Ratio of 204:205b |
|------------------------|----------|-----------------------|---------------------|
| Pd/CaCO ₃ | 1 atm | THF | 1:0.3 ^a |
| Pt/C | 1 atm | THF | 1: 1.8 |
| PtO ₂ | 1 atm | THF | 1:2.3 |
| Rh/AlO ₃ | 1 atm | THF | 0:1 |
| RuCl(PPh) ₃ | 1 atm | THF | 1:0.4 ^b |
| RuCl(PPh) ₃ | 80 psi | THF | 1:5.8 ^c |
| Pd/CaCO ₃ | 80 psi | THF | 1: 0.5 ^d |
| Rh/AlO ₃ | 80 psi | THF | 1: 0.76 |
| Rh/C | 80 psi | THF | 1:19.8 |
| PtO ₂ | 80 psi | THF | 1:1.9 |
| Pt/C | 80 psi | THF | 1:2.2 |
| Raney Ni | 80psi | MeOH/H ₂ O | 1:0.5 |
| Pd/C | 80 psi | AcOH | 1:0.7 |
| Pd/C | 80 psi | Toluene | 1: 0.7 |

Figure S2.2 Hydrogenation screening conditions and relative ratios of the products **CMVL (204)** to the hydrogenolysis product **205b** using Pd/C at various pressures of hydrogen gas. ^a Significant quantities of another product were formed in ca. 8–10% as determined via ¹H NMR spectroscopy. ^b Incomplete conversion.

S2.2.3 5-Methoxy-4-methylene-5-oxopentanoic acid (209c)



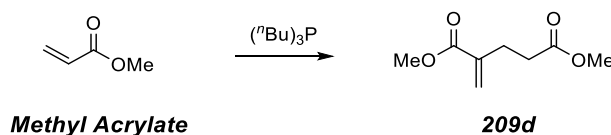
4-Carbomethoxyvalerolactone [**CMVL (204)**, 1.00 equiv, 1.00 g, 6.32 mmol] and anhydrous DCM (12 mL) were added to a 20 mL scintillation vial with a stir bar and capped with a rubber septum. DBU (1.20 equiv, 1.11 mL, 7.60 mmol) in DCM (2 mL)

was added dropwise over 5 minutes. After 20 hours the solution was diluted with EtOAc (~250 mL) and washed with 0.5 M HCl. The HCl wash was extracted with EtOAc (2x ~50 mL). The organic layers were combined, washed with brine, dried (MgSO₄), and concentrated to give a white solid (947 mg, 95% crude yield). This crude mixture could be polymerized without further purification. Additionally, a portion (697 mg) was purified via flash column chromatography (silica gel, 7:3 Hex: EtOAc) to give the carboxylic acid ester **209c** as a white solid (530 mg, 72% yield).

¹H NMR (500 MHz, CDCl₃) δ 11.34–10.10 (br s, 1H, -CO₂H), 6.22 (d, *J* = 1.1 Hz, 1H, MeCO₂CC=CH_{cis}H_{trans}), 5.63 (dt, *J* = 1.2, 1.2 Hz, 1H, MeCO₂CC=CH_{cis}H_{trans}), 3.76 (s, 3H, CO₂Me), 2.68–2.64 (m, 2H), and 2.60–2.57 (m, 2H).

mp: 54–58 °C (lit. reported as a liquid; however, the reported compound did contain noticeable impurities in the provided ¹H NMR spectrum⁶).

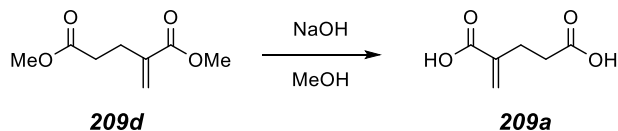
S2.2.4 Dimethyl 2-Methyleneglutarate (209d)



The synthesis of dimethyl 2-methyleneglutarate was adapted from Feng and Coward.⁷ Methyl acrylate (5.00 g, 58.1 mmol) was added to a 20-mL scintillation vial fitted with a stir bar and capped with a rubber septum. A stream of N₂ was bubbled through the solution for 20 minutes. The reaction mixture was cooled to 0 °C and tri-*n*-butylphosphine (0.100 equiv, 1.45 mL, 5.81 mmol) was added dropwise over the course of two minutes. The reaction mixture was allowed to stir under positive nitrogen pressure for 3 hours and subsequently allowed to stir for two days open to air to allow for the tri-*n*-butylphosphine to oxidize. This material was sequentially distilled two times under reduced pressure to afford dimethyl 2-methyleneglutarate (**209d**, 2.40 g, 48% yield) as a colorless oil, the ¹H NMR spectral of which were consistent with those reported.⁷

bp = 67–73 °C @ 0.16 Torr (lit. 95–98 °C/10–11 Torr)⁷

S2.2.5 2-Methylene glutaric acid (**209a**)

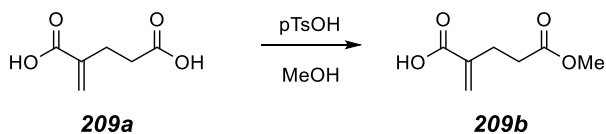


2-Methylene glutaric acid was synthesized from dimethyl 2-methylene glutarate according to Feng and Coward.⁷

¹H NMR (500 MHz DMSO-*d*₆) δ 12.31 (bs, 2H, CO₂H's), 6.04 (d, *J* = 1.5 Hz, 1H, =CH_{cis}H_{trans}), 5.60 (dt, *J* = 1.5, 1.5 Hz, 1H, =CH_{cis}H_{trans}), 2.44 (m, 2H), and 2.40–2.36 (m, 2H).

mp = 133–137 °C (lit. 130–132 °C).⁷

S2.2.6 5-Methoxy-2-methylene-5-oxopentanoic acid (**209b**)

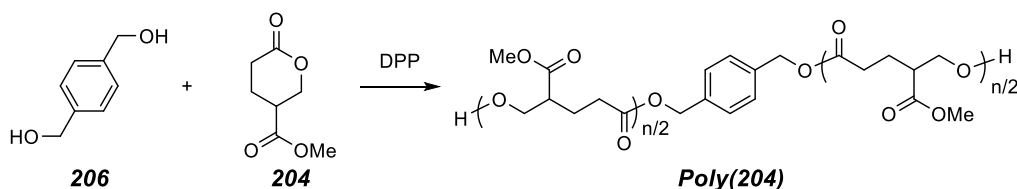


5-Methoxy-2-methylene-5-oxopentanoic acid (**209b**) was synthesized as described by the method of Tello-Alburto et. al.⁸ Briefly, 2-methyleneglutaric acid (500 mg, 3.47 mmol), *p*-toluenesulfonic acid (29.9 mg, 0.174 mmol), and MeOH (12 mL) were added to a 20-mL scintillation vial, capped, and allowed to stir for 17 h. The solution was concentrated and purified via column chromatography (silica, 7:3 Hex:EtOAc) to give 5-methoxy-2-methylene-5-oxopentanoic acid (**209b**, 441 mg, 80% yield) as a colorless oil.

¹H NMR (500 MHz, CDCl₃) δ 10.75 (bs, 1H, CO₂H), 6.22 (d, *J* = 1.1 Hz, 1H, =CH_{cis}H_{trans}), 5.63 (dt, *J* = 1.3, 1.3 Hz, 1H, =CH_{cis}H_{trans}), 3.77 (s, 3H, -CO₂Me), 2.65 (br t, *J* = 7.0 Hz, 2H, =CCH₂), and 2.56 (br t, *J* = 7 Hz, 2H, CH₂CO₂Me).

S2.3 Preparation and Characterization of Polymers

S2.3.1 Poly(CMVL) [poly(204)]



The following is a representative procedure. In a glovebox, benzene-1,4-dimethanol (**206**, 1.00 equiv, ~1.7 mg, 0.013 mmol), DPP (2.00 equiv, 6.4 mg, 0.025 mmol) were added to a 1-dram vial with a stir bar. 4-Carbomethoxyvalerolactone (**204**, **CMVL**, 500 equiv, 1.00 g, 6.33 mmol) was added, the vial was sealed with a Teflon-lined cap, and the solution was allowed to stir. After 36 h, the vial was broken, and the solid white nugget added to a 20-mL scintillation vial containing CHCl_3 (ca. 3 mL) and NEt_3 (ca. 10 μL). The solution was gently agitated on a nutator until the solid completely dissolved (typically 30-60 min), and the polymer was precipitated by dropwise addition of this solution into stirred, cold MeOH (ca. 15 mL). The majority of supernatant liquid was decanted from this suspension. The remaining solvent was removed from the precipitate on a rotary evaporator. The polymer was redissolved in CHCl_3 (ca. 2 mL) and precipitated, now by the addition of MeOH (ca. 15 mL) to the CHCl_3 solution. Decantation and drying under high vacuum at room temperature gave poly(4-carbomethoxyvalerolactone) [**poly(204)**] as a white powder. Typical mass recovery was in the range of 75-90% of the charged solids.

^1H NMR (500 MHz, CDCl_3): δ 7.35 (s, 4H, Ar), 5.11 (s, 4H, $-\text{OCH}_2\text{-Ar-CH}_2\text{O-}$), 4.23 [d, $J = 6.3$ Hz, 876H (438 repeat units (RUs), $\text{CO}_2\text{CH}_2^{\text{RU}}$], 3.71 [s, 1360H (453 RUs), $\text{CO}_2\text{CH}_3^{\text{RU}}$], 2.75 [dddd, $J = 8.7, 6.0, 6.0, 6.0$ Hz, 448H (448 RUs) $-\text{CHCO}_2\text{Me}^{\text{RU}}$], 2.39 [ddd, $J = 16.7, 8.6, 6.6$ Hz, 460H (460RU), $-\text{O}_2\text{CCH}_a\text{H}_b\text{CH}_2^{\text{RU}}$], 2.35 [ddd, $J = 16.7, 7.5, 7.5$ Hz, 460H (460RU), $-\text{O}_2\text{CCH}_a\text{H}_b\text{CH}_2^{\text{RU}}$], 1.92 [dddd, $J = 14.2, 8.2, 8.2, 6.6$ Hz, 460H

(460RU), $-\text{O}_2\text{CCH}_2\text{CH}_a\text{H}_b^{\text{RU}}$], and 1.87 [dddd, $J = 14.0, 8.5, 7.2, 5.4$ Hz, 442H (442 RU), $-\text{O}_2\text{CCH}_2\text{CH}_a\text{H}_b^{\text{RU}}$].

The M_n measured from end-group integration was $71.1 \text{ kg}\cdot\text{mol}^{-1}$

^{13}C NMR (125 MHz, CDCl_3): δ 172.9, 172.0, 64.1, 51.9, 43.6, 31.1, and 23.4.

IR (neat, selected peaks): 2957, 1721, 1459, 1436, 1247, 1154, and 1061 cm^{-1} .

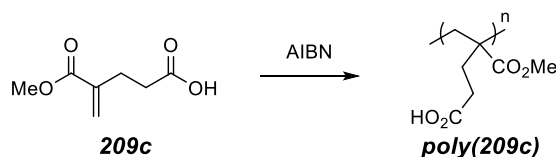
TGA: T_d 1% = $213 \text{ }^\circ\text{C}$; 5% = $263 \text{ }^\circ\text{C}$

DSC Cooling and ramping rates of $5 \text{ }^\circ\text{C}/\text{min}$: $T_g = -18 \text{ }^\circ\text{C}$, $T_c = 32 \text{ }^\circ\text{C}$, $T_m = 68, 86 \text{ }^\circ\text{C}$

Cooling and ramping rates of $10 \text{ }^\circ\text{C}/\text{min}$: $T_g = -17 \text{ }^\circ\text{C}$, $T_c = 43 \text{ }^\circ\text{C}$, $T_m = 73, 86 \text{ }^\circ\text{C}$

SEC PS-SEC (DMF): $M_n = 54.3 \text{ kg}\cdot\text{mol}^{-1}$, $M_w = 63.7 \text{ kg}\cdot\text{mol}^{-1}$, $D = 1.2$

S2.3.2 Poly(5-methoxy-4-methylene-5-oxopentanoic acid) [Poly(209c)]



Azobisisobutyronitrile (AIBN, 1.0 equiv, 1.6 mg, 0.0098 mmol), 5-methoxy-4-methylene-5-oxopentanoic acid (**209c**, 100 equiv, 158 mg, 1.00 mmol), and MeOH (1.00 mL) were added to a 1-dram vial fitted with a stir bar. A rubber septum was placed onto the vial, and the solution was degassed by slowly bubbling N_2 through the solution for 30 minutes. The rubber septum was quickly removed, the vial was sealed using a Teflon-lined cap, and the vial was placed in a heating bath and held at $65 \text{ }^\circ\text{C}$. After 24 h, the vial was cooled (freezer at ca. $-15 \text{ }^\circ\text{C}$ for 20 minutes) and opened. ^1H NMR spectroscopy showed ca. 68% conversion (32% remaining monomer in comparison to resonances for the polymer backbone). The polymer was precipitated by slow addition of the methanol solution to a stirred mixture of EtOAc:Hex ($\sim 5:1$). The resulting slurry was cooled, the supernatant liquid decanted, and the remaining viscous oil was heated *in vacuo* at $100 \text{ }^\circ\text{C}$ overnight to give poly(5-methoxy-4-methylene-5-oxopentanoic acid) [**poly(209c)**, 55 mg, 51% based on conversion] as a clear film. (Several attempts to effect this polymerization

in bulk (no added solvent) resulted in an insoluble, presumably crosslinked, material that swelled when CD₃OD was added.)

¹H NMR (500 MHz, CD₃OD): δ 4.94 (br s, 1H, OH), 3.72 (br s, 1.9H, CO₂Me), 3.63 (br s, 1.1H, CO₂Me'), and 2.8–1.4 (br m, 5.4H, CH₂'s).

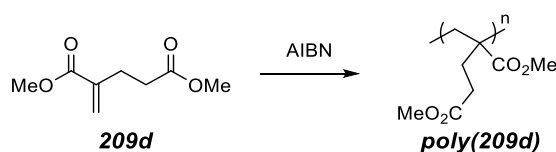
IR (neat, selected peaks): 3400–2500 (v br), 2953, 1703 (br), 1435, 1198, and 1159 cm⁻¹.

TGA *T*_d 1% = 190 °C, 5% = 253 °C

DSC *T*_g = 101 °C

SEC PS-SEC (DMF): *M*_n = 26.2 kg•mol⁻¹, *M*_w = 31.2 kg•mol⁻¹, *D* = 1.2

S2.3.3 Poly(dimethyl 2-methyleneglutarate) [Poly(209d)]



AIBN (1.0 eq, 1.6 mg, 0.010 mmol) and dimethyl 2-methyleneglutarate (**209d**, 100 equiv, 172 mg, 1.00 mmol) were added to a ½-dram vial containing a stir bar. A rubber septum was placed onto the vial and the monomer was degassed by slowly bubbling N₂ through the liquid for 30 minutes. The rubber septum was quickly removed, the vial was sealed using a Teflon-lined cap, and the vial was placed in a heating bath and held at 65 °C. After 24 h, the vial was cooled (freezer at ca. –15 °C for 20 minutes) and then opened to the air. The crude product was dissolved in CDCl₃ and ¹H NMR spectroscopy showed ca. 98.5% monomer conversion. The polymer was precipitated by slow addition of the CDCl₃ solution into a stirred, cold solution of hexanes:EtOAc (25:1). The resulting suspension was cooled, the supernatant liquid decanted, the residue rinsed with hexanes, and the remaining viscous oil heated *in vacuo* at 60 °C overnight to afford poly(dimethyl 2-methyleneglutarate)⁹ [**poly(209d)**] as a glassy solid.

¹H NMR (500 MHz, CDCl₃): δ 3.67 (br s, 4H, CO₂Me), 3.59 (br s, 2H, CO₂Me), and 2.7–1.2 (br m, 6.2H, CH₂'s).

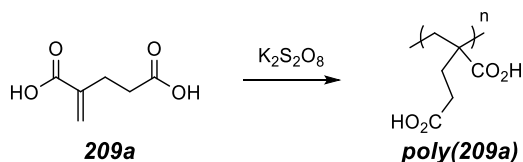
IR (neat, selected peaks): 2953, 1725, 1434, 1374, and 1157 cm⁻¹.

TGA *T*_d 1% = 171 °C, 5% = 267 °C

DSC *T*_g = 46 °C (lit. 63 °C)⁹

SEC PS-SEC (CHCl₃): *M*_n = 31.3 kg•mol⁻¹, *M*_w = 53.9 kg•mol⁻¹, *D* = 1.7

S2.3.4 Poly(2-methyleneglutaric acid) [Poly(209a)]



Potassium persulfate (1.0 equiv, 4.7 mg, 17 μmol), 2-methyleneglutaric acid (**209a**, 100 equiv, 250 mg, 1.74 mmol), and H₂O (1.6 mL) were added to a 1-dram vial with a stir bar. The vial was capped with a rubber septum and the contents were degassed by bubbling N₂ through the solution for 30 minutes. The rubber septum was quickly replaced with a Teflon-lined capped. The vial was placed in a bath at 65 °C for 24 h while stirring. The vial was allowed to cool and opened to the air. The solution was lyophilized and an aliquot was taken and analyzed by ¹H NMR spectroscopy (DMSO-*d*₆, 91% monomer conversion). The polymer was dissolved in MeOH (ca. 2 mL) and precipitated by slow addition into a stirred solution of EtOAc (ca. 18 mL). The suspension was placed in the freezer (ca. -20 °C) for 1 h and the excess solvent was then decanted. The polymer was dried under vacuum overnight at 70 °C and then at 100 °C for 6 h to give poly(2-methylene glutaric acid) [**poly(209a)**, 168 mg, 74% yield] as a white film.

¹H NMR (500 MHz, CD₃OD): δ 4.88 (br s, 3.1H, CO₂H's and CD₃OH) and 2.7–1.4 (v br m, 6H, methylenes).

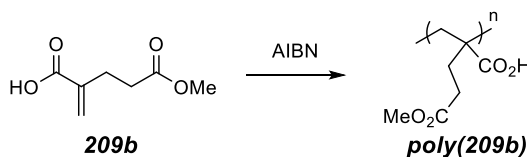
IR (neat, selected peaks): 3500–2500 (v br), 2934, 1695 (br), 1447, and 1406 cm⁻¹.

TGA T_d 1% = 175 °C, 5% = 204 °C

DSC T_g = 139 °C

SEC PS-SEC (DMF): M_n = 167 kg•mol⁻¹, M_w = 210 kg•mol⁻¹, D = 1.4

S2.3.5 Poly(5-methoxy-2-methylene-5-oxoglutaric acid) [Poly(9b)]



5-Methoxy-2-methylene-5-oxoglutaric acid (**209b**, 100 equiv, 158 mg, 1.00 mmol) and AIBN (1.0 equiv, 1.6 mg, 0.0098 mmol) were added to a ½ dram vial fitted with a stir bar. The vial was closed with a rubber septum and the contents were degassed by bubbling N₂ through the liquid monomer for 20 minutes. The septum was quickly replaced with a Teflon-lined cap. The vial was placed in a heating bath at 65 °C for 24 h while the contents were stirred. The vial was cooled (freezer, ca. -15 °C for 20 minutes) and then opened to the air. The residue was dissolved in CD₃OD and analyzed by ¹H NMR spectroscopy (88% conversion). The dissolved polymer was precipitated into EtOAc and the resulting slurry was centrifuged. The supernatant was decanted away and the residue was heated *in vacuo* at 100 °C overnight to give poly(5-methoxy-2-methylene-5-oxoglutaric acid) as a [**poly(209b)**, 81 mg, 57% yield] white powdery film.

¹H NMR (500 MHz, MeOD-*d*₄): δ 4.87 (br s, 3.1H, OH), 3.71 (br s, 2.4H, CO₂Me), 3.62 (v br shoulder, 0.6H, CO₂Me), and 2.8–1.4 (v br m, 6.1H, methylenes).

IR (neat, selected peaks): 3600–2400 (v br), 2951, 1703 (br), 1439, 1379, 1238, and 1164 cm⁻¹.

TGA T_d 1% = 170 °C, 5% = 216 °C

DSC T_g = 136 °C

SEC PS-SEC (DMF): M_n = 29.1 kg•mol⁻¹, M_w = 58.0 kg•mol⁻¹, D = 2.0

S2.4 Poly(204): Thermodynamics of Polymerization

In a glove box under nitrogen, 4-carbomethoxyvalerolactone (**204**, 200 equiv, 474 mg, 3.00 mmol) was added to a 3-mL volumetric flask. Benzene dimethanol (**206**, 1 equiv, 2.1 mg, 0.015 mmol) and diphenyl phosphoric acid (DPP, 2 equiv, 7.5 mg, 0.030 mmol) were dissolved in CHCl_3 (ca. 0.5 mL) and added to the volumetric flask. Two more CHCl_3 rinses (ca. 0.5 mL each) were added to the 2-dram vial prior to their addition to the volumetric flask containing **4**, and the flask was filled to 3.0 mL with additional CHCl_3 . The contents were thoroughly mixed and then divided into 23, separate, half-dram vials. Each vial was sealed with a Teflon cap, removed from the glove box, and the cap to thread connection wrapped with Teflon tape. The vials were placed in five, separate, pre-equilibrated heating baths at -15 , RT (23), 41, 53, and 68 °C. After 8 days for 23 °C, 41 °C, 53 °C, and 68 °C samples, or 11 days for the -15 °C samples, one sample was opened, and an aliquot was removed and immediately quenched by being added to a CDCl_3 solution of NEt_3 (ca. 2 $\mu\text{L}/\text{mL}$). Conversion was analyzed using ^1H NMR spectroscopy. This sequence was repeated the following day. In each case the conversion had not increased; therefore, the other vials at each temperature were analyzed by the same method. The enthalpy and entropy of polymerization (ΔH_p° and ΔS_p°) were determined using Van't Hoff analysis:

$$R \ln \left(\frac{[M]_{eq}}{[M]_0} \right) = \frac{\Delta H_p^\circ}{T} - \Delta S_p^\circ.$$

Initial monomer concentration was 1 M ($[M]_0 = 1 \text{ M}$). The polymerizations could not be as meaningfully performed in bulk because of the phase change to a semicrystalline polymer.^{10,11,12}

Table S2.1 Conversion vs. temperature for polymerization of **CMVL** to **poly(204)**. Polymerizations took place at **CMVL:benzenedimethanol:DPP** ratio of ca. 200:1:2. These data are graphically represented in Figure S2.2.

| Temperature (°C) | Inverse Temperature (1/K* 1000) | Conversion (%) | Temperature (°C) | Inverse Temperature (1/K* 1000) | Conversion (%) |
|------------------|---------------------------------|------------------------------------|------------------|---------------------------------|------------------------------------|
| -15 | 3.88 | a) 87.3 b) 87.7 c) 88.7 d) 88.0 | 53 | 3.07 | a) 45.6 b) 44.0 c) 47.3 d) 46.8 |
| 23 | 3.38 | a) 72.1 b) 70.0 c) 72.2 d) 72.4 | 68 | 2.93 | a) 34.1 b) 34.1 c) 34.6 |
| 42 | 3.17 | a) 56.8 b) 57.4 c) 57.1 d) 58.0 | | | |

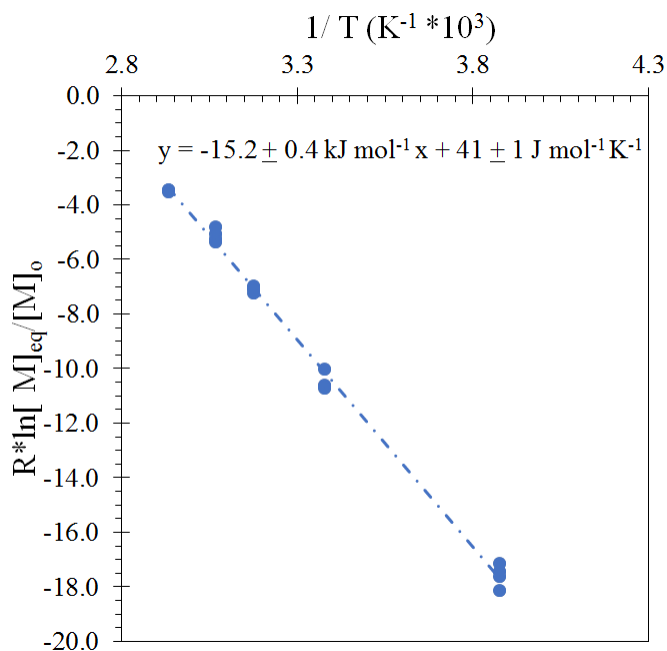


Figure S2.3 Van't Hoff plot of the temperature dependency of the equilibrium monomer concentration for ring-opening transesterification polymerization of **CMVL** to **poly(204)**. The monomer conversion at various temperatures are given above in Table S2.1. $\Delta H_p^0 = -15.2 \pm 0.4 \text{ kJ/mol}$, $\Delta S_p^0 = -41 \pm 1 \text{ J mol}^{-1} \text{ K}^{-1}$.

S2.5 Poly(204): Kinetics of Polymerization

Benzyl alcohol (5.4 μL , 5.2 μmol) and **CMVL (204)**, 1.65 g, 10.4 mmol were mixed in a 1-dram vial. Diphenyl phosphate [(PhO)₂PO₂H (DPP), 3.9 mg, 15.8 μmol] was added to three separate 1-dram vials (each vial containing 3.9 mg DPP) containing a stir bar. An aliquot of the benzyl alcohol/**CMVL** mixture was added (500 mg) to each vial, sequentially. The solid DPP had rapidly dissolved (ca. <30 sec); the reaction mixture viscosity had increased to the point that magnetic stirring stopped after ca. 2.5–3 h; the reaction mixture solidified after ca. 6 h. The raw data in Figure S2.3 suggest that the reaction kinetics continued to proceed without major discontinuity. Aliquots were removed from the stirred reaction mixture at various time points and quenched by the addition of a solution of NEt₃ in CDCl₃ (ca. 2 μL /1 mL). Analysis by ¹H NMR spectroscopy was used to determine the extent of monomer conversion.

The ratio of [M]₀/[BnOH] was determined at time zero and [M]₀'/[DPP] at time 10 minutes, where [M]₀'/[DPP] is the relative integration of the OCH₂ methylene protons in both the M (**CMVL**) (I_{MCH2}) and the small amount of **poly(204)** (I_{PCH2}) divided by the integration of the ortho protons of the two phenyl groups in DPP. *k*_{obs} was determined at early conversion (first 90 min) using the rate equation [M] = [M]₀ - *k*_{obs}t, where [M] = [I_{MCH2}]/(I_{MCH2} + I_{PCH2}) • [M]₀.

CMVL has a $\rho = 1.12$ g/mL, MW = 158 g/mol; thus, neat [M]₀ = 7.09 mol/L.

Table S2.2 Relative ratios of **CMVL**:BnOH:DPP observed upon ¹H NMR integrations. *k*_{obs} = 0.0193 ± 0.0015 M min⁻¹ or 1.16 ± 0.09 M h⁻¹ from the first 90 minutes of polymerization; for these experiments, t_{1/2} = 3.7 ± 0.2 h.

| Run | [M] ₀ /[BnOH] | [M] ₀ '/[DPP] | t _{1/2} (m) | <i>k</i> _{obs} (M min ⁻¹) |
|-----|--------------------------|--------------------------|----------------------|--|
| 1 | 198 | 202 | 227 | 0.0183 |
| 2 | 198 | 189 | 227 | 0.0186 |
| 3 | 198 | 170 | 203 | 0.0210 |

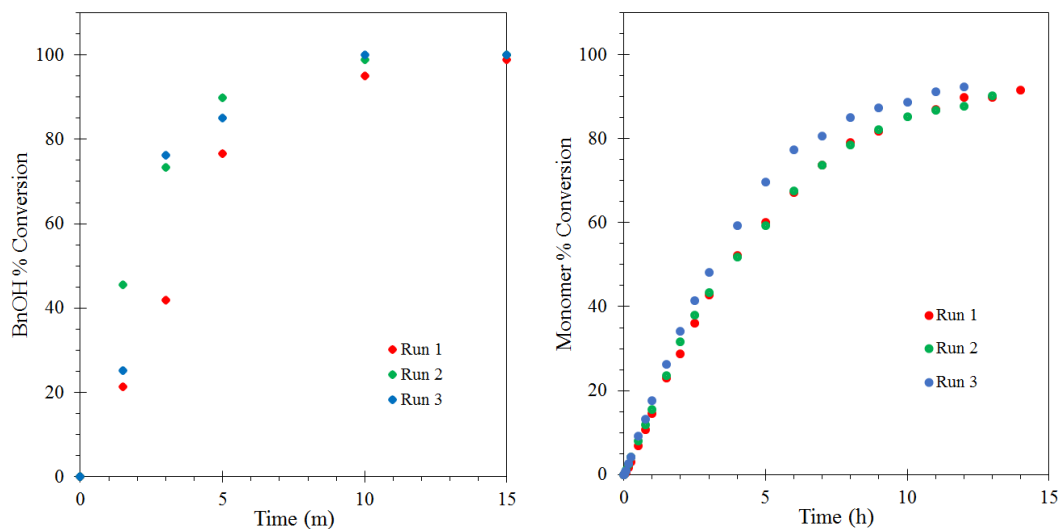


Figure S2.4 Left: Initiator conversion over time. Right: Monomer conversion over time (cf. Runs 1–3, Table S2.1). The $t_{1/2}$ of polymerization under these conditions was 219 ± 14 min. Together, these plots show that initiation is much faster than polymerization.

S2.6 Chemical Recyclability of Poly(204)

S2.6.1 CMVL recovery from poly(204) using Sn(Oct)₂

Poly(CMVL) [**poly(204)**, 704 mg, $M_n = \text{ca. } 70,000$ g/mol] and Sn(Oct)₂ (~2 μL) were placed into a 25-mL round bottom flask and distilled at 150 °C (external temperature) and 0.05 Torr. During the first 100 minutes, a majority (429 mg, 61% yield) of **CMVL** was recovered, and the overall rate of recovery slowed thereafter. After 23 h the total recovery of **CMVL** was 87% (614 mg). The residue remaining in the distillation flask, still a mostly white solid, was dissolved in CDCl₃ and analyzed via ¹H NMR spectroscopy. It contained mostly (ca. 94.5%) **poly(204)** along with a small amount (5.5%) of **9c**.

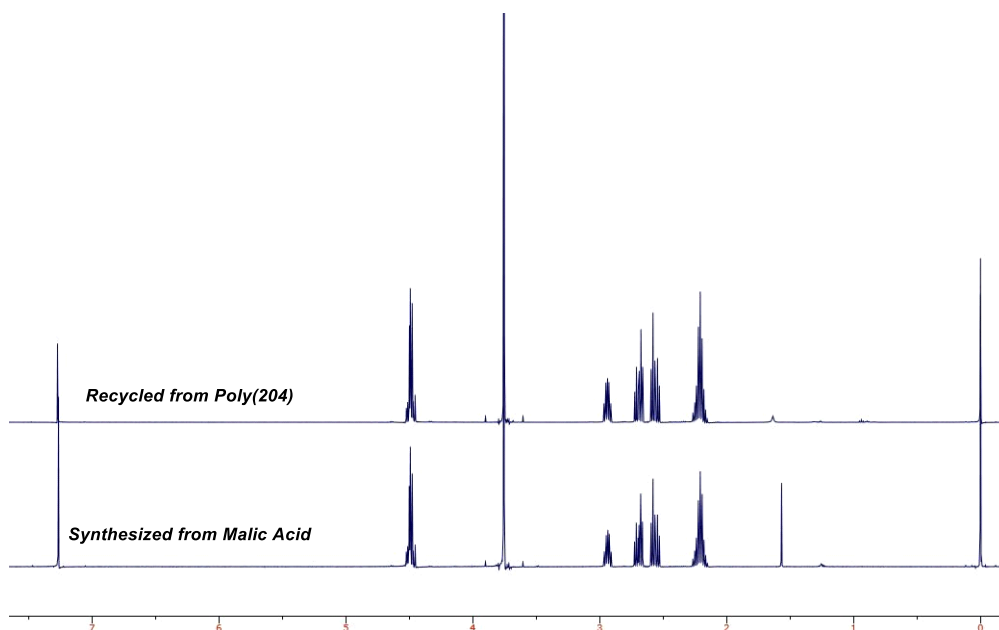


Figure S2.5 Overlay of ^1H NMR spectra of **CMVL** (top) recovered from the depolymerization of **poly(204)** using $\text{Sn}(\text{Oct})_2$ as a catalyst at $150\text{ }^\circ\text{C}$ and 0.05 Torr and (bottom) synthesized from malic acid.

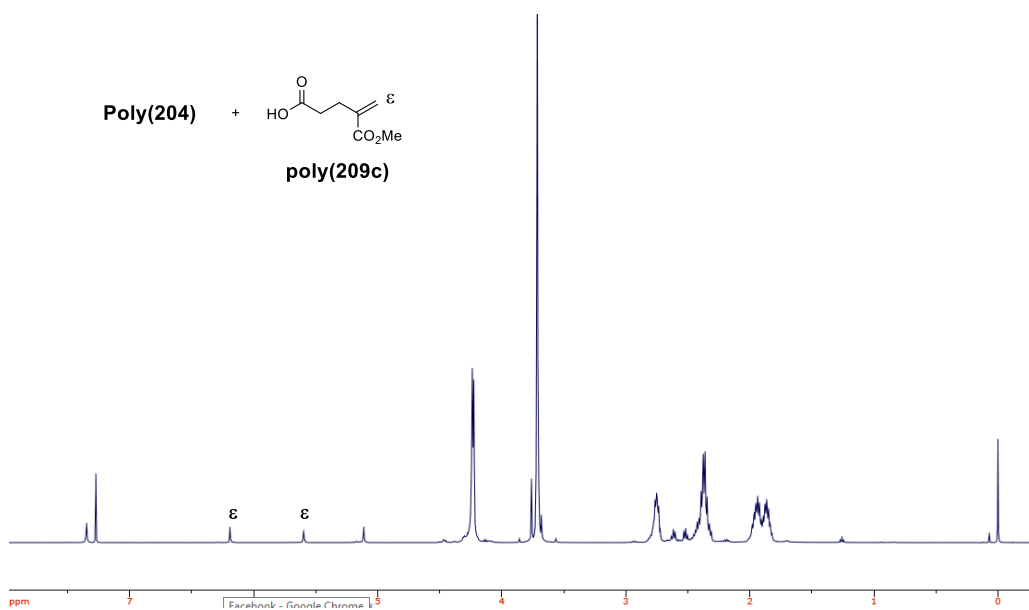
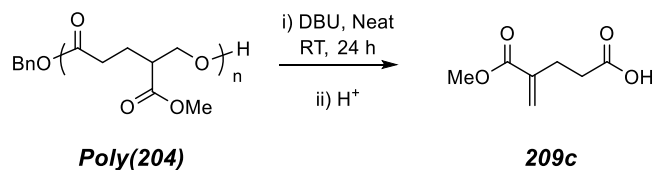


Figure S2.6 ^1H NMR spectrum of the remaining pot residue showing resonances for **poly(204)**-like species and some **209c** remaining in the distillation flask following the depolymerization of **poly(204)** using $\text{Sn}(\text{Oct})_2$ as a catalyst at $150\text{ }^\circ\text{C}$ and 0.05 torr .

S2.6.2 Production of 209c from poly(204) using DBU



Poly(204) (250 mg, 1.58 mmol of repeat units, $M_n = 22,000$ g/mol, initiated with BnOH), DBU (520 μ L, 3.48 mmol), and a stir bar were placed into a 1-dram vial and sealed with a Teflon-lined cap. The heterogeneous mixture was stirred until the polymer completely dissolved (ca. 24 h). The depolymerization mixture was diluted first with DCM (3 mL) followed by EtOAc (40 mL), and 0.3 M HCl was added. The acidic aqueous layer was extracted with EtOAc (2x 40 mL), and the combine organic layers were washed with brine, dried ($MgSO_4$), and concentrated to afford acid **209c** as a light-yellow oil that crystallized upon standing (221 mg, 88% yield).

NMR study of the DBU-promoted degradation of poly(204)

Poly(204) (25 mg, 30 repeat units, initiated with BnOH) and $CDCl_3$ (0.5 mL) were added to an NMR tube. An initial spectrum of the polymer was recorded, and DBU (50 μ L, a ca. 1:2 molar equivalents polymer repeat unit to DBU) was added. The NMR tube was capped and 1H NMR spectra were recorded at the indicated timepoints.

Initial formation of **CMVL (204)** and **208** was observed. Resonances for a terminal alkene in (shorter) polymers arising from mid-chain eliminative cleavage (**210**) was observed minutes after the addition of DBU. After 12 h **CMVL** was absent. After 2 days two major products, **209c** and dimer **212**, were present. Dimer **212** was slowly converted over the next ca. 50–60 days to give nearly full conversion to **209c**.

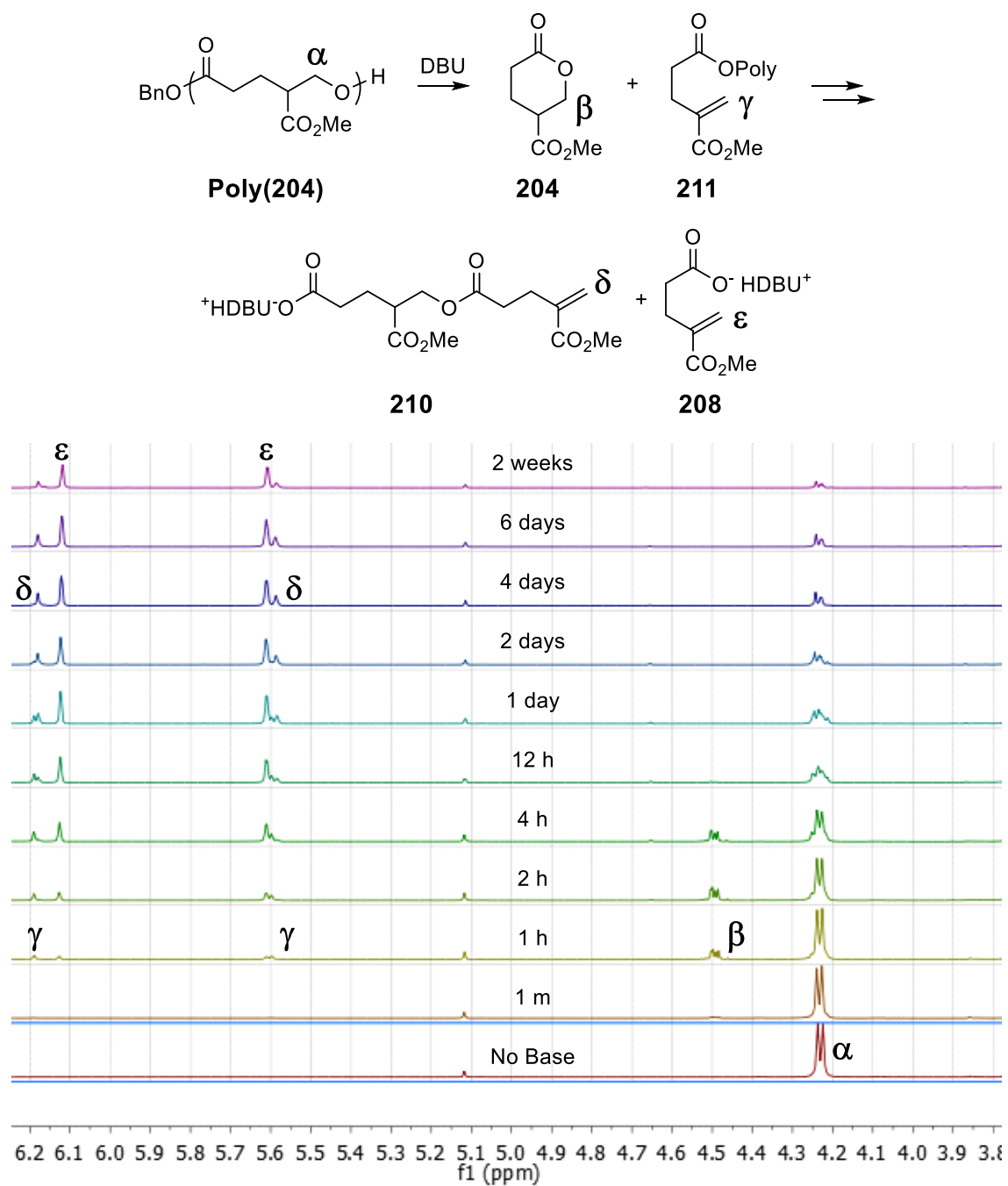
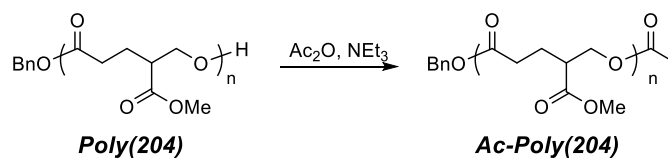


Figure S2.7 Overlaid ^1H NMR spectra (25 mg, **poly(204)**, 50 μL DBU, 0.5 mL CDCl_3) of DBU-promoted degradation of **poly(204)** over time.

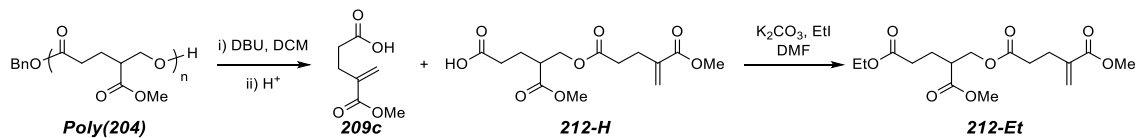
Preparation of the acetylated derivative **Ac-poly(204)** and NMR study of its DBU-promoted degradation.



Poly(204) (150 mg) and a stir bar were placed into a 2-mL vial followed by DCM (ca. 1 mL). Once the polymer dissolved, Ac₂O (35 μL, 0.37 mmol) and NEt₃ (79 μL, 0.57 mmol) were added. The vial was capped and allowed to stir overnight. After 16 h, the solution was precipitated into MeOH (ca. 10 mL), cooled, centrifuged, decanted, and concentrated *in vacuo* overnight at 40 °C to give **Ac-poly(204)** (111 mg, 74% yield).

NMR monitoring of the DBU degradation of **Ac-poly(204)** showed a similar amount of conversion to dimer **212** and **208** after two days as had been observed starting with **poly(204)**. However, there was no evidence of formation of **CMVL**, consistent with the requirement for a terminal hydroxyl group to enable a retro-ROTEP.

Ethyl Ester of the Dimer **212** (**212-Et**)



Poly(204) (50 mg, 0.316 mmol repeat units, $M_n = 22,000$ g/mol, initiated with BnOH) was placed into a 1/2-dram vial with a stir bar and dissolved in DCM (250 μL). DBU (55 μL, 0.367 mmol) was added, the vial was capped, and the mixture was stirred for 7 hours. The solution was diluted first with DCM (ca. 2 mL) followed by EtOAc (10 mL). The organic solution was acidified with 1.0 M HCl, washed (brine), dried (MgSO₄), and concentrated to give a 1.00:1.02 molar ratio of **209c** to dimer **212-H** (44 mg, 88% crude yield). A portion (20 mg, ~0.084 mmol **209c** and ~0.084 mmol of **212-H**) of this crude material was added to a 1-dram vial with a stir bar and dissolved in DMF (1.5 mL).

K_2CO_3 (33 mg, 0.24 mmol) and ethyl iodide (25 μ L, 0.31 mmol) were added, and the mixture was stirred. After 3 h, phenothiazine (~0.1 mg) was added. The mixture was concentrated *in vacuo*, diluted in EtOAc, washed with H_2O and brine, dried with $MgSO_4$, and concentrated under high vacuum overnight to afford a light brown oil (11.0 mg). A portion of the contents (8.0 mg) were purified by passage through a short column of silica gel [eluting first with Hex (not collected) followed by 1:1 EtOAc:Hex (collected)] and concentrated to afford **212-Et** as a light brown oil (7.4 mg, 0.022 mmol, 31% yield over 2 steps).

1H NMR (500 MHz, $CDCl_3$) δ 6.19 (d, $J = 1.1$ Hz, 1H, $=CH_{cis}H_{trans}$), 5.60 (dt, $J = 1.3$, 1.3 Hz, 1H, $=CH_{cis}H_{trans}$), 4.24 (d, $J = 6.4$ Hz, 2H, CO_2CH_2), 4.13 (q, $J = 7.1$ Hz, 2H, $CO_2CH_2CH_3$), 3.76 (s, 3H, CO_2Me), 3.71 (s, 3H, CO_2Me), 2.76 [dddd, $J = 8.7$, 6.1, 6.1, 6.1 Hz, 1H, $CHCO_2Me$], 2.64–2.60 (m, 2H), 2.54–2.50 (m, 2H), 2.38 [ddd, $J = 16.5$, 8.6, 6.5 Hz, 1H, $O_2CCH_aH_bCH_2CH$], 2.35 [ddd, $J = 16.5$, 8.2, 7.0 Hz, 1H, $O_2CCH_aH_bCH_2CH$], 1.95 [dddd, $J = 14.0$, 8.6, 8.6, 6.5 Hz, 1H, $-O_2CCH_2CH_aH_bCH$], 1.87 [dddd, $J = 14.1$, 8.6, 7.1, 5.5 Hz, 1H, $-O_2CCH_2CH_aH_bCH$], and 1.26 (t, $J = 7.1$ Hz, 3H, $CO_2CH_2CH_3$).

^{13}C NMR (125 MHz, $CDCl_3$) δ 173.3, 172.7, 172.4, 167.2, 138.8, 126.2, 64.4, 60.7, 52.1, 52.1, 44.0, 33.0, 31.7, 27.4, 23.9, and 14.3.

IR (neat, selected peaks): 2954, 1733, 1718 (sh), 1632, 1439, and 1161 cm^{-1} .

HRMS (ESI-TOF): Calculated for $(C_{16}H_{24}O_8Na)^+$ 367.1363; found: 367.1358.

S2.7 SEC, TGA, and DSC data of polymers

Poly(CMVL) [poly(204)]

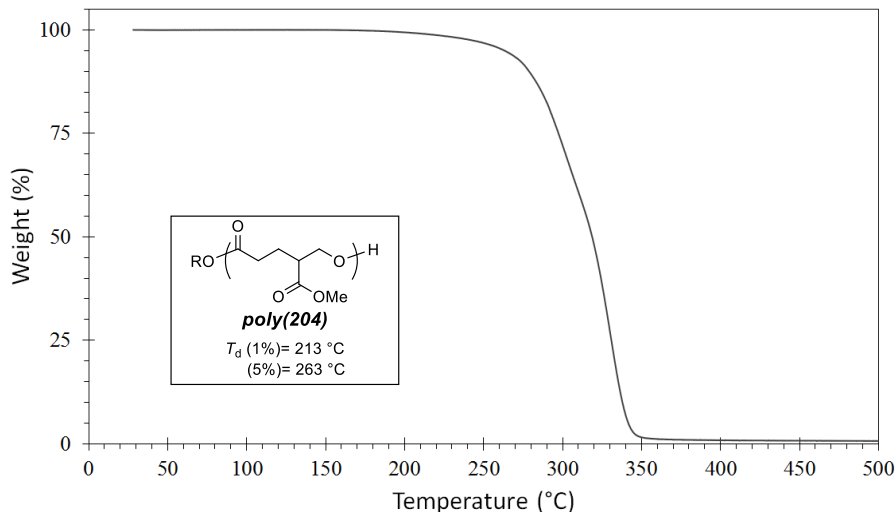


Figure S2.8 TGA thermogram of **poly(204)** at a heating rate increase of 10 °C/min. **Poly(204)** has a 1% mass loss at 213 °C and 5% mass loss at 263 °C.

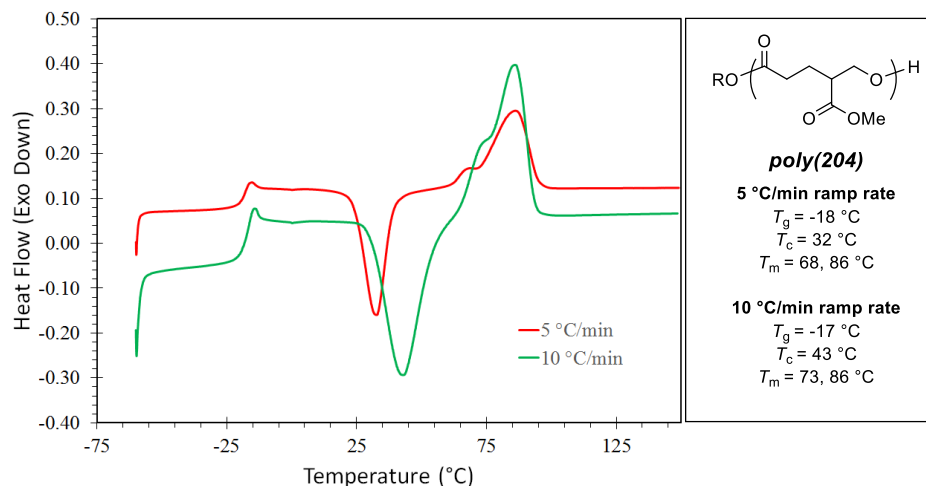


Figure S2.9 DSC thermograms of **poly(204)** taken on the second and third ramp of heating at 10 °C/min (green) and 5 °C/min (red), respectively. **Poly(204)** is a semicrystalline polymer with a $T_g = -18$ °C, $T_c = 32$ °C, and two T_m 's = 68 and 86 °C when taken at a heating rate of 5 °C/min. At 10 °C/min, the $T_g = -17$ °C, $T_c = 43$ °C, and T_m 's = 73 and 86 °C.

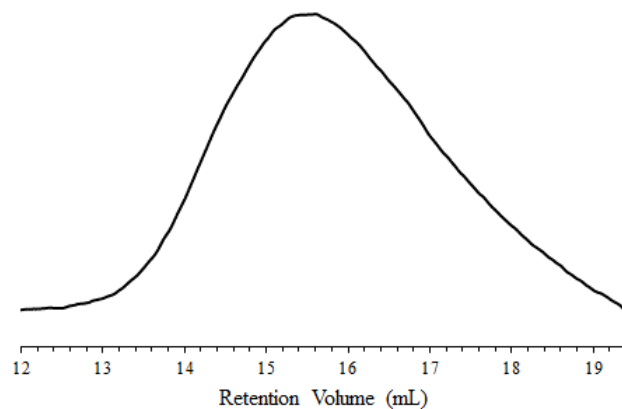


Figure S2.10 SEC trace of **poly(204)** polymerized neat using benzenedimethanol as an initiator and DPP as a catalyst. SEC was taken in DMF on a column calibrated using polystyrene standards. $M_n = 54.3 \text{ kg}\cdot\text{mol}^{-1}$, $M_w = 63.7 \text{ kg}\cdot\text{mol}^{-1}$, $D = 1.2$. [$M_n = 71.1 \text{ kg}\cdot\text{mol}^{-1}$ ($^1\text{H NMR}$)].

Poly(5-methoxy-4-methylene-5-oxopentanoic acid) [poly(209c)]

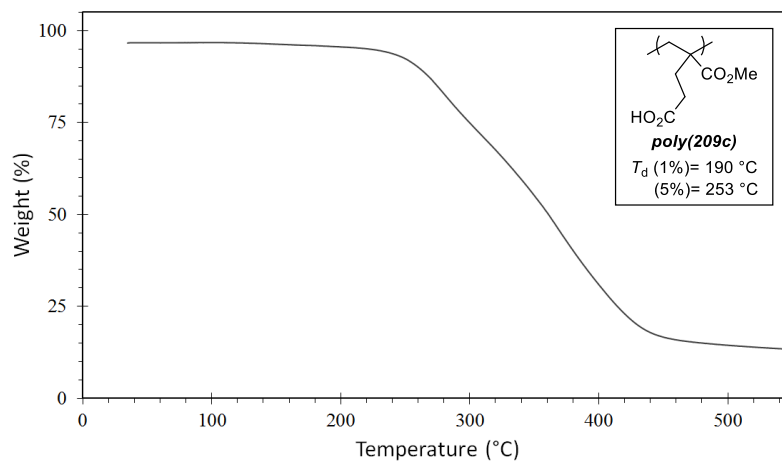


Figure S2.11 TGA thermogram of **poly(209c)** at a heating rate increase of $10 \text{ }^\circ\text{C}/\text{min}$ recorded after an initial heating cycle to $100 \text{ }^\circ\text{C}$ to remove water. This initial heating cycle removed 3.3% of the total mass. The second heating ramp showed a 1% mass loss at $190 \text{ }^\circ\text{C}$ and 5% mass loss at $253 \text{ }^\circ\text{C}$ for **poly(209c)**.

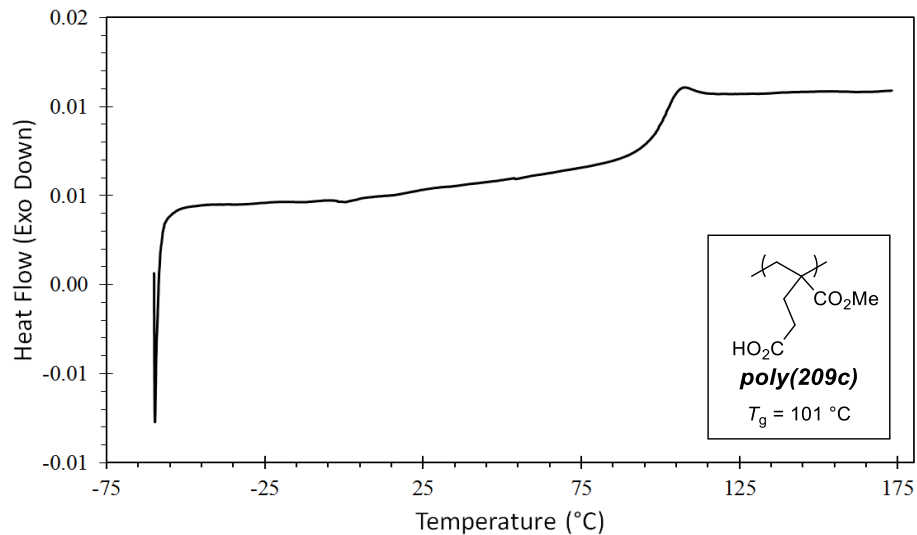


Figure S2.12 DSC trace of **poly(209c)** taken on the second cycle of heating at 10 °C/min. A hole was punched into the DSC pan in order to remove adsorbed water during the first heating cycle. The glass transition temperature (T_g) occurs at 101 °C.

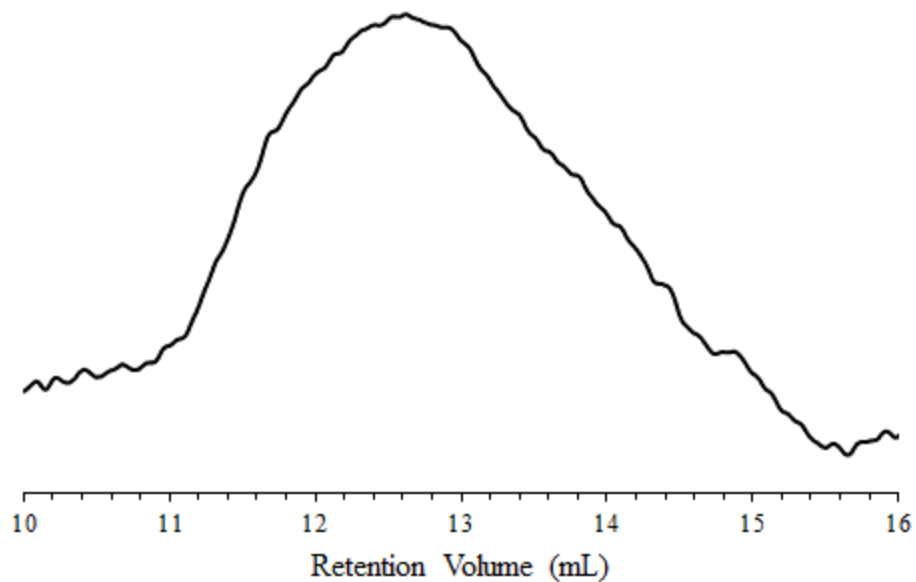


Figure S2.13 SEC trace of **poly(209c)** taken in DMF and calibrated using polystyrene standards. $M_n = 26.2 \text{ kg}\cdot\text{mol}^{-1}$, $M_w = 31.2 \text{ kg}\cdot\text{mol}^{-1}$, $D = 1.2$

Poly(dimethyl 2-methyleneglutarate) [poly(209d)]

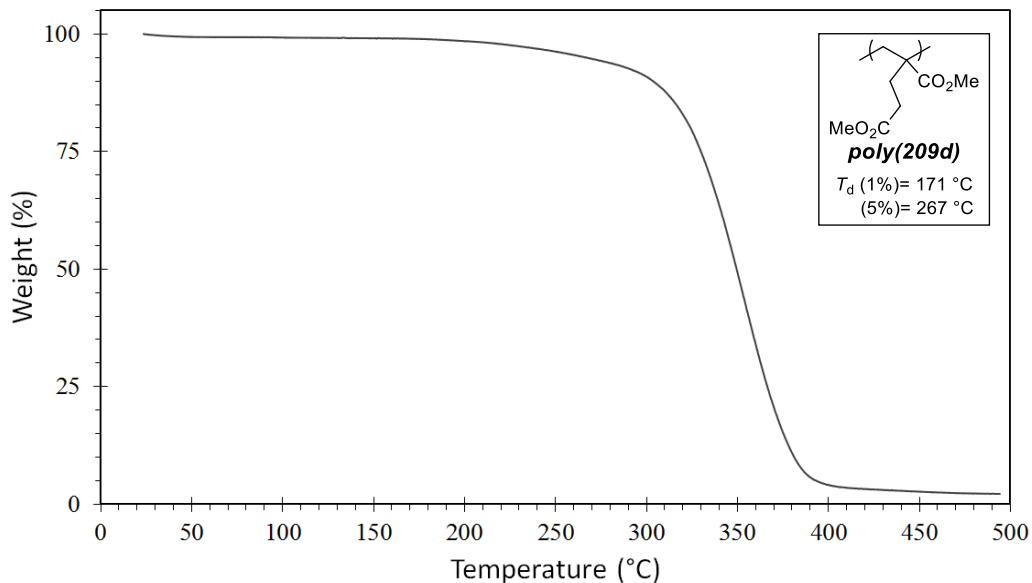


Figure S2.14 TGA thermogram of **poly(209d)** at an increase of 10 °C/min. **Poly(209d)** has a 1% mass loss at 171 °C and 5% mass loss at 267 °C.

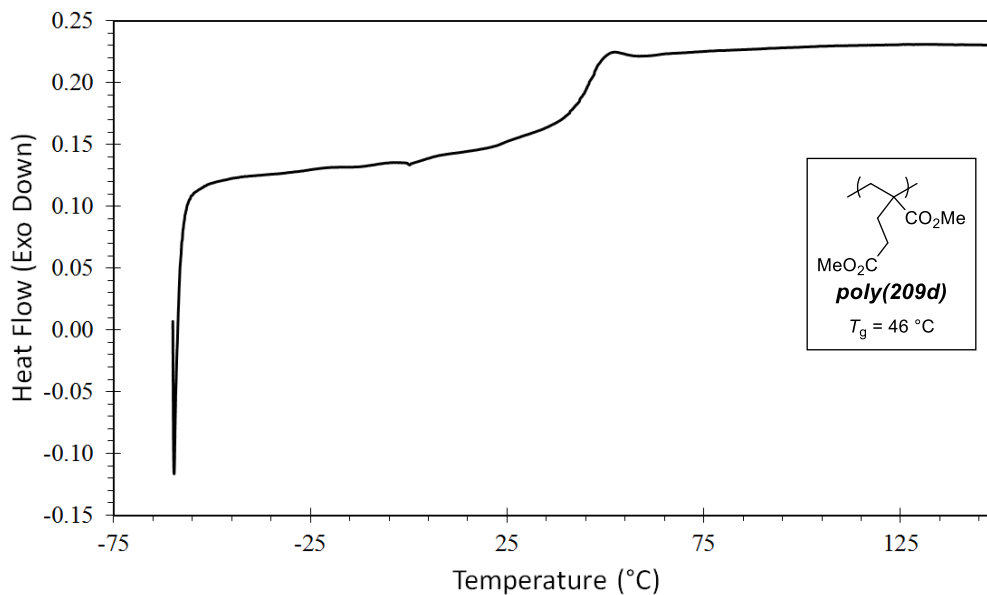


Figure S2.15 DSC trace of **poly(209d)** taken on the second cycle of heating at 10 °C/min. The glass transition temperature T_g occurs at 46 °C.

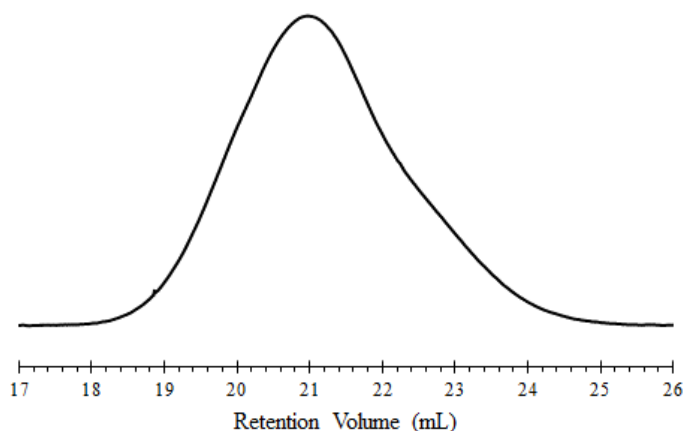


Figure S2.16 SEC trace of **poly(209d)** polymerized neat. SEC was taken in CHCl_3 , calibrated using polystyrene standards. $M_n = 31.3 \text{ kg}\cdot\text{mol}^{-1}$, $M_w = 53.9 \text{ kg}\cdot\text{mol}^{-1}$, $D = 1.7$.

Poly(2-methyleneglutaric acid) [poly(209a)]

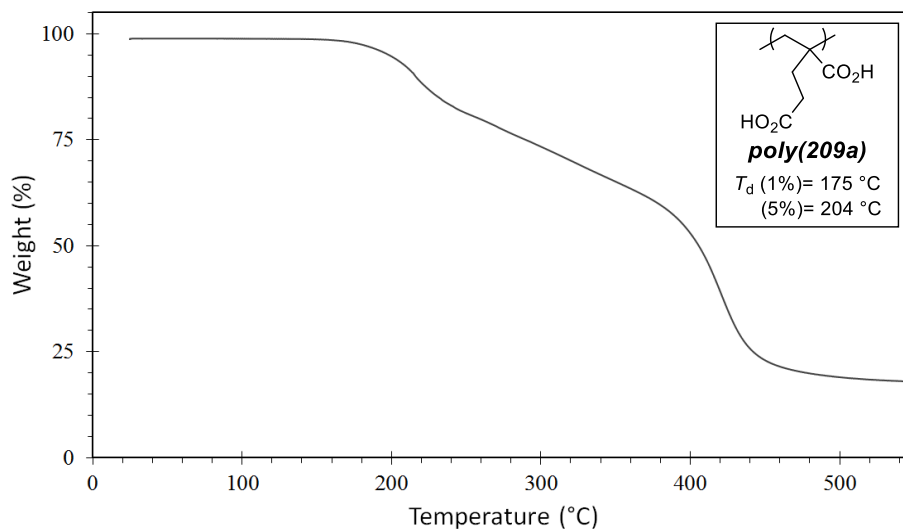


Figure S2.17 TGA thermogram of **poly(209a)** at a heating rate increase of $10 \text{ °C}/\text{min}$ recorded after an initial heating cycle to 100 °C to remove water. This initial heating cycle removed 1.2% of the total mass. The second heating ramp showed a 1% mass loss at 175 °C and 5% mass loss at 204 °C for **poly(209a)**.

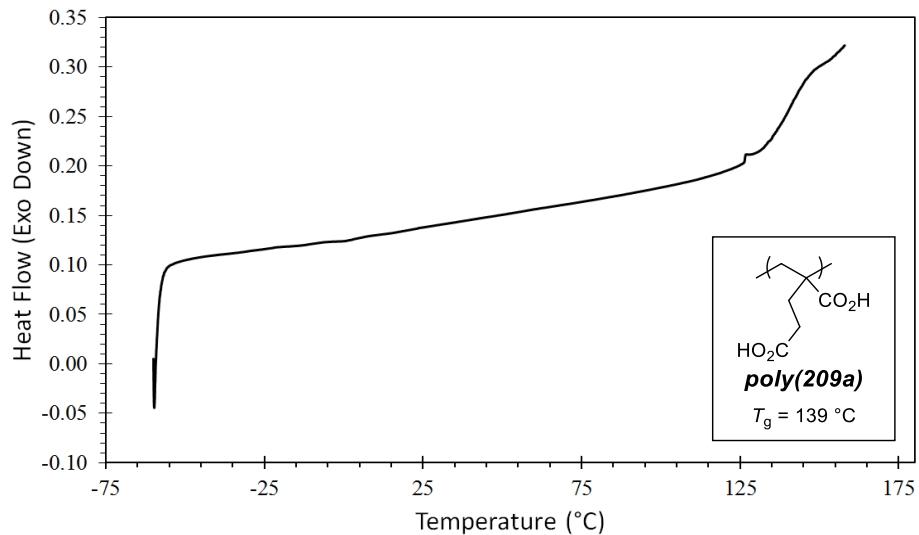


Figure S2.18 DSC trace of **poly(209a)** taken on the second cycle of heating at 10 °C/min. A hole was punched into the DSC pan in order to remove adsorbed water during the first heating cycle. The glass transition temperature (T_g) occurs at 139 °C.

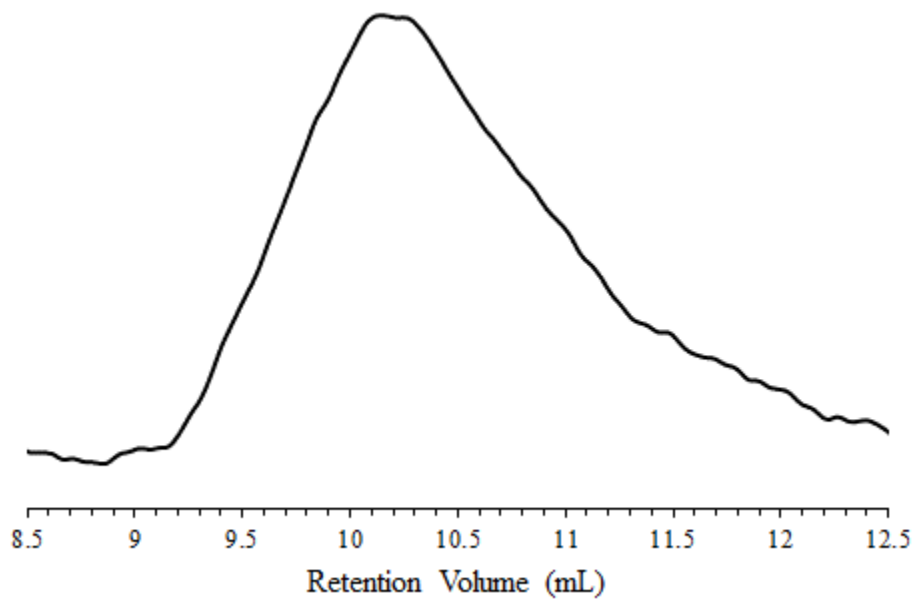


Figure S2.19 SEC trace of **poly(209a)**, prepared by polymerization in H₂O. SEC was taken in DMF, calibrated using polystyrene standards. $M_n = 167 \text{ kg}\cdot\text{mol}^{-1}$, $M_w = 210 \text{ kg}\cdot\text{mol}^{-1}$, $D = 1.4$.

Poly(5-methoxy-2-methylene-5-oxopentanoic acid) [poly(209b)]

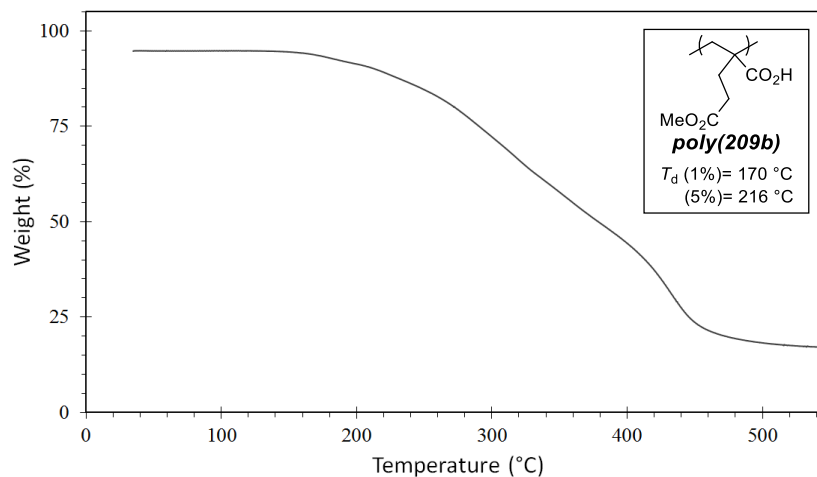


Figure S2.20 TGA thermogram of **poly(209b)** at a heating rate increase of 10 °C/min and recorded after an initial heating cycle to 100 °C to remove water. This initial heating cycle removed 5.3% of the total mass. The second heating ramp showed a 1% mass loss at 170 °C and 5% mass loss at 216 °C for **poly(209b)**.

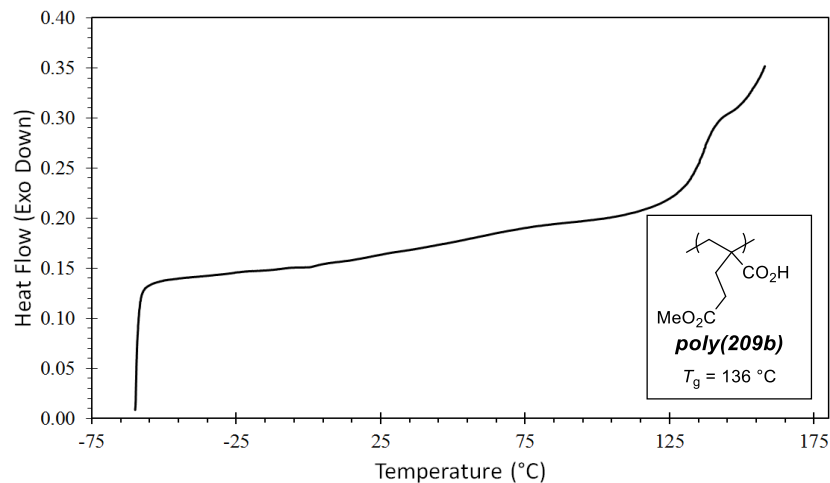


Figure S2.21 DSC trace of **poly(209b)** taken on the second ramp of heating at 10 °C/min. A hole was punched into the DSC pan to remove adsorbed water during the first heating cycle. The glass transition temperature (T_g) was observed at 136 °C.

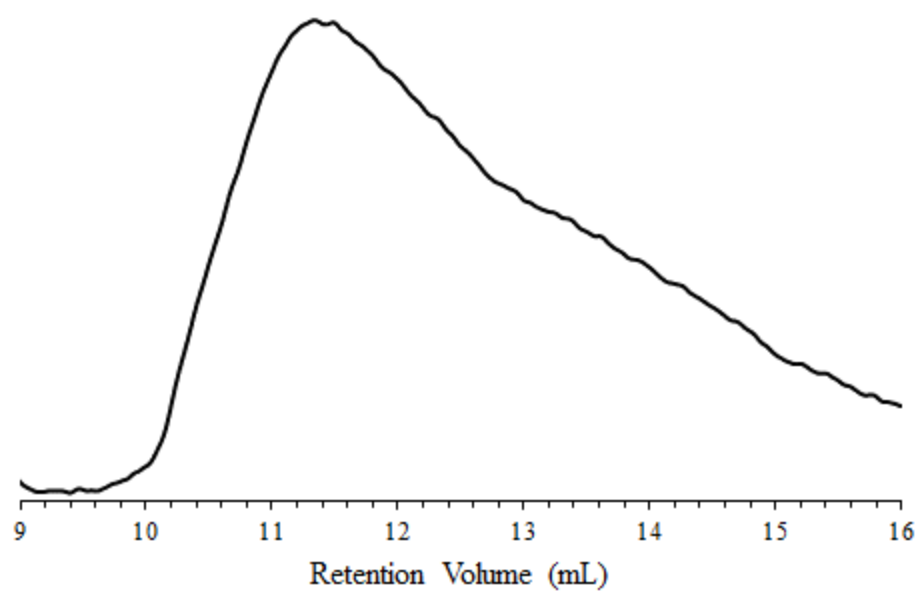


Figure S2.22 SEC trace of **poly(209b)** taken in DMF and calibrated using polystyrene standards. $M_n = 29.1 \text{ kg}\cdot\text{mol}^{-1}$, $M_w = 58.0 \text{ kg}\cdot\text{mol}^{-1}$, $D = 2.0$.

S2.8 References

- ¹ Hoye, T. R.; Hanson, P. R.; Vyvyan, J. R. A practical guide to first-order multiplet analysis in ¹H NMR spectroscopy. *J. Org. Chem.* **1994**, *59*, 4096–4103. (b) Hoye, T. R.; Zhao, H. A method for easily determining coupling constant (*J*) values: An addendum to "A Practical Guide to First-order Multiplet Analysis in ¹H NMR Spectroscopy." *J. Org. Chem.* **2002**, *67*, 4014–4016.
- ² Wiley, R. H.; Knabeschuh, L. H. 2-Pyrones. XIII. The chemistry of coumalic acid and its derivatives. *J. Am. Chem. Soc.* **1955**, *77*, 1615–1617.
- ³ Ashworth, L. W.; Bowden, M. C.; Dembofsky, B.; Levin, D.; Moss, W.; Robinson, E.; Szczur, N.; Virica, J. A new route for manufacture of 3-cyano-1-naphthalenecarboxylic acid. *Org. Process Res. Dev.* **2003**, *7*, 74–81.
- ⁴ Poisson, T.; Yamashita, Y.; Kobayashi, S. Catalytic asymmetric protonation of chiral calcium enolates via 1,4-addition of malonates. *J. Am. Chem. Soc.* **2010**, *132*, 7890–7892.
- ⁵ Foubelo, F.; Lloret, F.; Yus, M. Enolic radical derived from acetic acid: A useful radical alternative to acetate enolate in Michael-type reactions. *Tetrahedron* **1993**, *49*, 8465–8470.
- ⁶ Bartley, D. M.; Coward, J. K. *J. Org. Chem.* **2006**, *71*, 371–374.
- ⁷ Feng, Y.; Coward, J. K. Prodrug forms of *N*-[(4-deoxy-4-amino-10-methyl)pteroyl]glutamate- γ -[ψ P(O)(OH)]-glutarate, a potent inhibitor of Folylpoly- γ -glutamate synthetase: Synthesis and hydrolytic stability. *J. Med. Chem.*, **2006**, *49*, 770–788.
- ⁸ Tello-Aburto, R.; Lucero, A. N.; Rogelj, S. A catalytic approach to the MH-031 lactone: Application to the synthesis of geralcin analogs. *Tetrahedron Lett.* **2014**, *55*, 6266–6268.
- ⁹ Kobatake, S.; Yamada, B. Radical polymerization and copolymerization of methyl α -(2-carbomethoxyethyl)acrylate, a dimer of methyl acrylate, as a polymerizable α -substituted acrylate. *J. Polym. Sci. A Polym. Chem.* **1996**, *34*, 95–108.
- ¹⁰ Dainton, F. S.; Ivin, K. J. Some thermodynamic and kinetic aspects of addition polymerization *Q. Rev. Soc.* **1958**, *12*, 61–92.
- ¹¹ Olsen, P.; Odelius, K.; Albertsson, A.-C. Thermodynamic presynthetic considerations for ring-opening polymerization. *Biomacromolecules* **2016**, *17*, 699–709.
- ¹² Schneiderman, D. K.; Hillmyer, M. A. Aliphatic polyester block polymer design. *Macromolecules* **2016**, *49*, 2419–2428.

Appendix B. Supplementary information for Chapter 3 (S3)

The work in this chapter was performed in collaboration with Daniel E. Stasiw and
William B. Tolman

| | | |
|-------------|---|-----|
| S3.1 | General Experimental Protocols | 169 |
| S3.2 | Determination of Branch Density | 171 |
| S3.3 | Preparation and Characterization of non-Polymeric Compounds | 172 |
| S3.3.1 | 2-(2-Carbomethoxyethyl)propiolactone (isoCMVL)..... | 172 |
| S3.3.2 | Dimethyl 2-(acetoxymethyl)pentanedioate (<i>i</i>)..... | 173 |
| S3.3.3 | 5-Butyl 1-methyl 2-(acetoxymethyl)pentanedioate (S301)..... | 174 |
| S3.4 | Preparation and Characterization of Polymers | 175 |
| S3.4.1 | Exemplary polymerizations | 175 |
| S3.4.2 | Kinetics of polymerization | 177 |
| S3.4.3 | Degradation of EQ-PCMVL and P(isoCMVL) | 180 |
| S3.4.4 | Post-polymerization isomerization of PCMVL & P(isoCMVL) | 185 |
| S3.5 | Methanolysis and chemical recycling of EQ-PCMVL | 190 |
| S3.6 | Polymer SEC, TGA, and DSC data | 193 |
| S3.7 | References | 198 |

S3.1 General Experimental Protocols

Materials:

Chloroform and CDCl₃ used for experimentation was distilled from CaH₂, placed over 3 Å molecular sieves, and stored under N₂ in a glovebox prior to use. DBU was distilled from CaH₂ and stored over KOH. Benzyl alcohol was distilled from CaH₂ and stored under a N₂ atmosphere in a glovebox. **CMVL**,¹ **PCMVL** (from diphenyl phosphate catalysis),¹ acetylated **PCMVL**,¹ and zinc catalyst **302**² were prepared as previously described.

Instrumental methods:

NMR: ¹H and ¹³C NMR spectra were recorded using Bruker Avance 500 (500 MHz) and 400 (400 MHz) spectrometers. ¹H and ¹³C NMR chemical shifts using CDCl₃ are referenced to TMS at 0.00 ppm and to CDCl₃ (carbon resonance) at 77.16 ppm, respectively. Coupling constants were determined using previously described methods.³ Non-first-order multiplets in a ¹H NMR spectrum were assigned using the acronym 'nfom.' Proton data are presented in the following format: chemical shift (in ppm) followed by [multiplicity, coupling constant(s), relative number of protons (to the nearest whole integer), and substructural environment]. The proton(s) in each substructural environment is italicized: e.g., CH_aH_b.

ATR-FTIR: A Midac Prospect IR or a Bruker Alpha Platinum instruments, each fitted with an ATR stage, was used to measure Fourier transform infrared spectra. Measurements were commonly recorded with a four second acquisition time and sixteen scans.

Mass spectrometry of non-polymeric samples: High resolution mass spectra (HRMS) were collected on a Bruker BioTOF (ES-TOF) instrument in electrospray ionization mode (ESI) using PEG as an internal calibrant/standard.

Size Exclusion Chromatography (SEC): An Agilent 100 series SEC, fitted with an RI detector and three consecutive Varian PL gel Mixed C columns (25 cm length, 7.5 mm

inner diameter), was used to analyze the mass of polymeric samples. Each sample was dissolved at ca. $1 \text{ mg}\cdot\text{mL}^{-1}$ and eluted at $1 \text{ mL}\cdot\text{min}^{-1}$ with CHCl_3 . Polystyrene standards were used as calibrants to determine M_n , M_w , and \bar{D} of each sample.

Alternatively, an Agilent 1260 Series pump fitted with two consecutive Agilent PLgel MIXED-B columns (300 mm x 7.5 mm with 10 μm beads), an RI detector (Optilab rEX differential refractive index detector), and light scattering detector (Wyatt 18-angle DAWN HELEOS) were used to obtain M_n , M_w , and \bar{D} of samples using matrix-assisted laser light scattering data (MALS).

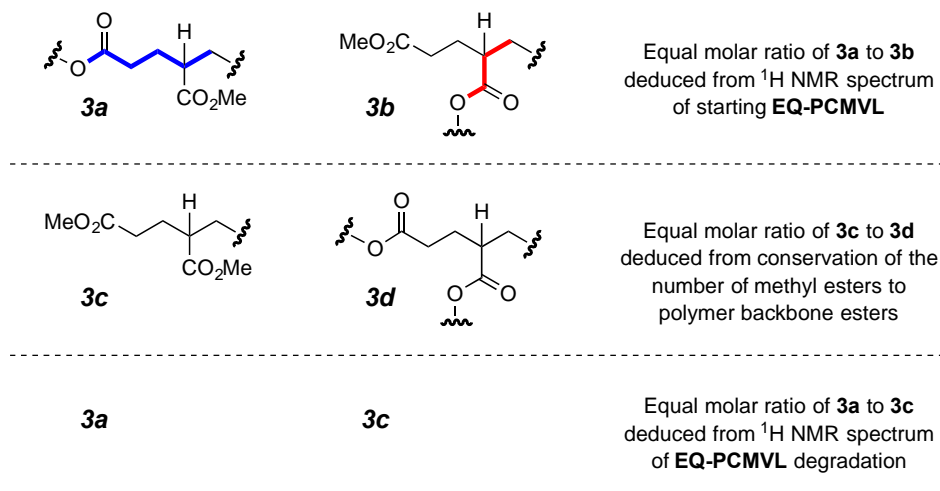
Thermogravimetric Analysis (TGA): A TA Instruments Q500 thermogravimetric analyzer using a heating rate of $10 \text{ }^\circ\text{C}\cdot\text{min}^{-1}$ under N_2 was used to analyze the thermal stability of polymeric materials. Typical sample sizes ranged from 3–8 mg.

Differential Scanning Calorimetry (DSC): A TA Instruments Q-1000 differential scanning calorimeter was used for analysis. Samples were hermetically sealed in aluminum pans. Samples were typically cooled to $-60 \text{ }^\circ\text{C}$, heated to $175 \text{ }^\circ\text{C}$ ($10 \text{ }^\circ\text{C}\cdot\text{min}^{-1}$), cooled to $-60 \text{ }^\circ\text{C}$ ($10 \text{ }^\circ\text{C}\cdot\text{min}^{-1}$), and reheated to $175 \text{ }^\circ\text{C}$ ($10 \text{ }^\circ\text{C}\cdot\text{min}^{-1}$). Glass transition temperatures (T_g) were recorded at the inflection point recorded during the second heating cycle.

Matrix-Assisted Laser Desorption/Ionization Time of Flight Mass Spectrometry (MALDI/TOF-MS): An AB-Sciex 5800 instrument was used in reflectron mode to obtain MALDI/TOF-MS spectra of low molecular weight polymer samples. Dihydroxybenzene (DHB) was used as a matrix. **PCMVL**, **EQ-PCMVL** and DHB were each dissolved in THF, combined in a ca. 1:2000 mass ratio of polymer to matrix, and applied to the target plate.

S3.2 Determination of Branch Density

The ^1H NMR spectrum of **EQ-PCMVL** after full isomerization showed an ca. 1:1 ratio of the two methyl ester resonances at δ 3.71 and 3.67 ppm (see footnote 9 in MS). This suggests that there is a 1:1 ratio of the monomethyl ester subunits **303a** (3.71) and **303b** (3.67), and some number of the dimethyl esters subunit **303c** (equal number of methoxy resonances at 3.71 and 3.67). Additionally, there should be an equivalent number of branch units (**303d**) to branch termini (**303c**) due to the conservation of methyl esters and backbone esters in the reaction mixture; free methanol was never observed in the NMR spectra of the reaction mixture over time. Finally, the degradation mixture from **EQ-PCMVL** (Figure S4) contains an ca. 1:1 ratio of subunits **301a** (from **303a**) and **301c** (from **3c**). Since the two subunits **303a** and **303c** eliminate to near completion [and subunits **303b** and **303c** do not fully eliminate (see discussion of **P(iso)CMVL**) degradation below)], the ratio of **301a**: **301c** in the degradation mixture is a reflection on the relative number of subunits of **303a** to **303c** in **EQ-PCMVL**, prior to degradation. Using the transitive law (if $a = b$ and $b = c$, then $a = c$), we conclude that **EQ-PCMVL** contains a nearly equimolar ratio of the four subunits **303a**, **303b**, **303c**, and **303d**.

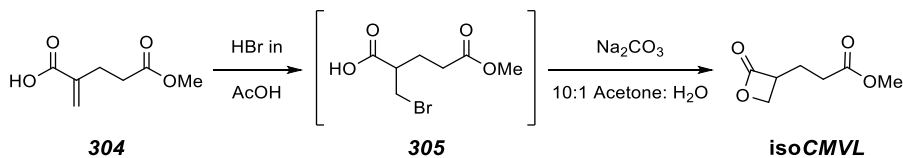


Therefore: $[\mathbf{3a}] \approx [\mathbf{3b}] \approx [\mathbf{3c}] \approx [\mathbf{3d}]$

Figure S3.1 Graphical summary of how we have deduced the degree of branching in **EQ-PCMVL**.

S3.3 Preparation and Characterization of non-Polymeric Compounds

S3.3.1 2-(2-Carbomethoxyethyl)propiolactone (isoCMVL)



5-Methoxy-2-methylene-5-oxopentanoic acid (**304**) was synthesized as previously described in three steps from methyl acrylate.^{1,4}

HBr in acetic acid (33 wt. %, 5 mL) was added to a 20-mL scintillation vial containing 5-methoxy-2-methylene-5-oxopentanoic acid (**304**, 472 mg, 2.99 mmol) and a stir bar. The vial was capped, and the mixture was stirred for 45 minutes and concentrated to give a mixture of acetic acid and 2-(bromomethyl)-5-methoxy-5-oxopentanoic acid (**305**) as light yellow oil. The oil was diluted in acetone (100 mL), and Na₂CO₃ (2.49 g, 23.5 mmol) and water (10 mL) were added. The solution was stirred for 2 h, and the mixture was concentrated in vacuo. Solid sodium sulfate was added to saturation, and the mixture was extracted with EtOAc (3 x ca. 50 mL). The organic layer was dried (MgSO₄) and concentrated to give a yellow oil that was further purified via MPLC (silica gel, 3:1 Hex:EtOAc) to give 2-(2-carbomethoxyethyl)propiolactone (*iso*CMVL, 218 mg, 46% yield over two steps) as a colorless oil.

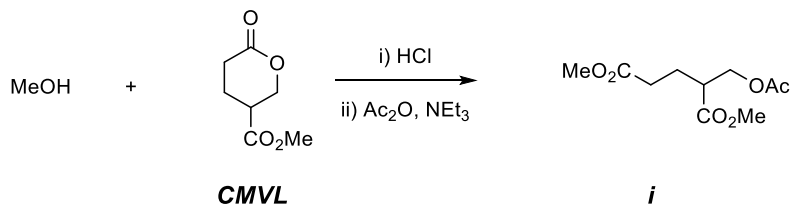
¹H NMR (400 MHz, CDCl₃) δ 4.40 (dd, *J* = 6.3, 5.4 Hz, 1H, CO₂H_aH_b), 4.06 (dd, *J* = 5.4, 4.5 Hz, 1H, CO₂H_aH_b), 3.79 (dddd, *J* = 7.9, 7.9, 6.4, 4.6 Hz, 1H, OCCHCH₂), 3.70 (s, 3H, CO₂CH₃), 2.55 (ddd, *J* = 16.7, 7.5, 6.5 Hz, 1 H, CH_aH_bCO₂Me), 2.49 (ddd, *J* = 16.7, 7.8, 7.1 Hz, 1 H, CH_aH_bCO₂Me), 2.17 (dddd, *J* = 14.2, 7.9, 7.1, 6.4 Hz, 1H, CHCH_cH_dCH₂), 2.13 (dddd, *J* = 14.2, 7.7, 7.7, 7.7 Hz, 1H, CHCH_cH_dCH₂).

¹³C NMR (125 MHz, CDCl₃) δ 172.8, 171.1, 65.2, 52.0, 51.3, 31.1, and 23.6.

IR (neat, selected peaks): 2878, 2943, 1740, 1726 (shoulder), and 1372 cm⁻¹.

HRMS (ESI-TOF): Calculated for (C₇H₁₀O₄Na)⁺ 181.0471; found: 181.0449.

S3.3.2 Dimethyl 2-(acetoxymethyl)pentanedioate (**i**)



4-Carbomethoxyvalerolactone (**CMVL**, 50.0 mg, 0.316 mmol), MeOH (50 equiv, 632 μ L, 15.8 mmol), and SOCl₂ (0.05 equiv, ca. 1 μ L, 0.01(6) mmol) were placed into a scintillation vial, capped, and stirred for 15 h at ambient temperature. Ac₂O (335 equiv, 10.0 mL, 106 mmol) and NEt₃ (50 equiv, 2.20 mL, 15.8 mmol) were added, and the reaction mixture was stirred for 24 h. The mixture was concentrated under high vacuum, diluted with EtOAc (30 mL), washed with NH₄Cl, NaHCO₃ and brine, dried (MgSO₄), and concentrated to afford **i** as a purple oil 5-methyl 1-methyl 2-(acetoxymethyl)pentanedioate (**i**, 48 mg, 67% yield).

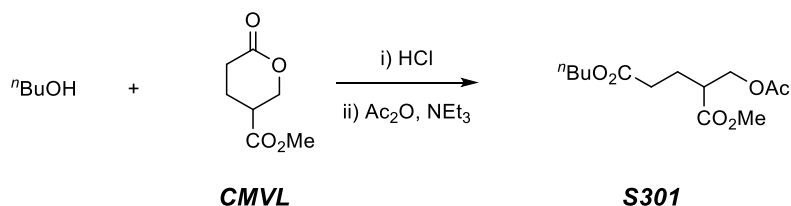
¹H NMR (500 MHz, CDCl₃) δ 4.24, (dd, J = 11.0, 6.9 Hz, 1H, H_aH_b OAc), 4.23 (dd, J = 11.1, 5.9 Hz, 1H, H_aH_b OAc), 3.72 (s, 3H, CHCO₂CH₃), 3.68 (s, 3H, CH₂CO₂CH₃), 2.77 (dddd, J = 8.8, 7.0, 5.7, 5.7 Hz, 1H, CHCO₂Me), 2.41 (ddd, J = 16.5, 8.6, 6.5 Hz, 1H, -O₂CCH_bH_cCH₂CH), 2.37 (ddd, J = 16.5, 8.2, 7.0 Hz, 1H, O₂CCH_bH_cCH₂CH), 2.05 (s, 3H, O₂CCH₃), 1.97 (dddd, J = 14.1, 8.4, 8.4, 6.5 Hz, 1H, -O₂CCH₂CH_dH_eCH), and 1.90 (dddd, J = 14.1, 8.6, 7.1, 5.5 Hz, 1H, -O₂CCH₂CH_dH_eCH).

¹³C NMR (125 MHz, CDCl₃) δ 173.3, 172.1, 170.8, 64.3, 54.1, 51.9, 44.0, 31.4, 23.9, and 20.9.

IR (neat, selected peaks) 2957, 1743, 1468, and 1440 cm⁻¹.

HRMS (ESI-TOF) Calculated for (C₁₀H₁₆O₆Na)⁺ 255.0845; found 255.0842.

S3.3.3 5-Butyl 1-methyl 2-(acetoxymethyl)pentanedioate (S301)



4-Carbomethoxyvalerolactone (**CMVL**, 235 mg, 1.49 mmol), nBuOH (10 mL), and DPP (ca. 1 mg, 0.004 mmol) were placed into a scintillation vial, capped, and stirred for 20 h at ambient temperature. The reaction mixture was transferred to a 250 mL round bottom flask, Ac₂O (100 mL) and NEt₃ (30 mL) were added, and the reaction mixture was stirred for 20 h. The mixture was concentrated *in vacuo*, diluted with EtOAc (30 mL), washed with NaHCO₃ and brine, dried (MgSO₄), and concentrated. The sample was further purified by a silica plug (EtOAc) and concentrated to give 5-butyl 1-methyl 2-(acetoxymethyl)pentanedioate (**S301**, 195 mg, 47% yield) as a purple oil.

¹H NMR (500 MHz, CDCl₃) δ 4.24, (dd, *J* = 11.0, 6.9 Hz, 1H, *H_aH_bOAc*), 4.23 (dd, *J* = 11.2, 6.0 Hz, 1H, *H_aH_bOAc*), 4.08 (t, *J* = 6.7, 2H, CO₂CH₂CH₂), 3.72 (s, 3H, CHCO₂CH₃), 2.77 (dddd, *J* = 8.7, 7.0, 5.7, 5.7 Hz, 1H, CHCO₂Me), 2.40 (ddd, *J* = 16.4, 8.6, 6.5 Hz, 1H, –O₂CCH_{*b*}H_{*c*}CH₂CH), 2.35 (ddd, *J* = 16.4, 8.3, 7.0 Hz, 1H, O₂CCH_{*b*}H_{*c*}CH₂CH), 2.05 (s, 3H, O₂CCH₃), 1.97 (dddd, *J* = 14.0, 8.4, 8.4, 6.5 Hz, 1H, –O₂CCH₂CH_{*d*}H_{*e*}CH), 1.90 (dddd, *J* = 14.1, 8.7, 7.1, 5.5 Hz, 1H, –O₂CCH₂CH_{*d*}H_{*e*}CH), 1.61 (m, 2H, CO₂CH₂CH₂), 1.37 (m, 2H, CO₂CH₂CH₂CH₂CH₃), and 0.94 (t, *J* = 7.4 Hz, CO₂CH₂CH₂CH₂CH₃).

¹³C NMR (125 MHz, CDCl₃) δ 173.3, 172.8, 170.8, 64.7, 64.3, 52.1, 44.0, 31.7, 30.8, 23.9, 20.9, 19.3, and 13.8.

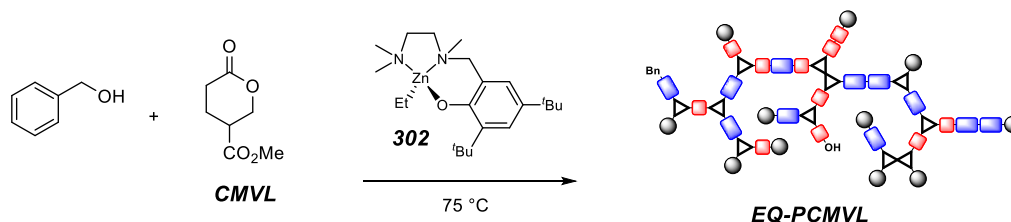
IR (neat, selected peaks) 2959, 2867, 1737, 1712 (shoulder), 1458, 1437, and 1370 cm⁻¹.

HRMS (ESI-TOF) Calculated for (C₁₃H₂₂O₆Na)⁺ 297.1309; found: 297.1328.

S3.4 Preparation and Characterization of Polymers

S3.4.1 Exemplary polymerizations

CMVL to EQ-PCMVL



Benzyl alcohol (1.0 equiv, 1.2 μL , 0.011 mmol), catalyst **302** (2.25 equiv, 10.0 mg, 0.0242 mmol), **CMVL** (595 equiv, 1.01 g, 6.37 mmol), and a stir bar were transferred to a 1-dram vial in a nitrogen-filled glovebox. The vial was sealed with a Teflon cap and held at 75 °C for 15 h. An aliquot of this viscous, homogenous sample showed >98% conversion via ^1H NMR spectroscopy. DCM (ca. 2 mL) was added to dissolve the contents of the vial, and the polymer was precipitated by dropwise addition into stirred MeOH (ca. 15 mL). This mixture was cooled in an ice bath and centrifuged, and the majority of supernatant liquid was decanted. The polymer was redissolved in DCM (ca. 2 mL) and reprecipitated, now by the addition of MeOH (ca. 15 mL) to the DCM solution. Cooling, centrifugation, decantation, and drying under high vacuum at 80 °C overnight gave **EQ-PCMVL** as a colorless, highly viscous material.

^1H NMR See assignments in the annotated spectrum

^{13}C NMR See spectrum

IR 2954, 1727, 1437, and 1154 cm^{-1}

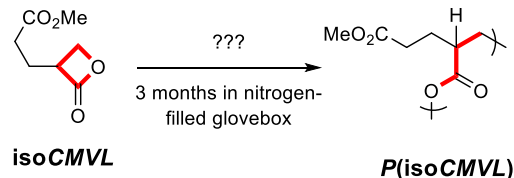
TGA T_d 1% = 241 °C; 5% = 270 °C

DSC T_g = -20 °C

SEC (CHCl_3 , PS calibration): M_n = 7.5 $\text{kg}\cdot\text{mol}^{-1}$, M_w = 12.3 $\text{kg}\cdot\text{mol}^{-1}$, D = 1.6

(THF, MALS): M_n = 11.1 $\text{kg}\cdot\text{mol}^{-1}$, M_w = 17.5 $\text{kg}\cdot\text{mol}^{-1}$, D = 1.6, dn/dc = 0.0563

*iso*CMVL to P(*iso*CMVL)



The polymerization of *iso*CMVL using catalysts like DPP, HCl, Zn(Et)₂, or Al(OiPr)₃ were unable to provide linear P(*iso*CMVL) and, instead, led to competitive formation of EQ-PCMVL. However, when *iso*CMVL was synthesized as described above, transferred using DCM to a vial, concentrated, and stored in a nitrogen-filled glovebox for 3 months, the *iso*CMVL had polymerized with ca. 67% conversion to P(*iso*CMVL). No isomerization to EQ-PCMVL was detected. This sample was dissolved in DCM (ca. 0.5 mL), and the polymer was precipitated by dropwise addition into 1:1 EtOAc:hexanes (ca. 5 mL). This suspension was cooled in an ice bath, centrifuged, and the majority of the supernatant was decanted. The polymer was resuspended in DCM, and reprecipitated by addition of EtOAc (ca. 2 mL) followed by hexanes (ca. 3 mL). This mixture was cooled and centrifuged, the supernatant was decanted. The remaining viscous liquid was placed under high vacuum at 75 °C for 12 h to give P(*iso*CMVL) as a clear highly viscous material.

¹H NMR See assignments in the annotated spectrum

¹³C NMR See spectrum

IR 2955, 1727, 1437, 1372, 1325, and 1152 cm⁻¹

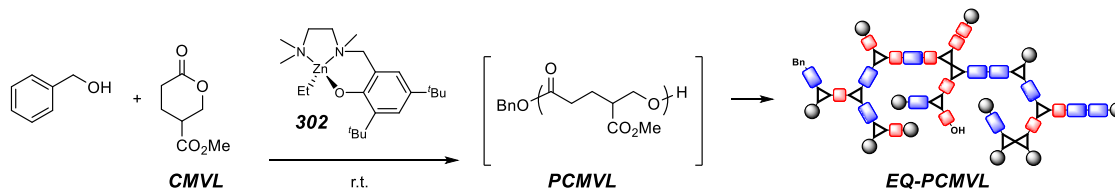
TGA *T*_d 1% = 245 °C; 5% = 270 °C

DSC *T*_g = -16 °C

SEC (CHCl₃, PS calibration): *M*_n = 16.3 kg•mol⁻¹, *M*_w = 20.3 kg•mol⁻¹, *D* = 1.3

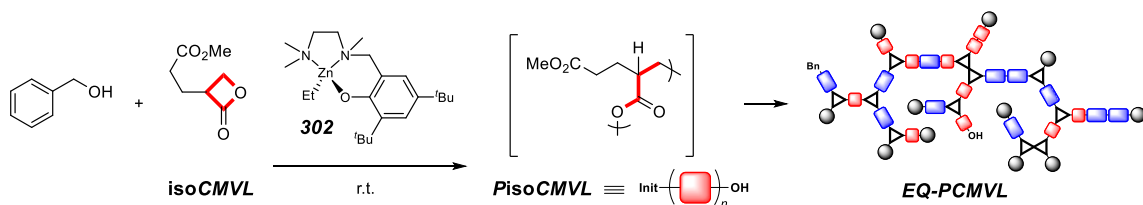
S3.4.2 Kinetics of polymerization

¹H NMR kinetic study of CMVL polymerization to EQ-PCMVL with catalyst **302**



The target concentrations for this experiment were: 3.35 M **CMVL**, 0.037 M internal standard, 0.087 M catalyst **302**, and 0.072 M benzyl alcohol. Thus, a solution of **CMVL** (50 equiv, ca. 400 μ L, 408 mg) and the internal standard bis-*para*-trimethylsilylbenzene (0.5 equiv, 6 mg) in 100 μ L of dry CDCl_3 were added to an NMR tube capped with a rubber septum. A solution of **302** (1.2 equiv, 28 mg) and benzyl alcohol (1 equiv, 6 mg) in 300 μ L of dry CDCl_3 was independently prepared. An initial spectrum of the **CMVL** and the internal standard was taken as a baseline. The NMR sample was removed from the spectrometer, and the solution of **302** and benzyl alcohol was injected into the NMR tube using an airtight syringe. The tube was shaken to mix the reagents and returned to the spectrometer. The polymerization was monitored over 48 h by comparing the integration of the methylene of **CMVL** at 4.16 δ and **PCMVL** 3.90 δ as well as by comparing the integration of the methyl ester CH_3 signal of **CMVL** at 3.42 δ , versus the two methyl resonances in the polymer repeat units at 3.39 δ and 3.35 δ . [Note: these chemical shifts are referenced to the TMS-groups in the internal standard, which was set to 0.00 ppm.] The reaction reached 90% monomer conversion after 1.4 h and maintained this conversion for the duration of the experiment.

^1H NMR kinetic study of *iso*CMVL polymerization to EQ-PCMVL with catalyst **302**



The targeted concentrations for this experiment were the same as those described above in the polymerization of **CMVL** to **EQ-PCMVL**. Benzyl alcohol (BnOH, 1 equiv, 0.7 μL , 0.007 mmol) and *iso*CMVL (47 equiv, 52 mg, 0.329 mmol), and a stir bar were added to a 1/2-dram vial in a nitrogen-filled glovebox. An aliquot of this mixture was dissolved in CDCl_3 and was measured to contain a 44:1 ratio of *iso*CMVL to BnOH. A stock solution of the internal standard bis-*para*-trimethylsilylbenzene and catalyst **302** was prepared. A 50 μL aliquot containing the standard (0.5 equiv, 0.75 mg, 0.0037 mmol) and **302** (1.2 equiv, 3.5 mg, 0.0085 mmol) was added to the vial. Aliquots (ca. 5 μL) were periodically removed at the indicated time points, diluted in CDCl_3 (0.55 mL), and analyzed by ^1H NMR spectroscopy.

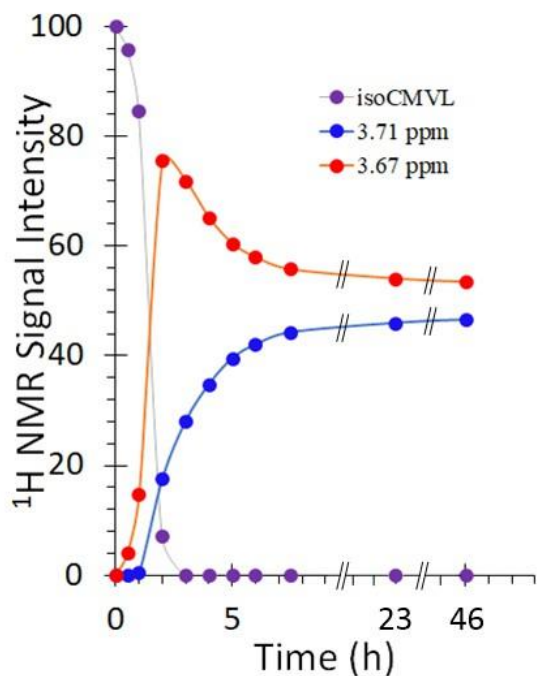


Figure S3.2 Kinetic plot for the polymerization of *iso*CMVL (50 equiv) initiated by benzyl alcohol (1 equiv) and catalyzed by zinc catalyst 302 (1.2 equiv). The plot shows full consumption of *iso*CMVL at ca. 1.5 h (similar to CMVL polymerization) with a slower rate of isomerization to EQ-PCVML (yet, still very similar to CMVL polymerization). [cf. Figure 3a in the manuscript for the analogous plot of CMVL polymerization.]

S3.4.3 Degradation of EQ-PCMVL and P(isoCMVL)

DBU promoted degradation of EQ-PCMVL

EQ-PCMVL (50 mg, 0.316 mmol of repeat units) *derived from CMVL polymerization*, DBU (200 μ L, 1.34 mmol), and a stir bar were placed into a 1/2-dram vial, capped, and allowed to stir at ambient temperature for 17 hours. A portion of the resulting crude mixture (ca. 50 μ L) was examined by ^1H NMR spectroscopy. The polymer was judged to be ca. 75% degraded, as measured by the integration of the oligomeric methylene protons at ca. 4.00–4.40 ppm vs. that of the vinylic protons from 5.08–6.13 ppm. Small portions of the conjugate acids of **301a–301d** (independently synthesized)¹ were each sequentially doped into this NMR sample and a spectrum taken at each interval (see Figure S3, below) to verify the identity of each degradation product.

In an analogous experiment, the DBU-promoted degradation of **EQ-PCMVL** *derived from isoCMVL* also produced the α -methyleneglutarates **301a–301d**.

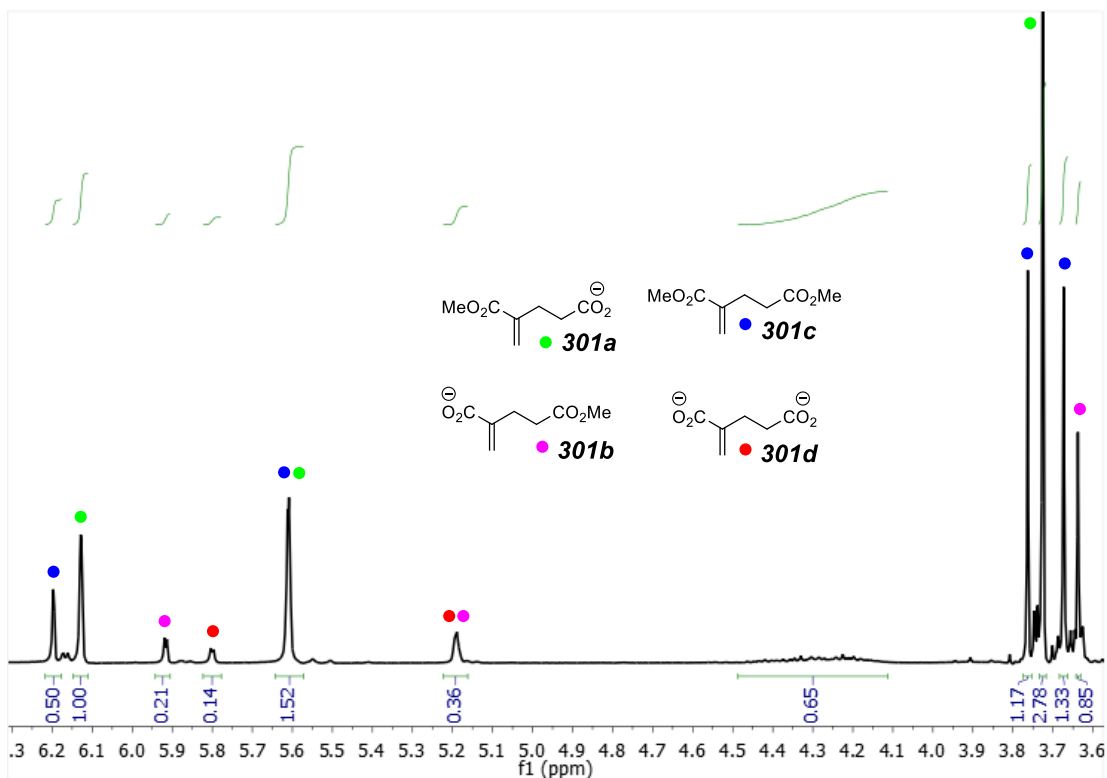
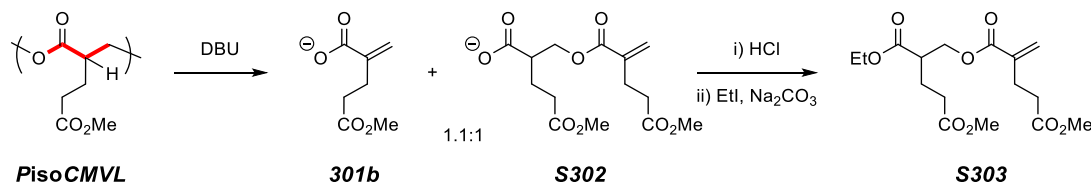


Figure S3.3 The final ¹H NMR spectrum of the crude degradation mixture generated by incubation with DBU (4.2 equiv per subunit of **EQ-PCMVL**) for 17 h. The assignments for each of the structures **301a–301d** were verified through subsequent, sequential doping of the sample giving rise to this spectrum with authentic samples of pure conjugate acids of **301a–301d**. The peaks between 4.50–4.10 ppm are consistent with the incomplete degradation.

Degradation of P(*iso*CMVL)

1-(2-(Ethoxycarbonyl)-5-methoxy-5-oxopentyl) 5-methyl 2-methylenepentanedioate (S5)



P(*iso*CMVL) [$M_n = 17 \text{ kg}\cdot\text{mol}^{-1}$ (CHCl₃ SEC), 17 mg, 0.11 mmol of repeat units], DBU (75 μL , 0.50 mmol), and a stir bar were placed into a 1/2-dram vial, capped, and allowed to stir for 18 h at ambient temperature. A small portion (ca. 20 μL) was dissolved in CDCl₃ (0.5 mL) and analyzed via ¹H NMR spectroscopy. This aliquot showed a 1.1:1 ratio of **301b** to **S302**. The identity of **301b** was confirmed by doping of the CDCl₃ solution with an authentic sample of 5-methoxy-2-methylene-5-oxopentanoic acid (protonated **301b**), and the presence of **S302** was deduced by the chemical modification described below.

The remaining DBU solution containing **301b** and **S302** was dissolved in DCM (2 mL) and EtOAc (6 mL), acidified with HCl (2 M), washed with brine, and concentrated to afford 10.1 mg of the protonated forms of **301b** and **S302**. This mixture was diluted in DMF (0.4 mL) in a 2-dram vial containing a stir bar. Na₂CO₃ (ca. 1.2 equiv per CO₂H, 5.2 mg, 0.050 mmol) was added followed by iodoethane (ca. 3.0 equiv per CO₂H, 10 μL , 0.125 mmol). The vial was capped, and the mixture was stirred for 24 h at ambient temperature. DMF and the remaining iodoethane were removed *in vacuo*, and the resulting white solid was dissolved in EtOAc (2 mL), washed with water and brine, dried with MgSO₄, and concentrated. The vial was placed under vacuum (0.1 mmHg) overnight to afford 1-(2-(ethoxycarbonyl)-5-methoxy-5-oxopentyl) 5-methyl 2-methylenepentanedioate as a light yellow oil (**S303**, 4.6 mg).

¹H NMR (500 MHz, CDCl₃) δ 6.18 (d, $J = 1.1$ Hz, 1H, =CH_{cis}H_{trans}), 5.62 (dt, $J = 1.3$, 1.3 Hz, 1H, =CH_{cis}H_{trans}), 4.32 (d, $J = 6.4$ Hz, 2H, =CCO₂CH₂CH), 4.17 (q, $J = 7.1$ Hz,

2H, CO₂CH₂CH₃), 3.68 (s, 3H, CO₂Me), 3.67 (s, 3H, CO₂Me), 2.81 [dddd, J = 8.9, 6.4, 6.4, 5.3 Hz, 1H, CHCO₂Et], 2.64–2.60 (m, 2H), 2.53–2.49 (m, 2H), 2.43 [ddd, J = 16.5, 8.6, 6.4 Hz, 1H, MeO₂CCH_aH_bCH₂CH], 2.38 [ddd, J = 16.5, 8.2, 7.1 Hz, 1H, MeO₂CCH_aH_bCH₂CH], 2.00 [dddd, J = 14.1, 8.9, 8.2, 6.4 Hz, 1H, MeO₂CCH₂CH_aH_bCH], 1.92 [dddd, J = 14.0, 8.6, 7.2, 5.4 Hz, 1H, MeO₂CCH₂CH_aH_bCH], and 1.26 (t, J = 7.1 Hz, 3H, CO₂CH₂CH₃).

¹³C NMR (125 MHz, CDCl₃) δ 173.19, 173.16, 172.8, 166.3, 138.6, 126.6, 64.8, 61.1, 51.9, 51.8, 44.1, 33.0, 31.4, 27.4, 23.9, and 14.3.

IR (neat, selected peaks) 2950, 2916, 1728 (s), 1632, 1437, and 1160 cm⁻¹.

HRMS (ESI-TOF) Calculated for (C₁₆H₂₄O₈Na)⁺ 367.1369; found: 367.1374.

Attempted retro-ROTEP degradation of EQ-PCMVL

EQ-PCMVL (41 mg) and $\text{Sn}(\text{Oct})_2$ (2 μL) were placed into a 5 mL round bottom flask and heated at 150 °C in a Kugelrohr distillation apparatus at 0.1 mmHg. After 18 h, ca. 0.4 mg of **CMVL** was recovered (^1H NMR spectroscopy), more $\text{Sn}(\text{Oct})_2$ (2 μL) was added, and the **EQ-PCMVL** mixture was heated again under vacuum. No additional distillate was observed after 12 h. More $\text{Sn}(\text{Oct})_2$ (6 μL) was added, and the flask was heated at 175 °C at 0.1 mmHg for an additional 12 h. Only $\text{Sn}(\text{Oct})_2$ was recovered. This experiment established that very few of the polymers contained their lone free hydroxyl group in a substructural environment capable of reverse-ROTEP fragmentation with ejection of the six-membered **CMVL** monomer.

S3.4.4 Post-polymerization isomerization of PCMV_L & P(isoCMV_L)

PCMV_L isomerization and MALDI TOF-MS analyses

In a nitrogen-filled glovebox, preformed, linear **PCMV_L** [75 mg, prepared by initiation with benzyl alcohol ($M_n = 2.54 \text{ kg}\cdot\text{mol}^{-1}$ from ^1H NMR spect)], zinc catalyst **302** (3.75 mg), CDCl_3 (50 mg), and a stir bar were placed into a ½-dram vial and sealed with a Teflon-lined cap. The vial was placed into a sand bath held at 80 °C and allowed to stir for 15 h. An aliquot was taken, dissolved in CDCl_3 , and analyzed via ^1H NMR spectroscopy. The aliquot showed an approximately 1:1 ratio of the two methyl ester resonances at 3.67 and 3.71 ppm, in addition to ca. 7% of depolymerized **CMV_L**. The reaction mixture was further diluted with DCM (ca. 0.5 mL) and precipitated into a stirring solution of 1:5 EtOAc:Hex (ca. 5 mL). This mixture was cooled in an ice bath and centrifuged, and the majority of supernatant liquid was decanted. The polymer was redissolved in DCM (ca. 0.5 mL) and reprecipitated, now by the addition of EtOAc (ca. 1 mL) followed by Hex (ca. 4 mL), to the DCM solution. Cooling, centrifugation, decantation, and drying under high vacuum at 80 °C overnight gave **EQ-PCMV_L** as a colorless, highly viscous material. Both **PCMV_L** and **EQ-PCMV_L** were analyzed via MALDI TOF-MS.

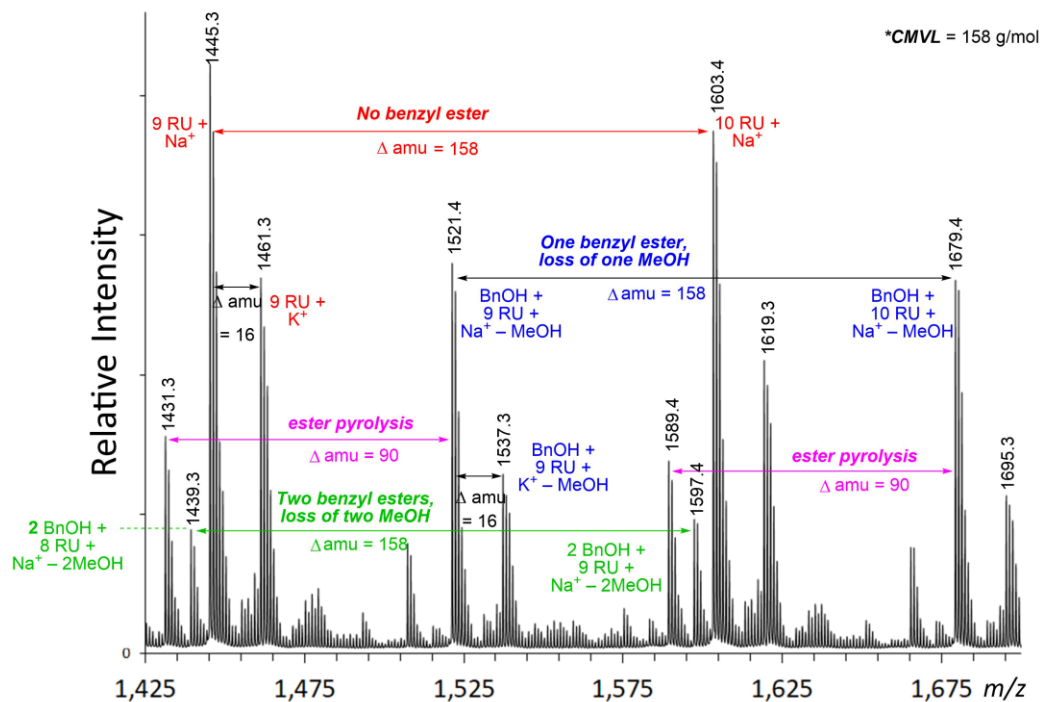
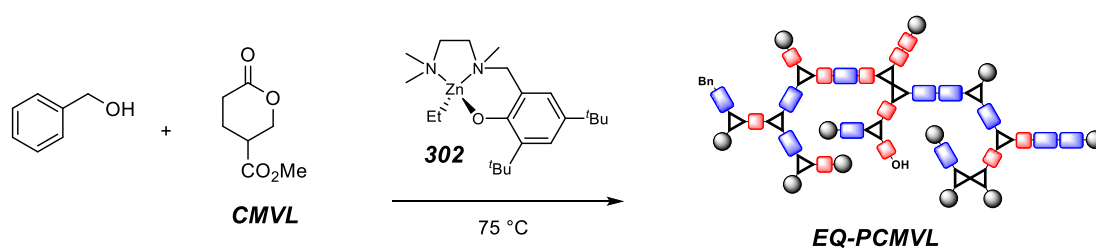


Figure S3.4 Expansion of a MALDI/TOF-MS spectrum (taken in reflectron mode) of **EQ-PCMVL** (Figure 3.6, isomerized from **PCMVL** with $M_n = 2.54 \text{ kg}\cdot\text{mol}^{-1}$ from ^1H NMR spectroscopy) using dihydroxybenzene as a matrix. **CMVL** molar mass = $158 \text{ g}\cdot\text{mol}^{-1}$.

Polymerization and isomerization parallel monitoring by SEC and ^1H NMR spectroscopy



4-Carbomethoxyvalerolactone (**CMVL**, 477 mg, 3.00 mmol), benzyl alcohol (0.7 μL , 6 μmol), and a stir bar were added to a 2 dram vial in a glovebox with a nitrogen environment. NNOZnEt (**302**, 6.2 mg, 12.6 μmol) was added, the vial was capped, the mixture was stirred at room temperature and aliquots were taken at the indicated timepoints. Each aliquot was dissolved in CDCl_3 , analyzed via ^1H NMR spectroscopy, concentrated *in vacuo*, resuspended in CHCl_3 , and analyzed via SEC. After 7 days, the polymer was precipitated 2x from methanol using precipitation method described above for **EQ-PCMVL**.

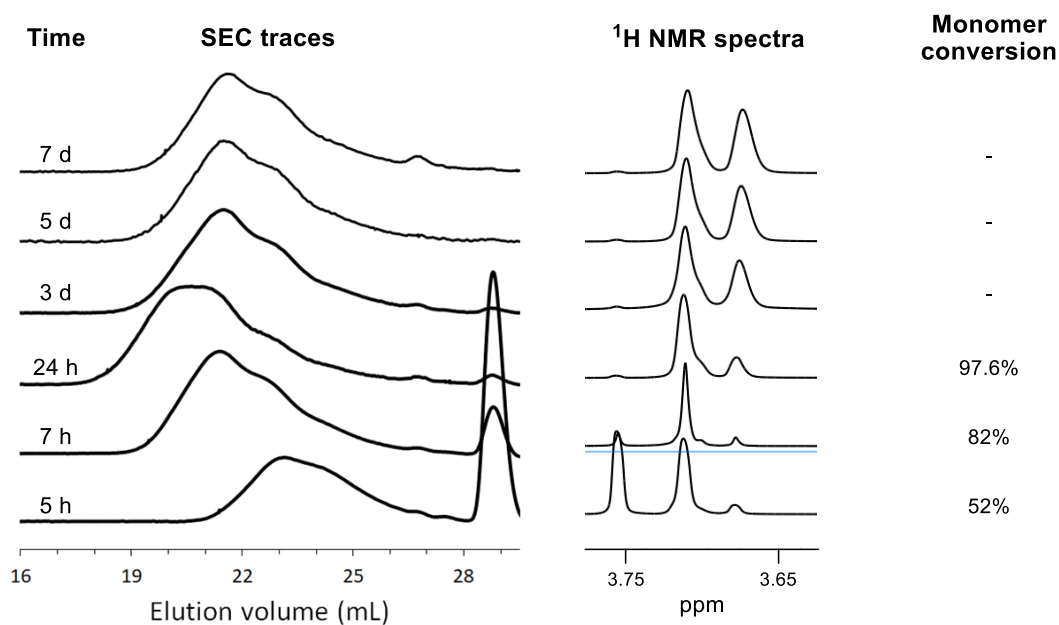
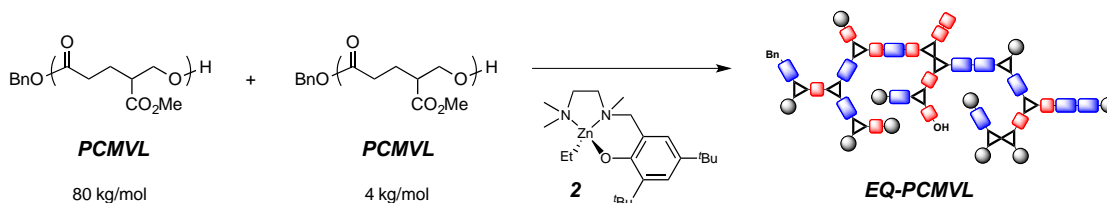


Figure S3.5 Parallel monitoring of polymerization and isomerization of **CMVL** with catalyst **302** by SEC and ^1H NMR spectroscopy.

Isomerization parallel monitoring by SEC and ¹H NMR spectroscopy



Equal masses of two samples of **PCMVL** having two significantly different molecular weights (20 mg, 80 kg/mol and 20 mg, 4 kg/mol, each made by polymerization of **CMVL** with diphenyl phosphate) were added to a 1-dram vial fitted with a stir bar in a nitrogen-filled glove box. CHCl₃ (245 mg, dried over CaH₂ distillation) was added. Catalyst **302** (3.2 mg) was added, the solution was stirred, and aliquots (ca. 10 μL) were removed and examined at the indicated timepoints. Each aliquot was diluted in CDCl₃, analyzed via ¹H NMR spectroscopy, concentrated *in vacuo*, redissolved in CHCl₃, and analyzed via SEC. A control experiment demonstrated that there was no appreciable amount of additional isomerization occurring during this handling protocol.

P(isoCMVL) isomerization by 302 in CDCl₃

P(isoCMVL) [10 mg, $M_n = 16.3 \text{ kg}\cdot\text{mol}^{-1}$ (SEC)] was added to a 1/2-dram vial and placed in a vacuum oven at 100 °C for two hours. The vial was transferred into a nitrogen-filled glovebox. Catalyst **302** (1.0 mg, 2.4 μmol) and CDCl₃ (30 μL) were added, the vial was sealed with a Teflon-line capped. The vial was heated in a sand bath held at 70 °C for 16 hours. The contents were dissolved in DCM (ca. 1 mL) and precipitated into a 2-dram vial filled with 1:1 EtOAc:Hex. The vial was cooled (−20 °C) and centrifuged, the solvent was decanted, and the residue was heated (ca. 75 °C) in a vacuum oven overnight to afford **EQ-PCMVL** (6 mg) as a colorless, viscous polymer.

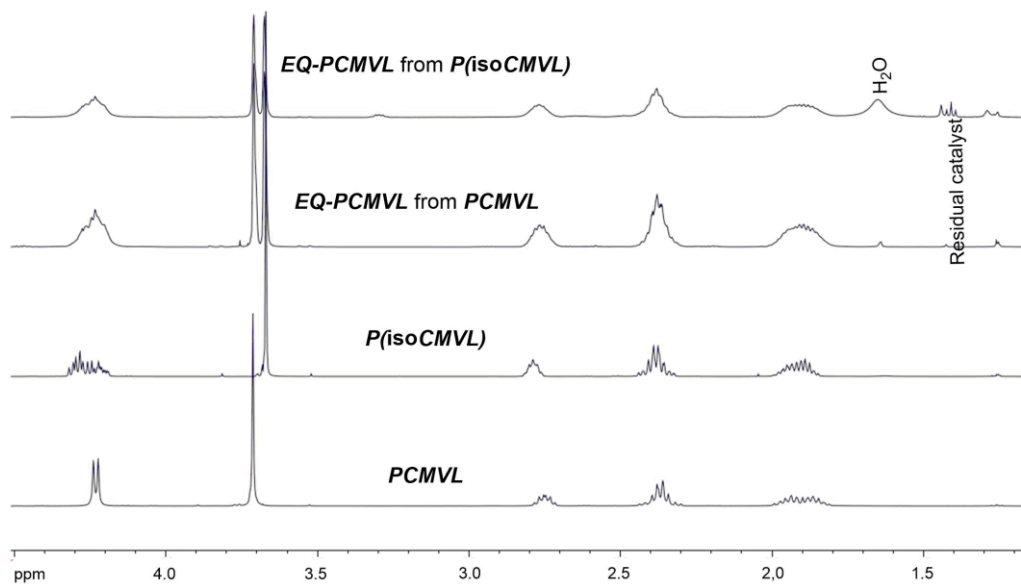
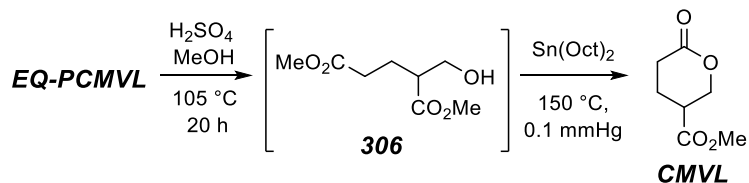


Figure S3.6 Overlaid ¹H NMR spectra of (bottom to top) **PCMV**, **P(isoCMVL)**, and isomerized **EQ-PCMV** [independently isomerized from **PCMV** and **P(isoCMVL)**].

S3.5 Methanolysis and chemical recycling of *EQ-PCMVL*



EQ-PCMVL (64 mg, $M_n = 91\text{ kg}\cdot\text{mol}^{-1}$), H_2SO_4 (5 μL), MeOH (2.5 mL), and a stir bar were added to an 8-mL culture tube and sealed with a Teflon-lined cap. The mixture was stirred at $105\text{ }^\circ\text{C}$ for 20 h, allowed to cool to room temperature, and concentrated to afford a mixture of **306**, **CMVL**, and some oligomeric **PCMVL**. The remaining oily residue was diluted in DCM, eluted through a plug of NaHCO_3 , and concentrated in a 5-mL round bottom flask. $\text{Sn}(\text{Oct})_2$ (2 μL) was added, and the mixture was placed at $75\text{ }^\circ\text{C}$ under vacuum for 7 h followed by Kugelrohr distillation at $130\text{ }^\circ\text{C}$ for 27 h for give **CMVL** (54 mg, 84% yield) as a colorless oil. The ^1H NMR spectrum of recycled **CMVL** did contain **306** in a 4:1 ratio (5-p051).

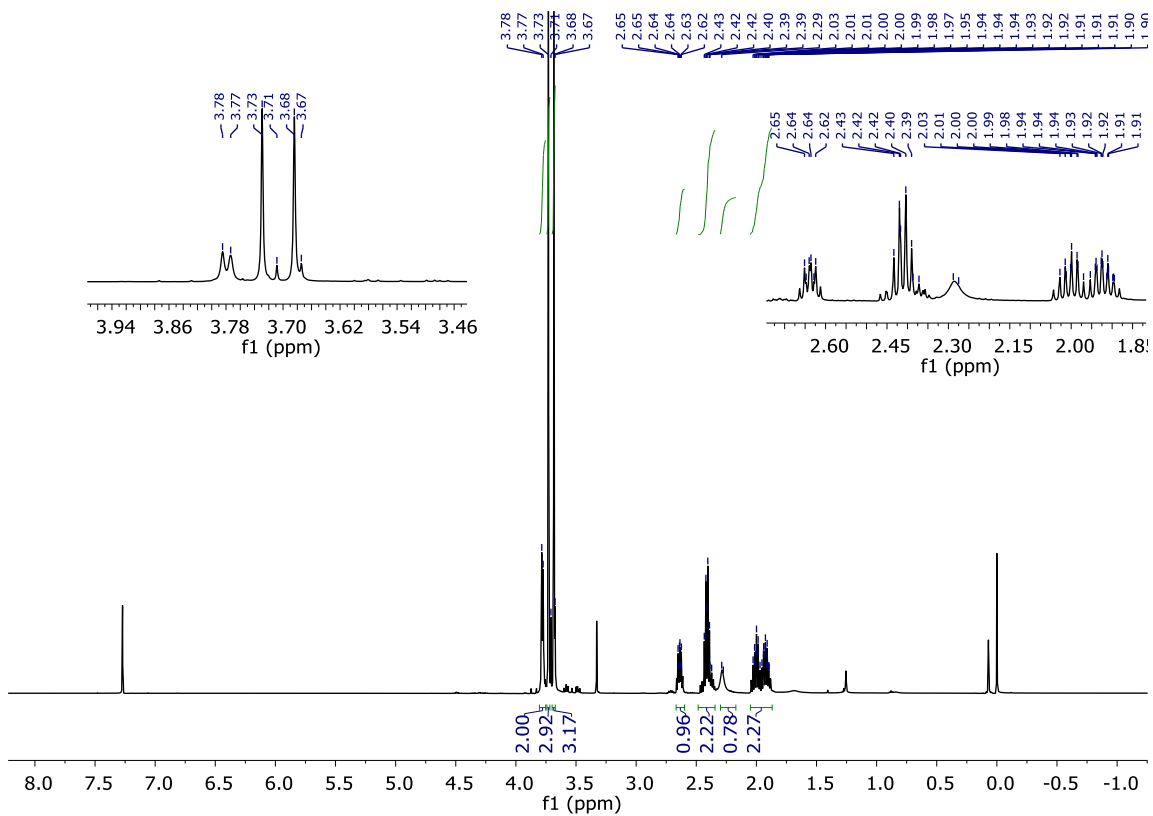


Figure S3.7 ^1H NMR spectrum of hydroxydimethyl ester **306**.

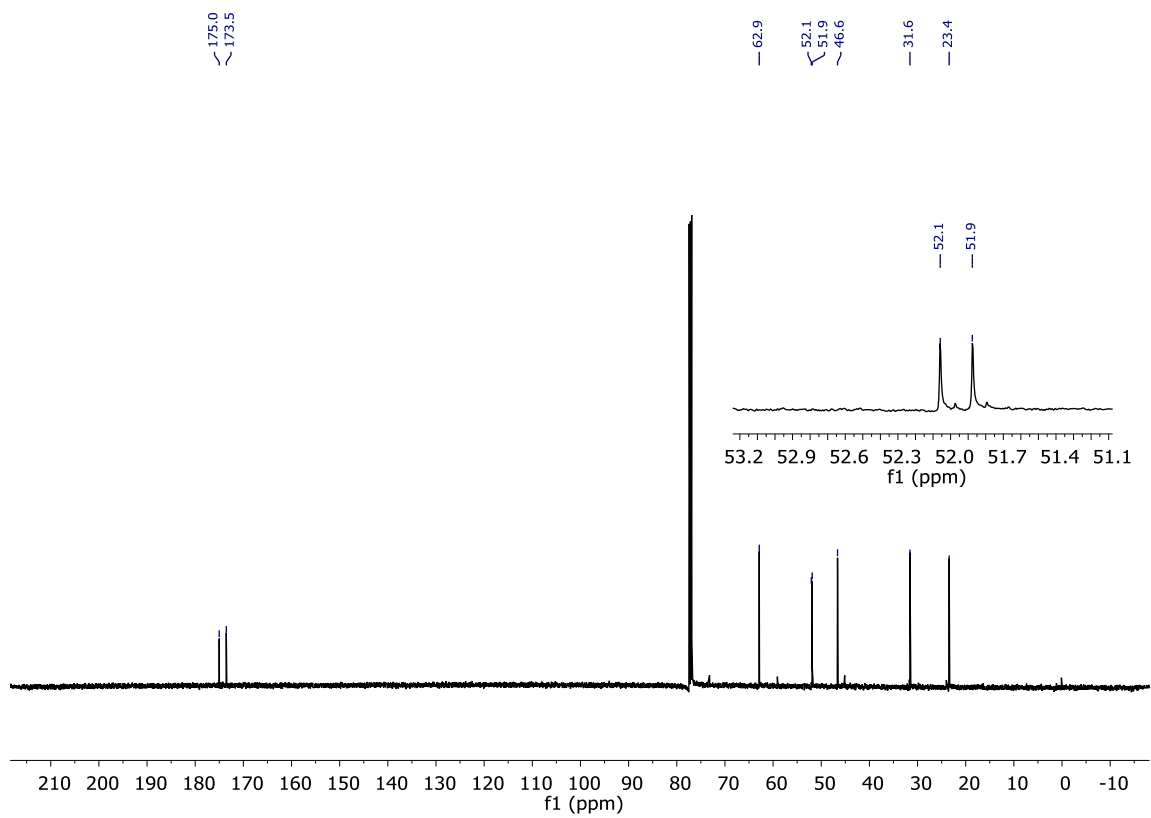


Figure S3.8 ^{13}C NMR spectrum of hydroxydimethyl ester **306**.

S3.6 Polymer SEC, TGA, and DSC data

EQ-PCMVL

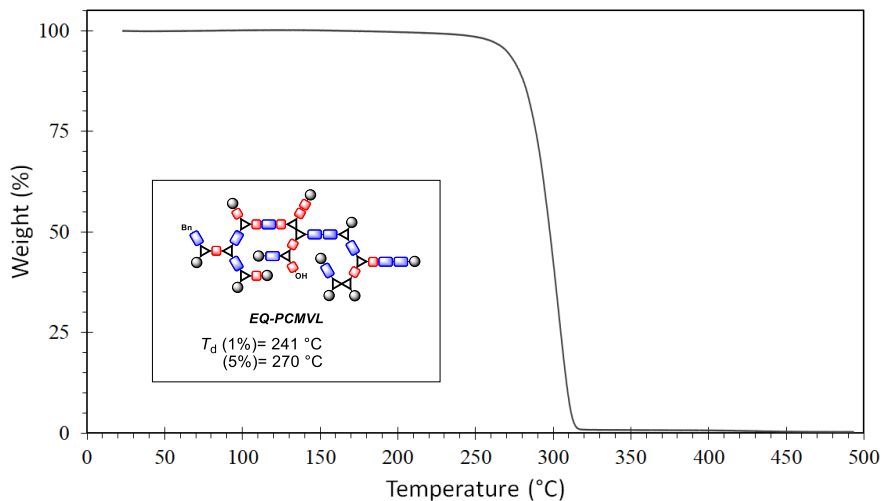


Figure S3.9 TGA thermogram of an **EQ-PCMVL** sample (prepared using a 595:1 ratio of **CMVL**: **BnOH**) at a heating rate of 10 °C/min. **EQ-PCMVL** has a 1% mass loss at 241 °C and 5% mass loss at 270 °C.

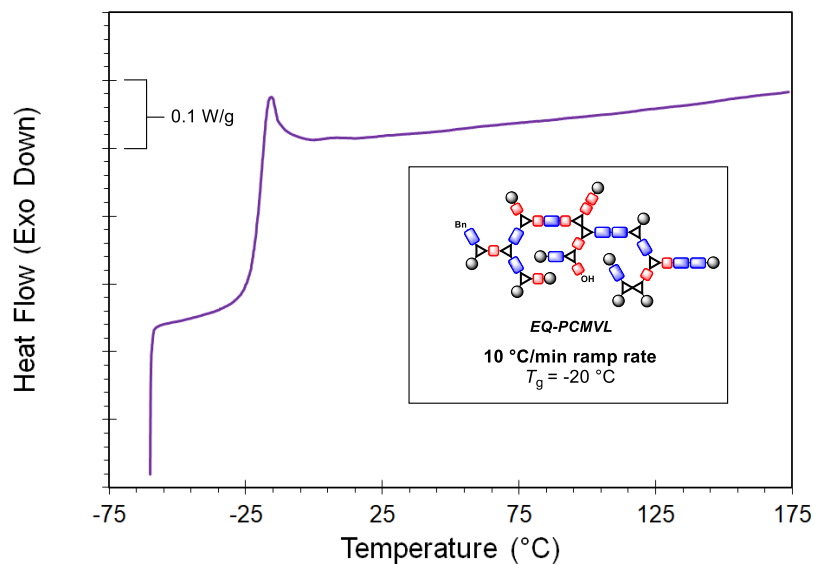


Figure S3.10 DSC thermogram of an **EQ-PCMVL** sample (prepared using a 595:1 ratio of **CMVL**: BnOH) taken on the second ramp of heating at 10 °C/min. **EQ-PCMVL** is an amorphous polymer with a $T_g = -20$ °C.

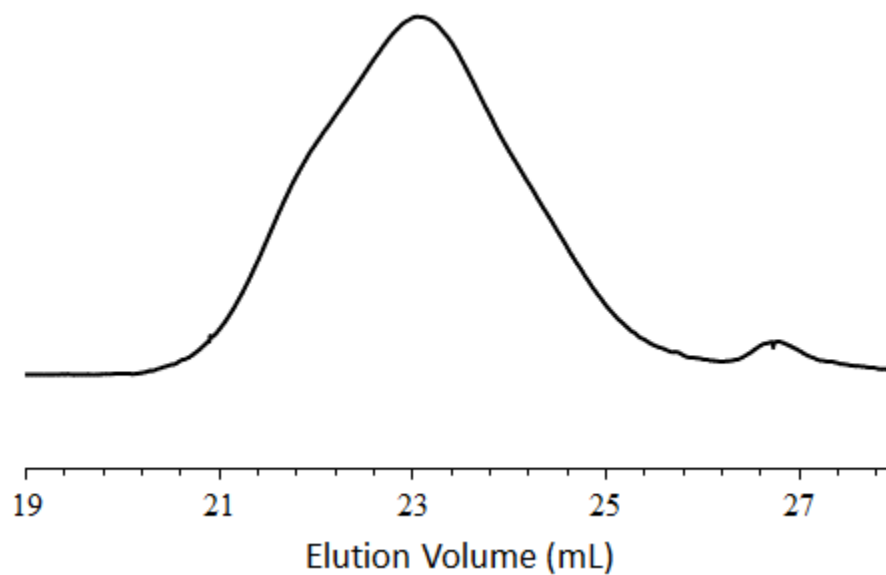


Figure S3.11 SEC trace of a precipitated **EQ-PCMVL** sample (prepared using a 595:1 ratio of **CMVL**: BnOH). SEC was taken in CHCl_3 on a column calibrated using polystyrene standards. $M_n = 7.4 \text{ kg}\cdot\text{mol}^{-1}$, $M_w = 12.3 \text{ kg}\cdot\text{mol}^{-1}$, $D = 1.6$.

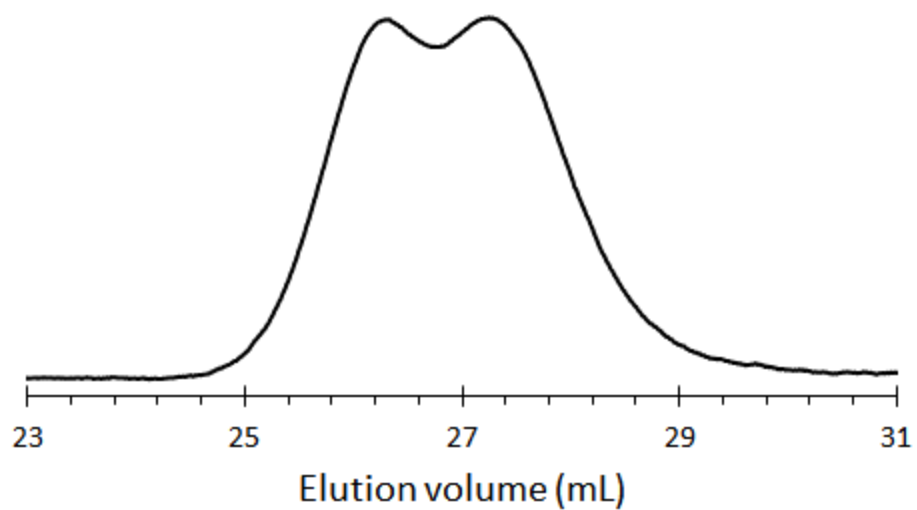


Figure S3.12 SEC trace of a precipitated **EQ-PCMVL** sample (prepared using a 595:1 ratio of **CMVL**: **BnOH**). SEC was taken in THF with MALS (not shown) and RI (shown) detection. $M_n = 10.9 \text{ kg}\cdot\text{mol}^{-1}$, $M_w = 17.2 \text{ kg}\cdot\text{mol}^{-1}$, $D = 1.6$, $dn/dc = 0.0563$. The bimodal nature is indicative of the presence of a population of cyclic polyesters.

P(*iso*)CMVL

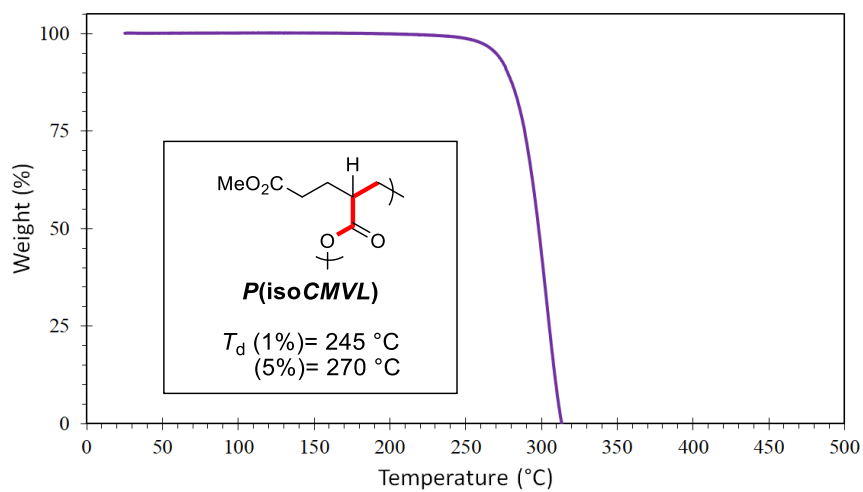


Figure S3.13 TGA thermogram of **P(*iso*)CMVL** ($M_n = 16.3 \text{ kg}\cdot\text{mol}^{-1}$, SEC) at a heating rate increase of $10 \text{ }^\circ\text{C}/\text{min}$. **P(*iso*)CMVL** has a 1% mass loss at $245 \text{ }^\circ\text{C}$ and 5% mass loss at $270 \text{ }^\circ\text{C}$.

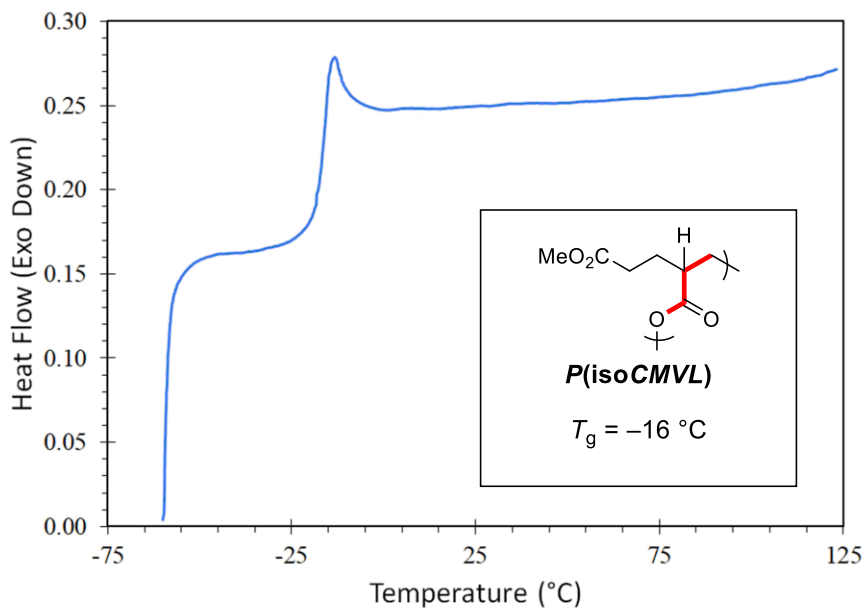


Figure S3.14 DSC thermogram of **P(*iso*CMVL)** ($M_n = 16.3 \text{ kg}\cdot\text{mol}^{-1}$, SEC) taken on the second ramp of heating at $10 \text{ }^\circ\text{C}/\text{min}$. **P(*iso*CMVL)** is an amorphous polymer with a $T_g = -16 \text{ }^\circ\text{C}$.

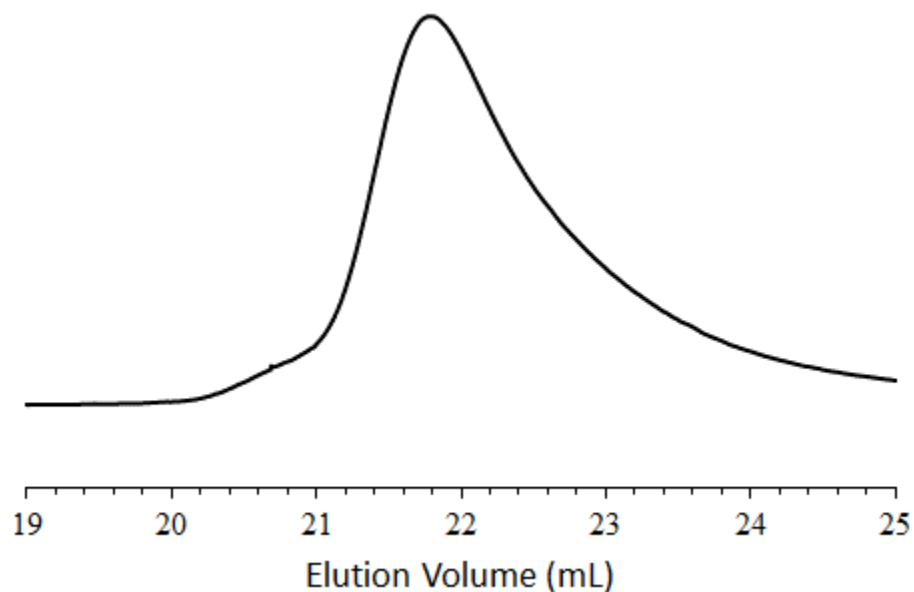


Figure S3.15 SEC trace of precipitated **P(*iso*CMVL)** that was polymerized when stored in a nitrogen-filled glovebox for three months. SEC was taken in CHCl_3 on a column calibrated using polystyrene standards. $M_n = 16.3 \text{ kg}\cdot\text{mol}^{-1}$, $M_w = 20.3 \text{ kg}\cdot\text{mol}^{-1}$, $D = 1.3$.

S3.7 References

- ¹ Fahnhorst, G. W.; Hoye, T. R. A carbomethoxylated polyvalerolactone from malic acid: Synthesis and divergent chemical recycling. *ACS Macro Lett.* **2018**, *7*, 143–147.
- ² Williams, C. K.; Breyfogle, L. E.; Kyung Choi, S.; Nam, W.; Young Jr., V. G.; Hillmyer, M. A.; Tolman, W. B. A highly active zinc catalyst for the controlled polymerization of lactide. *J. Am. Chem. Soc.* **2003**, *125*, 11350–11359.
- ³ Hoye, T. R.; Hanson, P. R.; Vyvyan, J. R. A practical guide to first-order multiplet analysis in ¹H NMR spectroscopy. *J. Org. Chem.* **1994**, *59*, 4096–4103. (b) Hoye, T. R.; Zhao, H. A Method for easily determining coupling constant (*J*) values: An addendum to "A practical guide to first-order multiplet analysis in ¹H NMR spectroscopy." *J. Org. Chem.* **2002**, *67*, 4014–4016.
- ⁴ Tello-Aburto, R.; Lucero, A. N.; Rogelj, S. A catalytic approach to the MH-031 lactone: Application to the synthesis of geraldin analogs. *Tetrahedron Lett.* **2014**, *55*, 6266–6268.

Appendix C. Supplementary information for Chapter 4 (S4)

| | |
|---|-----|
| S4.1 General Experimental Protocols | 200 |
| S4.2. Preparation and Characterization of non-Polymeric Compounds | 201 |
| S4.2.1. Pyrones | 201 |
| 5.2.2 4-Carboalkoxyvalerolactones and 5-Alkoxy-4-methyl-5-oxopentanoic acids .. | 207 |
| S4.3 Preparation and Characterization of Polymers | 220 |
| S4.4 Polymer testing | 232 |
| S4.4.1 Matrix-assisted laser desorption ionization time of flight (MALDI-TOF) | 232 |
| S4.4.2 Eliminative degradation..... | 234 |
| S.4.4.3 Differential scanning calorimetry annealing studies | 236 |
| S4.5 Polymer characterization data | 242 |
| S4.5.1 Size-exclusion chromatography..... | 242 |
| S4.5.2 Thermogravimetric analysis | 245 |
| S4.5.3 Differential scanning calorimetry | 248 |
| S4.5.4 Tensile testing..... | 250 |
| S4.6 References | 253 |

S4.1 General Experimental Protocols

Materials:

D,L-Malic acid ($\geq 99\%$) was used as received from Sigma Aldrich or Acros Organics. Solvents were used as received unless otherwise noted. Benzyl bromide (Aldrich), undecyl bromide (Alfa Aesar), and 2-ethylhexyl bromide (Aldrich) were used as received. BnOH was distilled over CaH_2 and stored under a N_2 atmosphere in a glovebox. Pd/C [5% (w/w)] was purchased from Engelhard and was used as received. Diphenyl phosphate [DPP; $(\text{PhO})_2\text{PO}_2\text{H}$] from Ark Pharm or Sigma Aldrich was placed in a vial containing a stir bar and the sample was stirred under high vacuum (ca. 0.1 mmHg) for 48 h before use.

Instrumental methods:

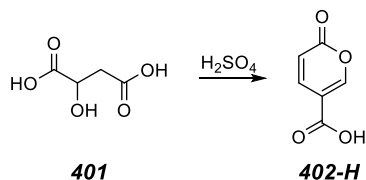
Nuclear Magnetic Resonance (NMR) spectroscopy, Attenuated Total Reflectance-Fourier Transform Infrared (ATR-FTIR) spectroscopy, High-Resolution Mass Spectrometry (HRMS), Size Exclusion Chromatography (SEC), Thermogravimetric Analysis (TGA), Differential Scanning Calorimetry (DSC), and Matrix-Assisted Laser Desorption/Ionization Time of Flight Mass Spectrometry (MALDI/TOF-MS) were analyzed using the instruments and protocols as outlined in the supporting information for Chapter 3.

Tensile Testing: High molar mass samples of **PCMeVL**, **PCEtVL**, **PCiPrVL**, and **PCnBuVL** were melt pressed at 120 °C for five minutes between two Teflon sheets and a square mold with a thickness of 0.2 mm. A dog-bone-shaped die was used to punch out samples for tensile testing with 0.2 mm thickness, ca. 20 mm gauge length, 5 mm gauge width, and 15 mm clamp width. Samples were pulled to the point of break with a rate of 50.0 $\text{mm}\cdot\text{min}^{-1}$ using a Shimadzu AGS-X Tensile Tester.

S4.2. Preparation and Characterization of non-Polymeric Compounds

S4.2.1. Pyrones

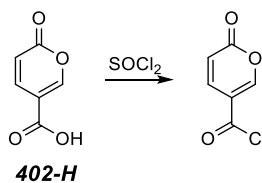
Coumalic Acid (**402-H**)



Coumalic acid was prepared using a modified procedure to Wiley and Smith.¹ Malic acid (400 g, 2.99 mol) was added portion-wise (ca. 25 g/10 min) to sulfuric acid (1 L) at 65 °C in a 3-L round bottom flask for 20 h. The contents were poured over ice (ca. 1.5 L), and the mixture was allowed to stand for 24 h. The mixture was filtered, and the filtered solid was thoroughly washed with cold water to afford coumalic acid as a tan powder (113 g, 54% yield). This powder was commonly 97–98% pure as determined by ¹H NMR spectroscopy and was often further purified by recrystallization in MeOH to give coumalic acid (**402-H**, 76.5 g, 37% yield) as a tan solid.

mp: begin to sublime at 170 °C, mp = 194–202 °C (lit. 206–209 °C).¹

Coumalic Acid Chloride



Coumalic acid (**402-H**, 2.79 g, 19.9 mmol) was refluxed in thionyl chloride (11.5 mL, 159 mmol) in a 25-mL round bottom flask until the solid was completely consumed (24–40 h). The reaction mixture was concentrated and distilled via bulb-to-bulb distillation to give coumalic acid chloride (2.83 g, 17.9 mmol, 90% yield) as a white solid. Because this compound degrades at room temperature in a day or so to a dark brown solid (sparingly soluble in CHCl₃) it was routinely used immediately after preparation.

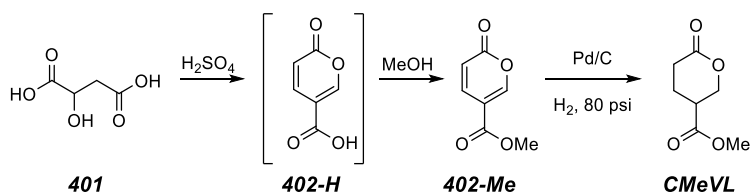
$^1\text{H NMR}$ (500 MHz, CDCl_3) δ 8.58, (dd, $J = 2.8, 1.1$ Hz, 1H, (CO)O-CH=C), 7.77 (dd, $J = 9.9, 2.8$ Hz, -CHCH(C=O)-), and 6.39 (dd, $J = 9.9, 1.1$ Hz, 1 H, -CHCH(C=O)-).

$^{13}\text{C NMR}$ (125 MHz, CDCl_3) δ 163.0, 162.8, 158.3, 140.3, 116.7, and 115.5.

IR 3089, 3065, 3035, 1732 (strong, with two shoulders), 1628 (med), 1556 (med), and 1267 (strong) cm^{-1} .

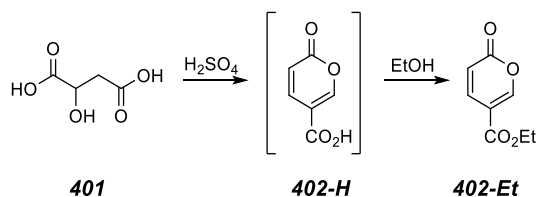
bp 105–115 °C at 0.15 mmHg

Methyl Coumalate (**402-Me**)



Methyl coumalate (**402-Me**) and 4-carbomethoxyvalerolactone (**CMeVL**) were synthesized by a procedure we previously described.²

Ethyl Coumalate (**402-Et**)



Ethyl coumalate (**402-Et**) was synthesized using an analogous procedure to that used for methyl coumalate.² D,L-Malic acid (**401**, 200.0 g, 745.7 mmol) was added portionwise (ca. 20 g/addition) over the course of one hour to a stirred solution of sulfuric acid (500 mL) in a 3-liter round-bottomed flask at 70 °C. The mixture was allowed to stir for 16 h, at which time the color had progressed to dark red. This mixture was placed into an ice bath. Once the internal temperature of the mixture reached 35–40 °C, ethanol (700 mL) was added dropwise at a rate to keep the reaction mixture between 35–50 °C (ca. 1.5 h). *Note: when the mixture was cooled further than 30–35 °C a precipitate, presumably coumalic acid, would begin to appear. Also, the addition of ethanol can generate a*

significant amount of heat. The solution was heated to 65 °C and stirred for 18 h. The solution was cooled and poured over ice (ca. 1.2 L), extracted with CHCl₃, washed (NaHCO₃ and brine), dried (MgSO₄), and concentrated to give a yellow liquid. The crude ethyl coumalate was distilled via bulb-to-bulb distillation (0.1 mm Hg, external bath temperature at 120 °C) with the first ca. 10% discarded. This fraction contained significant quantities of diethyl fumarate and diethyl maleate. The main fraction of distilled coumalate (76.0 g) was recrystallized (EtOAc:Hex, slowly cooled to -20 °C) to give ethyl coumalate (**402-Et**, 45.9 g, 273 mmol, 37% yield) as a white powder. The concentrated mother liquor could be distilled to provide additional ethyl coumalate.

¹H NMR (500 MHz, CDCl₃) δ 8.30 (dd, *J* = 2.6, 1.1 Hz, 1H, (CO)O-CH=C), 7.80 (dd, *J* = 9.8, 2.6 Hz, 1H, -CHCH(CO)-), 6.34 (dd, *J* = 9.8, 1.1 Hz, 1H, -CHCH(C=O)-), 4.34 (q, *J* = 7.1 Hz, 2H, -CH₂CH₃), and 1.36 (t, *J* = 7.1 Hz, 3H, -CH₂CH₃).

¹³C NMR (125 MHz, CDCl₃) δ 163.1, 160.0, 158.0, 141.9, 115.3, 112.2, 61.8, and 14.4.

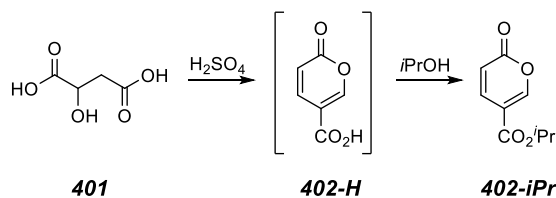
IR (neat, selected peaks): 3085, 3074, 2940, 1764 (med), 1745 (strong), 1698 (strong), 1634 (med), and 1556 (med) cm⁻¹.

HRMS Calculated for (C₈H₉O₄)⁺ 169.0495; found: 169.0491.

bp (bulb-to-bulb external temp): 120 °C @ 0.1 mmHg.

mp: 33 –36 °C (lit. = 35 °C).³

Isopropyl Coumalate (**402-iPr**)



Isopropyl coumalate was synthesized using a procedure analogous to that was used to prepare methyl coumalate.² D,L-Malic acid (**401**, 200.0 g, 745.7 mmol) was added portionwise (ca. 20 g/addition) over the course of 90 minutes to a stirred solution of sulfuric acid (500 mL) in a 3-liter round-bottomed flask at 70 °C. The mixture was

allowed to stir for 12 h, at which time the color had progressed to dark red. The mixture was placed into an ice bath. Once the internal temperature of the mixture reached 35–40 °C, isopropanol (950 mL) was added dropwise at a rate to keep the reaction mixture between 35–50 °C (ca. 1.5 h). *Note: when the mixture was cooled further than 30–35 °C a precipitate, presumably coumalic acid, began to appear. The addition of i-PrOH generates a significant amount of heat.* The solution was heated to 65 °C and stirred for 24 h. The solution was cooled and poured over ice (ca. 1.2 L), extracted with CHCl₃, washed (NaHCO₃ and brine), dried (MgSO₄), and concentrated to give a yellow solid. The crude coumalate was distilled via bulb-to-bulb distillation (0.1 mm Hg, external bath temperature at 120 °C) with the first ca. 10% discarded. This fraction contained significant quantities of the diisopropyl fumarate and diisopropyl maleate. The distilled coumalate (74.5 g) was recrystallized (pet ether) to give isopropyl coumalate (**402-iPr**, 49.7 g, 273 mmol, 37% yield) as white, needle-like crystals. The concentrated mother liquor could be distilled to recover additional isopropyl coumalate.

¹H NMR (500 MHz, CDCl₃) δ 8.28 (dd, *J* = 2.6, 1.1 Hz, 1H, (CO)O-CH=C), 7.79 (dd, *J* = 9.8, 2.6 Hz, 1H, -CHCH(C=O)-), 6.34 (dd, *J* = 9.8, 1.1 Hz, 1H, -CHCH(C=O)-), 5.21 (septet, *J* = 6.3 Hz, 1H, -CH(CH₃)₂), and 1.34 (d, *J* = 6.3 Hz, 6H, -CH(CH₃)₂).

¹³C NMR (125 MHz, CDCl₃) δ 162.6, 160.1, 158.0, 142.0, 115.3, 112.7, 69.6, and 22.0.

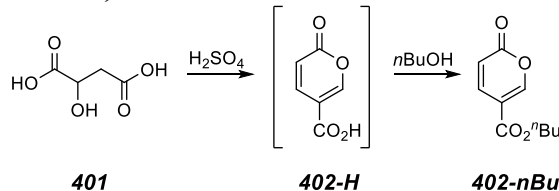
IR (neat, selected peaks): 3091, 2985, 1748 (strong), 1702 (strong), 1637 (med), 1556 (med), and 1429 (med) cm⁻¹.

bp (bulb-to-bulb external temp): 120 °C @ 0.1 mmHg.

mp: 44–47 °C (lit. = 44 °C).⁴

HRMS Calculated for (C₉H₁₁O₄)⁺ 183.0652; found: 183.0647.

n-Butyl Coumalate (**402-nBu**)



n-Butyl coumalate was synthesized using an analogous procedure to methyl coumalate.² D,L-Malic acid (**401**, 200.0 g, 745.7 mmol) was added portionwise (ca. 20 g/addition) over the course of one to two hours to a stirred solution of sulfuric acid (500 mL) in a 3-liter round bottom flask at 70 °C. The mixture was allowed to stir for 12 h, at which time the color had progressed to dark red. The mixture was placed into an ice bath. Once the internal temperature of the mixture reached 35–40 °C, *n*-butanol (700 mL) was added dropwise at a rate to keep the reaction mixture between 35–50 °C (ca. 1.5 h). *Note: when the mixture was cooled further than 30–35 °C a precipitate, presumably coumalic acid, appeared. The addition of n-butanol generates a significant amount of heat.* The solution was heated to 65 °C and stirred for 8 h. The solution was cooled and poured over ice (ca. 1.5 L), extracted with CHCl_3 , washed (NaHCO_3 and brine), dried (MgSO_4), and concentrated to give a yellow solid. The crude coumalate was distilled via bulb-to-bulb distillation (0.05 mm Hg, external bath temperature at 130 °C) with the first ca. 10% discarded. This fraction contained significant quantities of the dibutyl fumarate and dibutyl maleate. The distilled coumalate was recrystallized (pet ether) to give *n*-butyl coumalate (**402-nBu**, 86.7 g, 442 mmol, 59% yield) as white crystals. The concentrated mother liquor could be distilled to recover additional *n*-butyl coumalate.

¹H NMR (500 MHz, CDCl_3) δ 8.30 (dd, $J = 2.6, 1.1$ Hz, 1H, (CO)O-CH=C), 7.80 (dd, $J = 9.8, 2.6$ Hz, 1H, -CHCHCO), 6.34 (dd, $J = 9.8, 1.1$ Hz, 1H, -CHCH(C=O)-), 4.29 (t, $J = 6.7$ Hz, 2H, -(CO)O-CH₂CH₂), 1.71 (tt, $J = 7.6, 6.7$ Hz, 2H, -CH₂CH₂CH₂CH₃), 1.44 (qd, $J = 7.5, 7.5$ Hz, 2H, -CH₂CH₂CH₂CH₃), and 0.97 (t, $J = 7.5$ Hz, 3H, -CH₂CH₃).

¹³C NMR (125 MHz, CDCl_3) δ 163.1, 160.0, 158.1, 141.8, 115.4, 112.3, 65.6, 30.7, 19.3, and 13.8.

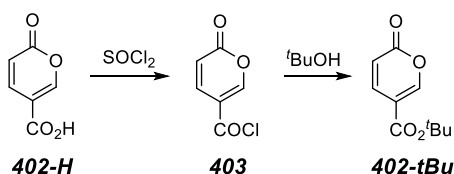
IR (neat, selected peaks): 3090, 2965, 2934, 2873, 1712 (br, strong), 1637 (med), 1553, 1429 (med) cm^{-1} .

bp 0.05 mm Hg, external bath temperature at 130 °C.

mp: 40–42 °C (lit. = 41 °C).⁴

HRMS Calculated for $(\text{C}_{10}\text{H}_{13}\text{O}_4)^+$ 197.0808; found: 197.0804.

***t*-Butyl Coumalate (402-tBu)**



Freshly prepared and distilled coumalic acid chloride (32.0 g, 203 mmol) was added to *tert*-butanol (550 mL) that was being stirred at 45 °C. After 30 minutes the reaction temperature was lowered to 30 °C and the solution was stirred overnight. After 15 h, the heterogeneous solution was filtered to give *tert*-butyl coumalate (**402-tBu**, 24.1 g, 61% yield) as an off-white powder. This sample was often used without further purification but also could be recrystallized in EtOAc.

^1H NMR (500 MHz, CDCl_3) δ 8.21 (dd, $J = 2.6, 1.1$ Hz, 1H, (CO)O-CH=C), 7.75 (dd, $J = 9.8, 2.6$ Hz, 1H, -CHCHCO), 6.32 (dd, $J = 9.8, 1.1$ Hz, 1H, -CHCH(C=O)-), 1.55 (s, 9H, -C(CH₃)₃).

^{13}C NMR (125 MHz, CDCl_3) δ 162.0, 160.2, 157.6, 142.0, 115.0, 113.4, 82.7, and 28.1.

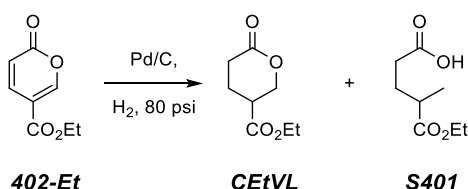
IR (neat, selected peaks) 3085, 2983, 2974, 1754 (strong), 1728 (med), 1706 (strong), 1622 (strong), 1576 (strong), and 1439 cm^{-1} .

mp: began to “sweat” at 124 °C and progressed to a black liquid until 150 °C, where it began to boil.

HRMS Calculated for $(\text{C}_{10}\text{H}_{13}\text{O}_4)^+$ 197.0808; found: 197.0803.

5.2.2 4-Carboalkoxyvalerolactones and 5-Alkoxy-4-methyl-5-oxopentanoic acids

4-Carboethoxyvalerolactone [Ethyl 6-oxotetrahydro-2H-pyran-3-carboxylate, **CEVL**] and 5-Ethoxy-4-methyl-5-oxopentanoic acid (**S401**)



Ethyl coumalate (**402-Et**, 40.0 g, 238 mmol) and Pd/C [3.0 g, 5% Pd/C] were placed into and sealed in a 500-mL Fisher-Porter vessel⁶. THF (250 mL) was added by being poured down the side of the reactor and the vessel was sealed. The headspace was pressurized with hydrogen gas (80 psi) and vented. Hydrogen was again added and frequently refilled to maintain the pressure between ca. 60–80 psi. When the reaction no longer consumed hydrogen (ca. 10 refills over ca. 16–24 h), the pressure was released, the mixture was filtered (Celite), and the filtrate was concentrated to afford ca. a 1.0:0.30 mixture of 4-carboethoxyvalerolactone (**CEVL**) and 5-ethoxy-2-methyl-5-oxopentanoic acid (**S401**). This mixture was diluted in EtOAc and washed with NaHCO₃ (3x). The aqueous bicarbonate layers were combined, saturated with NaCl, and extracted with EtOAc (1x). The combined organic layers were washed with brine, dried (MgSO₄), and concentrated to afford 4-carboethoxyvalerolactone (**CEVL**, 25.1 g, 146 mmol, 61% yield) as a colorless oil.

Typically, the lactone was stirred for ca. 1 h over CaH₂ at 50 °C under vacuum (0.05 mmHg–0.1 mmHg) and distilled *in vacuo*. This distillation over CaH₂ was repeated two to three times prior to polymerization. In each distillation, the first 5–10% of the distillate was discarded. In the last distillation, **CEVL** was distilled directly into a flame-dried scintillation vial and backfilled with N₂ prior to being capped with a Teflon-lined capped and placed into a glovebox.

A portion of the aqueous NaHCO₃ layer above was acidified with 3 M HCl and extracted with EtOAc (3x). The combined organic layers were washed with brine, dried (MgSO₄), and concentrated to give a colorless oil containing, predominantly, the 5-ethoxy-4-methyl-5-oxopentanoic acid (**S401**). A portion was further purified via MPLC (silica gel 7:3 Hex: EtOAc).

Data for CEVL

¹H NMR (500 MHz, CDCl₃) δ 4.50 (ddd, *J* = 11.4, 5.3, 0.9 Hz, 1H, (CO)O-CH_{eq}H_{ax}CH), 4.48 (dd, *J* = 11.6, 7.5 Hz, 1H, (CO)O-CH_{eq}H_{ax}CH), 4.20⁺ (dq, *J* = 11.1, 7.0 Hz, 1H, -CO₂CH_aH_bCH₃), 4.20⁻ (dq, *J* = 11.1, 7.0 Hz, 1H, -CO₂CH_aH_bCH₃), 2.92 (dddd, *J* = 7.7, 7.7, 6.6, 5.3 Hz, 1H, CH-CO₂Et), 2.69 (ddd, *J* = 17.5, 6.9, 6.9 Hz, 1H, -CH_aH_b(CO)OCH₂), 2.56 (ddd, *J* = 17.5, 7.5, 7.5 Hz, 1H, -CH_aH_b(CO)OCH₂), 2.22 (dddd, 1H, *J* = 13.9, 7.5, 7.5, 7.5 Hz, -O₂CCH₂H_{eq}CH_{ax}CH-), 2.19 (dddd, *J* = 14.0, 7.6, 7.6, 6.7, 0.9 Hz, 1H, -O₂CCH₂H_{ea}CH_{ax}CH), and 1.29 (t, *J* = 7.0 Hz, 3H, CO₂CH₂CH₃).

¹³C NMR (125 MHz, CDCl₃) δ 171.5, 170.5, 68.9, 61.6, 38.3, 28.3, 21.8, and 14.3.

IR (neat, selected peaks): 2982, 2908, 1723 (strong), 1459, 1371, and 1241 cm⁻¹.

bp: 111–114 °C @ 0.1 mmHg and 96–105 °C @ 0.05 mmHg.

HRMS: Calculated for (C₈H₁₂O₄Na)⁺ 195.0628; found: 195.0626

Data for 5-Ethoxy-4-methyl-5-oxopentanoic acid (**S401**)⁵

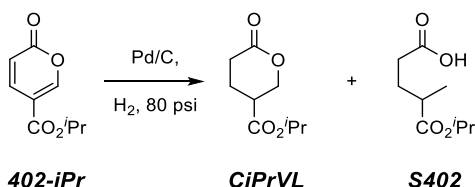
¹H NMR (500 MHz, CDCl₃) δ 11.32 (br s, 1H, -CO₂H), 4.14 (q, *J* = 7.1 Hz, 2H, CO₂CH₂CH₃), 2.50 (dq, *J* = 8.4, 7.0, 5.8 Hz, 1H, CHCO₂Et), 2.42 (ddd, *J* = 16.6, 8.6, 6.5 Hz, 1H, HO₂CCH_aH_b), 2.39 (ddd, *J* = 16.6, 8.3, 7.0 Hz, 1H, HO₂CCH_aH_b), 1.98 (dddd, *J* = 13.8, 8.3, 8.3, 6.6 Hz, 1H, CH_cH_dCHCO₂Et), 1.79 (dddd, *J* = 13.9, 8.7, 7.0, 5.9 Hz, CH_cH_dCHCO₂Et), and 1.26 (t, *J* = 7.1 Hz, 3H, CH₂CH₃), and 1.19 (d, *J* = 7.0 Hz, 3H, CH₃CHCO₂Et).

¹³C NMR (125 MHz, CDCl₃) δ 179.0, 176.0, 60.6, 38.8, 31.7, 28.4, 17.2, and 14.4.

IR (neat, selected peaks): 3450–2989 (br), 2974, 2938, 1729 (strong), and 1709 (strong) cm^{-1} .

HRMS Calculated for $(\text{C}_8\text{H}_{15}\text{O}_4)^+$ 175.0965; found: 175.0961.

4-Carboisopropoxyvalerolactone (*iso*-propyl 6-oxotetrahydro-2H-pyran-3-carboxylate, CiPrVL) and 5-*iso*-Propoxy-4-methyl-5-oxopentanoic acid (S402)



Isopropyl coumalate (**402-iPr**, 45.0 g, 247 mmol) and Pd/C [3.0 g, 5% Pd/C] were placed into a 500-mL Fisher-Porter pressure vessel⁶. THF (250 mL) was added by being poured down the side of the reactor and the vessel was sealed. The headspace was pressurized with hydrogen gas (80 psi) and vented. Hydrogen was again added and the mixture was stirred at ambient temperature. As the pressure fell, the headspace was refilled to ca. 60–80 psi. When the reaction no longer consumed hydrogen (ca. 10 refills over ca. 16–24 h), the final pressure was released, the mixture was filtered (Celite), and the filtrate was concentrated to afford ca. a 1.0:0.63 mixture of 4-carboisopropoxyvalerolactone (CiPrVL) and 5-isopropoxy-2-methyl-5-oxopentanoic acid (**S402**). The mixture was diluted in EtOAc and washed with NaHCO₃ (3x). The aqueous bicarbonate layers were combined, saturated with solid NaCl, and extracted with EtOAc (1x). The combined organic layers were washed with brine, dried (MgSO₄), and concentrated to afford 4-carboisopropoxyvalerolactone (**CiPrVL**, 26.5 g, 142 mmol, 58% yield) as a colorless oil.

CiPrVL was stirred for ca. 1 h over CaH₂ at 50 °C under vacuum (0.05 mmHg–0.1 mmHg) and distilled from CaH₂ *in vacuo* (two or three times) prior to polymerization. In each distillation, the first 5–10% of the distillate was discarded.

A portion of the aqueous NaHCO₃ layer above was acidified with 3 M HCl and extracted with EtOAc (3x). The combine organic layers were washed with brine, dried (MgSO₄), and concentrated to give a colorless oil containing, predominantly, 5-isopropoxy-4-

methyl-5-oxopentanoic acid (**S402**). A portion was further purified via MPLC (silica gel 7:3 Hex: EtOAc).

Data for CiPrVL

¹H NMR (500 MHz, CDCl₃) δ 5.06 (septet, *J* = 6.3 Hz, 1H, -CO₂CH(CH₃)₂), 4.49 (ddd, *J* = 11.5, 5.3, 1.0 Hz, 1H, (CO)O-CH_{eq}H_{ax}CH), 4.47 (dd, *J* = 11.5, 7.6 Hz, 1H, (CO)O-CH_{eq}H_{ax}CH), 2.88 (dddd, *J* = 7.7, 7.7, 6.6, 5.3 Hz, 1H, CH-CO₂ⁱPr), 2.68 (ddd, *J* = 17.5, 6.9, 6.9 Hz, 1H, -CH_aH_b(CO)OCH₂), 2.56 (ddd, *J* = 17.5, 7.5, 7.5 Hz, 1H, -CH_aH_b(CO)OCH₂), 2.21 (dddd, 1H, *J* = 13.9, 7.5, 7.5, 7.5 Hz, -O₂CCH₂H_{eq}CH_{ax}CH-), 2.19 (dddd, *J* = 14.0, 7.6, 7.6, 6.7, 1.0 Hz, 1H, -O₂CCH₂H_{ea}CH_{ax}CH), and 1.26 (d, *J* = 6.3 Hz, 6H, CO₂CH(CH₃)₂).

¹³C NMR (125 MHz, CDCl₃) δ 170.9, 170.6, 69.2, 69.0, 38.4, 28.3, 21.9, 21.84, and 21.78.

IR (neat, selected peaks): 2983, 2938, 1729 (strong) (with a shoulder), 1458, 1374, and 1171 cm⁻¹.

HRMS: Calculated for (C₉H₁₄O₄Na)⁺ 209.0784; found: 209.0781.

bp: 117–120 °C @ 0.05 mmHg.

Data for 5-isoPropoxy-4-methyl-5-oxopentanoic acid (**S402**)

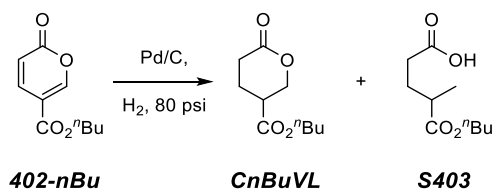
¹H NMR (500 MHz, CDCl₃) δ 10.99 (br s, 1H, -CO₂H), 5.01 [septet, *J* = 6.3 Hz, 1H, CO₂CH(CH₃)₂], 2.46 (dq, *J* = 8.4, 7.0, 5.8 Hz, 1H, CHCO₂ⁱPr), 2.42 (ddd, *J* = 16.4, 8.6, 6.5 Hz, 1H, HO₂CCH_aH_b), 2.38 (ddd, *J* = 16.5, 8.4, 7.0 Hz, 1H, HO₂CCH_aH_b), 1.96 (dddd, *J* = 13.9, 8.4, 8.4, 6.6 Hz, 1H, CH_cH_dCHCO₂ⁱPr), 1.77 (dddd, *J* = 13.9, 8.7, 7.0, 5.9 Hz, CH_cH_dCHCO₂ⁱPr), 1.24 [d, *J* = 6.3 Hz, 3H, CH(CH₃)₂], 1.23 [d, *J* = 6.3 Hz, 3H, CH(CH₃)₂], and 1.17 (d, *J* = 7.0 Hz, 3H, CH₃CHCO₂ⁱPr).

¹³C NMR (125 MHz, CDCl₃) δ 179.3, 175.6, 67.9, 39.0, 31.7, 28.3, 22.0, 21.9, and 17.2.

IR (neat, selected peaks): 3124 (br), 2979, 2934, 1723 (strong), 1707 (strong), 1445, 1415, 1167, 1105 cm⁻¹.

HRMS Calculated for (C₉H₁₇O₄)⁺ 189.1121; found: 189.1117.

Butyl 6-oxotetrahydro-2H-pyran-3-carboxylate (CnBuVL) and 2-Methyl-5-pentanedioic acid, 1-butyl ester (S403)



n-Butyl coumalate (**402-nBu**, 34.06 g, 173.7 mmol) and Pd/C [2.0 g, 5% Pd/C (wt. Pd/C/wt. coumalate)] were placed into a 500-mL Fisher-Porter pressure vessel⁶. THF (200 mL) was added by being poured carefully down the side of the reactor and the vessel was then sealed. The headspace was pressurized with hydrogen gas (80 psi) and vented. Hydrogen was again added and the mixture was stirred at ambient temperature. As the pressure fell, the headspace was refilled to ca. 60–80 psi. When the reaction no longer consumed hydrogen (ca. 8 refills over ca. 16–24 h), the final overpressure was released, the mixture was filtered (Celite), and the filtrate was concentrated to afford ca. a 1.0:0.67 mixture of 4-carbo-*n*-butoxyvalerolactone (**CnBuVL**) and 5-*n*-butoxy-2-methyl-5-oxopentanoic acid (**S403**). The mixture was diluted in EtOAc and washed with NaHCO₃ (3x). The combined organic layers were washed with brine, dried (MgSO₄), and concentrated. The mixture was distilled *in vacuo* over calcium hydride to afford 4-carbo-*n*-butoxyvalerolactone (**CnBuVL**, 19.86 g, 57% yield) as a colorless oil. **CnBuVL** was distilled *in vacuo* two more times from CaH₂ prior to polymerization. In each distillation, the first 5–10% of the distillate was discarded.

A portion of the aqueous NaHCO₃ layer from above was acidified with 3 M HCl and extracted with EtOAc (3x). The combine organic layers were washed with brine, dried (MgSO₄), and concentrated to give a colorless oil containing, predominantly, the 5-*n*-butoxy-4-methyl-5-oxopentanoic acid (**S403**). A portion was further purified via MPLC (silica gel 7:3 Hex: EtOAc).

Data for CnBuVL

¹H NMR (500 MHz, CDCl₃) δ 4.50 (ddd, *J* = 11.5, 5.3, 0.9 Hz, 1H, (CO)O-CH_{eq}H_{ax}CH), 4.48 (dd, *J* = 11.5, 7.6 Hz, 1H, (CO)O-CH_{eq}H_{ax}CH), 4.15 (t, *J* = 6.7 Hz, 2H, -

CO₂CH₂CH₂-), 2.92 (dddd, $J=7.7, 7.7, 6.6, 5.3$ Hz, 1H, CH-CO₂ⁿBu), 2.69 (ddd, $J=17.6, 6.9, 6.9$ Hz, 1H, -CH_aH_b(CO)OCH₂), 2.56 (ddd, $J=17.6, 7.5, 7.5$ Hz, 1H, -CH_aH_b(CO)OCH₂), 2.22 (dddd, 1H, $J=13.9, 7.6, 7.6, 7.6$ Hz, -O₂CCH₂H_{eq}CH_{ax}CH-), 2.19 (dddd, $J=14.0, 7.5, 7.5, 6.7, 0.9$ Hz, 1H, -O₂CCH₂H_{ea}CH_{ax}CH), 1.66–1.61 (m, 2H, -CH₂CH₂CH₂CH₃), 1.39 (br sext, $J=7.5$ Hz, 2H, -CH₂CH₂CH₂CH₃), and 0.94 (t, $J=7.4$ Hz, 3H, CO₂(CH₂)₂CH₃).

¹³C NMR (125 MHz, CDCl₃) δ 171.5, 170.5, 68.9, 65.5, 38.4, 30.7, 28.3, 21.8, 19.2, and 13.8.

IR (neat, selected peaks): 2960, 2935, 2878, 1726 (strong), 1459, 1172, and 1054 cm⁻¹.

HRMS: Calculated for (C₁₀H₁₆O₄Na)⁺ 223.0941; found: 223.0932.

bp: 140–143 °C @ 0.1 mmHg.

Data for 5-*n*-Butoxy-4-methyl-5-oxopentanoic acid (S403)

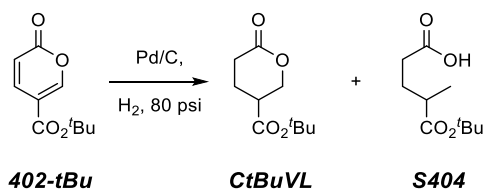
¹H NMR (500 MHz, CDCl₃) δ 10.6 (br s, 1H, -CO₂H), 4.08 (t, $J=6.7$ Hz, 2H, CO₂CH₂), 2.51 (dq, $J=8.4, 7.0, 5.7$ Hz, 1H, CHCO₂ⁿBu), 2.42 (ddd, $J=16.6, 8.7, 6.5$ Hz, 1H, HO₂CCH_aH_b), 2.39 (ddd, $J=16.5, 8.3, 6.9$ Hz, 1H, HO₂CCH_aH_b), 1.98 (dddd, $J=13.9, 8.3, 8.3, 6.6$ Hz, 1H, CH_cH_dCHCO₂ⁿBu), 1.83–1.75 (nfom, 2H, CH_cH_dCHCO₂ⁿBu), 1.64–1.58 (m, 2H, -CH₂CH₂CH₂CH₃), 1.38 (qt, $J=7.5, 7.5$ Hz, 2H, -CH₂CH₂CH₂CH₃), and 1.19 (d, $J=7.0$ Hz, 3H, CH₃CHCO₂ⁿBu), and 0.94 (t, $J=7.4$ Hz, 3H, CH₂CH₃).

¹³C NMR (125 MHz, CDCl₃) δ 178.6, 176.1, 64.5, 38.9, 31.6, 30.8, 28.4, 19.3, 17.3, and 13.9.

IR (neat, selected peaks): 3450–2989 (br), 2963, 2939, 1732 (strong), and 1715 (strong) cm⁻¹.

HRMS Calculated for (C₁₀H₁₉O₄)⁺ 203.1278; found: 203.1274.

4-Carbo-*t*-butoxyvalerolactone (*tert*-Butyl 6-oxotetrahydro-2H-pyran-3-carboxylate, (C'*t*BuVL) and 5-*t*-Butoxy-4-methyl-5-oxopentanoic acid (S404)



t-Butyl coumalate (**402-tBu** 1.02 g, 5.20 mmol), Pd/C (100 mg), and a stir bar were added to 6-dram vial. EtOAc (10 mL) was added by being poured carefully down the side of the vial. The vial was placed directly into a 150-mL Fisher-Porter pressure vessel⁶ and the apparatus was sealed. The headspace was pressurized with hydrogen gas (80 psi) and vented. Hydrogen was again added and the mixture was stirred at ambient temperature. When the reaction no longer consumed hydrogen, the final overpressure was released, the mixture was filtered (Celite), and the filtrate was concentrated to afford ca. a 1.0:0.52 mixture of 4-carbo-*t*-butoxyvalerolactone (**CtBuVL**) and 5-*t*-butoxy-2-methyl-5-oxopentanoic acid (**S404**). The mixture was diluted in EtOAc and washed with NaHCO₃ (3x). The combined organic layers were washed with brine, dried (MgSO₄), and concentrated to afford 4-carbo-*t*-butoxyvalerolactone (**CtBuVL**, 692 mg, 67% yield) as a colorless oil. **CtBuVL** was further dried and purified via MPLC (silica, 3:1 EtOAc:Hex) prior to polymerization. Additionally, the entire aqueous layers from extraction were combined, acidified (1M HCl), dried (MgSO₄), concentrated, and purified via MPLC (silica, 7:3 Hex:EtOAc) to afford 5-*t*-butoxy-4-methyl-5-oxopentanoic acid (**S404**, 265 mg, 26% yield) as a colorless oil.

Data for CtBuVL

¹H NMR (500 MHz, CDCl₃) δ 4.46 (ddd, *J* = 11.5, 5.2, 0.9 Hz, 1H, (CO)O-CH_{eq}H_{ax}CH), 4.43 (dd, *J* = 11.5, 7.8, Hz, 1H, (CO)O-CH_{eq}H_{ax}CH), 2.82 (dddd, *J* = 7.8, 7.8, 6.6, 5.2 Hz, 1H, CH-CO₂^{*t*}Bu), 2.67 (ddd, *J* = 17.5, 6.9, 6.9 Hz, 1H, -CH_aH_b(CO)OCH₂), 2.54 (ddd, *J* = 17.5, 7.5, 7.5 Hz, 1H, -CH_aH_b(CO)OCH₂), 2.22 (dddd, 1H, *J* = 13.9, 7.6, 7.6, 7.6 Hz, -O₂CCH₂H_aCH_bCH-), 2.19 (dddd, *J* = 14.0, 7.5, 7.5, 6.6, 1.0 Hz, 1H, -O₂CCH₂H_aCH_bCH), and 1.47 (s, 9H, CO₂^{*t*}Bu).

^{13}C NMR (125 MHz, CDCl_3) δ 170.8, 170.6, 82.2, 69.2, 39.1, 28.3, 28.1, and 21.8.

IR (neat, selected peaks): 2977, 2934, 1721 (strong), 1477, 1393, 1148, 1055 cm^{-1} .

HRMS: Calculated for $(\text{C}_{10}\text{H}_{16}\text{O}_4\text{Na})^+$ 223.0941; found: 223.0954.

Data for 5-tButoxy-4-methyl-5-oxopentanoic acid (S404)

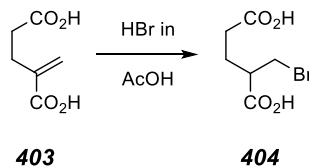
^1H NMR (500 MHz, CDCl_3) δ 10.4 (br s, 1H, $-\text{CO}_2\text{H}$), 2.45–2.33 (m, 3H, CHCO_2tBu and $\text{CH}_2\text{CO}_2\text{H}$), 1.93 (dddd, $J = 13.9, 8.4, 8.4, 6.4$ Hz, 1H, $\text{CH}_c\text{H}_d\text{CHCO}_2\text{tBu}$), 1.74 (dddd, $J = 14.0, 8.7, 7.0, 5.9$ Hz, 1H, $\text{CH}_c\text{H}_d\text{CHCO}_2\text{tBu}$), and 1.45 (s, 9H, tBu).

^{13}C NMR (125 MHz, CDCl_3) δ 179.3, 175.4, 80.5, 39.7, 31.8, 28.5, 28.2, and 17.3.

IR (neat, selected peaks): 3450–2989 (br), 2976, 2937, 1723 (strong), and 1709 (strong) cm^{-1} .

HRMS: Calculated for $(\text{C}_{10}\text{H}_{18}\text{O}_4\text{Na})^+$ 225.1097; found: 225.1088.

2-(Bromomethyl)glutaric acid (404)



2-Methyleneglutaric acid (**403**) was prepared as previously reported.^{2,7} This acid (10.00 g, 69.4 mmol), HBr in AcOH (48% w/v, 51 mL, 210 mmol), and a stir bar were added to an 8 oz. glass jar and sealed with a Teflon-lined cap. The contents were stirred for 20 h at ambient temperature. The reaction mixture was slowly poured into 600 mL of stirred DI H_2O , and the aqueous suspension was extracted with EtOAc (3x ca. 400 mL). The organic layers were combined, washed with H_2O (ca. 200 mL) and brine (ca. 400 mL), dried over MgSO_4 , and concentrated. Toluene (ca. 150 mL) was added to the light orange liquid to assist in the removal of acetic acid and placed under high vacuum to afford 2-(bromomethyl)glutaric acid (**404**, 13.64 g, 87% yield) as a white amorphous solid. This was stored in a freezer (ca. -30 $^\circ\text{C}$) and used without further purification.

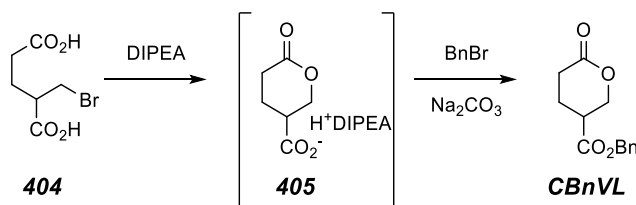
¹H NMR (500 MHz, DMSO-*d*₆) δ 12.75–11.93 (br s, 2H, CO₂H), 3.67 (dd, *J* = 10.0, 4.6 Hz, BrCH_aH_b), 3.60 (dd, *J* = 10.0, 7.3 Hz, BrCH_aH_b), 2.77 (dddd, *J* = 8.0, 7.3, 6.1, 4.6 Hz, 1H, BrCH₂CH), 2.29 (ddd, *J* = 16.6, 8.6, 6.7 Hz, 1H, CH_cH_dCO₂H), 2.26 (ddd, *J* = 16.6, 8.2, 7.1 Hz, 1H, CH_cH_dCO₂H), 1.81 (dddd, *J* = 13.8, 8.1, 8.1, 6.8 Hz, 1H CH_aH_bCH₂CO₂H), and 1.75 (dddd, *J* = 13.6, 8.6, 7.2, 6.0 Hz, 1H CH_aH_bCH₂CO₂H).

¹³C NMR (125 MHz, DMSO-*d*₆) δ 173.8, 173.6, 46.1, 34.3, 30.9, and 25.6.

IR (neat, selected peaks): 3340–2550 (br), 2923, 2854, 1688 (s), 1445, 1430, 1404, 1282, 1251, and 932 cm⁻¹.

mp: 103–109 °C

4-Carbobenzoxyvalerolactone (benzyl 6-oxotetrahydro-2H-pyran-3-carboxylate, CBnVL)



2-(Bromomethyl)glutaric acid (**404**, 1.0 equiv, 10.00 g, 44.46 mmol) and a stir bar were placed into a 500 mL round bottom flask. DCM (170 mL) was added followed by Hünig's base (3 equiv, 23.2 mL, 133.38 mmol) and the reaction mixture was stirred. After 16 h, the reaction mixture was concentrated *in vacuo* to afford a white slurry. The slurry was resuspended in DMF (200 mL) and benzyl bromide (1.5 equiv, 7.9 mL, 67 mmol) followed by Na₂CO₃ (3.0 equiv, 14.1 g, 130 mmol) were added. The heterogeneous mixture was stirred overnight at room temperature. The mixture was concentrated *in vacuo*, and the white residue was partitioned into EtOAc (ca. 600 mL) and water (ca. 100 mL). The organic layer was washed with NH₄Cl, NaHCO₃, and brine; dried with MgSO₄, and concentrated to leave a yellow oil. The oil was further purified via column chromatography (silica gel, gradient elution solvent EtOAc:Hex 9:1, 3:1, 1:1)

to afford 4-carbobenzoxyvalerolactone (**CBnVL**, 7.28 g, 70% yield) as a colorless, highly viscous oil.

¹H NMR (500 MHz, CDCl₃) δ 7.41–7.32 (m, 5H, *Ar*), 5.19 (d, *J* = 12.2 Hz, 1H, *ArCH_aH_b*), 5.16 (d, *J* = 12.2 Hz, 1H, *ArCH_aH_b*), 4.51 (ddd, *J* = 11.5, 5.6, 0.8 Hz, 1H, (CO)O-*CH_{eq}H_{ax}CH*), 4.48 (dd, *J* = 11.6, 7.2 Hz, 1H, (CO)O-*CH_{eq}H_{ax}CH*), 2.97 (dddd, *J* = 7.7, 7.7, 6.7, 5.6 Hz, 1H, *CH-CO₂Bn*), 2.67 (ddd, *J* = 17.5, 6.9, 6.9 Hz, 1H, -*CH_aH_b(CO)OCH₂*), 2.55 (ddd, *J* = 17.5, 7.5, 7.5 Hz, 1H, -*CH_aH_b(CO)OCH₂*), 2.23 (dddd, 1H, *J* = 13.9, 7.6, 7.6, 7.6 Hz, -O₂CCH₂*H_{eq}CH_{ax}CH-*), and 2.19 (dddd, *J* = 14.0, 7.5, 7.5, 6.7, 0.9 Hz, 1H, -O₂CCH₂*H_{ea}CH_{ax}CH*).

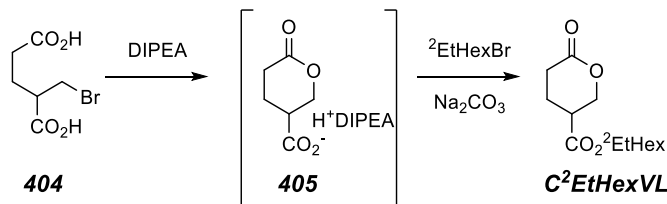
¹³C NMR (125 MHz, CDCl₃) δ 171.2, 170.4, 135.3, 128.85, 128.75, 128.4, 68.8, 67.3, 38.3, 28.2, and 21.8.

IR (neat, selected peaks): 3065, 3032, 2958, 2913, 1727 (s), 1498, 1241, 1155, and 1054 cm⁻¹.

HRMS: Calculated for (C₁₃H₁₄O₄Na)⁺ 257.0784; found: 257.0783.

bp: 194–199 °C @ 0.05 mmHg. Under these conditions, a small amount (ca. 5 mol%) of an elimination product is formed. Therefore, samples of this monomer used for the ROTEP were purified by MPLC.

4-Carbo(2-ethyl)hexoxyvalerolactone (2-ethylhexyl 6-oxotetrahydro-2H-pyran-3-carboxylate, **C²EtHexVL**)



2-(Bromomethyl)glutaric acid (**404**, 1.0 equiv, 1.50 g, 6.67 mmol) and a stir bar were placed into a 100-mL culture tube. DCM (20 mL) was added followed by Hünig's base (3 equiv, 3.5 mL, 20 mmol). The reaction mixture was stirred at ambient temperature for 20 h and concentrated *in vacuo* to afford a white slurry. The slurry was resuspended in DMF

(20 mL) and 1-bromo-2-ethylhexane (1.5 equiv, 1.8 mL, 10 mmol) followed by Na₂CO₃ (1.5 equiv, 1.06 g, 10 mmol) were added. The heterogeneous mixture was stirred at ambient temperature for 24 h, 35 °C for 20 h, and 55 °C for 40 h to achieve full conversion. The mixture was concentrated *in vacuo*, and the white residue was partitioned into EtOAc (ca. 80 mL) and water (ca. 30 mL). The organic layer was washed with NH₄Cl, NaHCO₃, and brine; dried with MgSO₄; and concentrated *in vacuo* to leave a yellow oil. The oil was further purified via column chromatography (silica gel, 1:3 EtOAc:Hex) to afford 4-carbo(2-ethyl)hexoxyvalerolactone (**C²EtHexVL**, 746 mg, 44% yield) as a colorless, highly viscous oil.

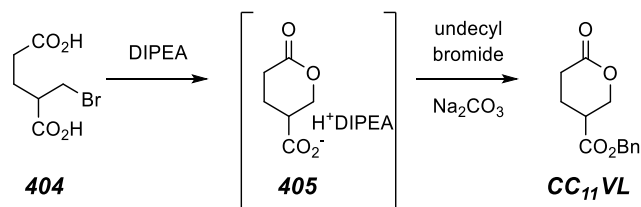
¹H NMR (500 MHz, CDCl₃) δ 4.51 (ddd, *J* = 11.5, 5.2, 1.0 Hz, 1H, (CO)O-CH_{eq}H_{ax}CH), 4.48 (dd, *J* = 11.5, 7.8 Hz, 1H, (CO)O-CH_{eq}H_{ax}CH), 4.08 (dd, *J* = 10.9, 5.7 Hz, 1H, CHCO₂CH_aH_b), 4.05 (dd, *J* = 11.0, 5.9 Hz, 1H, CHCO₂CH_aH_b), 2.93 (dddd, *J* = 7.8, 7.8, 6.8, 5.2 Hz, 1H, CH-CO₂Alk), 2.69 (ddd, *J* = 17.6, 6.9, 6.9 Hz, 1H, -CH_cH_d(CO)OCH₂), 2.57 (ddd, *J* = 17.6, 7.5, 7.5 Hz, 1H, -CH_cH_d(CO)OCH₂), 2.23 (dddd, 1H, *J* = 13.9, 7.6, 7.6, 7.6 Hz, -O₂CCH₂CH_{eq}H_{ax}CH-), 2.19 (dddd, *J* = 13.9, 7.6, 7.6, 6.7, 0.9 Hz, 1H, -O₂CCH₂CH_{eq}H_{ax}CH), 1.63–1.56 (m, 1H, CHCO₂CH₂CH), 1.39–1.24 (m, 8H), and 0.90 [t, *J* = 7.3 Hz, 6H, (CH₂CH₃)_a and (CH₂CH₃)_b].

¹³C NMR (125 MHz, CDCl₃) δ 171.5, 170.5, 68.9, 68.0, 38.8, 38.4, 30.5, 29.0, 28.2, 23.9, 23.1, 21.8, 14.2, and 11.1.

IR (neat, selected peaks): 2959, 2930, 2873, 2861, 1733, 1461, 1242, and 1196 cm⁻¹.

HRMS: Calculated for (C₁₄H₂₄O₄Na)⁺ 279.1567; found: 279.1565.

4-Carboundecoxyvalerolactone (undecyl 6-oxotetrahydro-2H-pyran-3-carboxylate, CC₁₁VL)



2-(Bromomethyl)glutaric acid (**404**, 1.0 equiv, 1.50 g, 6.67 mmol) and a stir bar were placed into a 100-mL culture tube. DCM (20 mL) was added followed by Hünig's base (3 equiv, 3.5 mL, 20 mmol). The reaction mixture was stirred at ambient temperature for 20 h and concentrated *in vacuo* to afford a white slurry. The slurry was resuspended in DMF (20 mL) and 1-bromoundecane (1.5 equiv, 2.4 mL, 10 mmol) followed by Na₂CO₃ (1.5 equiv, 1.06 g, 10 mmol) were added. The heterogeneous mixture was stirred at ambient temperature for 24 h followed by 35 °C for 20 h to achieve full conversion. The mixture was concentrated *in vacuo*, and the white residue was partitioned into EtOAc (ca. 80 mL) and water (ca. 30 mL). The organic layer was washed with NH₄Cl, NaHCO₃, and brine; dried with MgSO₄; and concentrated *in vacuo* to leave a yellow oil. The oil was further purified via column chromatography (silica gel, 1:3 EtOAc:Hex) to afford 4-carboundecoxyvalerolactone (**CC₁₁VL**, 825 mg, 42% yield) as a colorless, highly viscous oil.

¹H NMR (500 MHz, CDCl₃) δ 4.50 (ddd, *J* = 11.5, 5.2, 1.0 Hz, 1H, (CO)O-CH_{eq}H_{ax}CH), 4.47 (dd, *J* = 11.5, 7.7 Hz, 1H, (CO)O-CH_{eq}H_{ax}CH), 4.13 (t, *J* = 6.7 Hz, 1H, CO₂CH₂C₁₀H₂₁), 2.92 (dddd, *J* = 7.8, 7.8, 6.6, 5.2 Hz, 1H, CH-CO₂Alk), 2.69 (ddd, *J* = 17.6, 6.9, 6.9 Hz, 1H, CH_aH_b(CO)OCH₂), 2.56 (ddd, *J* = 17.6, 7.5, 7.5 Hz, 1H, -CH_aH_bCO₂CH₂), 2.23 (dddd, 1H, *J* = 13.9, 7.6, 7.6, 7.6 Hz, O₂CCH₂H_{eq}CH_{ax}CH-), 2.19 (dddd, *J* = 14.0, 7.6, 7.6, 6.7, 1.0 Hz, 1H, O₂CCH₂H_{ea}CH_{ax}CH), 1.64 (br app pent, *J* = 6.8 Hz, 2H, CO₂CH₂CH₂), 1.38–1.21 (m, 16H), and 0.88 (t, *J* = 7.0 Hz, 3H, CH₃)

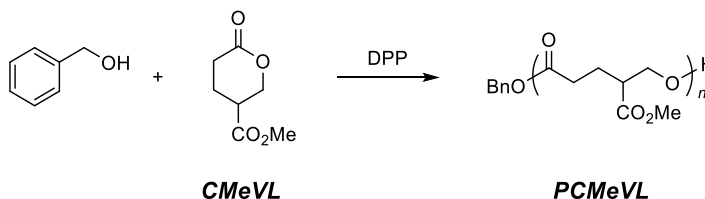
¹³C NMR (125 MHz, CDCl₃) δ 171.4, 170.5, 68.9, 65.8, 38.3, 32.0, 29.71, 29.68, 29.6, 29.4, 29.3, 28.6, 28.3, 26.0, 22.8, 21.8, and 14.3.

IR (neat, selected peaks): 2954, 2922, 2853, 1731, 1459, 1382, 1333, 1301, 1242, and 1058 cm^{-1} .

HRMS: Calculated for $(\text{C}_{17}\text{H}_{30}\text{O}_4\text{Na})^+$ 321.2036; found: 321.2028.

S4.3 Preparation and Characterization of Polymers

Poly(4-Carbomethoxyvalerolactone) (PCMeVL)



A low molecular weight sample (ca. $8 \text{ kg}\cdot\text{mol}^{-1}$) of PCMeVL was previously prepared.²

A higher molecular weight sample was prepared by the following procedure, which is essentially the same procedure used to synthesize higher MW polymers from three of the other monomers.

Benzyl alcohol (1.0 equiv, $8.9 \mu\text{L}$, 0.030 mmol), diphenyl phosphate [DPP, $(\text{PhO}_2)\text{PO}_2\text{H}$, 3.50 equiv, 75.8 mg , 0.300 mmol], and CMeVL (700 equiv, 9.503 g , 60.13 mmol , target polymer $M_n = 111 \text{ kg}\cdot\text{mol}^{-1}$), and a stir bar were sequentially added to a 50-mL culture tube in a nitrogen filled glovebox. The tube was sealed with a Teflon-lined cap and the mixture was stirred for 20 h at $70 \text{ }^\circ\text{C}$. The tube was opened and DCM (ca. 30 mL) and NEt_3 (ca. 2 mL) were added to the solidified reaction mass. The tube was capped and the suspension was heated at $70 \text{ }^\circ\text{C}$ until the polymer was fully dissolved (ca. 16 h). (^1H NMR analysis of an aliquot of the dissolved solution prior to precipitation showed 92% monomer conversion). The polymer was precipitated by dropwise addition into cooled, stirred MeOH (ca. 300 mL) into a 1-L Erlenmeyer flask. The contents were allowed to settle and after 15 min the supernatant was decanted, DCM (ca. 30 mL) and NEt_3 (ca. 0.1 mL) was added to redissolve the polymer and MeOH (ca. 300 mL) was slowly added to the stirred polymer/DCM solution to reprecipitate the polymer. The sample was once again cooled ($0 \text{ }^\circ\text{C}$) and allowed to stand (30 min), and the supernatant was decanted. The white-solid sample was placed under vacuum (ca. 0.1 mmHg) in a PTFE-lined aluminum pan at $110 \text{ }^\circ\text{C}$ for four hours to give poly(4-carbomethoxyvalerolactone) (PCMeVL, 8.36 g , 77% yield) as a white, cloudy disk. This sample was melt pressed ($120 \text{ }^\circ\text{C}$, 5 minutes)

and annealed at 35 °C (24 h) and then at RT (3 days) prior to its evaluation in mechanical testing.

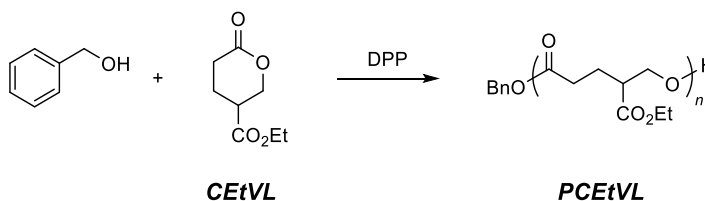
¹H NMR (500 MHz, CDCl₃): δ 7.39–7.31 (m, 5H, *Ar*), 5.12 (s, 2H, -OCH₂-*Ar*-CH₂O-), 4.23 [d, *J* = 6.3 Hz, 1222H (611 repeat units (RUs), CO₂CH₂^{RU}], 3.71 [s, 1830H (610 RUs), CO₂CH₃^{RU}], 2.75 [dddd, *J* = 8.7, 6.0, 6.0, 6.0 Hz, 602H (602 RUs) -CHCO₂Me^{RU}], 2.39 [ddd, *J* = 16.7, 8.6, 6.6 Hz, 605H (605RU), -O₂CCH_aH_bCH₂^{RU}], 2.35 [ddd, *J* = 16.7, 7.5, 7.5 Hz, 604H (604RU), -O₂CCH_aH_bCH₂^{RU}], 1.92 [dddd, *J* = 14.2, 8.2, 8.2, 6.6 Hz, 586H (586 RUs), -O₂CCH₂CH_aH_b^{RU}], and 1.87 [dddd, *J* = 14.0, 8.5, 7.2, 5.4 Hz, 616H (616 RU), -O₂CCH₂CH_aH_b^{RU}]. *M_n* (NMR) = 97 kg•mol⁻¹ (from analysis of the benzylic protons in the incorporated initiator). These data are quite consistent with those for a 71 kg•mol⁻¹ sample previously reported.²

The **¹³C NMR** and **IR** spectra and **TGA** thermogram were consistent with those previously reported.²

SEC (THF, MALS): *M_n* = 116 kg•mol⁻¹, *M_w* = 130 kg•mol⁻¹, *D* = 1.1, *dn/dc* = 0.0543

DSC (10 °C•min⁻¹): *T_g* = -10 °C, *T_m* = 49, 78 °C (Δ*H_m* = 35.4 J•mol⁻¹)

Poly[4-Carboethoxyvalerolactone] (PCEtVL)



In a nitrogen-filled glovebox, BnOH (1.0 equiv, 3.1 μL, 0.030 mmol), diphenyl phosphate [DPP, (PhO)₂PO₂H, 0.50 equiv, 3.8 mg, 0.015 mmol], 4-carboethoxyvalerolactone (**CEtVL**, 50.0 equiv, 258 mg, 1.50 mmol), and a stir bar were added sequentially to a 1-dram vial. The vial was sealed with a Teflon-lined cap and the mixture was stirred for 23 h at ambient temperature. At this time, an aliquot (ca. 3 mg) was dissolved in CDCl₃ (0.55 mL) with NEt₃ (ca. 1 μL) and analyzed via ¹H NMR spectroscopy, which indicated nearly complete monomer conversion. The vial was

removed from the glovebox and the sample was dissolved in NEt_3 (ca. 10 μL) and DCM (1–2 mL). The polymer was precipitated by dropwise addition into stirred MeOH (15 mL). The vial was cooled (0 $^\circ\text{C}$) and centrifuged, and the supernatant was decanted. DCM (ca. 1 mL) was added to redissolve the polymer and MeOH (ca. 15 mL) was slowly added to the stirred polymer/DCM solution to reprecipitate the polymer. The sample was once again cooled (0 $^\circ\text{C}$), centrifuged, decanted, and placed under vacuum (ca. 0.1 mmHg) at 60 $^\circ\text{C}$ to give poly(4-carboethoxyvalerolactone) (**PCEtVL**, 202 mg, 77% yield) as a slightly cloudy, waxy solid.

^1H NMR (500 MHz, CDCl_3) See i) the annotated spectrum and ii) the detailed line listing for **PCMeVL** above for the coupling constants typically seen for this family of polyesters. $M_n = 8.2 \text{ kg}\cdot\text{mol}^{-1}$ (from analysis of the benzylic protons in the incorporated initiator).

^{13}C NMR (125 MHz, CDCl_3) δ 172.6, 172.2, 64.5, 61.0, 44.0, 31.3, 23.7, and 14.3.

IR (neat, selected peaks): 2980, 2909, 1725 (strong), 1453, 1378, 1151 (strong), and 1020 cm^{-1} .

SEC (THF, MALS): $M_n = 14.5 \text{ kg}\cdot\text{mol}^{-1}$, $M_w = 15.5 \text{ kg}\cdot\text{mol}^{-1}$, $D = 1.06$, $dn/dc = 0.0598$.

TGA T_d 1% = 218 $^\circ\text{C}$, 5% = 249 $^\circ\text{C}$.

DSC Cooling and ramping rates of 5 $^\circ\text{C}/\text{min}$: $T_g = -29 \text{ }^\circ\text{C}$ [$T_m = 52 \text{ }^\circ\text{C}$ on initial heating cycle ($\Delta H_m = 6.4 \text{ J}\cdot\text{mol}^{-1}$)].

Cooling and ramping rates of 10 $^\circ\text{C}/\text{min}$: $T_g = -28 \text{ }^\circ\text{C}$

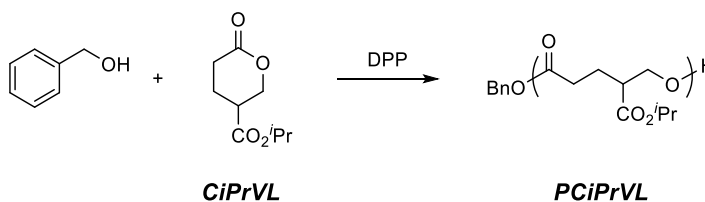
A higher molar mass sample was prepared in a similar fashion to **PCMeVL** using BnOH (1 equiv, 6.6 μL , 0.064 mmol), **CEtVL** (640 equiv, 7.00 g, 40.7 mmol), and DPP (3 equiv, 48.1 mg, 0.191 mmol). The polymer was heated to 70 $^\circ\text{C}$ for 22 h (93% monomer conversion), precipitated, and heated under vacuum as described for **PCMeVL** to give **PCEtVL** was a colorless, highly viscous liquid that solidified to a white, cloudy disk over three days at room temperature (5.45 g, 78% yield).

^1H NMR of higher MW sample $M_n = 110 \text{ kg}\cdot\text{mol}^{-1}$ (from analysis of the benzylic protons in the incorporated initiator) or $82 \text{ kg}\cdot\text{mol}^{-1}$ (integrated against the CH_2OH end group).

SEC of higher MW sample (THF, MALS): $M_n = 76.1 \text{ kg}\cdot\text{mol}^{-1}$, $M_w = 86.3 \text{ kg}\cdot\text{mol}^{-1}$, $D = 1.14$, $dn/dc = 0.0643$.

DSC ($10 \text{ }^\circ\text{C}\cdot\text{min}^{-1}$): $T_g = -26 \text{ }^\circ\text{C}$, $T_m = 50 \text{ }^\circ\text{C}$ ($\Delta H_m = 13.0 \text{ J}\cdot\text{mol}^{-1}$).

Poly(4-Carbo-*iso*-propoxyvalerolactone) (PCiPrVL)



In a nitrogen-filled glovebox, BnOH (1.0 equiv, $3.1 \mu\text{L}$, 0.030 mmol), diphenyl phosphate [DPP, $(\text{PhO})_2\text{PO}_2\text{H}$, 0.50 equiv, 3.8 mg , 0.015 mmol], 4-carboisopropoxyvalerolactone (**CiPrVL**, 50.0 equiv, 279 mg , 1.50 mmol), and a stir bar were added sequentially to a 1-dram vial. The vial was sealed with a Teflon-lined cap and the mixture was stirred for 24 h at ambient temperature. At this time, an aliquot of this waxy substance (ca. 3 mg) was dissolved in CDCl_3 (0.55 mL) with NEt_3 (ca. $1 \mu\text{L}$) and analyzed via ^1H NMR spectroscopy. The monomer conversion was observed to be 98%. The vial was removed from the glovebox and the sample was dissolved in NEt_3 (ca. $10 \mu\text{L}$) and DCM ($1\text{--}2 \text{ mL}$). The polymer was precipitated by dropwise addition of this solution into stirred MeOH (15 mL). The vial was cooled ($0 \text{ }^\circ\text{C}$) and centrifuged, and the supernatant was decanted. DCM (ca. 1 mL) was added to redissolve the polymer and MeOH (ca. 15 mL) was slowly added to the stirred polymer/DCM solution to reprecipitate the polymer. The sample was once again cooled ($0 \text{ }^\circ\text{C}$), the suspension centrifuged, the supernatant liquid decanted, and the remaining solid placed under

vacuum (ca. 0.1 mmHg) at 60 °C to give poly(4-carboisopropoxyvalerolactone) (**PCiPrVL**, 243 mg, 86% yield) as a cloudy, waxy solid.

¹H NMR (500 MHz, CDCl₃) See i) the annotated spectrum and ii) the detailed line listing for **PCMeVL** above for the coupling constants typically seen for this family of polyesters. $M_n = 8.9 \text{ kg}\cdot\text{mol}^{-1}$ (from analysis of the benzylic protons in the incorporated initiator).

¹³C NMR (125 MHz, CDCl₃) δ 172.3, 172.2, 68.5, 64.6, 44.2, 31.4, 23.8, and 21.9 (2x).

IR (neat, selected peaks): 2981, 2942, 1724 (strong), 1455, 1385, 1244, 1156 (strong), and 1052 (strong) cm⁻¹.

SEC (THF, MALS): $M_n = 14.9 \text{ kg}\cdot\text{mol}^{-1}$, $M_w = 15.4 \text{ kg}\cdot\text{mol}^{-1}$, $D = 1.0(3)$, $dn/dc = 0.0571$.

TGA T_d 1% = 228 °C, 5% = 269 °C.

DSC Cooling and ramping rates of 5 °C/min: $T_g = -24$ °C, $T_c = 36$ °C, $T_m = 62$ °C, ($\Delta H_m = 19.8 \text{ J}\cdot\text{mol}^{-1}$).

Cooling and ramping rates of 10 °C/min: $T_g = -22$ °C, $T_c = 49$ °C, $T_m = 67$ °C ($\Delta H_m = 3.6 \text{ J}\cdot\text{mol}^{-1}$)

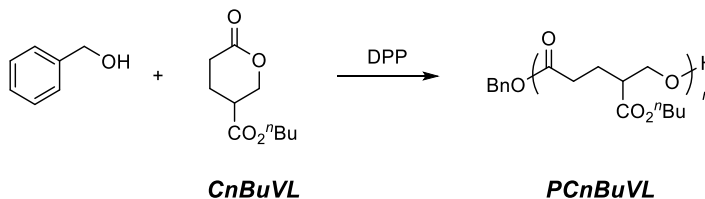
A higher molar mass sample was prepared in a similar fashion to that for **PCMeVL** using BnOH (1 equiv, 4.7 μ L, 0.046 mmol), **CiPrVL** (591 equiv, 5.00 g, 26.9 mmol), and DPP (3 equiv, 34.4 mg, 0.14 mmol). The polymer was heated to 70 °C for 7 h (90% monomer conversion), precipitated, and heated under vacuum as described for **PCMeVL** to give **PCiPrVL** as a white, cloudy disk (3.21 g, 64% yield).

¹H NMR (500 MHz, CDCl₃) $M_n = 78 \text{ kg}\cdot\text{mol}^{-1}$ (from analysis of the benzylic protons in the incorporated initiator).

SEC of higher MW (THF, MALS): $M_n = 56.6 \text{ kg}\cdot\text{mol}^{-1}$, $M_w = 64.8 \text{ kg}\cdot\text{mol}^{-1}$, $D = 1.15$, $dn/dc = 0.0639$.

DSC (10 °C \cdot min⁻¹): $T_g = -42$ °C, $T_m = 46, 56$ °C ($\Delta H_m = 19.3 \text{ J}\cdot\text{mol}^{-1}$)

Poly(4-Carbo-*n*-butylvalerolactone) (PCnBuVL)



In a nitrogen-filled glovebox, BnOH (1.0 equiv, 3.1 μL , 0.030 mmol), diphenyl phosphate [DPP, $(\text{PhO})_2\text{PO}_2\text{H}$, 0.50 equiv, 4.0 mg, 0.016 mmol], 4-carbo-*n*-butoxyvalerolactone (**CnBuVL**, 50.0 equiv, 300 mg, 1.50 mmol), and a stir bar were added sequentially to a 1-dram vial. The vial was sealed with a Teflon-lined cap and the mixture was stirred for 20 h at ambient temperature. At this time, an aliquot of this waxy sample (ca. 3 mg) was dissolved in CDCl_3 (0.55 mL) with NEt_3 (ca. 1 μL) and analyzed via ^1H NMR spectroscopy. The monomer conversion was measured to be 98%. The vial was removed from the glovebox and the sample was dissolved in NEt_3 (ca. 10 μL) and DCM (1–2 mL). The polymer was precipitated by dropwise addition into stirred MeOH (15 mL). The vial was cooled (0 $^\circ\text{C}$) and centrifuged, and the supernatant was decanted. DCM (ca. 1 mL) was added to redissolve the polymer and MeOH (ca. 15 mL) was slowly added to the stirred polymer/DCM solution to reprecipitate the polymer. The sample was again cooled (0 $^\circ\text{C}$), centrifuged, decanted, and placed under vacuum (ca. 0.1 mmHg) at 60 $^\circ\text{C}$ to give poly(4-carbo-*n*-butoxyvalerolactone) (**PCnBuVL**, 235 mg, 78% yield) as a cloudy, waxy solid.

^1H NMR (500 MHz, CDCl_3) See i) the annotated spectrum and ii) the detailed line listing for **PCMeVL** above for the coupling constants typically seen for this family of polyesters. $M_n = 9.7 \text{ kg}\cdot\text{mol}^{-1}$ (from analysis of the benzylic protons in the incorporated initiator).

^{13}C NMR (125 MHz, CDCl_3) δ 172.7, 172.3, 64.9, 64.5, 44.1, 31.4, 30.7, 23.7, 19.2, and 13.8. (for the 90 $\text{kg}\cdot\text{mol}^{-1}$ sample).

IR (neat, selected peaks): 2964, 2936, 2876, 1725 (strong), 1447, 1393, 1246, and 1145 (strong) cm^{-1} .

SEC (THF, MALS): $M_n = 19.4 \text{ kg}\cdot\text{mol}^{-1}$, $M_w = 28.3 \text{ kg}\cdot\text{mol}^{-1}$, $D = 1.4(6)$, $dn/dc = 0.0593$.

TGA T_d 1% = 252 °C, 5% = 292 °C.

DSC Cooling and heating rate of 5 °C/min: $T_g = -44$ °C, $T_c = 11$ °C, $T_m = 50$ °C ($\Delta H_m = 30.4 \text{ J}\cdot\text{mol}^{-1}$).

Cooling and heating rate of 10 °C/min: $T_g = -43$ °C, $T_c = 16$ °C, $T_m = 50$ °C ($\Delta H_m = 26.1 \text{ J}\cdot\text{mol}^{-1}$).

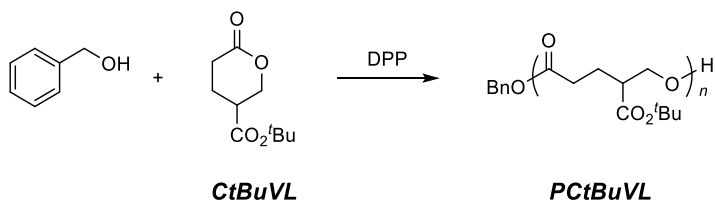
A higher molar mass sample was prepared in a similar fashion to that for **PCMeVL** using BnOH (1 equiv, 9.5 μL , 0.046 mmol), **CnBuVL** (550 equiv, 10.0 g, 50.0 mmol), and DPP (2.8 equiv, 63 mg, 0.25 mmol). The polymer was heated to 70 °C for 40 h (89% monomer conversion), precipitated, and heated under vacuum as described for **PCMeVL** to give **PCnBuVL** as a white, cloudy disk (7.24 g, 72% yield).

$^1\text{H NMR}$ (500 MHz, CDCl_3) $M_n = 93 \text{ kg}\cdot\text{mol}^{-1}$ (integrated against BnO-) or $900 \text{ kg}\cdot\text{mol}^{-1}$ (integrated against the CH_2OH end group).

SEC of higher MW (THF, MALS): $M_n = 75.0 \text{ kg}\cdot\text{mol}^{-1}$, $M_w = 90.3 \text{ kg}\cdot\text{mol}^{-1}$, $D = 1.21$, $dn/dc = 0.0635$.

DSC Heating rate of 10 °C $\cdot\text{min}^{-1}$: $T_g = -42$ °C, $T_m = 45$ °C, ($\Delta H_m = 23.5 \text{ J}\cdot\text{mol}^{-1}$).

Poly(4-Carbo-*t*-butylvalerolactone) (**PCtBuVL**)



In a nitrogen-filled glovebox, BnOH (1.0 equiv, 3.1 μL , 0.030 mmol), diphenyl phosphate [DPP, $(\text{PhO})_2\text{PO}_2\text{H}$, 0.50 equiv, 4.0 mg, 0.016 mmol], 4-carbo-*t*-

butoxyvalerolactone (**CtBuVL**, 50.0 equiv, 300 mg, 1.50 mmol), and a stir bar were added sequentially to a 1-dram vial. The vial was sealed with a Teflon-lined cap and the mixture was stirred for 20 h at ambient temperature. At this time, an aliquot (ca. 3 mg) was dissolved in CDCl₃ (0.55 mL) containing NEt₃ (ca. 1 μL) and analyzed via ¹H NMR spectroscopy. The monomer conversion was measured to be 97%. The vial was removed from the glovebox and the sample was dissolved in NEt₃ (ca. 10 μL) and DCM (1–2 mL). The polymer was precipitated by dropwise addition into stirred MeOH (15 mL). The vial was cooled (0 °C) and centrifuged, and the supernatant was decanted. DCM (ca. 1 mL) was added to resuspend the polymer and MeOH (ca. 15 mL) was slowly added to the stirred polymer/DCM solution to reprecipitate the polymer. This precipitation was repeated two more times because the chilled polymer/precipitation residue appeared to hold significant amounts of solvent. The four precipitations afforded poly(4-carbo-*t*-butoxyvalerolactone) (**PCtBuVL**, 98 mg, 32% yield) as a cloudy, hard solid.

¹H NMR (500 MHz, CDCl₃) See i) the annotated spectrum and ii) the detailed line listing for **PCMeVL** above for the coupling constants typically seen for this family of polyesters. $M_n = 11.7 \text{ kg}\cdot\text{mol}^{-1}$ (from analysis of the benzylic protons in the incorporated initiator).

¹³C NMR (125 MHz, CDCl₃) δ 172.3, 171.9, 81.4, 64.8, 45.0, 31.4, 28.2, and 24.9.

IR (neat, selected peaks): 2978, 2935, 1722 (strong), 1457, 1392, 1366, 1247, 1143 (strong), 1055, and 846 cm⁻¹.

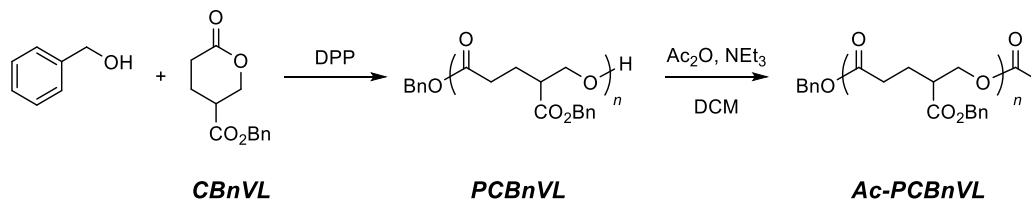
SEC (THF, MALS): $M_n = 15.6 \text{ kg}\cdot\text{mol}^{-1}$, $M_w = 18.0 \text{ kg}\cdot\text{mol}^{-1}$, $D = 1.15$, $dn/dc = 0.0431$.

TGA T_d 1% = 197 °C, 5% = 214 °C.

DSC Cooling and heating rate of 5 °C/min: $T_g = -7$ °C, $T_c = 44$ (on cool) °C, $T_m = 95$ °C ($\Delta H_m = 31.0 \text{ J}\cdot\text{mol}^{-1}$).

Cooling and heating rate of 10 °C/min: $T_g = -6$ °C, $T_c = 36$ °C (on cool), 37 (on ramp) °C, $T_m = 95$ °C ($\Delta H_m = 31.0 \text{ J}\cdot\text{mol}^{-1}$).

Poly(4-Carbobenzoxyvalerolactone) (**Ac-PCBnVL**)



In a nitrogen-filled glovebox, BnOH (1.0 equiv, 5.3 μ L, 0.051 mmol), diphenyl phosphate [DPP, (PhO)₂PO₂H, 0.50 equiv, 6.0 mg, 0.024 mmol], 4-carbobenzoxyvalerolactone (**CBnVL**, 50.0 equiv, 600 mg, 2.56 mmol), and a stir bar were added sequentially to a 1-dram vial. The vial was sealed with a Teflon-lined cap and the mixture was stirred for 24 h at ambient temperature. An aliquot of this viscous liquid sample (ca. 3 mg) was dissolved in CDCl₃ (0.55 mL) containing NEt₃ (ca. 1 μ L) and analyzed via ¹H NMR spectroscopy. The monomer conversion was measured to be 95%. The vial was removed from the glovebox and the sample was dissolved in DCM (2 mL). NEt₃ (100 μ L) and Ac₂O (100 μ L) were added and the solution was stirred. After 19 h the polymer was precipitated by dropwise addition into stirred MeOH (15 mL). The vial was cooled (0 °C) and centrifuged, and the supernatant was decanted. DCM (ca. 1 mL) was added to dissolve the polymer and MeOH (ca. 15 mL) was slowly added to the stirred solution to reprecipitate the polymer. The sample was once again cooled (0 °C), centrifuged, decanted, and placed under vacuum (ca. 0.1 mmHg) at 60 °C to give the end-capped poly(4-carbobenzoxyvalerolactone) (**Ac-PCBnVL**, 522 mg, 86% yield) as a tan, highly viscous liquid that slowly developed some cloudiness after ca. 3 weeks of storage at room temperature.

¹H NMR (500 MHz, CDCl₃) See i) the annotated spectrum and ii) the detailed line listing for **PCMeVL** above for the coupling constants typically seen for this family of polyesters. $M_n = 12.6 \text{ kg}\cdot\text{mol}^{-1}$ (from analysis of the benzylic protons in the incorporated initiator).

¹³C NMR (125 MHz, CDCl₃) δ 172.5, 172.1, 135.8, 128.7, 128.5, 128.4, 66.8, 64.4, 44.0, 31.2, and 23.6.

IR (neat, selected peaks): 3089, 3065, 3034, 2955, 1728 (strong), 1454, and 1148 (strong) cm^{-1} .

SEC (THF, MALS): $M_n = 10.3 \text{ kg}\cdot\text{mol}^{-1}$, $M_w = 10.9 \text{ kg}\cdot\text{mol}^{-1}$, $D = 1.05$, $dn/dc = 0.1190$.

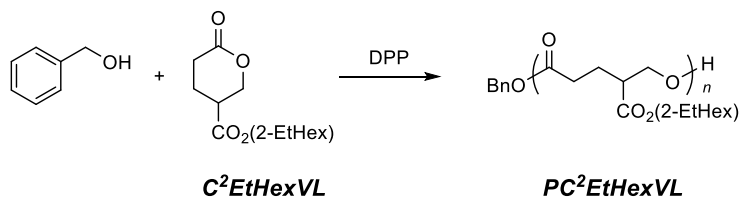
TGA T_d 1% = 289 °C, 5% = 307 °C.

DSC Cooling and heating rate of 5 °C/min: $T_g = -6$ °C [$T_m = 47$ °C on initial heating cycle, $4.4 \text{ J}\cdot\text{mol}^{-1}$]*

Cooling and heating rate of 10 °C/min: $T_g = -6$ °C.

*An SEC, taken two days after the preparation of **PCBnVL**, showed no presence of a melting characteristic. However, an SEC one month after its synthesis displayed a clear melting phenomenon at 47 °C.

Poly[4-Carbo(2-ethylhexyl)valerolactone] (**PC²EtHexVL**)



Benzyl alcohol (1.0 equiv, 2.1 μL , 0.020 mmol), diphenyl phosphate [DPP, $(\text{PhO})_2\text{PO}_2\text{H}$, 0.50 equiv, 2.5 mg, 0.010 mmol], and **C²EtHexVL** (50.0 equiv, 256 mg, 1.00 mmol), and a stir bar were sequentially added to a 1-dram vial in a nitrogen filled glovebox. The vial was sealed with a Teflon-lined cap and the polymerization was allowed to stir for 19 h. An aliquot of this viscous liquid sample, taken prior to precipitation, showed 97% monomer conversion via ^1H NMR spectroscopy. The procedure for precipitation and heating were followed as described above to give **PC²EtHexVL** (125 mg, 48% yield) as a highly viscous liquid.

^1H NMR (500 MHz, CDCl_3) See i) the annotated spectrum and ii) the detailed line listing for **PCMeVL** above for the coupling constants typically seen for this family of polyesters. $M_n = 13.3 \text{ kg}\cdot\text{mol}^{-1}$ (from analysis of the benzylic protons in the incorporated initiator).

^{13}C NMR (125 MHz, CDCl_3) δ 172.7, 172.2, 67.4, 64.5, 44.2, 38.8, 31.3, 30.4(4), 30.4(2), 29.0, 23.8, 23.7, 23.0, 14.2, 11.0. One aliphatic carbon appears as a pair of resonances with very similar chemical shifts, reflecting the mixture of diastereomers.

IR (neat, selected peaks): 2958, 2929, 2873, 2860, 1732 (strong), 1459, 1232, and 1153 cm^{-1} .

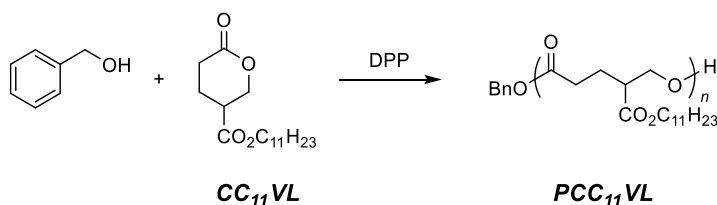
SEC (THF, MALS): $M_n = 16.0 \text{ kg}\cdot\text{mol}^{-1}$, $M_w = 18.6 \text{ kg}\cdot\text{mol}^{-1}$, $D = 1.2$, $dn/dc = 0.0550$.

TGA T_d 1% = 226 $^\circ\text{C}$, 5% = 268 $^\circ\text{C}$.

DSC Cooling and heating rate of 5 $^\circ\text{C}/\text{min}$: $T_g = -55$ $^\circ\text{C}$, $T_c = -29$ (on cooling) $^\circ\text{C}$, $T_m = -7$ $^\circ\text{C}$ ($\Delta H_m = 13.4 \text{ J}\cdot\text{mol}^{-1}$).

Cooling and heating rate of 10 $^\circ\text{C}/\text{min}$: $T_g = -54$ $^\circ\text{C}$, $T_c = -31$ $^\circ\text{C}$ (on cooling), 37 $^\circ\text{C}$ (on heating), $T_m = -5$ $^\circ\text{C}$ ($\Delta H_m = 9.6 \text{ J}\cdot\text{mol}^{-1}$).

Poly(4-Carboundecoxyvalerolactone) (**PCC₁₁VL**)



In a nitrogen-filled glovebox, BnOH (0.02 equiv, 2.1 μL , 0.020 mmol), diphenyl phosphate [DPP, $(\text{PhO})_2\text{PO}_2\text{H}$, 0.020 equiv, 5.0 mg, 0.020 mmol], 4-carboundecoxyvalerolactone (**CC₁₁VL**, 1 equiv, 298 mg, 1.00 mmol), and a stir bar were added sequentially to a 1 dram. The vial was sealed with a Teflon-lined cap and the mixture was stirred for 23 h at ambient temperature. An aliquot of this waxy solid sample (ca. 3 mg) was dissolved in CDCl_3 (0.55 mL) containing NEt_3 (ca. 1 μL) and analyzed by ^1H NMR spectroscopy. The monomer conversion was measured to be 98%. The vial was removed from the glovebox and the sample was dissolved in NEt_3 (ca. 10 μL) and DCM (1–2 mL). The polymer was precipitated by dropwise addition into stirred MeOH (15 mL). The vial was cooled (0 $^\circ\text{C}$) and centrifuged, and the supernatant was decanted.

DCM (ca. 1 mL) was added to dissolve the polymer and MeOH (ca. 15 mL) was slowly added to this stirred solution to reprecipitate the polymer. The sample was again cooled (0 °C), centrifuged, decanted, and placed under vacuum (ca. 0.1 mmHg) at 60 °C to give poly(4-carboundecoxyvalerolactone) (**PCC₁₁VL**) as a white, waxy solid (261 mg, 87% yield).

¹H NMR (500 MHz, CDCl₃) See i) the annotated spectrum and ii) the detailed line listing for **PCMeVL** above for the coupling constants typically seen for this family of polyesters. $M_n = 14.1 \text{ kg}\cdot\text{mol}^{-1}$ (from analysis of the benzylic protons in the incorporated initiator).

¹³C NMR (125 MHz, CDCl₃) δ 172.7, 172.3, 65.3, 64.6, 44.1, 32.1, 31.4, 29.8, 29.7, 29.5 (2x), 29.4, 28.7, 26.0, 23.7, 22.8, and 14.3.

IR (neat, selected peaks): 2954, 2921, 2853, 1729 (strong), 1465, 1889, and 1575 cm⁻¹.

SEC (THF, MALS): $M_n = 13.2 \text{ kg}\cdot\text{mol}^{-1}$, $M_w = 16.4 \text{ kg}\cdot\text{mol}^{-1}$, $D = 1.2$, $dn/dc = 0.0614$.

TGA T_d 1% = 236 °C, 5% = 268 °C.

DSC Cooling and heating rates of 5 °C/min: $T_g = <-75 \text{ °C}$, $T_c = 12 \text{ °C}$ (on cooling), $T_m = 55 \text{ °C}$ ($\Delta H_m = 28.2 \text{ J}\cdot\text{mol}^{-1}$).

Cooling and heating rates of 10 °C/min: $T_g = <-75 \text{ °C}$, $T_c = 16 \text{ °C}$ (on cooling), $T_m = 55 \text{ °C}$ ($\Delta H_m = 26.8 \text{ J}\cdot\text{mol}^{-1}$).

S4.4 Polymer testing

S4.4.1 Matrix-assisted laser desorption ionization time of flight (MALDI-TOF)

A low molecular sample for MALDI-TOF analysis was polymerized at 70 °C for 16 h using BnOH, **CnBuVL**, and DPP targeting a $M_n = \text{ca. } 2.5 \text{ kg}\cdot\text{mol}^{-1}$. **PCnBuVL** reached equilibrium conversion after ca. 2 to 3 h and was held at 70 °C for the additional 13 to 14 h.

The mass spectra of this sample contains 4 different series of peaks. The most intense series is associated with the linear **PCnBuVL** ($\text{BnOH} + n \cdot \text{CnBuVL} + \text{Na}^+$), and a second series attributed to ester pyrolysis of the polymer backbone ($18 + n \cdot \text{CnBuVL} + \text{Na}^+$) that occurs during the MALDI ionization, which we previously described.⁸ An additional two less intense series are present. These two series are indicative of intramolecular cyclization of the propagating hydroxy onto either the sidechain (loss of nBuOH) or the backbone esters (appears as loss of BnOH). These events, if occurring, would lead to broadening of the SEC distribution over time as observed in Figure 4.6c.

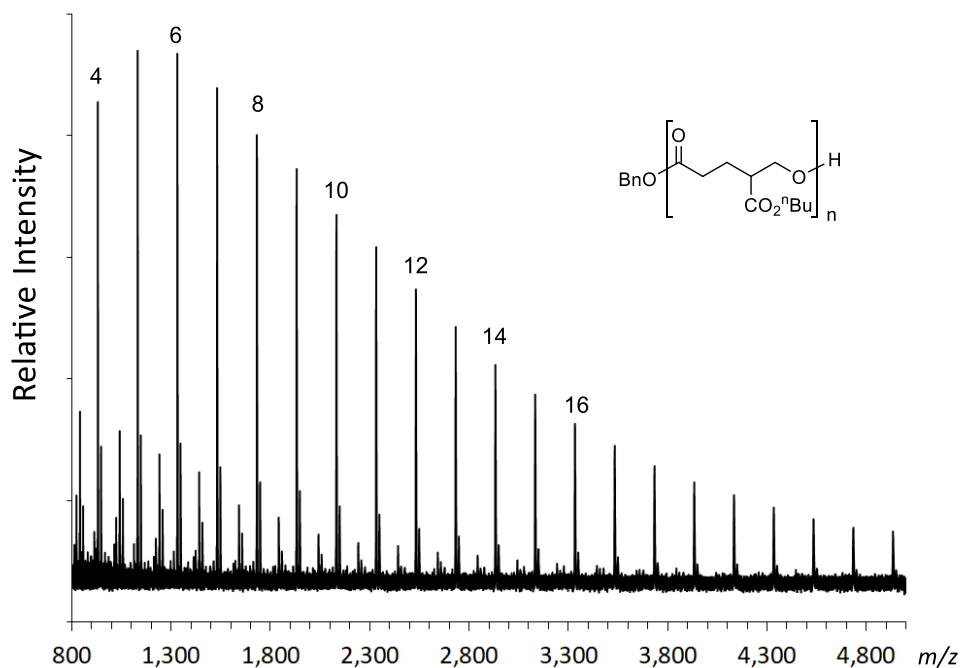


Figure S4.1 MALDI/TOF-MS spectrum taken in reflectron mode of **PCnBuVL** ($M_n = 3.1 \text{ kg}\cdot\text{mol}^{-1}$ from ^1H NMR spectroscopy) using dihydroxybenzene as a matrix. **CnBuVL** molar mass = $200 \text{ g}\cdot\text{mol}^{-1}$. See expansion in following Figure for a set of specific amu values across a representative pair of ions differing by one (or two) repeat units. See Figure 4.7 for an expansion of this MALDI spectrum.

S4.4.2 Eliminative degradation

The degradation of the **PCRVLs** (with larger $M_n = ca. 100 \text{ kg}\cdot\text{mol}^{-1}$) using an excess of 1,8-diazabicyclo[5.4.0]undec-7-ene (ca. 5 equiv, DBU) showed very small resonances suggestive of branching repeat units. These resonances were barely detectable via ^1H NMR spectroscopy but were similar to 2-methyleneglutarate species that we observed in the DBU degradation of a highly branched polyester derived from **CMeVL**.⁸ We prepared another sample of **PCMeVL** (described below) that was polymerized for a much longer period of time in order to (possibly) increase the concentration of the branch subunits. This would enable us to more easily detect the branching subunits of **PCRVL** and the degradation branching units using ^1H NMR spectroscopy.

The ^1H NMR spectrum of this newly prepared sample of **PCMeVL** showed a new, small methyl ester resonance (3.67 ppm) with in a 1:20 ratio to the larger methyl ester resonance observe for linear **PCMeVL** (3.71 ppm). Additionally, DBU degradation of this mixture showed the presence of small 2-methyleneglutarate derivatives (**S405**, **S406**, **S407**), which are again consistent with branch subunits (Figure S4.3).

Procedure

CMeVL (100 equiv, 178 mg, 1.13 mmol), BnOH (1 equiv, 1 μL , 0.01 mmol), diphenyl phosphate [7.6 mg, 0.03 mmol, DPP, $(\text{PhO})_2\text{PO}_2\text{H}$] and a stir bar were sequentially added to a 1-dram vial in a nitrogen-filled glovebox. The vial was sealed with a Teflon-lined cap placed into an oil bath at 85 $^\circ\text{C}$ for 4 days. The polymer was purified by precipitation as described above.

A portion of this **PCMeVL** (20 mg), DBU (200 μL), and a stir bar were placed in a 0.5-dram vial and capped. The mixture was stirred for 15 h, and an aliquot (ca. 20 μL) was dissolved in CDCl_3 (0.55 mL) and analyzed via ^1H NMR spectroscopy.

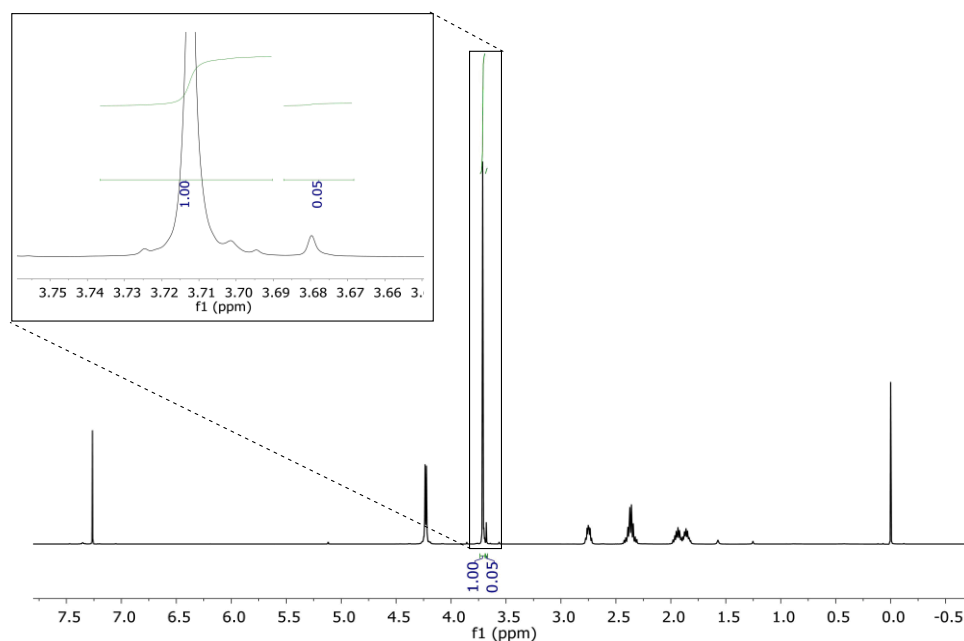


Figure S4.2 ^1H NMR spectrum of **PCMeVL** with ca. 100 repeat units per chain that was polymerized at 85 °C for 4 days. The inlay shows the presence of a smaller upfield methyl ester resonance suggestive of a small amount of branching.

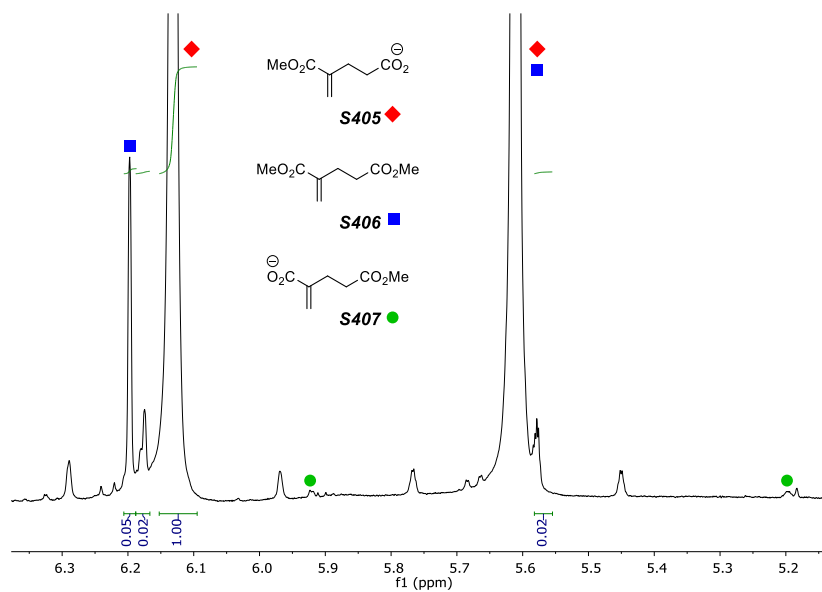


Figure S4.3 ^1H NMR spectrum of the crude degradation mixture using **PCMeVL** with DBU. The degraded **PCMeVL** sample was prepared using BnOH, **CMeVL**, and DPP (1:100:1), and the polymerization mixture was reactions for 4 days at 85 °C. The

spectrum of this degradation contains the main degradation product of **PCMeVL** (degraded to **S405**) and two smaller resonance of 2-methyleneglutarates **S406** and **S407** that arise from transesterification reactions of the sidechain methyl ester with the propagating hydroxy during the polymerization.⁸

S.4.4.3 Differential scanning calorimetry annealing studies

A sample of **PCMeVL**, **PCEtVL**, **PCiPrVL**, or **PCnBuVL** was heated to 150 °C (10 °C•min⁻¹), cooled (10 °C•min⁻¹) to the target temperature, and held at this temperature for 1 h. The sample was then cooled (or warmed) to 20 or 25 °C (10 °C•min⁻¹) and heated to 150 °C (10 °C•min⁻¹). The sample was again cooled to a new target temperature, and this sequence was repeated for a total of four or five temperatures. The annealing temperature for the subsequent experiments was chosen based on the annealing temperature that provided largest enthalpy of melting (ΔH_m) during the heating cycle.

DSC heating cycles were performed that varied the annealing times (at the determined annealing temperatures) to examine the aging of the **PCRVLs**. **PCRVL** samples were heated to 150 °C, cooled and held at the desired annealing temperature for the indicated time, cooled to 20 or 25 °C (10 °C•min⁻¹), reheated to 150 °C (10 °C•min⁻¹). The sample was again cooled to the determined annealing temperature, and this sequence was repeated for each timeframe.

PCMeVL

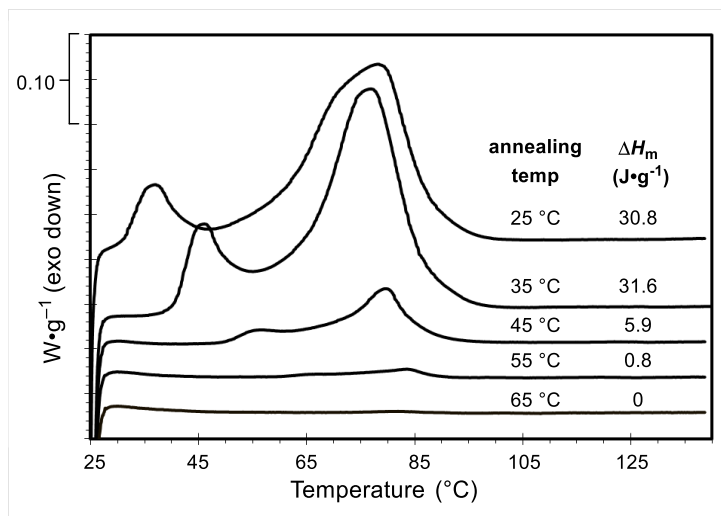


Figure S4.4 Annealing temperature screening. Vertically offset DSC thermograms of **PCMeVL** ($n = \text{ca. } 615$) annealed for 1 h at 25, 35, 45, 55, and 65 °C. The sample was heated to 150 °C, cooled to the indicated temperature ($10 \text{ }^\circ\text{C} \cdot \text{min}^{-1}$), annealed for one hour, further cooled to 25 °C ($10 \text{ }^\circ\text{C} \cdot \text{min}^{-1}$), and heated to 150 °C ($10 \text{ }^\circ\text{C} \cdot \text{min}^{-1}$, this heating cycle is shown for each annealing temperature). This heating cycle was immediately repeated for each annealing temperature.

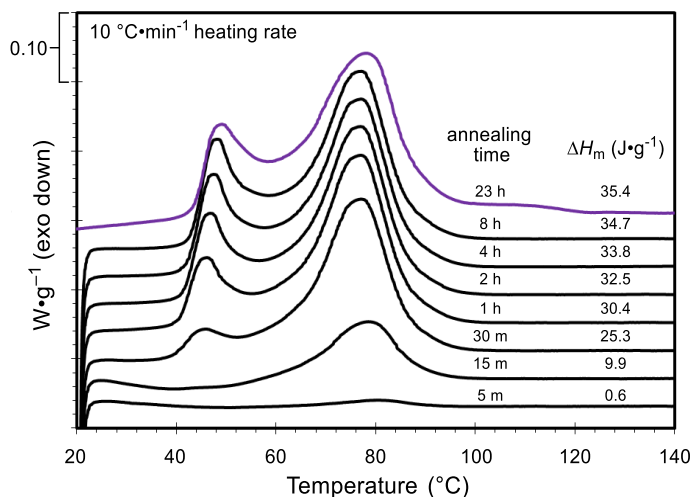


Figure S4.5 Annealing over time. Vertically offset DSC thermograms of **PCMeVL** ($n = \text{ca. } 615$) annealed at 35 °C for indicated time lengths. The sample was heated to 150 °C,

cooled to 35 °C (10 °C•min⁻¹), annealed for the indicated time, further cooled to 20 °C (10 °C•min⁻¹), and heated to 150 °C (10 °C•min⁻¹, this heating increase is shown above), and repeated for the each annealing time. The 23-h timepoint was prepared after melt pressing the bulk **PCMeVL** and annealing at 35 °C for 23 h. This prepared sample was later used for tensile testing. Each trace was integrated from 41–100 °C to determine ΔH_m .

PCEtVL

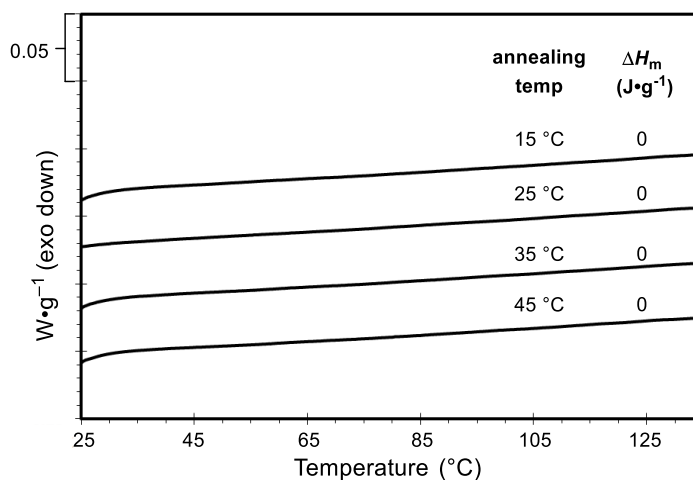


Figure S4.6 Annealing temperature screening. Vertically offset DSC thermograms of **PCEtVL** ($n = \text{ca. } 640$) annealed for 1 h at 25, 35, 45, 55, and 65 °C. The sample was heated to 150 °C, cooled to the indicated temperature (10 °C•min⁻¹), annealed for one hour, further cooled to 25 °C (10 °C•min⁻¹), and heated to 150 °C (10 °C•min⁻¹, this heating cycle is shown for each annealing temperature). This cycle was immediately repeated for each annealing temperature.

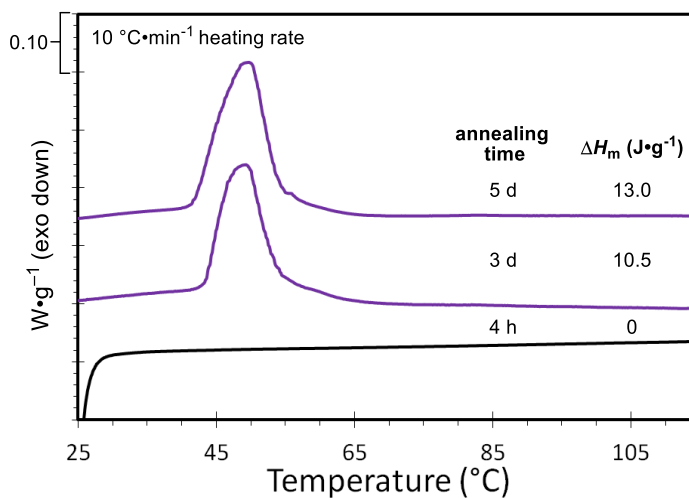


Figure S4.7 Annealing over time. Vertically offset DSC thermograms of **PCtVL** ($n =$ ca. 640) annealed at RT (ca. 22 °C) for indicated time lengths. The black sample was heated to 150 °C, cooled to 25 °C (10 °C•min⁻¹), annealed for 4 hours, and heated to 150 °C (10 °C•min⁻¹, this heating increase is shown above). The 3- and 5-day timepoints (purple) were prepared after melt pressing the bulk sample of **PCtVL** and annealing at RT (22 °C) for 3 and 5 days. This prepared sample was later used for tensile testing. Each trace was integrated from 39–65 °C determine ΔH_{ms} .

PCiPrVL

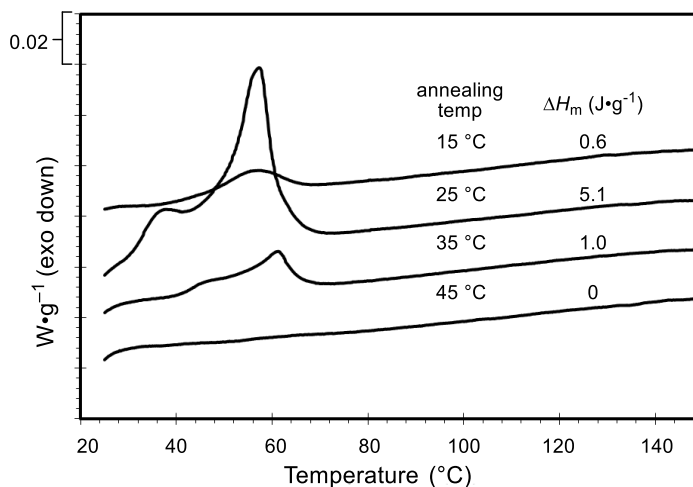


Figure S4.8 Annealing temperature screening. Vertically offset DSC thermograms of PCiPrVL ($n = ca. 420$) annealed for 1 h at 15, 25, 35, and 45 $^{\circ}C$. The sample was heated to 150 $^{\circ}C$, cooled to the indicated temperature (10 $^{\circ}C \cdot min^{-1}$), annealed for one hour, further cooled (or heated) to 20 $^{\circ}C$ (10 $^{\circ}C \cdot min^{-1}$), and heated to 150 $^{\circ}C$ (10 $^{\circ}C \cdot min^{-1}$, this heating increase is shown above). This was immediately repeated for each annealing temperature. Each trace was integrated from 31–67 $^{\circ}C$ to determine ΔH_m .

PCnBuVL

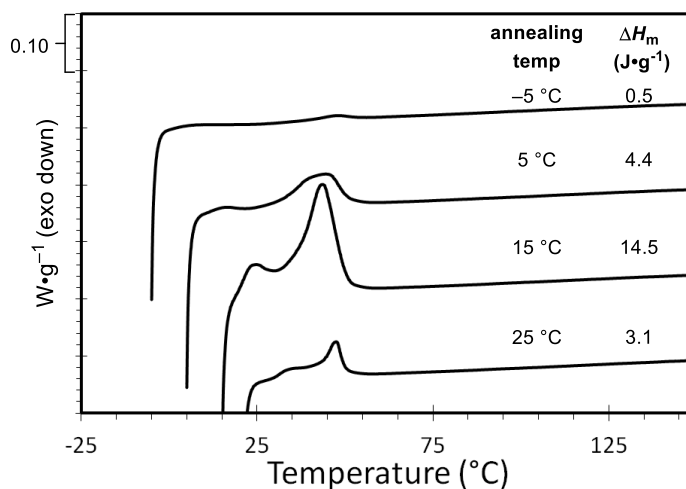


Figure S4.9 Annealing temperature screening. Vertically offset DSC thermograms of **PCnBuVL** ($n = \text{ca. } 465$) annealed for 1 h at 15, 25, 35, and 45 °C. The sample was heated to 150 °C, cooled to the indicated temperature ($10 \text{ }^\circ\text{C}\cdot\text{min}^{-1}$), annealed for one hour, further cooled to 25 °C ($10 \text{ }^\circ\text{C}\cdot\text{min}^{-1}$), and heated to 150 °C ($10 \text{ }^\circ\text{C}\cdot\text{min}^{-1}$, this heating increase is shown for each annealing temperature). This heating cycle was immediately repeated for each annealing temperature.

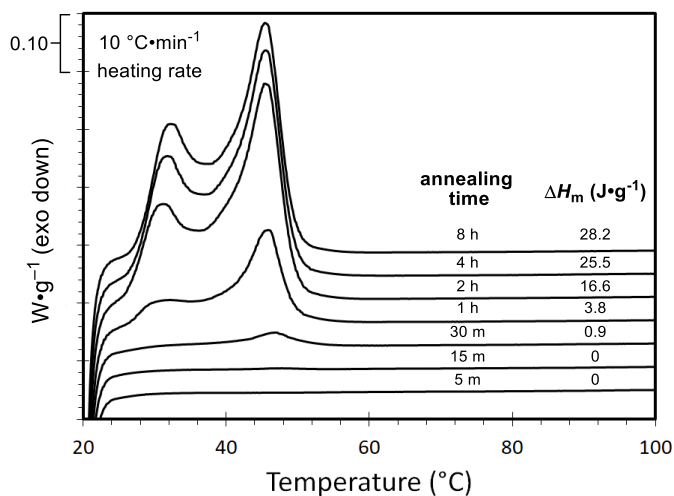
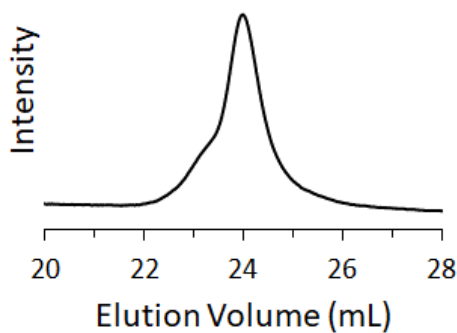


Figure S4.10 Annealing over time. Vertically offset DSC thermograms of **PCnBuVL** ($n = \text{ca. } 465$) annealed at RT (ca. 22 °C) for indicated time lengths. Each sample was heated to 150 °C, cooled to 22 °C ($10 \text{ }^\circ\text{C}\cdot\text{min}^{-1}$), annealed for the indicated time, and heated to 150 °C ($10 \text{ }^\circ\text{C}\cdot\text{min}^{-1}$, this heating increase is shown above). Each trace was integrated from 25–65 °C determine ΔH_m s.

S4.5 Polymer characterization data

S4.5.1 Size-exclusion chromatography

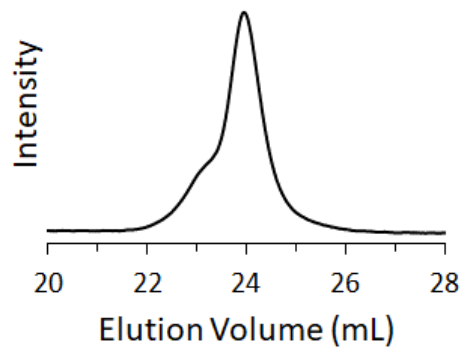
a) PCMeVL



$M_n = 115.6 \text{ kg}\cdot\text{mol}^{-1}$, $M_w = 129.9 \text{ kg}\cdot\text{mol}^{-1}$,

$\bar{D} = 1.12$

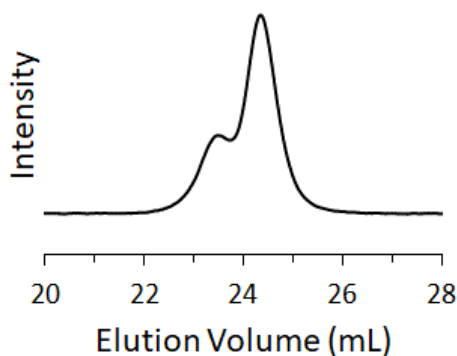
b) PCEtVL



$M_n = 76.1 \text{ kg}\cdot\text{mol}^{-1}$, $M_w = 86.3 \text{ kg}\cdot\text{mol}^{-1}$,

$\bar{D} = 1.14$

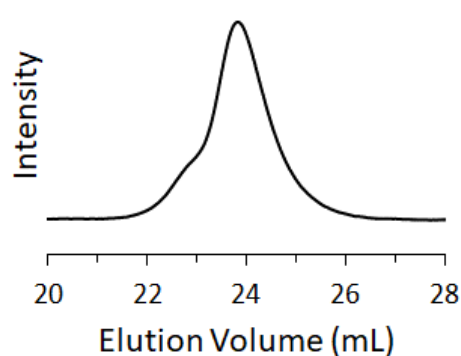
c) PCiPrVL



$M_n = 56.6 \text{ kg}\cdot\text{mol}^{-1}$, $M_w = 64.8 \text{ kg}\cdot\text{mol}^{-1}$,

$\bar{D} = 1.15$

d) PCnBuVL

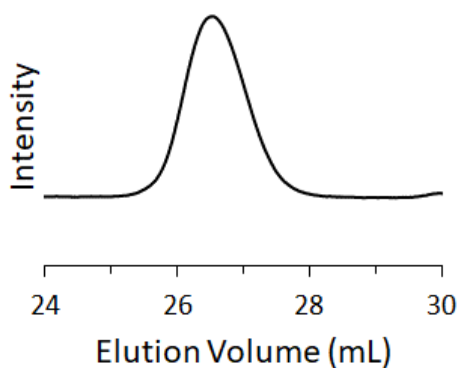


$M_n = 75.0 \text{ kg}\cdot\text{mol}^{-1}$, $M_w = 90.3 \text{ kg}\cdot\text{mol}^{-1}$,

$\bar{D} = 1.21$

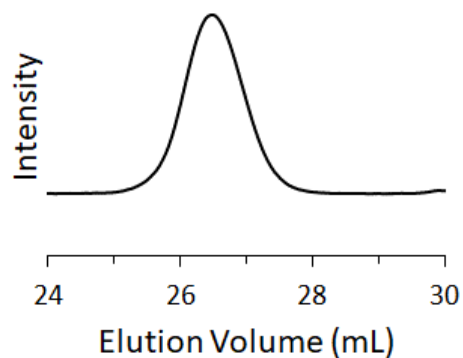
Figure S4.11 SEC chromatograms of PCRVLs with target of $M_n = 110 \text{ kg}\cdot\text{mol}^{-1}$. Each sample was polymerized at 70 °C to ca. 90% conversion and purified through precipitation. Samples were analyzed using a THF-SEC fitted with a MALS detector.

a) **PCtVL**



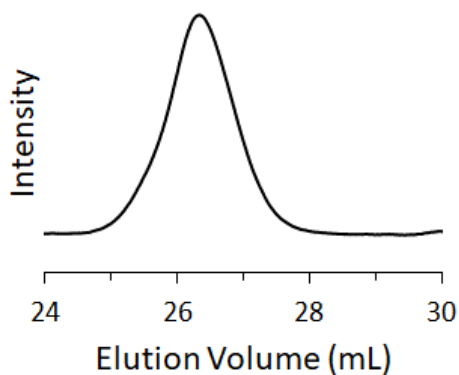
$M_n = 14.5 \text{ kg}\cdot\text{mol}^{-1}$, $M_w = 15.5 \text{ kg}\cdot\text{mol}^{-1}$,
 $\bar{D} = 1.06$

b) **PCiPrVL**



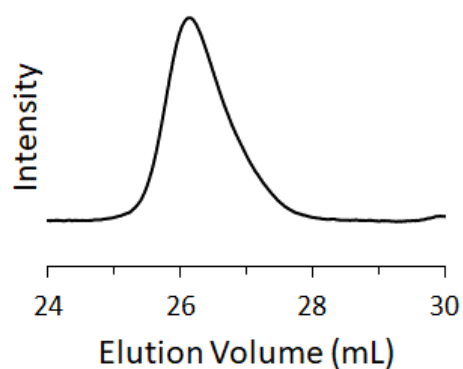
$M_n = 14.9 \text{ kg}\cdot\text{mol}^{-1}$, $M_w = 15.4 \text{ kg}\cdot\text{mol}^{-1}$,
 $\bar{D} = 1.03$

c) **PCnBuVL**



$M_n = 19.4 \text{ kg}\cdot\text{mol}^{-1}$, $M_w = 28.3 \text{ kg}\cdot\text{mol}^{-1}$,
 $\bar{D} = 1.46$

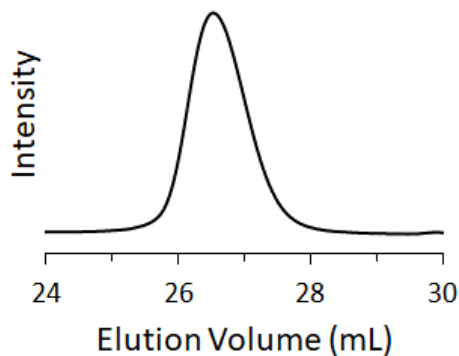
d) **PCtBuVL**



$M_n = 15.6 \text{ kg}\cdot\text{mol}^{-1}$, $M_w = 18.0 \text{ kg}\cdot\text{mol}^{-1}$,
 $\bar{D} = 1.15$

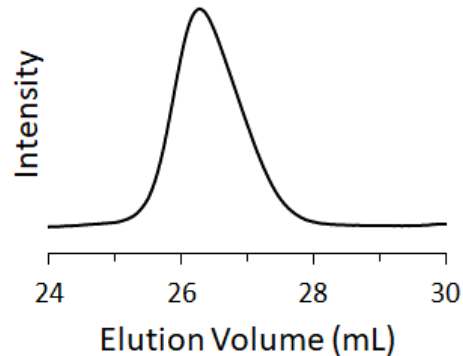
Figure S4.12 SEC chromatograms of **PCRVLs** with number average repeat unit = 50. Each sample was polymerized at room temperature and precipitated. Samples were analyzed using a THF-SEC fitted with a MALS detector.

e) PCBnVL



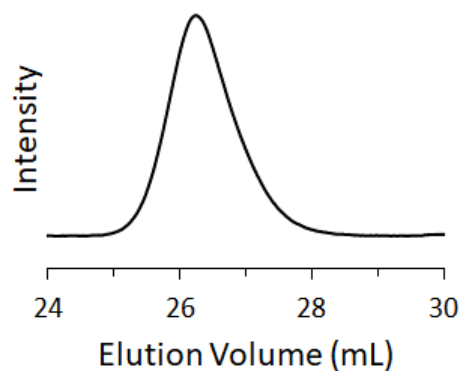
$$M_n = 10.3 \text{ kg}\cdot\text{mol}^{-1}, M_w = 10.9 \text{ kg}\cdot\text{mol}^{-1}, \\ D = 1.05$$

f) PC²EtHexVL



$$M_n = 16.0 \text{ kg}\cdot\text{mol}^{-1}, M_w = 18.6 \text{ kg}\cdot\text{mol}^{-1}, \\ D = 1.2$$

f) PCC₁₁VL



$$M_n = 13.2 \text{ kg}\cdot\text{mol}^{-1}, M_w = 16.4 \text{ kg}\cdot\text{mol}^{-1}, \\ D = 1.2, dn/dc = 0.0614$$

Figure S4.12 (continued). SEC chromatograms of PCRVLs with number average repeat unit = 50. Each sample was polymerized at room temperature and precipitated. Samples were analyzed a MALS detector.

S4.5.2 Thermogravimetric analysis

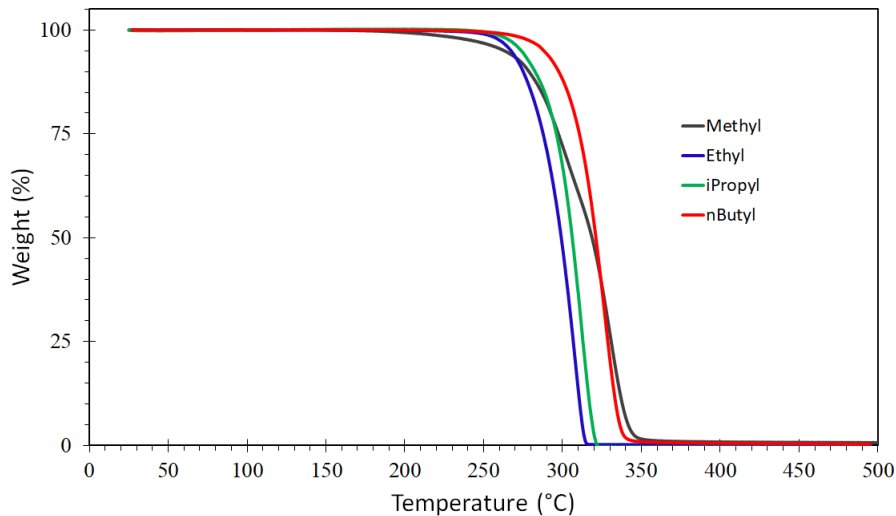


Figure S4.13 Overlaid TGA thermograms of high molecular weight **PCRVLs** ($M_w = 65\text{--}130 \text{ kg}\cdot\text{mol}^{-1}$). Samples were heated to 500 °C at a heating rate of 10 °C \cdot min $^{-1}$.

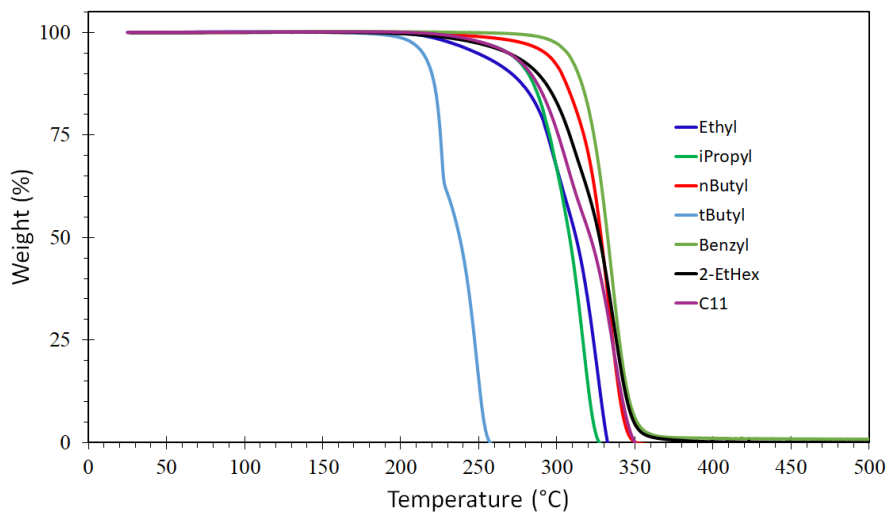
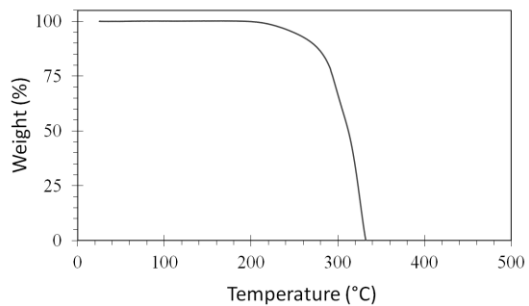
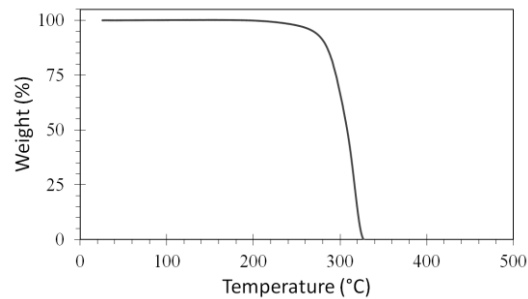


Figure S4.14 Overlaid TGA thermograms of **PCRVLs** with number average repeat units of 50. Samples were heated to 500 °C at a heating rate of 10 °C \cdot min $^{-1}$.

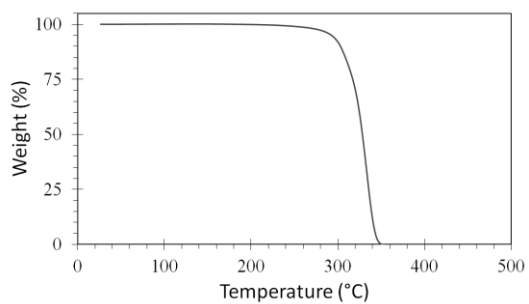
a) **PCEtVL**



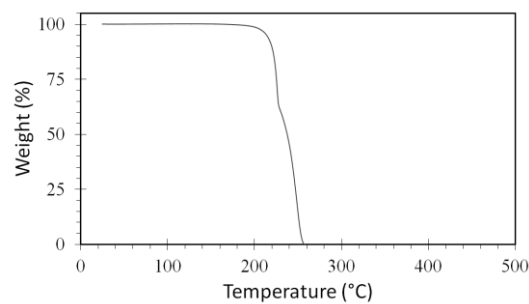
b) **PCiPrVL**



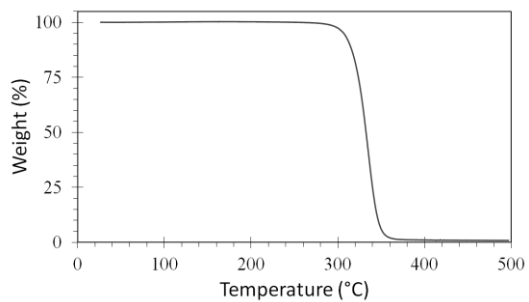
c) **PCnBuVL**



d) **PCtBuVL**



e) **PCBnVL**



f) **PC²EtHexVL**

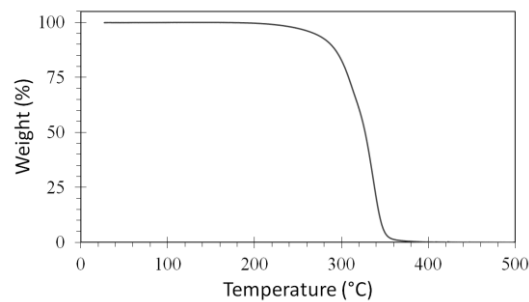
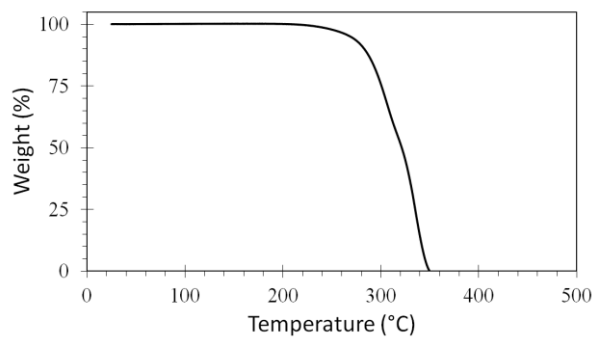


Figure S4.15 Individual TGA thermograms of **PCRVLs** with number average of 50 repeat units (same data as Figure S4.14 above). Samples were heated under nitrogen at a heating rate of 10 °C•min⁻¹.

g) **PCC₁₁VL**



h) Summary of TGA results of **PCRVLs** with $n = \text{ca. } 50$.

| | T_d (1%, 5% °C) | | T_d (1%, 5% °C) |
|----------------|----------------------|------------------------------|----------------------|
| PCMeVL | 213, 263 | PCtBuVL | 197, 214 |
| PCEtVL | 218, 249 | PCBnVL | 289, 307 |
| PCiPrVL | 228, 269 | PC²EtHexVL | 226, 269 |
| PCnBuVL | 252, 292 | PCC₁₁VL | 236, 268 |

Figure S4.15 (continued). Individual TGA thermograms of **PCRVLs** with number average of 50 repeat units (same data as Figure S4.14 above). Samples were heated under nitrogen at a heating rate of $10 \text{ }^\circ\text{C}\cdot\text{min}^{-1}$.

S4.5.3 Differential scanning calorimetry

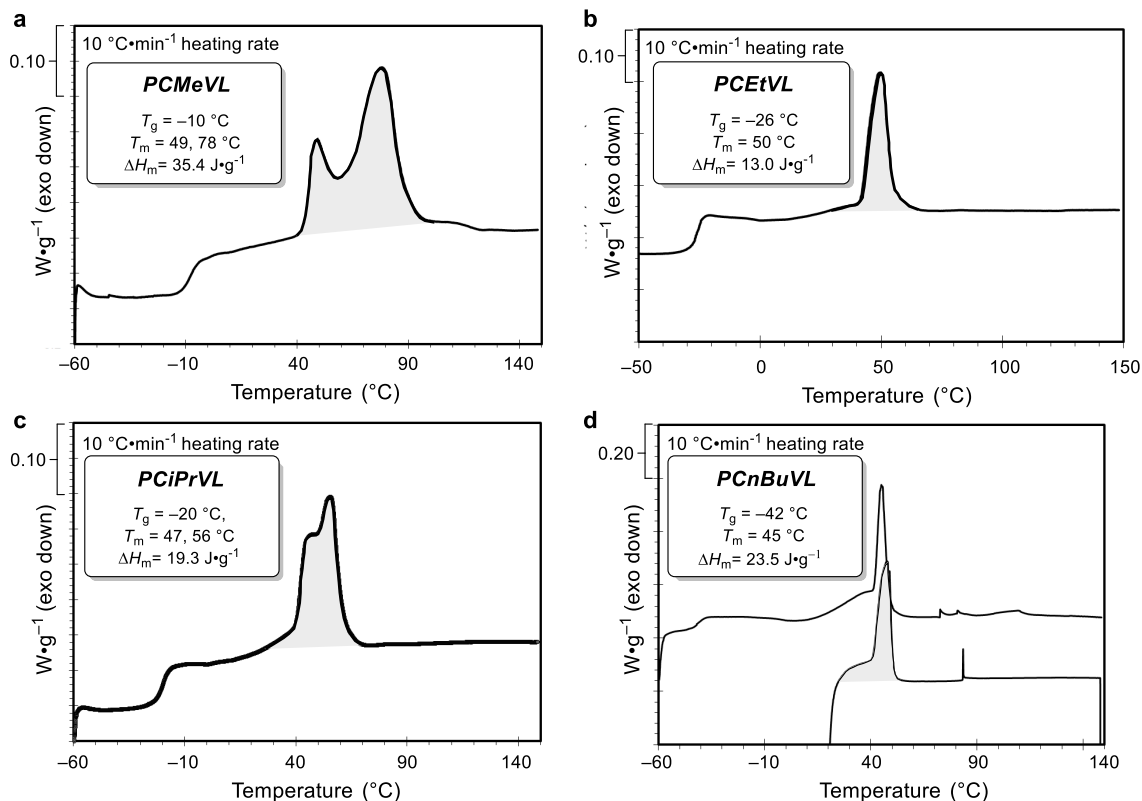
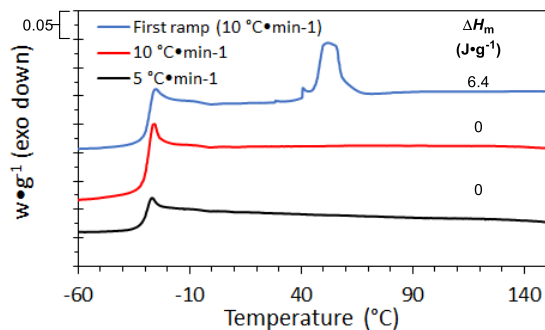
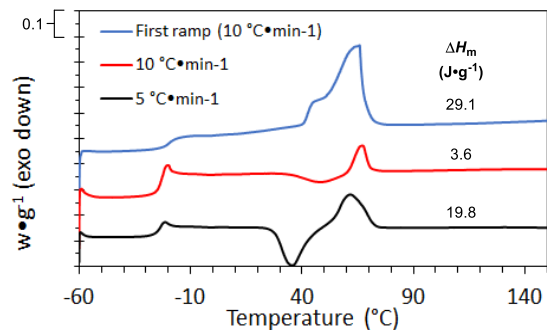


Figure S4.16 DSC thermograms of PCRVLs with molecular weight (M_n) $> 65 kg \cdot mol^{-1}$. DSC traces shown are taken from the first heating cycle. Each sample was annealed, cooled to $-60^{\circ}C$ and heated to $150^{\circ}C$ at a heating rate of $10^{\circ}C \cdot min^{-1}$. Due to the broadening of the melting exotherm of PCnBuVL while cooling to $-60^{\circ}C$, another DSC run was performed and cooled only to $20^{\circ}C$ prior to heating to $150^{\circ}C$. PCMeVL was annealed at $35^{\circ}C$ for 24 h followed by room temperature for 4 days. PCEtVL, PCiPrVL, and PCnBuVL was annealed at room temperature for 5 days. DSC measurements were taken before and after the indicated times to confirm little aging effects (prior to tensile testing) in the DSC behavior of each polymer.

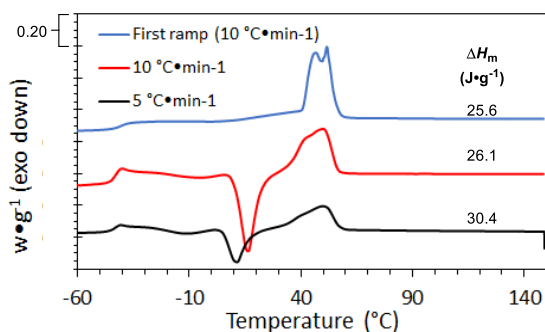
a) **PCEtVL**



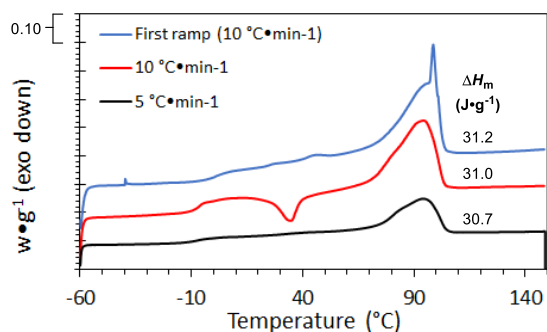
b) **PCiPrVL**



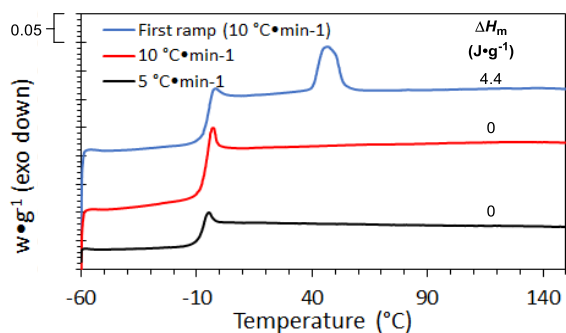
c) **PCnBuVL**



d) **PCtBuVL**



e) **PCBnVL**



f) **PC²EtHexVL**

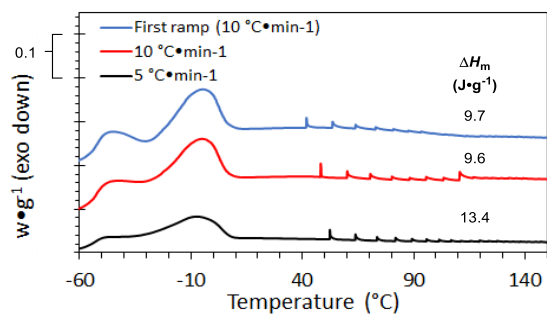
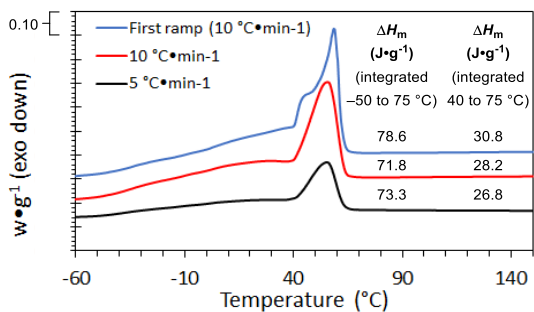


Figure S4.17 DSC thermograms of **PCRVLs** with number average of ca. 50 repeat units. DSC heating protocol described on next page.

g) PCC₁₁VL



DSC heating procedure: Samples were first cooled to $-60\text{ }^\circ\text{C}$, heated to $175\text{ }^\circ\text{C}$ at a rate of $10\text{ }^\circ\text{C}\cdot\text{min}^{-1}$ (listed as First ramp, blue), cooled to $-60\text{ }^\circ\text{C}$ at a rate of $10\text{ }^\circ\text{C}\cdot\text{min}^{-1}$, reheated to $175\text{ }^\circ\text{C}$ at a heating rate of $10\text{ }^\circ\text{C}\cdot\text{min}^{-1}$ (listed as $10\text{ }^\circ\text{C}\cdot\text{min}^{-1}$, red), cooled to $-60\text{ }^\circ\text{C}$ at a rate of $5\text{ }^\circ\text{C}\cdot\text{min}^{-1}$, and finally reheated to $175\text{ }^\circ\text{C}$ at a rate of $5\text{ }^\circ\text{C}\cdot\text{min}^{-1}$ (listed as $5\text{ }^\circ\text{C}\cdot\text{min}^{-1}$, black).

Figure S4.17 (continued). DSC thermograms of PCRVLs with number average of ca. 50 repeat units.

S4.5.4 Tensile testing

PCMeVL

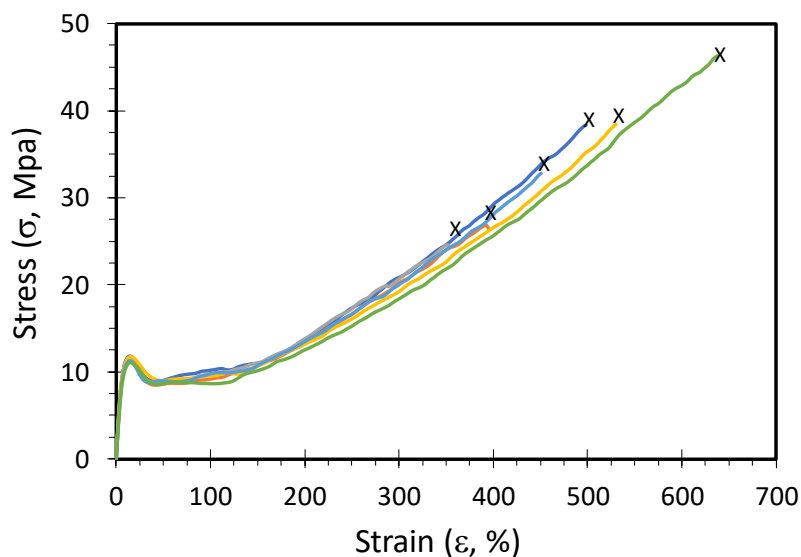


Figure S4.18 Tensile testing performance of PCMeVL [$M_w = 129.9\text{ kg}\cdot\text{mol}^{-1}$ (SEC-MALS)]. Dog-bone shaped samples (0.2 mm thickness, ca. 20 mm gauge length, 5 mm gauge width, and 15 clamp width) were pulled to the point of break (failure as indicated by X) with a rate of $50.0\text{ mm}\cdot\text{min}^{-1}$.

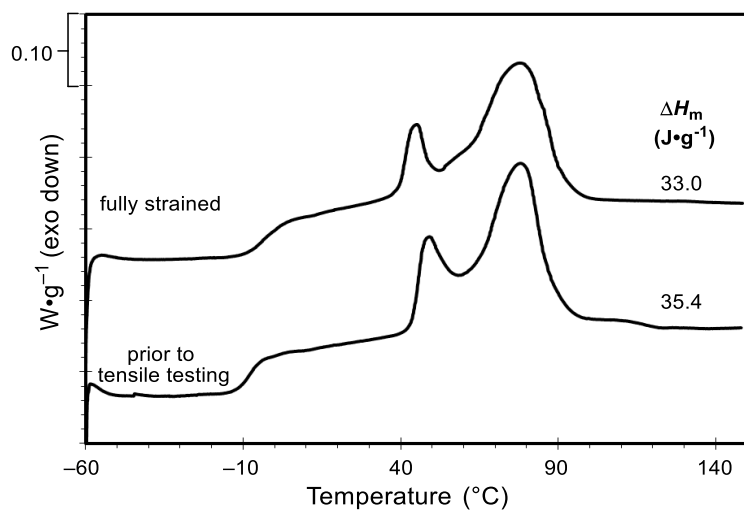


Figure S4.19 DSC of **PCMeVL** before and after tensile testing. For one mechanically stretched sample of **PCMeVL** (with the highest strain at break, green above), a whitening of the sample appeared. We took the DSC of the stretched and broken midsection of the sample (labeled fully strained) and found little evidence for strain-induced crystallization.

PCEtVL

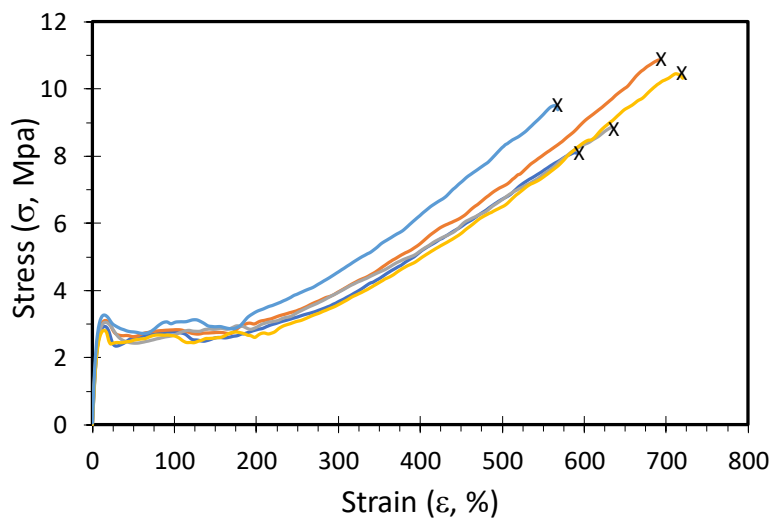


Figure S4.20 Tensile testing performance of **PCEtVL** [$M_w = 86.3 \text{ kg}\cdot\text{mol}^{-1}$ (SEC-MALS)]. Dog-bone shaped samples (0.2 mm thickness, ca. 20 mm gauge length, 5 mm gauge width, and 15 clamp width) were pulled to the point of break (failure as indicated by X) with a rate of $50.0 \text{ mm}\cdot\text{min}^{-1}$.

PCiPrVL

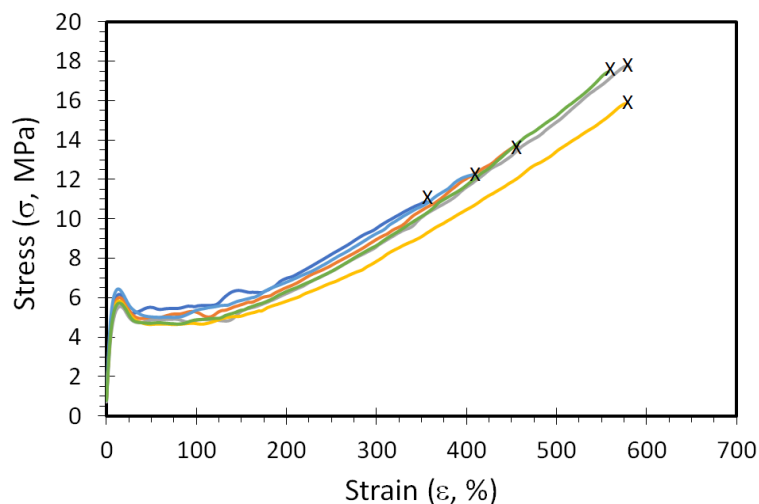


Figure S4.21 Tensile testing performance of **PCiPrVL** [$M_w = 64.8 \text{ kg}\cdot\text{mol}^{-1}$ (SEC-MALS)]. Dog-bone shaped samples (0.2 mm thickness, ca. 20 mm gauge length, 5 mm gauge width, and 15 clamp width) were pulled to the point of break (failure as indicated by X) with a rate of $50.0 \text{ mm}\cdot\text{min}^{-1}$.

PCnBuVL

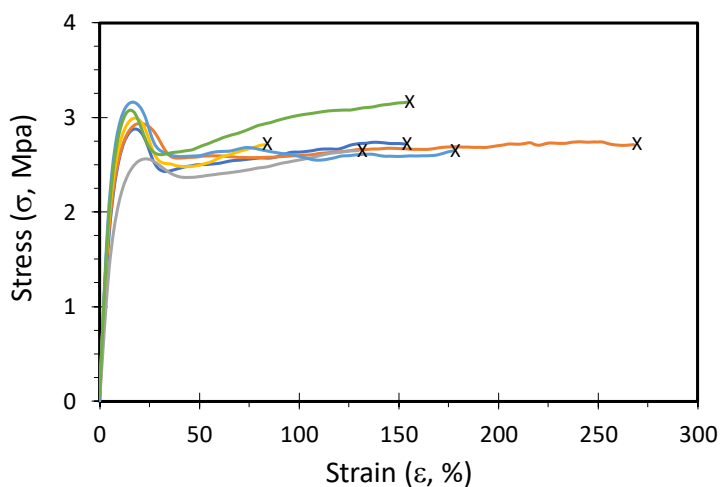


Figure S4.22 Tensile testing performance of **PCnBuVL** [$M_w = 90.3 \text{ kg}\cdot\text{mol}^{-1}$ (SEC-MALS)]. Dog-bone shaped samples (0.2 mm thickness, ca. 20 mm gauge length, 5 mm gauge width, and 15 clamp width) were pulled to the point of break (failure as indicated by X) with a rate of $50.0 \text{ mm}\cdot\text{min}^{-1}$.

S4.6 References

- ¹ Wiley, R. H.; Smith, N. R. Coumalic Acid. *Org. Synth.* **1951**, *31*, 23–24.
- ² Fahnhorst, G. W.; Hoye, T. R. A carbomethoxylated polyvalerolactone from malic acid: Synthesis and divergent chemical recycling. *ACS Macro Lett.* **2018**, 143–147.
- ³ Hendrickson, J. B.; Hussoin, M. S. Reactions of carboxylic acids with “phoshonium anhydrides.” *J. Org. Chem.* **1989**, *54*, 1144–1149.
- ⁴ Campbell, N. R.; Hunt, J. H. 220. Unsaturated lactones. Some esters of aconic and coumalic acids. *J. Chem. Soc.* **1947**, *0*, 1176–1179.
- ⁵ Durani, S.; Kapil, R. S. A novel rearrangement reaction: Single-step conversion of 2-(6-carboxy-3-oxoheptyl)-3,4-dihydro-6-methoxynaphthalen-1(2H)-one into 1-(3-carboxybutyl)-2-(2-carboxyethyl)-3,4-dihydro-6-methoxynaphthalene. *J. Chem. Soc. Perkin. Trans.* **1983**, 211–217.
- ⁶ Messerle, L. Convenient pressure reactors for organometallic reactivity studies. In *Experimental Organometallic Chemistry*; Wayda, A. L.; Daresnbourg, M. Y.; Eds.; ACS Symposium Series 357; American Chemical Society: Washington DC, pp 198–203, DOI: 10.1021/bk-1987-0357.ch007.
- ⁷ Feng, Y.; Coward, J. K. Prodrug forms of N-[(4-Deoxy-4-amino-10-methyl)pteroyl]glutamate- γ -[ψ P(O)(OH)]-glutarate, a potent inhibitor of Folylpoly- γ glutamate synthetase: Synthesis and hydrolytic stability. *J. Med. Chem.*, **2006**, *49*, 770–788.
- ⁸ Fahnhorst, G. W.; Stasiw, D. E.; Tolman, W. B.; Hoye, T. R. Isomerization of linear to hyperbranched polymers: Two isomeric lactones converge via metastable isostructural polyesters to a highly branched analogue *ACS Macro Lett.* **2018**, *7*, 1144–1148.

Appendix D. Supplementary information for Chapter 5 (S5)

| | |
|---|-----|
| S5.1 General Experimental Protocols | 255 |
| S5.2 Preparation, polymerization, and isomerization of compounds | 256 |
| S5.2.1 2-Carbomethoxyvalerolactone (501 ^{2Me}) preparation and polymerization.... | 256 |
| S5.2.2 2-Carboethoxyvalerolactone (501 ^{2Et}) preparation and polymerization..... | 258 |
| S5.2.3 2-Carbo- <i>n</i> -butoxyvalerolactone (501 ^{2nBu}) preparation and polymerization. | 259 |
| S5.2.4 5-Carbomethoxyvalerolactone (501 ^{5Me}) preparation and polymerization.... | 260 |
| S5.2.6 3-Carbomethoxycaprolactone (516 ^{3Me}) and 5-Carbomethoxycaprolactone (516 ^{5Me}) preparation and polymerization..... | 265 |
| S5.2.7 Dimethyl 3,5-dicarbomethoxycaprolactone (516 ^{3,5Me}) preparation and isomerization..... | 266 |
| S5.3 Polymer characterization data | 268 |
| S5.4 References | 271 |

S5.1 General Experimental Protocols

Materials

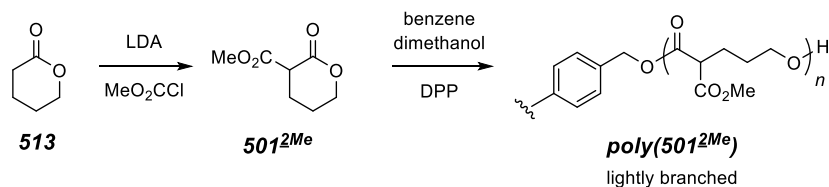
1-Bromoundecane (98%, Alfa Aesar), 2-ethylhexyl bromide (95%, Aldrich), benzyl bromide (98%, Aldrich), δ -valerolactone (**513**, technical grade, Aldrich), methyl chloroformate (Acros), *n*-butyl chloroformate (98%, Aldrich), methyl 4-hydroxybenzoate (Eastman), methyl 3-hydroxybenzoate (99%, Sigma-Aldrich), and dimethyl 5-hydroxyisophthalate (Aldrich) were purchased and used as received. δ -Valerolactone (technical grade, Aldrich) was distilled over CaH₂ and stored under N₂. THF was distilled over sodium/benzophenone and stored in a Schlenk flask under N₂.

Instrumental methods:

Nuclear Magnetic Resonance (NMR) spectroscopy, Attenuated Total Reflectance-Fourier Transform Infrared (ATR-FTIR) spectroscopy, High-Resolution Mass Spectrometry (HRMS), Size-Exclusion Chromatography (SEC), Thermogravimetric Analysis (TGA), Differential Scanning Calorimetry (DSC), and Matrix-Assisted Laser Desorption/Ionization Time of Flight Mass Spectrometry (MALDI/TOF-MS) were analyzed using the instruments and protocols as outlined in the supporting information for Chapter 3.

S5.2 Preparation, polymerization, and isomerization of compounds

S5.2.1 2-Carbomethoxyvalerolactone (**501^{2Me}**) preparation and polymerization



2-Carbomethoxyvalerolactone (**501^{2Me}**)

To a flame-dried, three-neck, 1-L flask containing a stir bar and a headspace filled with nitrogen, diisopropylamine (32 mL, 230 mmol) and THF (200 mL) were added, and the flask was capped with rubber septa. The flask was cooled in an acetone/dry-ice bath, and *n*BuLi (84.0 mL, 210 mmol) was slowly added over fifteen minutes so that the internal temperature of the reaction was kept below $-60\text{ }^\circ\text{C}$. The flask was removed from the dry-ice bath and was allowed to warm to $0\text{ }^\circ\text{C}$ over 25 minutes. The flask was returned to the dry-ice bath and a solution of δ -valerolactone (**513**, 9.3 mL, 93.0 mmol) in THF (100 mL) was added dropwise over the course of 25 minutes so that the internal temperature of the reaction was kept below $-65\text{ }^\circ\text{C}$. Methyl chloroformate (12.0 mL, 155 mmol) was added dropwise over 15 minutes. After full addition, the flask was removed from the dry ice bath, and the reaction mixture was allowed to warm to room temperature. During this warming, the reaction became very cloudy at ca. $-30\text{ }^\circ\text{C}$. The mixture was stirred at room temperature overnight was quenched by the addition of aqueous NH_4Cl (saturated, 300 mL) followed by H_2O (100 mL). The biphasic mixture was separated, and the aqueous layer was extracted with EtOAc (2x100 mL). The combined organic layers were washed with brine, dried with Na_2SO_4 , and concentrated to a yellow oil (9.196 g). This oil was further purified by column chromatography (silica, 1:1 EtOAc:Hex) to give 2-carbomethoxyvalerolactone (**501^{2Me}**, 4.22 g, 29% yield) as a colorless oil.

Spectroscopic data is consistent with a previous report.¹

¹H NMR (400 MHz, CDCl₃): δ 4.40 (ddd, *J* = 11.4, 7.0, 4.8 Hz, 1H, CO₂CH_aH_b), 4.37 (ddd, *J* = 11.4, 4.9, 0.9 Hz, 1H, CO₂CH_aH_b), 3.80 (s, 3H, CO₂Me), 3.58 (dd, *J* = 8.4, 7.5 Hz, 1H, CHCO₂), 2.28 (dddd, *J* = 14.0, 8.2, 8.2, 6.2 Hz, 1H, O₂CCHCH_aH_b), 2.18 (dddd, *J* = 13.6, 7.5, 6.0, 6.0, 0.9 Hz, 1H, O₂CCHCH_aH_b), 2.00 (dddd, 14.0, 6.4, 6.4, 6.4, 5.0 Hz, 1H, CO₂CH₂CH_aH_b), and 1.90 (dddd, *J* = 14.3, 8.3, 7.1, 6.0, 4.9 Hz, 1H, CO₂CH₂CH_aH_b).

Poly(2-carbomethoxyvalerolactone) [poly(501^{2Me})]

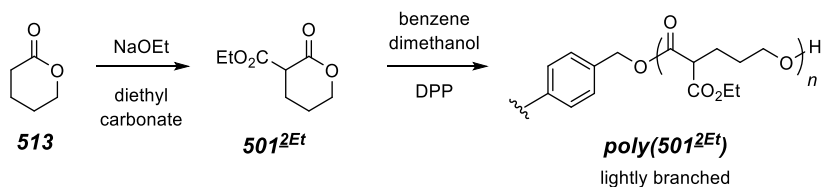
To a 2-dram vial fitted with a stir bar, 2-carbomethoxyvalerolactone (**501^{2Me}**, 315 mg, 1.99 mmol), benzene dimethanol (2.8 mg, 0.020 mmol), and diphenyl phosphate (DPP, 5.0 mg, 0.020 mmol) were added. The vial was capped and the solution was stirred overnight at ambient temperature. The mixture was dissolved in DCM (ca. 1 mL) and NEt₃ (ca. 10 μL), and the sample was precipitated by dropwise addition of this solution into stirred, cooled (0 °C) MeOH. The solution was decanted, and the remaining viscous liquid was dried *in vacuo* (60 °C, 0.1 mmHg) overnight to give poly(2-carbomethoxyvalerolactone) [**poly(501^{2Me})**] as a colorless, viscous oil.

¹H NMR (400 MHz, CDCl₃): δ 7.33 (s, 4H, Ar^{init}), 5.19 (d, *J* = 12.7 Hz, 2H, ArCH_aH_bO^{init}), 5.16 (d, *J* = 12.7 Hz, 2H, ArCH_aH_bO^{init}), 4.24–4.09 [br m, 107 H (53 RU), CO₂CH₂^{RU} (RU=repeat unit)], 3.74 [s, 142H (47 RU), CO₂Me^{RU}], 3.44–3.34 [br t (also contains a smaller, more downfield triplet also present), 55H (55 RU), CH(CO₂)₂^{RU}], 2.02–1.91 (br q, 123H (61 RU), CHCH₂^{RU}), and 1.74–1.65 (br m, 118H (64 RU), CO₂CH₂CH₂^{RU}].

TGA *T*_d 1% = 162 °C, 5% = 205 °C.

DSC Cooling and heating rates of 10 °C/min: *T*_g = –20 °C

S5.2.2 2-Carboethoxyvalerolactone (501^{2Et}) preparation and polymerization



2-Carboethoxyvalerolactone (501^{2Et})

2-Carboethoxyvalerolactone (501^{2Et}) was prepared according to a previous report by α -functionalizing valerolactone (**513**) with sodium ethoxide and diethyl carbonate. Prior to polymerization, 510^{2Et} was distilled over CaH_2 .

Spectroscopic data is consistent with a previous report.²

$^1\text{H NMR}$ (500 MHz, CDCl_3): δ 4.40 (ddd, $J = 11.5, 7.0, 4.7, 0.5$ Hz, 1H, $\text{CO}_2\text{CH}_a\text{H}_b\text{CH}_2$), 4.37 (ddd, $J = 11.4, 6.5, 4.9, 0.8$ Hz, 1H, $\text{CO}_2\text{CH}_a\text{H}_b$), 4.26 (dq, $J = 10.8, 7.2$ Hz, 1H, $\text{CO}_2\text{CH}_a\text{H}_b\text{CH}_3$), 4.24 (dq, $J = 10.8, 7.2$ Hz, 1H, $\text{CO}_2\text{CH}_a\text{H}_b\text{CH}_3$), 3.56 (dd, $J = 8.3, 7.5$ Hz, 1H, CHCO_2), 2.27 (dddd, $J = 13.6, 8.2, 8.2, 6.2, 0.4$ Hz, 1H, $\text{O}_2\text{CCHCH}_a\text{H}_b$), 2.18 (dddd, $J = 13.7, 7.5, 7.5, 6.0, 0.9$ Hz, 1H, $\text{O}_2\text{CCHCH}_a\text{H}_b$), 2.00 (dddd, 14.4, 6.4, 6.4, 6.4, 5.0 Hz, 1H, $\text{CO}_2\text{CH}_2\text{CH}_a\text{H}_b$), and 1.90 (dddd, $J = 14.4, 8.2, 7.0, 6.1, 4.9$ Hz, 1H, $\text{CO}_2\text{CH}_2\text{CH}_a\text{H}_b$), 1.31 (t, $J = 7.1$ Hz, 3H, $\text{CO}_2\text{CH}_2\text{CH}_3$).

Poly(2-carboethoxyvalerolactone) [poly(501^{2Et})]

To a flame-dried, scintillation vial fitted with a stir bar, 2-carboethoxyvalerolactone (501^{2Et} , 600 equiv, 1.00 g, 5.81 mmol), benzene dimethanol (1 equiv, 1.3 mg, 0.010 mmol), and diphenyl phosphate (29.1 mg, 0.117 mmol) were added. The mixture was stirred at ambient temperature for 30 h, and the polymer sample was purified by precipitation as described for poly(501^{2Me}) to give poly(2-carboethoxyvalerolactone) [poly(501^{2Et})] as a highly viscous, colorless oil.

$^1\text{H NMR}$ (500 MHz, CDCl_3): δ 7.33 (s, 4H, Ar^{init}), 5.19 (d, $J = 12.7$ Hz, 2H, $\text{ArCH}_a\text{H}_b\text{O}^{init}$), 5.15 (d, $J = 12.7$ Hz, 2H, $\text{ArCH}_a\text{H}_b\text{O}^{init}$), 4.24–4.09 [m, 1670 H (418 RU), $\text{CO}_2\text{CH}_2\text{CH}_2^{\text{RU}} + \text{CO}_2\text{CH}_2\text{CH}_3^{\text{RU}}$ (RU=repeat unit)], 3.37–3.32 [br t, $J = 7.5$ Hz, 393H

(393 RU), $CH(CO_2-)^{RU}$, 1.98–1.91 (m, 806H (403 RU), $CHCH_2^{RU}$), 1.73–1.65 (br m, 811H (405 RU), $CO_2CH_2CH_2^{RU}$), 1.27 [t (with smaller upfield triplet), $J = 7.1$ Hz, 1200H (400 RU) $CO_2CH_2CH_3$].

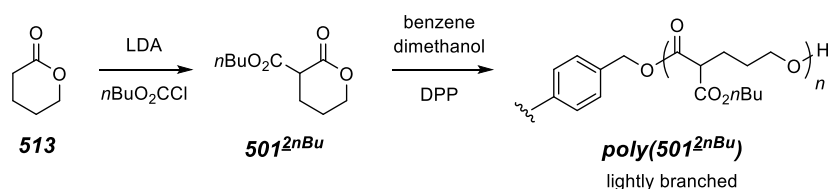
^{13}C NMR (125 MHz, $CDCl_3$): 169.15, 169.09, 64.8, 61.7, 51.4, 26.4, 25.2, and 14.2 (see spectrum for smaller resonances present in ca. 10% relative intensity).

IR (neat, selected peaks) 2977, 2942, 2874, 1727 (s), 1724 (s), 1449, and 1150 (s) cm^{-1} .

TGA T_d 1% = 233 °C, 5% = 296 °C.

DSC Cooling and heating rates of 10 °C/min: $T_g = -34$ °C

S5.2.3 2-Carbo-*n*-butoxyvalerolactone (**501^{2nBu}**) preparation and polymerization



2-Carbo-*n*-butoxyvalerolactone (**501^{2nBu}**)

Lactone **502^{2nBu}** was prepared as described for 2-carbomethoxyvalerolactone (**501^{2Me}**) this time using LDA and *n*-butyl chloroformate.

1H NMR (400 MHz, $CDCl_3$): δ 4.40 (dd, $J = 11.3, 4.8$ Hz, 1H, $CO_2CH_aH_b$), 4.36 (ddd, $J = 11.5, 5.0, 0.9$ Hz, 1H, $CO_2CH_aH_b$), 4.2 (dt, $J = 10.8, 6.7$ Hz, 1H, $CO_2CH_aH_b(CH_2)_2CH_3$), 4.18 (dt, $J = 10.8, 6.7$ Hz, 1H, $CO_2CH_aH_b(CH_2)_2CH_3$), 3.56 (dd, $J = 8.2, 7.6$ Hz, 1H, $CHCO_2$), 2.27 (dddd, $J = 13.6, 8.1, 8.1, 6.3$ Hz, 1H, $O_2CCHCH_aH_b$), 2.17 (dddd, $J = 13.7, 7.5, 7.5, 6.0, 0.9$ Hz, 1H, $O_2CCHCH_aH_b$), 2.00 (dddd, 14.4, 6.4, 6.4, 6.4, 5.0 Hz (couplings deduced from **501^{2Et}**), 1H, $CO_2CH_2CH_aH_b$), and 1.90 (dddd, $J = 14.4, 8.2, 7.0, 6.1, 4.9$ Hz (couplings deduced from **501^{2Et}**), 1H, $CO_2CH_2CH_aH_b$), 1.65 (br p, , $J = 7.0$ Hz, 2H, $CO_2CH_2CH_2CH_2CH_3$), 1.39 (br. sext, $J = 7.3$ Hz, 2H, $CO_2CH_2CH_2CH_2CH_3$), and 0.94 (t, $J = 7.4$ Hz, 3H, CH_3).

Poly(2-carbo-*n*-butoxyvalerolactone) [poly(**501**^{2nBu})]

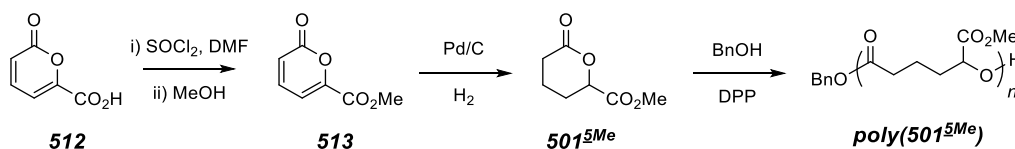
To a flame-dried, 2-dram vial fitted with a stir bar, **501**^{2nBu} (224 mg, 1.12 mmol), benzene dimethanol (7.0 mg, 0.051 mmol), and diphenyl phosphate (5.0 mg, 0.020 mmol) were added. The mixture was stirred at ambient temperature overnight, and the polymer was purified by precipitation as described for **poly(501**^{2Me}) to give poly(2-carbo-*n*-butoxyvalerolactone) [poly(**501**^{2nBu})] as a highly viscous oil.

¹H NMR (400 MHz, CDCl₃): See the line listing for **poly(501**^{2Me}) and **poly(501**^{2Et}) above and attached spectrum for the chemical shifts and resonances typically seen for this family of polyesters

TGA T_d 1% = 173 °C, 5% = 241 °C.

DSC Cooling and heating rates of 10 °C/min: $T_g = -46$ °C

S5.2.4 5-Carbomethoxyvalerolactone (**501**^{5Me}) preparation and polymerization



2-oxo-2H-pyran-6-carboxylic acid (**512**) was prepared as described by Wiley and Hart, and methyl 2-oxo-2H-pyran-6-carboxylate (**513**) was prepared using a modified procedure to which they also described.³

Methyl 2-oxo-2H-pyran-6-carboxylate (**513**)

2-oxo-2H-pyran-6-carboxylic acid (**512**, 500 mg, 3.57 mmol), thionyl chloride (SOCl₂, 780 μ L, 10.71 mmol), and a stir bar were added to a 20-mL scintillation vial. A drop of DMF was added and the reaction was stirred at 50 °C until homogeneous (ca 8 h). The reaction mixture was concentrated to a brown solid. The solid was cooled to 0 °C and MeOH (7.0 mL) was added to the vial to afford a homogenous solution. The capped vial was capped and within minutes, a precipitate began to form. After 20 minutes, the solution was placed into a freezer (ca. -20 °C) to further promote precipitation of the product.

After 1 h, the mixture was filtered to give methyl 2-oxo-2H-pyran-6-carboxylate (**513**, 379 mg, 69% yield) as a white, flaky solid.

$^1\text{H NMR}$ (500 MHz, CDCl_3) δ 7.41 (dd, $J = 9.4, 6.6$ Hz, 1H, $\text{CH}=\text{CHCO}_2$), 7.10 (dd, $J = 6.5, 1.0$ Hz, 1H, $\text{CO}_2\text{C}(\text{CO}_2\text{Me})=\text{CH}$), 6.55 (dd, $J = 9.4, 1.0$ Hz, $\text{CH}=\text{CO}_2$) and 3.94 (s, 3H, $-\text{CO}_2\text{Me}$)

$^{13}\text{C NMR}$ (125 MHz, CDCl_3) δ 160.0, 159.8, 149.6, 141.8, 121.2, 110.0, and 53.3.

mp: 122–124 °C (lit. 124–125 °C)³

5-Carbomethoxyvalerolactone (methyl 6-oxotetrahydro-2H-pyran-2-carboxylate, **501^{5Me})**

5-Carbomethoxyvalerolactone (**507^{5Me}**) was prepared as described by Wiley and Hart.³ 2-Oxo-2H-pyran-6-carboxylate (**513-Me**, 350 mg, 2.27 mmol), Pd/C (30 mg, 5% Pd/C), and a stir bar were added to a 1-mL scintillation vial. THF (3 mL) and acetone (3 mL) were added carefully along the sides of the vial, and the vial was placed into a 150-mL Fisher-Porter tube. The tube was sealed, hydrogen gas was admitted, the gas was vented, hydrogen was readmitted (80 psi), and the reaction mixture was stirred. Aliquots were diluted with CDCl_3 and analyzed via $^1\text{H NMR}$ spectroscopy. These aliquots showed ca. 35% conversion at both 12 h and 24 hours. Additional Pd/C (50 mg) was added, and the Fisher-Porter tube was re-pressurized. The reaction mixture no longer consumed hydrogen gas after 4 h, and at this time, the Fisher-Porter tube was depressurized, filtered through Celite, and concentrated to a highly viscous oil. The oil was further purified via MPLC (silica, 1:1 EtOAc:Hex) to give 5-carbomethoxyvalerolactone (**507^{5Me}**, 281 mg, 81% yield) as a clear, highly viscous oil.

$^1\text{H NMR}$ (500 MHz, CDCl_3) δ 4.97 (dd, $J = 5.8, 4.7$ Hz, 1H, CO_2CH), 3.83 (s, 3H, CO_2Me), 2.63 (dddd, $J = 18.2, 6.9, 6.0, 0.8$ Hz, 1H, $\text{CH}_a\text{H}_b\text{CO}_2\text{CH}$), 2.58 (ddd, $J = 18.2, 7.7, 7.7$ Hz, 1H, $\text{CH}_a\text{H}_b\text{CO}_2\text{CH}$), 2.16 (dddd, $J = 14.3, 8.3, 6.0, 5.2$ Hz, 1H), 2.04 (dq, $J = 14.3, 5.7, 1.4$, 1H), and 1.92–1.86 (m, 2H).

$^{13}\text{C NMR}$ (125 MHz, CDCl_3) δ 170.3, 169.2, 77.0, 52.9, 29.7, 25.1, and 17.7.

Poly(5-carbomethoxyvalerolactone) [Poly(501**^{5Me})]**

In a nitrogen-filled glovebox, BnOH (1.0 equiv, 2.6 μ L, 0.025 mmol), diphenyl phosphate [DPP, (PhO)₂PO₂H, 0.50 equiv, 3.2 mg, 0.013 mmol], 5-carbomethoxyvalerolactone (**501**^{5Me}, 28 equiv, 112 mg, 0.709 mmol), and a stir bar were added sequentially to a 1-dram vial. The vial was sealed with a Teflon-lined cap and the mixture was stirred for 23 h at ambient temperature. At this time, an aliquot (ca. 3 mg) was dissolved in CDCl₃ (0.55 mL) with NEt₃ (ca. 1 μ L) and analyzed via ¹H NMR spectroscopy, which indicated ca. 15% monomer conversion. The vial was placed into an oil bath at 55 °C for 70 h (89% monomer conversion). The vial was removed from the oil bath, and the sample was dissolved in NEt₃ (ca. 10 μ L) and DCM (1–2 mL). The polymer was precipitated by dropwise addition into stirred 5:1 Hex:EtOAc (15 mL). The vial was cooled (0 °C) and centrifuged, and the supernatant was decanted. DCM (ca. 1 mL) was added to redissolve the polymer and 5:1 Hex:EtOAc (ca. 15 mL) was slowly added to the stirred polymer/DCM solution to reprecipitate the polymer. The sample was once again cooled (0 °C), centrifuged, decanted, and placed under vacuum (ca. 0.1 mmHg) at 60 °C for 10 h to give poly(5-carbomethoxyvalerolactone) (**poly(501**^{5Me}), 69 mg, 60% yield) as a light yellow, viscous oil.

¹H NMR (500 MHz, CDCl₃): δ 7.39–7.31 (m, 5H, Ar), 5.12 (s, 2H, ArCH₂O), 5.01 [dd, J = 7.4, 5.0 Hz, 26H (26 repeat units (RUs), CO₂CHCO₂Me)], 4.20 [dd, J = 7.5, 3.7, 1H, HOCHCO₂Me (End group)], 3.75 [s, 75H (25 RUs), CO₂CH₃^{RU}], 2.52–2.38 [m, 53H (27 RUs), -CH₂CO₂Me^{RU}], 1.98–1.84 [m, 55H (28 RUs)], 1.98–1.84 [m, 55H (28 RUs)], and 1.83–1.69 [m, 55H (28 RUs)].

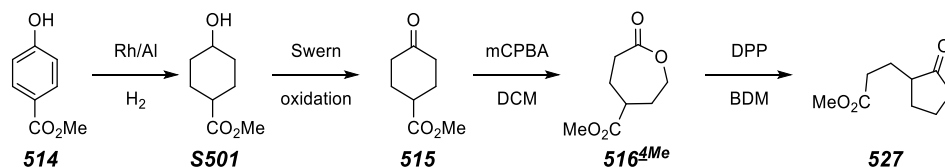
¹³C NMR (500 MHz, CDCl₃): δ 172.5, 170.4, 72.0, 52.4, 33.2, 30.3, 20.5 and 20.6 (there are many resonances we attribute to benzyl ester and the first benzyl ester-RU).

IR (neat, selected peaks) 2955, 2874, 1732 (strong), 1438, 1206 (med), 1148 (strong), and 1086 (med) cm⁻¹.

TGA T_d 1% = 183 °C, 5% = 260 °C.

DSC Cooling and heating rates of 5 °C/min: T_g = -5 °C

S5.2.5 4-Carbomethoxycaprolactone (**516**^{4Me}) preparation and isomerization



Methyl 4-hydroxybenzoate (514) was hydrogenated to **S501** according to literature precedent.⁴

4-Carbomethoxycyclohexanone (methyl 4-oxocyclohexane-1-carboxylate, **515**^{4Me})

DMSO (2 equiv, 1.8 mL, 52 mmol) and DCM (24 mL) were placed into a flame-dried, two-neck, 500-mL round bottom flask fitted with a stir bar. Rubber septa were added, and the headspace of the flask was purged by slowly bubbling nitrogen gas into the headspace over the course of ca. 20 min. The flask was cooled in a dry ice-acetone bath (15 minutes). Oxalyl chloride [(COCl)₂, 1.5 equiv, 2.8 mL, 39 mmol] in DCM (20 mL) was added dropwise over ca. 10 minutes. Alcohol **S501** (1 equiv, 4.08 g, 25.8 mmol) in DCM (25 mL) was added over 25 minutes, and the reaction mixture was stirred for an additional 30 minutes. NEt₃ (4 equiv, 14.4 mL, 103 mmol) was added dropwise over ca. 5 minutes, and the flask was removed from the cold bath and slowly allowed to warm to room temperature overnight. The mixture was concentrated; the white solid was suspended in DCM; and the organic layer was washed (NH₄Cl and brine), dried (MgSO₄), and concentrated to afford 4-carbomethoxycyclohexanone (**515**^{4Me}, 4.08 g, quantitative) as a light-yellow oil that was used without further purification. Spectroscopic data matched those previously reported.⁵

4-Carbomethoxycaprolactone (Methyl 7-oxooxepane-4-carboxylate, **516**^{4Me})

4-Carbomethoxycyclohexanone (**515**, 400 mg, 2.56 mmol) was placed into a 20-mL scintillation vial and dissolved in DCM (6 mL) and saturated NaHCO₃ (aq, 6 mL). mCPBA (70% by mass, 1.16 g, 4.71 mmol) was added portionwise over 5 minutes. After 4 h, another portion of mCPBA (500 mg) was added and the solution was stirred

overnight. The aqueous phase was removed via pipette and the organic phase placed into the freezer. The cold organic phase was filtered, diluted in EtOAc, washed [NaSO₃ (2x), NaHCO₃ (2x), brine (1x)], dried (MgSO₄), and concentrated to give a wet white solid containing a 1:1 mixture (254 mg) of lactone and m-chlorobenzoic acid. The crude mixture was purified via column chromatography (silica, 1:1 EtOAc: Hex) to give methyl 7-oxooxepane-4-carboxylate (**516**^{4Me}, 182 mg, 41% yield) as a colorless oil.

¹H NMR (500 MHz, CDCl₃) δ 4.38 (ddd, *J* = 13.3, 7.3, 1.6 Hz, 1H, CO₂CH_aH_b), 4.20 (ddd, *J* = 13.3, 8.8, 1.4 Hz, 1H, CO₂CH_aH_b), 3.72 (s, 3H, -CO₂Me), 2.79 (ddd, *J* = 14.4, 9.2, 1.7 Hz, 1H, CH_aH_bCO₂), 2.72 (tdd, *J* = 9.3, 4.1, 4.1 Hz, 1H, -CHCO₂Me), 2.62 (ddd, *J* = 14.4, 11.0, 1.9 Hz, 1H, CH_aH_bCO₂), 2.19 (dddd, *J* = 15.7, 7.0, 4.2, 1.3, 1.3 Hz, 1H, -CH₂CH₂CO₂), 2.15–2.06 (m, 2H, CO₂CH₂CH₂), 1.97 (dddd, *J* = 14.7, 11.0, 9.3, 1.8 Hz, -CH₂CH₂CO₂).

¹³C NMR (125 MHz, CDCl₃) δ 175.1, 174.1, 66.8, 52.3, 44.1, 32.3, 31.5, and 25.0.

IR (neat, selected peaks): 2954, 2872, 1722 (strong), 1169 (strong), and 1069 (strong) cm⁻¹.

HRMS: Calculated for (C₈H₁₂O₄Na)⁺ 195.0628; found: 195.0632.

Methyl 3-(2-oxotetrahydrofuran-3-yl)propanoate (522)

4-Carbomethoxycaprolactone (**516**^{4Me}, 50.0 equiv, 100 mg, 0.581 mmol), benzene dimethanol (1 equiv, 1.6 mg, 0.012 mmol), and diphenyl phosphate [DPP, (PhO)₂PO₂H, 1 equiv, 2.9 mg, 0.012 mmol], and a stir bar were placed in 0.5-dram vial, and the vial was capped. The contents were stirred were for 48 h at ambient temperature, and an aliquot was taken (ca. 2 mg), diluted in CDCl₃, and analyzed via ¹H NMR spectroscopy. The spectrum showed complete consumption of **516**^{4Me}, ca. 67% conversion to butyrolactone **522**, and additional resonances corresponding to what appeared to be an oligomeric material. The vial was again capped and heated at 45 °C for 24 h and another ¹H NMR spectrum of an aliquot was taken, which showed no change in the ratio of products. A portion of this

reaction mixture was purified by MPLC (silica, 1:1 EtOAc:Hex) to give methyl 3-(2-oxotetrahydrofuran-3-yl)propanoate (**522**) as a colorless oil.

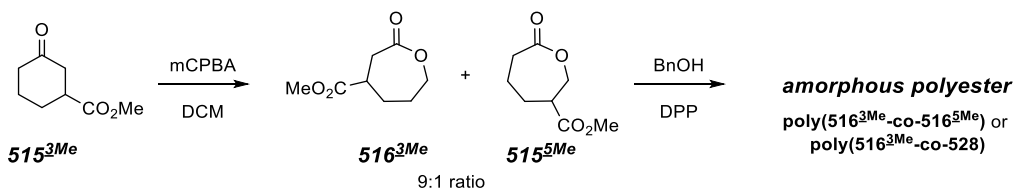
$^1\text{H NMR}$ (500 MHz, CDCl_3) δ 4.36 (ddd, $J = 9.2, 8.3, 2.6$ Hz, 1H, $\text{CO}_2\text{CH}_a\text{H}_b$), 4.19 (ddd, $J = 9.8, 9.1, 6.6$ Hz, 1H, $\text{CO}_2\text{CH}_a\text{H}_b$), 3.69 (s, 3H, CO_2Me), 2.61 (dddd, $J = 10.5, 8.7, 7.9, 6.4$ Hz, 1H, CHCO_2CH_2), 2.54 (dd, $J = 7.1, 1.6$ Hz, 1H, $\text{MeCO}_2\text{CH}_c\text{H}_d$), 2.52 (dd, $J = 7.0, 1.2$ Hz, 1H, $\text{MeCO}_2\text{CH}_c\text{H}_d$), 2.42 (dddd, $J = 12.6, 8.6, 6.6, 2.7$ Hz, 1H, $\text{CO}_2\text{CH}_2\text{CH}_e\text{H}_f$), 2.16 (dddd, $J = 14.2, 7.9, 7.1, 6.4$ Hz, 1H, $\text{MeCO}_2\text{CH}_2\text{CH}_g\text{H}_h$), 1.96 (dddd, $J = 12.6, 10.6, 9.8, 8.5$ Hz, 1H, $\text{CO}_2\text{CH}_2\text{CH}_e\text{H}_f$), and 1.84 (dddd, $J = 14.1, 8.0, 7.6, 7.3$ Hz, $\text{MeCO}_2\text{CH}_2\text{CH}_g\text{H}_h$).

$^{13}\text{C NMR}$ (125 MHz, CDCl_3) δ 178.8, 173.3, 66.5, 51.9, 38.5, 31.6, 28.9, and 25.6.

IR (neat, selected peaks): 2954, 1768, 1735 (strong), 1438, 1376, 1174, 1152 cm^{-1} .

HRMS: Calculated for $(\text{C}_8\text{H}_{12}\text{O}_4\text{Na})^+$ 195.0628; found: 195.0633

S5.2.6 3-Carbomethoxycaprolactone (**516**^{3Me}) and 5-Carbomethoxy-caprolactone (**516**^{5Me}) preparation and polymerization



3-Carbomethoxycyclohexanone [Methyl 3-oxocyclohexane-1-carboxylate, **515**^{3Me}]

3-Carbomethoxycyclohexanone (**515**^{3Me}) was prepared in an analogous fashion to 4-carbomethoxycyclohexanone (**515**^{4Me}) as described above to afford a light-yellow oil that was used without further purification. Spectroscopic characterization was consistent with previous reports.⁶

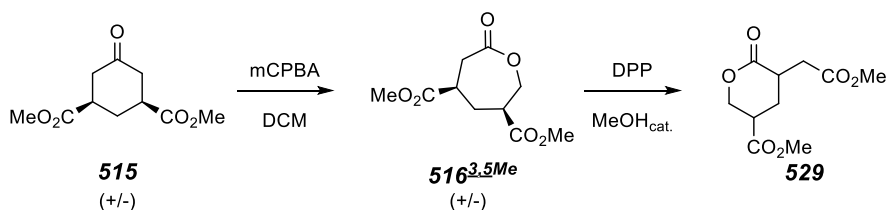
3-Carbomethoxycaprolactone (**516**^{3Me})

A Baeyer-Villiger oxidation of **515**^{3Me} was performed as described for 4-carbomethoxycaprolactone above to give a ca. 9:1 mixture of **516**^{3Me} to **516**^{5Me}. A small portion of this mixture was purified by MPLC (silica, 1:3 EtOAc:Hex)

¹H NMR (500 MHz, CDCl₃) δ 4.30 (dddd, *J* = 12.9, 6.0, 1.8, 0.9 Hz, 1H, CO₂CH_aH_b), 4.22 (ddd, *J* = 12.9, 9.4, 1.1 Hz, 1H, CO₂CH_aH_b), 3.72 (s, 3H, CO₂Me), 2.93 (ddd, *J* = 14.0, 2.8, 1.2 Hz, 1H, CH_aH_bCO₂CH₂), 2.89 (dd, *J* = 14.1, 9.9 Hz, 1H, CH_aH_bCO₂CH₂), 2.73 [m, 1H, CH(CO₂Me)CH₂CO₂], 2.22–2.15 (m, 1H), 2.10–2.02 (m, 1H), and 1.91–1.80 (m, 2H).

¹³C NMR (125 MHz, CDCl₃) δ 174.0, 173.5, 68.8, 52.5, 39.5, 36.6, 31.8, and 27.9.

S5.2.7 Dimethyl 3,5-dicarbomethoxycaprolactone (dimethyl cis-7-oxooxepane-3,5-dicarboxylate, **516**^{3,5Me}) preparation and isomerization



Dimethyl 5-oxocyclohexane-1,3-dicarboxylate (**515**^{3,5Me}) was prepared using a Swern oxidation as described above for 4-carbomethoxycyclohexanone (**515**^{4Me}). The mixture of products, which contained “dehydroxylated product”⁷ was purified by recrystallization (EtOAc) to give 5-oxocyclohexane-1,3-dicarboxylate (**515**^{3,5Me}) as white needles [**mp** = 121–123 °C (Lit. = 118.5–122 °C)⁸].

3,5-Dicarbomethoxycaprolactone (**516**^{3,5Me})

3,5-Dicarbomethoxycaprolactone (**516**^{3,5Me}) from dimethyl 3,5-dicarbomethoxycyclohexanone (**515**^{3,5Me}, 289 mg, 1.34 mmol) was synthesized in an analogous fashion to methyl 4-carbomethoxycaprolactone (**516**^{3,5Me}) as described above. The crude product was purified by MPLC (silica, 1:1 Hex:EtOAc) to give dimethyl 3,5-dicarbomethoxycaprolactone (**516**^{3,5Me}, 187 mg, 61% yield) as an amorphous solid.

¹H NMR (500 MHz, CDCl₃) δ 4.55 (ddd, *J* = 13.1, 1.9, 1.9 Hz, 1H, CO₂H_aH_b), 4.28 (ddd, *J* = 13.2, 9.5, 0.6 Hz, 1H, CO₂H_aH_b), 3.74 (s, 3H, CO₂Me), 3.73 (s, 3H, CO₂Me), 3.00 (ddd, *J* = 14.2, 1.9, 1.9 Hz, 1H, CH_cH_dCO₂), 2.90 (dd, *J* = 14.2, 11.6 Hz, 1H, CH_cH_dCO₂), 2.85 (dddd, *J* = 13.1, 9.4, 3.6, 2.1 Hz, 1H, CO₂CH₂CH), 2.76 (ddd, *J* = 11.8, 11.8, 3.5, 2.0 Hz, 1H, CHCH₂CO₂CH₂), 2.59 (dddd, *J* = 13.9, 5.2, 3.4, 1.7 Hz, 1H, CHCH_eH_fCH), and 1.96 (ddd, *J* = 14.0, 12.0, 12.0 Hz, CHCH_eH_fCH). *HSQC and COSY were used to determine the proton environment.*

¹³C NMR (125 MHz, CDCl₃) δ 173.3, 172.5, 171.6, 68.5, 52.7, 52.6, 44.5, 38.9, 36.1, and 34.5.

IR (neat, selected peaks): 2956, 1732, 1436, 1265, 1187, and 1167 cm⁻¹.

HRMS: Calculated for (C₁₀H₁₄O₆Na)⁺ 253.0683; found: 253.0659.

Methyl 5-(2-methoxy-2-oxoethyl)-6-oxotetrahydro-2H-pyran-3-carboxylate (529)

3,5-Dicarbomethoxycaprolactone (**516**^{3,5Me}, 26.1 mg, 0.113 mmol), MeOH (ca. 1 μL), diphenyl phosphate (DPP, 1 mg, 0.005 mmol), CDCl₃ (150 μL), and a stir bar were placed in a 1-dram vial. The vial was capped, and the mixture was stirred at ambient temperature for three days. The solution was purified by MPLC (1:1 EtOAc:Hex) to give 3,5-dicarbomethoxycaprolactone (**516**^{3,5Me}, 22.7 mg, 87% yield) as a colorless oil.

¹H NMR (500 MHz, CDCl₃) δ 4.55 (dd, *J* = 11.5, 5.3 Hz, 1H, CO₂CH_aH_b), 4.49 (ddd, *J* = 11.5, 8.4, 1.0 Hz, 1H, CO₂CH_aH_b), 3.76 (s, 3H, CO₂Me), 3.72 (s, 3H, CO₂Me), 3.11 (dddd, *J* = 11.7, 8.1, 5.9, 5.9 Hz, 1H, CO₂CH₂CH), 3.04 (dddd, *J* = 8.4, 8.4, 5.3, 5.4 Hz, 1H, MeO₂CCH₂CH), 2.77 (dd, *J* = 17.1, 5.7 Hz, 1H, MeO₂CCH_cH_d), 2.65 (dd, *J* = 17.1, 6.0 Hz, 1H, MeO₂CCH_cH_d), 2.48 (dddd, *J* = 13.8, 8.1, 5.4, 0.9 Hz, 1H, CHCH_eH_fCH), and 1.92 (ddd, *J* = 13.8, 11.7, 8.5 Hz, 1H, CHCH_eH_fCH).

¹³C NMR (125 MHz, CDCl₃) δ 173.0, 171.9, 171.8, 67.6, 52.7, 52.2, 38.2, 35.2, 34.0, and 27.0.

IR (neat, selected peaks): 2956, 1733 (strong), 1454, 1200, 1157 cm⁻¹.

HRMS: Calculated for (C₁₀H₁₄O₆Na)⁺ 253.0683; found: 253.0669

S5.3 Polymer characterization data

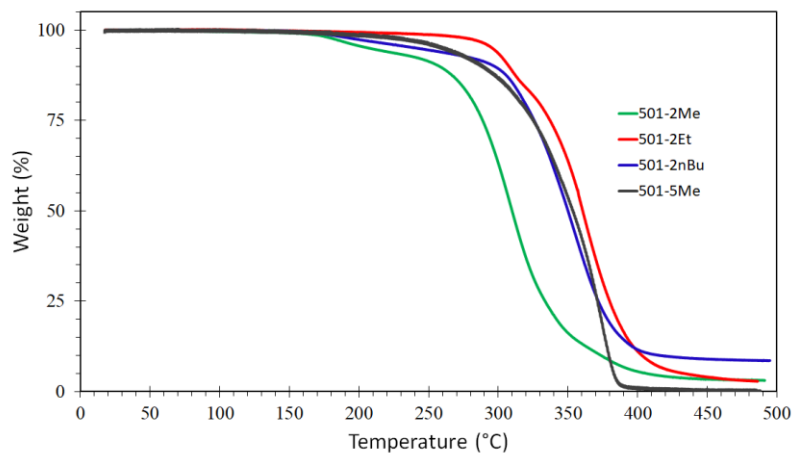


Figure S5.1 Thermogravimetric analysis of **501^{2Me}**, **501^{2Et}**, **501^{2nBu}**, and **501^{5Me}**.

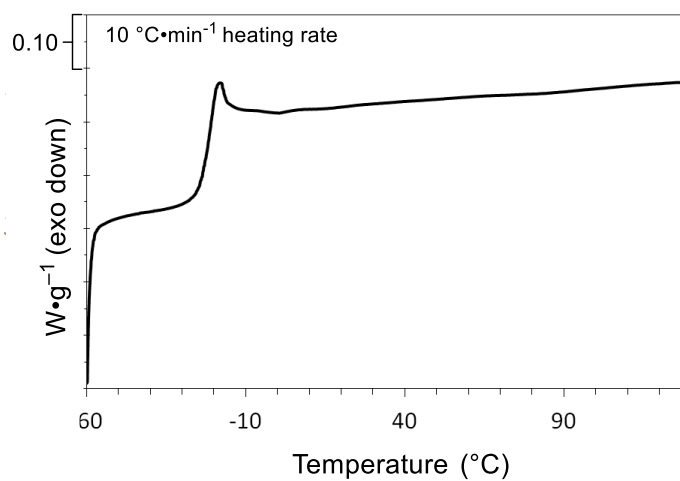


Figure S5.2 DSC thermogram of **poly(501^{2Me})**. This data was collected on the second heating cycle at a heating rate of 10 °C·min⁻¹. The T_g for **poly(501^{2Me})** occurs at -20 °C.

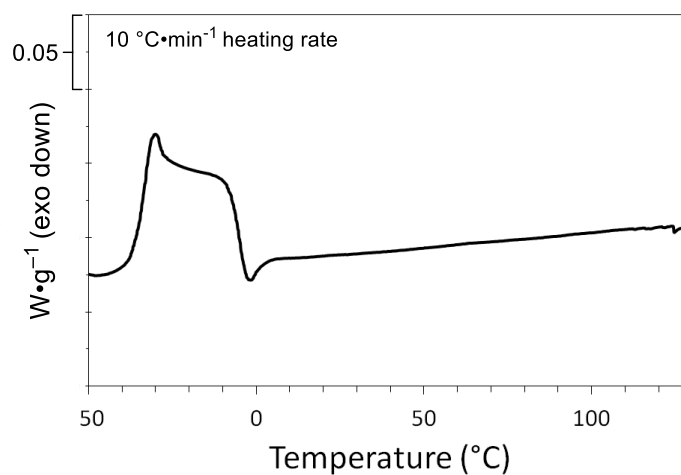


Figure S5.3 DSC thermogram of **poly(501^{2Et})**. This data was collected on the second heating cycle at a heating rate of 10 °C·min⁻¹. The T_g for **poly(501^{2Et})** occurs at -34 °C and contains an interesting exotherm at -5 °C.

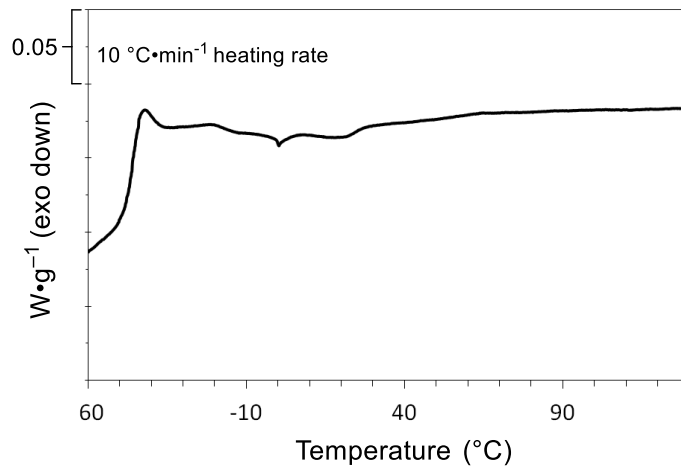


Figure S5.4 DSC thermogram of **poly(501^{2nBu})**. This data was collected on the second heating cycle with a heating rate of 10 °C·min⁻¹. The T_g for **poly(501^{2nBu})** occurs at -46 °C.

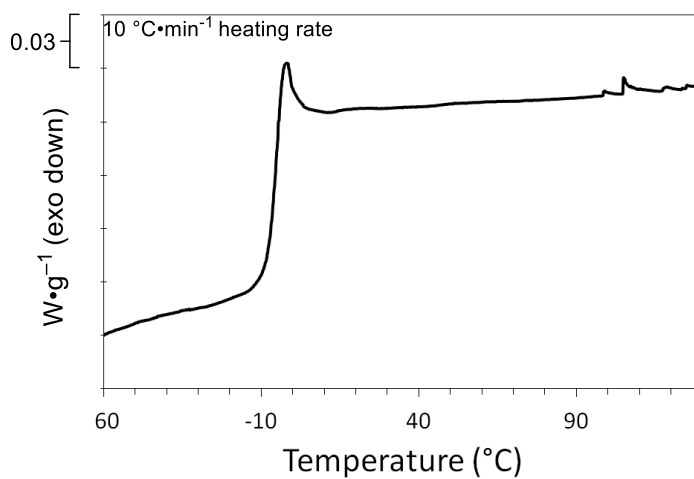


Figure S5.5 DSC thermogram of **poly(501⁵Me)**. This data was collected on the second heating cycle with a heating rate of 10 °C·min⁻¹. The T_g for **poly(501⁵Me)** occurs at -5 °C.

S5.4 References

- ¹ Jakubec, P.; Farley, A. J. M.; Dixon, D. J. Towards the total synthesis of keramaphidin B. *Beilstein J. Org. Chem.* **2016**, *12*, 1096–1100.
- ² Wright, J. L.; Caprathe, B. W.; Downing, D. M.; Glase, S. A.; Heffner, T. G.; Jaen, J. C.; Johnson, S. J.; Kesten, S. R.; MacKenzie, R. G.; Meltzer, L. T.; Pugsley, T. A.; Smith, S. J.; Wise, L. D.; Wustrow, D. J. The discovery and structure-activity relationships of 1,2,3,6-tetrahydro-4-phenyl-1-[(arylcyclohexenyl)alkyl]pyridines. Dopamine autoreceptor agonists and potential antipsychotic agents. *J. Med. Chem.* **1994**, *37*, 3523–3533.
- ³ Wiley, R. H.; Hart, A. J. 2-Pyrones. IX. 2-Pyrone-6-carboxylic acid and its derivatives. *J. Am. Chem. Soc.* **1954**, *76*, 1943–1944.
- ⁴ Charlton, J. L.; Sayeed, V. A.; Lypka, G. N. Xanthocyclines: 5-Oxaanthracyclines (7,8,9,10-tetrahydrobenzo[b]xanthen-12-one). *Can. J. Chem.* **1982**, *60*, 1996–2001.
- ⁵ Cregge, R. J.; Lentz, N. L.; Sabol, J. S. Conformationally restricted leukotriene antagonists. Synthesis of chiral 4-hydroxy-4-alkylcyclohexanecarboxylic acids as Leukotriene D4 analogues. *J. Org. Chem.* **1991**, *56*, 1758–1763.
- ⁶ Moteki, S. A.; Usui, A.; Zhang, T.; Soloria Alvarado, C. R.; Maruoka, K. Site-selective oxidation of unactivated C_{sp3}-H bonds with hypervalent iodine(III) reagents. *Angew. Chem. Int. Ed.* **2013**, *52*, 8657–8660.
- ⁷ Breining, S. R.; Melvin, M.; Bhatti, B. S.; Byrd, G. D.; Kiser, M. N.; Hepler, C. D.; Hooker, D. N.; Zhang, J.; Reynolds, L. A.; Benson, L. R.; Fedorov, N. B.; Sidach, S. S.; Pike Mitchener, J.; Lucero, L. M.; Lukas, R. J.; Whiteaker, P.; Yohannes, D. Structure-activity studies of 7-heteroaryl-3-azabicyclo[3.3.1]non-6-enes: A novel class of highly potent nicotinic receptor ligands. *J. Med. Chem.* **2012**, *55*, 9929–9945.
- ⁸ Gensler, W. J.; Solomon, H. P. Synthesis of chaminic acid. *J. Org. Chem.* **1973**, *38*, 1726–1731.

Appendix E. Supporting information for Chapter 6 (S6)

Parts of this supporting information was performed and prepared by Dr. Nicolas Ball-Jones

| | | |
|--------------|---|------------|
| S6.1 | General experimental protocols | 273 |
| S6.2. | Small molecule and monomer synthesis | 275 |
| S6.2.1 | (<i>Z</i>)-3-Methylpenta-2,4-dienoic acid (606-H) | 275 |
| S6.2.2 | Methyl (<i>Z</i>)-3-Methylpenta-2,4-dienoate (606-Me) | 276 |
| S6.2.3 | Ethyl (<i>Z</i>)-3-Methylpenta-2,4-dienoate (606-Et)..... | 277 |
| S6.2.4 | Butyl (<i>Z</i>)-3-Methylpenta-2,4-dienoate (606-ⁿBu)..... | 278 |
| S6.2.5 | <i>tert</i> -Butyl (<i>Z</i>)-3-Methylpenta-2,4-dienoate (606-^tBu)..... | 279 |
| S6.2.6 | 3-Methylpenta-2,4-dienamide (614-NH₂) | 280 |
| S6.2.7 | <i>N</i> ,3-Dimethylpenta-2,4-dienamide (614-NHMe)..... | 282 |
| S6.2.8 | <i>N,N</i> ,3-Trimethylpenta-2,4-dienamide (614-NMe₂)..... | 284 |
| S6.3 | Polymer synthesis | 286 |
| S6.3.1 | Poly(methyl isoprenecarboxylate) [poly(606-Me)] | 286 |
| S6.3.2 | Poly(ethyl isoprenecarboxylate) [poly(606-Et)] | 289 |
| S6.3.3 | Poly(<i>n</i> -butyl isoprenecarboxylic acid) [poly(606-ⁿBu)] | 291 |
| S6.3.4 | Poly(<i>t</i> -butyl ester isoprenecarboxylate) [poly(606-^tBu)] | 292 |
| S6.3.5 | Poly(carboxamide) [poly(614-R ¹ R ²)]..... | 294 |
| S6.4. | Polymer characterization data | 295 |
| S6.4.1 | Size exclusion chromatography | 295 |
| S6.4.2 | Thermogravimetric analysis | 296 |
| S6.4.4 | Linear viscoelastic (rheological) measurements..... | 301 |
| S6.5 | References | 306 |

S6.1 General experimental protocols

Anhydrous THF, DCM, and diethyl ether were taken immediately prior to use from a column of activated alumina. Reported reaction temperatures are the temperature of the external heating or cooling bath.

Instrumental methods:

NMR: ^1H and ^{13}C NMR spectra were recorded on a Bruker Avance 500 (500 MHz) or a Varian Inova 500 (500 MHz) spectrometers. ^1H NMR chemical shifts in CDCl_3 are referenced to TMS (δ 0.00 ppm). Non-first-order multiplets in ^1H NMR spectra have been identified as 'nfom.' The following format is used to report resonances: chemical shift in ppm [multiplicity, coupling constant(s) in Hz, integral, and assignment]. ^1H NMR assignments are indicated by the substructural environment (e.g., CH_aH_b). Coupling constant analysis was led by methods we have described elsewhere.¹ ^{13}C NMR chemical shifts for spectra recorded in CDCl_3 are referenced to the carbon resonance in CDCl_3 (δ 77.16).

ATR-FTIR: Fourier transform infrared (FTIR) spectra were recorded with a Bruker Alpha Platinum ATR-FTIR instrument (diamond single-bounce crystal). Typically 16 scans were acquired and a 4 s acquisition time was used.

Mass spectrometry of non-polymeric samples: MS measurements were made using electron impact ionization on an Agilent 5975 MSD at 70 eV GC-MS. The column stationary phase was an Agilent HP-5 with a 0.25 μm film thickness, 30 m long, \times 0.32 mm i.d.

Size Exclusion Chromatography (SEC): SEC was conducted on a liquid chromatograph (Agilent 1100 series) fitted with a refractive index detector (HP1047A). Polymer samples were dissolved in CHCl_3 (1-2 $\text{mg}\cdot\text{mL}^{-1}$) and eluted through three successive Varian PLgel Mixed C columns (7.5 mm id; 25 cm l) at 35 $^\circ\text{C}$ at a flow rate of 1 $\text{mL}\cdot\text{min}^{-1}$. Dispersity and mass-average molar mass of the samples were referenced to polystyrene standards.

Thermogravimetric Analysis (TGA): TGA was performed (TA Instruments Q500) at a heating rate of 10 °C•min⁻¹ under an atmosphere of nitrogen. The sample size was 5–15 mg.

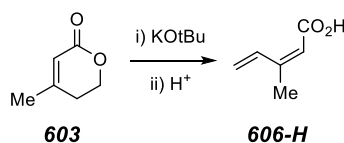
Differential Scanning Calorimetry (DSC): Differential scanning calorimetry (TA Instruments Q-1000 DSC) was performed on samples hermetically sealed in aluminum pans. Each sample was heated to 250 °C, cooled to -60 °C, and reheated to 250 °C. Glass transition temperatures were taken as the inflection point and are reported as measured on the second (or third) heating cycle.

Linear Viscosity (Rheology) Measurements: A 0.50 g sample of solid polymer was placed onto the bottom rheometer plate (2.5 cm d) held at the desired reference temperature (70 °C above the T_g). The top plate was manually lowered under a steady rate sweep at a frequency of 0.1/s for approximately 2 full rotations to prepare the sample for the measurements. A dynamic strain sweep was taken at this temperature to ensure linearity within the sample. The dynamic linear viscoelastic measurements were carried out within the linear viscoelastic regime at temperatures in the range from 10 to 125 °C. The dynamic measurements were conducted in the range of 0.1–100 rad/s at a strain of 1%. A gap of approximately 1.0 mm was used to minimize edge effects. The rheological measurements were carried out under an atmosphere of nitrogen to minimize oxidative events of the polymer samples during testing. Entanglement molecular weights were approximated using the equation $M_e = \frac{4}{5} \frac{\rho RT}{G_N}$. The plateau moduli were calculated using the minimum of tan delta vs G' .

S6.2. Small molecule and monomer synthesis

S6.2.1 (Z)-3-Methylpenta-2,4-dienoic acid (**606-H**)

Synthesized following a modified literature procedure.²



To a 50 mL two-neck round bottom flask equipped with a stir bar was added potassium metal (1.08 equiv, 0.487 g, 12.5 mmol), followed by dry, warm *tert*-butanol (10.1 equiv, 11.2 mL, 117 mmol). A bubbler was affixed to allow for the escape of hydrogen gas and the mixture was stirred under a slight positive pressure of nitrogen. After one hour at room temperature, the mixture was heated to 80 °C and stirred for 21 h until complete dissolution of the solid potassium had occurred. This solution of potassium *tert*-butoxide (1.06 M) was added rapidly to a stirring solution of 4-methyl-5,6-dihydro-2*H*-pyran-2-one (**603**, 1 equiv, 1.3 g, 11.6 mmol) in diethyl ether (8 mL). Immediate appearance of a precipitate was observed. The solid was collected by filtration (1.77 g). Analysis by ¹H NMR spectroscopy (D₂O) indicated the solid to contain potassium (*Z*)-3-methylpenta-2,4-dienoate (**606-K**), potassium formate (a few percent), and potassium (*Z*)-5-hydroxy-3-methylpent-2-enoate. The purity of **606-K** was judged to be ca. 90%.

Alternatively, commercially available potassium *tert*-butoxide was used to synthesize **606-K**. Anhydromevalanolactone (**603**, 1 equiv, 6.06 g, 54.1 mmol) was dissolved in diethyl ether (15 mL) and added to a cooled (0 °C) solution of *tert*-butoxide (6.67 g, 59.6 mmol) in *tert*-butanol (20 mL) and diethyl ether (15 mL) in a 250 mL round bottom flask. A precipitate formed nearly immediately. After being stirred for approximately 10 minutes, the slurry was filtered, and the solid was rinsed thoroughly with diethyl ether. The crude mixture (8.70 g) was recovered as a tan solid. Similar purity was observed as described above. This material was used without further purification. (The yield of acid **606-H**, obtained by the acidification procedure described below, was 5.34 g or 88%.)

The salt **606-K** (35 g) was dissolved in water (200 mL) and diethyl ether (100 mL) was added. Aqueous hydrochloric acid was added to this mixture until the pH of the aqueous portion fell to ca. 3). The aqueous portion was extracted with additional diethyl ether. The combined organic layers were dried over MgSO₄, filtered, and concentrated to provide acid **606-H** (20 g, 77% yield).

The material could be molecularly distilled in a sublimation apparatus held at ca. 210 °C at ca. 1 torr. Acid (**606-H**) was found to be somewhat sensitive to light and was stored in the dark.

¹H NMR (500 MHz, CDCl₃) δ 12.06 (br s, CO₂H), 7.80 (ddd, *J* = 17.6, 10.9, 0.9 Hz, 1H, CH₂=CHR), 5.76 (br dq, *J* = 1.4, 1.4 Hz, 1H, =CHCO₂H), 5.65 (ddd, *J* = 17.6, 1.3, 0.8 Hz, 1H, CH_ZH_E=CHR), 5.49 (ddd, *J* = 10.9, 1.4, 1.4 Hz, 1H, CH_ZH_E=CHR), and 2.05 (d, *J* = 1.3 Hz, 3H).

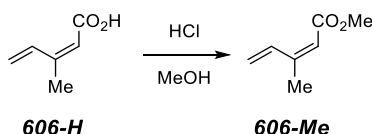
¹³C NMR (125 MHz, CDCl₃) δ 171.8, 153.5, 133.9, 121.6, 117.5, and 20.6.

IR (neat, selected peaks): 2984, 2962, 1684, 1633, 1587, and 1427, 1395 cm⁻¹.

mp: 68–73 °C.

GC-MS (30 m x 0.25 mm ID, HP-5, 50 °C/2.0 min/20 °C min⁻¹ /250 °C) *t_R* = 3.38 min; MS [70 eV, *m/z* (rel int)]: 112 (96, M⁺), 111 (100, M⁺-H), 97 (62, M⁺-Me), and 94 (36, M⁺-H₂O).

S6.2.2 Methyl (*Z*)-3-Methylpenta-2,4-dienoate (**606-Me**)



To an 80 mL screw cap topped culture tube equipped with a stir bar was added methanol (28 equiv, 25 mL, 0.6 mol) and thionyl chloride (25 mol %, 0.4 mL, 5.51 mmol). After five minutes, (*Z*)-3-methylpenta-2,4-dienoic acid (**606-H**, 1 equiv, 2.44 g, 21.8 mmol) was added followed by phenothiazine (7 mol %, 0.03 g, 0.15 mmol). The tube was capped and stirred at 76 °C for 18 h and allowed to cool. The contents were added to a

saturated solution of sodium bicarbonate (100 mL) followed by extraction with diethyl ether (100 mL x 3). The organic layers were combined, dried (MgSO₄), and concentrated *in vacuo*. ¹H NMR analysis of an aliquot of this crude reaction product indicated that all of the acid had been consumed. This material was distilled at ambient temperature under reduced pressure (1.5 torr) into a flask cooled in a -78 °C bath to afford methyl (*Z*)-3-methylpenta-2,4-dienoate (**606-Me**, 2.18 g, 17.3 mmol, 79% yield). Visual inspection of the reaction mixture when no phenothiazine was added led us to conclude that polymerization had occurred.

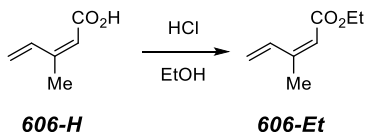
¹H NMR (500 MHz, CDCl₃) δ 7.81 (ddd, *J* = 17.6, 10.9, 0.8 Hz, 1H, CH₂=CHR), 5.74 (qddd, *J* = 1.4, 1.4, 0.7, 0.7 Hz, 1H, =CHCO₂Me), 5.61 (br ddd, *J* = 17.6, 1.3, 0.7 Hz, 1H, CH_ZH_E=CHR), 5.47 (ddd, *J* = 10.9, 1.5, 1.5 Hz, 1H, CH_ZH_E=CHR), 3.72 (s, 3H, OMe), and 2.02 (d, *J* = 1.4 Hz, 3H, =CMe).

¹³C NMR (125 MHz, CDCl₃) δ 166.6, 151.0, 134.0, 120.8, 117.8, 51.2, and 20.4.

IR (neat, selected peaks): 3095, 1710, 1637, and 1590 cm⁻¹.

GC-MS (30 m x 0.25 mm ID, HP-5, 50 °C/2.0 min/20 °C min⁻¹ /250 °C) *t*_R = 2.73 min; MS [70 eV, *m/z* (rel int)]: 126 (100, M⁺), 125 (80, M⁺-H), 111 (72, M⁺-Me), 95 (99, M⁺-OMe), and 67 (99, M⁺-CO₂Me).

S6.2.3 Ethyl (*Z*)-3-Methylpenta-2,4-dienoate (**606-Et**)



To an 80 mL screw cap topped culture tube equipped with a stir bar was added ethanol (19 equiv, 50 mL, 0.85 mol) and thionyl chloride (24 mol %, 0.8 mL, 11 mmol). After five minutes, (*Z*)-3-methylpenta-2,4-dienoic acid (1 equiv, 4.7 g, 43 mmol) was added followed by phenothiazine (3 mol %, 0.03 g, 0.15 mmol). The tube was capped and stirred at 86 °C for 18 h and allowed to cool. The contents were added to a saturated solution of sodium bicarbonate (100 mL) and then extracted with diethyl ether (100 mL x 3). The organic layers were combined, dried (MgSO₄), and concentrated *in vacuo*. This

material was distilled at 35 °C under reduced pressure (1.5 torr) into a flask cooled in a –78 °C bath to afford ethyl (*Z*)-3-methylpenta-2,4-dienoate (**606-Et**, 3.52 g, 25.2 mmol, 59% yield, 91:9 mixture of *Z*:*E* isomers).

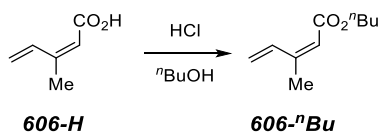
¹H NMR (500 MHz, CDCl₃) δ 7.81 (ddd, *J* = 17.6, 10.9, 0.8 Hz, 1H, CH₂=CHR), 5.72 (qddd, *J* = 1.4, 1.4, 0.8, 0.8 Hz, 1H, =CHCO₂Me), 5.59 (br ddd, *J* = 17.6, 1.3, 0.7 Hz, 1H, CH_ZH_E=CHR), 5.45 (ddd, *J* = 10.9, 1.4, 1.4 Hz, 1H, CH_ZH_E=CHR), 4.17 (q, *J* = 7.1 Hz, 2H, OCH₂CH₃), 2.00 (d, *J* = 1.4 Hz, 3H, =CMe), and 1.28 (t, *J* = 7.1 Hz, 3H, OCH₂CH₃).

¹³C NMR (125 MHz, CDCl₃) δ 166.1, 150.6, 133.9, 120.5, 118.1, 59.8, 20.2, and 14.3.

IR (neat, selected peaks): 2977, 1710, 1634, and 1590 cm⁻¹.

GC-MS (30 m x 0.25 mm ID, HP-5, 50 °C/2.0 min/20 °C min⁻¹ /250 °C) *t*_R = 3.48 min; MS [70 eV, *m/z* (rel int)]: 140 (57, M⁺), 139 (10, M⁺-H), 112 (75, M⁺-CH₂=CH₂), 111 (78, M⁺-Et), 95 (100, M⁺-OEt), and 67 (99, M⁺-CO₂Et).

S6.2.4 Butyl (*Z*)-3-Methylpenta-2,4-dienoate (**606-ⁿBu**)



Thionyl chloride (0.13 equiv, 1 mL, 13.8 mmol) was added in dropwise fashion to a 200 mL heavy-walled glass pressure tube containing *n*-butanol (10 equiv, 100 mL, 1.08 mol). The tube was capped, and the mixture was stirred for five minutes to allow generation of anhydrous HCl. (*Z*)-3-Methylpenta-2,4-dienoic acid (1 equiv, 4.7 g, 42 mmol) was added in one portion. The pressure tube was recapped and heated to 100 °C. After 18 h the mixture was allowed to cool, and the butanol solution was partitioned between saturated potassium carbonate (100 mL) and methylene chloride. The aqueous layer was extracted 3x with dichloromethane, and the organic layers were combined, dried over MgSO₄, and concentrated. Phenothiazine (0.1 g) was added to minimize polymerization and this material was distilled under reduced pressure to afford butyl (*Z*)-3-methylpenta-2,4-dienoate (**606-ⁿBu**, 4.8 g, 34.3 mmol, 81.7% yield, 86:14 mixture of *Z*:*E* isomers (¹H NMR analysis).

¹H NMR (500 MHz, CDCl₃) δ 7.81 (ddd, *J* = 17.6, 10.9, 0.8 Hz, 1H, CH₂=CHR), 5.73 (qddd, *J* = 1.4, 1.4, 0.7, 0.7 Hz, 1H, =CHCO₂Me), 5.59 (br ddd, *J* = 17.6, 1.3, 0.7 Hz, 1H, CH₂H_E=CHR), 5.44 (ddd, *J* = 10.9, 1.4, 1.4 Hz, 1H, CH₂H_E=CHR), 4.11 (t, *J* = 6.7 Hz, 2H, OCH₂CH₂), 2.00 (d, *J* = 1.3 Hz, 3H, =CMe), 1.64 (br pent, *J* = 7.1 Hz, 2H, OCH₂CH₂CH₂), 1.40 (br sextet, *J* = 7.5 Hz, 2H, CH₂CH₂CH₃), and 0.94 (t, *J* = 7.4 Hz, 3H, CH₂CH₃).

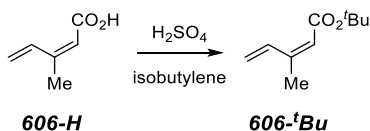
¹³C NMR (125 MHz, CDCl₃) δ 166.2, 150.5, 134.0, 120.5, 118.2, 63.8, 30.8, 20.3, 19.3 and 13.7.

IR (neat, selected peaks): 3095, 2959, 2878, 1709, 1636, 1591, 1460, and 1381 cm⁻¹.

bp: 65 °C (1.5 torr).

GC-MS (30 m x 0.25 mm ID, HP-5, 50 °C/2.0 min/20 °C min⁻¹/250 °C) *t_R* = 5.08 min; MS [70 eV, *m/z* (rel int)]: 168 (10, M⁺), 112 (78, M⁺-butene), 111 (57, M⁺-Bu), 95 (51, M⁺-OBu), and 67 (31, M⁺-CO₂Et).

S6.2.5 *tert*-Butyl (*Z*)-3-Methylpenta-2,4-dienoate (**606-^tBu**)



(*Z*)-3-Methylpenta-2,4-dienoic acid (3.00 g, 26.7 mmol) was added to an 80 mL screw cap culture tube equipped with a stir bar. The solution was cooled to -78 °C and isobutylene (15 equivalents, 38 mL, 400 mmol), which had been pre-condensed in a graduated cylinder, was added. Concentrated sulfuric acid (0.2 equivalents, 280 μL, 5.34 mmol) was added, the culture tube was capped, and the mixture was stirred for 7 h at 35 °C. No starting **606-H** remained (¹H NMR analysis). The culture tube was cooled to -78 °C, opened, and approximately 20 mL of diethyl ether and 20 mL of saturated sodium bicarbonate (gas evolution) were added. The mixture was allowed to warm to ambient temperature to allow for slow evaporation of excess isobutylene over ca. 1 h while stirring. The remaining contents were diluted into ca. 100 mL of diethyl ether, washed with saturated sodium bicarbonate and brine, dried (MgSO₄), and concentrated to leave a

yellow oil (4.73 g). Phenothiazine (0.1 g) was added and this crude material was distilled under reduced pressure (0.7 torr) to afford *tert*-butyl (*Z*)-3-methylpenta-2,4-dienoate (**606-*t*Bu**, 3.54 g, 21.7 mmol, 78.9% yield).

¹H NMR (500 MHz, CDCl₃) δ 7.77 (ddd, *J* = 17.6, 10.9, 0.9 Hz, 1H, CH₂=CHR), 5.66 (qddd, *J* = 1.4, 1.4, 0.7, 0.7 Hz, 1H, =CHCO₂Me), 5.57 (br ddd, *J* = 17.6, 1.4, 0.8 Hz, 1H, CH_ZH_E=CHR), 5.40 (ddd, *J* = 10.9, 1.5, 1.5 Hz, 1H, CH_ZH_E=CHR), 1.97 (d, *J* = 1.3 Hz, 3H, =CMe), and 1.48 (s, 9H, O(CH₃)₃).

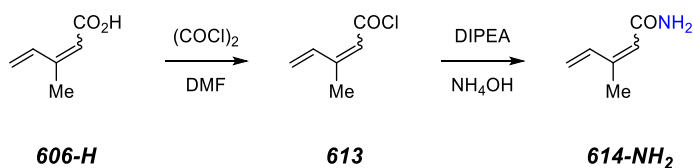
¹³C NMR (125 MHz, CDCl₃) δ 165.7, 149.4, 134.1, 120.2, 120.1, 80.1, 28.4, and 20.3.

IR (neat, selected peaks): 2987, 1706, 1637, and 1591 cm⁻¹.

bp: 27 °C (0.7 torr).

GC-MS (30 m x 0.25 mm ID, HP-5, 50 °C/2.0 min/20 °C min⁻¹/250 °C) *t*_R = 4.10 min; MS [70 eV, *m/z* (rel int)]: 112 (100, M⁺-isobutylene), 111 (55, M⁺-C(Me)₃), 95 (63, M⁺-O^tBu), and 67 (24, M⁺-CO₂^tBu).

S6.2.6 3-Methylpenta-2,4-dienamide (**614-NH₂**)



(*Z*)-3-Methylpenta-2,4-dienoic acid (7.00 g, 62.5 mmol) and THF (100 mL) were added to a 250-mL round bottom flask containing a stir bar. The reaction was stirred and oxalyl chloride (1.1 equiv, 5.8 mL, 68.8 mmol) and DMF (10 μL) were added. The reaction mixture was monitored visually through the evolution of gas. Once the bubbling ceased, the flask was cooled to 0 °C and Hünig's base (2 equiv, 21.7 mL, 125 mmol) was added dropwise followed by the addition of aqueous ammonium hydroxide (27% by volume, 3 equiv, 12.5 mL, 188 mmol). After 10 minutes, the heterogeneous solution was diluted with DCM (150 mL), EtOAc (100 mL) and water (50 mL); washed with aqueous HCl (0.5 M), NaHCO₃, and brine; and dried over MgSO₄. The solution was concentrated, the solid was diluted (EtOAc) and eluted through a plug of basic alumina, and the product

recrystallized (toluene) to give a 4:1 mixture of *Z*:*E* isomers of 3-methylpenta-2,4-dienamide (**614-NH₂**, 3.19 g, 46% yield) as white needles.

¹H NMR (500 MHz, CDCl₃) δ 7.76 (ddd, *J* = 17.6, 10.9, 0.8 Hz, 1H, CH₂=CHR), 5.69 (qddd, *J* = 1.4, 1.4, 0.7, 0.7 Hz, 1H, =CHCO), 5.59–5.29 (br s, 2H, -NH₂), 5.57 (ddd, *J* = 17.6, 1.3, 0.7 Hz, 1H, CH₂H_E=CHR), 5.40 (ddd, *J* = 10.9, 1.5, 1.5 Hz, 1H, CH₂H_E=CHR), and 1.97 (d, *J* = 1.3 Hz, 3H, =CMe).

¹³C NMR (125 MHz, CDCl₃) δ 168.3, 147.7, 134.2, 119.94, 119.86, and 20.3

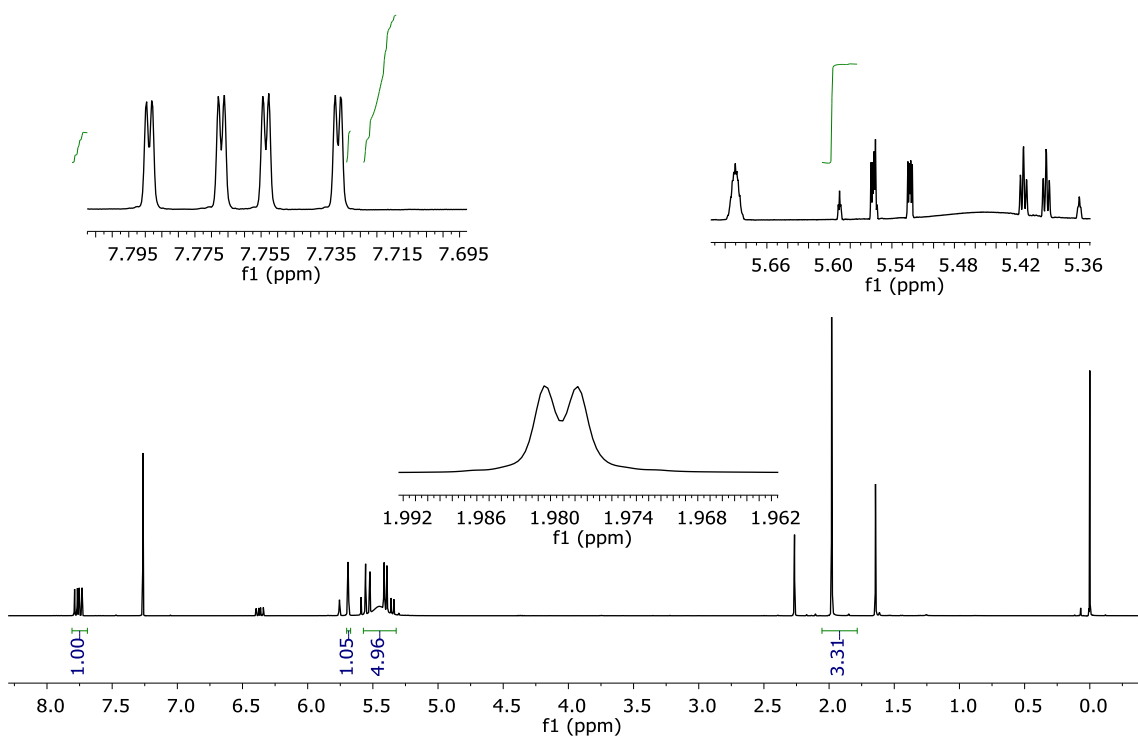


Figure S6.1 ¹H NMR spectrum of isoprenecarboxamide **614-NH₂**.

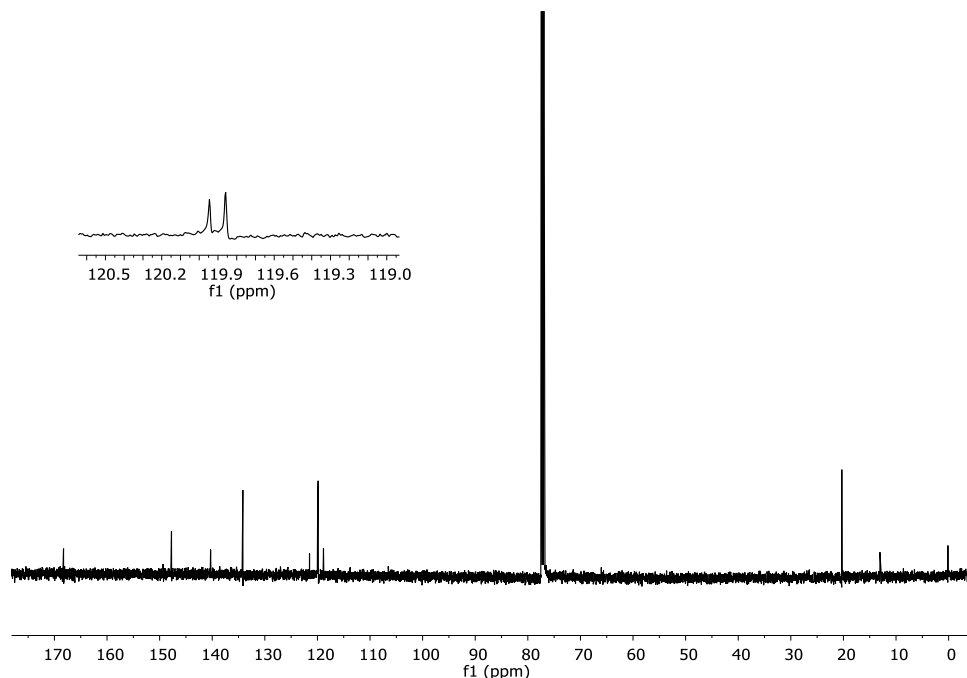
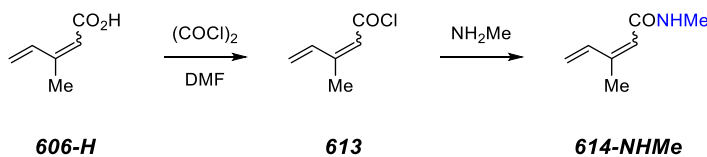


Figure S6.2 ^{13}C NMR spectrum of isoprenecarboxamide **614-NH₂**.

S6.2.7 *N*,3-Dimethylpenta-2,4-dienamide (**614-NHMe**)



(*Z*)-3-Methylpenta-2,4-dienoic acid (5.00 g, 44.6 mmol) and THF (40 mL) were added to a 100-mL round bottom flask containing a stir bar. The reaction was stirred and oxalyl chloride (1.1 equiv, 4.2 mL, 49.1 mmol) and DMF (10 μL) were sequentially added. The reaction mixture was monitored visually through the evolution of gas. Once the bubbling ceased, the flask was cooled (0 $^\circ\text{C}$), and methylamine (40% by volume in H_2O , 4 equiv, 16 mL, 180 mmol) was added. After 20 minutes, the mixture was concentrated (to remove THF), diluted with EtOAc, and washed with brine. The brine layer was back extracted with EtOAc, and the combine organic layers were dried (MgSO_4). The mixture was concentrated to give crude *N*,3-dimethylpenta-2,4-dienamide (**614-NHMe**, 2.76 g, 49% yield) as a colorless liquid (99.5:0.5 *Z:E*). Amide **614-NHMe** was distilled using bulb-to-bulb distillation (K \ddot{u} gelrohr) prior to polymerization.

¹H NMR (500 MHz, CDCl₃) δ 7.76 (ddd, *J* = 17.6, 10.9, 0.8 Hz, 1H, CH₂=CHR), 5.71–5.49 (br s, 1H, -NHMe), 5.63 (qddd, *J* = 1.4, 1.4, 0.7, 0.7 Hz, 1H, =CHCO), 5.49 (ddd, *J* = 17.6, 1.3, 0.7 Hz, 1H, CH₂H_E=CHR), 5.36 (ddd, *J* = 10.9, 1.5, 1.5 Hz, 1H, CH₂H_E=CHR), 2.85 (s, 3H, NHMe), and 1.95 (d, *J* = 1.3 Hz, 3H, =CMe). *Note: the shims on this sample were poor. The *J*-values were deduced from spectra of other isoprenecarboxamide monomers.

¹³C NMR (125 MHz, CDCl₃) δ 167.2, 145.2, 134.4, 121.3, 119.1, 26.3, and 20.2.

bp 145 °C @ 0.3 Torr

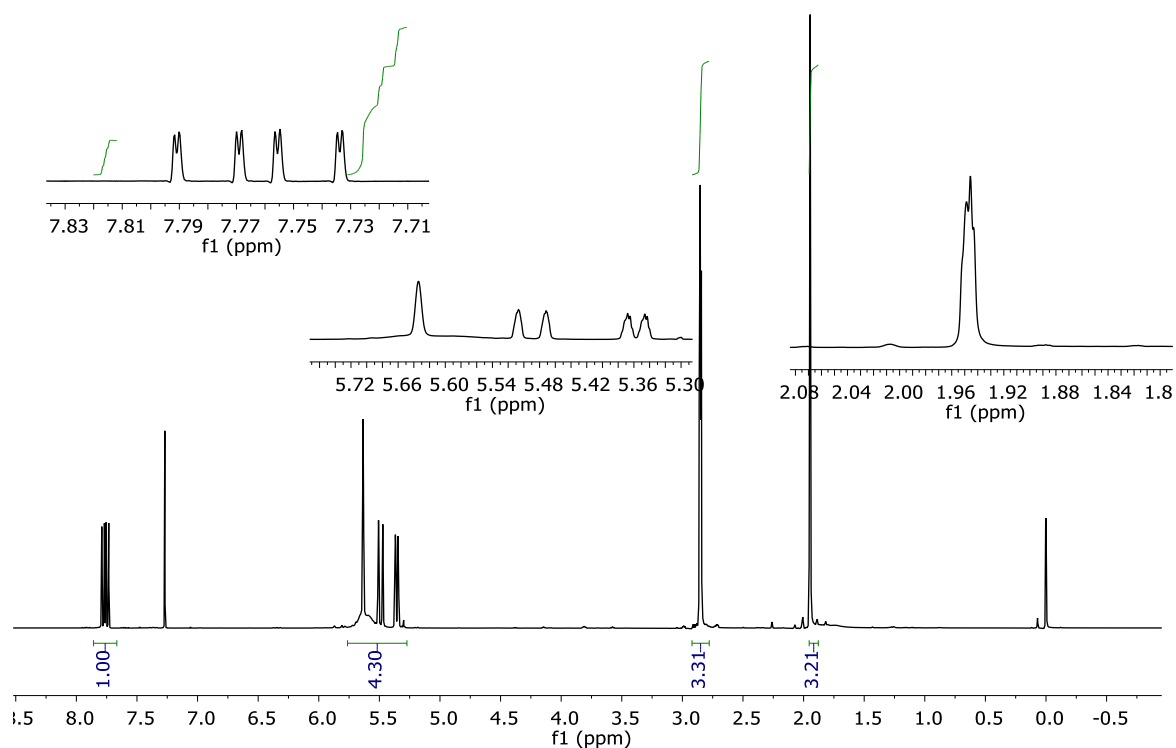


Figure S6.3 ¹H NMR spectrum of isoprenecarboxamide **614-NHMe**.

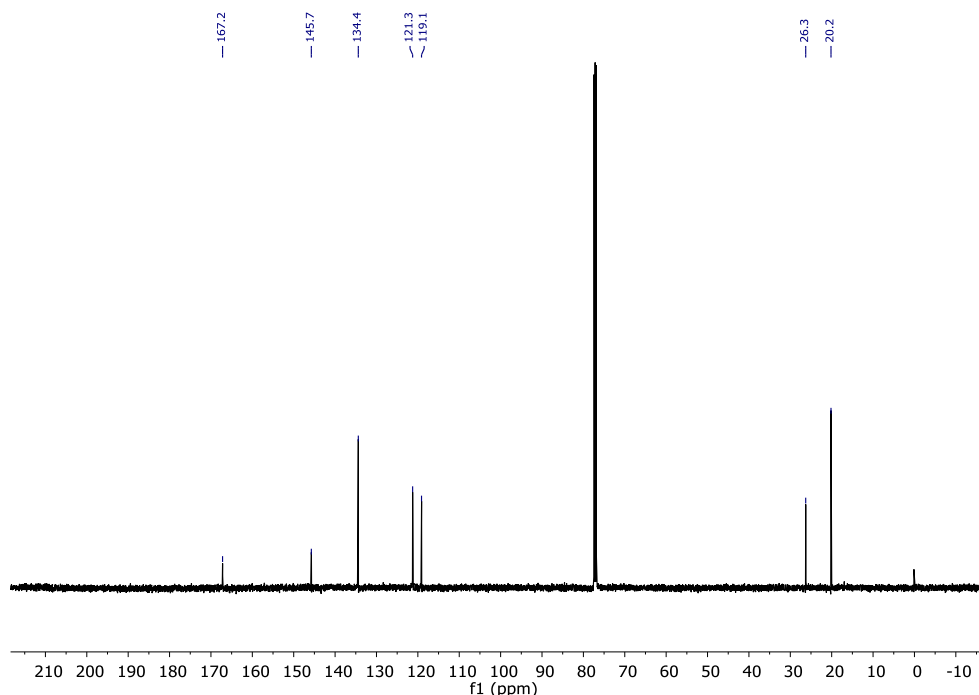
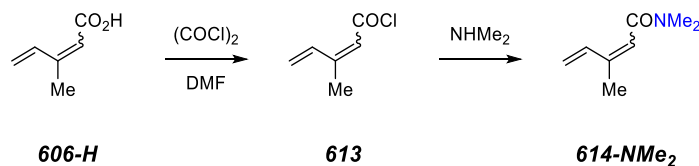


Figure S6.4 ^{13}C NMR spectrum of isoprenecarboxamide **614-NHMe**.

S6.2.8 *N,N*,3-Trimethylpenta-2,4-dienamide (**614-NMe₂**)



(*Z*)-3-Methylpenta-2,4-dienoic acid (7.00 g, 62.5 mmol) and THF (40 mL) were added to a 250-mL round bottom flask containing a stir bar. The reaction was stirred and oxalyl chloride (1.2 equiv, 6.4 mL, 75.0 mmol) and DMF (10 μL) were added. The reaction mixture was monitored visually through the evolution of gas. Once the bubbling ceased, the flask was cooled to 0 $^{\circ}\text{C}$ and dimethylamine (in THF, which was prepared from bubbling gaseous dimethylamine into THF to saturation). After 3 hours, the reaction mixture was concentrated, diluted with EtOAc, washed (1M HCl, NaHCO_3 , brine, dried (MgSO_4), and concentrated. The crude product was distilled 2x to afford *N,N*,3-trimethylpenta-2,4-dienamide (**614-NMe₂**, 3.41 g, 39% yield) as a colorless oil. **Quite a

bit of this sample was spilt into oil that was removed in the distillation process. This could be a contributing reason why the yield was sub-par.

¹H NMR (500 MHz, CDCl₃) δ 6.97 (ddd, *J* = 17.6, 10.9, 0.7 Hz, 1H, CH₂=CHR), 5.91 (qddd, *J* = 1.4, 1.4, 0.7, 0.7 Hz, 1H, =CHCO), 5.42 (ddd, *J* = 17.6, 1.3, 0.7 Hz, 1H, CH₂H_E=CHR), 5.28 (ddd, *J* = 10.8, 1.4, 1.4 Hz, 1H, CH₂H_E=CHR), 3.01 (s, 3H, N(CH₃)₂), 3.00 [s, 3H, N(CH₃)₂], and 1.95 (d, *J* = 1.4 Hz, 3H, =CMe).

bp 113 °C @ 1.2 Torr

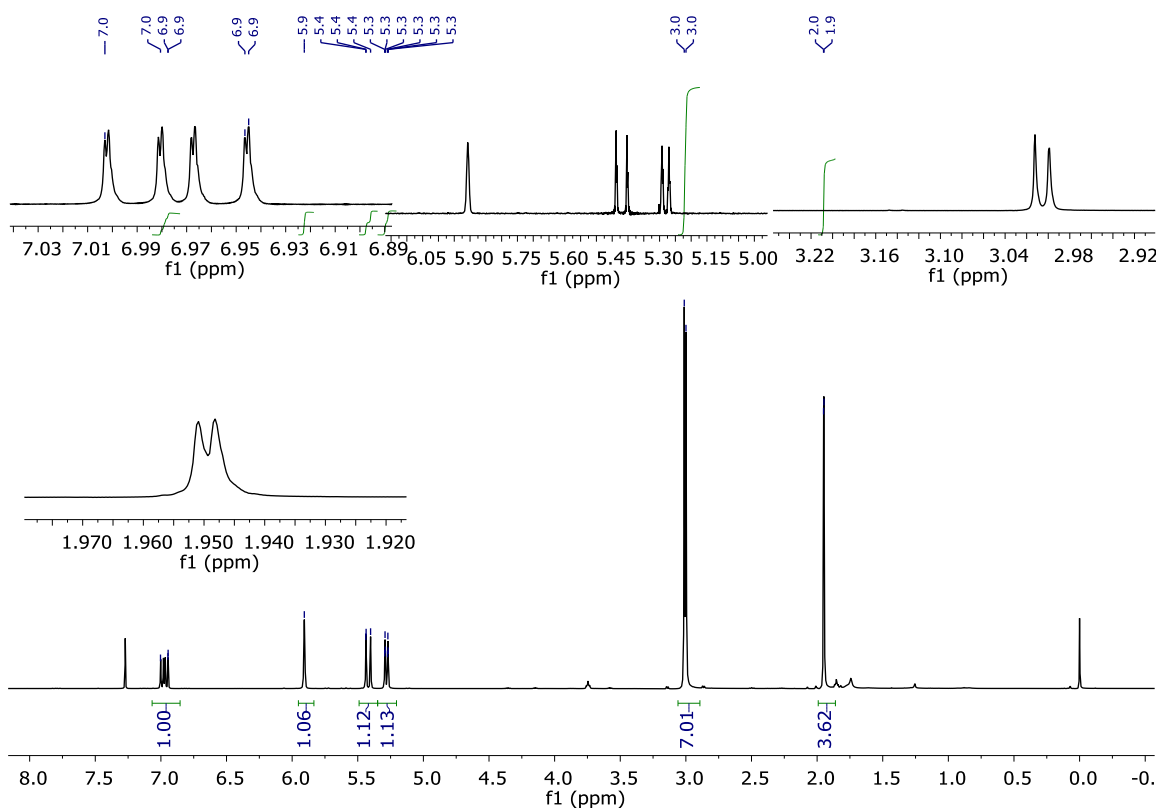


Figure S6.5 ¹H NMR spectrum of isprenecarboxamide **614-NMe₂**.

S6.3 Polymer synthesis

S6.3.1 Poly(methyl isoprenecarboxylate) [poly(606-Me)]

Procedure for AIBN initiated free radical polymerization of (*Z*)-3-methylpenta-2,4-dienoate (606-Me)

A stock solution of methyl (*Z*)-3-methylpenta-2,4-dienoate (**606-Me**, 0.21 g, 1.66 mmol) and (*E*)-2,2'-(diazene-1,2-diyl)bis(2-methylpropanenitrile) (AIBN, 4.1 mg, 0.025 mmol) was prepared. After the full dissolution of AIBN in the diene, the stock solution was dispensed into a series of 2 mL ampules (51 mg each). To each of these was added one of four solvents (benzene, acetonitrile, toluene, and methanol; 0.12 mL). The ampule was degassed through a series of three freeze-pump-thaw cycles and sealed under vacuum with a torch. The ampule was heated at 65 °C for 48 h. The ampule was allowed to cool to ambient temperature and a portion of the contents was analyzed by ¹H NMR spectroscopy to determine the conversion. The remainder of the reaction mixture was freed of solvent *in vacuo* and then analyzed by SEC to determine the molecular weight and dispersity.

*Polymerization for **614-NR¹R²** followed the procedure described for **606-Me**.

Procedure for nitroxide-mediated radical polymerization (NMP) of (*Z*)-3-methylpenta-2,4-dienoate (**606-Me**)

To a 10 mL Schlenk flask was added *N*-(*tert*-butyl)-*N*-(2-methyl-1-phenylpropyl)-*O*-(1-phenylethyl)hydroxylamine (1 equiv, 25.7 mg, 0.079 mmol) and methyl (*Z*)-3-methylpenta-2,4-dienoate [**606-Me** (before known as ICAM)] (100 equiv, 1 g, 7.93 mmol). The solution was degassed through three freeze-pump-thaw cycles and then heated at 110 °C. Aliquots were taken at intervals to monitor conversion (¹H NMR) and M_n and dispersity (D) (SEC).

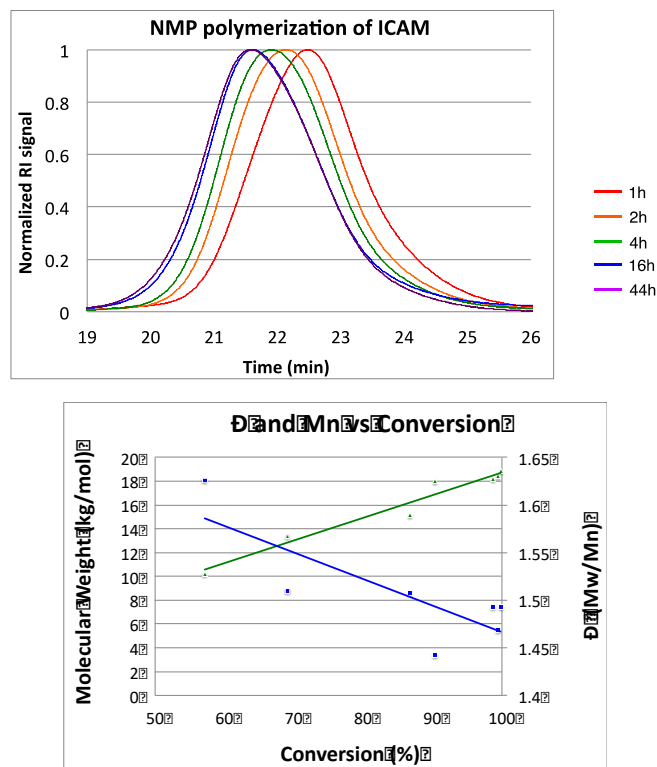
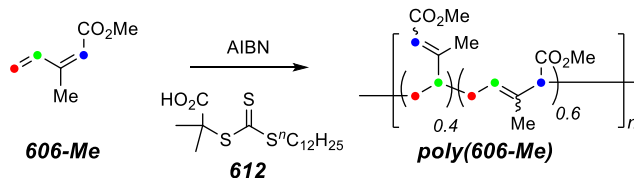


Figure S6.6 Normalized SEC chromatograms and corresponding dispersity (D) and molecular weights of aliquots taken from a nitroxide-mediated radical polymerization (NMP). (**ICAM** = **606-Me**)

Poly(methyl isprenecarboxylate) [poly(606-Me)]



AIBN (0.08 equiv, 0.16 mg, 1.0 μmol) was added as a stock solution in DCM (10 $\text{mg}\cdot\text{mL}^{-1}$) to a 10 mL Schlenk flask. The DCM was removed under reduced pressure and 2-[[dodecylthio]carbonothioyl]thio-2-methylpropanoic acid (DDMAT, **612**, 1.0 equiv, 4.3 mg, 12 μmol) and methyl (*Z*)-3-methylpenta-2,4-dienoate (**606-Me**, 1000 equiv, 1.50 g, 11.9 mmol) were added. The headspace was degassed through several freeze-pump-thaw cycles, under static vacuum, until bubbling no longer was observed during thawing. Nitrogen was then admitted and the flask was heated in an oil bath held at 95 °C. Aliquots were periodically withdrawn under nitrogen flow. ¹H NMR analysis of each crude aliquot relied, principally, on integration of the following resonances: 7.81—H4 in the starting **606-Me**; 6.40—H4 in a small amount of the *E*-isomer of **606-Me** (*E*-**6-Me**) that appears during the polymerization; and 4.9–6.0, the superposition of the single alkene proton arising from both the 1,4- and 1,2-modes of addition in the PMIC polymer as well as protons H₂, H_{5E}, and H_{5Z} in both **606-Me** and *E*-**606-Me**. ¹H NMR analysis of the crude aliquots indicated >94% conversion of the monomer after 5 days. The flask was allowed to cool to ambient temperature, the residue was dissolved in dichloromethane, and the polymer was precipitated by addition to swirled methanol held at 0 °C. The resulting slurry was cooled (-20 °C), centrifuged, decanted, and rendered free of solvent under vacuum overnight at 70 °C to provide 1.26 g of PMIC (84% yield). This product was judged to arise from a 42:58 ratio of 1,2- and 1,4-modes of polymerization [cf. "y" vs. "x", respectively, in the structure of poly(**606-Me**)] across the conjugated diene based on integration of ¹H NMR resonances from 5.83–5.37 ppm (from moieties arising from 1,2-addition) and 5.37–4.92 ppm (from moieties arising from 1,4-addition). A nearly identical ratio for the 1,2- and 1,4-modes was seen in the relative intensities of the ¹³C NMR resonances for the conjugated (167.0–165.5 ppm) vs. unconjugated (174.2–173.0 ppm) carbonyl carbons.

¹H NMR (500 MHz, CDCl₃): δ 5.84–4.97 (m, 1.0H, HC=), 3.84–3.50 (m, 3.1H, OCH₃), 3.08–1.16 (m, 6.2H, three C_{sp3}H protons on the backbone and allylic methyl groups).

¹³C NMR (125 MHz, CDCl₃): δ 174.1–173.1, 166.9–165.5, 161.9–159.0, 135.0–132.0, 126.6–124.6, 120.0–116.5, 54.4–53.8, 51.3–52.3, 50.9–50.5, 48–43, 38–27.5, 20.0–18.5, and 15.5–12.8.

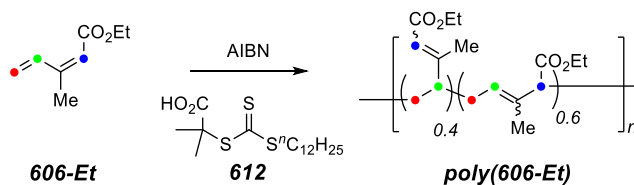
IR (neat, selected peaks): 2950, 1728, 1715, 1643, and 1433 cm⁻¹.

DSC $T_g = 34$ °C

SEC PS-GPC (CHCl₃): $M_n = 152,000$ g mol⁻¹, $M_w = 228,000$ g mol⁻¹, $\mathcal{D} = 1.5$

Linear Viscoelastic Measurements: $T_{ref} = 110$ °C, $G_N = 1.53 \times 10^5$ Pa, $M_e = 17.0$ kDa

S6.3.2 Poly(ethyl isoprenecarboxylate) [poly(606-Et)]



AIBN (0.08 equiv, 0.14 mg, 0.9 μmol) was added as a stock solution in DCM (10 mg•mL⁻¹) to a 10 mL Schlenk flask. The DCM was removed under reduced pressure and 2-[[dodecylthio]carbonothioyl]thio-2-methylpropanoic acid (DDMAT, **612**, 1.0 equiv, 3.9 mg, 10.7 μmol) and ethyl (Z)-3-methylpenta-2,4-dienoate (**606-Et**, 1000 equiv, 1.50 g, 10.7 mmol) were added. The headspace was degassed through several freeze-pump-thaw cycles, under static vacuum, until bubbling no longer was observed during thawing. Nitrogen was then admitted, and the flask was heated in an oil bath held at 95 °C.

Aliquots were periodically withdrawn under nitrogen flow. As with the examples above, ¹H NMR analysis of the crude aliquots indicated >98% conversion of the monomer after 4 days. The flask was allowed to cool to ambient temperature, the residue was dissolved in dichloromethane, and the polymer was precipitated by addition to swirled methanol held at 0 °C. The resulting slurry was cooled in (-20 °C), centrifuged, decanted, and

rendered free of solvent under vacuum overnight at 70 °C to provide 1.18 g of **poly(606-Et)** (79% yield).

This product was also judged to arise from a 42:58 ratio of 1,2- and 1,4-modes of polymerization (cf. "y" vs. "x", respectively) across the conjugated diene based on integration of ¹H NMR resonances from 5.85–5.38 ppm (from moieties arising from 1,2-addition) and 5.38–4.97 ppm (from moieties arising from 1,4-addition). A nearly identical ratio for the 1,2- and 1,4-modes was seen in the relative intensities of the ¹³C NMR resonances for the conjugated (166.8–165.0 ppm) vs. unconjugated (173.0–172.5 ppm) carbonyl carbons.

¹H NMR (500 MHz, CDCl₃): δ 5.8–5.0 (m, 1.0H), 4.3–3.7 (m, 2.2H, OCH₂CH₃), 3.5–1.2 (m, 9.2H, three C_{sp3}H protons on the backbone, allylic methyl groups, and CH₂CH₃).

¹³C NMR (125 MHz, CDCl₃): δ 173.6–172.5, 166.5–165.0, 162.0–159.0, 135.0–132.0, 126.5–124.5, 120.3–116.5, 60.5–60.0, 59.6–59.0, 54.5–53.9, 52.5–51.6, 48–43, 38–27.5, 20.0–18.5, and 14.5–13.0.

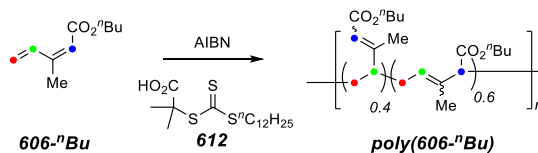
IR (neat, selected peaks): 2979, 1726, 1713, and 1641 cm⁻¹.

DSC $T_g = 10$ °C

SEC PS-GPC (CHCl₃): $M_n = 101,000$ g•mol⁻¹, $M_w = 157,000$ g•mol⁻¹, $\mathcal{D} = 1.6$

Linear Viscoelasticity Measurements: $T_{ref} = 85$ °C $G_N = 1.11 \cdot 10^5$ Pa, $M_e = 21.5$ kg•mol⁻¹

S6.3.3 Poly(*n*-butyl isprenecarboxylic acid) [poly(**606-ⁿBu**)]



AIBN (0.08 equiv, 0.14 mg, 0.7 μmol) was added as a stock solution in DCM (10 $\text{mg}\cdot\text{mL}^{-1}$) to a 10 mL Schlenk flask. The DCM was removed under reduced pressure and 2-[(dodecylthio)carbonothioyl]thio}-2-methylpropanoic acid (DDMAT, **612**, 1.0 equiv, 10.8 mg, 29.6 μmol) and *tert*-butyl (*Z*)-3-methylpenta-2,4-dienoate (**606-ⁿBu**, 300 equiv, 1.50 g, 8.93 mmol) were added. The headspace was degassed through several freeze-pump-thaw cycles, under static vacuum, until bubbling no longer was observed during thawing. Nitrogen was then admitted and the flask, which was heated in an oil bath held at 115 $^{\circ}\text{C}$. Aliquots were periodically withdrawn under nitrogen flow. As with the examples above, ^1H NMR analysis of the crude aliquots indicated >90% conversion of the monomer after 7 days, and the M_n , M_w , and D were analyzed ($M_n = 69,000 \text{ g mol}^{-1}$, $M_w = 90,000 \text{ g mol}^{-1}$, $D = 1.3$). To demonstrate the livingness of this polymerization, more **606-ⁿBu** (320 eq, 1.6 g, 9.5 mmol) was added and the same freeze-pump-thaw cycles were performed. After introduction of nitrogen into the headspace, the Schlenk flask was placed into an oil bath at 95 $^{\circ}\text{C}$. ^1H NMR analysis of the crude aliquots indicated >90% conversion of the monomer after 6 days. The flask was allowed to cool to ambient temperature and the residue was dissolved in dichloromethane and the polymer was precipitated by addition to swirled methanol held at 0 $^{\circ}\text{C}$. The resulting slurry was cooled (-20 $^{\circ}\text{C}$), centrifuged, decanted, and rendered free of solvent under vacuum overnight at 70 $^{\circ}\text{C}$ to provide 1.96 g of **poly(606-ⁿBu)** (63% yield). This sample was judged to be a 41:59 mixture of 1,2:1,4 addition products based on integration of ^1H NMR peaks from 5.90–5.40 ppm (1,2 addition) and 5.40–4.95 ppm (1,4 addition). A nearly identical ratio was seen for the 1,2- and 1,4-modes in the relative intensities of the ^{13}C NMR resonances for the conjugated (166.8–165.1 ppm) vs. unconjugated (173.7–172.5 ppm) carbonyl carbons.

^1H NMR (500 MHz, CDCl_3): δ 5.8–5.0 (m, 1.0H), 4.1–3.9 (m, 2.1H, OCH_2CH_2), 3.6–1.2 (m, 10.5H, three $\text{C}_{\text{sp}^3}\text{H}$ protons on the backbone, the allylic methyl groups, and $\text{OCH}_2\text{CH}_2\text{CH}_2$), and 0.97–0.87 (br t, $J = 7$ Hz, 3.0H, $\text{CH}_2\text{CH}_2\text{CH}_3$).

^{13}C NMR (125 MHz, CDCl_3): δ 173.8–172.6, 166.6–165.2, 161.8–159.3, 135.0–132.3, 127.0–124.4, 120.0–116.7, 64.4–63.9, 63.6–63.0, 54.8–54.0, 52.6–51.6, 48.1–43.9, 38–27.0, 19.8–18.6, and 14.5–13.0.

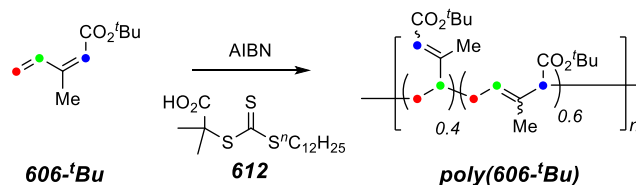
IR (neat, selected peaks): 2979, 1726, 1713, and 1641 cm^{-1} .

DSC $T_g = -19\text{ }^\circ\text{C}$

SEC PS-GPC (CHCl_3): $M_n = 115,000\text{ g}\cdot\text{mol}^{-1}$, $M_w = 188,000\text{ g}\cdot\text{mol}^{-1}$, $D = 1.6$

Linear Viscoelasticity Measurements: $T_{\text{ref}} = 50\text{ }^\circ\text{C}$, $G_N = 5.56 \cdot 10^5\text{ Pa}$, $M_e = 40.9\text{ kg}\cdot\text{mol}^{-1}$

S6.3.4 Poly(*t*-butyl ester isoprenecarboxylate) [poly(606-*t*Bu)]



AIBN (0.08 equiv, 0.12 mg, $0.7\text{ }\mu\text{mol}$) was added as a stock solution in DCM ($10\text{ mg}\cdot\text{mL}^{-1}$) to a 2 mL Schlenk flask. The DCM was removed under reduced pressure and DDMAT (**612**, 1.0 equiv, 3.2 mg, $8.9\text{ }\mu\text{mol}$) and *tert*-butyl (*Z*)-3-methylpenta-2,4-dienoate (**606-*t*Bu**, 1000 equiv, 1.50 g, 8.93 mmol) were added. The headspace was degassed through several freeze-pump-thaw cycles, under static vacuum, until bubbling no longer was observed during thawing. Nitrogen was then admitted and the flask, which was heated in an oil bath held at $115\text{ }^\circ\text{C}$. Aliquots were periodically withdrawn under nitrogen flow. As with the examples above, ^1H NMR analysis of the crude aliquots indicated $>90\%$ conversion of the monomer after 4 days. The flask was allowed to cool to ambient temperature, the residue was dissolved in dichloromethane, and the polymer was

precipitated by addition to swirled methanol held at 0 °C. The resulting slurry was cooled (-20 °C), centrifuged, decanted, and rendered free of solvent under vacuum overnight at 70 °C to provide 1.22 g of **poly(606-*t*Bu)** (81% yield).

This sample was judged to be a 40:60 mixture of 1,2:1,4-addition products based on integration of ¹H NMR peaks from 5.79–5.37 ppm (1,2 addition) and 5.37–4.94 ppm (1,4 addition). A nearly identical ratio was seen for the 1,2- and 1,4-modes in the relative intensities of the ¹³C NMR resonances for the conjugated (166.6–164.8 ppm) vs. unconjugated (173.4–172.0 ppm) carbonyl carbons.

¹H NMR (500 MHz, CDCl₃): δ 5.8–5.0 (m, 1.0H), 4.1–1.8 (m, 3.2H, all C_{sp3}H protons on the backbone), 1.8–1.5 (m, 2.6H, the allylic methyl groups), and 1.5–1.3 (m, 9.2H, O[CH₃]₃).

¹³C NMR (125 MHz, CDCl₃): δ 172.9–172.1, 166.2–164.9, 160.2–158.4, 135.4–132.9, 127.5–124.4, 121.6–118.0, 80.6–78.7, 55.8–55.1, 52.4–53.6, 48.1–47.1, 45.8–44.6, 38.4–31.5, 29.6–27.6, 20.0–19.0, and 15.1–12.9.

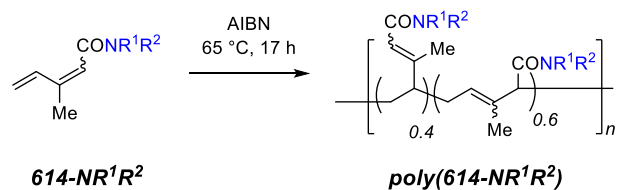
IR (neat, selected peaks): 2976, 1722, 1710, 1641, and 1454 cm⁻¹.

DSC *T_g* = 55 °C

SEC PS-GPC (CHCl₃): *M_n* = 170,000 g•mol⁻¹, *M_w* = 260,000 g•mol⁻¹, *Đ* = 1.5

Linear Viscoelasticity Measurements: *T_{ref}* = 125 °C, *G_N* = 6.59*10⁵ Pa, *M_e* = 38.7 kg•mol⁻¹

S6.3.5 Poly(carboxamide) [poly(614-R¹R²)]



3-Methylpenta-2,4-dienamides (**614-NR¹R²**) were polymerized using the protocol described for the radical (no RAFT agent) polymerization of **606-Me** and was precipitated by first diluting the sample in DMF followed by precipitation into a combination of EtOAc and Hex. Each sample was filtered and heated at 100 °C under high vacuum overnight.

S6.4. Polymer characterization data

S6.4.1 Size exclusion chromatography

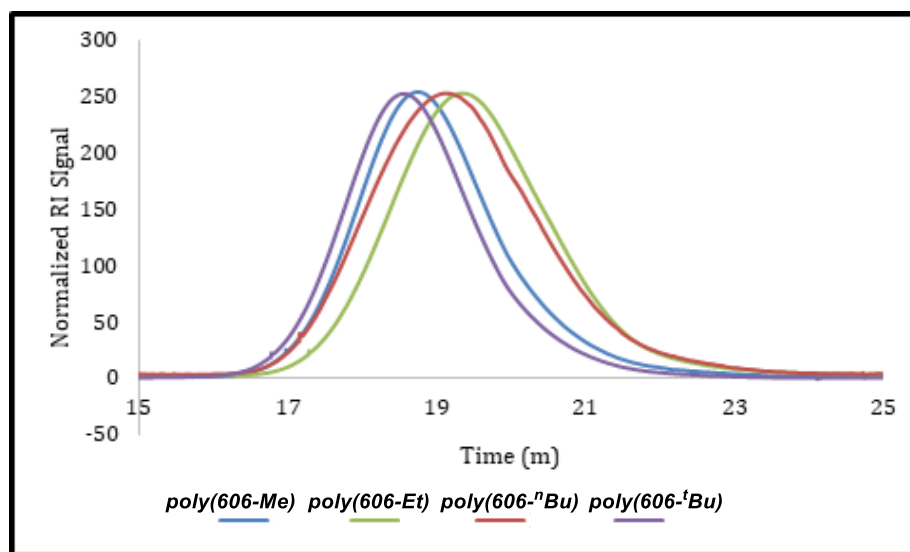


Figure S6.7 Overlay of the SEC chromatograms of the poly(isoprenecarboxylic acid esters) (PS calibration in CHCl_3). Molecular weights (M_n) of **poly(606-Me)**, **poly(606-Et)**, **poly(606-nBu)**, and **poly(606-tBu)**, correspond to 152, 101, 115, 170 $\text{kg}\cdot\text{mol}^{-1}$, respectively.

S6.4.2 Thermogravimetric analysis

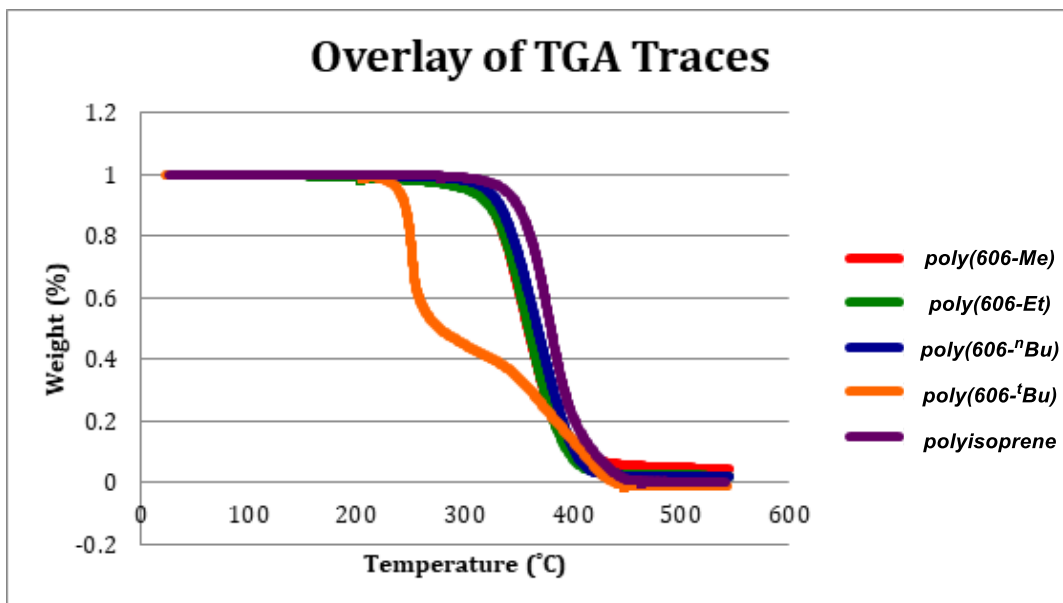


Figure S6.8 Overlay of the TGA traces of the poly(isoprenecarboxylic acid esters) **poly(606-Me)**, **poly(606-Et)**, **poly(606-nBu)**, **poly(606-iBu)**, and polyisoprene correspond to 152, 101, 115, 170 kg•mol⁻¹, respectively. The sample size for each was between 10-20 mg. **Poly(606-iBu)** shows two modes of degradation, the first indicative of the thermal loss of isobutylene.

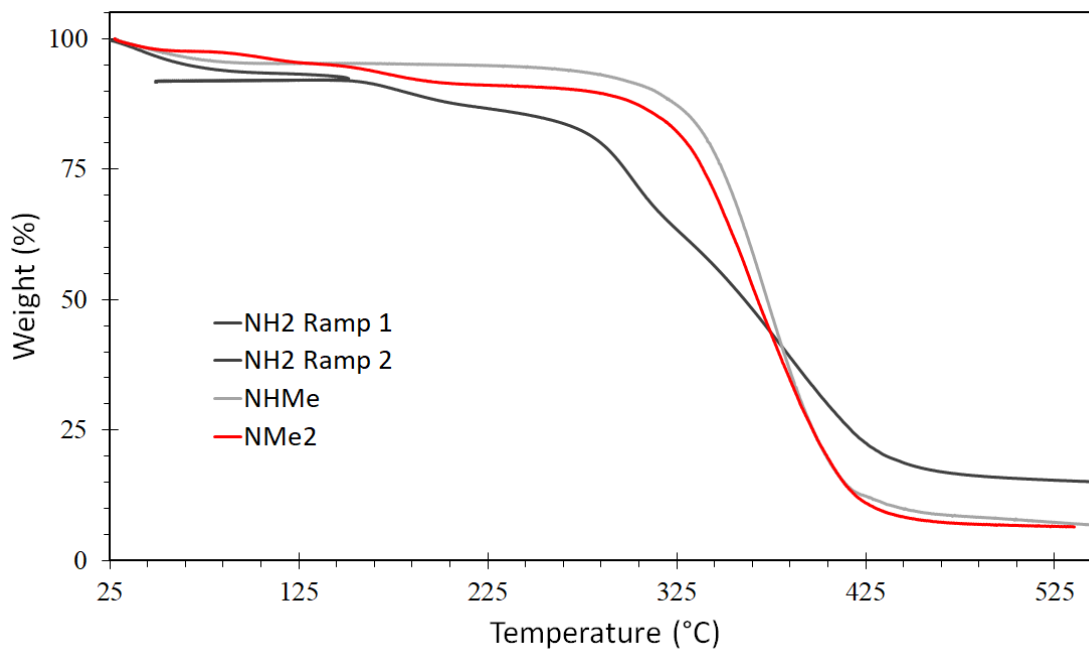


Figure S6.9 Overlay of the TGA traces of the poly(isoprenecarboxamides) **poly(614-H₂)**, **poly(614-HMe)**, and **poly(614-Me₂)**, prepared from radical polymerization (no RAFT agent).

S6.4.3 Differential scanning calorimetry

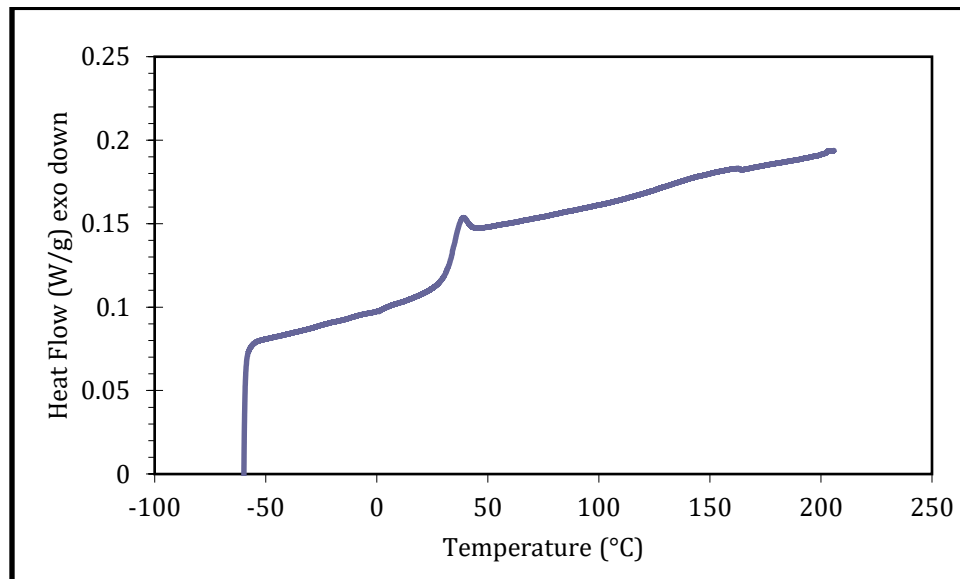


Figure S6.10 DSC thermogram of **poly(606-Me)** (methyl ester, $M_n = 152,000 \text{ g mol}^{-1}$). Glass transition temperature observed at 34 °C.

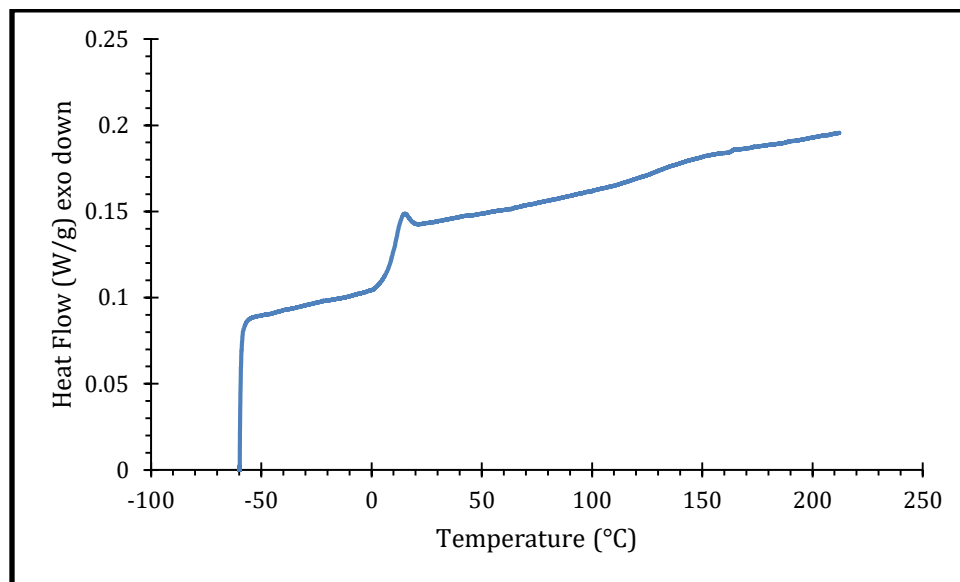


Figure S6.11 DSC thermogram of **poly(606-Et)** (ethyl ester, $M_n = 101,000 \text{ g mol}^{-1}$). Glass transition temperature observed at 16 °C.

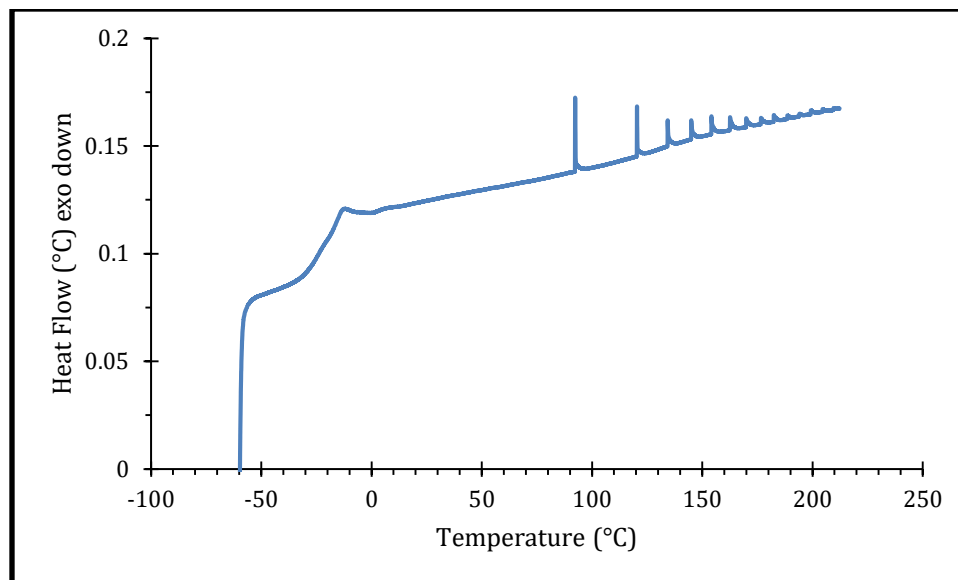


Figure S6.12 DSC thermogram of **poly(606-*n*Bu)** (*n*-butyl ester, $M_n = 115,000 \text{ g mol}^{-1}$). Glass transition temperature observed at $-19 \text{ }^\circ\text{C}$.

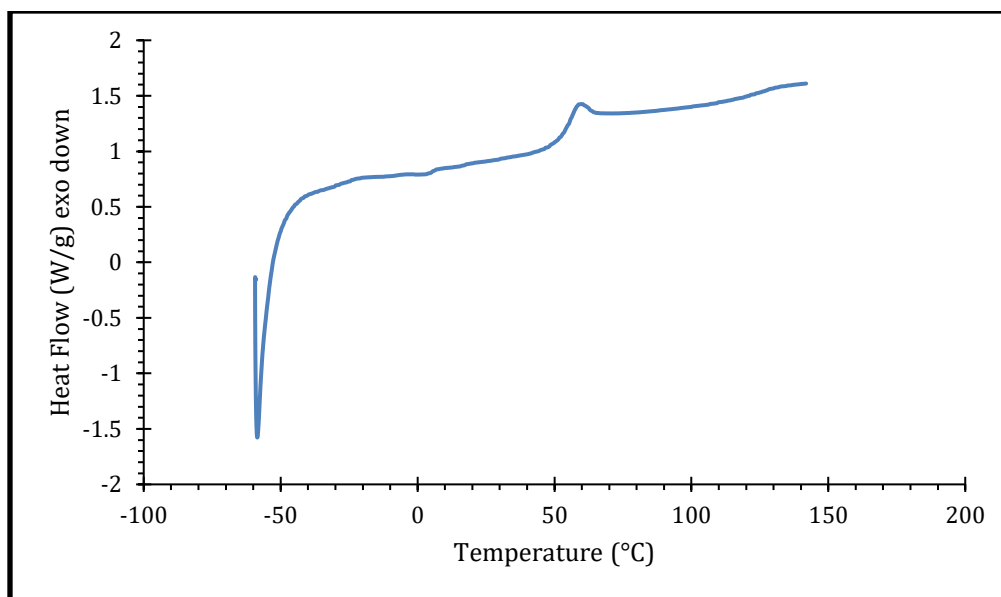


Figure S6.13 DSC thermogram of **poly(606-*t*Bu)** (*t*-butyl ester, $M_n = 170,000 \text{ g mol}^{-1}$). Glass transition temperature observed at $55 \text{ }^\circ\text{C}$.

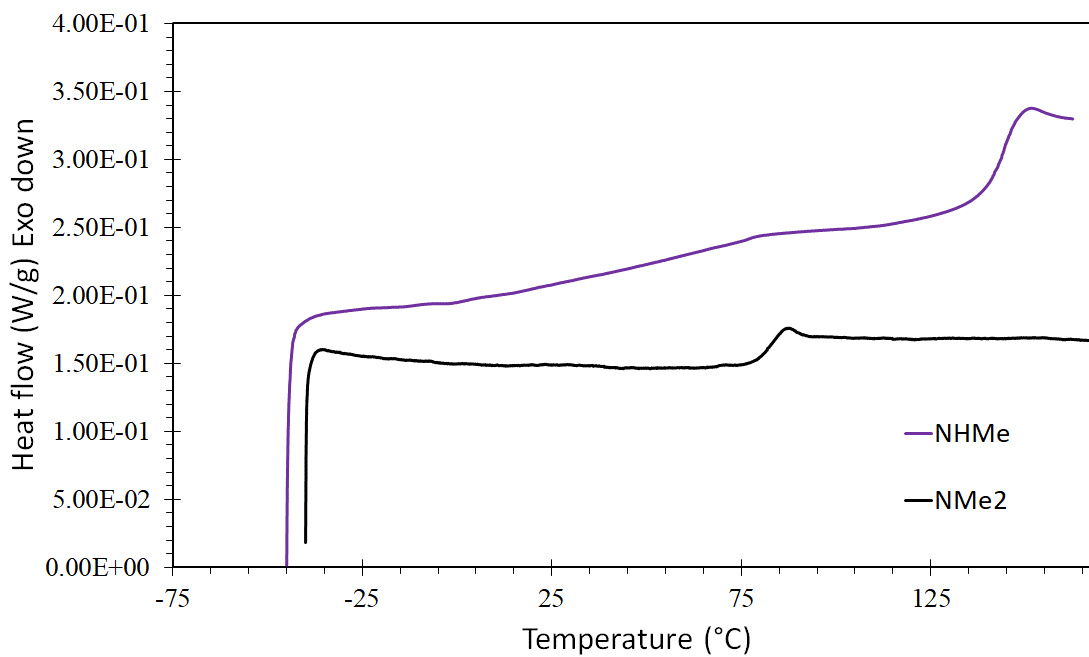


Figure S6.14 Overlaid DSC thermogram of **poly(614-NHMe)** and **poly(614-NMe₂)** prepared from radical polymerization. Glass transition temperature observed at 147 and 87 °C, respectively.

S6.4.4 Linear viscoelastic (rheological) measurements

poly(606-Me)

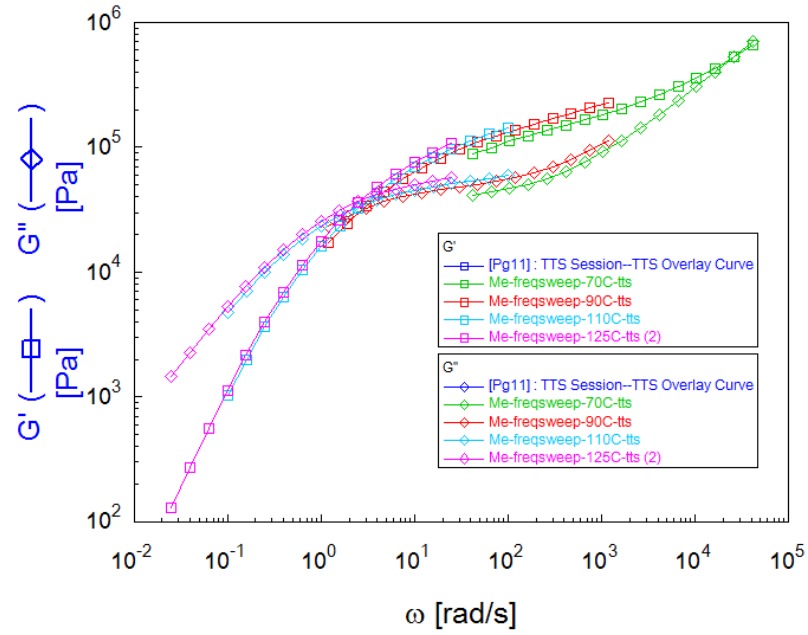


Figure S6.15 Time-temperature superposition plot of **poly(606-Me)** ($M_n = 152,000$ g/mol) referenced at 110 °C ($T_g = 38$ °C). Temperatures covered in this test ranged from 70 °C to 125 °C.

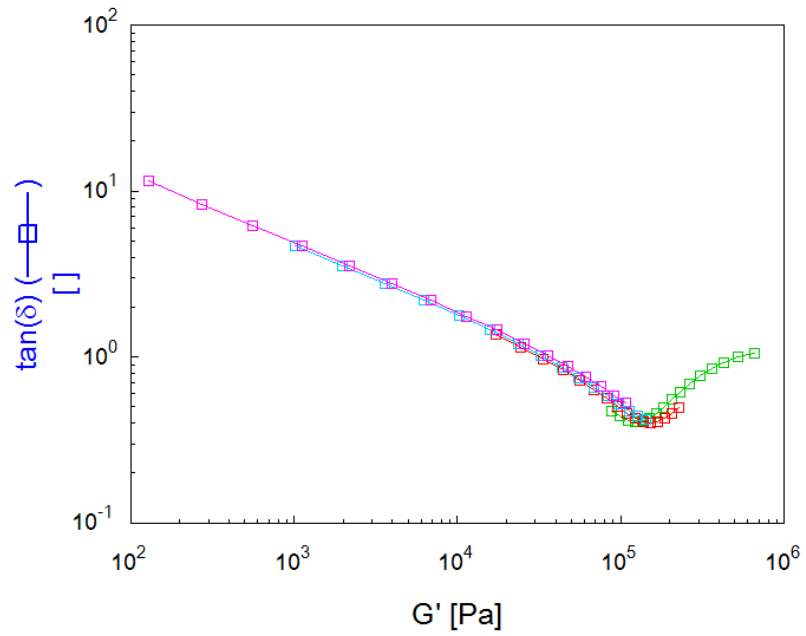


Figure S6.16 Tan delta vs elastic modulus for **poly(606-Me)**. Plateau modulus approximated at 1.11×10^5 Pa. $M_e = 17,000$ g mol⁻¹.

poly(606-Et)

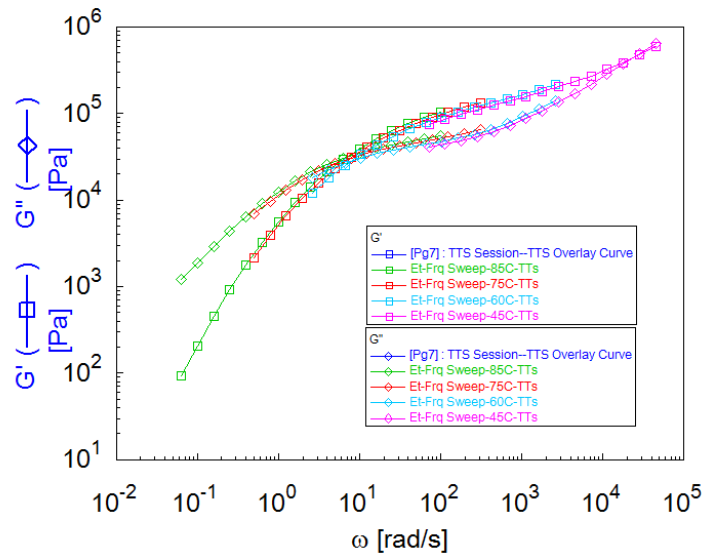


Figure S6.17 Time-Temperature Superposition plot of **poly(606-Et)** ($M_n = 101,000$ g/mol) referenced at 85 °C ($T_g = 16$ °C). Temperatures covered in this test ranged from 45 °C to 85 °C.

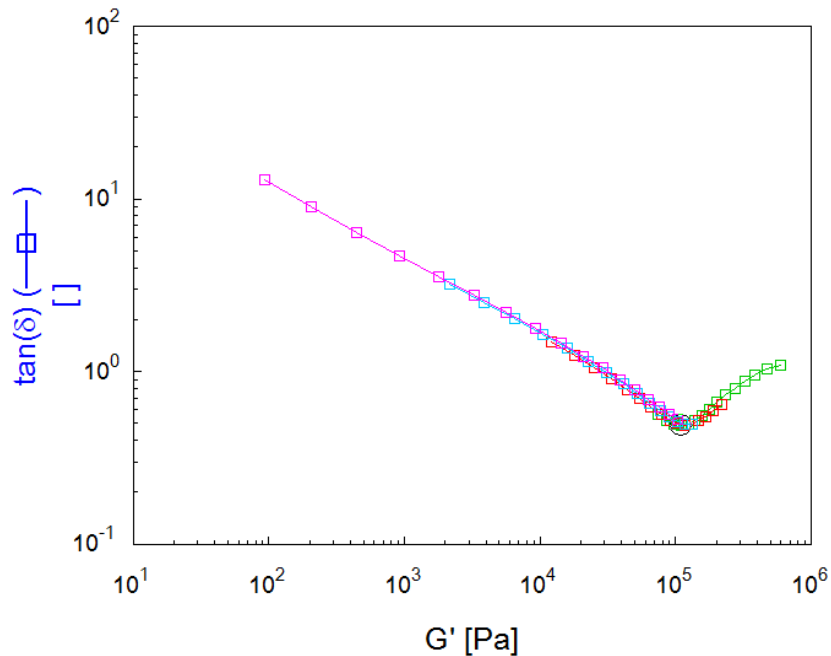


Figure S6.18 Tan Delta vs Elastic Modulus for **poly(606-Et)**. Plateau modulus approximated at 1.11×10^5 Pa. $M_e = 21,100$ g mol $^{-1}$.

poly(606-ⁿBu)

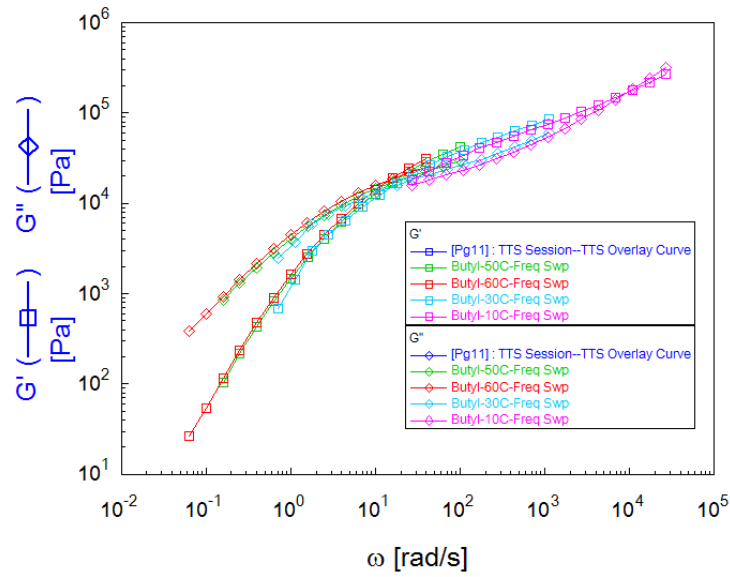


Figure S6.19 Time-Temperature Superposition plot of **poly(606-ⁿBu)** ($M_n = 115,000$ g/mol) referenced at 50 °C ($T_g = -16$ °C). Temperatures covered in this test ranged from 10 °C to 60 °C.

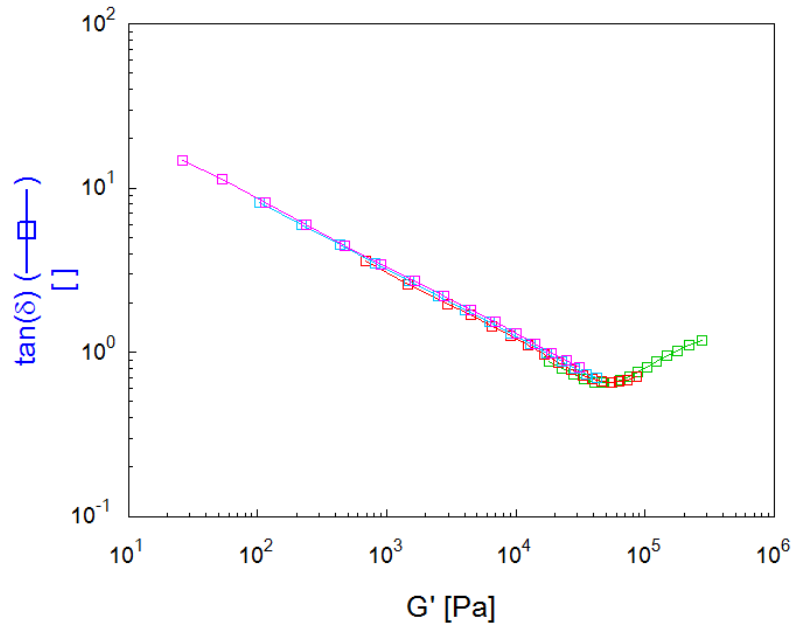


Figure S6.20 Tan Delta vs Elastic Modulus for **poly(606-ⁿBu)**. Plateau Modulus approximated at 5.56×10^5 Pa. $M_e = 40,900$ g mol⁻¹.

poly(606-*t*Bu)

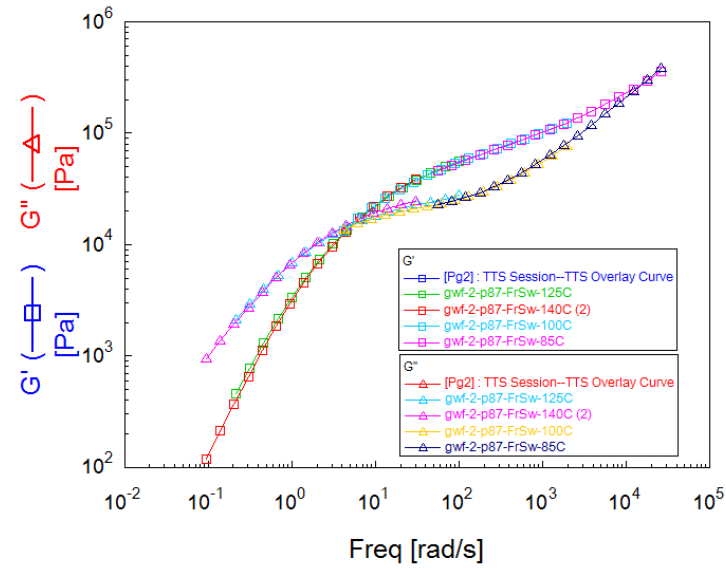


Figure S6.21 Time-Temperature Superposition plot of **poly(606-*t*Bu)** ($M_n = 180,000$ g/mol) referenced at 125 °C ($T_g = 55$ °C). Temperatures covered in this test ranged from 85 °C to 140 °C.

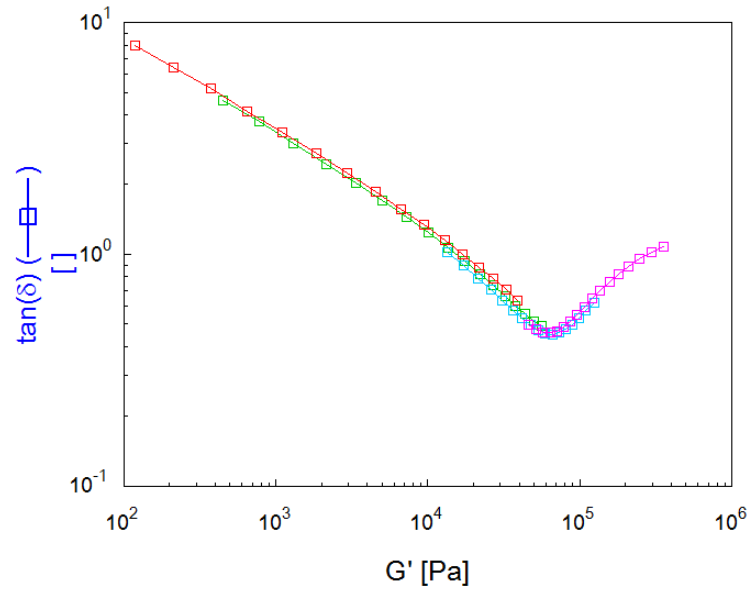


Figure S6.22 Tan Delta vs Elastic Modulus for **poly(606-*t*Bu)**. Plateau Modulus approximated at 6.59×10^4 Pa. $M_e = 38,700$ g mol $^{-1}$.

S6.5 References

- ¹ (a) Hoye, T. R.; Hanson, P. R.; Vyvyan, J. R. *J. Org. Chem.* **1994**, *59*, 4096–4103. (b) Hoye, T. R.; Zhao, H. *J. Org. Chem.* **2002**, *67*, 4014–4016.
- ² (a) Moriconi, E. J.; Meyer, W. C. *J. Org. Chem.* **1971**, *36*, 2841–2849. (b) Cornforth, J. W.; Cornforth, R. H.; Popjak, G.; Gore, I. Y. *Biochem. J.* **1958**, *69*, 146–155.

Appendix F. Supporting information for Chapter 7 (S7)

| | |
|---|-----|
| S7.1 Instrumental methods | 308 |
| S7.2 Preparation and characterization of monomers | 309 |
| S7.2.1 Butane-1,4-diyl (2Z,2'Z)-bis(3-methylpenta-2,4-dienoate) (ICA-XL) | 310 |
| S7.3 Preparation of (dried) hydrogel powders and their (swollen) hydrogels | 312 |
| S7.3.1. Synthesis of the dried hydrogels..... | 312 |
| S7.3.2 A representative procedure for the synthesis of a cross-linked poly(acrylic acid) powder (90% sodiated). | 315 |
| S7.4 Characterization of (dried) hydrogel powders and their (swollen) hydrogels | 317 |
| S7.4.1 Sodiated poly(isoprenecarboxylate) hydrogels [Gel(ICA-H/Na)] | 317 |
| S.7.4.2 Sodiated poly(acrylate) hydrogels [Gel(AA-H/Na)]..... | 324 |
| S.7.4.3 Potassiated poly(isoprenecarboxylate) hydrogels [Gel(ICA-H/K)] | 327 |
| S.7.4.3 Lithiated poly(isoprenecarboxylate) hydrogels [Gel(ICA-H/Li)] | 329 |
| S.7.5 References | 331 |

S7.1 Instrumental methods

NMR: ^1H and ^{13}C NMR spectra were taken on a Bruker Avance 500 (500 MHz) spectrometer. Chemical shifts for ^1H NMR taken in CDCl_3 are referenced to TMS (δ 0.00 ppm). ^1H NMR resonances are reported as follows: chemical shift in ppm [multiplicity, coupling constant(s) in Hz, integral, and structural assignment]. Coupling constant analysis was determined as we have described previously.¹ Substructural environment (e.g., CH_aH_b) was used to specify the proton assignments. The carbon resonance in CDCl_3 (δ 77.16) was used as the reference for ^{13}C NMR chemical shifts.

ATR-FTIR: Fourier transform infrared (FTIR) spectra were taken with a Bruker Alpha Platinum ATR-FTIR instrument fitted with a diamond single-bounce crystal. Typical spectra were collected using 16 scans and 4 s acquisition time.

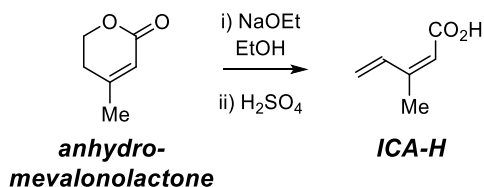
Mass spectrometry of monomers: Electron ionization (EI) MS measurements were taken on an Agilent 5975 MSD at 70 eV GC-MS. An Agilent HP-5 column 30 m long, \times 0.32 mm i.d., with a 0.25 μm film thickness was used as the column stationary phase. The crosslinking agent **ICA-XL** was analyzed via high resolution mass spectroscopy (HRMS) by dissolving the sample in MeOH and injecting it into a Bruker BioTOF (ES-TOF) instrument. PEG was used as an internal standard/calibrant.

Thermogravimetric analysis (TGA): Several sodiated isoprenecarboxylate gels [**Gel(ICA-H/Na)**] were analyzed by TGA using a TA instruments Q500 analyzer. The gels were heated under nitrogen gas at a heating rate of 10 $^\circ\text{C}\cdot\text{min}^{-1}$. Sample masses ranged from ca. 5–10 mg.

Scanning electron microscopy (SEM): SEM images were taken on a field emission gun-SEM Hibachi SU8230 instrument. Samples were sputter coated with iridium (ca. 2–3 nm) prior to imaging. Particle sizes were manually measured using software on the instrument. Particle sizes were determined using the longest end-to-end distance.

S7.2 Preparation and characterization of monomers

S7.2.1 Isoprenecarboxylic acid [(*Z*)-3-methylpenta-2,4-dienoic acid, **ICA-H**]



Anhydrous ethanol (1.65 L) was added to a flame-dried, 3 L round-bottom flask fitted with a stir bar. Sodium metal (1.30 equiv, 16.0 g, 697 mmol) was cut and added portion-wise. Upon full dissolution of sodium, anhydromevalonolactone (1 equiv, 60.00 g, 535.8 mmol) was added dropwise over the course of ca. 10 minutes (a light-yellow color was noticeable immediately upon addition of the first few drops, and this continued to darken over the course of the reaction). The reaction mixture was allowed to stir for 24 h and was concentrated under reduced pressure. The solid residue was dissolved in H₂O (ca. 600 mL) and washed once with Et₂O, which was discarded. Concentrated hydrochloric acid (1.4 equiv, 64.4 mL, 750.1 mmol) was added to the aqueous layer and a white solid began to precipitate out of solution. The aqueous-solid mixture was extracted with EtOAc (3x), and the combined organic layers were washed (brine), dried (MgSO₄), and concentrated to afford a white solid (55.3 g, 92% crude yield). The white solid was recrystallized by first dissolving **ICA-H** in EtOH (ca. 100 mL) at room temperature followed by the addition of H₂O (ca. 500 mL) until the cloud point was just barely reached. This EtOH:H₂O solution was placed into the freezer (ca. -20 °C) overnight and filtered to afford isoprenecarboxylic acid (**ICA-H**, 45.8 g, 77% yield) as white needles.

Note: In some instances, recrystallized **ICA-H** was not fully soluble in CDCl₃ (ca. 95% soluble). Analysis via ¹H NMR spectroscopy (DMSO-*d*₆) showed that small amounts of polymerization (ca. 0.5–1%) had occurred. In these cases, the polymer could easily be removed by suspending crude **ICA-H** in DCM, filtering the suspension through Celite, and concentrating the filtrate to afford a clean sample of **ICA-H**. The ¹H NMR data for

this material was essentially identical to that previously reported,² the full characterization data are reproduced here for convenience.

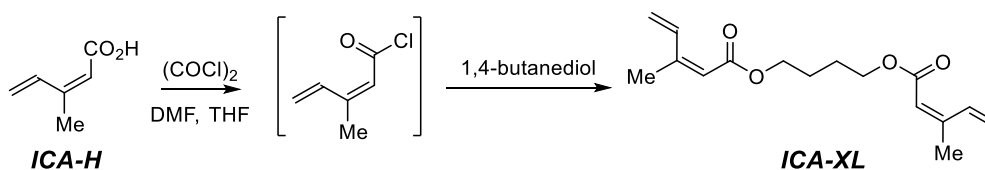
¹H NMR (500 MHz, CDCl₃) δ 12.06 (br s, CO₂H), 7.80 (ddd, *J* = 17.6, 10.9, 0.9 Hz, 1H, CH₂=CHR), 5.76 (br dq, *J* = 1.4, 1.4 Hz, 1H, =CHCO₂H), 5.65 (ddd, *J* = 17.6, 1.3, 0.8 Hz, 1H, CH₂H_E=CHR), 5.49 (ddd, *J* = 10.9, 1.4, 1.4 Hz, 1H, CH₂H_E=CHR), and 2.05 (d, *J* = 1.3 Hz, 3H).

¹³C NMR (125 MHz, CDCl₃) δ 171.8, 153.5, 133.9, 121.6, 117.5, and 20.6.

IR (neat, selected peaks): 2984, 2962, 1684, 1633, 1587, 1427, and 1395 cm⁻¹.²

mp: 67–71 °C (Lit. mp 68–73 °C).²

S7.2.1 Butane-1,4-diyl (2*Z*,2'*Z*)-bis(3-methylpenta-2,4-dienoate) (ICA-XL)



Isoprenecarboxylic acid (**ICA-H**, 1.50 g, 13.4 mmol), THF (5 mL), and DMF (10 μL) were added to a 6-dram vial fitted with a stir bar. Oxalyl chloride (1.05 equiv, 1.20 mL, 14.1 mmol) was added dropwise open to air over the course of ca. 15 minutes. The reaction progress was monitored by observing the bubbling of CO₂. In the initial performance of this experiment, once bubbling appeared to have stopped (~20 minutes), an aliquot was taken for NMR analysis. The spectrum showed >96% conversion to the acid chloride as determined by, for example, the upfield shift of the proton at C4 from 7.80 ppm to 7.42 ppm. 1,4-Butanediol (0.400 equiv, 478 μL, 5.36 mmol) was added, the headspace of the vial was flushed nitrogen, the vial was capped, and the solution was allowed to stir for 21 h. The mixture was diluted in Et₂O, washed with NaHCO₃ (2x) and brine, dried (MgSO₄), and concentrated to give 1.71 g of a lightly yellow colored oil. A portion (606 mg) was purified via MPLC (silica, 15:1 Hex:EtOAc) and concentrated to give butane-1,4-diyl (2*Z*,2'*Z*)-bis(3-methylpenta-2,4-dienoate) (**ICA-XL**) as a white solid

(449 mg, 85% yield based on the amount of diol used). On one subsequent occasion the sample of the bis-ester **ICA-XL** polymerized as the MPLC fraction was being concentrated. Subsequently, a small amount of phenothiazine (~0.1 mg) was added to the relevant MPLC fractions prior to final concentration. Such samples were routinely stored in a freezer (ca. -20 °C) and no deterioration was noted over the course of 8 months.

¹H NMR (500 MHz, CDCl₃) δ 7.80 (ddd, *J* = 17.6, 10.9, 1.0 Hz, 2H, CH₂=CHR), 5.72 (m, 1H, =CHCO₂), 5.60 (dddq, *J* = 17.6, 1.3, 0.7, 0.4 Hz, 2H, CH_ZH_E=CHR), 5.45 (ddd, *J* = 10.9, 1.5, 1.5 Hz, 2H, CH_ZH_E=CHR), 4.15-4.13 (nfom, 4H), 2.01 (d, *J* = 1.3 Hz, 3H), and 1.79-1.75 (nfom, 4H).

¹³C NMR (125 MHz, CDCl₃) δ 166.2, 151.1, 134.1, 120.8, 118.1, 63.6, 25.6, and 20.4.

IR (neat, selected peaks): 3029, 2973, 2957, 1698, 1633, 1588, 1462, and 1348 cm⁻¹.

mp: 32–35 °C.

GC-MS (30 m x 0.25 mm ID, HP-5, 50 °C/2.0 min/20 °C min⁻¹ /250 °C) *t_R* = 9.92 min;

MS [70 eV, *m/z* (rel int)]: 278 (1, M⁺), 263 (1, M⁺-Me), 167 (26, M⁺

O₂CCH=CMeCH=CH₂), and 95 (100, (CO)CH=CMeCH=CH₂).

HRMS (ESI-TOF): Calculated for (C₁₆H₂O₄Na)⁺ 301.1410; found: 301.1383.

S7.3 Preparation of (dried) hydrogel powders and their (swollen) hydrogels

S7.3.1. Synthesis of the dried hydrogels

i. A representative procedure for the synthesis of a cross-linked poly(isoprenecarboxylate) powder (90% sodiated).

2,2'-Azobis(2-methylpropionitrile) (AIBN, 0.01 equiv, 6.4 mg, 0.04 mmol), (Z)-3-methylpenta-2,4-dienoic acid (**ICA-H**, 1.00 equiv, 448 mg, 4.00 mmol), and MeOH (400 μ L) were added to a 1-dram vial. Sodium hydroxide was added via a titrated solution (455 μ L, 7.9 M, 0.900 equiv, 3.60 mmol) to deprotonate 90% of the carboxylic acid groups to sodium carboxylates. An additional portion of water (155 μ L) was added to bring the total volume of water to 600 μ L. The cross-linking agent, butane-1,4-diyl (2Z,2'Z)-bis(3-methylpenta-2,4-dienoate) (**ICA-XL**, 0.01 equiv, 11.2 mg, 0.04 mmol) was added in MeOH (200 μ L). The headspace was evacuated using several freeze-pump-thaw cycles until gas evolution was no longer observed upon thawing. Nitrogen gas was admitted, and the vial was sealed with a Teflon-lined screw-cap. The vial was placed into a sand bath held at 65 °C for 24 hours. It was not unusual for polymerization mixtures to be slightly cloudy at room temperature when preparing the initial reaction mixture. However, the solution became homogeneous and clear quickly after being heated.

The vial was allowed to cool, and the resulting gel was transferred to a 6-dram vial. To remove impurities not incorporated into the polymeric network, water (ca. 14 mL) was added to further swell the gel [when the extent of ionization of the polymer was less than 50%, aqueous MeOH (ca. 1:1) was used instead of pure water]. Acetone was added (ca. 3 mL), the mixture was shaken, the vial was allowed to stand until a top liquid layer was clearly evident, and that supernatant aqueous acetone liquid was removed by pipet. This process was repeated ca. 6-8 times, using increasingly larger volumes of acetone, until that liquid layer was not cloudy. A wet, white solid remained. This material was placed under vacuum for ca. 24 hours at 70 °C and ground to a fine white powder using a

mortar and pestle. This powder was placed back into the vacuum oven at 70 °C until the mass of the sample no longer decreased (typically 24–48 h).

Polymerizations using different extents of carboxylic acid ionization were performed under essentially identical conditions (0.01 equiv AIBN, 0.01 equiv cross-linking agent, 65 °C for 24 h, ca. 3.3 M monomer concentration in 1:1 MeOH:H₂O). Overall mass recovery of final dried powder was typically in the range of 70-90%.

Polymerization of isoprenecarboxylate and its sodium salt in the absence of a cross-linking agent to determine conversion (monomer consumption) by ¹H NMR analysis. (Z)-3-Methylpenta-2,4-dienoic acid (**ICA-H**, 1.0 equiv, 56 mg, 0.5 mmol) and 2,2'-azobis(2-methylpropionitrile) (AIBN, 0.01 equiv, 0.8 mg, 0.005 mmol, 75 μL of a 0.065 M solution in MeOH) were placed in each of a series of 1/2-dram vials. Sodium hydroxide (pre-titrated 7.9 M solution in H₂O) corresponding to 0.10, 0.25, 0.50, 0.75, and 0.90 equiv was added. Additional H₂O was added so that the sum of each solution contained 75 μL of H₂O total. Each vial was submitted to three freeze-pump-thaw cycles, and the headspace of each was filled with nitrogen and quickly closed with a Teflon-lined screw cap. All vials were then placed into a sand bath at 65 °C. After 24 h the vials were opened to air and an aliquot of each was taken to monitor the conversion of each polymerization via ¹H NMR spectroscopy. The results are summarized in Table S7.1.

Table S7.1 Monomer conversion of crude polymerization mixtures (determined by ^1H NMR analysis) using various initiator ratios and percentages of sodium carboxylate. Allowing the polymerization to proceed for longer times (e.g., 48 instead of 24 h) resulted in little change in the overall monomer conversion.

| run # | mol% AIBN | % ionization | monomer conversion |
|-------|-----------|--------------|--------------------|
| 1 | 1.0 | 10 | 97 |
| 2 | 1.0 | 25 | 91 |
| 3 | 1.0 | 50 | 91 |
| 4 | 1.0 | 75 | 81 |
| 5 | 1.0 | 90 | 69 |
| 6 | 0.10 | 50 | 38 |
| 7 | 0.25 | 50 | 35 |
| 8 | 0.50 | 50 | 78 |
| 9 | 1.00 | 50 | 90 |

Li⁺ or K⁺ counterions. Lithiated and potassiated samples of cross-linked poly(isoprenecarboxylate) were prepared in an analogous fashion. However, because of the limited solubility of LiOH in water, solid LiOH-monohydrate was used rather than an aqueous stock solution in order to achieve final concentrations of reactants consistent with those described above for sodium counterions.

Gels with different of cross-linking densities. Sodiated (90%) isoprenecarboxylic acid hydrogel powders were prepared as described above using 0.1, 0.5, 2.5, and 5.0 mol% crosslinking densities; 5.5, 27.8, and 55.6 mg of the bis-dienoate **ICA-XL**, respectively, were used. When 10 mol% (111.2 mg) of **ICA-XL** was used, a non-homogenous reaction mixture was observed that gave qualitative evidence suggestive of a non-homogeneous extent and nature of cross-linking.

S7.3.2 A representative procedure for the synthesis of a cross-linked poly(acrylic acid) powder (90% sodiated).

A procedure very similar to that described above for the synthesis of 90% sodiated poly(isoprenecarboxylate) hydrogel was followed, using the following amounts of reactants and initiator: acrylic acid (1.00 equiv, 432 mg, 6.00 mmol), 2,2'-azobis(2-methylpropionitrile) (AIBN, 0.010 equiv, 9.6 mg, 0.060 mmol, added via stock solution in 200 μL of MeOH), sodium hydroxide (0.90 equiv, 684 μL , 5.4 mmol), 1,4-butanediol diacrylate (0.01 equiv, 12.5 μL , 0.06 mmol in 400 μL of MeOH) in a total of 900 μL of MeOH and 900 μL of water.

b. Swelling of dried hydrogels procedure

Determination of swelling ratios (SR) (or degree of swelling). For each of the following types of swelling experiments was determined by mass measurements: $\text{SR} = m_{\text{gel}}/m_{\text{polymer}}$, where m_{gel} is the total mass of water (or salt or buffer solution) and polymer in the fully swollen gel and m_{polymer} is mass of the dry polymer. This process was performed twice for each polymer sample, and the reported SRs are an average of the four measurements (2 swelling times * 2 samples).

In deionized (DI) H₂O. A portion (~25 mg) of the above cross-linked powder was allowed to swell in DI water for 30 minutes in a 6-dram vial. The solution was then centrifuged, and the top layer of excess water was removed by pipette followed by gently dabbing with a moist paper towel. This process was repeated by addition a second portion of water to the vial, shaking the contents, incubating again for 30 minutes, re-centrifuging, and removing the excess water as above.

In solutions of NaCl, KCl, and CaCl₂. For swelling experiments in NaCl, KCl, and CaCl₂ solutions, 0.17 M solutions [1.0% (w/w) NaCl, 1.3% (w/w) KCl, and 1.9% CaCl₂ (w/w)] were prepared. The above DI water procedure was followed, but a 2- instead of 6-dram vial was used because of the reduced swelling in these salt solutions.

50 %Na to 90 %Na swelling in deionized (DI) H₂O study. Two samples (ca. 25 mg) each of 50 %Na **Gel(ICA-H/Na)** and **Gel(AA-H/Na)** prepared as previously described were

each placed in a 6-dram vial followed by DI H₂O (ca. 15 mL). After 15 minutes, NaOH (0.4 equiv) in DI H₂O [1.025 M, ca. 80 μ L for the **Gel(ICA-H/Na)** and ca. 125 μ L for **Gel(AA-H/Na)**] was added, and the samples were allowed to swell for ca. 17 h. The samples were centrifuged, the top H₂O layer was removed by pipette followed by dabbing with a paper towel. The mass gained by the gels (m_{gel}) from the addition of more sodium carboxylates upon addition of the NaOH solution were taken into account when calculating the swelling ratios of these samples. The two 90 %Na **Gel(ICA-H/Na)** samples prepared in this way had swelling ratios of 255x and 260x, and the two 90 %Na **Gel(AA-H/Na)** samples prepared in this way had swelling ratios of 101x and 109x. These swelling ratios are within error of those obtained using for the material made directly by starting with a 10:90 RCO₂H:RCO₂Na ratio of monomers as described above.

In solutions of different pH. For swelling experiments at different pH's, the following buffers, each at a buffer concentration = 0.050 M, were used: (i) pH = 2.4 (from a 1:1 molar ratio of H₃PO₄ and NaH₂PO₄•H₂O); (ii) pH = 4.5 (from a 2:1 molar ratio of AcOH and NaOH); (iii) pH = 6.6 (from a 1:1 molar ratio of NaH₂PO₄•H₂O and [Na₂HPO₄•(H₂O)₇]); (iv) pH = 8.3 [from a 1:2 molar ratio of HCl and tris(hydroxymethyl)aminomethane (tris)]; (v) pH = 9.9 (from a 1:1 molar ratio of Na₂CO₃ and NaHCO₃); and (vi) pH = 11.5 (from a 1:1 molar ratio of Na₂HPO₄•(H₂O)₇ and NaOH). Solid NaCl was added to each solution to an ionic strength of 0.225 M. The pH of each stock solution was measured prior to use in swelling experiments using an *Oakton pH 1100 series* pH detector. The procedure described above for swelling in DI water was followed for the buffer solutions, except that a 2- instead of 6-dram vial was used because of the reduced swelling in these buffer solutions. Samples at 25 %Na were used for both the ICA and acrylic acid gels.

S7.4 Characterization of (dried) hydrogel powders and their (swollen) hydrogels

S7.4.1 Sodiated poly(isoprenecarboxylate) hydrogels [Gel(ICA-H/Na)]

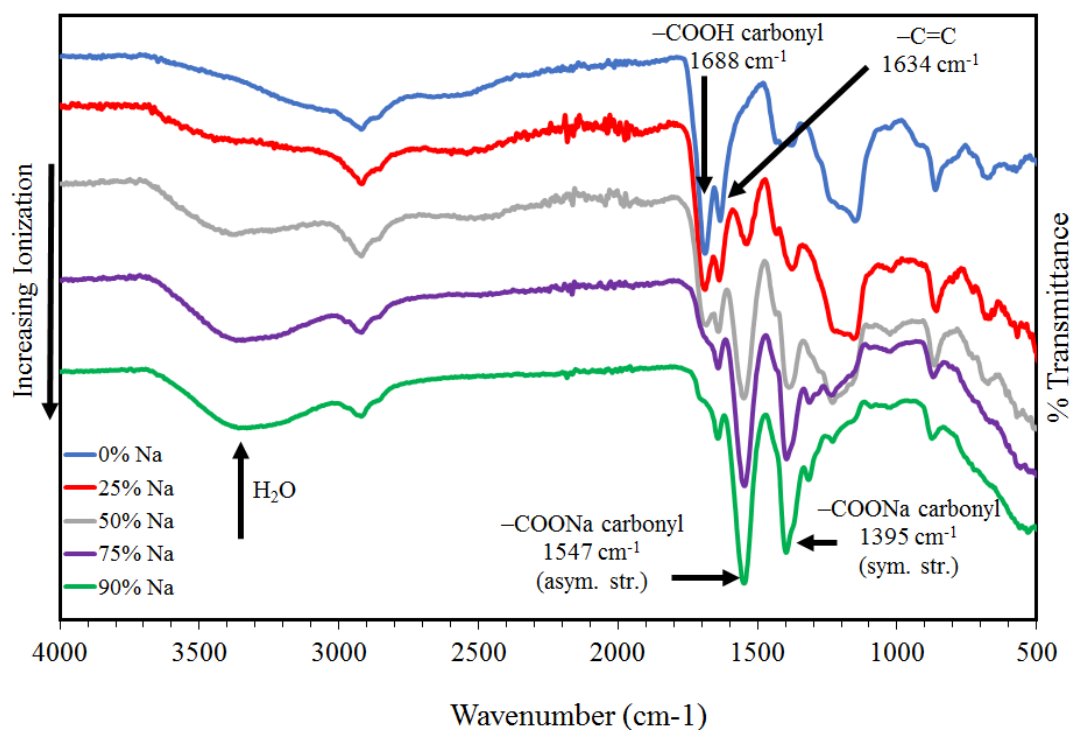


Figure S7.1 IR spectra of sodiated dried hydrogel powders [Gel(ICA-H/Na)] of varying levels (%) of ionization. Spectra of samples with higher levels of ionization show (i) decreased intensity of the $\text{-CO}_2\text{H}$ carbonyl stretch at 1688 cm^{-1} , (ii) increased intensity of the two $\text{-CO}_2\text{Na}$ carbonyl stretches at 1547 (asymmetric) and 1395 (symmetric) cm^{-1} ,³ and (iii) increased intensity in the broad -OH stretch at ca. 3300 cm^{-1} due to a greater amount of residual H_2O in the samples having higher ionization levels.

Table S7.2 Swelling ratios for sodiated isoprenecarboxylate hydrogels [Gel(ICA-H/Na)] at ionization levels ranging from 10–90% in DI water, in 0.17 M NaCl, and in 0.17 M KCl solutions.

| Di H ₂ O Solution | | | | 0.17 M NaCl in H ₂ O Solution | | | | | |
|------------------------------|----------------|--------|-----------------------|--|--------------|----------------|--------|-----------------------|-------------------|
| % Ionization | Swelling Ratio | | Average (each sample) | Average | % Ionization | Swelling Ratio | | Average (each sample) | Average |
| | 30 min | 60 min | | | | 30 min | 60 min | | |
| 10 (a) | 1.9 | 1.4 | 1.6 | 2.0 ± 0.9 | 10 (a) | - | - | - | - |
| (b) | 3.2 | 1.4 | 2.4 | | (b) | - | - | - | |
| 25 (a) | 84.7 | 80.7 | 82.7 | 80.9 ± 5.9 | 25 (a) | 9.5 | 8.5 | 9.0 | 10.4 ± 1.7 |
| (b) | 85.6 | 72.7 | 79.1 | | (b) | 12.2 | 11.5 | 11.9 | |
| 50 (a) | 136.3 | 137.6 | 137.0 | 137.2 ± 0.9 | 50 (a) | 16.5 | 13.0 | 14.7 | 15.8 ± 1.9 |
| (b) | 136.4 | 138.6 | 137.5 | | (b) | 17.0 | 16.9 | 17.0 | |
| 75 (a) | 189.2 | 174.9 | 182.0 | 178.1 ± 6.4 | 75 (a) | 36.4 | 37.6 | 37.0 | 36.4 ± 0.8 |
| (b) | 174.9 | 173.5 | 174.1 | | (b) | 36.0 | 35.8 | 35.9 | |
| 90 (a) | 245.1 | 245.4 | 245.2 | 257.9 ± 15.3 | 90 (a) | 53.1 | 52.3 | 52.7 | 51.9 ± 1.0 |
| (b) | 276.2 | 264.8 | 270.5 | | (b) | 51.4 | 50.8 | 51.1 | |

| 0.17 M KCl in H ₂ O Solution | | | | |
|---|----------------|--------|-----------------------|-------------------|
| % Ionization | Swelling Ratio | | Average (each sample) | Average |
| | 30 min | 60 min | | |
| 10 (a) | - | - | - | - |
| (b) | - | - | - | |
| 25 (a) | 6.5 | 6.3 | 6.4 | 5.2 ± 1.5 |
| (b) | 4.4 | 3.6 | 4.0 | |
| 50 (a) | 21.6 | 21.7 | 21.7 | 22.4 ± 0.5 |
| (b) | 22.5 | 22.6 | 22.6 | |
| 75 (a) | 36.4 | 36.6 | 36.5 | 36.1 ± 0.5 |
| (b) | 35.5 | 36.0 | 35.8 | |
| 90 (a) | 49.0 | 47.4 | 48.2 | 48.1 ± 0.8 |
| (b) | 47.3 | 48.6 | 48.0 | |

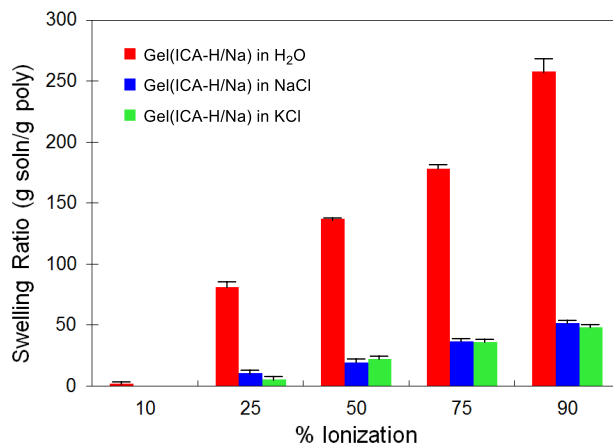


Figure S7.2 Graph of swelling ratio data (Table S7.2) for sodiated poly(isoprenecarboxylate) hydrogels [Gel(ICA-H/Na)] at ionization levels ranging from 10–90% in DI water (red), in 0.17 M NaCl (blue), and in 0.17 M KCl (green) solutions. This shows an increase in swelling ratio with increasing ionization in addition to a decrease in swelling ratio ca. 5 times in salt solutions relative to the swelling ratio in DI water.

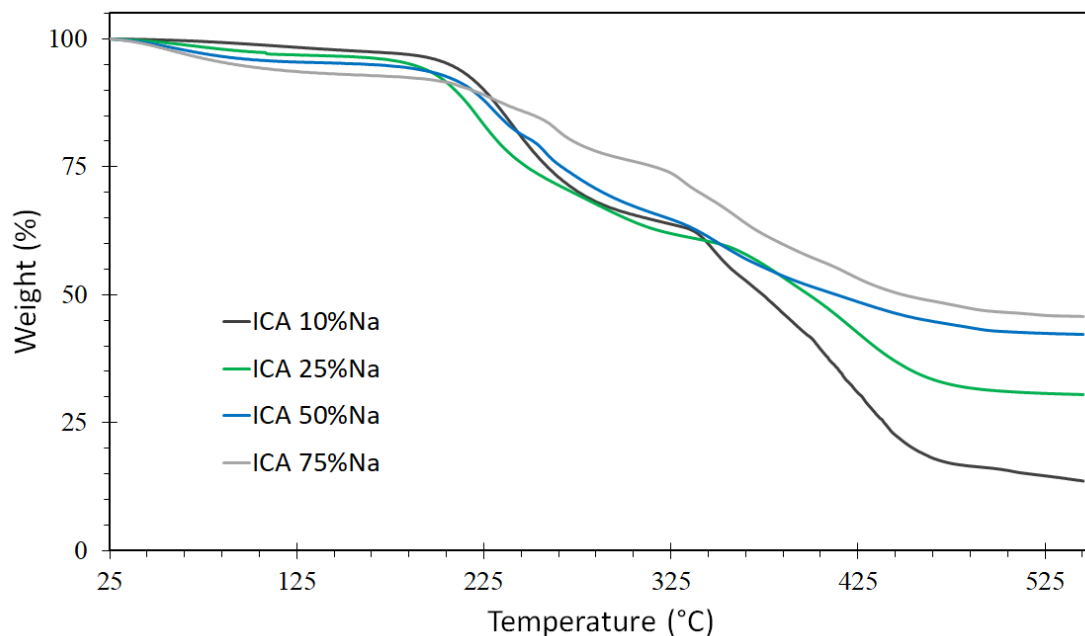
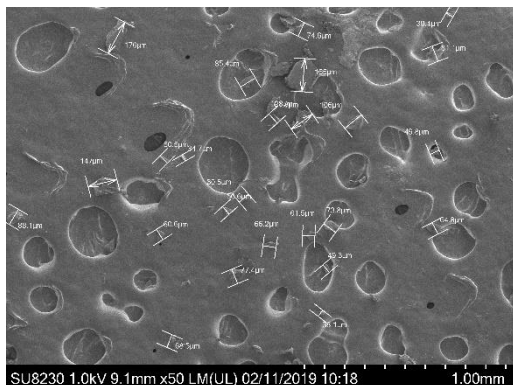


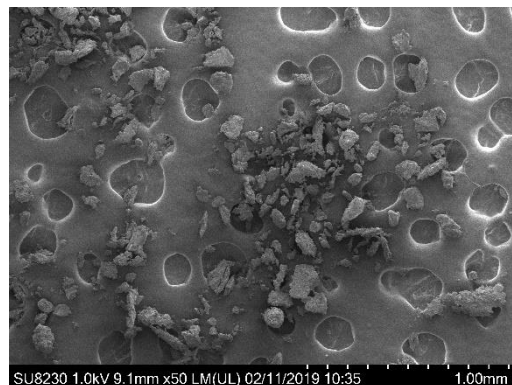
Figure S7.3 Thermogravimetric analysis (TGA) of Gel(ICA-H/Na) with varied levels of sodiation. For increasing levels of %Na, there is a higher level of mass loss from 25–150 °C, suggestive of an increasing amount of H₂O present in the gels with higher levels of %Na. This is supported with the IR spectra of these gels as shown in Figure 2c.

i. SEM images of **Gel(ICA-H/Na)**

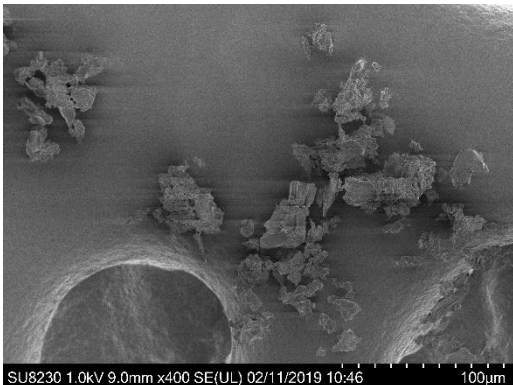
a) 10 %Na



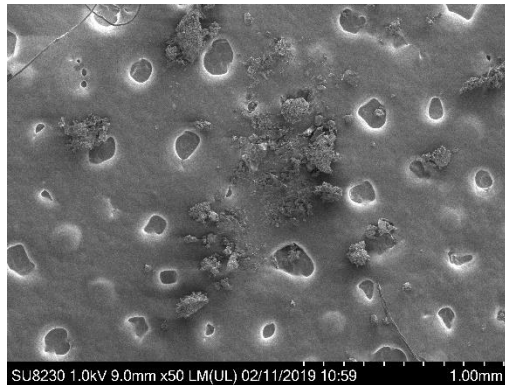
b) 25 %Na



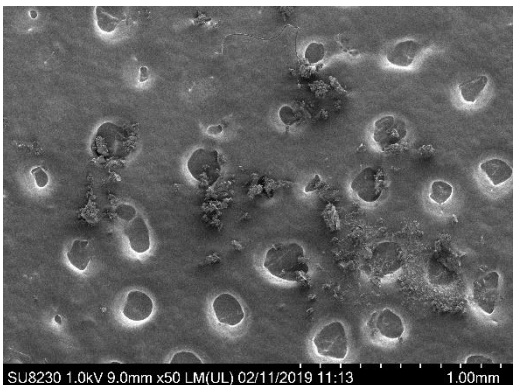
c) 50 %Na



d) 75 %Na



e) 90 %Na

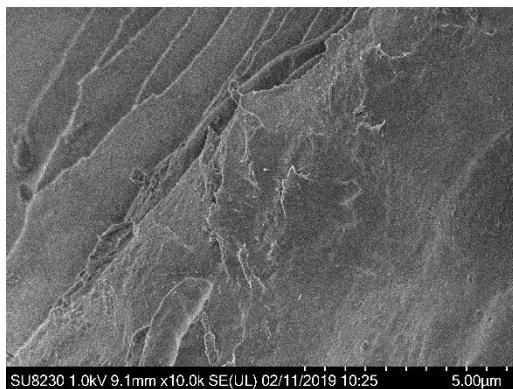


f) Tabulated particles sizes of **Gel(ICA-H/Na)** found from SEM images

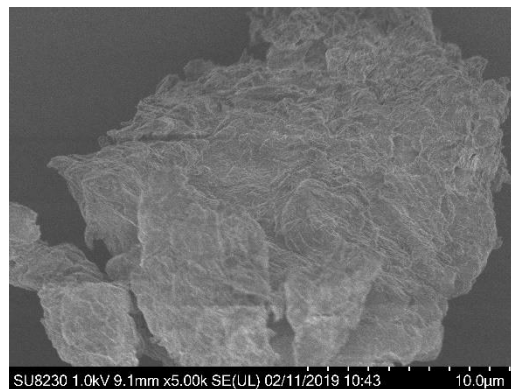
| | 10 | 25 | 50 | 75 | 90 %Na |
|---------------------|---------|---------|---------|---------|---------|
| avg. ± st.dev. (μm) | 83 ± 41 | 83 ± 54 | 32 ± 68 | 81 ± 68 | 31 ± 30 |
| max. (μm) | 176 | 301 | 350 | 285 | 131 |
| min. (μm) | 34 | 10 | 6 | 5 | 4 |

Figure S7.4 Representative SEM images of dried sodiated ICA gels (1% cross-link density) used to determine the relative particle sizes (note the low magnification) of each **Gel(ICA-H/Na)** [see table in bottom-right of figure (f)].

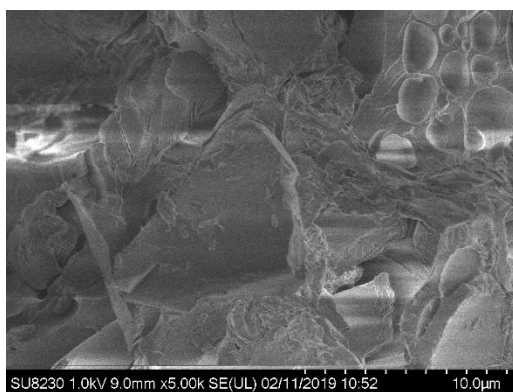
a) 10 %Na



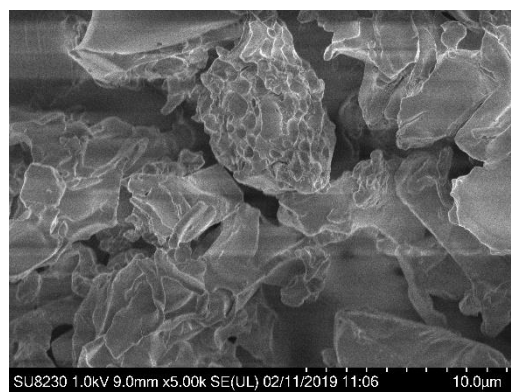
b) 25 %Na



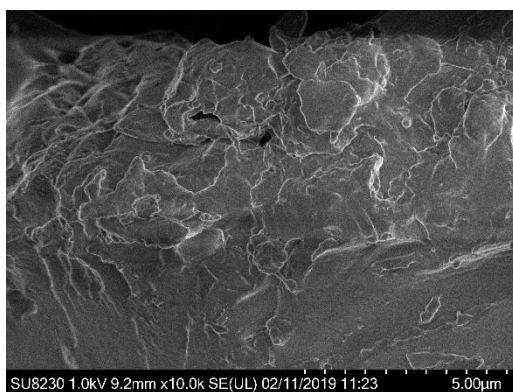
c) 50 %Na



d) 75 %Na



e) 90 %Na (i)



e) 90 %Na (ii)

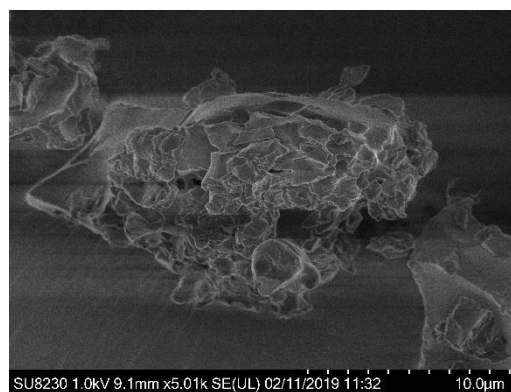


Figure S7.5 Representative, high-resolution SEM images of dried sodiated ICA gels (1% cross-link density).

Variation in the amount of cross-linking agent used in the preparation of hydrogel powders and swollen gels.

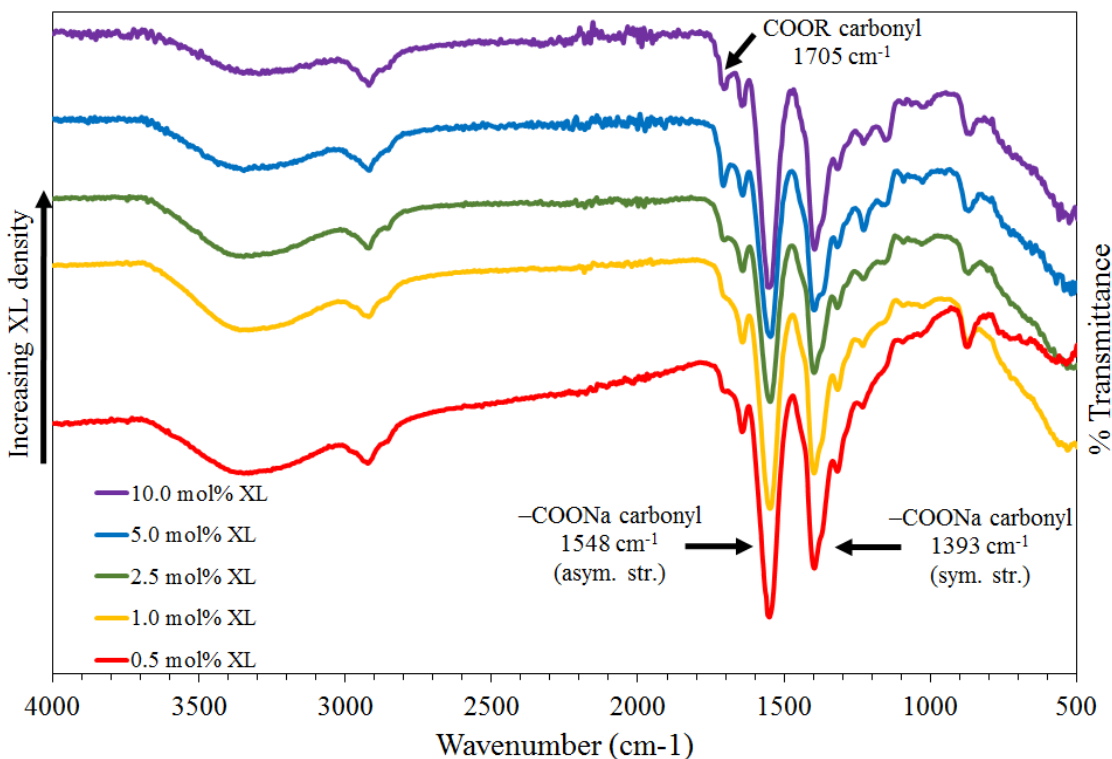


Figure S7.6 IR spectra of dried hydrogel powders that vary in the amount of cross-linking agent from 0.5–10 mol% of ICA-XL. All gels were synthesized with sodiated poly(isoprenecarboxylates) at 90% ionization. Spectra of samples show the $\text{-CO}_2\text{Na}$ carbonyl stretches at 1547 (asymmetric) and 1395 (symmetric) cm^{-1} and a broad -OH stretch at ca. 3300 cm^{-1} from H_2O that has been retained in the oven-dried gel. At higher cross-link densities, the $\text{-CO}_2\text{R}$ carbonyl stretch of the cross-linking agent is observed at 1705 cm^{-1} . The intensity of this band in the dried hydrogels prepared using 5 and 10 mol% of the cross-linker were very similar, suggestive of incomplete incorporation of the bis-dienoate ester.

Table S7.3 Swelling ratios for hydrogels made using 0.5 to 10 mol% of the cross-linking agent ICA-XL (90 %Na). The swelling ratios were recorded in DI water, in 0.17 M NaCl, and in 0.17 M KCl solutions.

| DI H ₂ O | | | | 0.17 M NaCl | | | | | |
|---------------------|----------------|--------|-----------------------|---------------------|-------------------|----------------|-------------|-----------------------|-------------------|
| % Crosslink Agent | Swelling Ratio | | Average (each sample) | Average | % Crosslink Agent | Swelling Ratio | | Average (each sample) | Average |
| | 30 min | 60 min | | | | 30 min | 60 min | | |
| 0.5 (a) | >400 | >400 | >400 | >400 | 0.5 (a) | 53.7 | 54.3 | 54.0 | 58.8 ± 5.5 |
| (b) | - | - | - | - | (b) | 63.3 | 63.9 | 63.6 | - |
| 1.0 (a) | 245.1 | 245.4 | 245.2 | 257.9 ± 15.3 | 1.0 (a) | 53.1 | 52.3 | 52.7 | 51.9 ± 1.0 |
| (b) | 276.2 | 264.8 | 270.5 | - | (b) | 51.4 | 50.8 | 51.1 | - |
| 2.5 (a) | 191.0 | 179.9 | 185.9 | 184.8 ± 5.9 | 2.5 (a) | 46.6 | 47.1 | 46.8 | 47.7 ± 1.1 |
| (b) | 187.4 | 179.9 | 183.7 | - | (b) | 48.4 | 48.9 | 48.6 | - |
| 5.0 (a) | 118.3 | 111.6 | 114.9 | 116.1 ± 3.1 | 5.0 (a) | 37.4 | 34.0 | 35.7 | 35.0 ± 2.0 |
| (b) | 117.5 | 117.0 | 117.2 | - | (b) | 35.7 | 32.9 | 32.4 | - |
| 10.0 (a) | 105.4 | 105.6 | 105.5 | 111.4 ± 6.9 | 10.0 (a) | 34.9 | 34.7 | 34.8 | 35.2 ± 0.5 |
| (b) | 118.7 | 115.9 | 117.3 | - | (b) | 35.5 | 35.7 | 35.6 | - |

| 0.17 M KCl | | | | |
|-------------------|----------------|--------|-----------------------|-------------------|
| % Crosslink Agent | Swelling Ratio | | Average (each sample) | Average |
| | 30 min | 60 min | | |
| 0.5 (a) | 66.5 | 56.8 | 61.7 | 61.3 ± 7.7 |
| (b) | 69.1 | 52.9 | 61.0 | - |
| 1.0 (a) | 49.0 | 47.4 | 48.2 | 48.1 ± 0.8 |
| (b) | 47.3 | 48.6 | 48.0 | - |
| 2.5 (a) | 48.2 | 50.8 | 49.5 | 49.3 ± 1.1 |
| (b) | 49.1 | 49.1 | 49.1 | - |
| 5.0 (a) | 39.2 | 37.5 | 38.4 | 39.5 ± 1.6 |
| (b) | 41.5 | 39.6 | 40.6 | - |
| 10.0 (a) | 35.5 | 36.7 | 36.1 | 35.2 ± 1.7 |
| (b) | 32.7 | 36.0 | 34.3 | - |

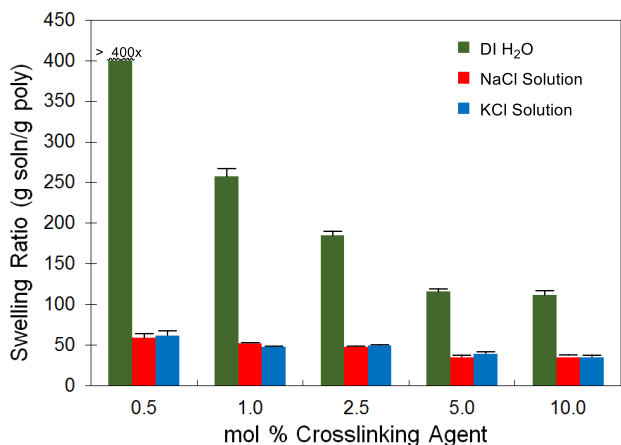


Figure S7.7 Graph of swelling ratios (SRs) (Table S7.3) for hydrogels prepared using 0.5 to 10 mol% of the cross-linking agent ICA-XL (90 %Na). The SRs were measured in DI water (green), in 0.17 M NaCl (red), and in 0.17 M KCl (blue) solutions.

S.7.4.2 Sodiated poly(acrylate) hydrogels [Gel(AA-H/Na)]

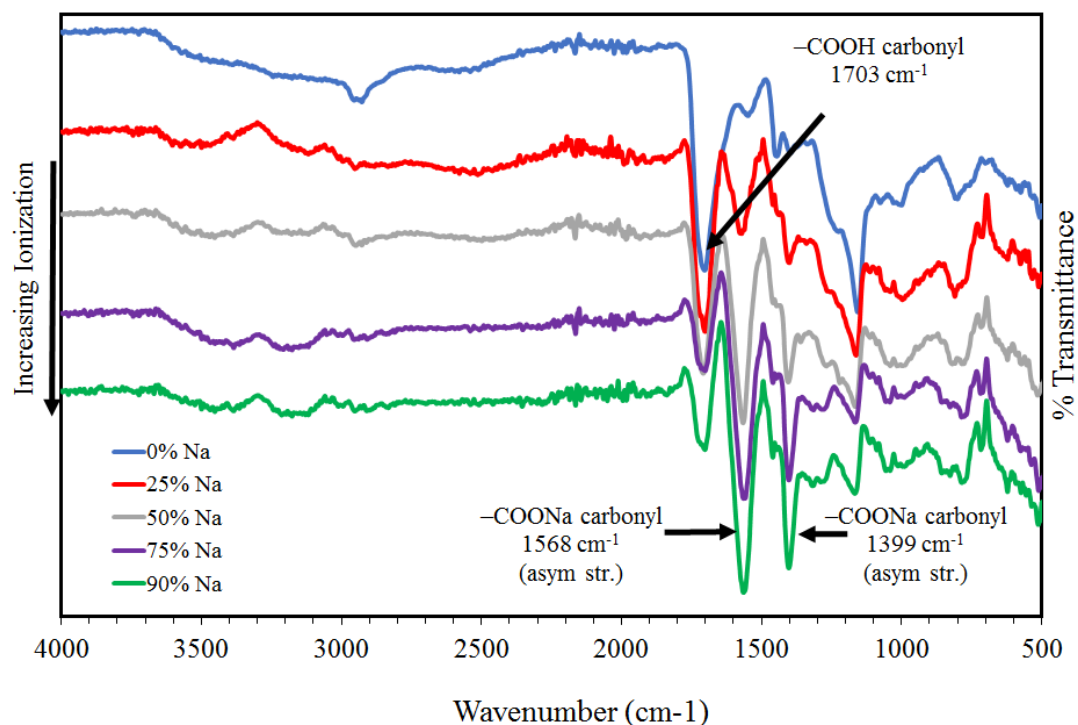


Figure S7.8 IR spectra of dried poly(acrylate) hydrogels [Gel(AA-H/Na)] of varying ionization with NaOH. The spectra show (i) the decrease in the $\text{-CO}_2\text{H}$ carbonyl stretch at 1703 cm^{-1} and (ii) an increase in the two $\text{-CO}_2\text{Na}$ carbonyl stretches at 1566 (asymmetric) and 1399 (symmetric) cm^{-1} .

Table S7.4 Swelling ratios for sodiated poly(acrylate) hydrogels [Gel(AA-H/Na)] at ionizations ranging from 10–90% in DI water, in 0.17 M NaCl, and in 0.17 M KCl solutions.

Poly(sodio acrylate)

| DI H ₂ O Solution | | | | | 0.17 M NaCl in H ₂ O Solution | | | | |
|------------------------------|----------------|--------|-----------------------|-------------|--|----------------|--------|-----------------------|----------------|
| % Ionization | Swelling Ratio | | Average (each sample) | Average | % Ionization | Swelling Ratio | | Average (each sample) | Average Groups |
| | 30 min | 60 min | | | | 30 min | 60 min | | |
| 10 (a) | 78.3 | 72.1 | 75.2 | 76.0 ± 3.2 | 10 (a) | 13.1 | 15.0 | 14.0 | 13.2 ± 1.4 |
| (b) | 78.8 | 74.8 | 76.8 | | (b) | 13.0 | 11.6 | 12.3 | |
| 25 (a) | 124.8 | 118.4 | 121.6 | 113.2 ± 8.9 | 25 (a) | 24.2 | 23.6 | 23.9 | 23.9 ± 0.3 |
| (b) | 107.5 | 102.2 | 104.8 | | (b) | 23.8 | 23.9 | 23.8 | |
| 50 (a) | 153.0 | 165.5 | 159.3 | 151.8 ± 8.7 | 50 (a) | 39.4 | 38.9 | 39.2 | 37.3 ± 2.2 |
| (b) | 145.6 | 143.3 | 144.4 | | (b) | 35.0 | 35.9 | 35.4 | |
| 75 (a) | 124.5 | 108.6 | 116.6 | 113.8 ± 6.4 | 75 (a) | 34.7 | 33.3 | 34.0 | 34.8 ± 1.0 |
| (b) | 110.8 | 111.2 | 111.0 | | (b) | 35.5 | 35.6 | 35.5 | |
| 90 (a) | 107.0 | 109.1 | 108.0 | 105.9 ± 2.9 | 90 (a) | 30.9 | 28.8 | 29.8 | 31.1 ± 2.3 |
| (b) | 101.3 | 106.3 | 103.8 | | (b) | 34.3 | 30.6 | 32.5 | |

0.17 M KCl in H₂O Solution

| % Ionization | Swelling Ratio | | Average (each sample) | Average |
|--------------|----------------|--------|-----------------------|------------|
| | 30 min | 60 min | | |
| 10 (a) | 7.5 | 7.7 | 7.6 | 7.7 ± 0.2 |
| (b) | 7.7 | 7.7 | 7.9 | |
| 25 (a) | 23.9 | 24.1 | 24.0 | 23.0 ± 1.2 |
| (b) | 21.8 | 22.2 | 22.0 | |
| 50 (a) | 36.7 | 35.6 | 36.1 | 35.7 ± 0.7 |
| (b) | 35.1 | 35.3 | 35.2 | |
| 75 (a) | 34.8 | 38.0 | 36.4 | 34.4 ± 2.7 |
| (b) | 32.7 | 32.0 | 32.3 | |
| 90 (a) | 34.6 | 31.9 | 33.2 | 34.1 ± 1.6 |
| (b) | 35.5 | 34.5 | 35.0 | |

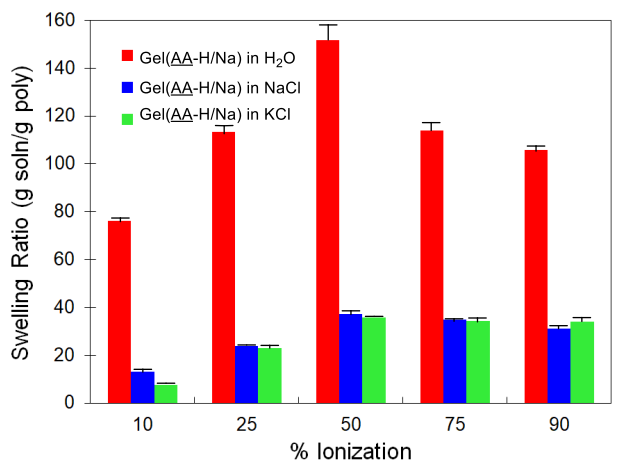


Figure S7.9 Graph of swelling ratio data (Table S7.4) for sodiated poly(acrylate) hydrogels [Gel(AA-H/Na)] at ionization levels ranging from 10–90% in DI water (red), in 0.17 M NaCl (blue), and in 0.17 M KCl (green) solutions. This shows an increase in swelling ratio with increasing ionization in addition to a decrease in swelling ratio ca. 3–5 times in salt solutions relative to the swelling ratio in DI water.

i. Swelling vs. pH comparison of **Gel(ICA-H/Na)** and **Gel(AA-H/Na)**

Table S7.5 Swelling ratios for sodiated hydrogels [**Gel(ICA-H/Na)** and **Gel(AA-H/Na)**] at 25% ionization in pH solutions ranging from 2.4-9.9 ([buffer] = 0.05 M $I = 0.225$ M).

pH Effects

Gel(ICA-H/Na)

| pH | Swelling Ratio | | Average (each sample) | Average |
|---------|----------------|--------|--------------------------|-------------------|
| | 30 min | 60 min | | |
| 2.4 (a) | 1.4 | 1.0 | 1.2 | 1.1 ± 0.4 |
| (b) | 0.6 | 1.3 | 0.9 | |
| 4.4 (a) | 6.0 | 4.1 | 5.1 | 5.3 ± 0.9 |
| (b) | 6.4 | 4.6 | 5.5 | |
| 6.6 (a) | 38.4 | 38.0 | 38.2 | 39.2 ± 1.2 |
| (b) | 40.7 | 40.5 | 40.6 | |
| 8.3 (a) | 43.4 | 37.9 | 40.6 | 43.0 ± 3.1 |
| (b) | 44.7 | 46.1 | 45.4 | |
| 9.9 (a) | 54.9 | 51.7 | 53.3 | 49.9 ± 4.2 |
| (b) | 49.3 | 43.5 | 46.4 | |

Gel(AA-H/Na)

| pH | Swelling Ratio | | Average (each sample) | Average |
|---------|----------------|--------|--------------------------|-------------------|
| | 30 m | 60 min | | |
| 2.4 (a) | 3.5 | 1.9 | 2.7 | 2.8 ± 0.6 |
| (b) | 3.2 | 2.7 | 2.9 | |
| 4.4 (a) | 16.6 | 15.0 | 15.8 | 17.4 ± 1.7 |
| (b) | 19.3 | 18.8 | 19.0 | |
| 6.6 (a) | 36.7 | 37.1 | 36.9 | 35.9 ± 1.3 |
| (b) | 36.1 | 33.7 | 34.9 | |
| 8.3 (a) | 34.7 | 34.9 | 34.8 | 35.4 ± 1.1 |
| (b) | 34.8 | 37.4 | 36.1 | |
| 9.9 (a) | 34.2 | 34.0 | 34.1 | 35.4 ± 1.1 |
| (b) | 37.8 | 35.6 | 36.7 | |

S.7.4.3 Potassiated poly(isoprenecarboxylate) hydrogels [Gel(ICA-H/K)]

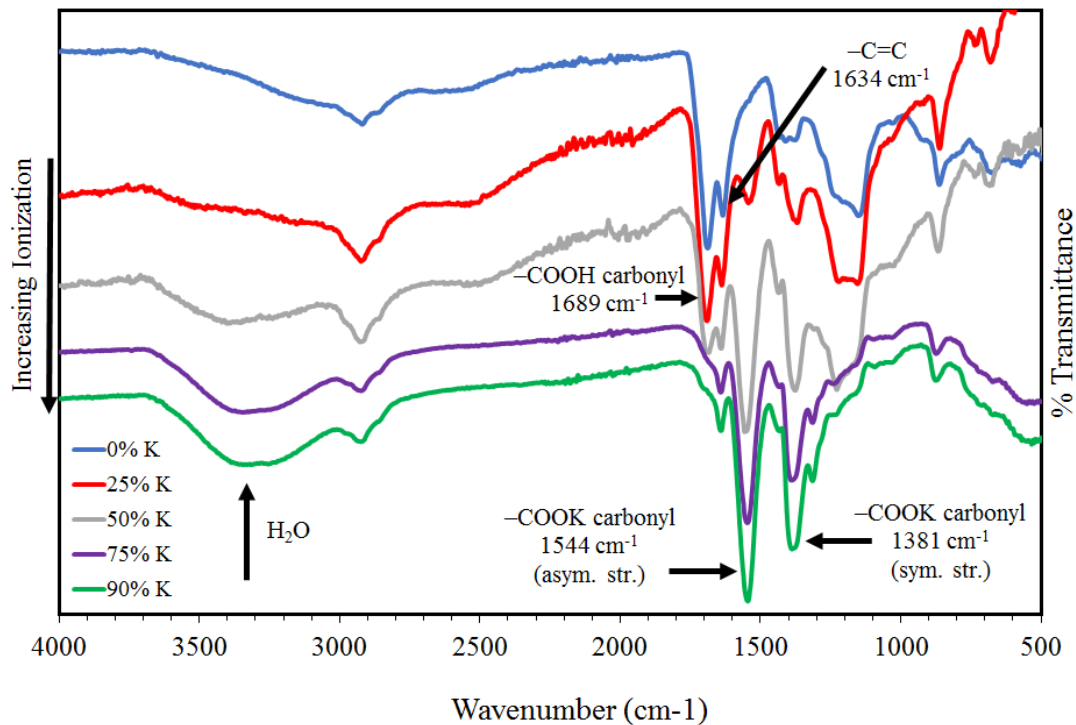


Figure S7.10 IR spectra of dried potassiated hydrogel powders [Gel(ICA-H/K)] of varying % ionization. Spectra of samples with higher levels of ionization show (i) decreased intensity of the -CO₂H carbonyl stretch at 1689 cm⁻¹, (ii) increased intensity of the two -CO₂Na carbonyl stretches at 1544 (asymmetric) and 1381 (symmetric) cm⁻¹, and (iii) increased intensity in the broad -OH stretch at ca. 3300 cm⁻¹ due to a greater amount of residual H₂O in the samples having higher ionization levels.

Table S7.6 Swelling ratios for potassiated isoprenecarboxylate hydrogels [**Gel(ICA-H/K)**] at ionization levels ranging from 10–90% in DI water, in 0.17 M NaCl, and in 0.17 M KCl solutions.

| DI H ₂ O Solution | | | | | 0.17 M NaCl in H ₂ O Solution | | | | |
|------------------------------|----------------|--------|-----------------------|------------------|--|----------------|--------|-----------------------|----------------|
| % Ionization | Swelling Ratio | | Average (each sample) | Average | % Ionization | Swelling Ratio | | Average (each sample) | Average |
| | 30 min | 60 min | | | | 30 min | 60 min | | |
| 10 (a) | 1.6 | 2.0 | 1.8 | 1.6 ± 0.3 | 10 (a) | - | - | - | - |
| (b) | 1.5 | 1.3 | 1.4 | | (b) | - | - | - | |
| 25 (a) | 36.0 | 39.1 | 37.5 | 42.9 ± 6.3 | 25 (a) | 7.2 | 7.2 | 7.2 | 6.8 ± 0.5 |
| (b) | 47.5 | 49.0 | 48.2 | | (b) | 6.7 | 6.2 | 6.5 | |
| 50 (a) | 140.6 | 147.4 | 144.0 | 146.4 ± 4.2 | 50 (a) | 21.2 | 16.9 | 19.1 | 21.1 ± 3.3 |
| (b) | 150.4 | 147.1 | 148.7 | | (b) | 24.9 | 21.5 | 23.2 | |
| 75 (a) | 230.5 | 220.3 | 225.4 | 218.6 ± 9.1 | 75 (a) | 38.7 | 35.9 | 37.3 | 39.2 ± 5.0 |
| (b) | 209.4 | 214.2 | 221.8 | | (b) | 46.3 | 44.2 | 45.2 | |
| 90 (a) | 238.2 | 246.5 | 242.3 | 224.3 ± 21.1 | (c) | 34.8 | 35.0 | 34.9 | 45.6 ± 0.3 |
| (b) | 207.3 | 205.3 | 206.3 | | 90 (a) | 45.2 | 45.8 | 45.5 | |
| | | | | | (b) | 45.6 | 45.7 | 45.7 | |

| 0.17 M KCl in H ₂ O Solution | | | | |
|---|----------------|--------|-----------------------|----------------|
| % Ionization | Swelling Ratio | | Average (each sample) | Average |
| | 30 min | 60 min | | |
| 10 (a) | - | - | - | - |
| (b) | - | - | - | |
| 25 (a) | 4.5 | 4.2 | 4.4 | 3.1 ± 0.5 |
| (b) | 3.3 | 4.0 | 3.6 | |
| 50 (a) | 26.4 | 28.3 | 27.3 | 28.1 ± 1.2 |
| (b) | 28.6 | 29.1 | 28.8 | |
| 75 (a) | 44.6 | 42.6 | 43.6 | 42.9 ± 1.4 |
| (b) | 43.2 | 41.2 | 42.2 | |
| 90 (a) | 45.5 | 45.9 | 45.7 | 44.1 ± 2.0 |
| (b) | 42.9 | 41.8 | 42.4 | |

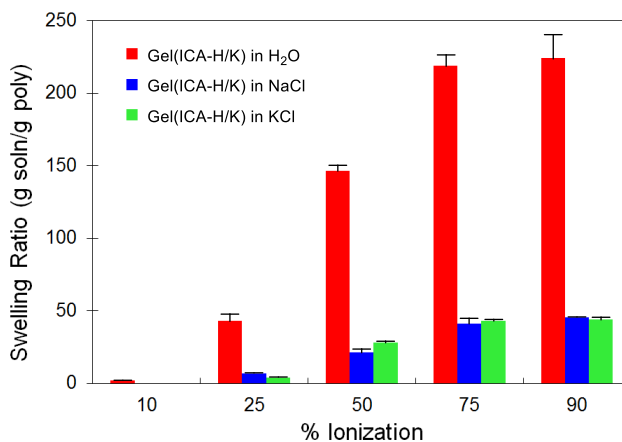


Figure S7.11 Graph of swelling ratio data (Table S7.6) for potassiated poly(isoprene-carboxylate) hydrogels [**Gel(ICA-H/K)**] at ionization levels ranging from 10–90% in DI water (red), in 0.17 M NaCl (blue), and in 0.17 M KCl (green) solutions. This shows an increase in swelling ratio with increasing ionization in addition to a decrease (ca. 5 times) in swelling ratio in salt solutions relative to the swelling ratio in DI water.

S.7.4.3 Lithiated poly(isoprenecarboxylate) hydrogels [Gel(ICA-H/Li)]

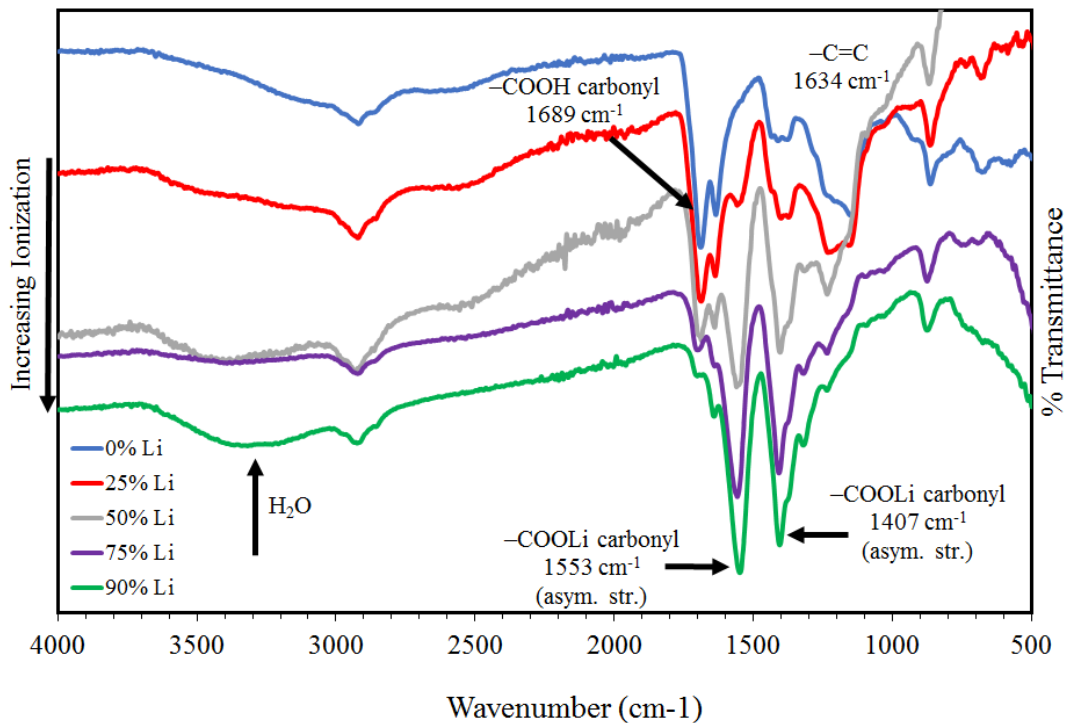


Figure S7.12 IR spectra of lithiated dried hydrogel powders [Gel(ICA-H/Li)] of varying % ionization. Spectra of samples with higher levels of ionization show (i) decreased intensity of the $\text{-CO}_2\text{H}$ carbonyl stretch at 1689 cm^{-1} , (ii) increased intensity of the two $\text{-CO}_2\text{Li}$ carbonyl stretches at 1553 (asymmetric) and 1407 (symmetric) cm^{-1} , and (iii) increased intensity in the broad -OH stretch at ca. 3300 cm^{-1} due to a greater amount of residual H_2O in the samples having higher ionization levels.

Table S7.7 Swelling ratios for lithiated poly(isoprenecarboxylate) hydrogels [**Gel(ICA-H/Li)**] at ionization levels ranging from 10–90% in DI water, in 0.17 M NaCl, and in 0.17 M KCl solutions. The 10% ionization samples in DI H₂O continued to increase in swelling ratio at 30 and 60 minutes; results shown are for *90 and **120 minutes.

| DI H ₂ O Solution | | | | | 0.17 M NaCl in H ₂ O Solution | | | | |
|------------------------------|----------------|--------|-----------------------|--------------|--|----------------|--------|-----------------------|------------|
| % Ionization | Swelling Ratio | | Average (each sample) | Average | % Ionization | Swelling Ratio | | Average (each sample) | Average |
| | 30 min | 60 min | | | | 30 min | 60 min | | |
| 10 (a) | 12.5* | 12.4** | 12.4 | 13.2 ± 0.9 | 10 (a) | - | - | - | - |
| (b) | 14.2* | 13.7** | 13.9 | | (b) | - | - | - | |
| 25 (a) | 60.2 | 59.7 | 59.9 | 55.9 ± 5.0 | 25 (a) | 6.6 | 5.6 | 6.1 | 5.4 ± 0.9 |
| (b) | 53.8 | 49.8 | 51.8 | | (b) | 4.8 | 4.8 | 4.8 | |
| 50 (a) | 165.9 | 169.5 | 167.7 | 171.3 ± 4.8 | 50 (a) | 28.1 | 26.0 | 27.1 | 26.8 ± 1.0 |
| (b) | 177.1 | 172.7 | 174.9 | | (b) | 27.2 | 26.1 | 26.6 | |
| 75 (a) | 201.2 | 203.0 | 202.1 | 212.3 ± 11.8 | 75 (a) | 46.8 | 45.3 | 46.1 | 45.1 ± 1.6 |
| (b) | 222.3 | 222.8 | 222.6 | | (b) | 43.0 | 45.3 | 44.2 | |
| 90 (a) | 321.0 | 311.1 | 316.1 | 321.9 ± 11.9 | 90 (a) | 57.4 | 55.7 | 56.5 | 55.9 ± 1.0 |
| (b) | 316.9 | 338.7 | 327.8 | | (b) | 54.8 | 55.7 | 55.2 | |

| 0.17 M KCl in H ₂ O Solution | | | | |
|---|----------------|--------|-----------------------|------------|
| % Ionization | Swelling Ratio | | Average (each sample) | Average |
| | 30 min | 60 min | | |
| 10 (a) | - | - | - | - |
| (b) | - | - | - | |
| 25 (a) | 3.5 | 2.8 | 3.2 | 3.1 ± 0.3 |
| (b) | 3.1 | 3.1 | 3.1 | |
| 50 (a) | 27.1 | 28.2 | 27.7 | 28.0 ± 1.2 |
| (b) | 27.1 | 29.6 | 28.3 | |
| 75 (a) | 45.0 | 44.5 | 44.8 | 43.4 ± 1.7 |
| (b) | 42.6 | 41.5 | 42.1 | |
| 90 (a) | 54.6 | 54.5 | 54.6 | 54.0 ± 0.7 |
| (b) | 53.8 | 53.4 | 53.4 | |

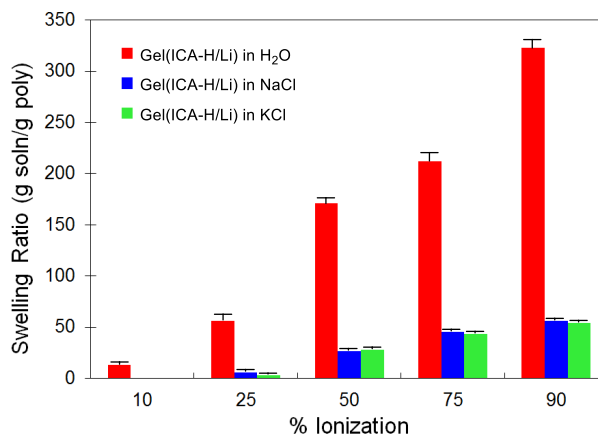


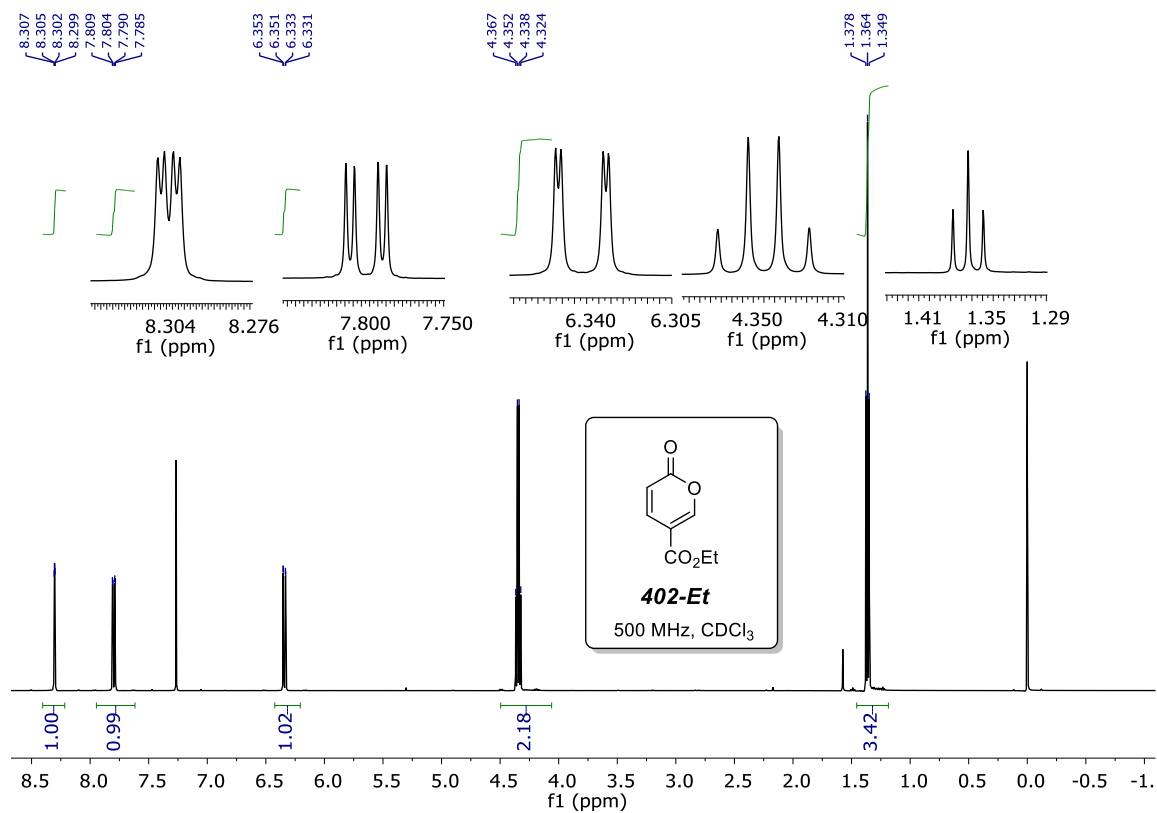
Figure S7.13 Graph of swelling ratio data (Table S7.7) for lithiated poly(isoprenecarboxylate) hydrogels [**Gel(ICA-H/Li)**] at ionization levels ranging from 10–90% in DI water (red), in 0.17 M NaCl (blue), and in 0.17 M KCl (green) solutions. This shows an increase in swelling ratio with increasing ionization in addition to a decrease (ca. 5 times) in swelling ratio in salt solutions relative to the swelling ratio in DI water.

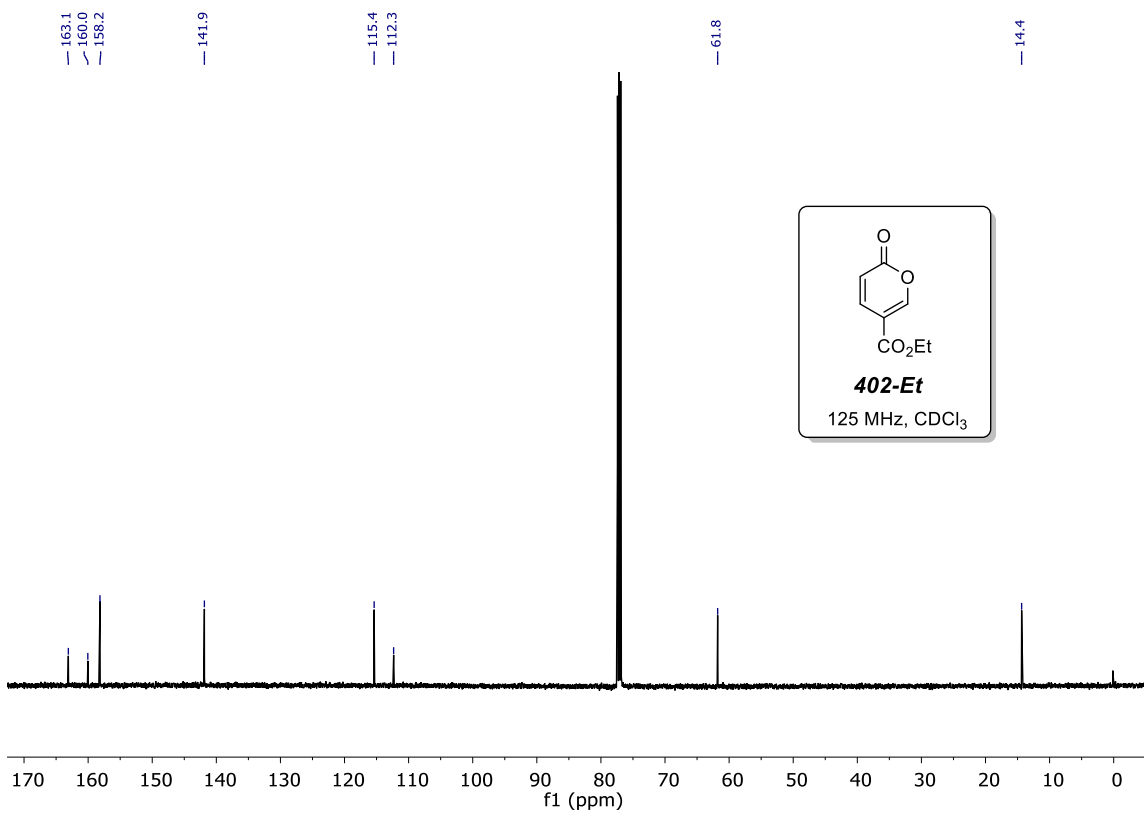
S7.5 References

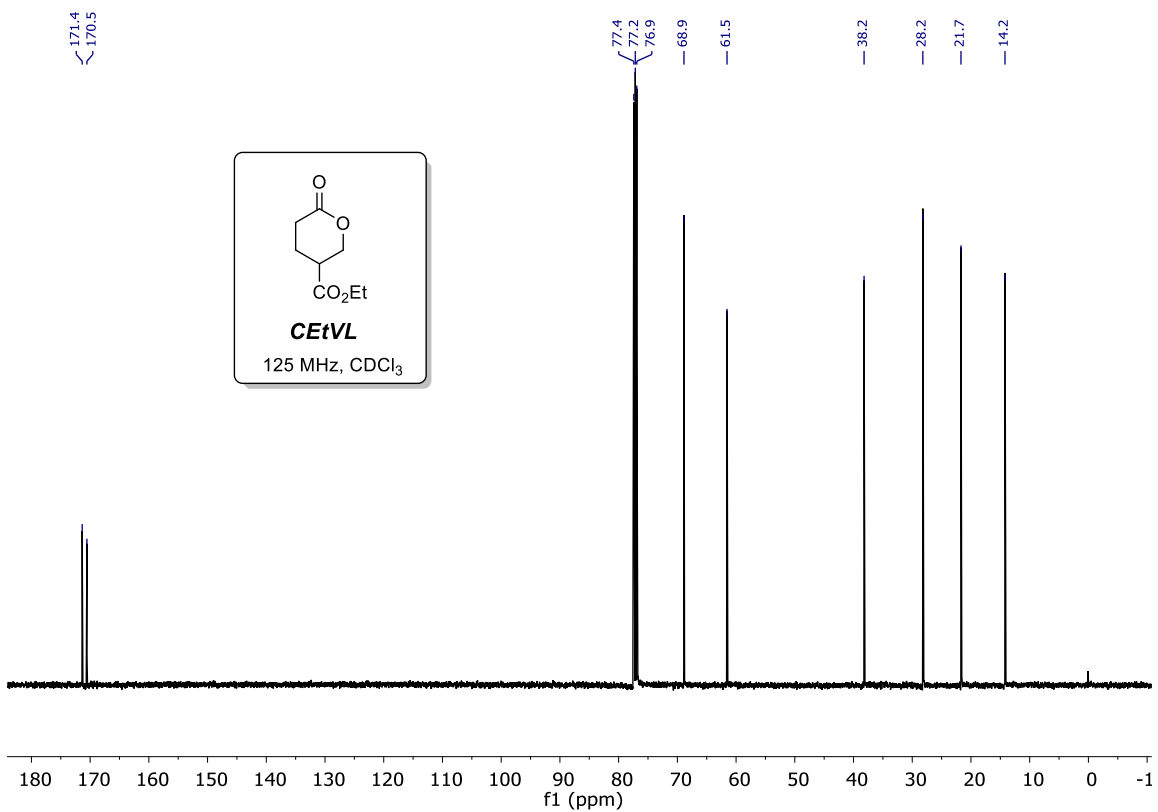
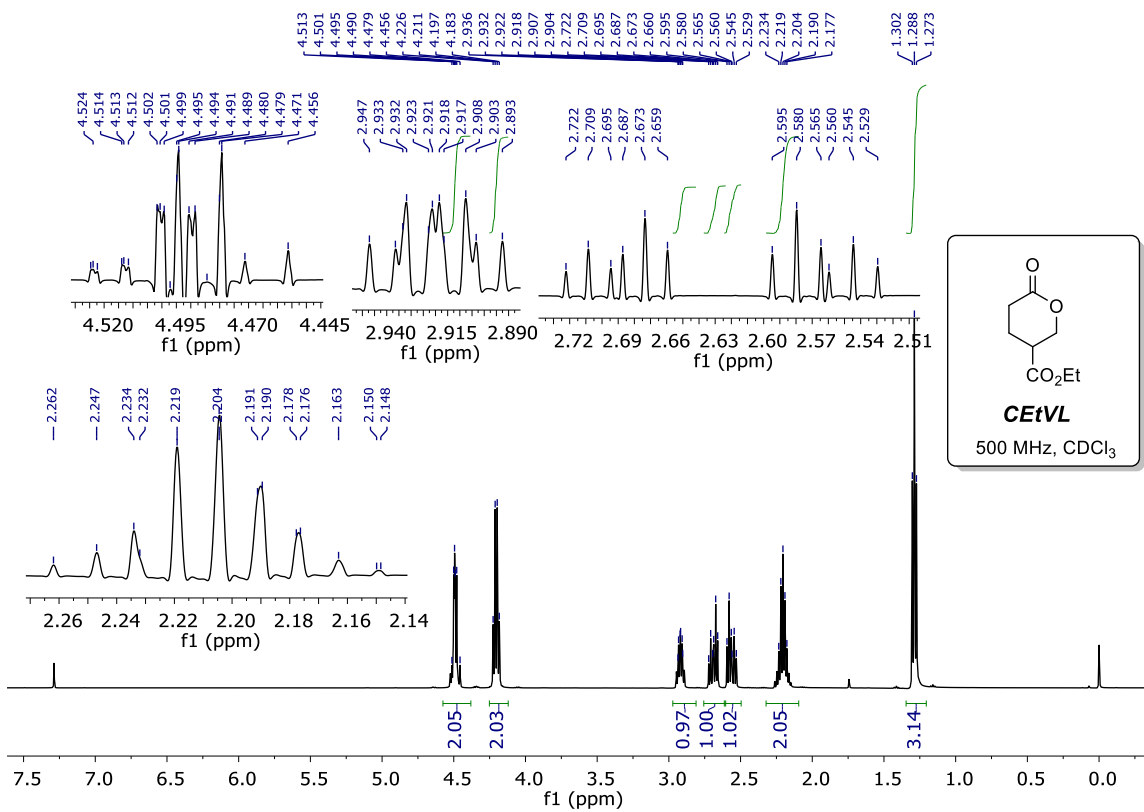
- ¹ (a) Hoye, T. R.; Hanson, P. R.; Vyvyan, J. R. *J. Org. Chem.* **1994**, *59*, 4096–4103. (b) Hoye, T. R.; Zhao, H. *J. Org. Chem.* **2002**, *67*, 4014–4016.
- ² Ball-Jones, N. R.; Fahnhorst, G. W.; Hoye, T. R. *ACS Macro Lett.* **2016**, *5*, 1128–1131.
- ³ Max, J. J.; Chapados, C. *J. Phys. Chem. A* **2004**, *108*, 3324–3337.

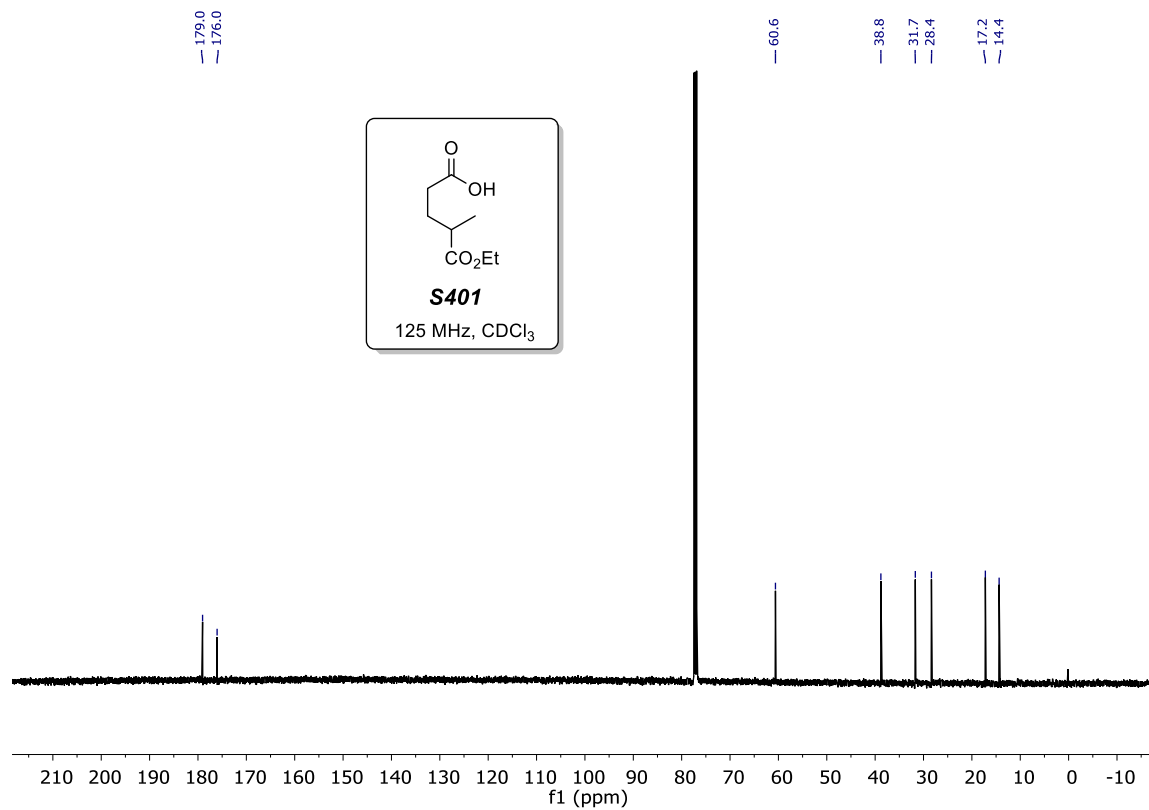
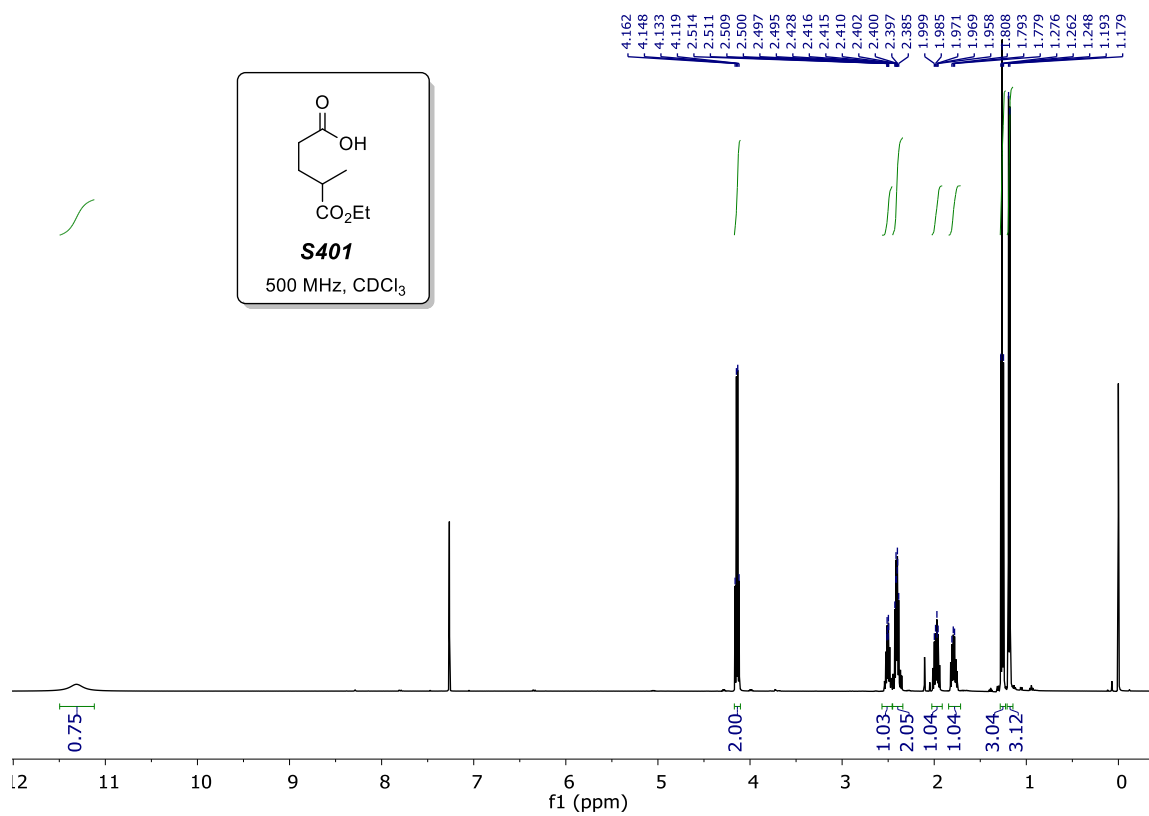
Appendix G. Copies of NMR spectra for Chapter 4 and 5

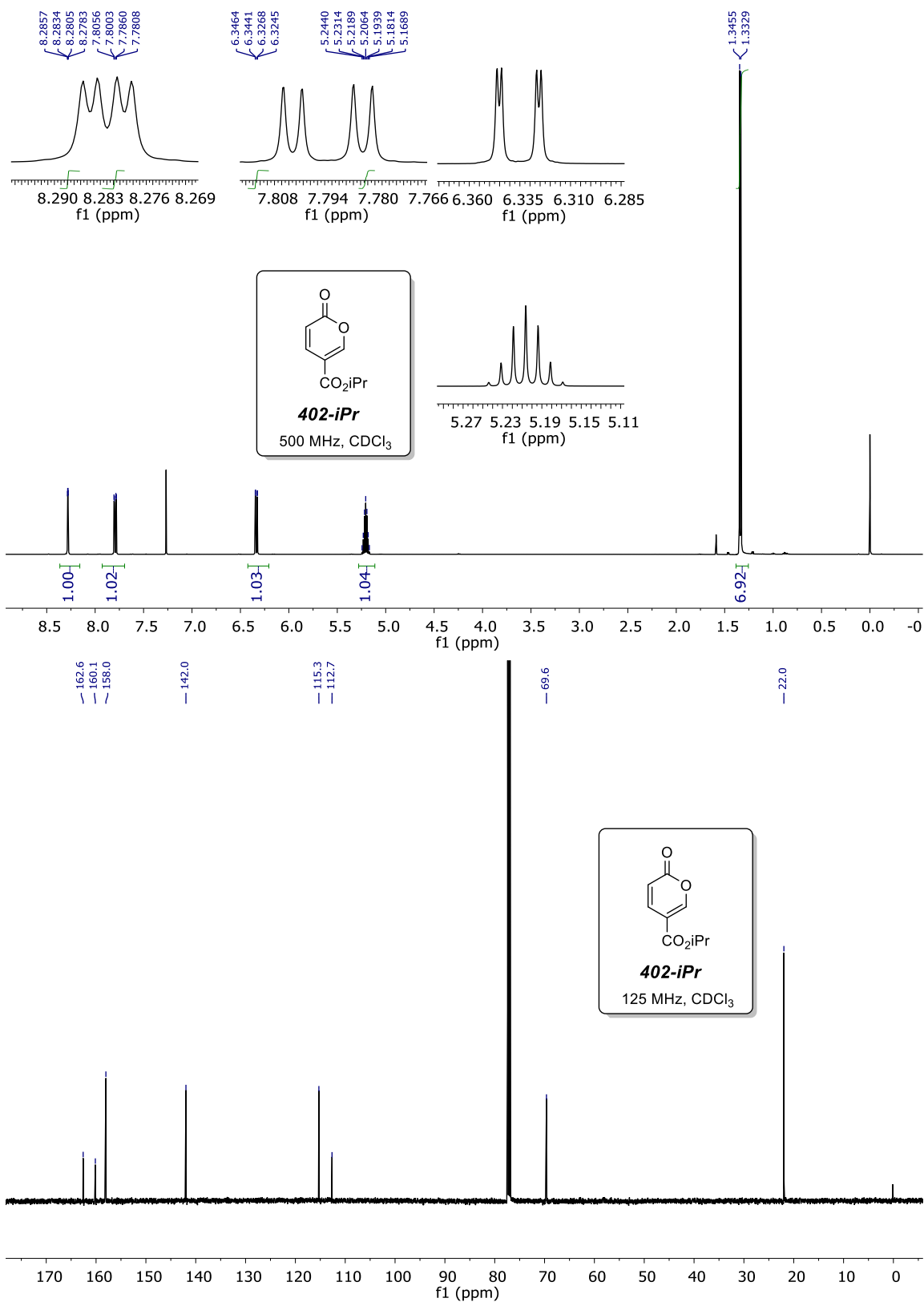
S8.1 Small molecule spectra for Chapter 4

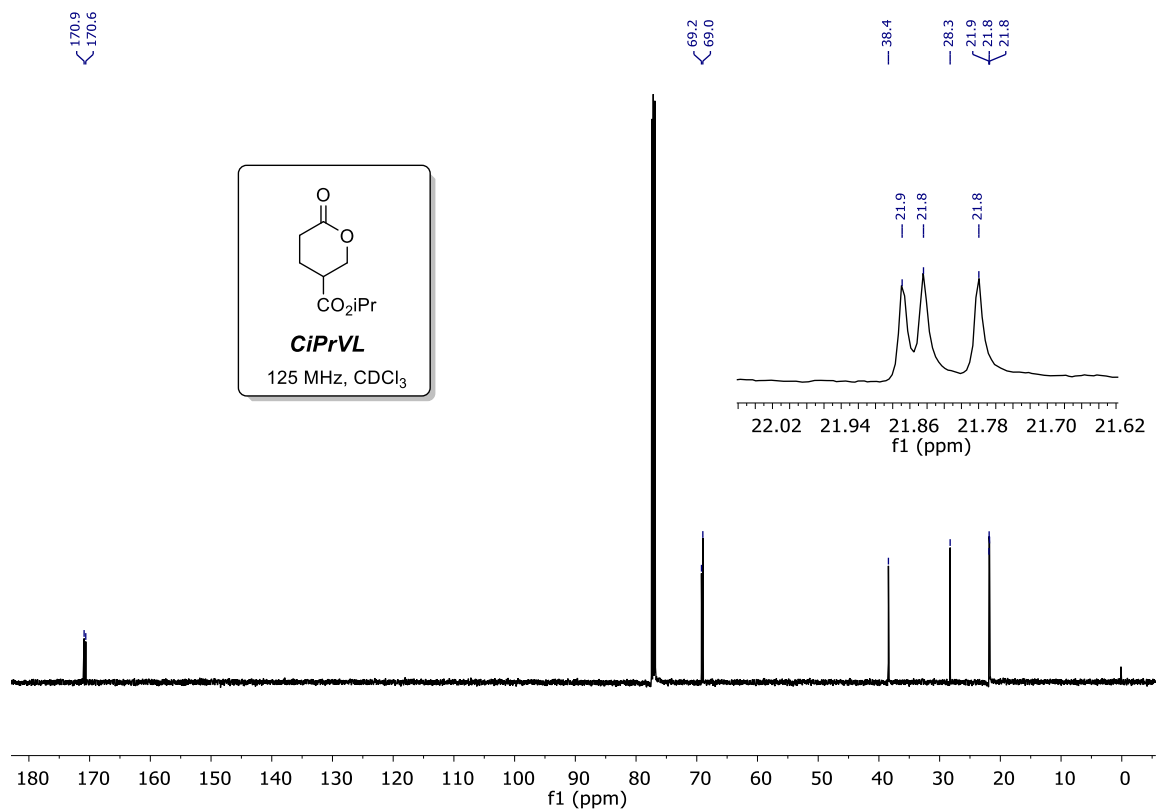
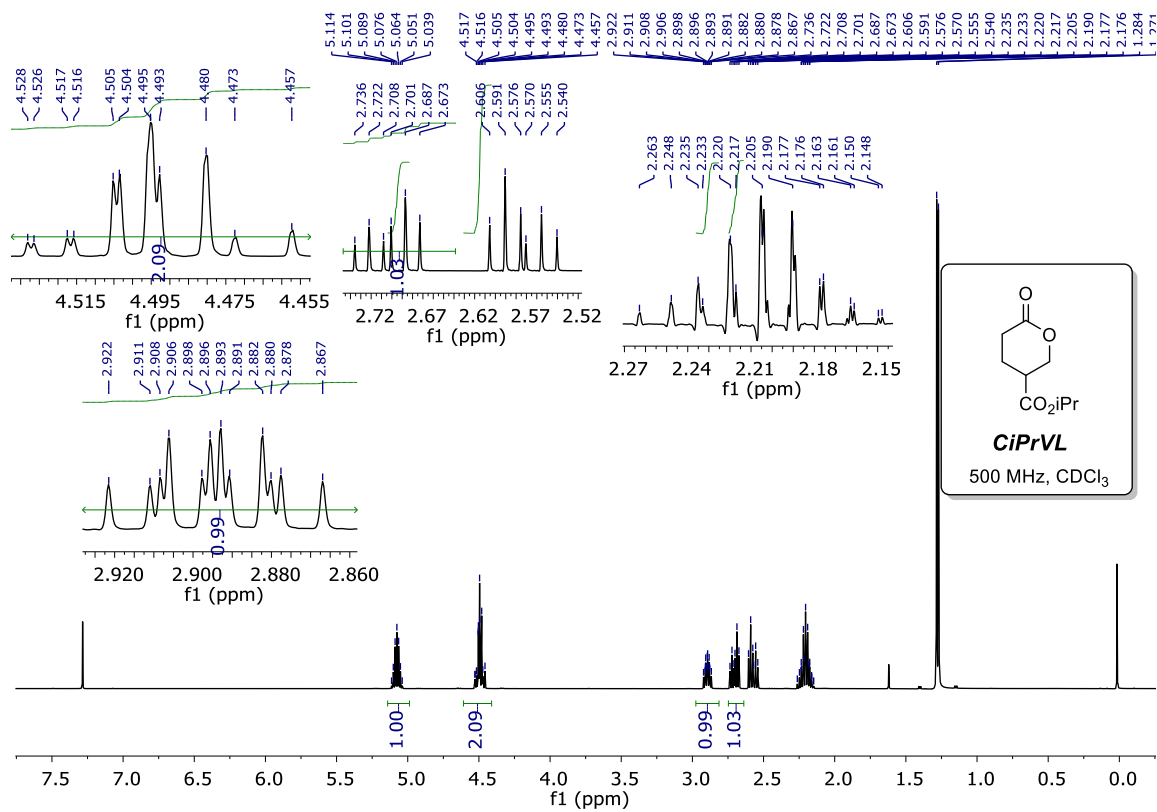


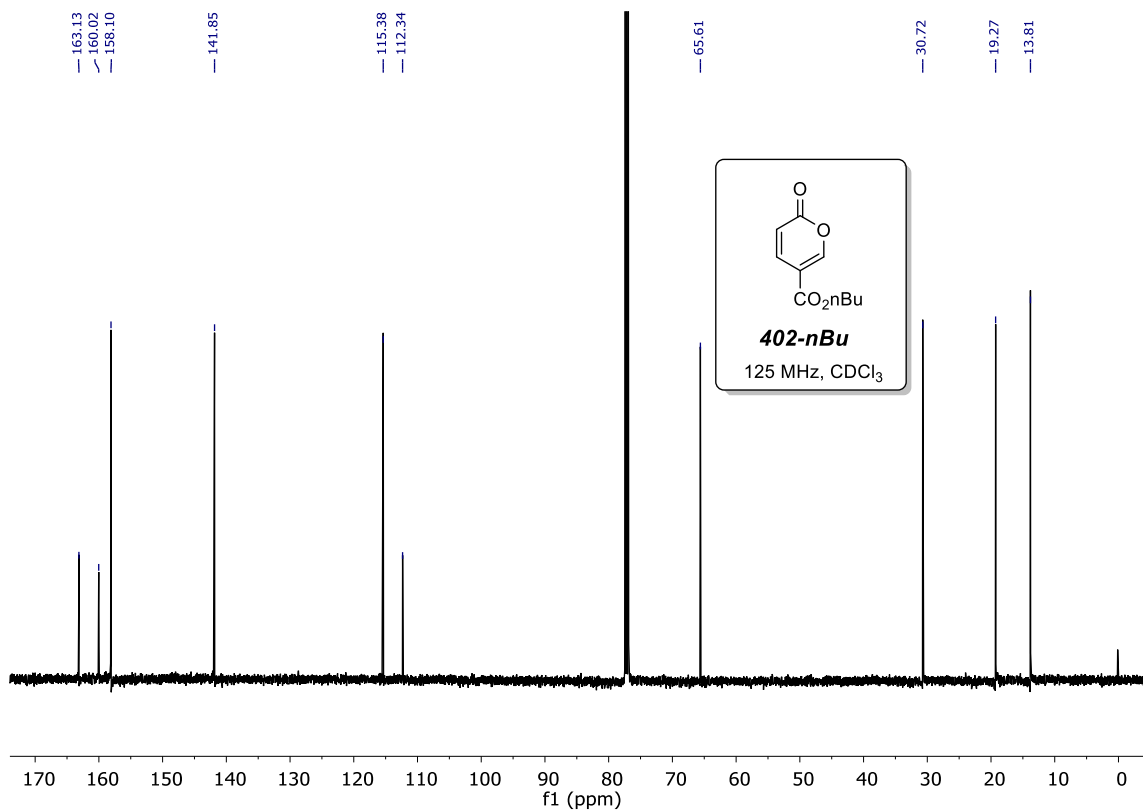
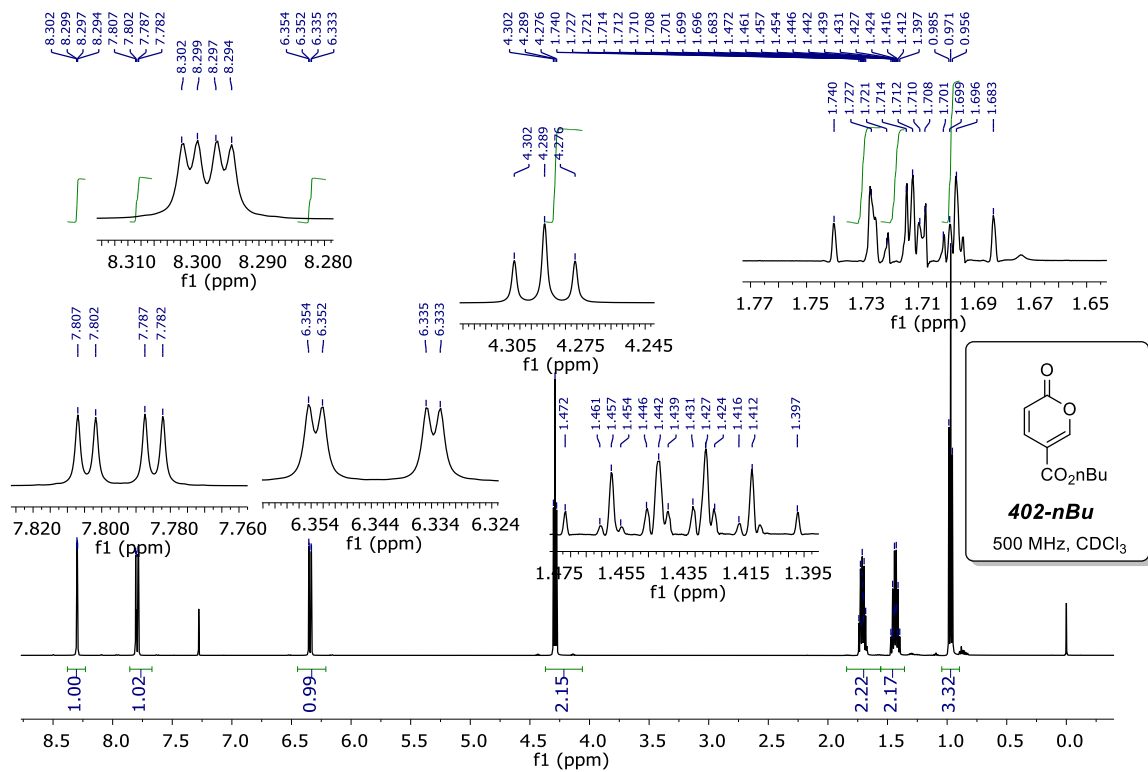


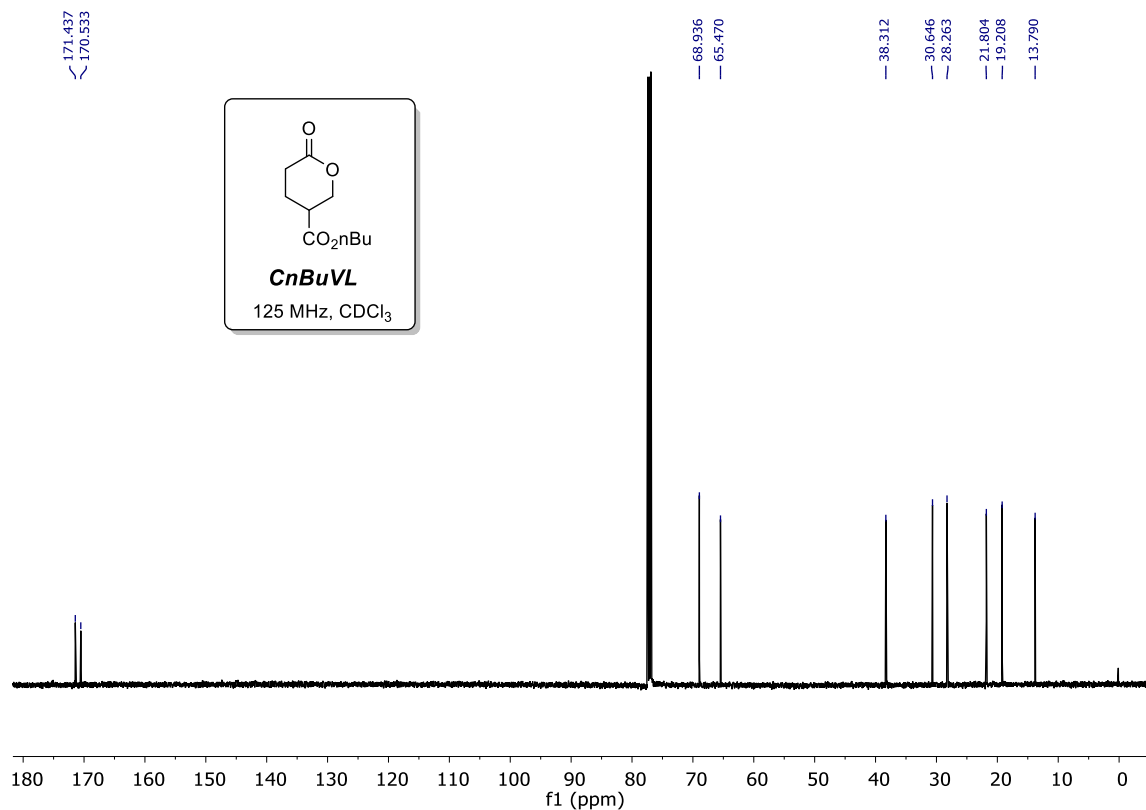
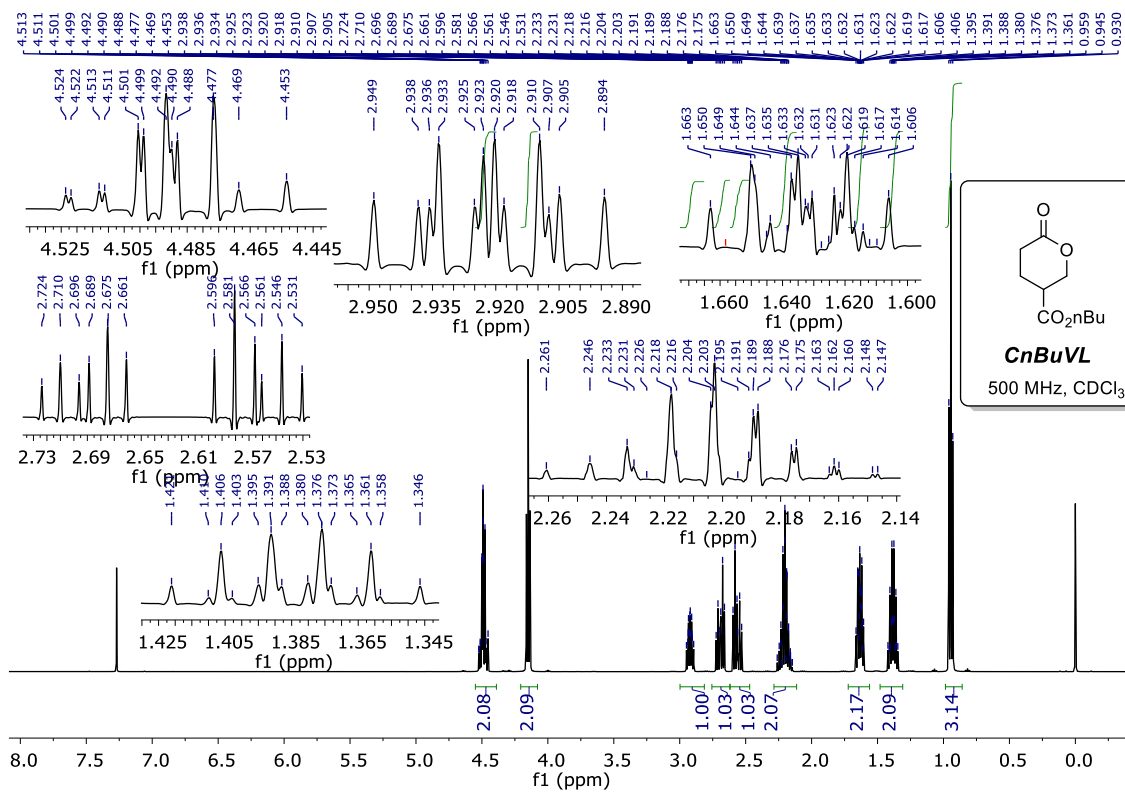


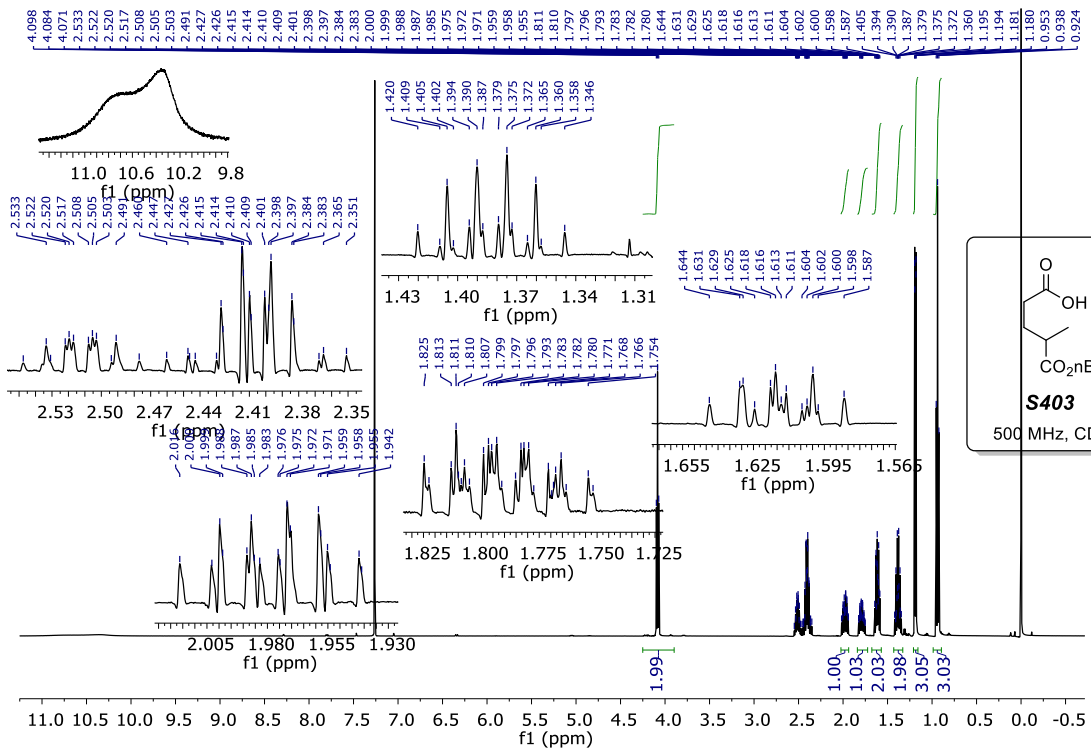


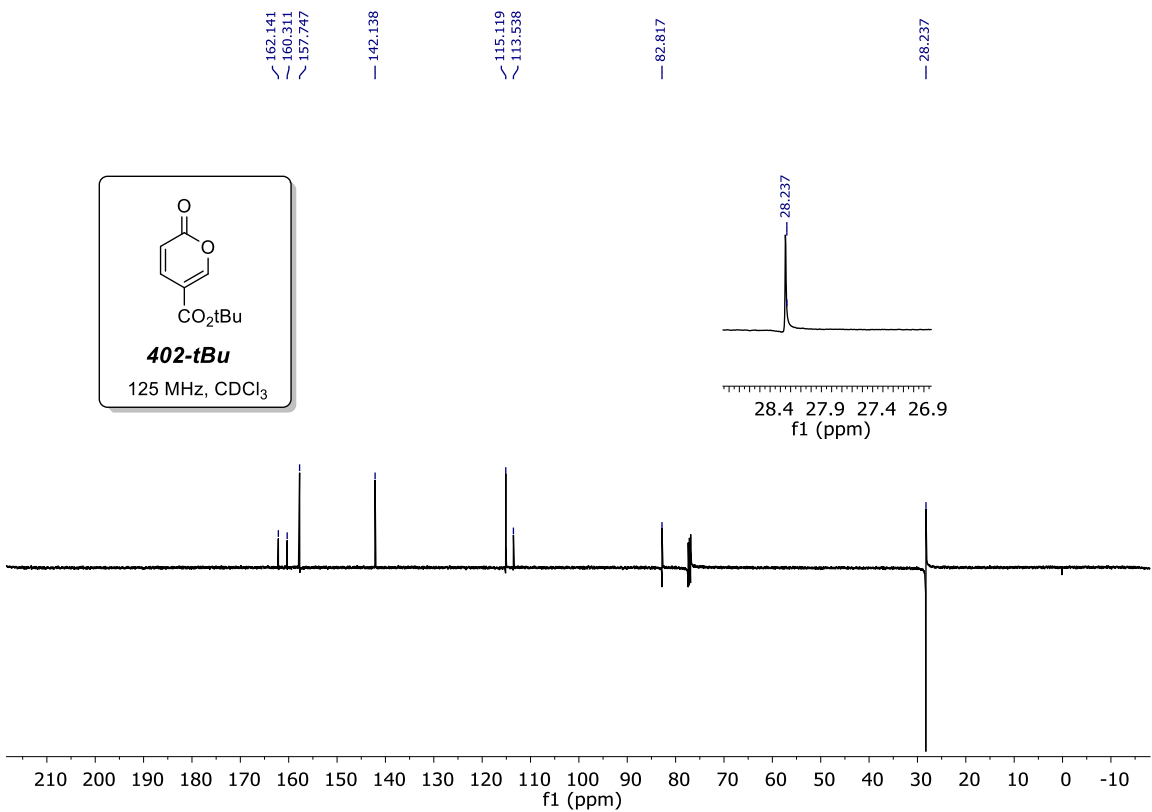
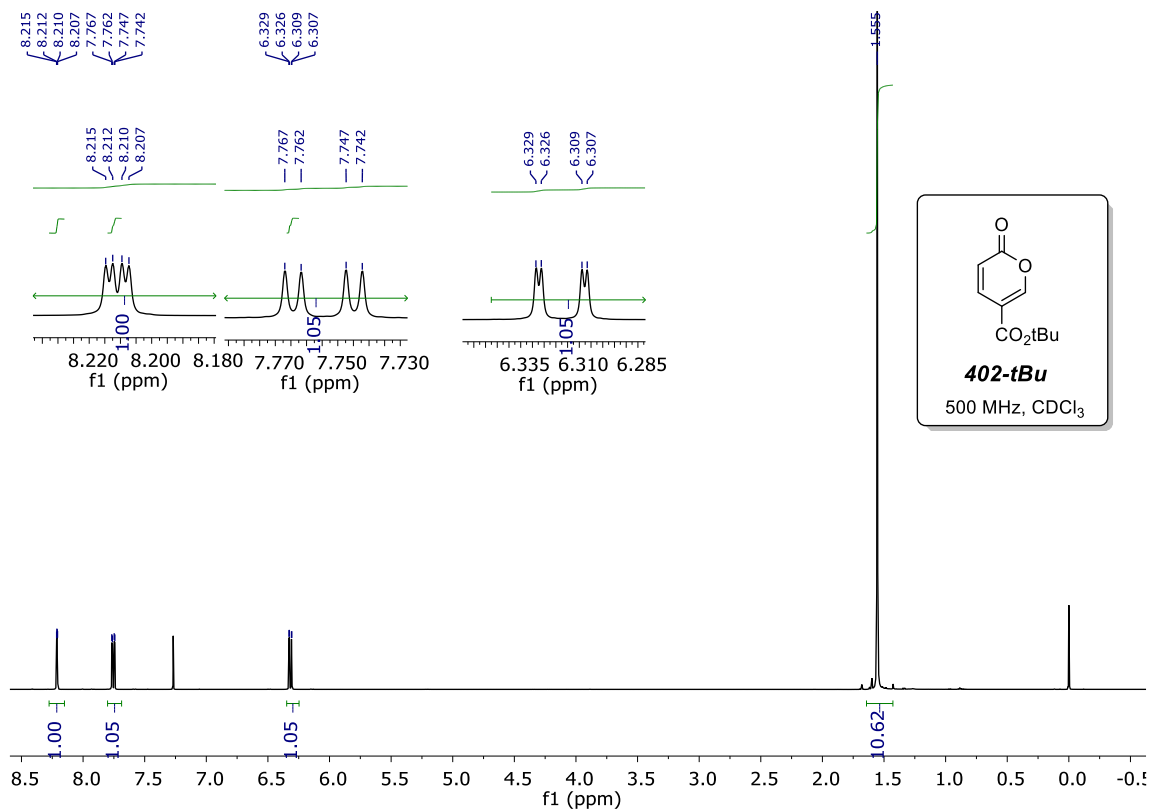


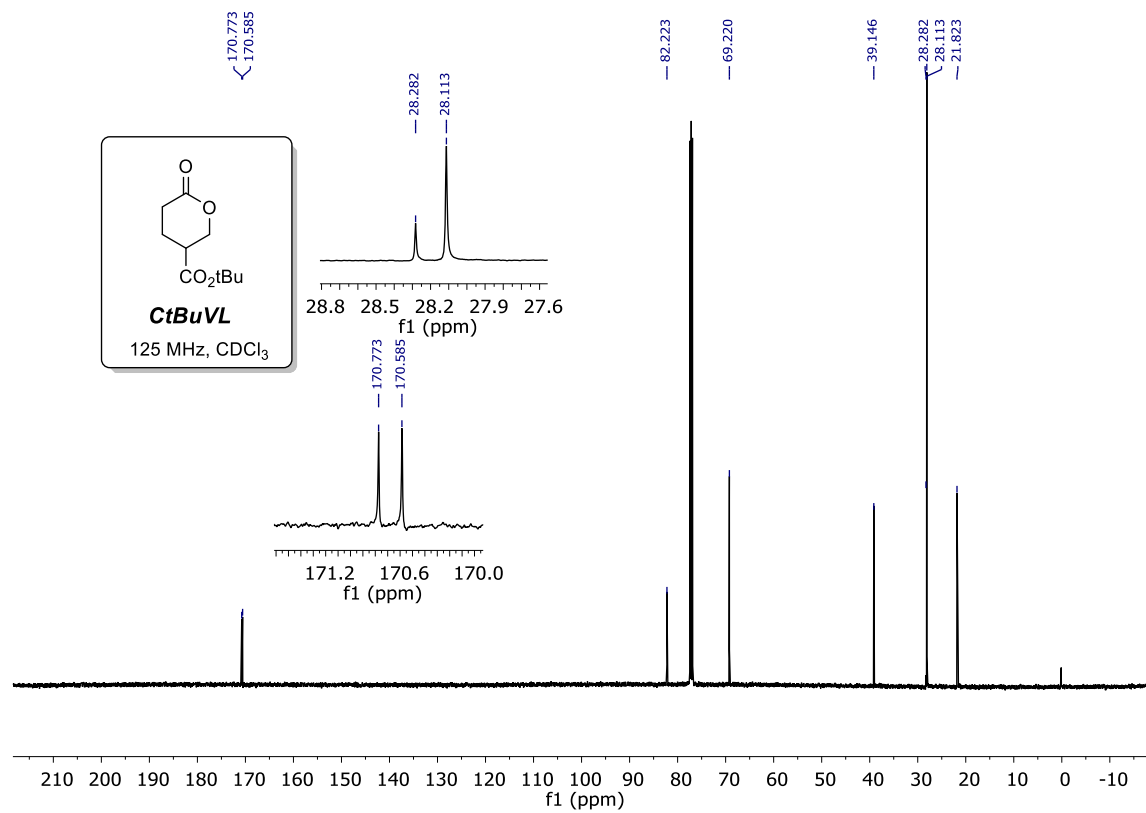
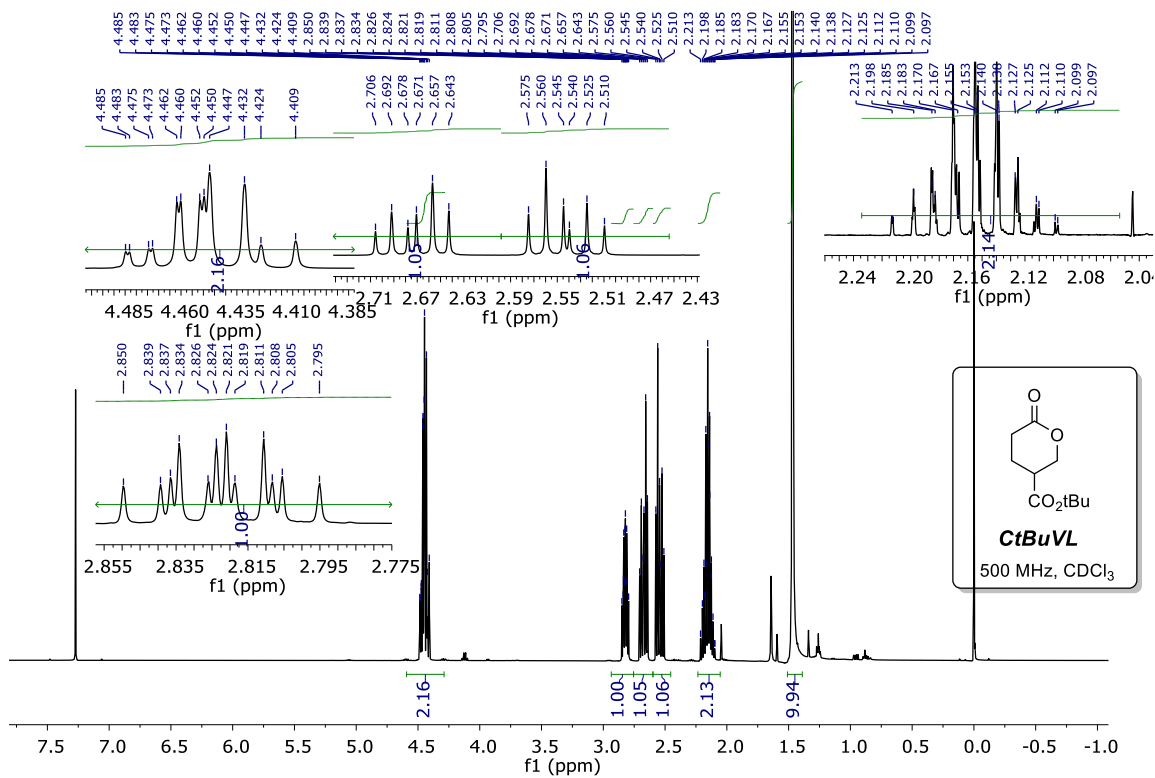


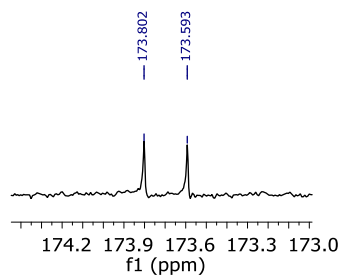
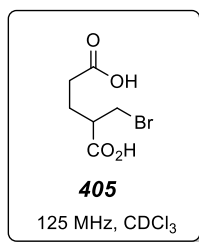
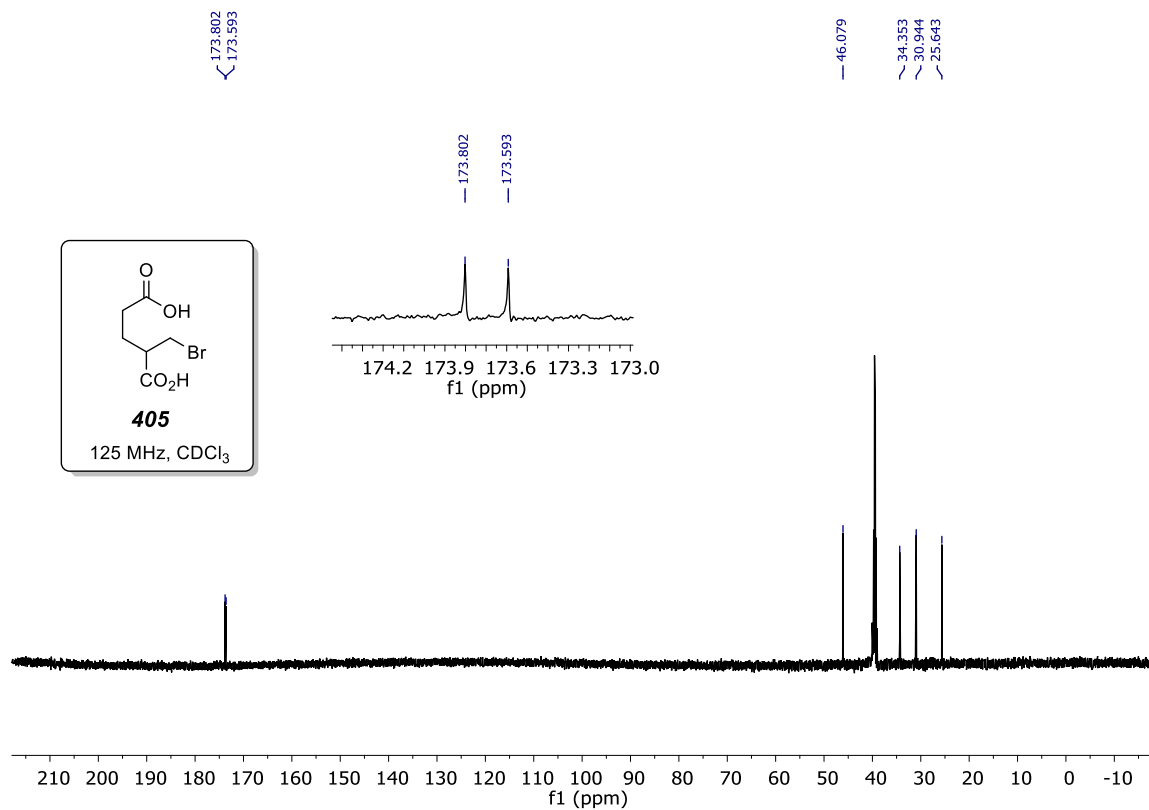
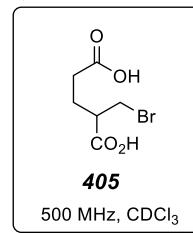
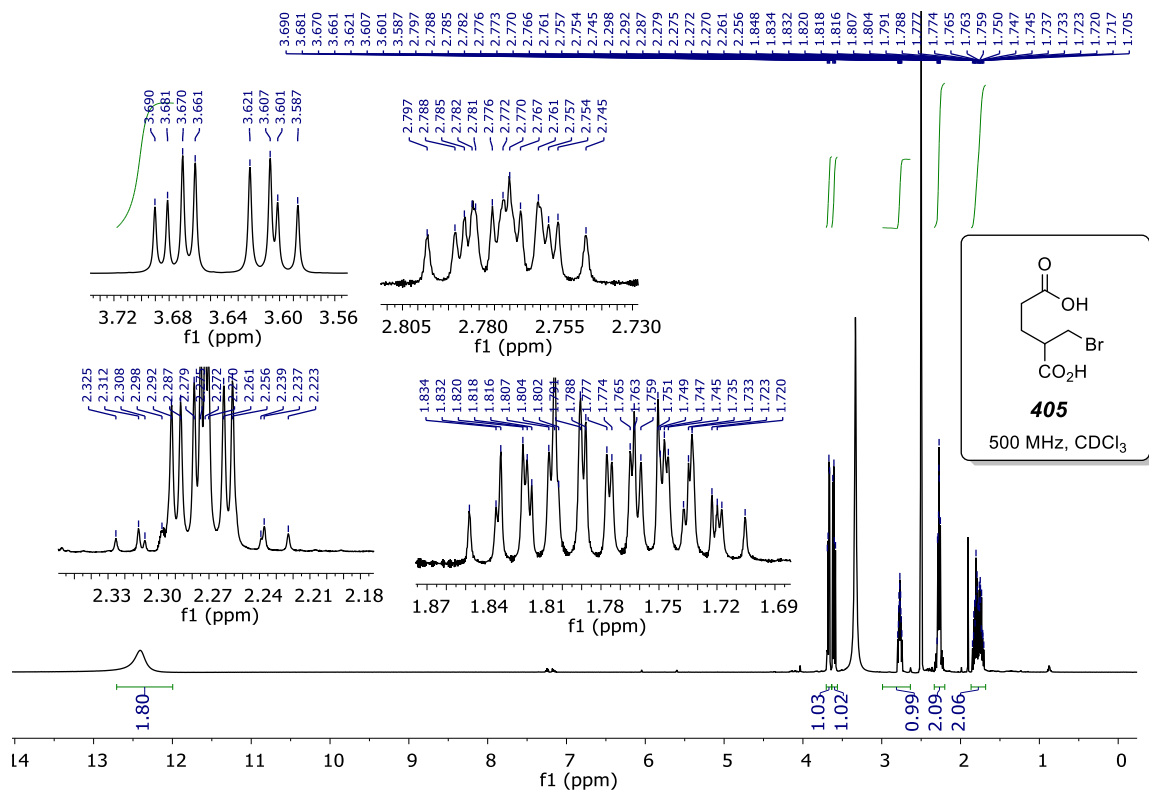


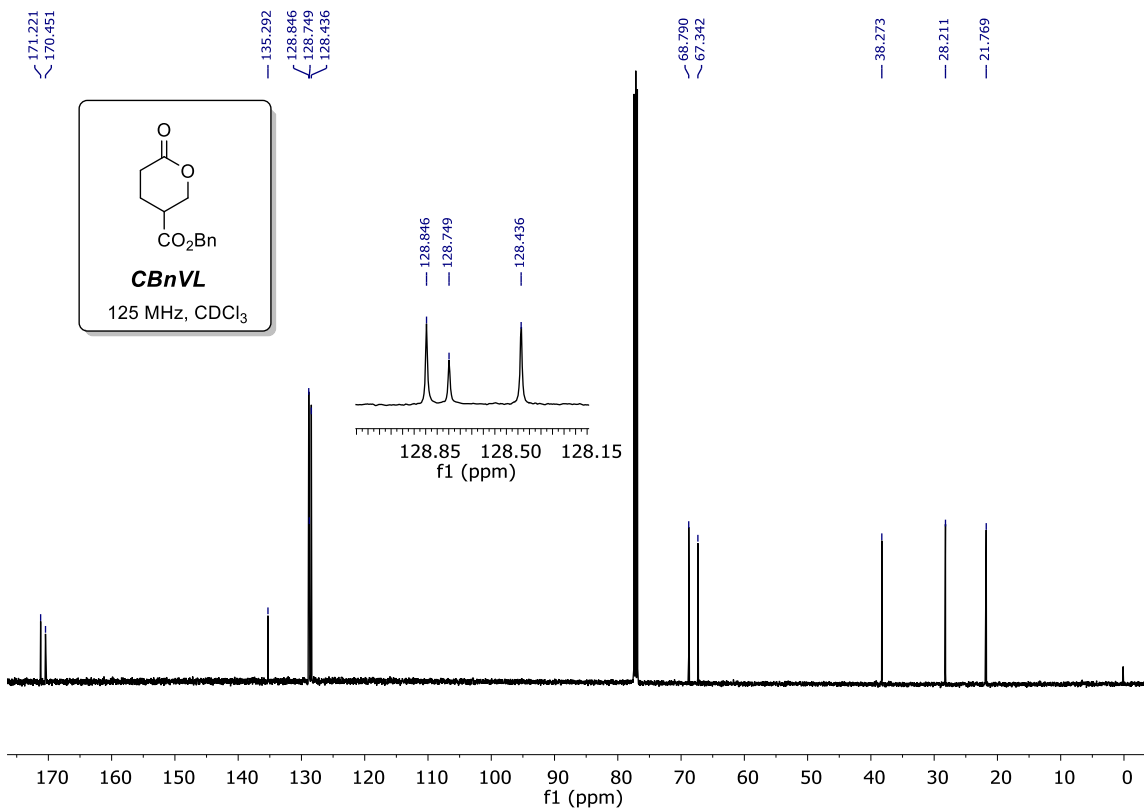
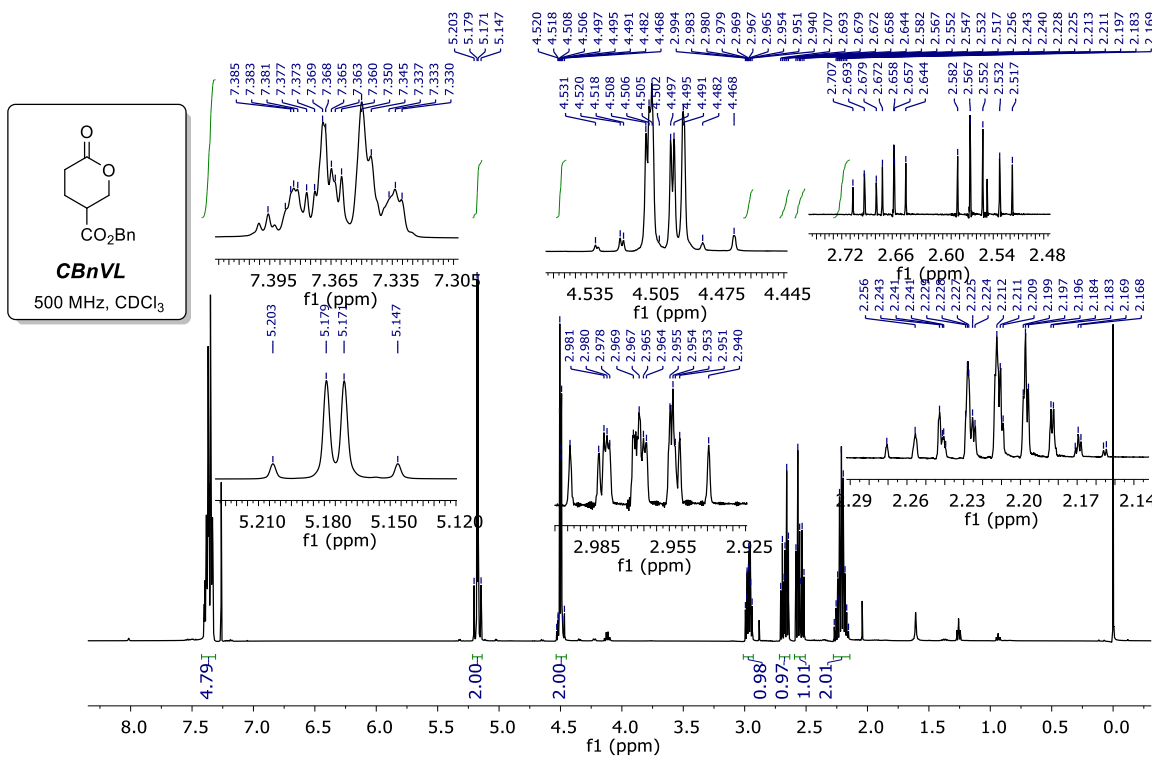


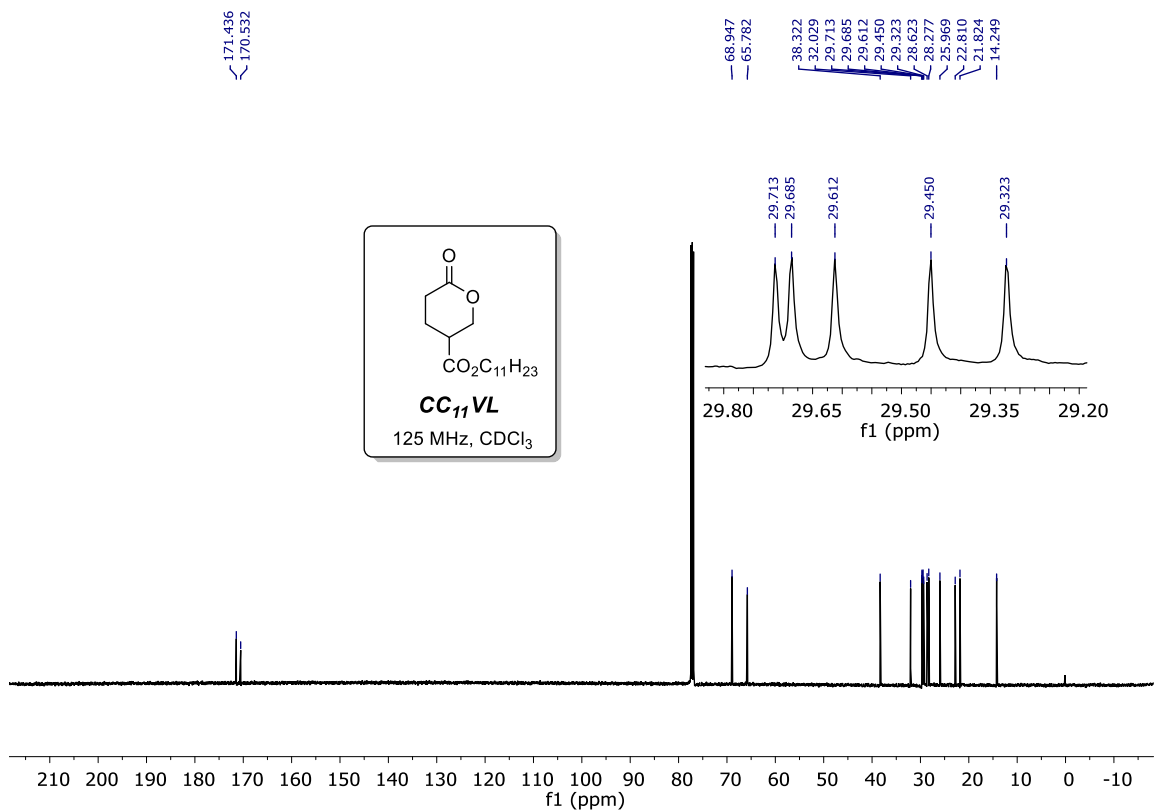
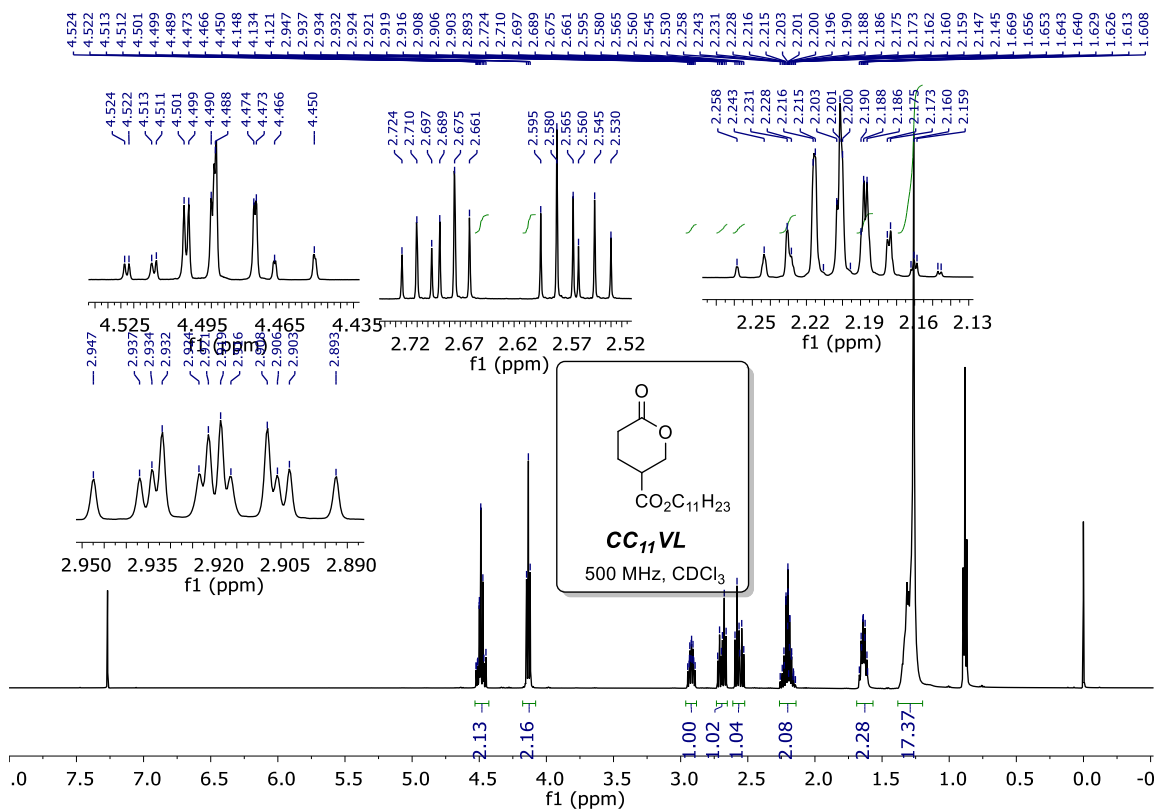


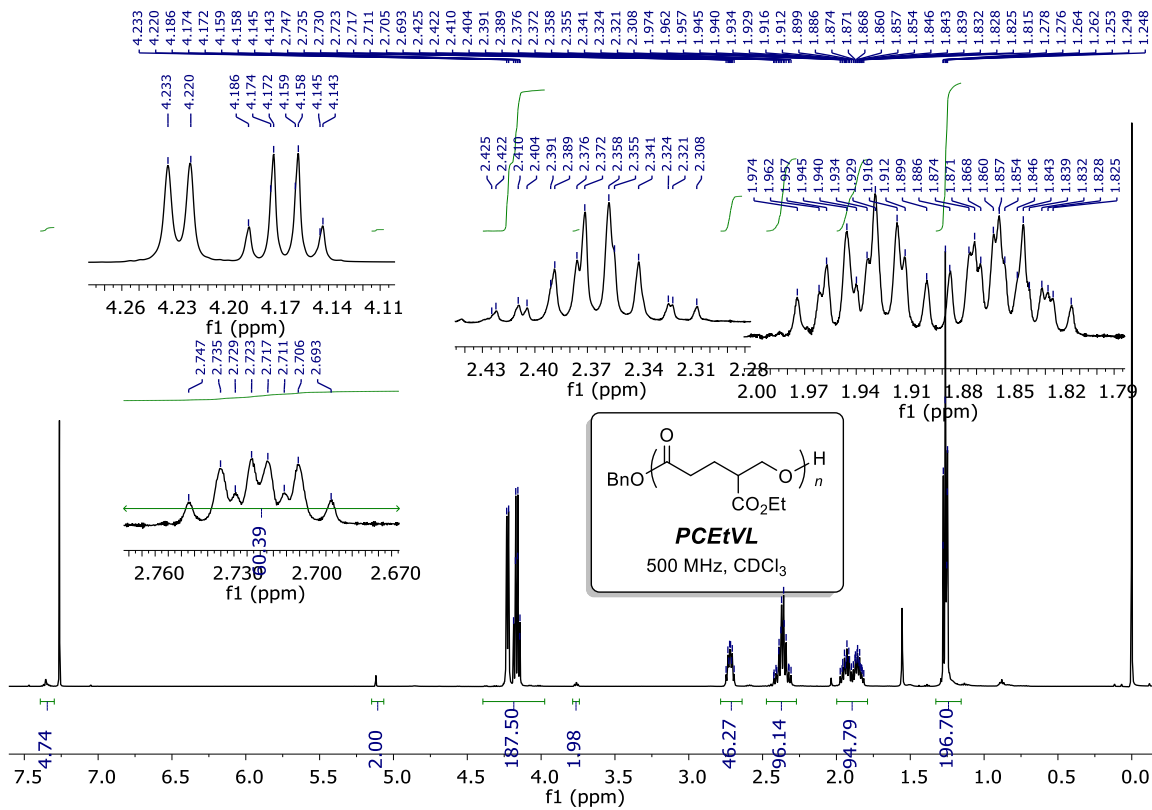




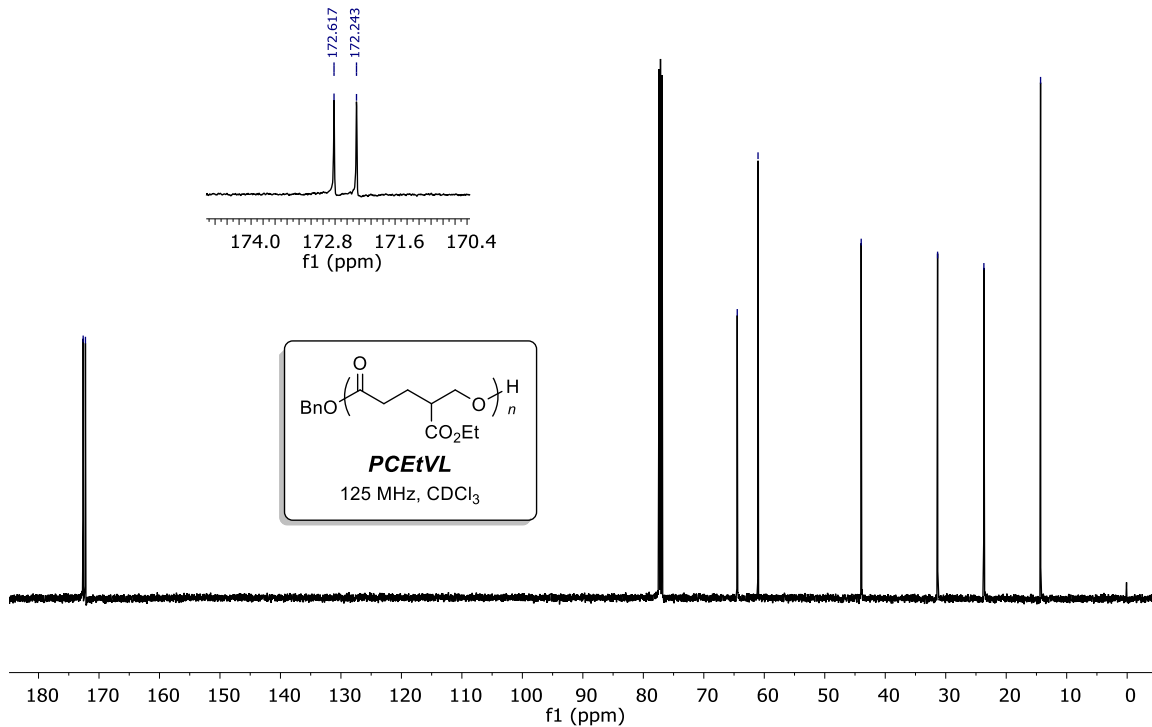


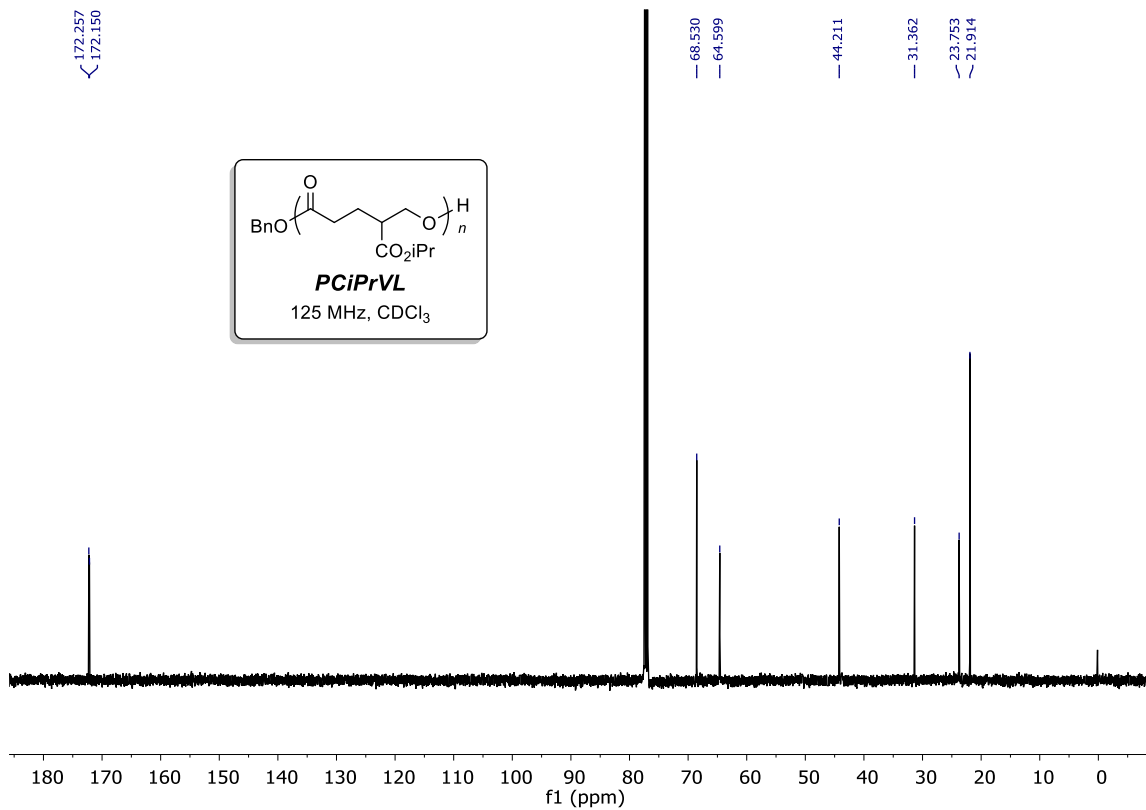
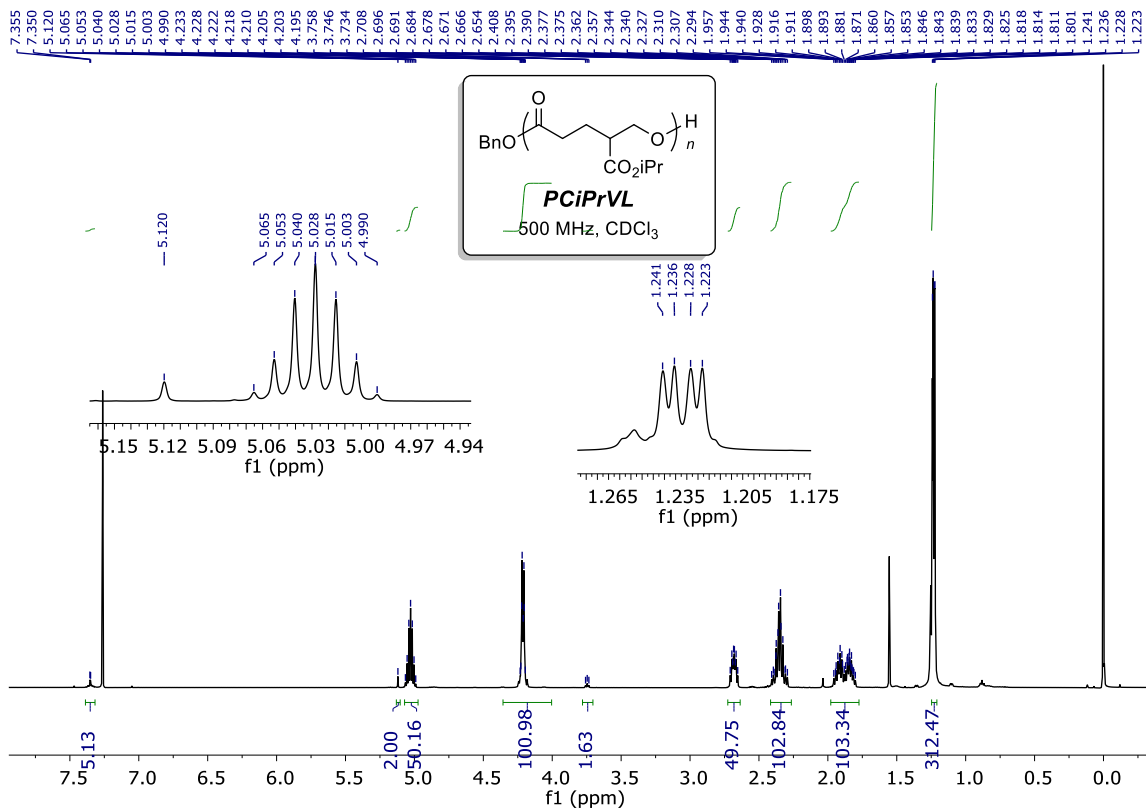


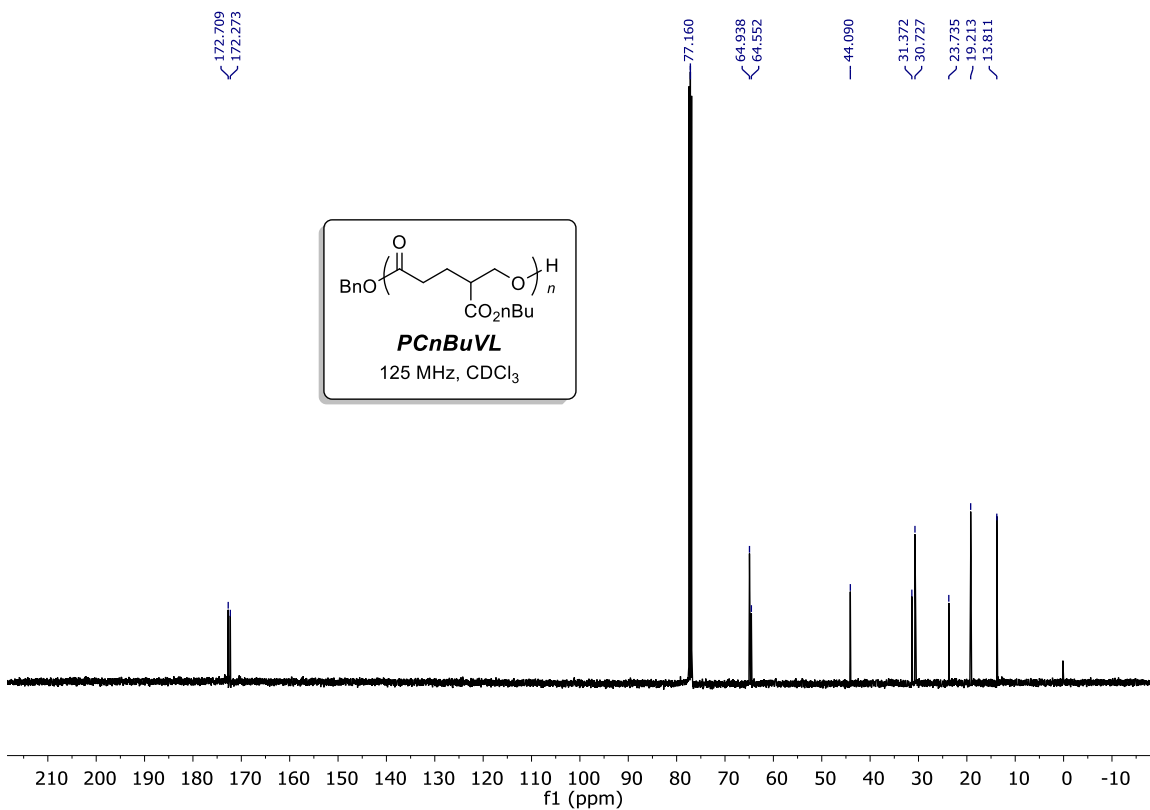
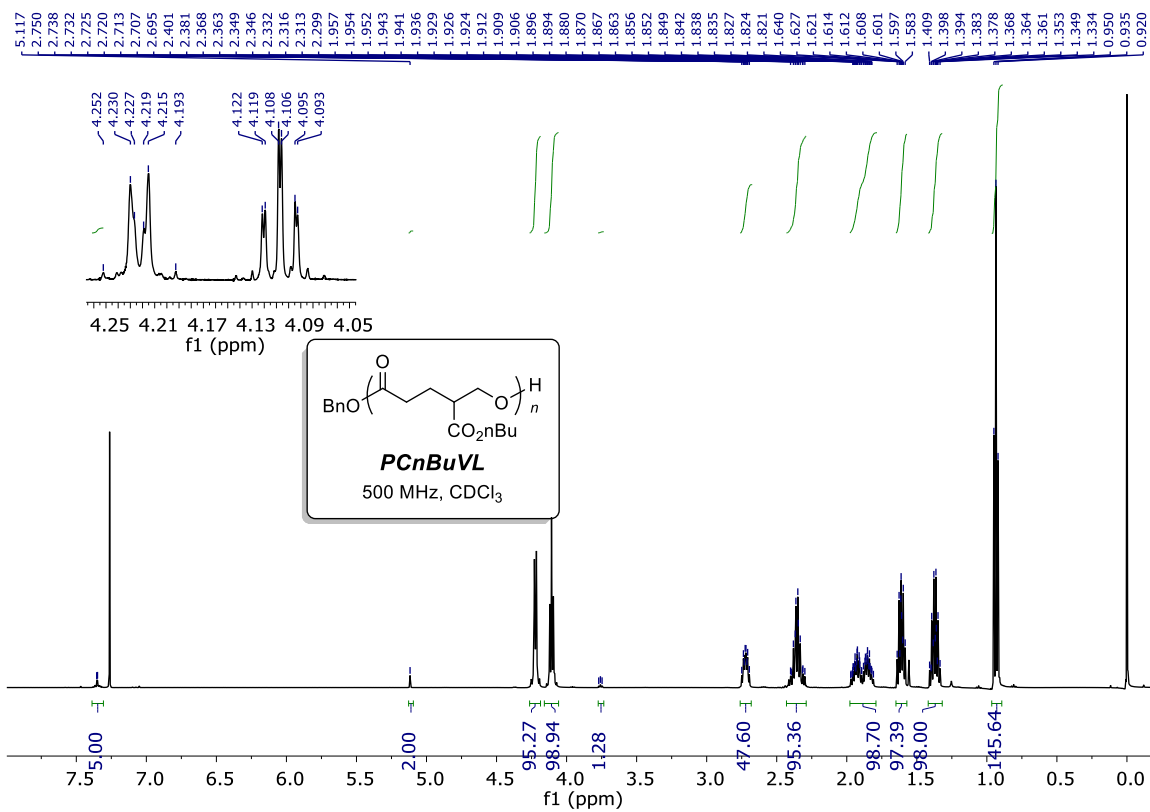


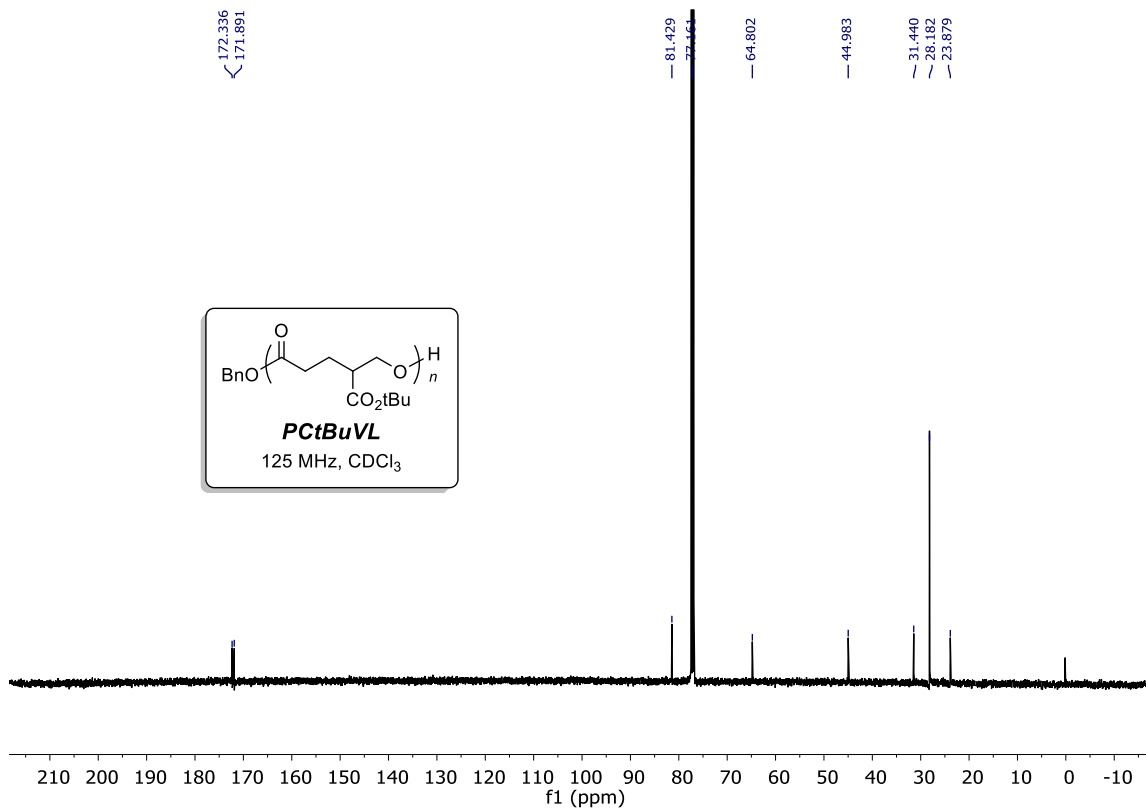
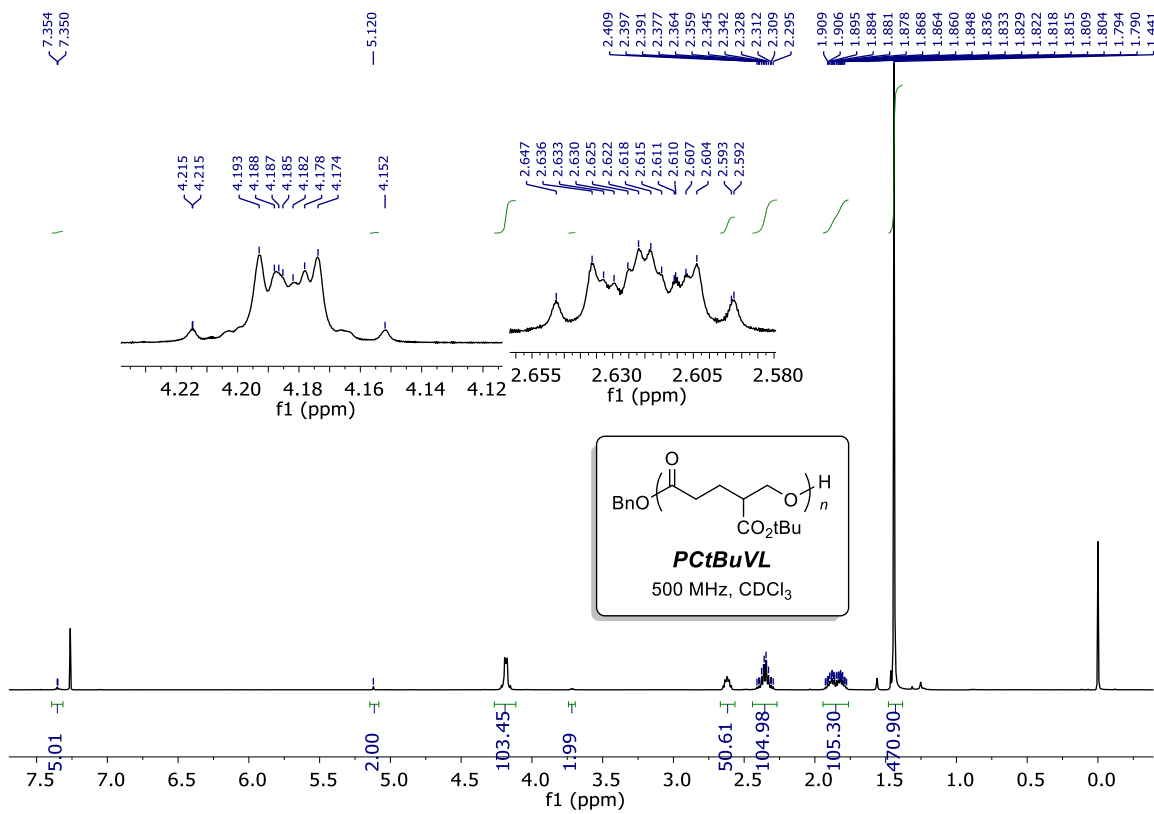


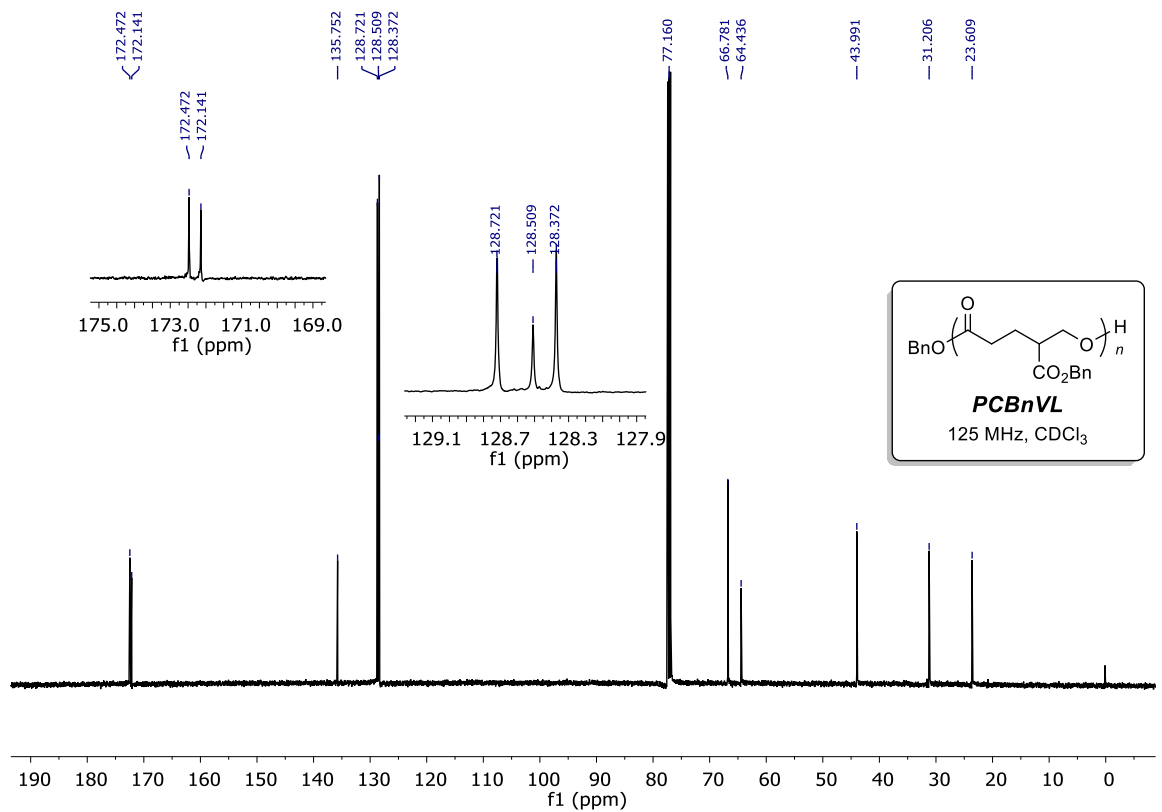
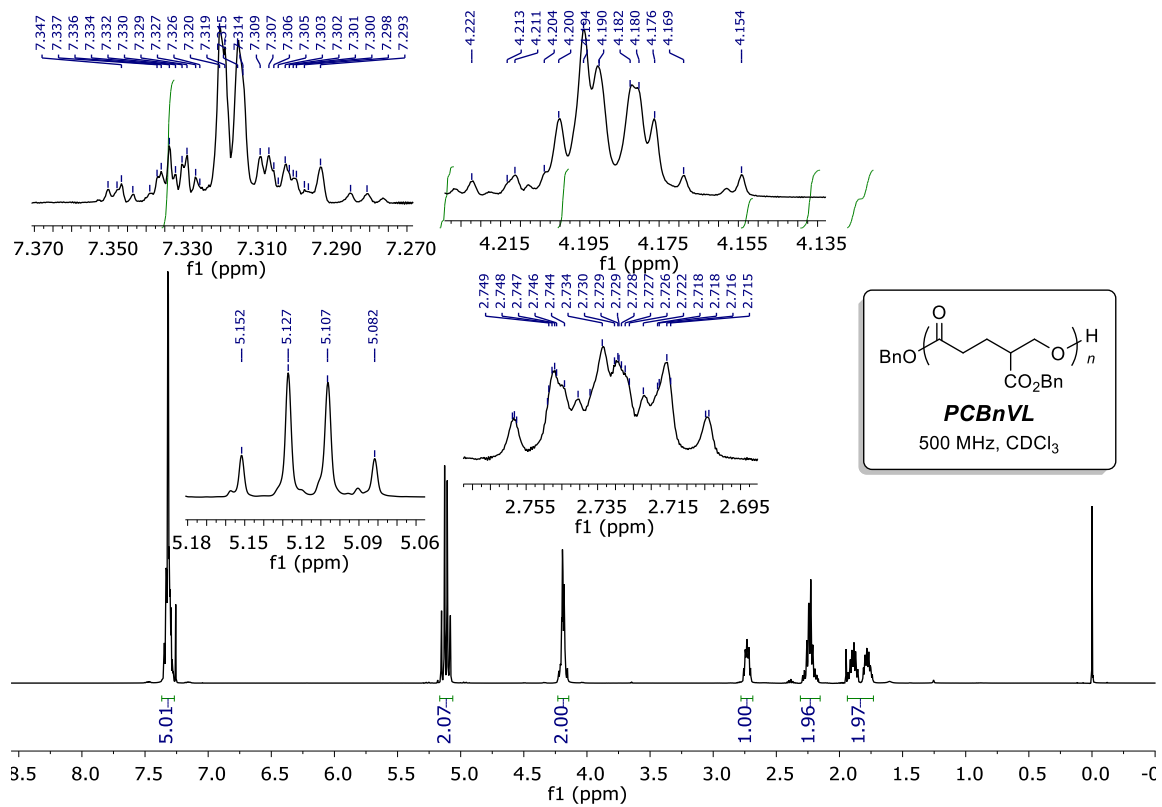
172.617
 172.243
 64.470
 61.036
 43.976
 31.347
 23.694
 14.321



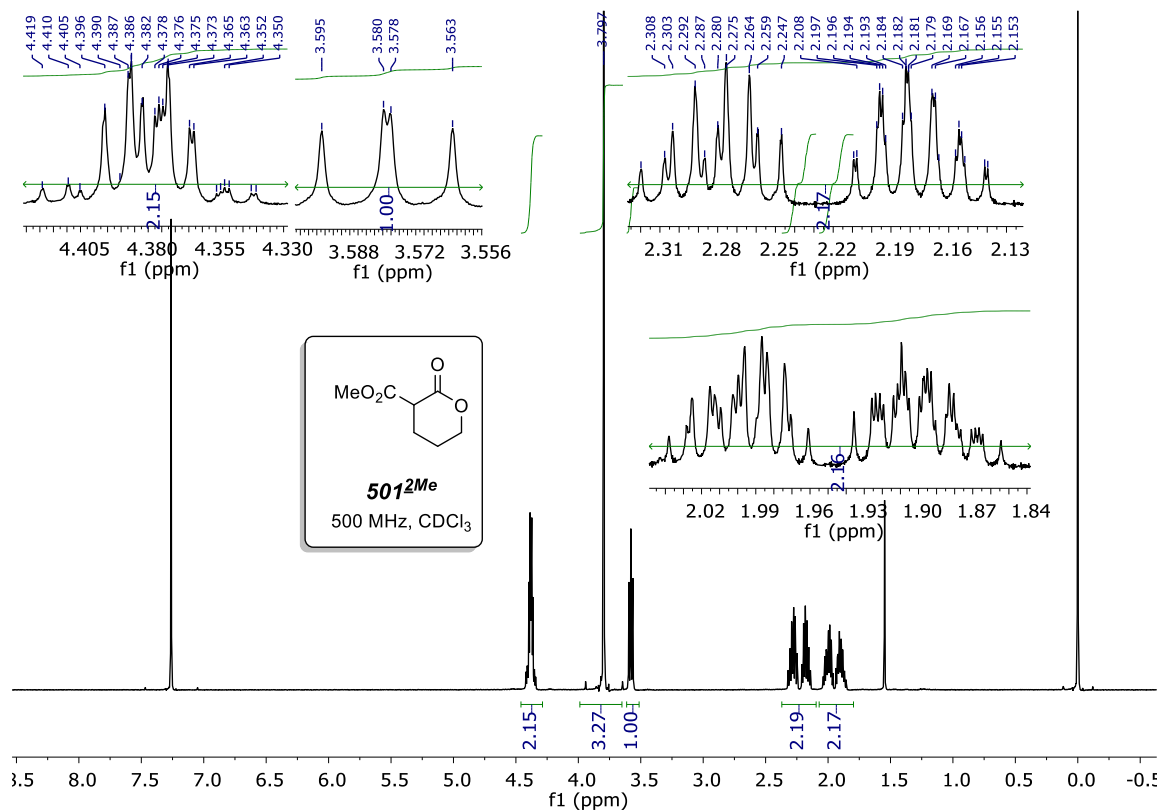


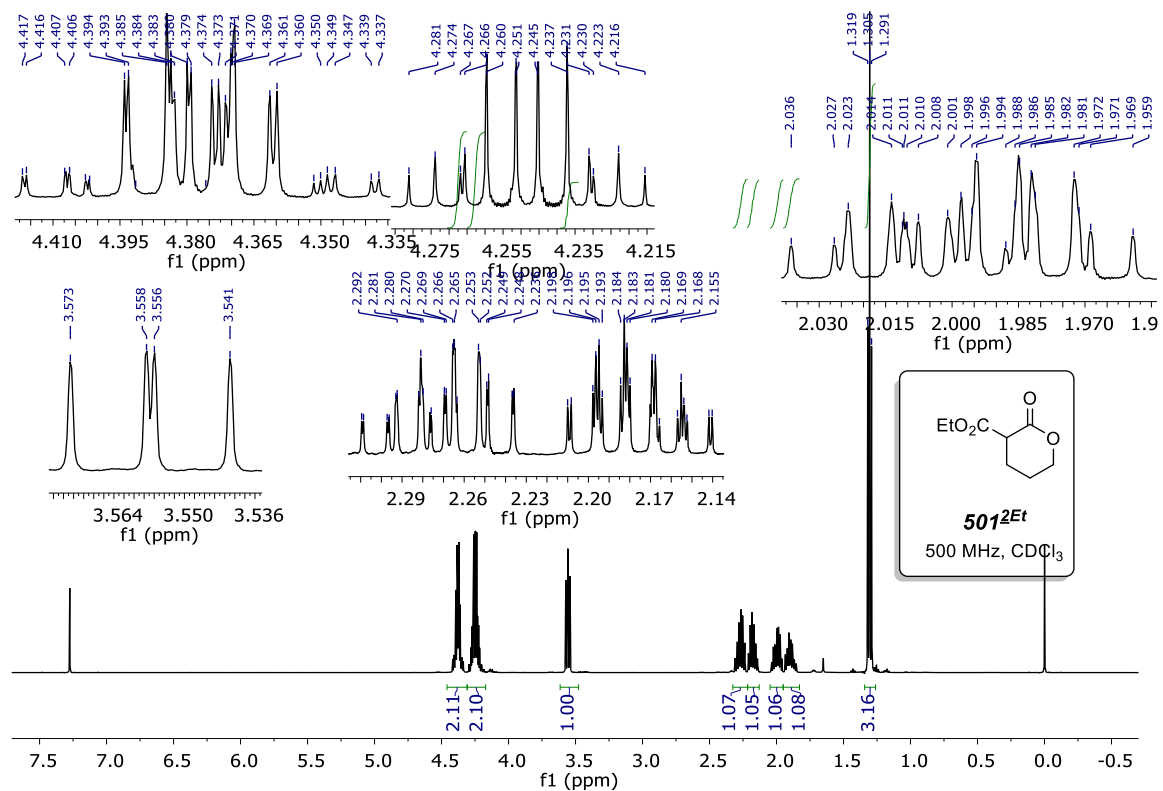
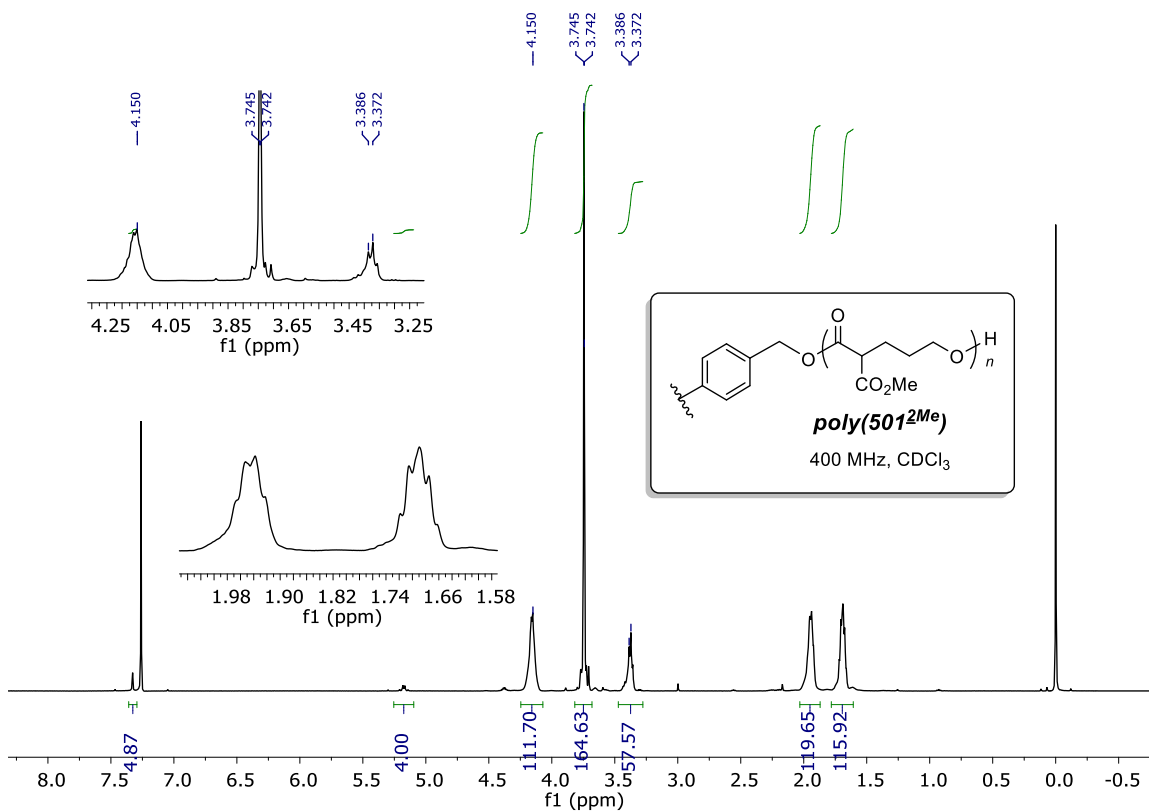


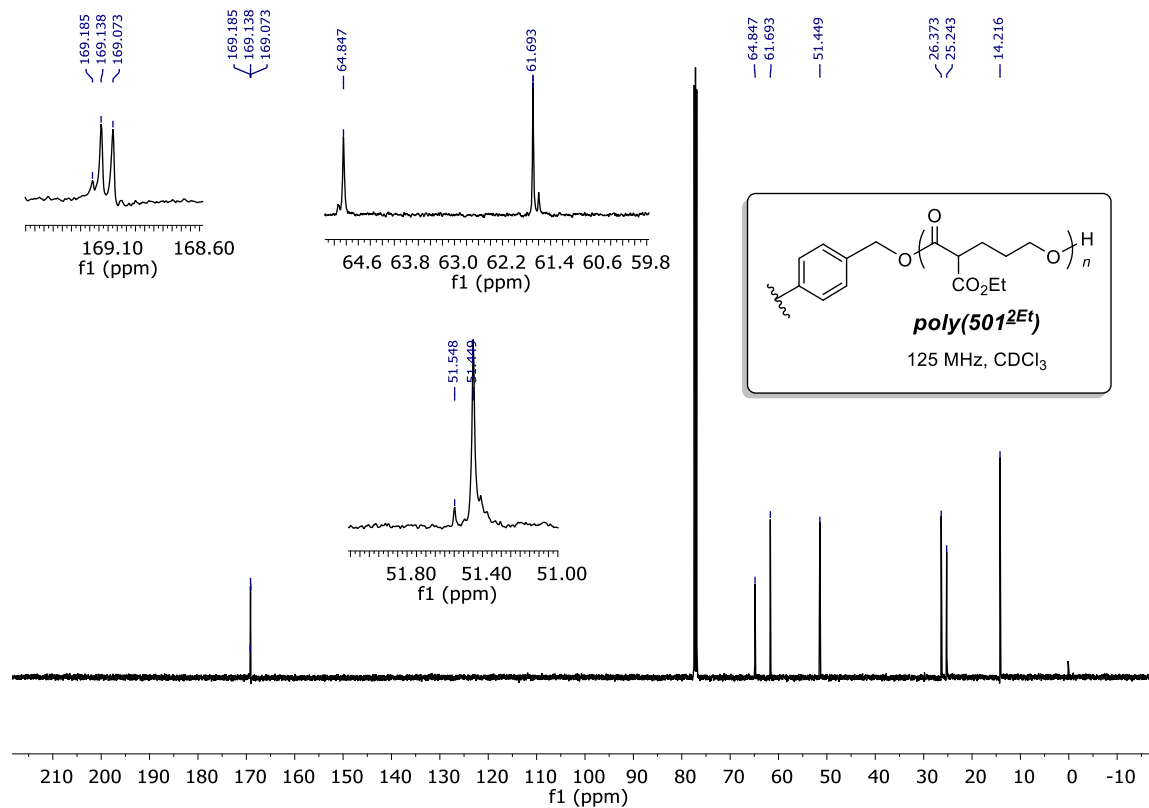
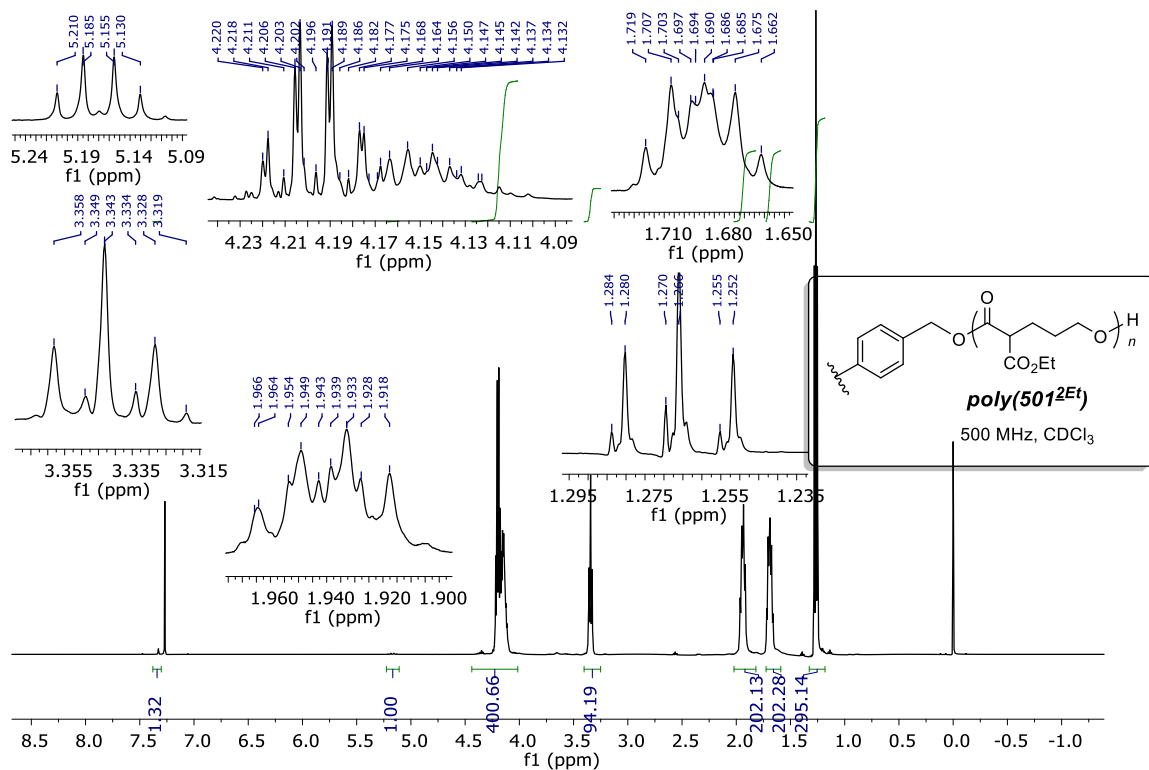


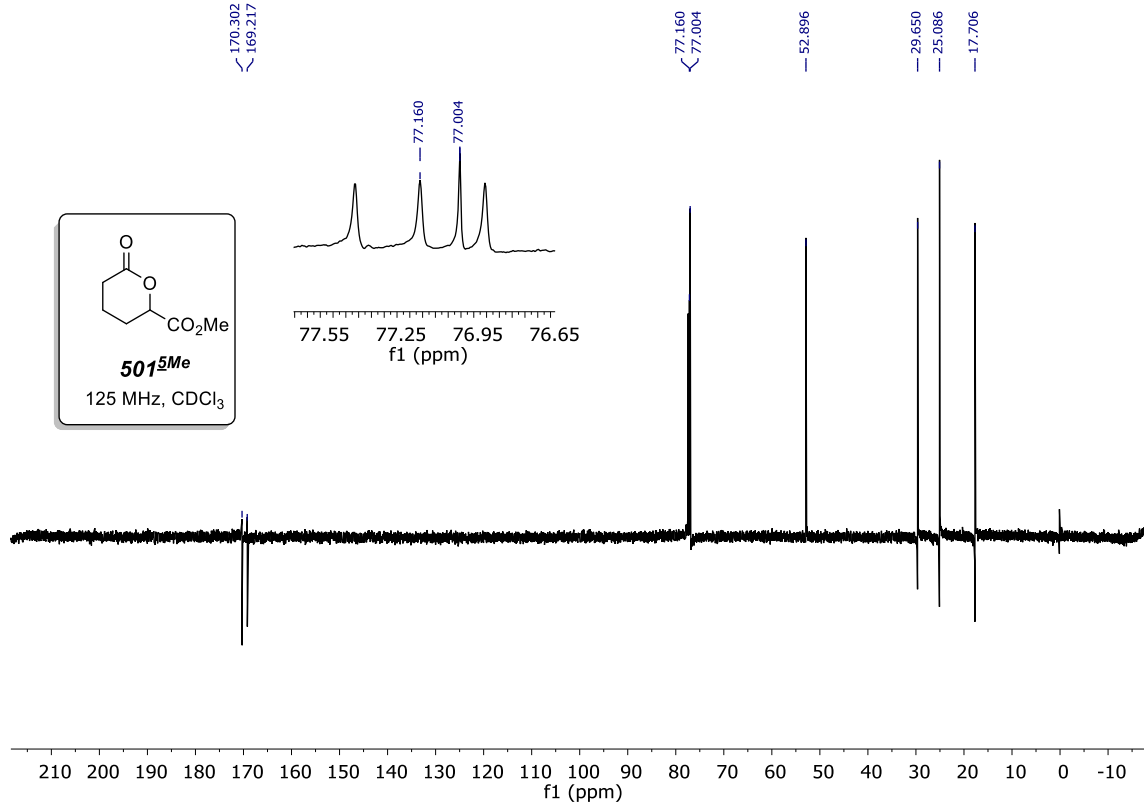
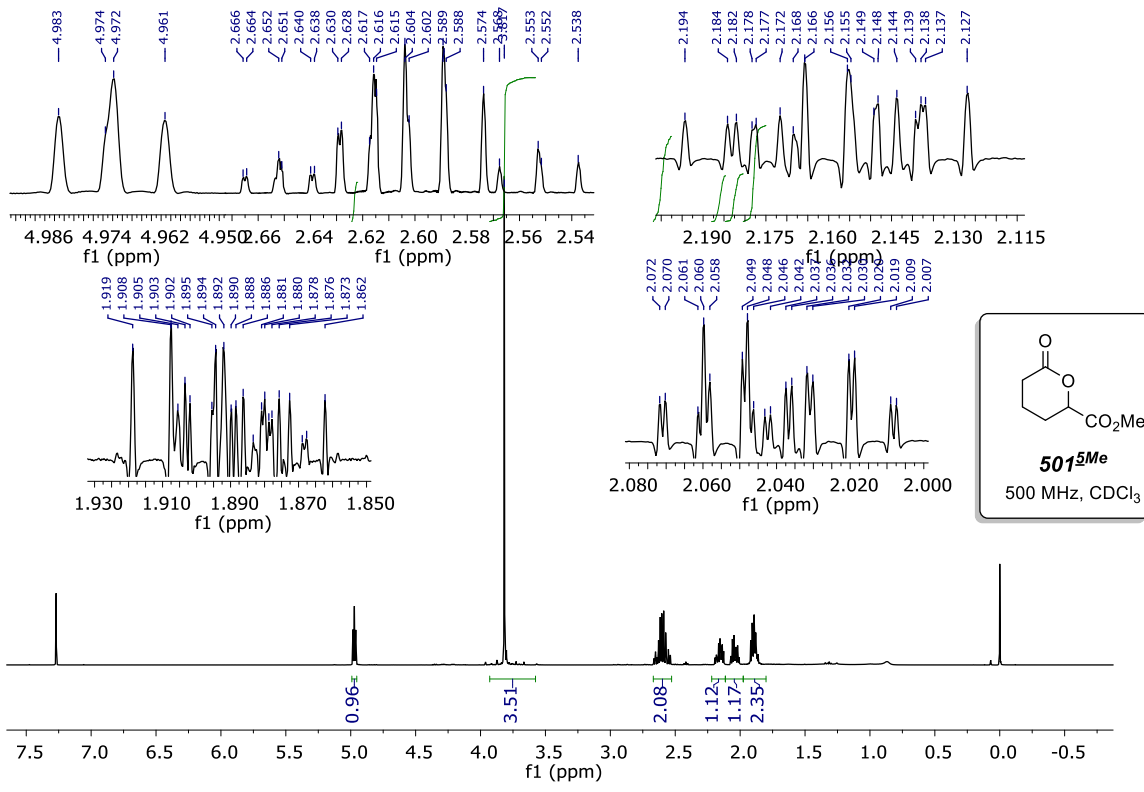


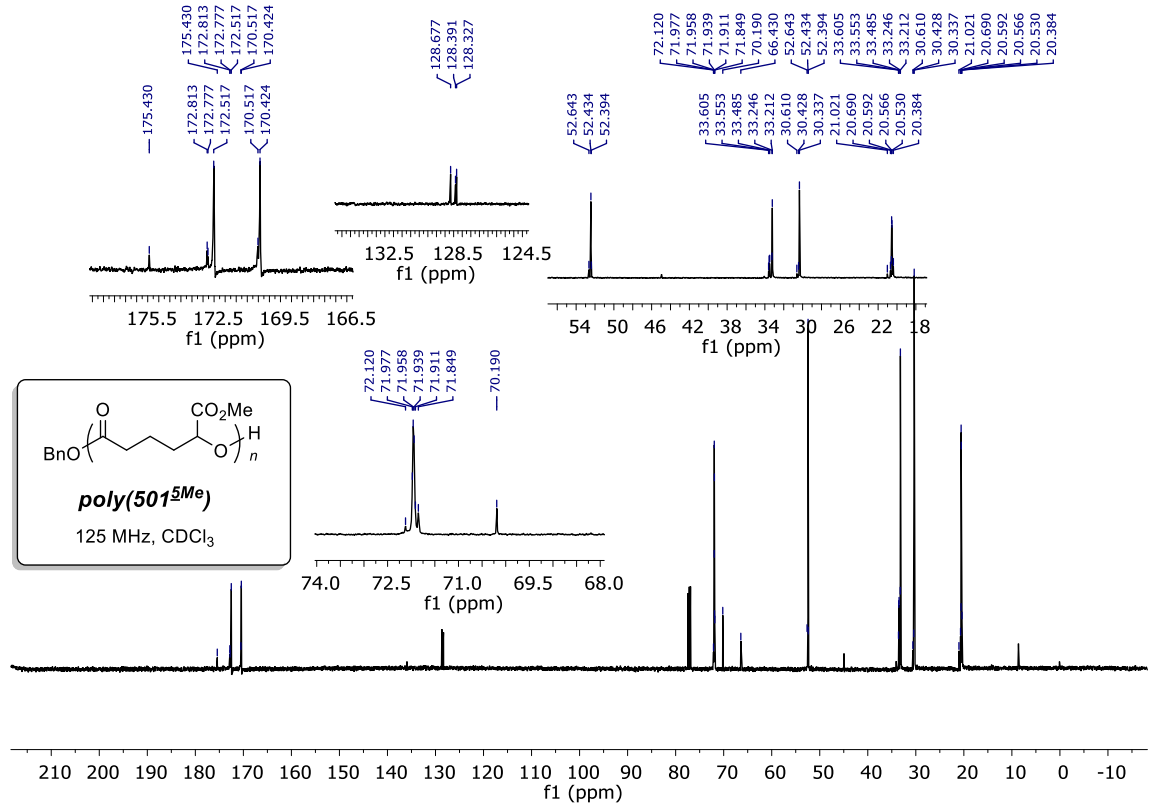
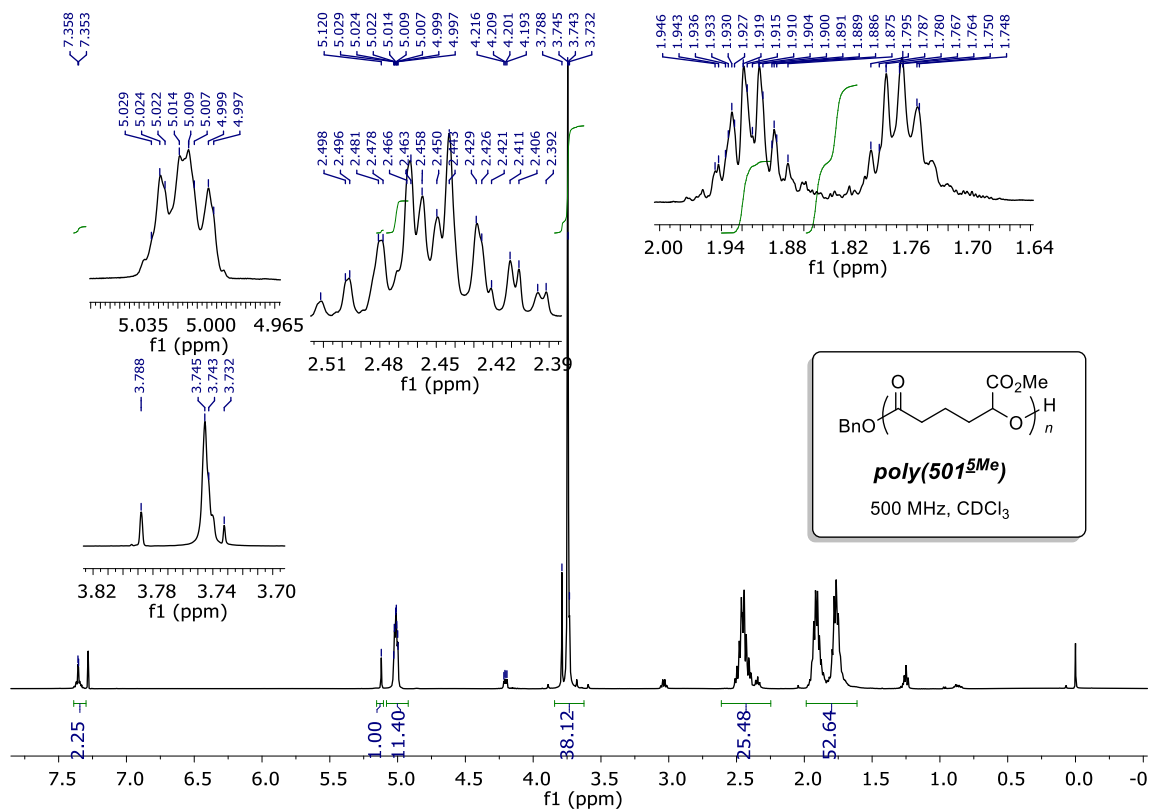
S8.3 Carboalkoxylated valerolactones: Small molecules and Polymer



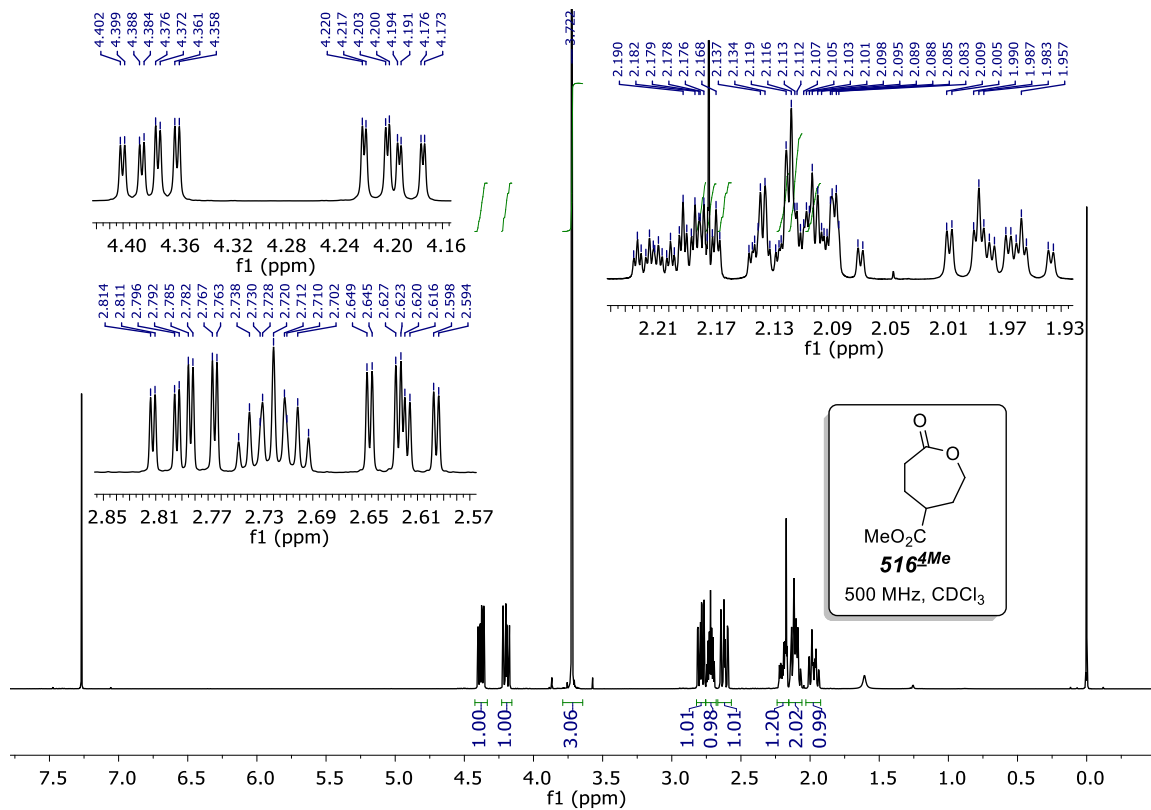


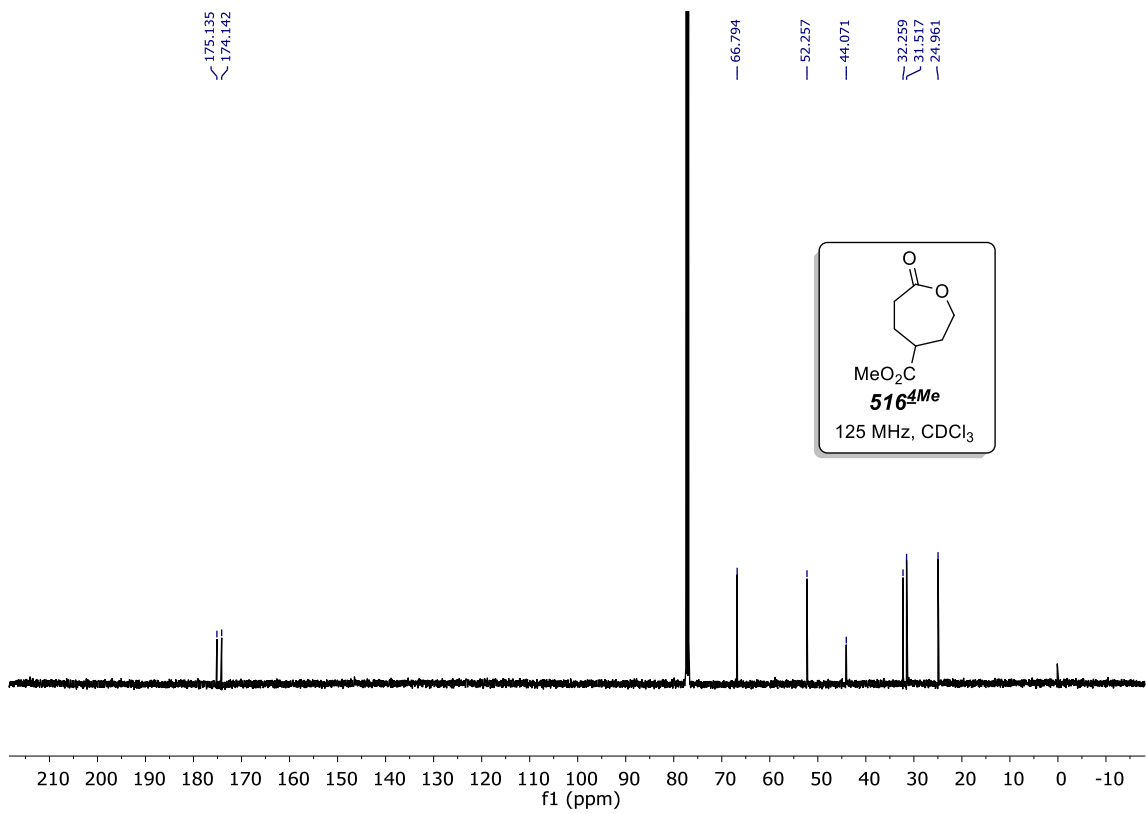


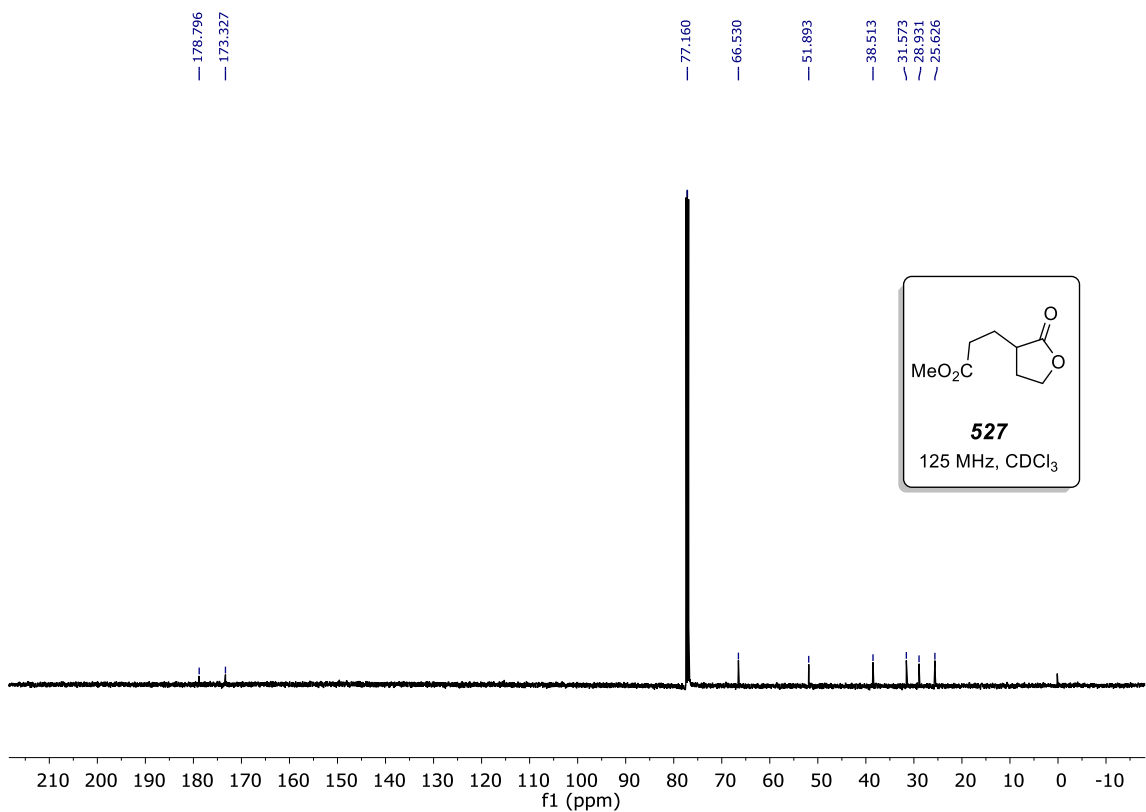
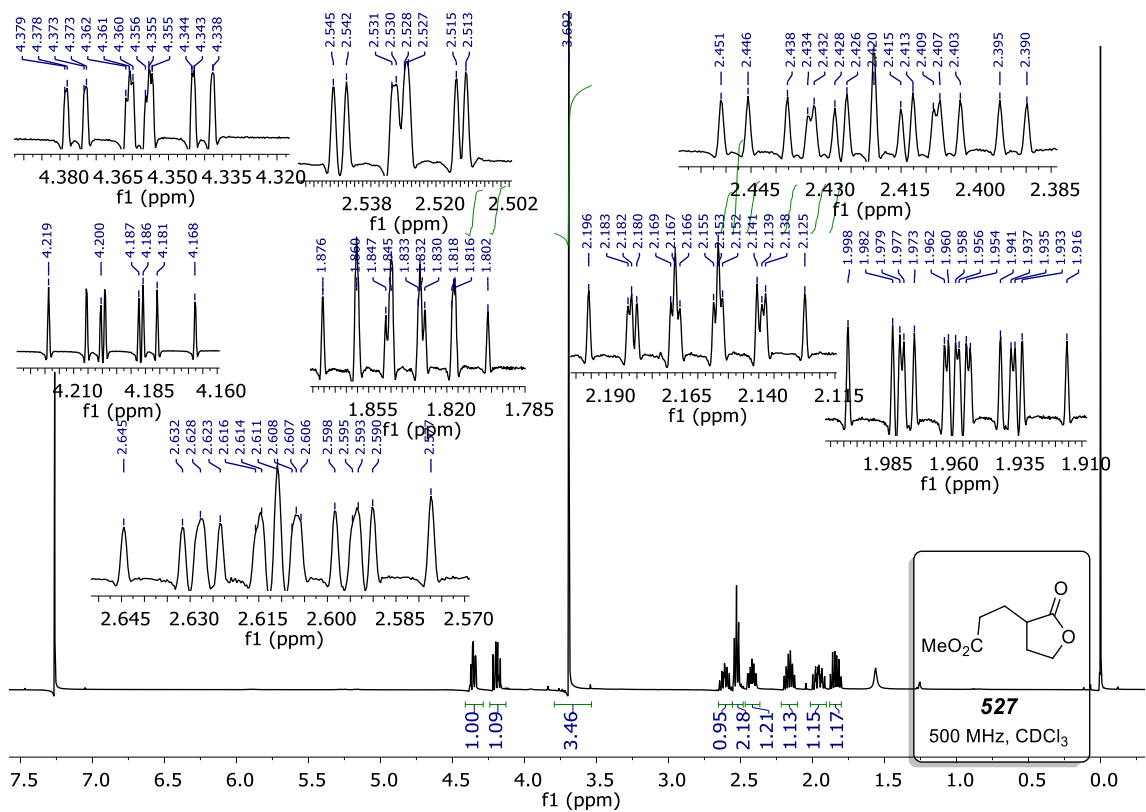


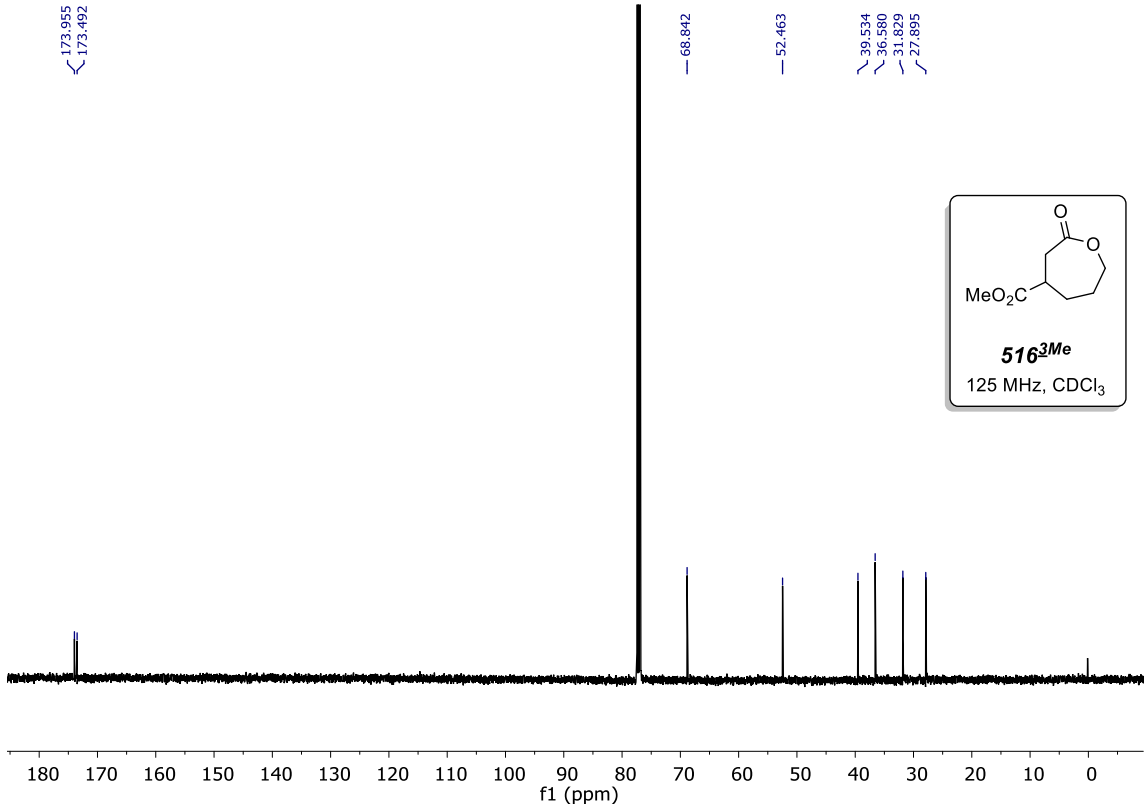
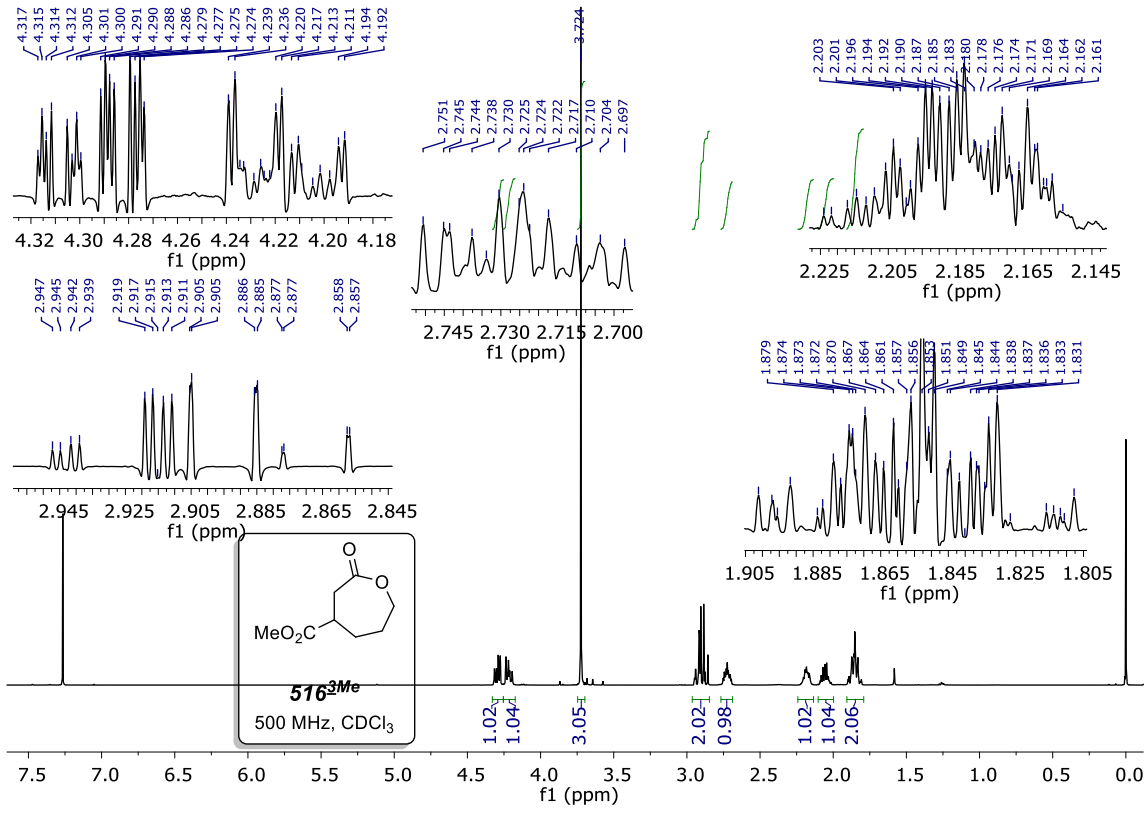


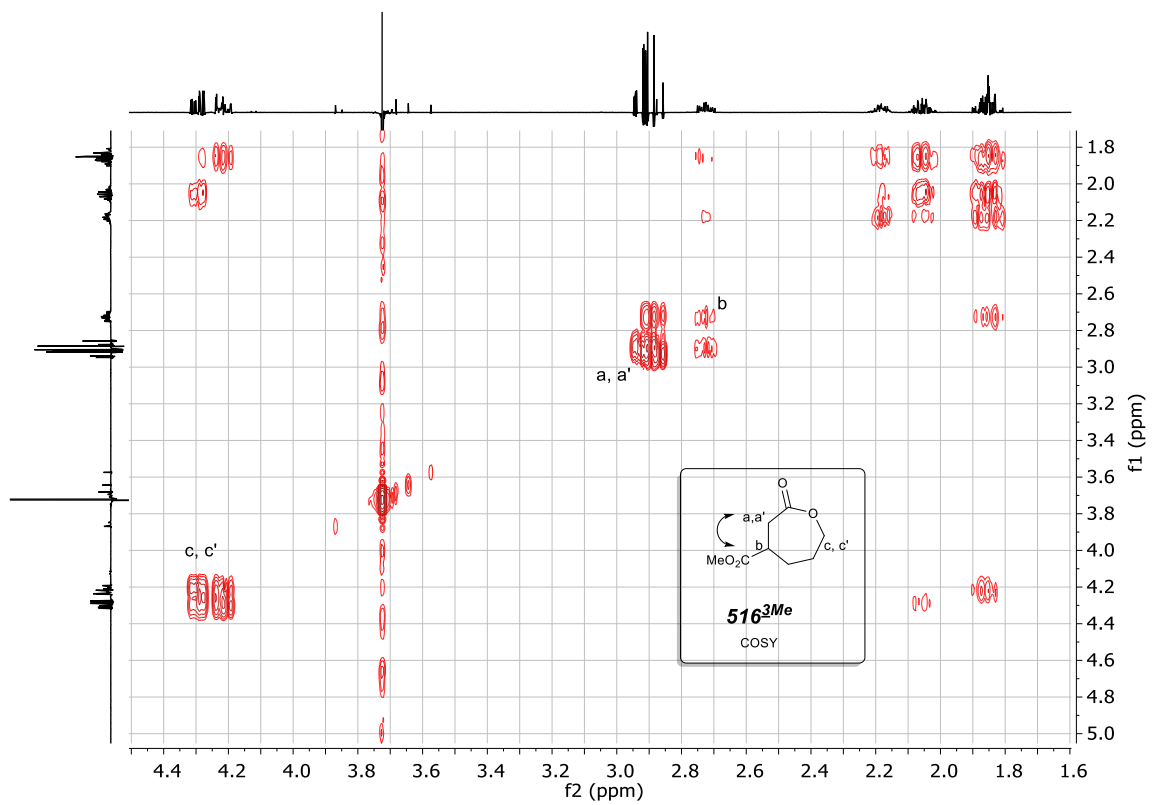
S8.4 Carboalkoxylated caprolactones: Small molecules

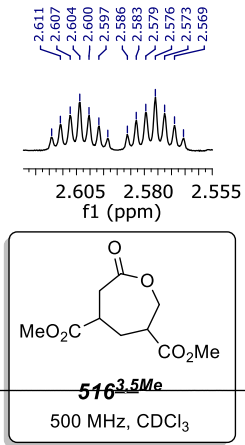
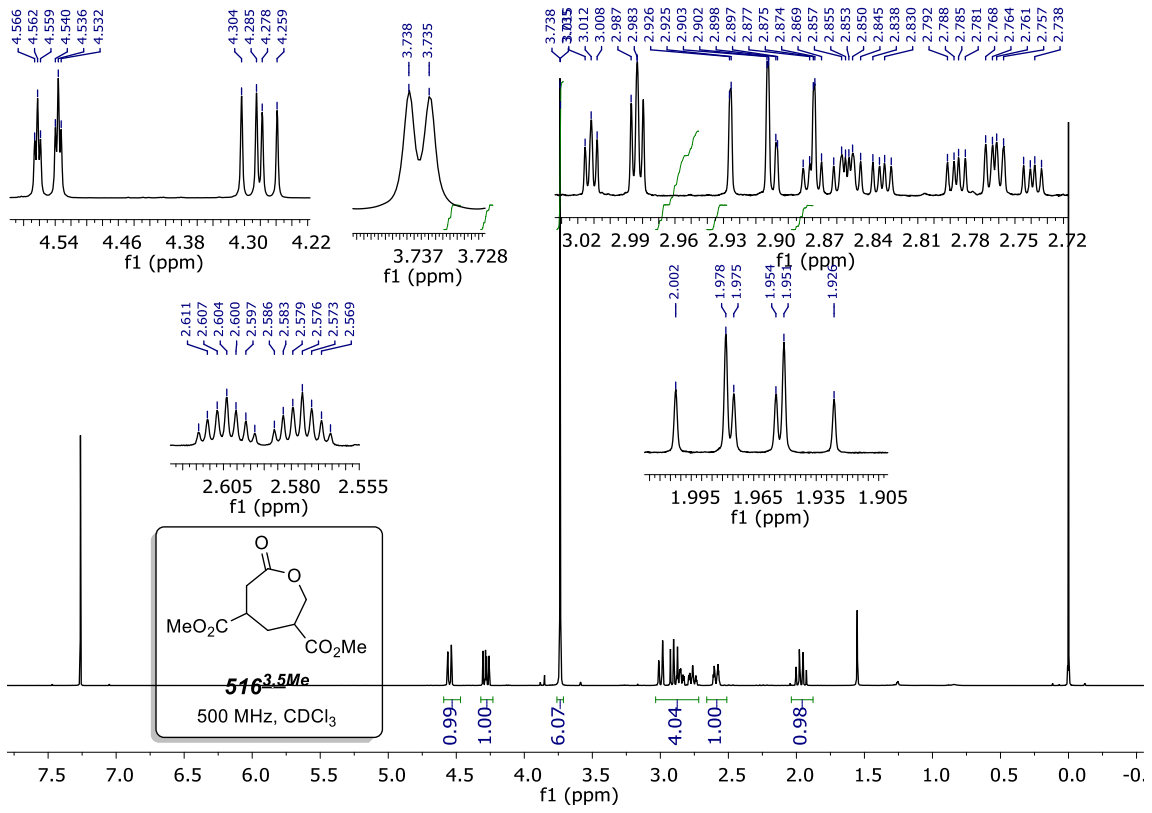












173.250, 172.483, 171.609

77.159, 68.476, 52.739, 52.634, 44.499, 38.889, 36.094, 34.527

